Control and performance studies on the differential compound engine

Hall, J.

Award date:
1989

Awarding institution:
University of Bath

CONTROL AND PERFORMANCE STUDIES ON THE DIFFERENTIAL COMPOUND ENGINE

submitted by J. Hall
for the degree of Ph.D
of the University of Bath
1989

ProQuest LLC
789 East Eisenhower Parkway
P.O. Box 1346
Ann Arbor, MI 48106-1346

SUMMARY

This thesis reports on experimental and theoretical work on the differential compound engine (DCE), an integrated engine-transmission system, with particular emphasis on optimisation and control.

The first part of the thesis explains the requirements of engine-transmission systems for heavy vehicles, then reviews alternative prime movers and transmissions, and the increasing use of electronic engine-transmission control.

The second part discusses the characteristics of the DCE and the matching process for DCE design, then describes the current Leyland 520DCE research prototype and test installation. Experimental steady state optimisation and mapping, followed by transient testwork, are then reported.

The third part of the thesis initially covers the development of a dynamic simulation specifically intended for control system design. This simulation was used for the evaluation of optimisation methods, and the development of control systems ultimately implemented on the 520DCE prototype. More advanced control designs based on identified models and predictive control techniques were also evaluated.

The final part summarises the findings of the above research, and gives specific recommendations for future work on the DCE concept.

ACKNOWLEDGEMENTS

I would like to express my gratitude and best wishes to the following people:

Professor Frank Wallace for his support, guidance and enthusiasm throughout the project

Professor Cliff Burrows for guidance in control aspects of the project

The SERC, who provided both sponsorship and project funding

Tony Elley and Keith Britton for their efforts in developing the experimental prototype and relieving much of the burden of detailed rig and installation design

Thomas Roelle, for his hard work in developing transient data handling software

Ian Marsh, William Alexander and Peter Prest, for advice and practical assistance, particularly with electronics problems

David Barker, for assistance with computer hardware and communications

The School secretarial and administrative staff, particularly Hazel Ford and Jan Thomas, also Sue White for her very competent typing.

Finally I would like to thank my parents and Victoria for their continual support and encouragement.

CONTENTS

NOTATION

SYMBOLS

A	area
Cv,Cp	specific heat capacities
Cd	discharge coefficient
d	dead time
e	error
E	tractive effort
h	specific enthalpy
j	sq.root of -1
m	mass
N	rotational speed
p	pressure
r	radius; reference input
R	gas constant .287kJ/kgK
s	Laplace variable
t	time
T	absolute temperature; time period
u	control input; specific internal energy
w	noise/disturbance input
v	velocity
V	volume
y	output
z	discrete system Laplace variable
γ	ratio of specific heats (isentropic index)
Δ	difference
δ	delay
ρ	density

τ torque; time constant

SUBSCRIPTS

ANN	annulus
cbyp	compressor bypass
c,comp	compressor
ebyp	engine bypass
e,eng	engine
mr	model reference
mv	multivariable
o/s	output shaft
pc	planet carrier
s	sampling
SUN	sunwheel
turb	turbine

SUPERSCRIPTS

•	derivative wrt time
*	predicted
^	estimated
T	transpose

ABBREVIATIONS

AC	alternating current
ADC	analog/digital converter
AFR	air/fuel ratio
BMEP	brake mean effective pressure
BNC	standard co-axial cable connector
BSFC	brake specific fuel consumption
CAT	charge air temperature

CO	carbon monoxide
CVT	continuously-variable transmission
DAC	digital/analog converter
DC	direct current
DI	direct injection
FAD	free air delivery
FBR	fuelling/boost ratio
FIR	finite impulse response
GCW	gross combination weight
HC	hydrocarbons
KE	kinetic energy
LRPC	long range predictive control
mps	mean piston speed
NDMF	non-dimensional massflow
NOx	oxides of Nitrogen
PID	proportional, integral, derivative
PRBS	pseudo-random binary sequence
SISO	single input - single output
SNL	start of needle lift
SOC	start of combustion
TC,TC/A	turbocharged, turbocharged/aftercooled
VG	variable geometry
ZOH	zero-order hold

1.INTRODUCTION

1.1 Powertrain requirements for commercial vehicles

1.2 Viable prime movers

1.2.1 The Diesel engine

1.2.2 The automotive gas turbine

1.2.3 The Stirling engine

1.3 Diesel engine-transmission systems

1.3.1 Multi-ratio gearboxes

1.3.2 Mechanical continuously-variable transmissions (CVT)

1.3.3 Hydrostatic CVT

1.3.4 Integrated powertrains

1.4 Control of engine-transmission systems

1.5 The research programme

1. INTRODUCTION

1.1 POWERTRAIN REQUIREMENTS FOR COMMERCIAL VEHICLES

The general requirements of powertrains for road-based commercial vehicles (light/heavy truck, bus or coach) are similar, though there may be variations in absolute terms. These requirements are described in turn below; for simplicity only the heavy truck will be considered. Legislative limits on truck weight (or gross combination weight - GCW) vary, but a typical figure is 40 tonnes, and the limits seem unlikely to increase greatly in the foreseeable future. The order of discussion below does not imply an order of importance - all the requirements must be considered together to produce a successful powertrain.

(i) Peak power

Heavy-duty vehicles typically use power/weight ratios of 5-8 kW/tonne GCW. Lower ratios imply that the powertrain will be operated at high load factors. This is important in achieving good vehicle fuel economy, partly because prime movers are generally most efficient near to full load (this applies to alternatives such as the gas turbine as well as to the Diesel engine), but also because higher load factors lead to lower and steadier speeds under normal conditions. Nevertheless, typical truck power/weight ratios are slowly increasing, possibly due to more demanding traffic conditions or time constraints (driver hours legislation). Taking the median value of 6.5 kW/t, the 40t truck would require a 260kW powertrain.

(ii) Peak tractive effort

This requirement is determined by "gradeability", the ability of the vehicle to ascend a given gradient or move away on a given gradient - this distinction is important for engines which cannot develop their full torque during the short clutch engagement time. Typically ascent of 30

per cent gradients is the requirement for heavy duty trucks; for the 40t truck this implies a peak tractive effort of about 120kN. Fig.1.1 shows a vehicle speed/effort map for the 260kW 40t truck geared for a reasonable top speed of 110km/h. The ratio of peak/rated tractive effort is thus approximately 14. The figure also shows the tractive effort curve for an "ideal" powertrain which can produce rated power at all vehicle speeds.

(iii) Efficiency

Fuel costs are a major part of commercial vehicle operating costs. High fuel efficiency is thus of great importance. Since commercial vehicle powertrains must operate over a wide speed and load range (the regions of greatest importance depend upon the application), fuel efficiency must not only have a competetively high peak value, it must also remain high over the operating range.

(iv) Driveability

This refers to the powertrain's ability to accelerate and decelerate the vehicle quickly and smoothly, without appreciable delays between a change in the driver's demand and the powertrain response. Obviously increasing the vehicle power/weight ratio will improve acceleration, but this is constrained by efficiency requirements as indicated above. Ideally, a powertrain of a given rated power should be able instantaneously to develop any demanded power level up to this rated power.

Engine braking is an important requirement in commercial vehicles, to give the driver more sensitive control of vehicle speed via a single pedal, and to supplement service (wheel) brakes under prolonged braking (for example, when descending hills).

(v) Emissions and noise control

It is difficult to discuss either of these constraints without explicitly considering the Diesel engine rather than keeping to a general discussion. While the Diesel engine completely dominates the heavy truck field, emissions and noise legislation will reflect what is realistically achievable by the Diesel engine, new limits gradually tightening only as existing ones are met. Nevertheless, these limits are steadily reducing. The "problem" emissions are NOx, CO, HC and particulates, plus visible smoke (related to HC and particulates). Legislation differs around the world (being generally most stringent in the U.S. and Japan), but is generally based upon transient drive cycle tests. NOx and particulates currently pose the major challenge. Fig.1.2 [1] shows the range of test cycle particulate and NOx emissions for current Diesel engine types, with predictions for future DI engines having electronic FIE, low oil consumption, and particulate traps. As shown, particulate traps will be required in order to meet proposed legislative limits.

Ultimately, noise is a less severe challenge. Legislation is based upon drive-by tests of the complete vehicle, so that engine-mounted shields and/or vehicle-mounted enclosures may be used. However, these imply increased weight, plus installation and maintainance difficulties, so work on the engine itself is important if limits can be met without shielding. This would mainly involve the use of dynamic structural analysis in engine design, and the use of alternative materials with high internal damping. While combustion is the main noise source in Diesel engines, efficiency and emissions are the primary concerns in combustion system development, and noise considerations traditionally come a poor third.

(vi) "Life cost"

The "life cost" of a powertrain is a complex combination of many factors, including initial purchase price and maintainance costs, durability (rebuild intervals) and fuel efficiency. Increased powertrain complexity and higher ratings may therefore be unacceptable unless durability can be maintained and manufacturing costs controlled. However, as indicated earlier, all the factors previously discussed are important, so for example increased complexity may be accepted if it gives improved driveability or efficiency.

(vii) Power density and storage density

For commercial vehicles power density should be considered in terms of power/powertrain weight and power/powertrain "box" volume. A typical Diesel powertrain for the 40t truck would weigh in the order of 1t, while the payload would be about 25t. Although powertrain differences therefore make only a small difference to the available payload weight, improvements are welcomed.

Powertrain box volume shape and size are important for installation reasons. Similarly the storage density of the energy source is obviously important in terms of weight and bulk - the best example of this is the unsuitability of electric traction for road vehicles owing to the low storage density of currently-available batteries.

1.2 VIABLE PRIME MOVERS

There appear to be three viable prime movers for heavy commercial vehicles; the Diesel engine, the automotive two shaft gas turbine (free turbine engine) and the Stirling engine. Each will now be described with

reference to the requirements listed above, showing why the Diesel engine is completely dominant.

1.2.1 The Diesel engine

The widespread use of the Diesel engine is due to its existence and continual development from the outset of the internal combustion engine industry. In naturally-aspirated form it offers simplicity, durability and good fuel efficiency. In recent decades, the major changes in Diesel engine technology have been associated directly or indirectly with turbomachinery developments, described below. A distinction should first be made between direct and indirect injection (DI,IDI), two and four-stroke engines. DI systems are favoured for heavy-duty Diesels since fuel consumption tends to be lower. Only one major manufacturer (GM) continues to produce two-stroke automotive Diesels; the turbomachinery developments discussed below are not in general applicable to the two-stroke since peak brake mean effective pressure (BMEP) is limited (thermal limits). An exception is variable geometry turbocharging, which might help to meet the two-stroke's sensitive scavenging requirements.

(i) Turbocharging

Turbocharging increases charge air density, and thus increases the peak BMEP achievable given a fixed minimum air/fuel ratio (AFR). Furthermore, since turbocharged engines will generally operate at higher AFRs and higher ratios of brake/friction power than naturally-aspirated engines of the same rated power, their brake thermal efficiency will also be higher.

For heavy vehicle applications the turbocharger is matched to give "torque rise", that is, increasing peak BMEP with falling speed. Torque rise may be defined as:

torque rise = (maximum BMEP - rated BMEP) / rated BMEP (1.1)

It is important to know the speed range over which this torque rise occurs, particularly since re-matching for increased maximum BMEP often necessitates a reduction in rated speed due to turbocharger speed limits.

Typical turbocharged heavy-duty Diesel engines have a torque rise of 10 - 20 per cent, with peak BMEP up to about 14 bar, as sketched in fig.1.3. This is a major improvement upon naturally-aspirated engine torque curves which are at best essentially flat, and is very important in matching engine and transmission to achieve a tractive effort curve with good driveability.

(ii) Charge cooling and increased injection pressure

To achieve higher ratings and torque rise, charge cooling is employed. Provided adequate heat rejection can be achieved without excessive charge cooler pressure losses, charge air density is increased. Importantly, thermal loading is also reduced, which allows fuelling to increase in line with the air mass flow increase and/or improves durability [2].

Current turbocharged charge cooled engines operate with peak BMEPs up to about 17 bar, and torque rise of 20 - 30 per cent (fig.1.3).

The high fuellings which correspond to these high ratings require increased fuel injection pressures to maintain short injection periods for good heat release characteristics. Increased injection pressures have been found to improve thermal efficiency, smoke and particulate emissions [3]. Unit injectors are increasingly used, and quiescent combustion systems may be considered, giving improved volumetric efficiency and potentially improved thermal efficiency (due to reduced pumping loss and heat rejection) compared to swirl port systems.

The BMEP limit for engines with single stage turbochargers appears to be 18 - 21 bar, regardless of whether fixed geometry (or nozzleless) turbochargers or variable geometry (VG) / sequential turbocharging is used. In [4] a limit of about 18 bar was suggested. In [5] peak BMEPs of 20 bar were achieved at low engine speeds, however, the turbocharger had been matched primarily for this and rated speed had to be reduced to prevent compressor overspeed (although a VG turbine might overcome this). The "upper limit" torque curve for single stage turbocharging in fig.1.3 reflects the latter peak BMEP. Two stage turbocharging will not be considered here, but if current trends in heavy-duty Diesel ratings continue then this technique will be warranted by the early 1990's. The boost pressure ratio required for a BMEP rating in the above range is firstly dependent upon the minimum AFR allowed by the combustion system (that is, the mass of fuel which may be injected for a given mass of air) and the resulting brake thermal efficiency (that is, the work produced using the above fuel). Secondly, the required boost ratio is dependent upon the degree of charge cooling employed, since it is charge air density which must be increased and density varies linearly with temperature as well as pressure. The derivation of an algebraic expression for the required boost pressure as a function of BMEP and the above factors (minimum AFR, brake thermal efficiency and charge air cooling) is straightforward, but too lengthy for inclusion here. In practice, current engines operating at 18 - 21 bar BMEP would require boost pressure ratios of 2.5 - 3.0.

The above discussion of increasing ratings has not considered the effects upon transient response. For engine operating at the above peak boost ratios there may be a major shortfall between transient torque and the

peak steady state torque at a given speed, impairing driveability. This is particularly a problem when moving from light to full load, for example when moving away from rest. Turbocharger (and thus boost) response is chiefly dependent upon matching and inertia/friction.

(iii) Variable geometry (VG) and sequential turbocharging

Both of these techniques alter the turbocharger match (continuously or in discrete steps) over the engine operating range, giving improved engine torque rise and efficiency, improved transient response (with a suitable control system) and potential emissions reductions [6-10].

Turbocharger turbines for automotive applications are invariably of the radial inflow type due to the small sizes involved and the requirement for low cost. Nozzleless casings are commonly used to broaden the flow range of the unit. Alternative VG arrangements have been proposed, broadly in three categories:

(a) swivelling nozzles

(b) variable tongue or volute area - achieved by sliding or hinged flaps in the turbine inlet, or by a flexible shroud used to "tighten" the volute.

(c) sliding nozzles - an annular nozzle ring is moved axially across the rotor inlet, gradually changing the turbine from nozzleless to fixed nozzled type. Opposing pairs of rings may be used to give more progressive variation.

Approaches (b) and (c) were considered in order to achieve cheaper and more durable VG than swivel nozzles. Approach (c) was successful as reported in [7,8]. Further details may be found in [11]. However, swivelling nozzles seem likely to have the greatest commercial success

[12,13].

Sequential turbocharging techniques were first investigated for medium speed and quick-running marine engines, which may operate for long periods at any point in a very wide power range. The only published study for truck applications is [10]. This used two conventional turbochargers in series, as shown in fig.1.4, with a pulse converter arrangement to retain pulse operation with a simple pipework layout. Unequal size turbochargers are required for greatest matching flexibility. In [10] the larger unit operated continuously, and was supplemented by the smaller unit at high engine speeds to prevent overspeeding. The larger turbocharger in the sequential arrangement can thus be smaller than the turbocharger in a comparable single-turbocharger arrangement. This enables improved low speed torque and transient response.

Since sequential turbocharging allows a greater change in turbocharger match than VG turbocharging, it should achieve greater improvements in low speed torque. However, the VG system is more progressive, and would seem to have greater potential to improve transient response. Both systems are likely to be of future interest.

It is appropriate at this point to illustrate the reductions in brake specific fuel consumption (BSFC) achieved by these advances in Diesel engine technology. Fig.1.5 shows the BSFC range of current engines [14,15]; as ratings increase compounding becomes more worthwhile, and is now under development by several manufacturers.

(iv) Turbocompounding

This refers to a system whereby some of the exhaust enthalpy is recovered as shaft power by an expander and drive train. Three primary

decisions must be made in designing a turbocompound engine:

(a) expander type - the usual choice is between radial and axial turbines, although positive displacement devices have been advocated. As with turbocharger turbines, the choice of radial types would be expected (as adopted by Cummins [15]) however, Caterpillar [14] developed and used a high efficiency axial compound turbine in a 225 kW truck engine.

(b) turbomachinery layout - the compound turbine may be configured in parallel or in series (preceding or following) with the turbocharger turbine. In [14] it was concluded that several arrangements could give equal design point efficiencies, but in both [14] and [15] a series configuration was used, with the turbocharger first. This gives the most rapid engine response to load changes. With this configuration the axial compound turbine gives a simpler installation, since turbocharger turbine outlet and compound turbine inlet flows are both axial.

(c) drivetrain layout - compound turbines for heavy-duty Diesel engines typically operate up to 50 000 rev/min, requiring a speed reduction of about 25:1 to the crankshaft. Cummins and Caterpillar [14,15] both used layshaft gear drives. Whether the compound turbine is geared to the front of the engine (where the main fuel pump/camshaft gear drives are usually located) or to the rear (where torsional amplitudes are lower - "nodal" drive), some torsional isolation is required, probably a fluid coupling. The use of a toroidal continuously-variable transmission (traction CVT) in the drivetrain, operating at an intermediate speed, has been reported by Hino [16]. This would allow the compound turbine to operate at high efficiencies (best blade/speed ratio) regardless of engine speed.

The three arrangements - front drive, rear drive and CVT drive - are shown in figs.1.6(a)-(c).

The addition of a compound turbine to a conventional turbocharged charge cooled engine typically can improve peak thermal efficiency by about 5 - 7 per cent as shown in fig.1.5. High turbomachinery and drivetrain efficiencies are required to realise these gains. Driveability may also be improved, by increased torque rise and low speed transient response. This is because the back pressure imposed by the compound turbine allows the use of a smaller turbocharger turbine without overspeeding at high engine speeds.

A possible alternative or addition to turbocompounding is the use of Rankine bottoming cycles [17] (fig.1.7). These utilise heat from the exhaust in a secondary closed loop system with feedpump and expander (again geared to the crankshaft). The inclusion of a regenerator in the loop gives better energy utilisation than turbocompounding, but the system appears too bulky for automotive applications, and must have appreciable thermal inertia, impairing transient power.

(v) Insulation

Insulation of the Diesel engine has been considered to reduce cooling system requirements and improve thermal efficiency. In practice most of the reduced heat loss to coolant is rejected to the exhaust rather than appearing as shaft power. Hence insulation is most attractive for turbocompound engines; anticipated reductions in BSFC with insulation are shown in fig.1.5 [14,19,20].

The main components to be insulated in DI Diesels are the piston crown, liner top, flame deck and exhaust ports. However, the type of insulation to be used - ceramic material type, monolithic or coating application, incorporation of air gaps - is the subject of much research. Furthermore

the manufacture of engineering ceramics and the design of ceramic engine components require new approaches, while there may be further difficulties associated with lubrication at elevated temperatures.

While insulation is undoubtedly worthwhile for highly-rated compound engines, ceramic components will only be adopted as reliable design/manufacturing methods plus acceptable cost and durability are developed.

1.2.2 The automotive gas turbine

Gas turbines for automotive applications normally have the following main features (fig.1.8):

(i) Free turbine layout

A compressor (usually radial) and turbine (axial or radial) are mounted on a common shaft, forming a self-supporting "gas generator". This turbine is followed by a free power turbine (axial or radial) with step-down gears to the output shaft.

(ii) Regenerator or heat exchanger

To improve thermal efficiency, some form of heat exchange is used between exhaust gases leaving the power turbine and compressed air entering the combustion chamber (burner). A rotating regenerator is commonly used, as shown in fig.1.8(a). More complex cycles incorporating multi-stage compressors with intercooling, and reheat between turbines enable design point efficiencies to be maintained down to low powers [21], but the simpler heat-exchange cycle of fig.1.8 is generally favoured for cost and durability reasons.

(iii) Variable geometry (VG) power turbine nozzles

Consideration of the ideal heat-exchange cycle [21] shows that thermal efficiency increases with peak cycle temperature (burner exit / turbine inlet), and this is also true of the practical engine. Thus thermal efficiency will deteriorate at part load as peak temperatures fall. By introducing VG nozzles into the power turbine, its swallowing capacity can be reduced at part load, altering the gas generator condition to a higher turbine inlet temperature, and thus improving efficiency.

For automotive applications the VG nozzles have two further important uses. Firstly, transient response, which would normally require acceleration of the gas generator to achieve higher output powers, can be improved by closing the nozzles to directly increase temperature rather than gas generator speed. Carefully-designed control systems are required [22,23]. Secondly, if the nozzles are rotated such that the power turbine inlet flow impinges on the back of the blades, then substantial engine braking can be obtained.

Alternative systems have been considered to improve part-load efficiency. The GM "power transfer" system employed an electro-hydraulically actuated clutch between gas generator and power turbine (geared such that the power turbine side ran more slowly). Partial engagement of the clutch forces the gas generator to operate at a lower speed, higher load - and thus higher efficiency - condition. Power turbine VG is therefore not required. Also, by locking the clutch, the compressor can absorb shaft power, giving engine braking. A modern equivalent might use a CVT to reduce power transfer losses.

The automotive gas turbine offers high power density, low noise and

vibration, and a torque curve superior to that of high torque rise Diesel engines (fig.1.9). Peak thermal efficiencies of about 35 per cent are achievable with metal-based alloy components, and ceramic components allowing higher peak cycle temperatures may enable this to be increased towards 40 per cent. However, as indicated earlier typical turbocharged charge cooled Diesel peak efficiencies are now 42-44 per cent; also gas turbine efficiencies fall off more rapidly at light load.

Fuel costs and manufacturing costs are thus major obstacles at present. The low emissions and multifuel capability (although constrained by fouling problems with low-grade fuels) of the continuous combustion system may conceivably lead to future re-evaluation of the automotive gas turbine.

1.2.3 The Stirling engine [17,24]

In a Stirling engine, the following basic processes are applied to a working fluid operating in a closed loop in a positive displacement machine with external combustion (fig.1.10).

(i) Isothermal compression with heat rejection at a low temperature to a cooler (cycle points 1-2)

(ii) Transfer of the working fluid at constant volume through a regenerator where it picks up heat from the previous cycle (2-3)

(iii) Isothermal expansion with heat addition at a high temperature from external combustion (3-4)

(iv) Transfer of the working fluid at constant volume through a regenerator, to which it rejects heat (4-1)

It may be noted that if the regenerator heat transfers in (ii) and (iv) were equal, the cycle would have the Carnot efficiency, that is the

highest possible efficiency for any cycle with the given maximum and minimum temperatures.

The practical Stirling engine uses reciprocating cross-head pistons and has non-ideal heat exchange, so falls short of the ideal cycle of fig.1.10 and has typically less than half the Carnot efficiency. A typical automotive Stirling engine is shown in fig.1.11. This uses double -acting pistons in a U4 configuration. The working fluid passes from the underside ("cold space") of each piston via regenerator and heater tubes to the top side ("hot space") of the next piston. There is a heater, regenerator and cooler section between each successive cylinder, and the working fluid thus progresses around the whole engine.

To achieve acceptable power density for automotive use, gases with high heat capacity and low flow losses - usually hydrogen or helium - are used, at mean working pressures up to 200 bar. This raises the major technical problem of the automotive Stirling engine: sealing to prevent the egress of these light gases at these pressures is extremely difficult. An equally major problem is the high cost associated with the "hot space" components, where expensive materials must be used at the high temperatures required for good efficiency.

Automotive Stirling engines can achieve thermal efficiencies comparable with current Diesel engines, and have a similar torque characteristic (fig.1.9) with a wider speed range. Emissions and noise are very low owing to the continuous external combustion, and as with the gas turbine this also gives multifuel capability, subject to fouling considerations.

Quite sophisticated control systems are required for good driveability. Simply regulating fuel flow gives slow response due to thermal inertia.

The favoured approach is to vary the working fluid mean pressure, typically between 50 and 200 bar, while keeping combustion chamber temperature more nearly constant.

In summary, the automotive Stirling engine offers comparable fuel economy, driveability and power density to the Diesel engine, with reduced emissions and noise. Its commercial application has been ruled out by high manufacturing costs and technical problems such as piston rod sealing.

1.3 DIESEL ENGINE-TRANSMISSION SYSTEMS

The preceding sections have established the reasons for the dominance of the Diesel engine as a prime mover for heavy vehicles. Nevertheless, the Diesel torque characteristic shown in fig.1.9 is far removed from the tractive effort curve of fig.1.1. This section covers transmission systems employed to bridge this gap.

1.3.1 Multi-ratio gearboxes

This is the simplest and most common form of transmission. For heavy trucks a gearbox and two-speed rear axle are usual, giving 7-16 ratios in all. A more powerful and/or higher torque rise engine allows the use of fewer ratios, and vice versa. This gives a good approximation to the ideal constant power hyperbola (an example for the 40t, 260kW, truck is sketched in fig.1.12), particularly since transmission efficiency falls off only slightly in the lower gears, but driveability is impaired by the need for gearchanges. Typical transmission efficiencies are 91-96 per cent.

Semi-automatic (pre-selector) gearboxes common in lower torque

applications where frequent gearchanging would be required (mainly buses). These are usually compound epicyclic trains with hydraulically actuated clutches or brake bands.

Computer-aided gearshifting is increasingly being offered for heavy trucks, combining conventional layshaft gearbox technology with microprocessor "advice" on optimum gear selection, and sometimes electro-hydraulic clutch/gearlever actuation. Improving driving technique in this way can significantly improve vehicle fuel consumption with little new technology [25].

1.3.2 Mechanical continuously-variable transmissions (CVT)

Mechanical CVTs may be classified into two types [26]:

(i) Traction drive ("Perbury" or "toroidal" CVT)

Drive is transmitted between an opposing pair of toroidally surfaced discs by a set of rollers. The rollers are located such that they can be tilted, varying the rolling radii on the two discs and thus the relative speed of the discs.

(ii) Friction drive

This consists either of a flat belt in tension or steel vee-belt in thrust between two variable diameter pullies. As the pulleys are moved axially, so the diameter covered by the belt varies and the speed ratio changes.

CVT efficiency is typically 85-92 per cent over the speed range, rather lower than conventional geartrains. However, with appropriate control systems (microprocessor-based) the prime mover can be made to operate at its peak efficiency for any given power output, so vehicle fuel efficiency may be improved. Furthermore, vehicle acceleration may be

improved as the prime mover has only to move to its rated power once, the CVT ratio then varying continuously as the vehicle speed rises. With a stepped transmission the prime mover must repeatedly traverse its torque curve, so that the mean power available during acceleration is probably in the region of 70 per cent of rated power. For commercial vehicles the CVT might lead to the use of smaller engines with lower rated power, probably re-matched since high torque rise is not required, and designed to withstand more frequent operation at rated power.

CVTs are currently only available in small passenger cars, with much lower powers (about 50kW) and torque ranges than required for heavy vehicles. Commercial vehicle developments have been restricted to traction CVT trials in a 16t bus, with incorporation into a regenerative braking driveline [27]. The tractive effort curve approaches the constant power hyperbola (with the 10-15 per cent power loss mentioned above), but peak torque and minimum speed are limited, and the gap to zero speed must be covered by a clutch or torque converter.

1.3.3 Hydrostatic CVT

Hydrostatic transmissions fundamentally comprise a hydrostatic (that is, positive displacement) pump driven by the prime mover, supplying fluid to a hydrostatic motor driving the load. For a vehicle transmission the pump and motor must both operate at variable speed and load if the prime mover is to operate near peak efficiency over its power range. Furthermore, the hydrostatic system efficiency will fall with fluid pressure. Thus variable displacement pump and motor (for example, variable swash axial piston machines) must be used to maintain efficiency, with a control system to ensure that the pump and motor

displacements give optimum prime mover conditions at a given load (vehicle) condition. Nevertheless, transmission efficiencies are poor at the extreme speed/ load conditions.

A combined gear/hydrostatic transmission has been proposed which gives improved efficiencies, since it allows a high proportion of the power to be transmitted through an epicyclic geartrain (fig.1.13(a)); again at the extremities of the range power flows through the hydrostatic system and efficiency falls considerably [28]. A tractive effort curve for a turbocharged Diesel engine with this hydrostatic shunt transmission is shown in fig.1.13(b). The hydrostatic machines have a maximum pressure limit and typically a 4:1 turndown range in displacement. Hence the torque rise of the system is typically about 3.5:1 over a 4 or 5:1 speed range. From fig.1.13(b) it is evident that a stepped transmission (at least three ratios) would be required in series with the hydrostatic shunt to meet the tractive effort requirements of the 40t truck.

As with the mechanical CVT, the low transmission efficiencies may be outweighed in some applications by the ability to operate the prime mover on its locus of maximum efficiency over the power range. Studies have been carried out for bus applications, again incorporating regenerative braking (hydraulic accumulation) in many cases. Commercial use of hydrostatic transmissions is currently limited to special applications where the vehicle layout precludes the use of mechanical transmissions (for example, the combine harvester).

1.3.4 Integrated powertrains

The preceding sections have considered vehicle transmission systems which may be used to overcome the inherently unsuitable torque characteristics of the turbocharged Diesel engine. Two integrated Diesel engine-transmission systems are described below which are designed specifically to approach the ideal stepless constant power characteristic.

(i) The differentially-supercharged Diesel engine (DDE) [29]

The DDE, as developed by Perkins in the 1960's, is shown schematically in fig.1.14(a). The system consists of a Diesel engine, compressor and output shaft connected through a fully-floating epicyclic gear. The component connections are such that at a fixed engine speed the compressor and output shaft speeds are differentially related. It is important to recognise that this is a torque-dividing or torque-balancing system, not a speed-dividing system. Thus at steady state engine, compressor and output (load) torque are all in fixed proportion. The relative speeds are determined by the torque level and component match (compatibility of compressor and engine air massflows). The speed/boost range imposed on the compressor is wide, and this led to the use of a positive displacement (screw-type) rather than centrifugal compressor.In the Perkins prototypes, the output shaft was "overdriven", covering a wider speed range than the engine, and thus improving driveability. It is also worth pointing out that since compressor torque (and thus boost) varies with engine torque, the problem of excessive part-load compressor power consumption due to unnecessarily high boost pressures which affects conventionally supercharged engines does not apply to the DDE.

The Perkins DDE was matched for a peak BMEP of 17.6 bar, much higher than

achieved by production turbocharged engines at that time. Rated BMEP was set relatively low, at 9.66 bar, in order to achieve a high torque rise of 82 per cent. The torque rise at the output shaft was similar (due to the above gear relations); the output shaft peak torque speed was 43.5 per cent of maximum speed. A two-speed gearbox and torque converter were used in tandem with the DDE, giving an adequate traction curve. The tractive effort curve, "scaled-up" to a rated power of 260kW, is shown in fig.1.14(b).

It is difficult to justify the use of low rated BMEP (and thus low specific power) in an engine designed to withstand high peak BMEP, except perhaps to argue that the high torque rise characteristic improves driveability to the extent that lower rated power is acceptable.

As was seen earlier, it is now possible to achieve the above peak DDE rating with conventional turbocharged charge cooled Diesels. If one accepts the use of low rated BMEP (achieved by tailoring the maximum fuelling curve), then current turbocharged engines could be matched to equal the torque rise, speed range and rated power achieved with differential supercharging. The DDE might retain superior transient response compared to a highly-turbocharged engine, but as discussed earlier, the latter may be improved by VG turbocharging.

(ii) The differential compound engine (DCE) [30-32]

The Wallace DCE has the same basis as the DDE above, namely a Diesel engine with differentially-drivencompressor. However, the addition of an engine air bypass and compounding turbine (as illustrated in fig.1.15(a)) gives greatly increased matching flexibility, and enables a close approach to the ideal stepless constant power characteristic down to a

low output shaft speed.

The DCE is the subject of the research reported in this thesis, and its principles and characteristics will be discussed in later chapters. At this point it is appropriate to list the main features of the DCE, and the advantages they confer.

(a) Highly-rated Diesel engine

Because the engine is supercharged, as with the DDE, high ratings may be used as required (within the engine mechanical limits), giving high power density and good indicated thermal efficiency as in highly-turbocharged engines. In the DCE, the engine torque rise is no longer the main source of the output torque rise, so the high speed de-rating used in the DDE is unnecessary.

(b) Differentially-driven compressor, and engine air bypass

The differentially-driven compressor provides increasing air flow as output shaft speed decreases. In the DCE this is used partly to increase the engine boost ratio for a degree of engine torque rise, but chiefly is passed via an engine bypass directly to the compound turbine, giving a torque conversion effect. The output shaft may then be run down to low speed (typically 20 per cent of maximum speed) with increasing bypass flow and turbine power.

The mechanically-driven compressor potentially gives better transient response than a free-running turbocharger.

(c) Compound turbine

Over much of the DCE operating range the main function of the compound turbine is the same as that in a conventional turbocompound Diesel engine, namely to increase system power and efficiency by

recovering work from exhaust gas enthalpy. Since there is no turbocharger, the available enthalpy is much greater, and its recovery much more important. At low output speed/high load conditions the turbine has the equally vital role, indicated above, of providing substantial output torque rise.

The use of a high-efficiency turbine CVT to maximise turbine exhaust gas energy utilisation is crucial to both system efficiency and the tractive effort characteristic. At typical ratings the maximum power transmitted by the CVT (the maximum turbine power) is about half the rated DCE power. As in the Hino CVT turbocompound scheme mentioned earlier in this chapter, the CVT could run at an intermediate speed in the reduction train, with a resultant reduction in bulk and, probably, cost.

The use of turbine VG is extremely valuable for continuous steady state optimisation of the system operating condition, and to improve transient boost response.

(d) Torque converter

To cover the range between minimum output shaft speed and zero speed, an hydrodynamic torque converter is proposed, with a lock-up clutch. This gives a continuous (stepless) tractive effort curve.

A tractive effort curve for a 260kW DCE, with a torque converter (peak torque ratio 3.6:1 as in the DDE prototype) operating only below 20 per cent of full speed, is shown in fig.1.15(b).

The DCE provides an excellent stepless traction curve for heavy vehicles. Given high turbomachinery efficiencies, output shaft thermal efficiency is comparable to that of turbocharged and turbocompound engines with

conventional transmissions. Being a compound scheme, the DCE could immediately take advantage of developments in engine insulation, with the improvements in efficiency forecast earlier (fig.1.5).
At present some integral features of the DCE concept (turbine CVT, VG turbine nozzles and positive displacement compressor) prevent its commercial adoption on the grounds of cost and novelty. However, as the technology of these components is developed for other applications, their combination in the DCE may become commercially viable.

1.4 CONTROL OF ENGINE-TRANSMISSION SYSTEMS [33-35]

With the advent of the cheap general purpose microprocessor, and the decreasing cost of electronic sensors, engine and transmission control systems have become increasingly sophisticated. As with most developments in this field, the use of electronic controls is justified by improvements in fuel efficiency, engine power and response, emissions, and noise/vibration/harshness (NVH).

Electronic controls may be introduced in two ways:
(i) For more precise control of existing parameters - a good example of this is electronic timing control in spark ignition engines
(ii) For the control of novel parameters - such as VG turbochargers, or CVTs.

Spark ignition engines have generally led the way in electronic control, particularly of fuel injection, spark timing (for economy, NOx or knock control) and exhaust gas recirculation (EGR - also mainly for NOx control). Diesel engines are now following, primarily with fuel injection equipment (FIE) control, as efficiency requirements and emissions

legislation tighten. Two classes of electronic Diesel FIE may be defined:

(i) Analogue actuation

Here a conventional pump-pipe-nozzle system, or a "first-generation" unit injector system with a common control rack, is operated by a pneumatic, solenoid or hydraulic actuator, which is electronically controlled. Separate actuators and mechanisms may be used to alter injection timing.

(ii) Digital

Here electronic unit injectors control fuelling by pulsewidth modulation (PWM). The injector supply is held at a high pressure, so that the quantity of fuel injected depends upon the pulsewidth of a digital signal admitting fuel to the injector. Injection timing control is effected simply by controlling the pulse timing with respect to the engine angular position signal. This is in effect an electronic development of the Cummins mechanical "pressure-time" (P-T) system.

The control microprocessor can then carry out the following functions:

(i) Speed governing - including precise (isochronous) governing for special applications and power take-offs. Acceleration control may also be applied to improve fuel economy in unladen heavy-duty vehicles.

(ii) Maximum fuelling control - with boost-related limits for smoke-limiting, compensation for fuel temperature, and special features such as a time-limited higher fuelling mode.

(iii) Timing control - for economy, emissions or noise control, usually according to a pre-set schedule rather than any feedback parameter.

Further controls will follow if engine developments such as VG turbochargers and variable charge cooling are adopted. Advisory controls such as computer-aided gearshifting mentioned earlier, are already in production. The interaction between the effects of the various controls

will require an integrated approach to control system design.

A major part of the work reported in this thesis was the development of control designs and design techniques for the DCE, which in prototype form employs electronic fuelling, timing, and turbine VG control.

1.5 THE RESEARCH PROGRAMME

The work carried out by the writer formed part of a major DCE research project, which was itself conducted in parallel with other commercially-funded DCE studies at Bath. The work had two broad objectives:

(i) To continue experimental investigations on a recently-commissioned DCE research prototype, beginning with steady state optimisation and component mapping, and leading to transient testing. Underlying this work was the need for experimental data for comparison with simulations.

(ii) To investigate the control of the DCE for optimum steady state efficiency and transient response, leading to the design and implementation of a microprocessor-based control system on the prototype. The multivariable nature of the DCE, that is the interaction between the effects of the control inputs (fuelling, turbine VG and injection timing), had long been recognised, and it was intended ultimately to investigate control designs which would take these multivariable effects into account.

LIST OF FIGURES

TRACTIVE EFFORT CURVE - TYPICAL REQUIREMENTS FIG. 1.1

[40t truck
6.5kW/t
110km/h at rated power
30% gradeability]

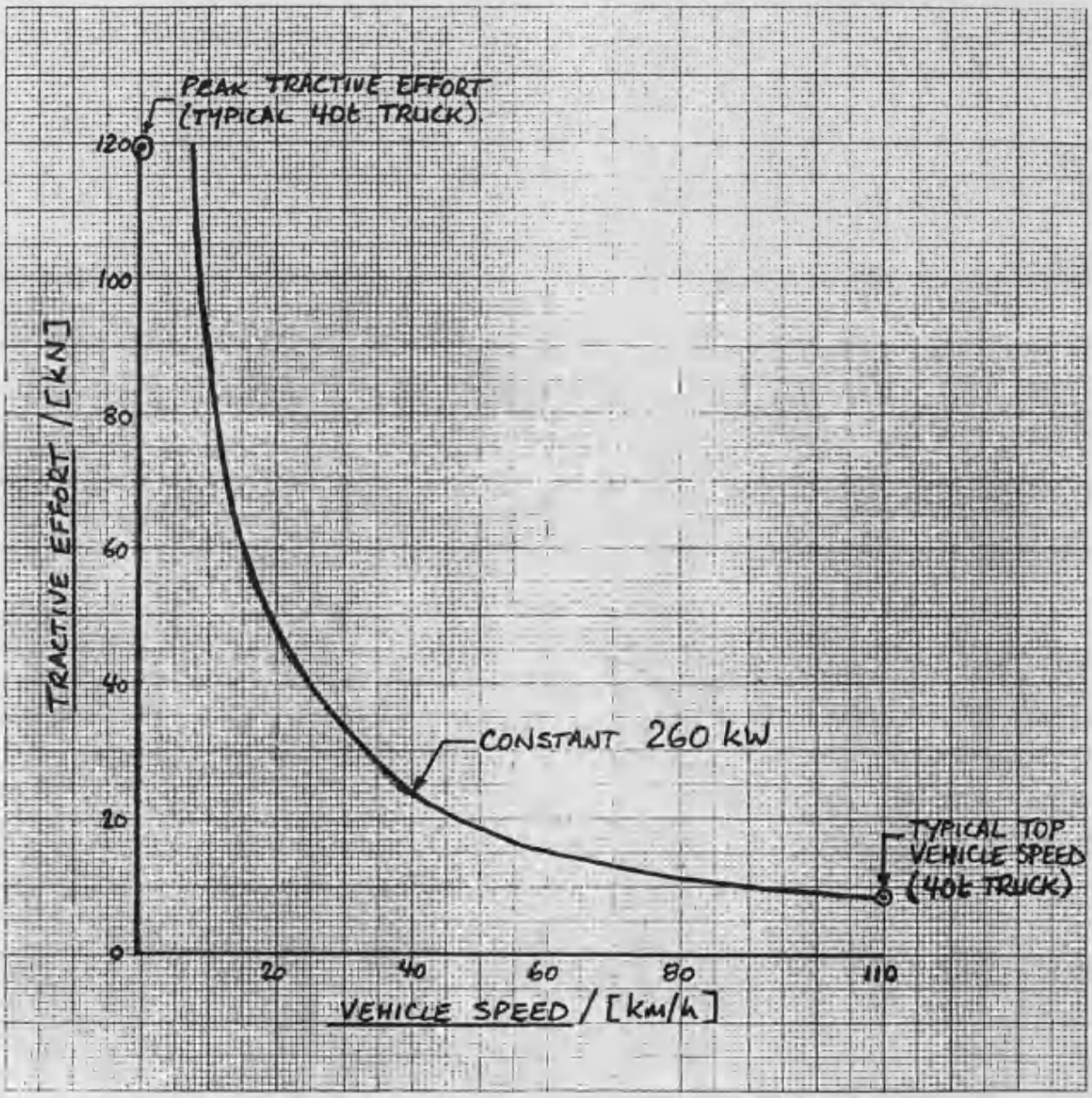

PARTICULATE-NOx TRADE-OFF OVER
U.S. HEAVY-DUTY TEST CYCLE

FIG. 1.2

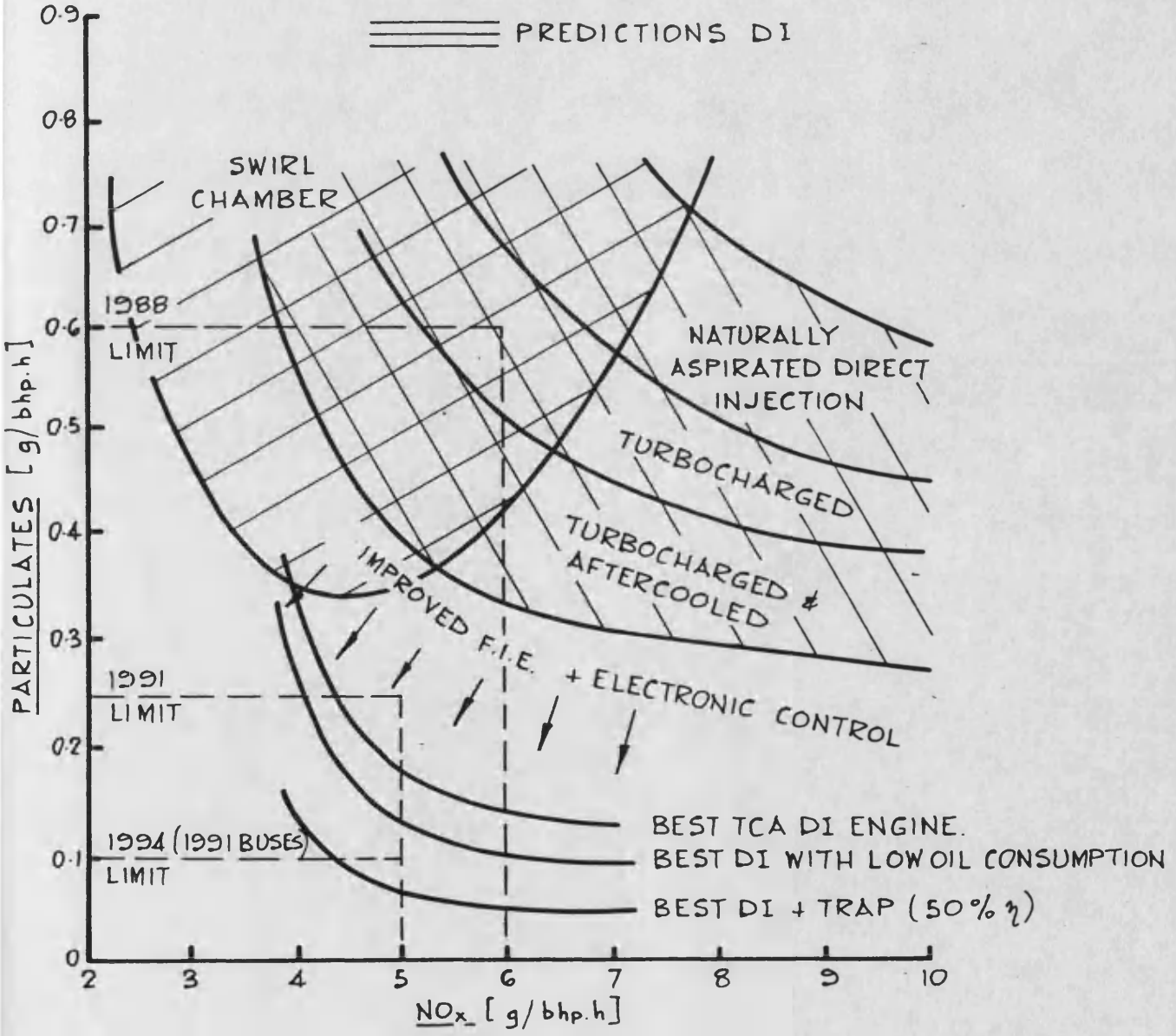

TYPICAL HEAVY-DUTY DIESEL ENGINE RATINGS FIG. 1.3

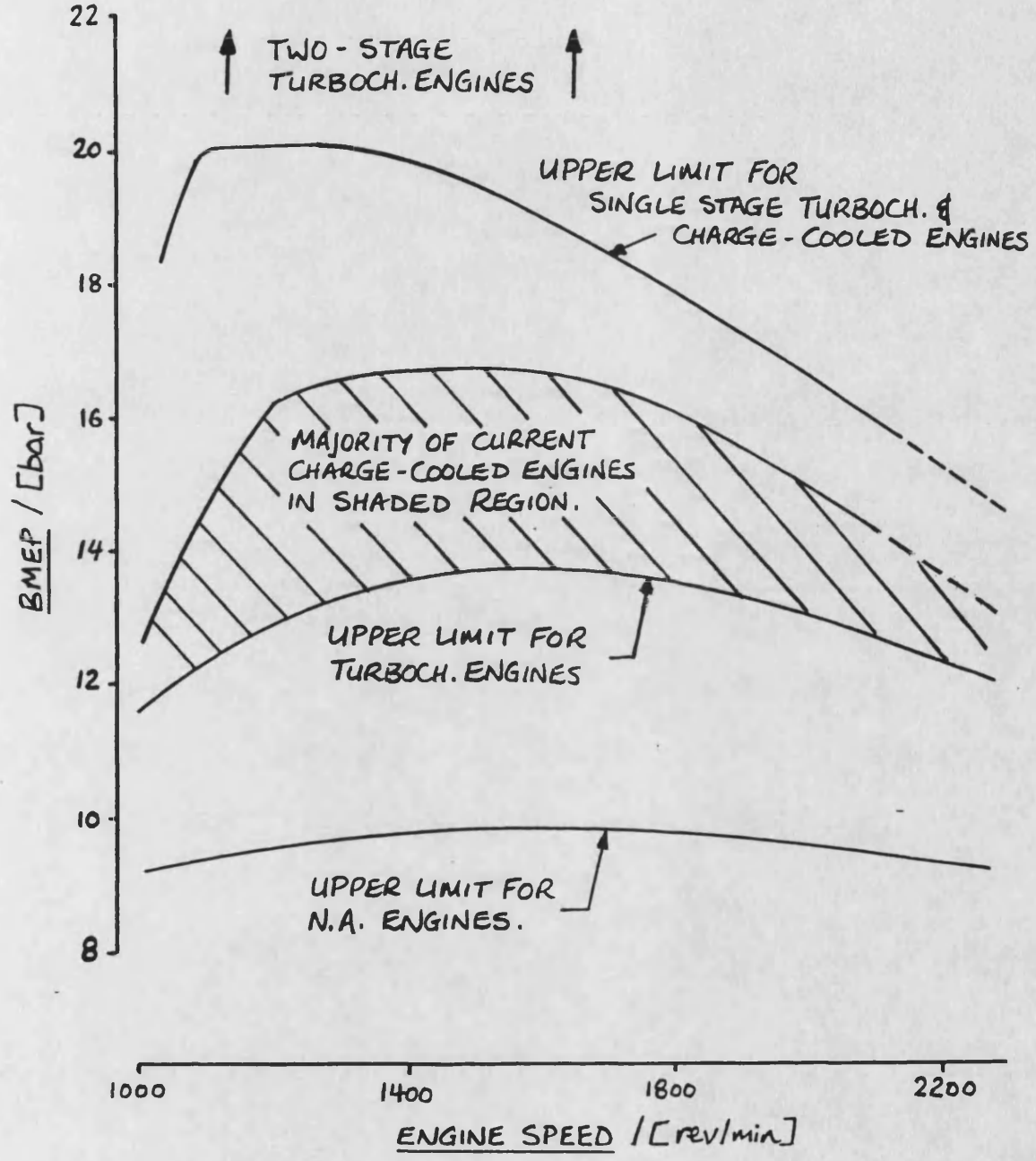

SEQUENTIAL TURBOCHARGING ARRANGEMENT FIG. 1.4

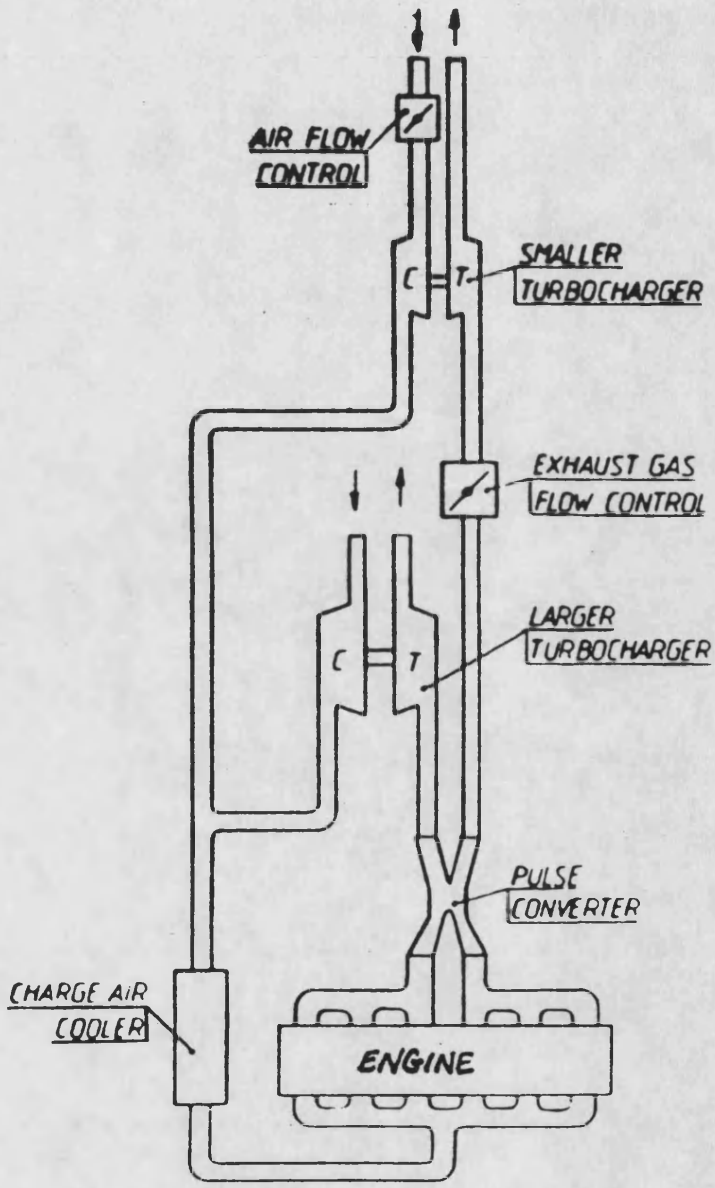

REDUCTIONS IN SPECIFIC FUEL CONSUMPTION FIG. 1.5

TC	turbocharged
TCC	..and charge cooled
VG	..with variable geometry t/c.
TCM	turbocompound
ITCM	insulated turbocompound

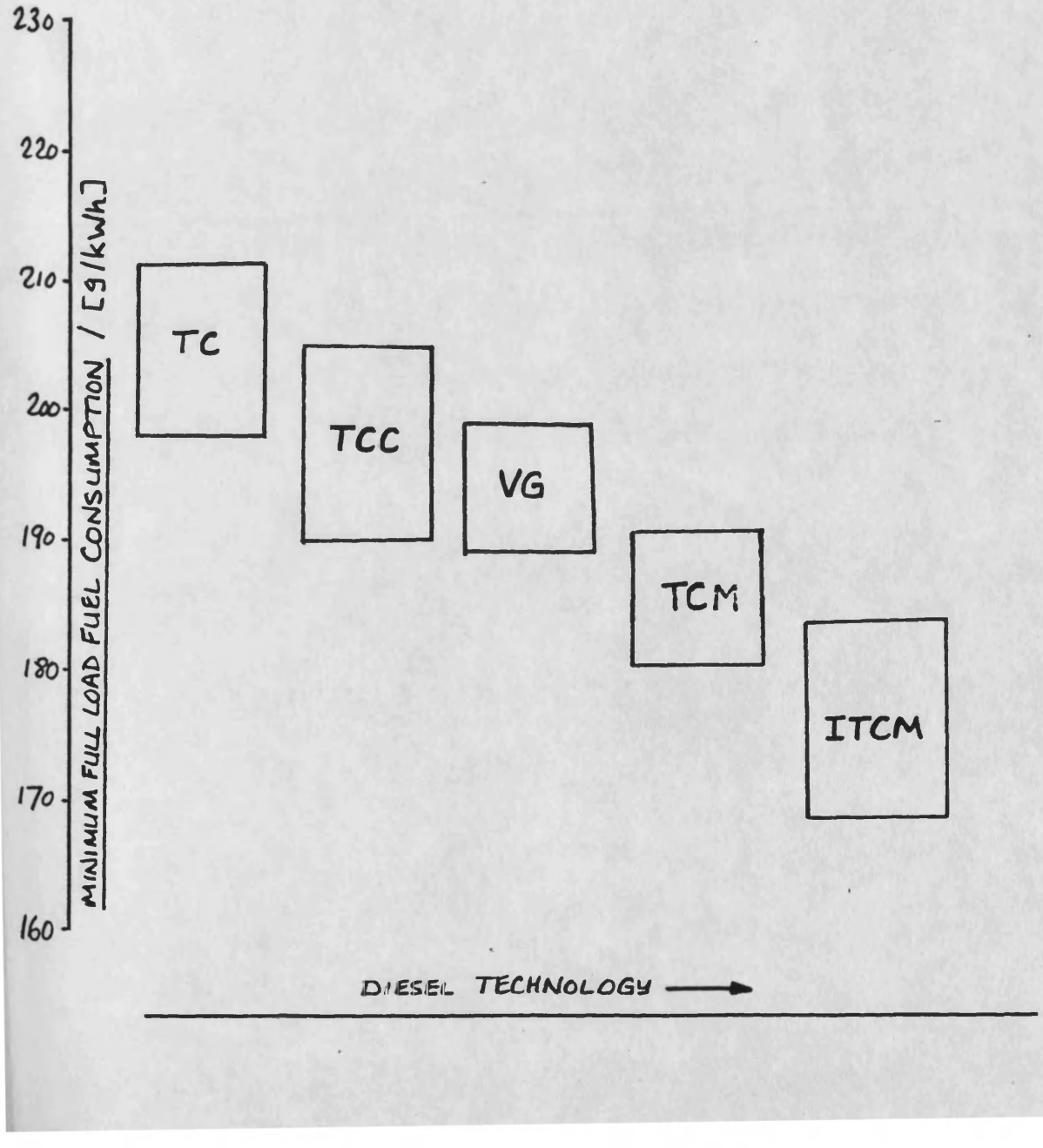

AUTOMOTIVE TURBOCOMPOUND ARRANGEMENTS FIG. 1.6

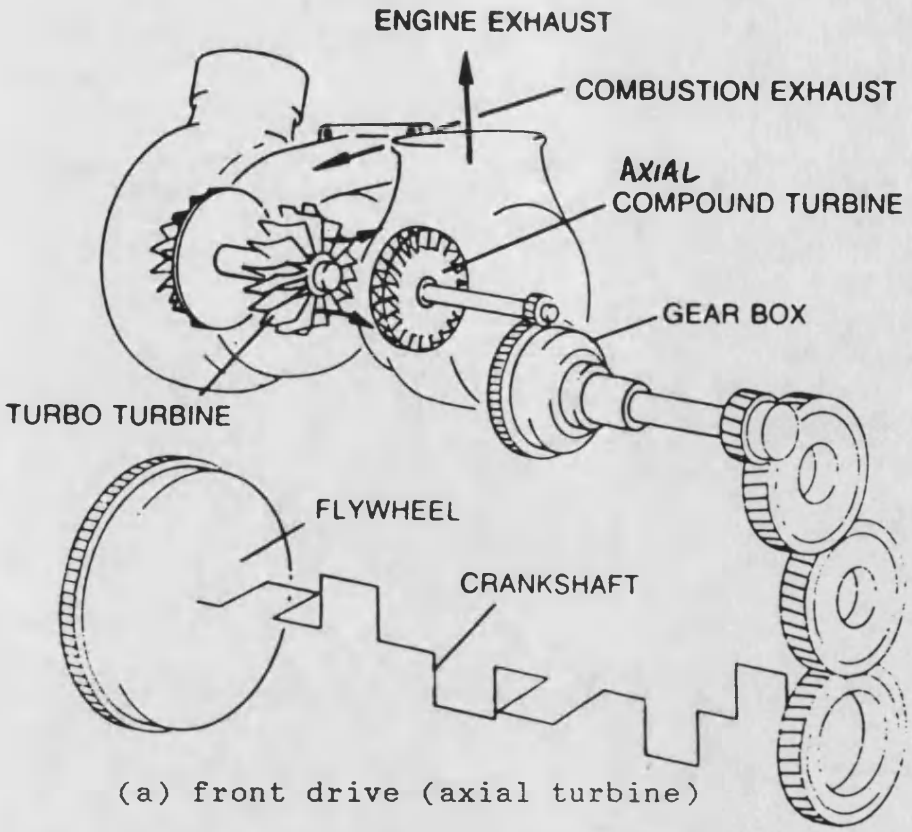

(a) front drive (axial turbine)

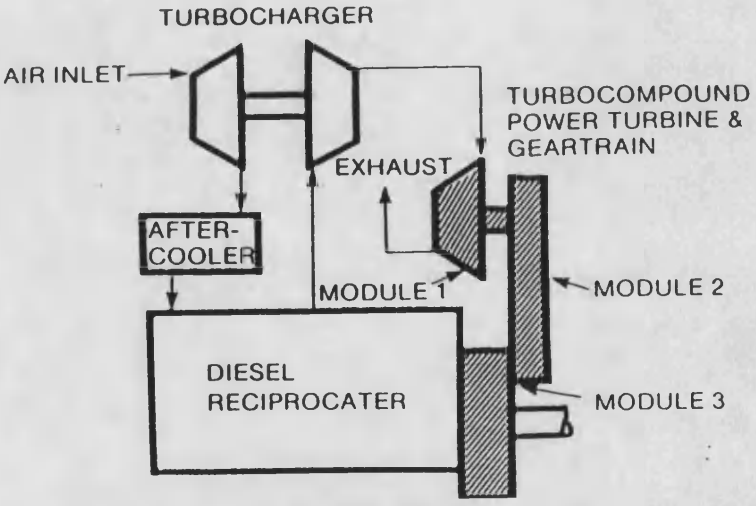

(b) rear (nodal) drive

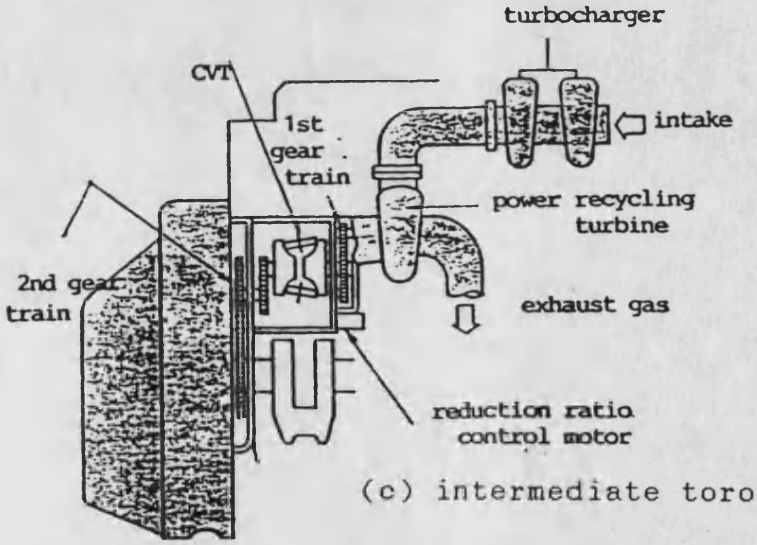

(c) intermediate toroidal CVT

AUTOMOTIVE RANKINE BOTTOMING CYCLE ARRANGEMENT FIG. 1.7

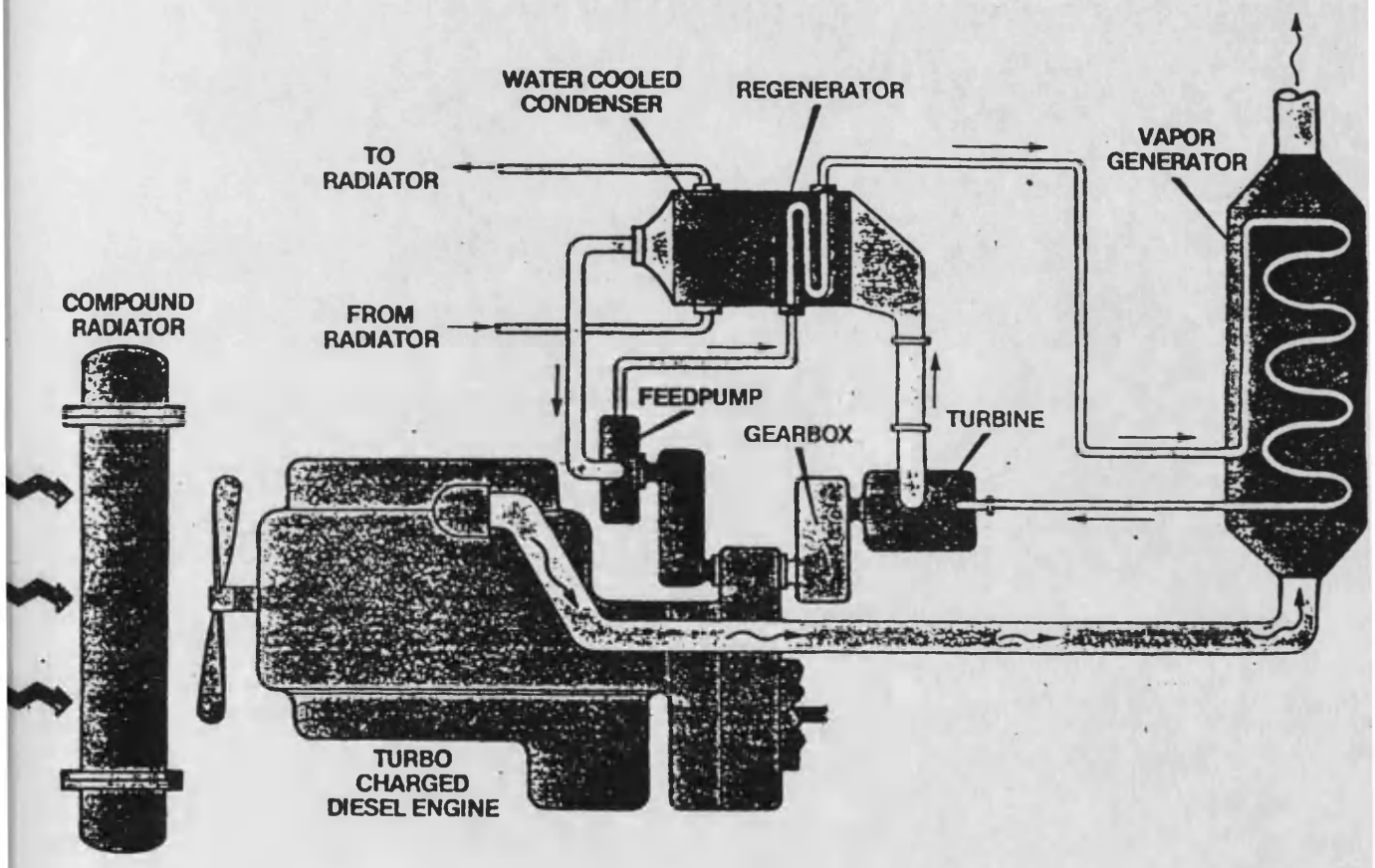

FIG. 1.8

AUTOMOTIVE GAS TURBINE

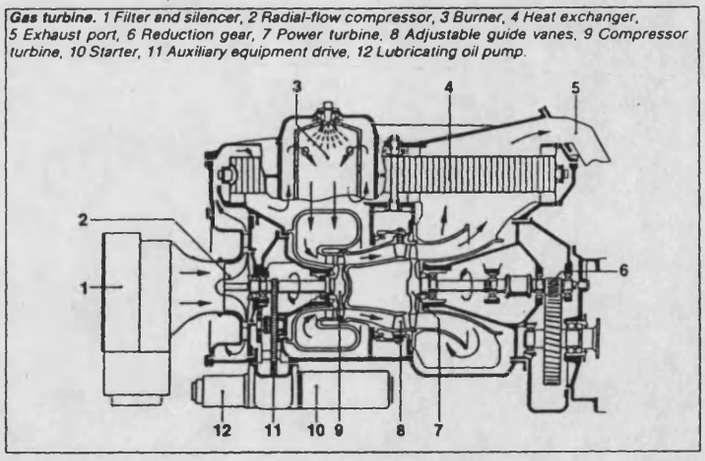

Gas turbine. *1 Filter and silencer, 2 Radial-flow compressor, 3 Burner, 4 Heat exchanger, 5 Exhaust port, 6 Reduction gear, 7 Power turbine, 8 Adjustable guide vanes, 9 Compressor turbine, 10 Starter, 11 Auxiliary equipment drive, 12 Lubricating oil pump.*

(a) TYPICAL DESIGN

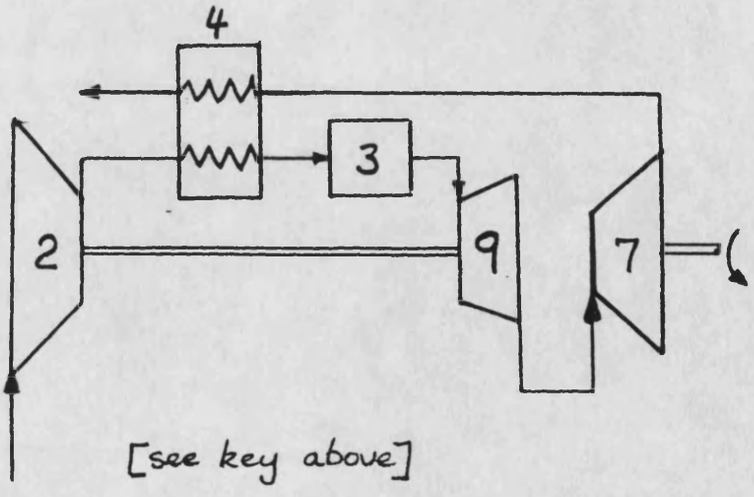

(b) CYCLE DIAGRAM FOR ABOVE ENGINE
(free turbine engine with heat exchange)

TYPICAL PRIME MOVER TORQUE CURVES FIG. 1.9

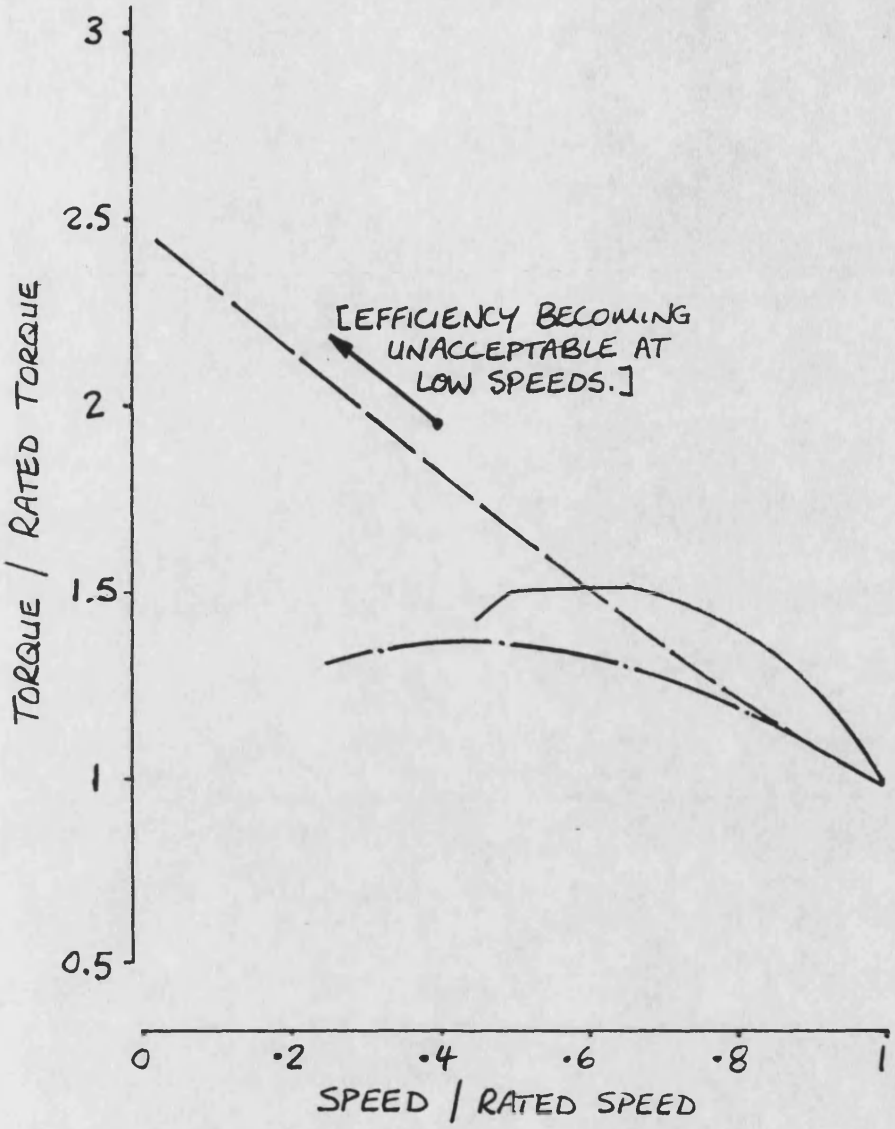

——— HIGH TORQUE RISE TURBOCH. DIESEL.

— — — TWO SHAFT GAS TURBINE.

——·—— STIRLING ENGINE.

STIRLING CYCLE - BASIC PROCESSES FIG. 1.1Ø

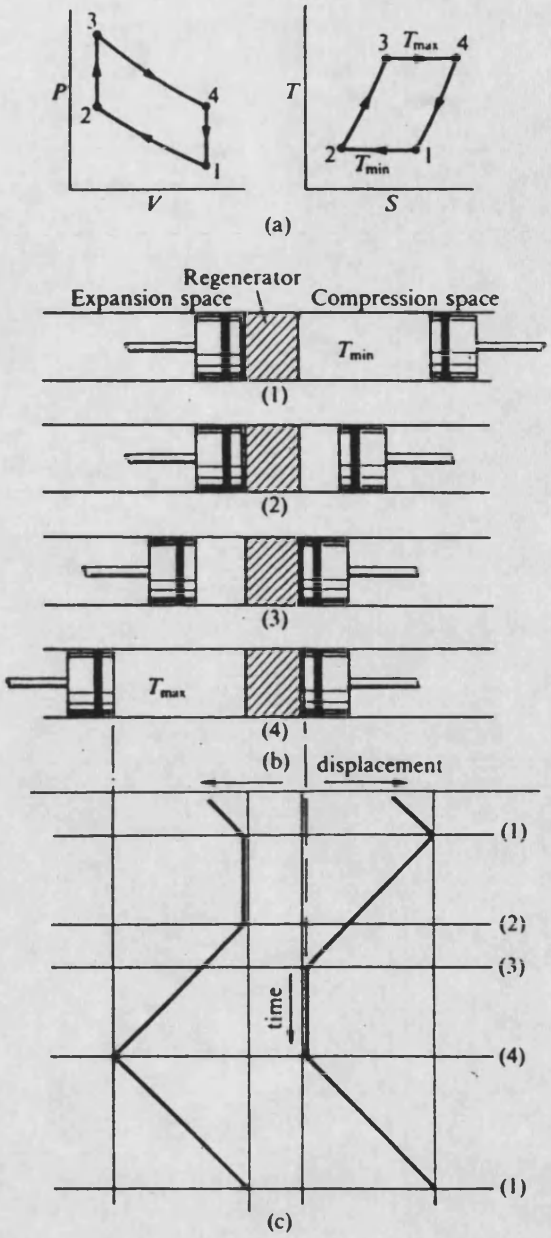

(a) P-V and T-S diagrams

(b) 'Ideal' piston arrangements at the terminal points of the cycle

(c) Time - displacement diagram

AUTOMOTIVE STIRLING ENGINE (U4 configuration) FIG. 1.11

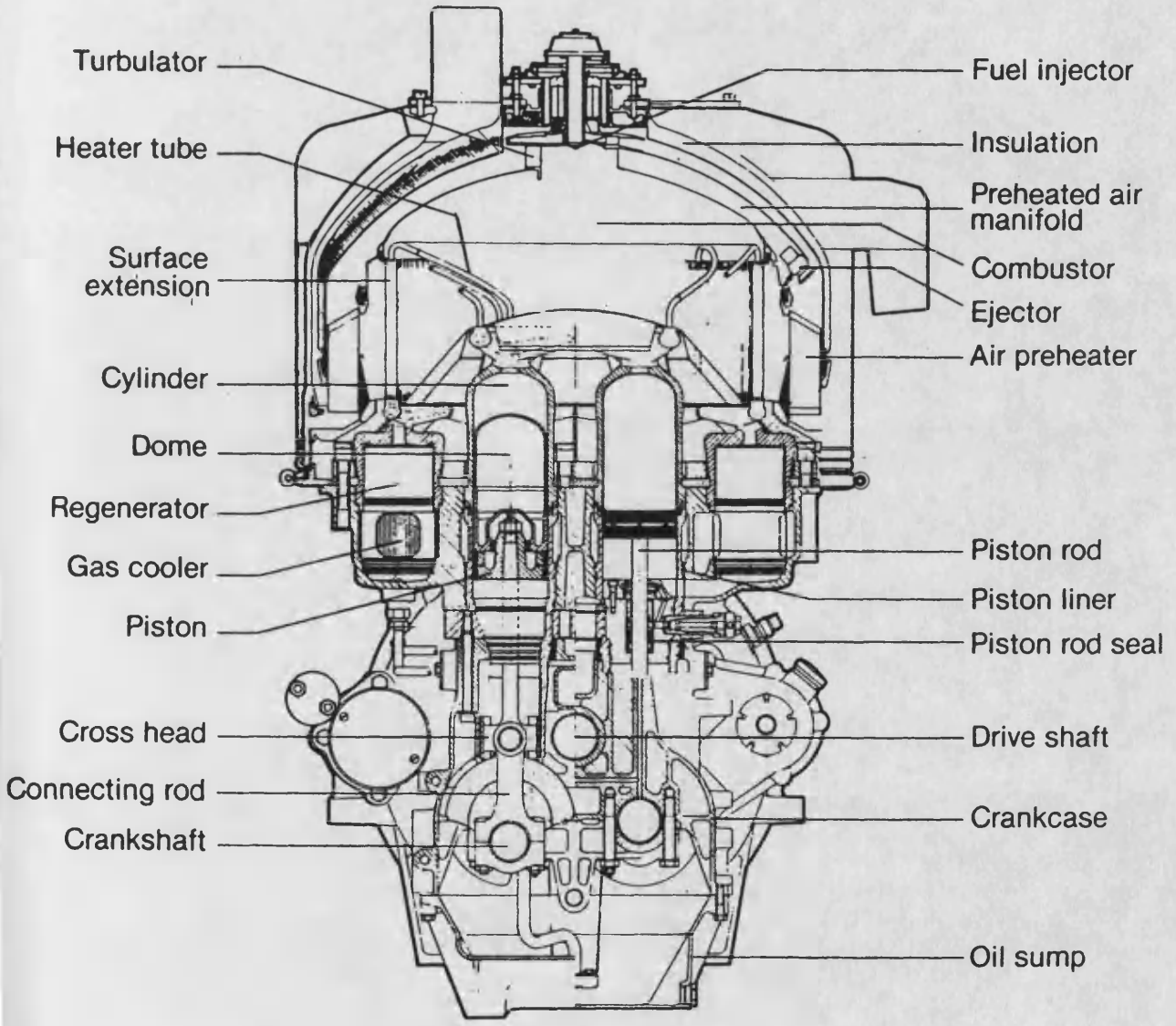

TURBOCHARGED DIESEL + STEPPED TRANSMISSION
TYPICAL TRACTIVE EFFORT CURVE

FIG. 1.12

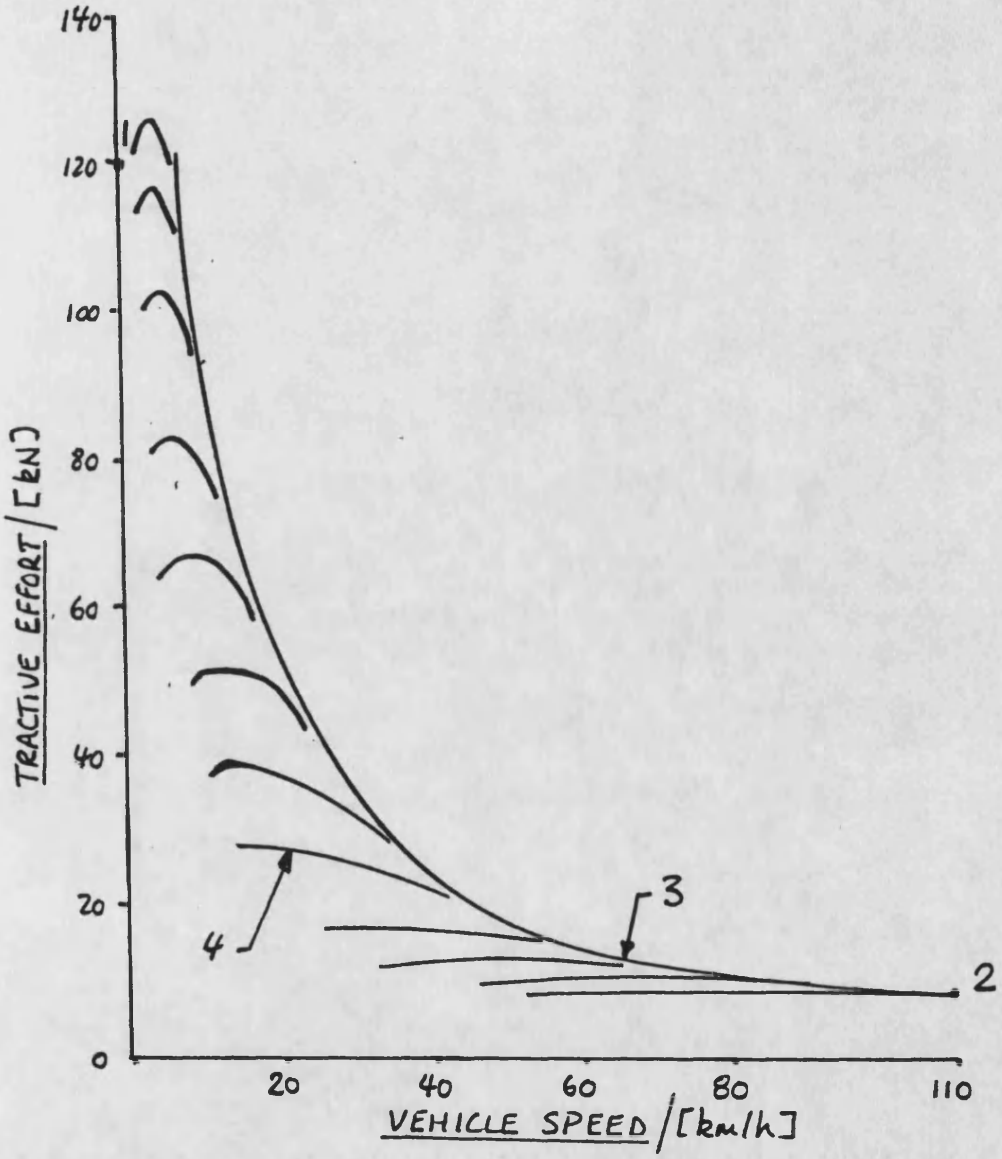

1. 40 t truck, 30% gradeability
2. typical vehicle max. speed.
3. 260kW hyperbola.
4. stepped transmission tractive effort curve.

HYDROSTATIC SHUNT TRANSMISSION SYSTEM FIG. 1.13

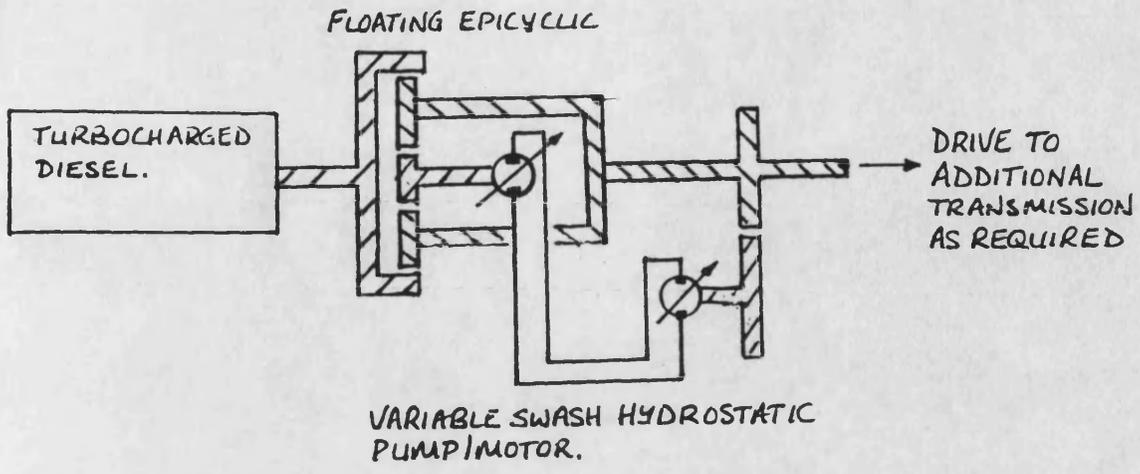

(a) SYSTEM SCHEMATIC

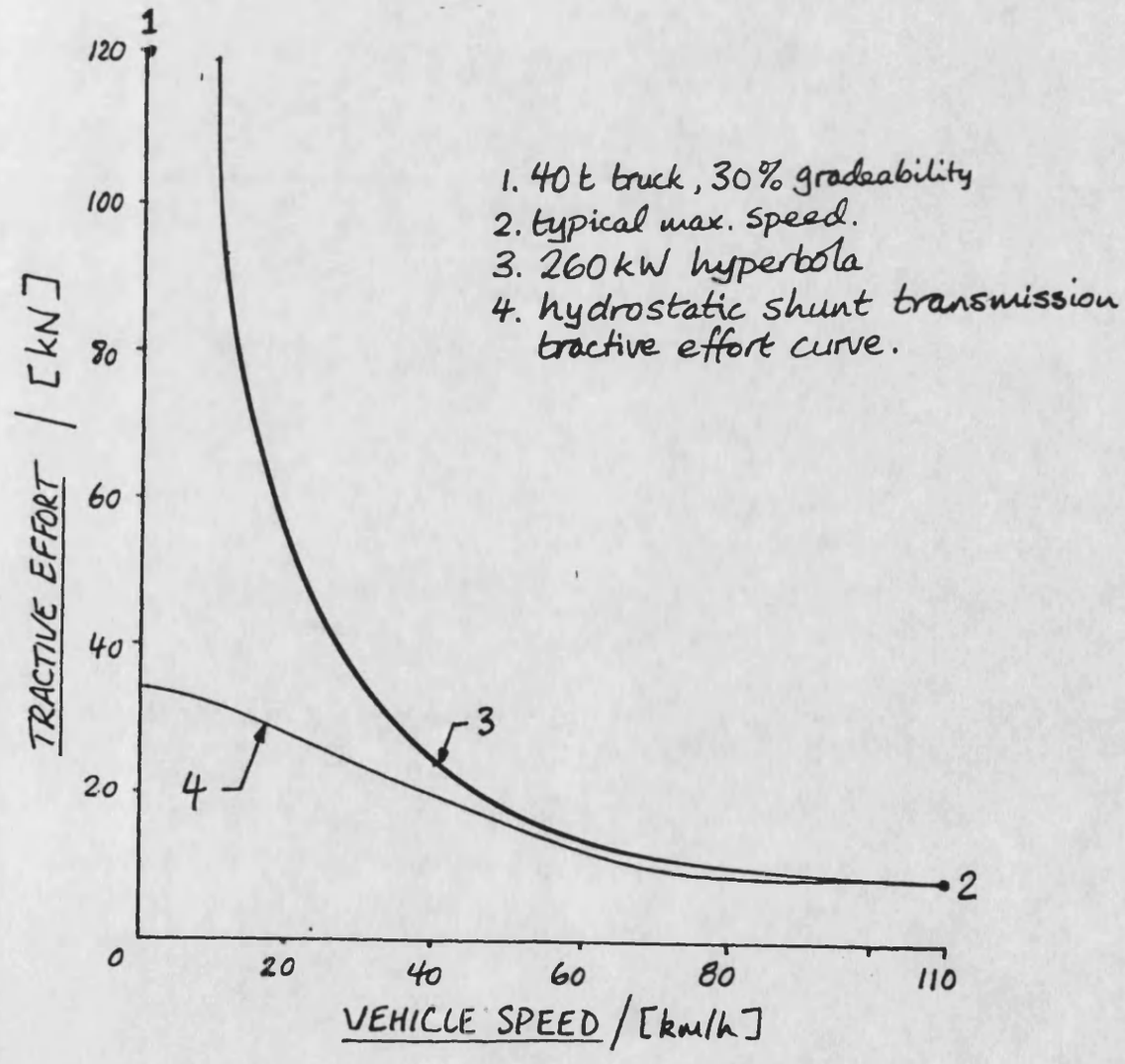

(b) TYPICAL TRACTIVE EFFORT CURVE

DIFFERENTIALLY-SUPERCHARGED ENGINE (DDE) FIG. 1.14

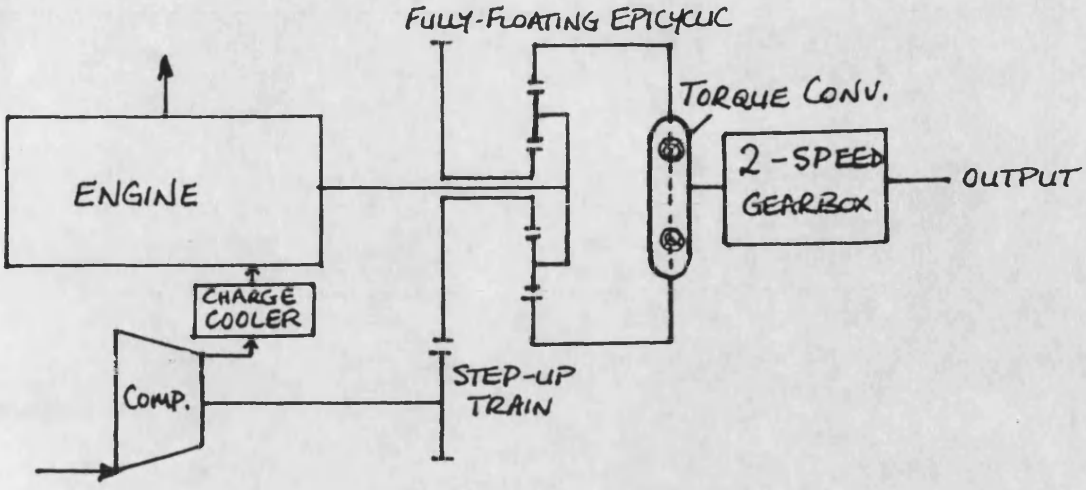

(a) SYSTEM SCHEMATIC

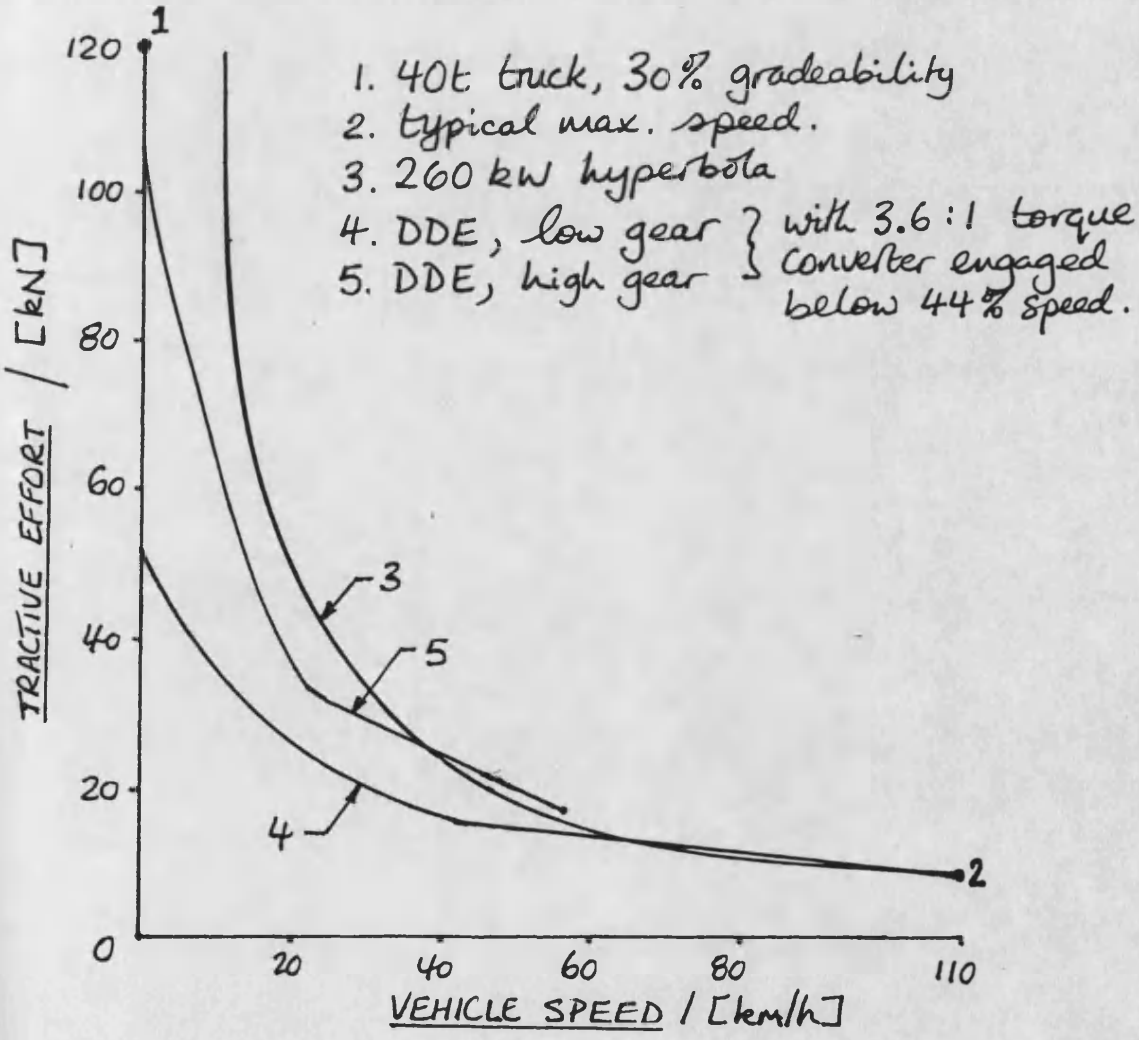

(b) TYPICAL TRACTIVE EFFORT CURVE

DIFFERENTIAL COMPOUND ENGINE (DCE) FIG. 1.15

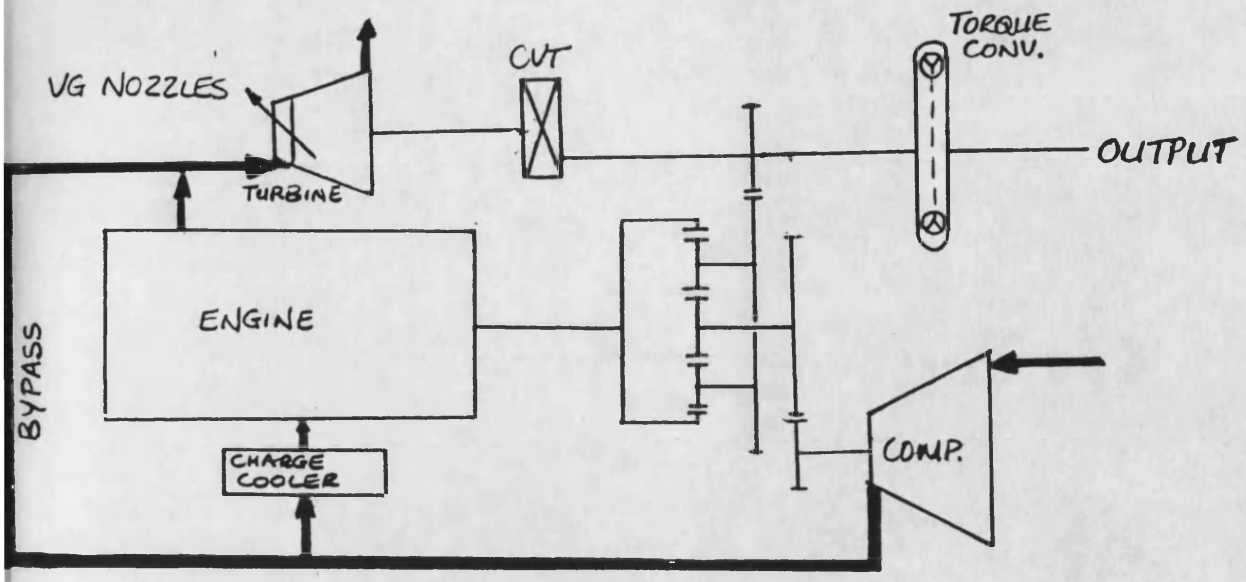

(a) SYSTEM SCHEMATIC

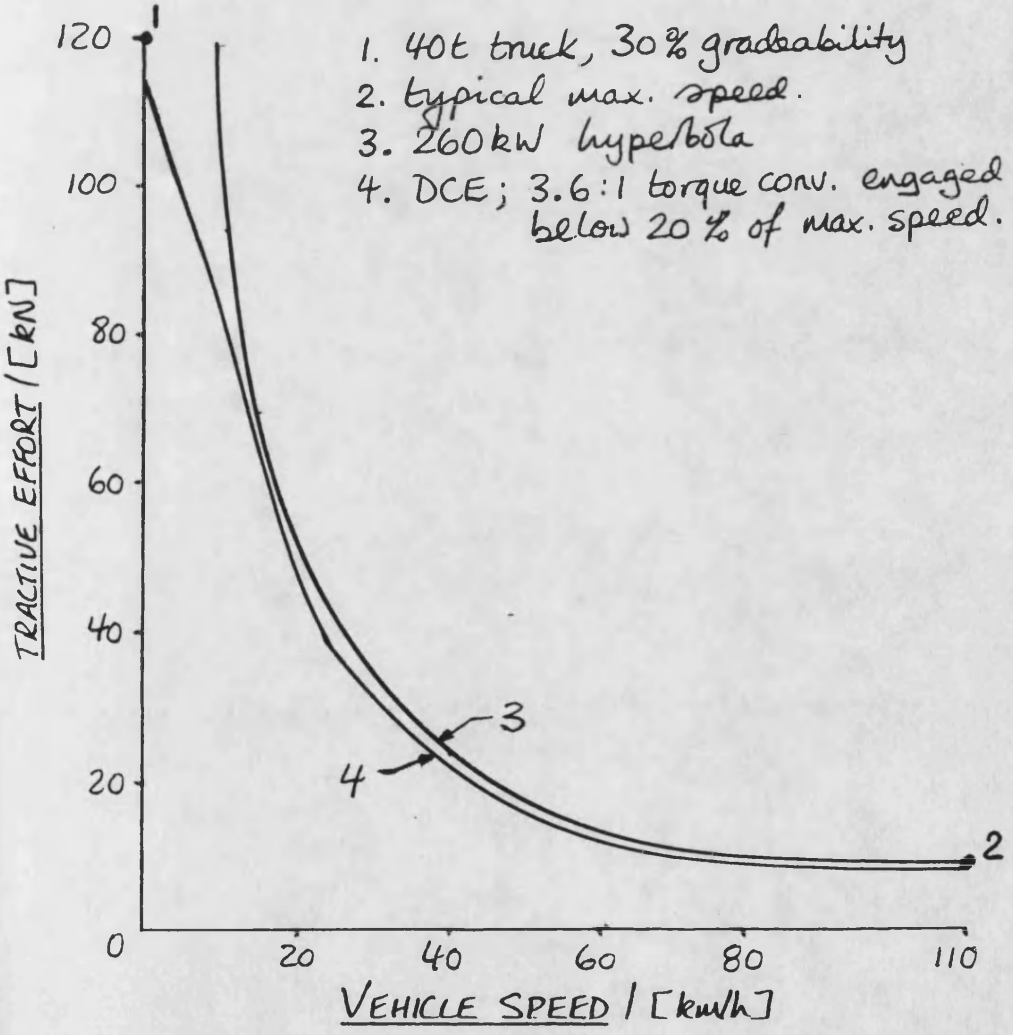

(b) TYPICAL TRACTIVE EFFORT CURVE

CHAPTER 2 - CONTENTS

2. PROTOTYPE AND INSTALLATION

2.1 GENERAL

The current laboratory research prototype DCE (the "520DCE") was first commissioned in 1985. A very detailed mechanical description of the 520DCE and test installation may be found in [36]; further information on the analogue electronics and actuator systems design may be found in [37]. The writer joined the project in 1987 and was responsible for re-commissioning the 520DCE following a gearbox failure, and subsequent development of the prototype/test facility plus experimental test work.

This chapter first describes the design and matching process for the DCE, followed by a relatively brief description of the 520DCE and test installation, with details of modifications and extensions made under the writer's direction. Finally the predicted performance of the 520DCE prototype is presented, for comparison with test results in the next chapter.

2.2 PROTOTYPE DESIGN

2.2.1 Component Selection and Matching

(i) Basic objectives

The fundamental principles of the 520DCE were introduced in Chapter 1, where the DCE was shown to have an excellent torque-speed characteristic for heavy-duty automotive applications owing to the method of coupling and matching quite conventional Diesel engine/turbomachinery components.

It was intended that this research prototype should be rated in the power range of current "premium" heavy-duty Diesel engines

(typically 200-300 kW, but gradually increasing) and achieve steady-state performance and efficiency representative of a production DCE, to demonstrate the concept and support previous claims based upon simulation results. The selection of components was made under tight financial constraints for a powertrain of this complexity; this meant firstly that the individual detail development of major components was out of the question, and secondly that major components available from the previous DCE prototype build or other related projects would be selected if their modification for the purpose were more economic than procurement of new components.

(ii) Epicyclic Configuration

The first decision was the configuration of engine, compressor, turbine and output driveshaft around the epicyclic geartrain. Considering first the engine, compressor and output shaft, these must be connected to the epicyclic such that the differential effect between compressor and output shaft speeds at fixed engine speed is obtained. At this point it is appropriate briefly to introduce the relationships of a free epicyclic gearset. Figure 2.1 shows the meshing points of the annulus, one planetary gear and the sunwheel in schematic form. The speed relations between annulus (ANN), planet carrier (PC) and sunwheel (SUN) are found by considering displacement compatibility at the two meshing points A and B. This leads to the speed equation

$$N_{SUN} = (R + 1).N_{pc} - R.N_{ANN} \qquad (2.1)$$

where R = no. of teeth on Annulus/no. of teeth in Sunwheel.

(Which reflects the fact that any two epicyclic speeds may be defined independently, the third then being dependent.) While the relative epicyclic gear speeds are set by equation (2.1) and the

choice of R, the components may of course be connected via layshaft gear trains to achieve any necessary speeds. The design path will become clear later. The steady-state torque relations between the gears are obtained from the equilibrium of forces on any planet. Neglecting friction, it is found that annulus, planet carrier and sunwheel torques are all in proportion. Again the epicyclic torque ratios depend upon R, but the ratio of component torques also depends upon any additional layshaft trains. It is worth stressing that while the speed relations (displacement compatibility) must hold under all conditions, the proportionality between torques (force equilibrium) does not apply under changing speed conditions.

There are a considerable number of possible combinations of senses of shaft rotations, torques and power flows, as summarised in [38]. For the DCE, power input is required to one shaft (from the engine), and power output from two shafts (to the compressor and output load). As noted above, compressor and output shafts must be differentially related. This still leaves a range of suitable arrangements for the DCE, and the remaining guideline is to match the highest epicyclic speeds with the highest required component speeds to reduce the ratio of step-up layshaft trains.

Fig. 2.2(a) shows the chosen arrangement for the DCE; this is a velocity vector diagram about the axis of any planet, and shows qualitatively the differential effect. For comparison the arrangement used for the DDE is shown in fig. 2.2(b). It may simply be noted that there is considerable flexibility in the epicyclic-component arrangement, and the designer can choose the

layout to suit the configurations of the major components (engine layout, compressor type and sense of rotation and so on) and installation constraints for a particular application.

(iii) Turbine location

Having determined the layout (although not yet the gear ratios) for engine, compressor and output shaft, the turbine location must be chosen. The turbine may be geared (via a continuously variable transmission - CVT - in the complete design seen in Chapter 1, or by a fixed gear train in the prototype) either into the epicyclic or directly into the output shaft. In an early paper on the DCE concept [30] it was shown that if one considers the "ideal" DCE in which the engine remains at its rated condition over the full output shaft speed range, then at zero output shaft speed the compressor speed will be increased from its rated value by a factor which is inversely proportional to the fraction of rated epicyclic input power being consumed by the compressor. In short, the smaller the ratio between rated compressor (sunwheel) power and rated annulus power, the greater the overspeed ratio imposed upon the compressor. This argument was repeated with reference to the 520DCE design in [36].

The implication is that if the turbine contribution were added to the annulus with the engine input, then the rated compressor power fraction would diminish, and the imposed compressor speed range would increase. Compressor speed range is a particular problem for centrifugal types, which have surge and choke restrictions, but is a problem for centrifugal and positive displacement compressors alike since high efficiencies are obtained only over a small part of the operating range. Thus the turbine must be geared in after the epicyclic, directly to the output shaft.

More straightforward reasoning leads to the same conclusion. In the above argument it was postulated that boost pressure should remain fixed at full output load over the output speed range. In a practical application boost may be allowed to vary somewhat, but the ratio of boost at stall to that at rated conditions is limited. At the rated condition it is necessary to use a reasonably high boost to achieve a good specific power output from the DCE and to obtain positive conditions (excess of turbine over compressor power) with consequent good system thermal efficiency. At the stall condition the maximum boost pressure is limited by the design of the turbomachinery and by mechanical (BMEP and cylinder pressure) limits on the engine, whose geometric compression ratio cannot be reduced indefinitely since it must be able to start and operate efficiently at light loads. As will be seen, the 520DCE was designed to have compressor pressure ratios of 3.17 at the rated condition and 3.95 at peak output torque (the ratio of these values is 1.25). In a study for a much more highly-rated DCE for military applications [39] the rated and peak torque compressor pressure ratios were 4.73 and 6.63 respectively (ratio 1.4). Thus boost rises typically by 25 - 40 per cent rated to peak torque conditions. If one takes the analytically convenient case of a positive displacement compressor as used in the 520DCE, this type of compressor has the characteristic that compressor torque is approximately proportional to boost pressure ratio. Hence compressor (and sunwheel) torque will rise by 25 - 40 per cent. As explained above, steady-state epicyclic torques are all in proportion (neglecting gear losses).

Therefore, if both power sources (engine and turbine) feed the output shaft through the epicyclic, then the DCE output shaft torque (being purely the planet carrier torque) will rise by 25 - 40 per cent from rated to peak torque speeds. The primary feature of the DCE, namely very high torque rise giving almost constant output shaft power, would then be lost. This is the reason why the DDE (lacking a compounding turbine) used low BMEP at the rated condition in conjunction with high peak BMEP. As discussed in Chapter 1, in the final version of the DDE the rated BMEP was 9.66 bar, compared to the peak BMEP of 17.6 bar, a ratio of 1.82. The output shaft torque rise was thus also approximately 1.82, giving good driveability (with two-speed gearbox and torque convertor), but only at the expense of rather low specific power.

(iv) Design point matching

The 520DCE matching process will now be described with brief reference to the main features of the components used and the reasons for their selection. Further description of the components will follow in subsection 2.2.

The basis of the DCE design is the engine and its chosen rating. The targets for the prototype output power mentioned earlier implied an engine rating in the region of 250kW. The chosen engine type was four-stroke, direct injection (DI), which dominates the heavy-duty automotive field. The original DCE scheme [30] used an opposed-piston two-stroke engine, which was acceptable because the mechanical compressor drive in the DCE would enable self-starting and adequate scavenging at all conditions - reference to the epicyclic vector diagram (fig 2.2a) shows qualitatively that if the output shaft were loaded then the

compressor speed would be more than adequate for the engine cranking speed. However, this scheme used separate engine exhaust and bypass air turbines so that the necessary pressure gradient for scavenging was achievable. In current DCE schemes exhaust and bypass flows are mixed so that mean compressor delivery pressures and engine exhaust pressures are nearly equal at steady-state; given the unavoidable charge cooler pressure drop, the engine must therefore be subject to an adverse pressure gradient. Hence a two-stroke engine would now be unsuitable, even if the inherent problem of thermal loading at high boost ratios could be overcome.

An available Leyland 500 series engine was selected, the turbocharged (520) version having been designed to withstand BMEP similar to those envisaged for the DCE. Importantly its integral block-head design and oil-cooled pistons allowed 150 bar cylinder pressure (no head gasket) and increased thermal loading without modifications. Reduced compression ratio pistons were specified to stay within the 150bar limit at the proposed ratings. The 520 is a relatively small (8.2 litres), high speed (rated at 2600 rev/min) design for highly-rated applications. Current trends are towards slower-running engines (1900-2100 rev/min) for reasons of reduced noise and friction, and to enable short injection and combustion periods (in terms of crank angle duration). It may be noted, however, that the "displacement rate" at rated speed of the 520, that is the air consumption assuming unity volumetric efficiency, is for example equal to that of a 10.2 litre engine at a rated speed of 2100 rev/min. Thus the 520 is "equivalent" in this sense to current engines rated for similar power output. In fact, a subsequent study [40] for a DCE for heavy truck

applications was based upon the 10 litre Cummins L10 engine (rated at 2100 rev/min), and the component selection and matching was very similar to that for the 520DCE.

The choice of design point for the DCE is not obvious. Turbocharged heavy-duty Diesels are commonly matched for high boost at mid-speed (with a reasonable surge margin) rather than peak compressor efficiency. In the DCE the engine/compressor match depends upon the choice of engine rating (implying boost and massflow), which must account for factors such as the compressor speed range and efficiency characteristics. The 520DCE design point was chosen to be the rated output condition, and matching was carried out using available or predicted component steady-state data with a simple iterative matching program developed for the DCE, analogous to conventional engine-turbomachinery matching programs. The main guidelines are described below.

At the DCE rated condition, the engine should be at its rated condition, and bypass flow (which will increase at lower speeds to improve torque back-up) should be minimal, that is engine and compressor massflows should approximately match. It may be noted from the earlier observation that higher rated compressor power/engine power implies lower compressor speed range, that some bypassing here would involve higher compressor power and this reduce the compressor speed range requirements. However, the compressor-bypass-turbine "torque conversion" effect is inefficient, so this would imply an unacceptable loss of system efficiency. In addition to matched air flows, the compressor must achieve sufficient boost for an adequate engine air/fuel ratio.

These two requirements are interdependent, the relation being the engine swallowing capacity characteristic at its rated speed.

The chosen engine rating at the design point was 15 bar BMEP (giving 266kW, a 35 per cent increase over the most highly-rated turbocharged production 520), acceptable in terms of engine durability whilst enabling significant compounding (with a turbine CVT). The required engine boost ratio is dependent upon many factors, including the desired air/fuel ratio (AFR), the volumetric efficiency and brake thermal efficiency of the engine, and inlet manifold air temperature. This last is in turn a function of the compressor isentropic efficiency and the degree of charge cooling employed. While the rated AFR will be the "worst case" at steady-state, it should still be sufficiently high that there is an adequate margin for transient response (engine/compressor acceleration) above the smoke-limited minimum AFR.

In this case an engine boost ratio of 3. was selected by simulation, giving a compressor boost ratio of 3.17 with the assumed charge cooler loss. From the compressor characteristics this determined the rated compressor torque. The required relative gear ratios of the engine and compressor were thus determined from their rated torques. Simulation again gave the compressor speed required for rated compressor and engine massflows to match at this boost ratio. Then since engine (annulus) speed and compressor (sunwheel) speed were known, this predetermined the planet carrier speed. The final design point output shaft speed was then given by the step-up ratio used from the planet carrier.

Finally, the turbine gear ratio (fixed in the prototype case) was chosen to match the rated turbine speed to the design point output shaft speed.

(v) Off-design point operation

Having set the design point it was necessary to investigate the consequences over the DCE operating envelope. In concept, the DCE would provide increasing output shaft torque down to zero output shaft speed by holding the engine at its design point (rated) condition and using the bypass flow generated by the overspeeded compressor to drive the turbine. The practical constraint is on the speed range of the compressor. As indicated earlier, the compressor overspeed ratio is inversely related to the ratio of compressor to engine power at the design point. At the above rating the overspeed ratio would be large. To maintain a reasonable compressor speed range, there are two practical solutions:

(a) Increase the minimum output shaft speed from zero (true stall) to some fraction of the rated speed.

(b) allow the engine speed to decrease to some extent with output shaft speed at full load.

The effect of each may be seen using the epicyclic speed vector diagram Fig. 2.2a. Both measures were adopted for the 520DCE. The "design stall" output shaft speed was taken to be one-fifth of rated speed; in a vehicle application the gap to zero speed would be bridged by a torque converter as used in the DDE, locked up above the design stall speed. BMEP is allowed to rise (maximum 20bar) with decreasing engine speed to limit the reduction in power. Nevertheless, the resulting speed range was still

excessive for current centrifugal compressor designs, whose limitations were noted earlier. Thus a positive displacement compressor was used. While the best current positive displacement compressors have isentropic efficiencies typically 5-10 percentage points lower than centrifugal types, this is offset somewhat by their lower speed, removing probably one layshaft from the step-up train; with its associated power loss. The difference is further reduced by the generally wider regions of high efficiency in the positive displacement compressor operating map. However, positive displacement compressors all pose problems of increased bulk, cost and noise in comparison to centrifugal compressors. Screw, vane and spiral compressor offer the highest efficiencies, by virtue of having some internal compression, in contrast to the Roots type which works purely by displacement into a high pressure region. Development of the DDE led to the final use of a screw-type compressor for reasons of its good performance and availability in well-developed form. A screw-type compressor was used for the 520DCE as a relatively high efficiency prototype unit with the required flow range and peak boost ratio became available .

This is commercially the highest-cost option because of its complex rotor forms and close tolerances; however, in the DDE project, and in the cost analysis undertaken by Cummins for the L10 DCE design, it was considered that the use of a screw compressor would be economically feasible in mass production.

The final consideration is of rotational inertia for transient response. The 520DCE screw compressor inertia is approximately 0.1 kgm^2. The inertia for a centrifugal compressor of the same

massflow operating at similar speeds to the 520DCE turbine (up to 50,000 rev/min) would be of the order of 0.001 kgm^2. The ratio of compressor inertiae is thus of the order of

$$0.1/0.001 = 100$$

The referred inertia at the sunwheel depends upon the relative speeds, which in this case differ by a factor of approximately 5. The ratio of referred inertiae is thus roughly $100/5^2 = 4$ (This excludes the additional inertiae associated with the centrifugal compressor's extra step-up gear). However, the compressor is not accelerated in isolation - its inertia is only part of the combined engine/compressor/geartrain inertia which must be accelerated to increase to DCE power output. Thus the extra screw compressor inertia causes a less profound increase in the effective inertia of the engine-compressor combination than might initially be expected.

Having set the engine/compressor conditions at the design point (rated) and at the "stall" (peak torque) point, this defined the operating limits (rated and peak boost, massflow and inlet temperatures) of the turbine. It also defined the compressor boost and massflow - and therefore the turbine boost and massflow - at these two points. Since both conditions cannot be met with a fixed turbine swallowing characteristic, and because it is highly desirable to be able to optimise boost/massflow conditions over the operating range of the DCE, a variable geometry (VG) turbine is required. A fixed geometry turbine could be used, rematching engine, compressor and turbine together to achieve the best compromise over the operating range. Experience shows that turbines with VG nozzles have a small isentropic

efficiency deficit away from the optimum setting in comparison to nozzleless turbines (this deficit is also seen with fixed-nozzled turbines). Thus the loss in system efficiency incurred with a fixed geometry turbine, which would result from the inability to re-optimise the system boost/massflow balance at any operating condition, would be offset somewhat by generally improved turbine efficiency. In commercial terms the reduced complexity and cost of a fixed geometry turbine would be attractive. Indeed, the later Cummins L10 DCE study included a comparison of a VG scheme and a rematched fixed geometry scheme [41]. However, for research purposes VG was unquestionably required in order that the DCE concept could be thoroughly investigated.

Radial and axial turbines would both be acceptable in this application. Past experience of variable geometry-nozzled axial turbines for automotive gas turbine engines has more recently been augmented by widespread development of VG radial turbines for turbochargers. Radial turbines are usually credited with the higher efficiency and lower cost in this size range, but in a recent turbocompound engine design [14] an axial compound turbine was preferred (handling approximately half the peak massflow of the 520DCE, although at lower pressure ratios).

In the 520DCE case a VG radial turbine was already available from the previous DCE prototype, having the necessary boost and flow range for the 520DCE, and this was retained.

Having described the 520DCE component selection and matching process in general terms, the chosen components will now be described in detail.

2.2.2 Component Descriptions

2.2.2.1 Engine

The engine is a modified Leyland "520", as described below:

Type : Leyland 510/77/1. Fixed head design (rebuilt with later type strengthened block) Cross flow four-stroke six-cylinder (in-line) Diesel. Water-cooled.

Bore x stroke : 118 x 125mm

Swept vol : 8.2 litres

Compression ratio : 12.8 (reduced from standard turbocharged 520 ratio of 15.3 by piston machining)

Valve timing : IVO 10 deg. BTDC IVC 50 deg. ABDC

EVO 46 deg. BBDC EVC 14 deg. ATDC

(overlap 24 deg.)

Combustion system : Direct Injection. High swirl (spiral port), 2-valves per cylinder. Toroidal piston bowl.

Full load speed range : 800-2600 rev/min

Cylinder pressure limit : 150 bar

Exhaust temperature limit : 700^{o}C

Fuel Injection Equipment :-

Pump : Sigma RZMSP - 6D - 110T - 101R - 735 - 1

(In-line type)

11mm dia. plunger x 11mm lift.

All governing elements removed.

Injectors : American Bosch AKN - 120M - D6547B

Nozzles : 4 hole, American Bosch 186 - 7

Engine ratings (design conditions) :

max. power 15 bar BMEP at 2600 rev/min (266kW)

max. torque 20 bar BMEP at 1673 rev/min (299kW)

It was noted earlier that the above 266kW rating represents a 35 per cent increase over the highest turbocharged 520 output. Standard design features of the 520, such as piston crown oil jet cooling and good coolant flow near the top ring reversal position (enabled by the fixed head design) allowed the uprating without modifications, at least for research purposes. The reduced compression ratio was chosen by simulation to allow 20 bar BMEP within the 150 bar cylinder pressure list, taking due account of the use of variable injection timing. Fuelling and timing control forms part of the test installation, discussed later (subsection 2.2).

A revised exhaust manifold was required to suit the DCE installation, allowing mixing of engine exhaust and bypass air before entry to the (twin-entry) turbine. Pulse-preserving manifolds are commonly used in automotive turbocharged engines giving maximum turbine power and transient response. It has been suggested however, that even for engines with favourable cylinder groupings (such as the six-cylinder four-stroke used here), a constant pressure system would give a higher turbine power at boost ratios in excess of 3 [42]. This is because the additional pulse energy at the turbine in a pulse manifold system would no longer compensate for the drop in turbine efficiency during the associated high pressure excursion.

As noted above the 520DCE boost ratios exceed 3 over the speed range at full load, with a peak design ratio of 3.95. For this reason, and for simplicity of design, a constant pressure system was used. The system (including bypass air mixing) is shown schematically in fig. 2.3(a).

The manifold was fabricated as a straight 4" diameter pipe, with individual stub pipes butt-welded to it (no protrusion). The stub pipe length was chosen simply to give easy installation and some flexibility. Total manifold volume is 8 litres. The exhaust gases pass via a bellows joint (the turbine is rigidly mounted to the gearbox and thus to the floor; the engine is resiliently mounted) to give a mixing plenum (volume 8 litres) . The combined exhaust and bypass flows then enter the turbine. Although the large exhaust system volume (approximately 20 litres in total) will damp pulsations to a negligible level, one might anticipate uneven admission between the twin turbine entries as a result of the plenum layout. In a fully-optimised system the following points would be important :

(i) The need to mix engine exhaust and bypass flows

(ii) The need for "constant pressure" turbine inlet conditions at the relatively high pressure ratios used in DCE schemes

(iii) The improvement in scavenging which can be obtained with a pulse manifold

and the DCE exhaust/bypass system might then look like fig. 2.3(b) (for a six-cylinder, four-stroke engine). Two pulse manifolds meet in a simple pulse converter. The bypass air is then admitted in the mixing section or plenum. Thus the turbine inlet conditions are steady, while the engine scavenging is "isolated" from the higher pressure bypass flow. This is a matter for detail development.

The 520DCE manifold was originally a one-piece fabrication. On removal during the test programme, significant distortion was noted, causing angular misalignment of the stub pipe flanges. It was therefore modified to two half-manifolds with a central flange joint, to restore correct flange-head seating. Exhaust gaskets were replaced once (before

the manifold modification) following leakage at high load (4 bar boost and 700 deg.C exhaust temperature) but gasket life at these conditions would not generally be a problem.

2.2.2.2 Compressor

The compressor is a CompAir Industrial type 1200 rotary screw positive displacement unit. It has high efficiencies for its type, and importantly is of the dry screw type: the rotor faces have a hard Teflon surface coating and are unlubricated. Oil contamination of the delivered air would cause fouling of the inlet system, and in a practical application would be a major source of particulate/HC emissions. The unit is water cooled.

The extreme design conditions for the compressor occur at the peak torque ("stall") point:

max. speed : 11500 rev/min

max. pressure ratio : 3.95

mass flow : 52.2 kg/min (at the above speed and pressure ratio)

max. delivery temperature : 220 deg.C

max. power consumption : 173 kW

This compressor was formerly a CompAir prototype, and performance data were obtained from CompAir. Fig. 2.4 shows the free air delivery as a function of compressor speed and delivery pressure. Being a positive displacement device the influence of delivery pressure is slight. Unfortunately the CompAir data did not include the low speed range or the extreme high speed range (9000-11500 rev/min), but the relationship was linear and could therefore be extrapolated with reasonable confidence. Fig. 2.5 shows the compressor power consumption as a

function of speed and delivery pressure. Again the data is restricted in range but the relationship is linear. Reduction of the data to a speed : torque basis would show that torque is related to boost and is nearly independent of speed. Fig. 2.6 shows compressor efficiency contours (ratio of isentropic work to actual shaft work) over the boost : massflow (or, approximately, speed) operating range. The design points (rated and "stall") are marked, and it can be seen that the unit is best matched for 520DCE operation near full load. The peak efficiency recorded was 77 per cent.

During the experimental programme some inlet system fouling was noted. This was attributable to oil leakage past the rotor seals at light load (low boost ratios), but could no doubt be improved by detail development of the seal arrangement and oil drainage system. Some light load oil leakage from bearings to rotor is accepted in production turbochargers.

2.2.2.3 Turbine

The turbine is a modified Napier C-045B twin-entry radial inflow type. The extreme design conditions for the turbine boost ratio and massflow occur at the "stall" point:

max. pressure ratio 3.95

max. massflow : 54 kg/min

While the maximum turbine speed is 50,000 rev/min, obtaining in the prototype only at the rated output shaft speed, but in the conceptual 520DCE with turbine CVT obtaining virtually over the full output speed range at maximum torque.

The original modifications to the turbine were made for previous DCE prototypes, as indicated earlier. These were :

(i) turbine wheel and shroud modifications for pressure ratios up to 4 and massflows over the DCE range of operation - now suitable for the 520DCE

(ii) modification of the centre causing bearing arrangement and turbine shaft to operate as a power turbine rather than as part of a turbocharger (which implies altered balancing problems and increased axial thrust since there is no opposing compressor axial thrust). The standard laminated sleeve bearings were replaced by ball-race bearings. These bearings have an impractically short life except for research purposes, but rolling element bearings with acceptable life have been demonstrated in numerous production turbomachines

(iii) Modification from fixed nozzles to a VG nozzle arrangement. The design employs sixteen profiled vanes, equispaced around the wheel inlet, swivelling in plain bushes. The initial arrangement is shown in Fig. 2.7, and a detail view of one vane/bush/actuating arm is shown in Fig. 2.8. Each vane has a pivot shaft which protrudes through a pressed-in plain bush (the vane and shaft is a one-piece machined component in stainless steel En57; the bushes are phosphor-bronze). The vanes are retained in the bushes by clamp/actuating arms (the clamping arrangement can be seen clearly in section B-B of Fig. 2.7). The arms are linked by spring steel (En 45A) strips to a peripheral actuating ring. The actuating rings moves around three roller bearings fixed to the turbine casing. The spring strip accommodates the change in relative position of the arm and ring as they move through different arcs.

The arrangement worked well for a considerable time, but rapidly deteriorated towards the end of the steady-state test programme as the

highest operating temperatures (inlet gas temperatures up to 650 deg.C) were encountered. At these conditions the vane shafts seized into their bushes, due to oxidation build-up, causing buckling and failure of the spring steel strips. It was thus necessary to change the bushing arrangement; the design had to provide :

(i) jam-free movement through nozzle angles of 30 degrees with unbalanced actuating forces (the actuating arm imposes a lateral force on the pivot/bush rather than a pure torque).

(ii) Retention of the bush (and thus of the vane and actuating arm, allowing for thermal expansion over a 650 deg.C temperature range.

(iii) Sealing at differential pressures up to 3 bar, with gas temperatures up to 650 deg.C.

Various alternative designs were considered, as summarised below:

(i) Same materials, increased clearances

That is the bush internal diameter could be increased slightly. While this would be very simple, increased gas leakage would result, and the possibility of jamming due to tilting of the shafts in the bushes would be increased. Furthermore, there would still be the possibility of oxidation leading to seizure.

(ii) Two-piece plain bush (fig. 2.9a)

The aim here is to maintain good sealing. The design could consist either of two phosphor-bronze bushes directly end-bearing on each other, or as shown with other materials separated by a sealing/bearing ring, possibly made of stellite. Clearances are exaggerated in the figure for clarity. Retention is by the rear (right hand side of diagram) bush fit only; the rest of the assembly is retained onto the rear bush when the actuating arms is clamped on. However, there remains the possibility of seizure

onto the bushes if phosphor-bronze is retained, with equal risk of tilting and jamming.

(iii) High-temperature bearing materials

The final alternative is to improve the material specification. Graphite was considered, but oxidises at about 550 deg.C in air. Morganite Special Carbons Ltd. offered a Silicon Carbide bearing material, capable of operating up to 1000 deg.C. However, this is a brittle, low thermal expansion material (coefficient of thermal expansion 4.1 x 10^{-6} per deg.C compared to 11x10^{6} per deg.C for Mild Steels and 18 x 10^{-6} for stainless steels). Press or shrink fits were thus precluded. A two-piece top hat form bush (fig. 2.9(b)) could be used, all retained between the vane and the clamped-on actuating arm, the "brims" preventing steel-steel contact. At high temperatures the bush would be loose in the casing, while the shaft would have to be a sliding fit in the bush (implying it would be loose at low temperatures). Additionally the design would need to allow for shrinkage during sintering of about 18 per cent [18]. The figure shows a sealing ring which might be incorporated.

Clearly the requirement was for a material of similar thermal expansivity to mild steel and stainless steel, with good bearing properties and high temperature capability. A combination of Stellite (Cobalt-base) alloys was finally selected in consultation with Deloro Stellite Ltd. The thermal expansivity of the alloys is approximately 14 x 10^{-6} per deg.C, allowing the use of a plain, press-fit bush without excessive shaft clearances and leakage. The bushes were made from Stellite 6. The external diameter was ground for a cold press fit (B.S. H7 p6) into the existing casing holes. The vane shafts were reduced in diameter over their full-length, plasma sprayed with Stellite 31, then

ground back to leave a 0.020" coating. The finished shaft diameter gave an average running fit (B.S. H8 f8) at the "tightest" case thermal expansion (highest temperature). This provides better sealing (closer fit) at higher boost pressure, since boost and temperature tend to rise together in this application.

Whilst the turbine was dismantled, it was decided to revise the actuating arrangement in order to

(i) ease re-assembly - with the existing design it would be necessary to assemble the sixteen actuating arms to the ring with the spring links, and fit the complete assembly to the turbine. Ideally one would fit each arm to its shaft individually before installing the ring, which obscures the arm-shaft clamping bolts.

(ii) provide a more positive action - when the spring links are "pushing" the actuating arms, fouling at the vane edges and in the bushes causes the spring links to flex, since the actuating force far exceeds their buckling stiffness. Their behaviour and life under computer control at high frequencies was therefore of concern.

One possible design followed that of a variable nozzle turbocharger turbine designed by Garret Automotive [12, 13], which used actuating arms ending in simple cam forms, engaged in an internally-toothed actuating ring. The cam form ensured that the actuating arms remained fully engaged with actuating ring, as they described their smaller arcs. For the DCE turbine the design would have involved the manufacture of cam-shaped tips for the existing actuating arms, although the actuating ring already incorporated suitable "teeth" as part of the original design. However, a simpler design was chosen, using a peg and slot

arrangement as sketched in fig. 2.10. This used the original arms, with a straight slot. The slot length was made significantly greater than the calculated travel of the peg, ensuring that even with positioning discrepancies (for example, some arms are reversed to allow access to the clamping screw) the peg does not reach the slot ends, and nozzle movement is purely determined by the hydraulic actuator limits as before. The actuator forms part of the test installation, described in subsection 2.2. The pegs are 4mm diameter silver steel, tapped into the actuating ring. Too large a clearance between peg and slot would cause a "deadband" on reversal and might allow vane "flutter", the converse might lead to seizure under continuous computer control. A free running fit (B.S. D9 h9) was used, treating peg and slot differential thermal expansion as negligible. The stellite shaft-bush interface should operate safely unlubricated. The peg-slot faces were sprayed with a high temperature (up to 800 deg.C) aluminium-based anti-seize compound on assembly, as a precaution.

The revised VG design operated for the remainder of the test programme with no problems. It was also noted that even after significant running (and thus potential fouling and seizure) the required actuation force remained very small.

Fig. 2.11 shows the partially-dismantled turbine, with the VG nozzles set to the two extremes of their range.

2.2.2.4 Gearbox

The combined epicyclic/layshaft geartrain was manufactured by Allen Gears Ltd. for an earlier DCE prototype, and was modified by the manufacturer to suit the 520DCE component matching. The gearbox is a free-standing unit, typical of industrial/marine installations rather than automotive, but suitable for a research prototype.

The geartrain arrangement is shown in Fig. 2.12, including the single-stage compressor step-up and the two stage fixed step-up to the turbine. Gearshaft speeds are shown for the design rated and (in brackets) stall conditions. The imposed relations between engine, compressor and output shaft speeds are shown in fig. 2.13.

The gearbox suffered two failures during initial testwork [36]. As noted earlier the writer became responsible for the prototype during the second rebuild, and no problems have occurred since these two faults were rectified.

2.2.2.5 Charge Cooler

Charge cooling is effected by an air-water heat exchanger :
SERCK AM11/JFL 30.

The coolant (pond water) is thermostatically controlled for an inlet manifold air temperature of 50 deg.C. This is unrepresentative of usual automotive air-water charge coolers which are closer to fixed effectiveness, but gives better repeatability in the face of varying pond water temperatures. Furthermore, there is now a trend towards constant inlet temperature control in automotive installations, using thermostatic switching to take charge cooler water from alternative

parts of the engine coolant circuit. This becomes increasingly important as ratings increase; a charge cooler set to give the required charge density and thermal loading at full power will give excessively low charge low temperatures at part load, leading to long delay periods, with consequent poor combustion efficiency and high rates of pressure rise.

The thermostatic control on the prototype allows the charge air temperature to drift by up to +/-5 deg.C over the operating range, but this is accepted. There will also be unavoidable excursions (due to thermostat response and charge cooler thermal inertia) during transients.

The quoted charge cooler pressure drop at the design point (rated) condition was :
1.5 psi (0.1 bar) at 3 bar, 28.6 kg/min air flow

2.2.2.6 Dynamometer

Twin hydrostatic pumps are driven from the DCE output shaft via a two-way splitter gearbox. The use of hydrostatic dynamometers for engine testing is not common, D.C. machines or eddy-current regenerative motors are more usual. However, the considerable expertise in fluid power at Bath had led to the use of hydrostatic pumps on the previous DCE prototype and other installations.

The hydrostatic pump can absorb a constant maximum torque over its speed range. Because of the DCE rising torque characteristic, the "corner power" (product of the peak torque with the maximum speed) requirement was high. The use of the splitter box allowed two available identical

pumps to be used in parallel, rather than purchasing a single pump with the high corner power.

Pumps :

2 off Sauer - Sundstrand SPV25 variable swash axial-piston hydrostatic pumps.

Rated speed : 2400 rev/min

Rated power : 230 kW EACH at 350 bar absorption

Splitter Box :

Wareing-Rigby RT276

Rated speed : input 3409 rev/min, output 2440 rev/min

Rated power : 275 kW

The pumps are controlled by loading pressure, at fixed swash angle. Each pump is loaded by an Abex Denison R4V pressure relief valve. The two relief valves are controlled by a common Abex Denison SE 03 solenoid pressure control valve. The boost supply to the hydrostatic pump inlets provided by a single independent electrically-driven boost pump.

Further details of the installation, and of the use of hydrostatic pumps generally in this type of application, may be found in [37].

Control of the dynamometer is discussed in sub-section 2.3.5.

2.2.3 Design Performance Predictions

Having described the 520DCE matching and component selection, it is appropriate at this point briefly to present the design performance

predictions for the 520DCE without CVT, that is, the prototype configuration. These predictions were obtained using CSPDCE (described in Chapter 5) and are taken from [36], where they are discussed in detail.

The basic design conditions for the 520DCE with CVT may be summarised as:

(i) Rated

Engine : 2600 rev/min, 15 bar BMEP (266kW), 3.boost ratio

Compressor : 6606 rev/min, 0.477 kg/s, 74kW, 3.17 pressure ratio

Turbine : 50,000 rev/min, 660 deg.C inlet, 102 kW, 3.17 pressure ratio

Output shaft : 3409 rev/min, 769 Nm (275 kW)

(ii) "Stall"

Engine : 1673 rev/min, 20 bar BMEP (229 kW), 3.8 boost ratio

Compressor : 11,500 rev/min, 0.87 kg/s, 173 kW, 3.95 pressure ratio

Turbine : 46,500 rev/min, 414 deg.C inlet, 156 kW, 3.95 pressure ratio

Output shaft : 682 rev/min, 2718 Nm (194 kW)

For the prototype 520DCE with fixed turbine gear ratio, the rated engine design conditions are unchanged, but the design stall conditions become:

(iii) "Stall", no CVT

Engine : as (ii)

Compressor : as (ii)

Turbine : 10,000 rev/min, 52 kW, 3.95 pressure ratio

Output shaft : 682 rev/min, 1400 Nm (100kW)

Fig. 2.14 shows the predicted optimum steady-state engine speeds over the output shaft speed/torque range of the 520DCE with fixed turbine gear ratio. The predicted limiting torque curve (LTC) is the locus of peak torques available over the speed range within the various engineering constraints (discussed in Chapter 3), and obviously runs from the design stall to rated conditions.

Fig. 2.15 shows the corresponding contours of optimum engine boost ratio.

Fig. 2.6 shows the resulting bypass massflows at the optimum conditions.

Fig. 2.17 shows the optimum output shaft brake thermal efficiency contours.

The above data will be compared with experimental results in Chapter 3, and so are not discussed here.

2.3 TEST INSTALLATION

2.3.1. General Test Facility Requirements

The testing of engine-transmission systems demands a careful and consistent approach to test facility design if the results are to be obtained easily and to be of practical use. The major obstacles to effective testwork are inaccuracy and unrepeatability of test results, poor control of the test parameters and unreliability/poor damage prevention systems in the test facility.

(i) Accuracy

The required accuracy of each test bed measurement should be considered with regard to the significance of the parameter,

likely repeatability limits of the parameter, and the error build-up in derived data which use several measurements (for example, specific fuel consumption, or differential heat flows). Calibration procedures are important, particularly where sensors exhibit non-linearities. The accuracy of nominally linear sensors which have small non-linearities can be maximised by calibrating over the range of typical values rather than the full range of the sensor. Inherently non-linear sensors, such as orifice plates, are accurate only over a limited range, since their sensitivity varies with the magnitude of the sensed parameter. It is important to calibrate as far as possible under test conditions. The most significant factor in engine testing is variation with temperature, but unfortunately it is usually impractical to calibrate, for example, pressure sensors at normal operating temperatures. In these cases the sensors may be cooled during testing to approach calibration conditions more closely, or sensors with low temperature drift must be specified. Finally the in situ calibration of sensors (incorporating the complete sensor-wire-readout chain) will account for wire/connector losses.

It may also be noted that the use of standard measurement techniques will facilitate comparison of results with other test installations. An example of this is the widespread use of the Bosch smoke measurement system for steady-state engine testing.

(ii) Repeatability

To achieve repeatability it is first necessary to install reliable measurement systems (irrespective of the chosen accuracy) without drift over time. All relevant parameters must then be controlled as closely as possible. For engine testing relevant parameters

include oil, coolant and fuel temperatures and fuel quality; ambient conditions are important, but while inlet air temperatures may be controlled, the effects of ambient pressure must be accepted, and standard correction factors may be applied in certain cases.

(iii) Control of test parameters

The speed, accuracy and repeatability of testing of complex engine/transmission systems is dependent upon the quality of the control systems used. The automatic control of "external" influences such as coolant temperatures, inlet air temperatures and so on is an obvious necessity. Tight, stable control of the major test parameters such as load torque or speed is also vital.

(iv) Reliability/damage prevention

Unreliable measurement systems waste testing time both by causing delays for rectification and by invalidating previous results if the failure has been progressive. All measurement systems have finite reliability and life; it is therefore inevitable that a complex, highly instrumented prototype such as the DCE will be prone to delays through sensor failure. This must be minimised by the use of well-proven measurement techniques and equipment, by improving the senor environment (mounting for reduced vibration, heat shielding and so on), and by regular inspection and calibration.

Where it is possible to exceed the operating limits of the test installation or the engine under test, some form of automatic monitoring system is a necessity. This must give a clear indication of the fault and allow the operator to take action wherever possible. Failing this the test rig must be

automatically shutdown in a way which minimises any potential damage.

2.3.2 Layout of 520DCE Installation

The layout of the 520DCE prototype was predetermined by

(i) The gearbox shaft locations - in particular the compressor shaft exits the rear of the gearbox whereas the engine and turbine input shafts are to the front

(ii) The component package dimensions

(iii) The need to fit torquemeters to certain shafts

The final layout is shown in Fig. 2.18. The general height of the rig is as low as possible, constrained by the need for oil sumps below the gearbox and compressor, and by the downward-facing compressor air outlet. The compressor was installed as close as possible to the gearbox, allowing room solely for flexible couplings. The dynamometer splitter gearbox could not be installed alongside the compressor, thus the output shaft is much longer than is required to install the torquemeter. The engine propshaft length was set by the inclusion of a torquemeter and the need for flexible couplings.

The resulting large overall length of the rig determined the choice of the following :

(i) Component Mounting

A one-piece bedframe was impracticable; all components were mounted on independent bedframes. The gearbox, compressor and dynamometer bedframes were bolted rigidly to the cell floor, while the turbine was initially mounted directly onto the gearbox. Later, with the installation of a turbine torquemeter, the turbine

was rigidly mounted to the floor via a pedestal. The engine, having reciprocating forces, was resiliently mounted to its bedframe, which was bolted rigidly to the floor.

(ii) Gas Pipework (Fig. 2.19)

Relatively large diameter pipework was used to achieve air/exhaust system losses representative of a compact "production" DCE. This would give realistic steady-state performance (apart from pressure waves, but as explained earlier a constant pressure exhaust system was intended from the outset), at the expense of transient response (volume filling). One useful result of the pipework layout was the improved theoretical accuracy of the gas flow measurements (longer straight runs) and pressure measurements (less fluctuation).

2.3.3 Couplings (Fig. 2.18)

The differing coupling arrangements around the system warrant some discussion.

(i) Engine to Gearbox

A torsional vibration (t.v.) analysis was undertaken by Holset to determine the effect of engine excitation upon the 520DCE. This led to the fitment of a torsionally flexible half coupling at the flywheel. A t.v. analysis in this context usually considers the excitation over the normal operating speed range, at maximum (or maximum and zero) torque. Resonances on start-up and shutdown are thus ignored.

The above coupling also provides lateral freedom at the engine end; a gear coupling is used at the gearbox end. The torquemeter extends from the gear coupling roughly to the mid-point of the

shaft. Here a rigid coupling (to prevent whirling) connects the torquemeter to the engine shaft. A compression coupling (Fenner Taperlock) was used, since press or shrink-fitting might damage the torquemeter strain gauges.

This gave problems under certain rapid shutdown conditions. It had been noted [36] that a previous unkeyed (Simplatroll ETP) bush had been prone to slippage on start-up. In the keyed Taperlock case, it seemed that fractional slippage also occurred, whereupon the shutdown resonance torque was borne by the key, causing brittle fracture of the bush initiated at the sharp keyway corner. There is a design weakness in that the keyway position on the bush bore coincides with a compression bolt aperture on the outer diameter, putting a stress-raiser and the minimum component thickness at the same point.

Despite careful attention to fitting and bedding-in the coupling, three failures occurred, all during uncontrolled shutdowns.

Strengthening of the coupling might have referred the damage to a more expensive component; to cure the problem the use of a torsionally-soft coupling would have to be reassessed. Conversely, replacement of the taperlock bush was cheap and quick. Having thus decided to accept the bush as an occasional "frangible link", no further failures occurred. It was notable that this final coupling was chosen from the available spares as the only one in which the keyway did not coincide with a compression bolt aperture.

(ii) Gearbox - dynamometer

The output shaft uses gear couplings at each end to allow for misalignment. As noted above the shaft is long, and incorporates a torquemeter. Again a compression coupling (Simplatroll ETP) is used, but no problems have been experienced. It may be noted here that the use of gear rather than resilient flexible couplings is preferred where a torquemeter is fitted, to avoid imposing bending forces upon it.

(iii) Gearbox - compressor

No torquemeter was fitted to the compressor shaft. It was therefore quite acceptable to use "Autoflex" flexring-type couplings, as demanded by the high speed range of this shaft.

(iv) Turbine - gearbox

The turbine was initially close-coupled to the gearbox. The turbine shaft drive end is splined, and was connected to a similar gearbox input spline via a nitrided sleeve coupling. This allows some angular misalignment and axial float. Since the turbine and high speed geartrain are nominally isolated from engine torsional excitation by the engine-gearbox coupling, no torsional isolation was used.

With the later installation of a turbine torquemeter, the coupling arrangement was revised. Given the need to retain splined couplings at turbine output and gearbox input, and the high speeds involved (50,000 rev/min), a suspended torquemeter would be highly prone to whirling, and thus a pedestal torquemeter was required. On each side of the torquemeter, "tordisc" diaphragm couplings (giving good radial location with low bending forces) were bolted to quill shafts. The quill shafts were flanged and jig-bored to match the Tordisc couplings (fitted bolts were used), and

internally-splined and nitrided to match the turbine and gearbox splines. The quill shaft lengths (4") were chosen to give adequate misalignment capacity within constraints of overall installation length. Given the existing spline diameter, the quill shaft outside diameter was set at 1"; at 50,000 rev/min this gave a peripheral speed of 66 m/s, more than twice the limit of commercially-available oil seals. A two-stage oil baffle and catcher arrangement was devised which minimised oil loss, but retained the ability to remove the torquemeter and couplings for inspection/calibration without disturbing the carefully-aligned turbine and associated pipework.

2.3.4 Services

The following is a brief summary of the test installation services- again a detailed description may be found in [36].

(i) Lubrication

The engine lubrication system was augmented by an oil-cooler, exchanging heat directly with cooling pond water.

The compressor has an external lubrication system comprising an electrically-driven gear pump (giving the required flowrate) and a relief valve (giving the required supply pressure). No oil cooler is required.

The gearbox, turbine bearings and splitter box can all use the same lubricating oil, and thus share a common external system. An electrically-driven vortex pump is used; a combination of valved supply and bypass lines is used to give the required pressures and flowrates to each component. A pond water oil cooler is included since there is significant heat rejection in these components.

(ii) Cooling

All heat exchangers pass heat to an external cooling pond. The pond water is filtered through gauze strainers. The engine coolant circulates in a closed loop controlled by the standard engine thermostat. This jacket water then rejects heat to pond water. All other components (charge cooler, compressor water jacket and so on) use pond water directly.

(iii) Compressed Air

The common Wolfson laboratory compressed air supply is used. The steady-state and transient smoke meters both need purge air to prevent fouling. The turbine requires a cooling air supply to the rear of the wheel (normally bled from the compressor in a complete turbocharger assembly). Water traps/filters and pressure regulators are included in each line as required.

(iv) Hydraulic supply

The prototype has three electro-hydraulic actuators, described in the next sub-section. These use a common supply comprising an electrically-driven pump, relief valve and filter, though individual filters are also included for each actuator. An hydraulic accumulator is incorporated to maintain servo pressure when the actuators are moving.

(v) Electrical Services

Electrical supplies within the cell are :

(a) d.c. The engine uses a 24V battery supply (alternator removed to reduce parasitic losses and avoid possible unrepeatability), boosted by an external charger to prevent "drop-out" during high current drains (e.g. starting). 12/24V d.c. requirements within the cell are taken from the batteries.

(b) 240V a.c. Mains supply is required for some safety/shutdown functions.

(c) 415V 3-phase This is required for the electrically-driven lubricating oil, hydraulics and coolant services.

2.3.5 Actuators and Control Boards

2.3.5.1 General

The prototype has four active controls, operating on:

(i) Fuel rack

(ii) Turbine VG nozzles

(iii) Static injection timing

(iv) Dynamometer loading conditions

There is also Manual control of

(v) Bypass valve closure

With modifications made during the steady-state test programme, controls (i), (ii) and (iii) above now use a common design of electro-hydraulic circuit, shown schematically in fig. 2.20. Each comprises an analogue control board, Moog servovalve and hydraulic ram, with feedback by A.C. linear variable displacement transformer (LVDT) and A.C. carrier-amplifier card. The main differences are in the "front-end", that is the way in which the servovalve currently is calculated by the analogue control board. In each case the control stage of the board arrives at a position demand; this is compared with the position feedback from the LVDT, and any error results in a proportional current from the valve driver stage to the board. This current sets the fluid flowrate at the servovalve, and the hydraulic ram "integrates" this flowrate until the actuator position feedback reaches the required position.

Details of the control loops and the actuator design are given for each control in turn, followed by a note on the bypass valve and a description of the dynamometer control system.

2.3.5.2 Fuel rack control (Figs. 2.21 and 2.22)

All governing elements were removed from the fuel injection pump; the hydraulic ram drives a unison plate which operates the rack directly, and also drives the LVDT, as shown in Fig. 2.21. The ram end stops coincide with the physical limits of the rack. 10V corresponds to maximum fuelling; the other extreme position is set at 0V, although fuelling actually begins at 3V owing to the large deadband formerly used to ensure positive fuel shut-off with a mechanical governor.

The rack position demand may be generated in one of three ways (Fig. 2.22)

(i) Rack demand

That is, direct position demand, giving direct control of fuelling (quantity of fuel per shot). As shown in Fig. 2.20, the feedforward input may be set either manually (potentiometer), or from an external voltage source (computer or signal generator).

(ii) Engine speed demand

The feedforward input is interpreted as an engine speed demand (currently 10V corresponds to 3000 rev/min), and the rack position is proportional to the error between feedforward and feedback engine speeds. This is analogous to a mechanical allspeed governor.

(iii) Fuel flowrate demand

The rack position demand is set by a proportional and integral control to keep the fuel volume flowrate (gross fuel consumption)

constant. The feedback signal is generated by a vane-type flowmeter.

Each of the above modes is subject to a variable absolute rack limit which may also be set either manually or by external voltage input. A more detailed description of the electronic governor may be found in [36, 43].

2.3.5.3 Turbine VG control (Figs. 2.23 and 2.24)

The turbine VG design was described in subsection 2.2.2.4. The VG nozzles are actuated by a unison ring; this is driven via a crank mechanism which enables the use of linear hydraulic ram and LVDT (Fig. 2.23). The feedback was originally provided by a D.C. type LVDT with on-board conditioning [36], but this implied a low temperature limit. Despite the use of insulating mounting washers and compressed air blast to reduce the effects of heat transfer from the turbine, this LVDT eventually failed, and was replaced by an A.C. type LVDT with remote A.C. carrier-amplifier card (in common with the other actuators). The temperature limit for the latter LVDT was 125 deg.C, which allowed the air blast to be dispensed with. The control board was redesigned to suit the new feedback arrangement; the circuit diagram is shown in Fig. 2.24. The minimum and maximum VG restrictions correspond to 0 and 10V respectively.

Only the basic positional loop is available, that is, direct VG position demand.

2.3.5.4 Static injection timing control (Figs. 2.21 and 2.25

Injection timing control is effected by driving the fuel pump via a collar which can be moved axially along a helically-splined shaft. Thus as the collar axial position is changed, so is the relative angular position of the fuel pump camshaft and the engine geartrain. The design was based upon the arrangement, and some of the parts, used in the Gardner 6LXCT Diesel engine. Fig. 2.25 shows the general arrangement of the unit. The unit was installed in place of the service air compressor (to the rear of the fuel pump in Fig 2.21). The output shaft from the unit is attached to the fuel pump camshaft by a spring-disc coupling and clamp. The collar is driven by a yoke and external arm, attached to a linear hydraulic ram and LVDT. The unit gives a total angular range of 22 deg.C crank, 0V corresponding to full retard, 10V to full advance. It is set up such that 7V corresponds to the standard Leyland 520 static injection timing, giving more capacity for retard than advance (in anticipation of the need to reduce cylinder pressure at high loads).

The unit is subject to harsh 3rd order impulses from the fuel pump. These are transmitted through the complete mechanism, and tend to be stiffly-opposed, rather than damped, by the high hydraulic actuator force (a friction damper is incorporated in the manually-operated Gardener installation). This caused various problems due to vibration loosening components and linkages, with eventual fracture of the hydraulic ram. Revised fasteners, and a ram area increase of approximately 50 per cent (constrained by the dimensions of surrounding parts) were successful. The yoke assembly and the straight splines (which are only fully meshed at full advance) showed only slight wear over the test programme, despite the greatly increased injection forces at the 520DCE engine ratings.

2.3.5.5 Bypass valve

A bypass valve has been proposed in all DCE schemes since it provides an extra degree of freedom in optimising performance. However, simulation studies have found there to be no advantage in its use during steady-state operation. At the design stage of the 520DCE a bypass valve was included for possible future investigations. A manually-operated butterfly valve was fitted, but no steady-state experimental investigations were thought worthwhile, and its transient use in the 520DCE (with a suitable actuator) was ruled out by simulation studies (Chapter 7).

2.3.5.6 Dynamometer control (Fig. 2.26)

The fundamental dynamometer control mode is constant load torque. As shown in Fig 2.26 a proportional and integral (PI) controller is used to set dynamometer servovalve current (and thus loading pressure) according to the error between demanded load torque and a feedback signal from the conditioned output shaft torquemeter signal.

Output shaft speed control is obtained by closing a speed feedback loop around the torque loop. The demand input to the torque loop is generated by PI control of the error between demanded and feedback output shaft speed.

The final "windage" mode gives rising load torque demand with increasing speed. A linear function is used (as sketched in Fig. 2.26), where both the offset and slope may be controlled actively. Alone, this is of limited value, but it may be augmented with an inertia simulator to provide vehicle simulation using analogue electronics, as in [37]. A more direct approach to vehicle simulation, where the computer

controlling a transient test also computes digital road load plus inertia simulation inputs to the basic torque loop, is discussed in Chapter 4 which covers 520DCE transient testwork.

2.3.6 Steady-State Instrumentation

The instrumentation used for steady-state testwork is described in the following groups:

(i) Speed

(ii) Torque/power

(iii) Pressure

(iv) Fuel flow

($\dot{v}$) Gas flow

(vi) Temperature

(vii) Smoke

(viii) Position/displacement

Accuracies of individual instrumentation and of derived data are summarised in table 2.1. Calibration factors are given in Table 2.2.

2.3.6.1 Speed measurement

Rotational speeds in the 520DCE installation are predominantly measured by toothed wheel and inductive (magnetic) pick-up, with frequency to voltage (F-V) conversion. Separate sensors are used for control loop feedback and data acquisition/safety monitoring, to provide a degree of fail-safety. Optical pick-ups are used to give once/rev rotation counter signals, but these are prone to fouling, so are unsafe for more critical uses.

2.3.6.2 Torque/power measurement

Engine torque is measured by a suspended strain-gauge transducer (EEL Saunders-Roe TT2.4DC torque transducer). Bridge excitation and signal are transmitted via silver slip rings and silver-graphite sprung bushes. Double springs were fitted to reduce brush bounce (at the expense of increased wear), but recurrent fouling in the poor test environment was a problem. The torquemeter was reconditioned during the test programme, but the loan of a similar unit from within the school was pre-arranged to minimise downtime.

Output shaft torque us also measured by a suspended strain-gauge transducer (Vibrometer TG 200/B). Here the stator and rotor signals are inductively-coupled, so that brush bounce and fouling problems are eliminated.

The installation of a compressor torque transducer was prohibited by space constraints (see section 2.3.2) and by cost. Detailed experimental power consumption data were supplied for the compressor by the manufacturer, so that compressor power (and thus torque) could be inferred from pressure ratio and speed.

Turbine power was initially inferred from measured massflow and temperature drop (enthalpy change) by making the common assumption of negligible heat rejection. This neglects turbine mechanical losses, which are then included with the gearbox losses in the overall power balance. The enthalpy measurements proved unreliable (as discussed in Chapter 3) so that a turbine torquemeter was fitted later in the test programme. Owing to the high speeds (up to 50,000 rev/min) involved, the range of available torquemeters was small. A Torquemeters Ltd. "Torquetronic" ET12MS unit was purchased. This works on the phase

displacement principle; inductive pick-ups detect the phase difference between toothed wheels at each end of the torsion shaft. The "torquetronic" system is a development of this principle which uses multiple pick-ups in the form of internally-toothed rings. If radial movements of the shaft cause an early signal at one tooth this is compensated by a late signal from the opposite tooth. This enables spring couplings to be used without the resulting radial shaft movements affecting accuracy.

For calibration purposes the stator assembly (normally locked to the main causing) may be rotated by a miniature electric motor, so that a phase displacement signal is generated with the torsion shaft stationary ("static calibration"). Because of the high speeds involved, there may be a small change in the zero torque datum (ZTD) over the speed range. This dynamic calibration is carried out by the manufacturer. A comprehensive microprocessor-based conditioning unit (type 603 readout) includes digital storage of the ZTD and static calibration data.

The ET12MS unit uses grease-packed bearings, suitable for continuous operation up to 40,000 rev/min, and intermittent operation up to 50,000 rev/min (higher speed units use a pressure-lubrication system - with a prohibitive increase in cost). The bearings are thermocoupled; excessive temperatures would indicate incipient bearing failure and/or heat soak from the turbine, but no such problems were encountered.

2.3.6.3 Pressure measurement

Two gas pressure transducers are used (Druck PDCR strain gauge type), in the compressor and turbine plenums. Both are water-cooled. Pressures elsewhere in the system are obtained by water/mercury manometers,

referenced either to the compressor plenum or to atmosphere as appropriate. Single-point wall tappings are generally used. Owing to the large pipework diameters used, the measured static pressures will be close to the stagnation pressures, especially in the plenums.

Cylinder pressure is measured by a flush-mounted piezoelectric transducer (Kistler 6121) and charge amplifier. This is calibrated using a dynamic compressed gas realease rig.

2.3.6.4 Fuel flow measurement

Steady-state fuel consumption measurements were made using a dead-weight system. This comprised a simple balance with fuel drawn from a beaker on one side, and weights on the other. Tipping of the scales triggers an opto-switch which starts and stops a timer-counter. This records elapsed time and total engine and output shaft revolutions (from once/rev pick-ups), so that fuel consumption is based upon mean speeds. Being a gravimetric device, fuel temperatures need not be measured. A float chamber was included in the fuel system to maintain constant lift pump pressure and fuel pump element filling regardless of whether the fuel was drawn from the weigh-gear or the day tank.

2.3.6.5 Gas flow measurement

For steady-state testing, gas flow was measured by orifice plate and manometer. It is necessary to measure flow through the compressor and the engine. The difference is then the bypass flow, whilst the turbine flow is the sum of compressor gas flow and fuel flow.

Compressor flow is measured by an open-ended orifice, engine flow by in-line orifice. These were installed as closely as possible to BS1042

[44]; errors introduced by deviation from the standard are estimated in table 2.1. Compressor flow may also be inferred from the manufacturer's data, given compressor speed and delivery pressure. The compressor flow range is wide; a compressibility correction was included in the data reduction software written by Prince [36]. The calculated bypass flow is error-prone being the difference between two often similar readings. However, since the range of flows is very wide (from about 20 Kg/min at the design stall condition through zero to negative flow at some conditions), the accuracy of a direct bypass orifice measurement would be poor.

2.3.6.6 Temperature measurement

Chromel-Alumel (K-type) thermocouples are used throughout, of 1/16" diameter. These are mineral-insulated and sheathed. Shrouds are used to prevent radiation from nearby surfaces which are above the current gas temperature, and to stagnate flow in the region of the probe - however, as noted earlier the pipework volumes are such that static and stagnation conditions are nearly identical.

2.3.6.7 Smoke measurement

Steady-state smoke was measured by Bosch manual sampling pump and comparator. The pump was initially installed strictly to the Bosch specification, placing it in a dangerous location adjacent to the engine and turbine. It was later installed outside the cell, permanently connected to the sampling nozzle, but purged by compressor air. A change over globe valve isolated the purge air supply when sampling, and isolates the sample pump otherwise. Cross-checks showed that this installation did not affect the results obtained.

No gaseous or particulate emission measurements were made - these would be inappropriate to this research prototype. Data for a modern engine with a fully-matched combustion system, operating at similar air/fuel ratios and cylinder pressures would be of more relevance.

2.3.6.8 Displacement measurement

Actuator position measurements are simply taken from the LVDT feedback signals.

Injector needle lift is sensed by an integral transducer (UTD Systems instrumental injector) and remote conditioning (Bentley Nevada proximitor).

2.3.7 Transient instrumentation

Much of the above steady-state instrumentation was suitable for transient data recording. However, the following parameters required additional instrumentation:

(i) Fuel flow

(ii) Gas flow

(iii) Smoke

2.3.7.1 Transient fuel flow measurement

Two types of transient fuel flowmeter are commonly used: gravimetric beaker systems and volumetric turbine/positive displacement meters. The former basically comprises a fuel beaker mounted on a load cell, fuel flowrate being calculated from the derivative of the load cell signal. This has the advantage of excellent response, but is expensive (being made commercially only in small numbers for specified use) and suffers a discontinuity if the beaker needs refilling during a prolonged

transient. A larger beaker size would imply a larger load cell with loss of accuracy in short transients.

Volumetric flowmeters are inexpensive and widely available, being used in process industries. The flowmeter size must be matched closely to the expected flow range to maximise accuracy and response. A volumetric flowmeter was already fitted as part of the electronic governor system, but this was of insufficient accuracy and pulse rate for transient instrumentation purposes. Other common measurement principles are less suitable; thermal mass flowmeters have limited accuracy and slow dynamic response while electromagnetic meters cannot work with fuel oil. Coriolis flow meters operate on the principle that fluid flowing in a moving (vibrating) tube will exert a measurable twisting force on the tube in proportion to the mass flow. This gives very accurate massflow measurement, but the units are expensive and bulky.

It was decided to use a volumetric flowmeter. An additional requirement (apart from flow range and response) was a small pressure drop, to maintain a positive head at the engine lift pump (gravity-fed from the day tank). This led to the choice of a Litremeter LM24 unit, which has excess flow range but acceptable pressure drop. This has a Pelton wheel rotor producing a pulse output linear to volume flowrate, followed by remote F-V conversion. Accuracy and calibration factors are given in tables 2.1 and 2.2 respectively. Dynamic response data were not available, but the rotor is of nylon, running in low friction sapphire bearings, and the pulse output is several Hertz even at the lowest flowrate.

The meter was cross-calibrated against the fuel weighgear; the manufacturer's calibration was found to be within +/- 0.5% of the weighgear result over the range of interest, using the standard fuel density correction with temperature.

2.3.7.2 Transient gas flow measurement

To reduce costs it was decided to calculate transient compressor flow from transient compressor speed and pressure data and manufacturer's experimental data. Although these data were obtained at steady-state, they should hold reasonably well during transients since the compressor is a positive displacement machine.

For transient engine airflow, an ITT Barton 7403 turbine meter was selected to satisfy flow range, pressure drop and accuracy requirements. This required pipework diameter reduction from 4" to 3", achieved by taper sections upstream and downstream of the unit. The unit incorporated an on-board frequency to direct current transmitter, which was followed by a remote current to voltage converter. The meter was calibrated by the manufacturer; this calibration agreed reasonably well with orifice plate results during cross-checks. Since the orifice plate accuracy was reduced by the presence of the turbine meter, the manufacturer's calibration was used.

2.3.7.3 Transient smoke measurement

The transient opacity meter is of the Celesco type, as described below. The measuring section passes the full exhaust flow. A collimated light source and photo-electric detector are positioned opposite each other. The reduction in detected light is converted to opacity or smoke density units. The meter and conditioning were built in-house for an earlier project and are fully described in [11].

The lenses are swept by compressed air to reduce fouling. Fouling is simply shown up by a non-zero opacity reading with the engine shutdown; both lenses may be removed for cleaning without disturbing their alignment. A closed coolant circuit of distilled water is used to prevent overheating of the light source and detector. Both air pressure and coolant flow are monitored, with visual failure warnings.

The opacity meter was cross-calibrated against the Bosch sampling system at steady-state, as shown in Fig. 2.27. The maximum smoke achieved was limited, so the calibration from the previous installation [11] is superimposed to extend the curve to higher opacities which may obtain transiently.

2.3.8 Monitoring/Shutdown System

A complex rig such as the DCE prototype requires a comprehensive monitoring and warning/automatic shutdown system to prevent damage. Three shutdown devices were installed :

(i) Fuel shut-off

This is the most commonly-used device, which simply cuts the power supply to the fuel rack servovalve, causing the rack to be closed by mechanical bias in the servovalve. It is used for normal shutdown as well as emergency situations. In addition to a push button on the control rack, lanyards are provided on each cell wall which have the same effect.

(ii) Engine air shut-off

This is affected by a drop-arm, normally supported by a solenoid. It is applied in situations where a rapid shutdown is required, or where the engine must be positively stopped. It forms a vital back-up to fuel shut-off in the event of the rack jamming open, or some combustible fluid (e.g. compressor oil leak) being aspirated.

(iii) Compressor brake

This comprises an industrial hydraulic (fully-retracting) disc brake attached to the compressor drive shaft. Its purpose is to prevent compressor reversal - being sized for operation up to 12000 rev/min it must never be applied at speed.

It follows that, being safety devices, each must itself fail-safe in the event of power loss, that is, fuel shuts off, air shuts off, but the compressor brake is not applied.

The complexity of the decisions involved in automating these shutdown devices led to the use of a microprocessor-based system. The system layout is shown schematically in Fig. 2.28.

The incoming signals are conditioned and read by the microprocessor through "versatile interface adaptors" (VIAs). The monitored parameters and corresponding shutdown action are listed in table 2.3. Where the signals are derived from analogue instrumentation (e.g. speeds), warning and shutdown levels can be adjusted by changing the comparator settings in the shutdown system. Other inputs are purely make/break circuits driven by pressure/temperature/level switches - in most cases the switches themselves may be adjusted.

Wherever possible, automatic shutdown is preceded by a warning set below the absolute limit of the parameter in question. Warning/shutdown trip codes are stored in order of occurrence and may be scrolled through on a digital display.

2.3.9 Data Acquisition and Reduction

2.3.9.1 Steady-state

For the main steady-state mapping work, existing BASIC software ("DDERUN" and "DCETAB") written by Prince [36] was used. This was implemented on a PET 3032 microcomputer. Since a large proportion of the instruments had no analogue output signals available (e.g manometer and temperature readings), all the data were manually input via an interactive menu.

For other steady-state tests where different data reduction was required, software was written for latterly-available IBM PC-AT compatible microcomputers, using FORTRAN or C. To avoid repetition, these short programmes are presented with the corresponding testwork in Chapter 3.

2.3.9.2 Transient

For transient data acquisition, an IBM PC-AT compatible-based system was purchased with general purpose acquisition software:

Machine : Opus PCV 6/10 MHz PC-AT compatible

Input/output : Analog Devices RTI-860 Analog to Digital Convertor (ADC)-
12 bit, 16 channel (single-ended) input
Analog Devices RTI-802 Digital to Analog Convertor (DAC)-
12 bit, 8 channel output

(A more detailed description of these boards may be found in their technical manuals [45, 46]).

Data Acquisition Software : Laboratory Technologies Corporation "LabTech Notebook" version 4

This is a menu-driven software package used to set up input/output (i/o) channels for the above hardware, and scaling plus disk storage of the acquired data. It has additional facilities for open-loop outputs, and simple process control. Details of the package may be found in [47].

The chosen i/o boards work with D.C. voltage signals (selectable unipolar or bipolar, 5 or 10V), thus being compatible with instrumentation signals from the 520DCE installation, which were standardised as 0-10V.

The transient data acquisition layout is shown in schematic form in Fig. 2.29. The data acquisition system is also used to run the transient from a prepared data file, setting feedforward inputs to the 520DCE digital controller and to the dynamometer control boards. A number of the inputs to the data acquisition system are also feedback signals for the controller. This microcomputer-based controller will be described in Chapter 4.

The parameters recorded by the data acquisition system are listed in table 2.4, together with scaling factors to engineering units.

The above software includes only very limited data reduction and plotting capabilities, requiring further add-on packages. In view of the specialised nature of the DCE data reduction (including, for example, computation of compressor air flow and power from arrays), it was decided to write the necessary software in-house.

The data reduction software ("DATRED") and plotting software ("PLOTT") were developed by T.Rolle to the writer's specification. Listings of

the code, and documentation, may be found in [48]. The software is written in FORTRAN, except for HP-GL plotter commands - only the HP7470A plotter is supported.

CHAPTER 2 LIST OF FIGURES

CHAPTER 2 LIST OF TABLES

TABLE 2.1

ACCURACIES

1. "RAW" DATA

PARAMETER	INSTRUMENT ACCURACY	READING DISCRIMINATION	TOTAL (worst case)
SPEEDS			
(timer/counter averaged)	accurate	± 1 in 5000 (typical)	accurate
TORQUES			
Engine	± 0.2 %	± 1 in 400-1400	± 0.5 %
Output Shaft	± 0.2 %	± 1 in 200-1000	± 0.7 %
Turbine	± 0.1 %	± 1 Nmm in 10 Nm (typical)	± 0.1 %
PRESSURES			
Compr.plenum	± 0.2 %	± 1 mbar in 1-4 bar	± 0.3 %
Ambient	accurate	± 1 mbar in 1 bar	± 0.1 %
FUEL FLOWRATE			
balance/timer	accurate	± 1 in 300 (typical)	± 0.3 %
flowmeter	± 0.5 %	(analogue voltage)	± 0.5 %
TEMPERATURES			
Inlet side		± 2 in 300-500 K	± 0.6 %
Exhaust side (see note i)		± 2 in 600-900 K	± 0.3 %

2. DERIVED DATA

PARAMETER	SOURCES	TOTAL ACCURACY (worst case)
POWER		
Engine	(torque,speed)	± 0.5 %
Output Shaft	(torque,speed)	± 0.7 %
Compressor	(pressure ratio,speed,map)	± 0.5 % (note ii)
Turbine	(torque,speed)	± 0.1 % (note iv)
THERMAL EFFICIENCY		
Engine	(torque,speed,fuel flow)	± 0.8 %
Output Shaft	(torque,speed,fuel flow)	± 1.0 %

TABLE 2.1 (contd.)

PARAMETER	SOURCES	TOTAL ACCURACY (worst case)
ISENTROPIC EFFICIENCY		
Compressor	(temperature,pressure ratio,index)	± 2.%
Turbine	(temperature,pressure ratio,index)	± 4.%(notes i,iii)

NOTES

(i) Turbine inlet temperatures depend on mixing of engine exhaust and bypass flows - an average of two thermocouples is used. Accuracy of the result varies with the amount of bypass flow.

(ii) This assumes negligible error in the data supplied by CompAir, and in interpolation/extrapolation from the data points.

(iii) The isentropic index depends upon the proportions of exhaust and bypass flows as well as temperatures. A numerical approximation is made in the data reduction software.

(iv) This applies only to turbine powers based on torque measurements, not on enthalpy calculations.

TABLE 2.2

CALIBRATION FACTORS

The following is a summary of calibration factors for the 520DCE instrumentation. Each factor is given as engineering units per Volt.

SPEEDS [rev/min/V]

Engine	300
Output shaft	350
Compressor	1200

TORQUES [Nm/V]

Engine	148.6
Output shaft	200
Turbine	5

PRESSURES [bar g./V]

Compressor plenum	0.4
Turbine plenum	0.3
Cylinder pressure	17.82

FLOWS [cu.m/s/V]

Engine air	0.03411
Fuel	6.67 E-6

OTHER

Opacity	10 [%/V]

TABLE 2.3

DCE MONITORING & SHUTDOWN SYSTEM CODES

Code no.	Parameter	Status	Action
1	Compressor high speed	Warning	
2	Engine high speed	Warning	
3	Output high speed	Warning	
4	High Boost	Warning	
5	Compressor low speed	Warning	
9	Compressor Overspeed	Shutdown	F + A
10	Engine Overspeed	Shutdown	F + A
11	Ouput Overspeed	Shutdown	F + A
12	Over Boost	Shutdown	F + A
13	Compressor Reversal	Shutdown	F + B
17	Dyno. Oil Pres.	Shutdown	F
18	Allen Gearbox Oil Pres.	Shutdown	F
19	Compressor Oil Pres.	Shutdown	F
20	Dyno. Oil Temp	Warning	
21	Compressor Oil Temp	Warning	
22	Allen Gearbox Oil Temp	Warning	
23	Compressor Oil Level	Warning	
24	Allen Gearbox Oil Level	Warning	
25	Turbine Cooling/Purge Air Pres.	Warning	
26	Day Tank Fuel Level	Warning	
27	Engine Coolant Leak	Shutdown	F
28	Engine Water Pres.	Warning	
29	Dyno. Oil Level	Warning	
30	Dyno. Water Pres.	Warning	
31	Servo. Oil Pres.	Shutdown	F
33	Engine Coolant Temp	Warning	
34	Engine Oil Temp	Warning	
35	Engine Oil Pres.	Shutdown	F

F - FUEL SHUT-OFF
A - AIR SHUT-OFF
B - COMPRESSOR BRAKE ACTIVATED.

TABLE 2.4

TRANSIENT DATA INPUTS AND SCALING

ADC channel	Software I/face channel	Parameter	Scaling [engg. units at 10V]
0	1	demand	10V (ie 100% demand)
1	2	o/s torque	2000 Nm
2	3	o/s speed	3500 rev/min
3	4	engine speed	3000 rev/min
4	5	compr.plenum pres.	4 bar g.
5	6	turbine plen.pres.	3 bar g.
6	7	engine torque	1486 Nm
7	8	fuel flow	6.67 E-5 cu.m/s
8	9	engine airflow	0.341 cu.m/s
9	10	opacity	100 %
10	11	rack position	10 V (ie full rack)
11	12	VG nozzle position	10 V (ie full restrn)
12	13	timing position	10 V (ie full advn.)
13	14	(spare)	
14	15	(spare)	
15	16	(spare)	

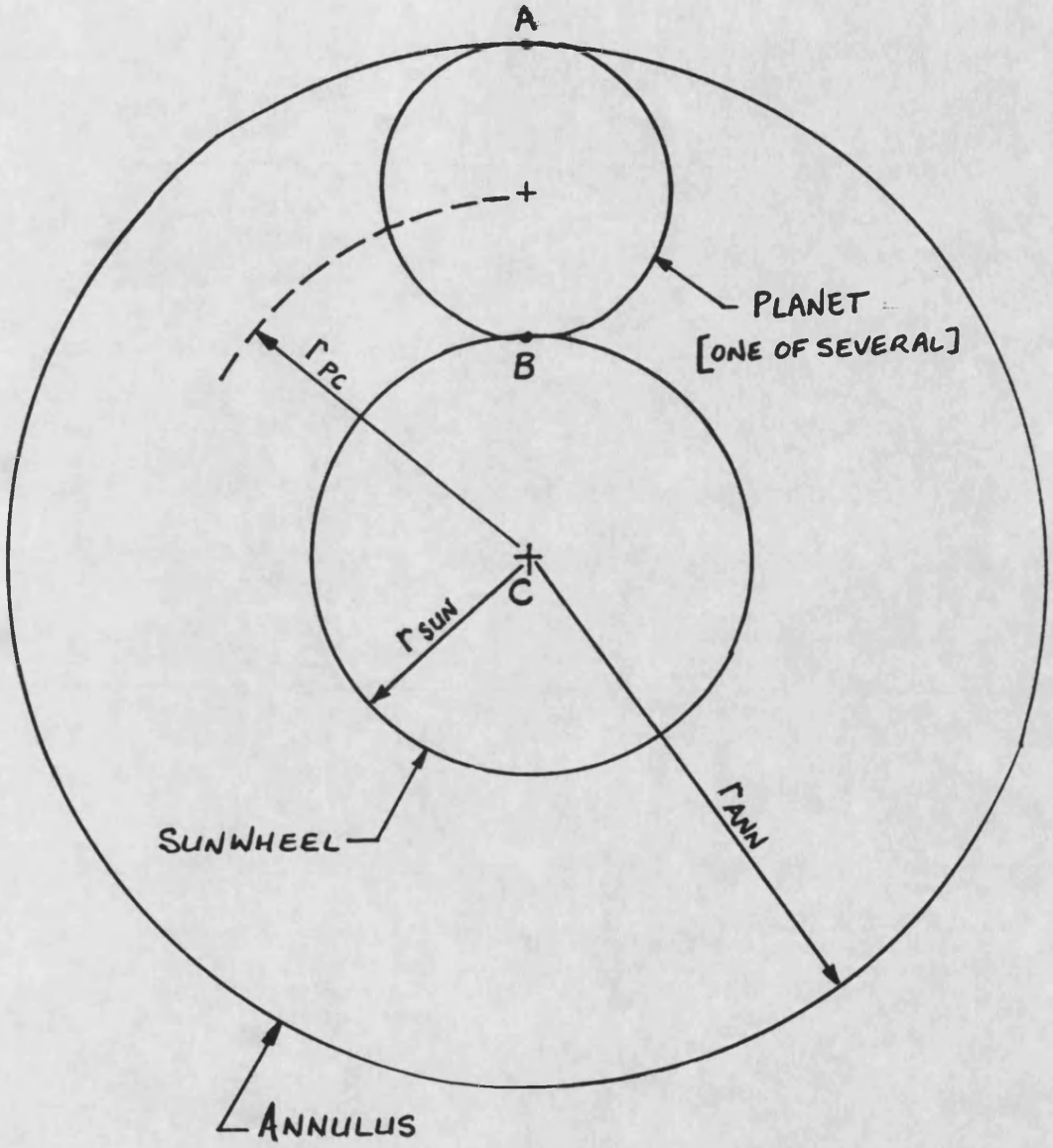

FIG. 2.1 EPICYCLIC GEARSET SCHEMATIC

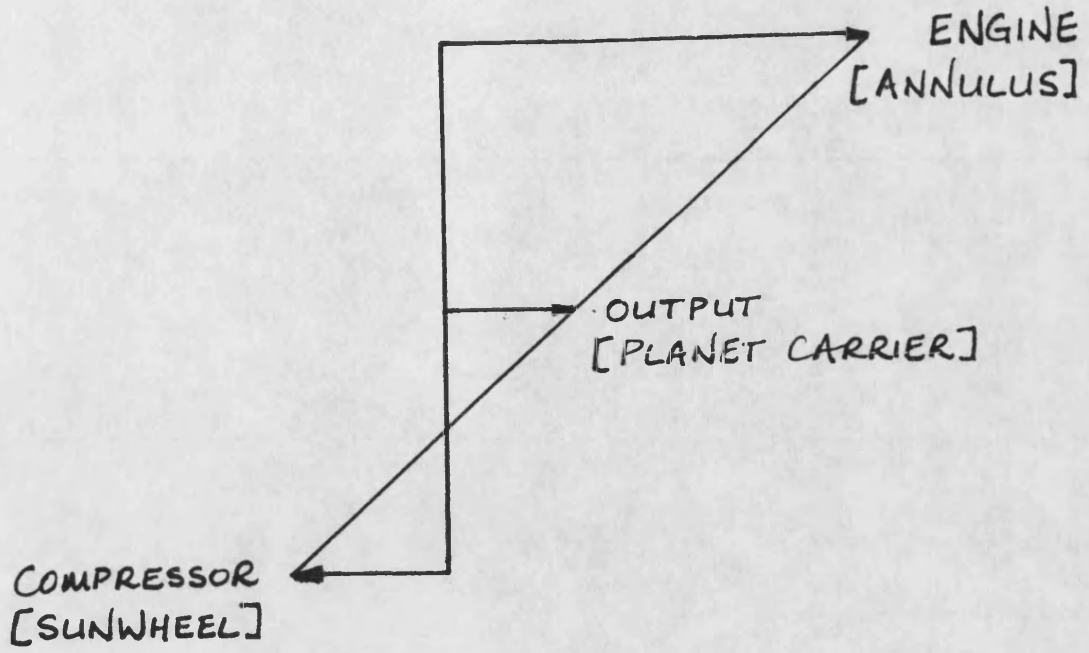

(a) 520DCE.

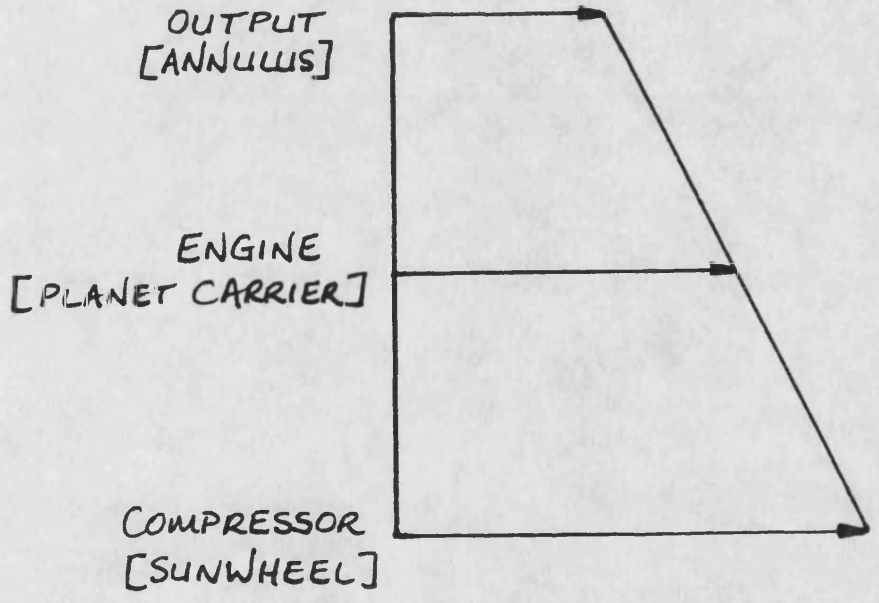

(b) PERKINS DDE.

FIG. 2.2 EPICYCLIC VELOCITY VECTOR DIAGRAMS.

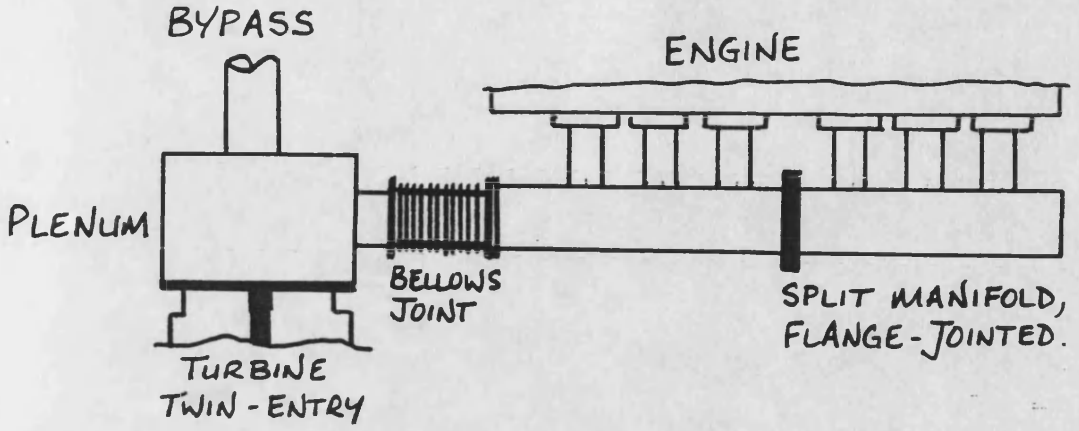

(A). 520DCE EXHAUST/BYPASS/TURBINE INLET

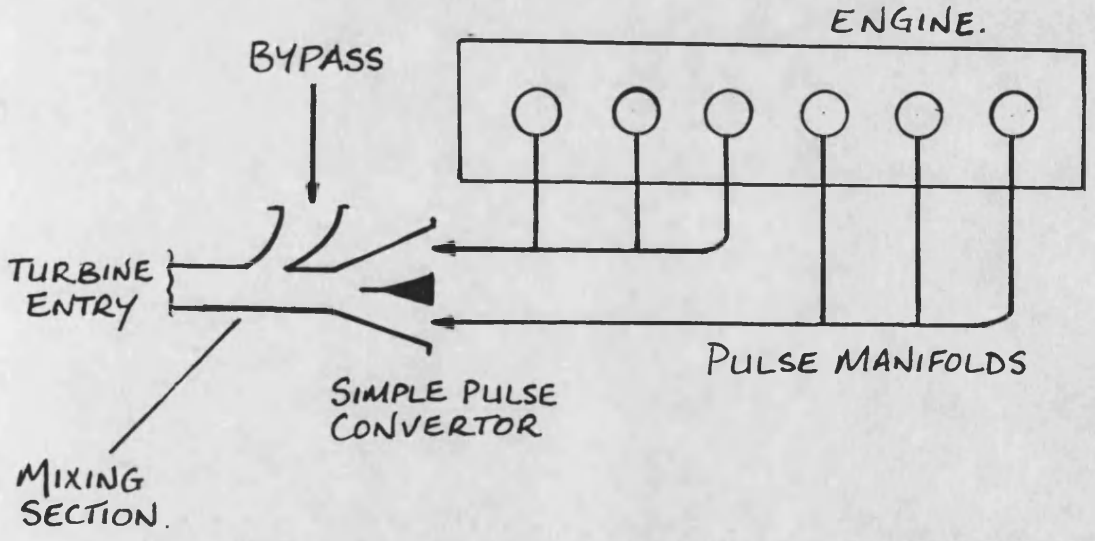

(B). SUGGESTED PULSE CONVERTOR SYSTEM.

FIG. 2.3 520DCE EXHAUST SYSTEM

FIG. 2.4 CompAir 1200 Volume Flowrates

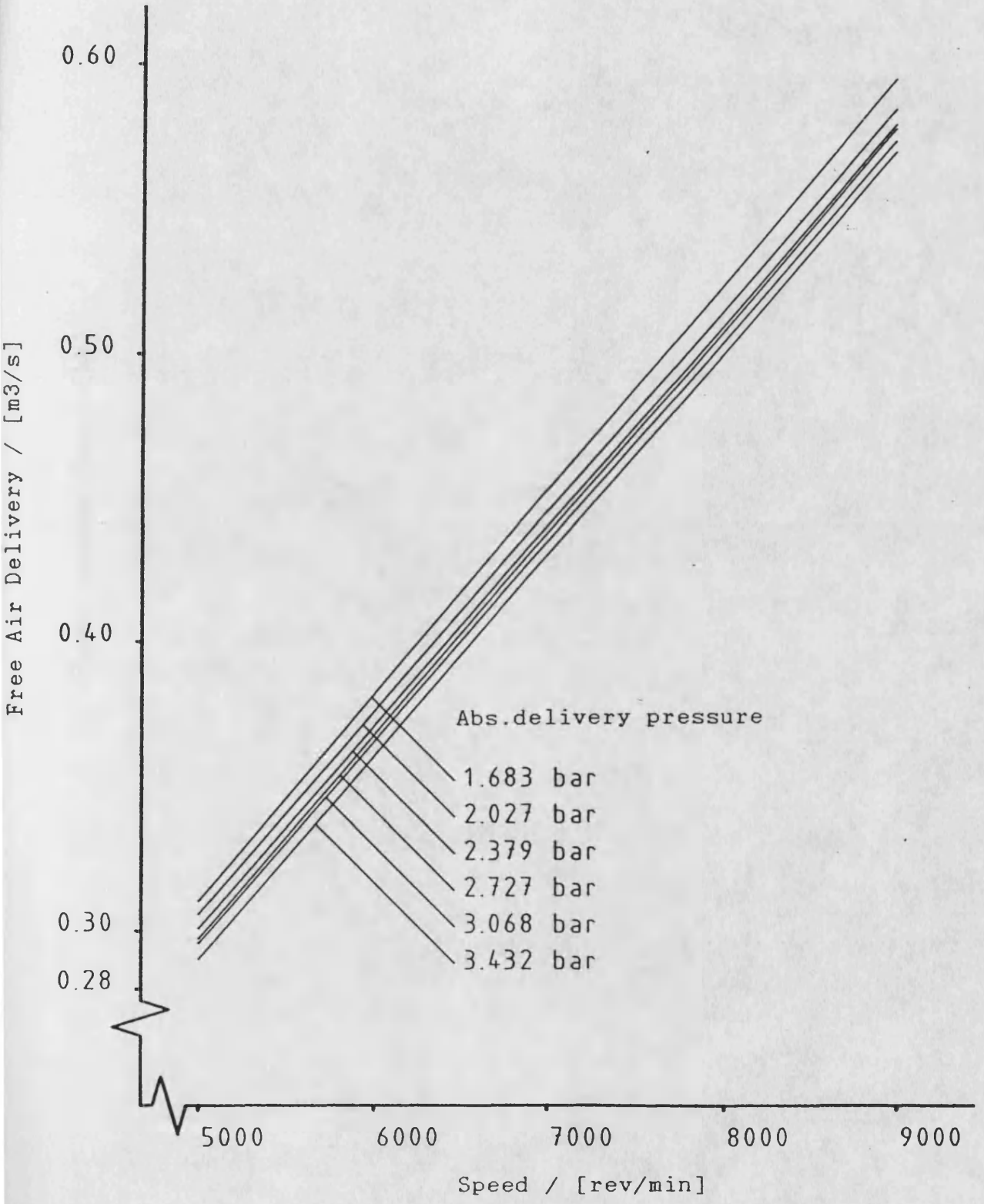

FIG. 2.5 CompAir 1200 Power Consumption

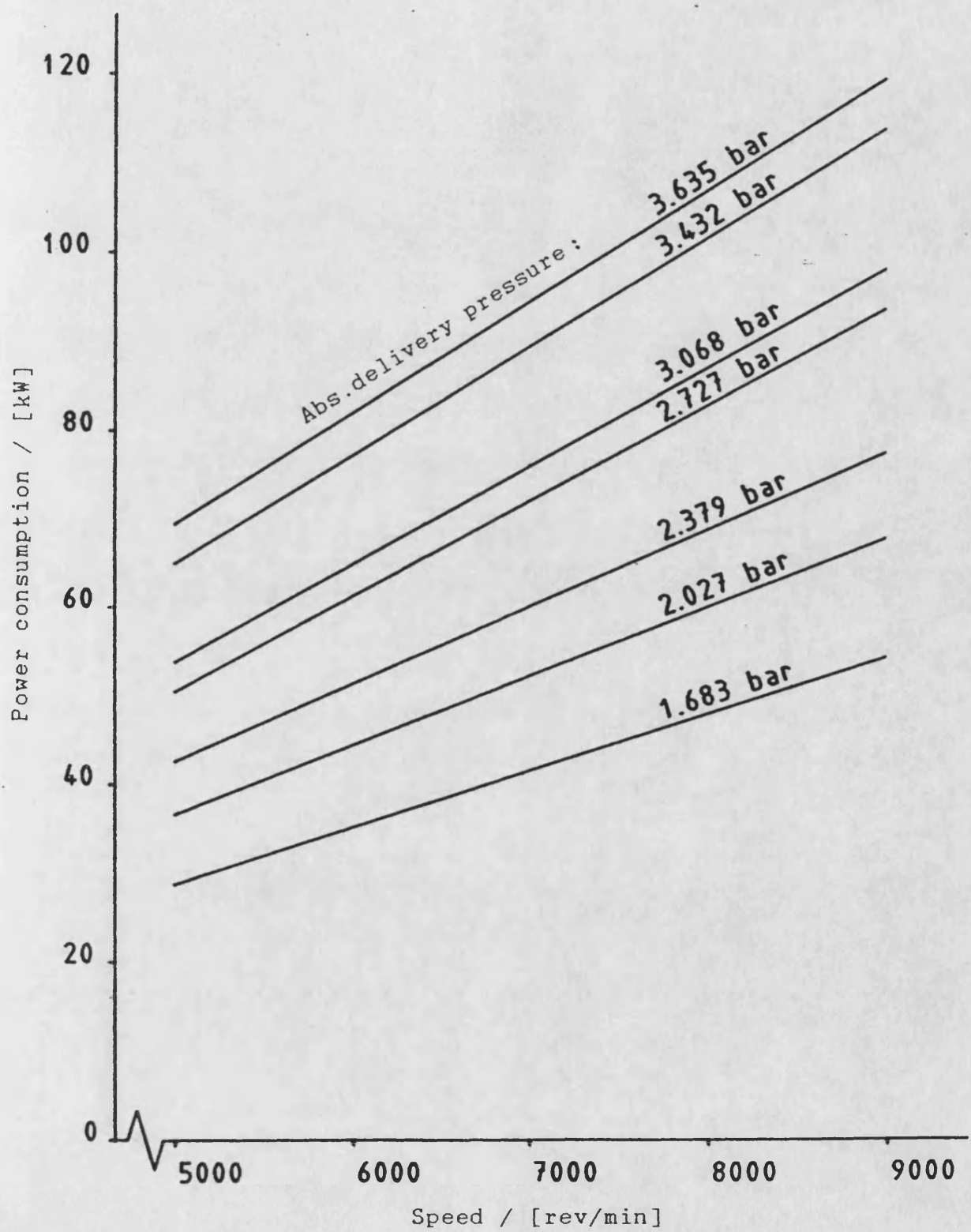

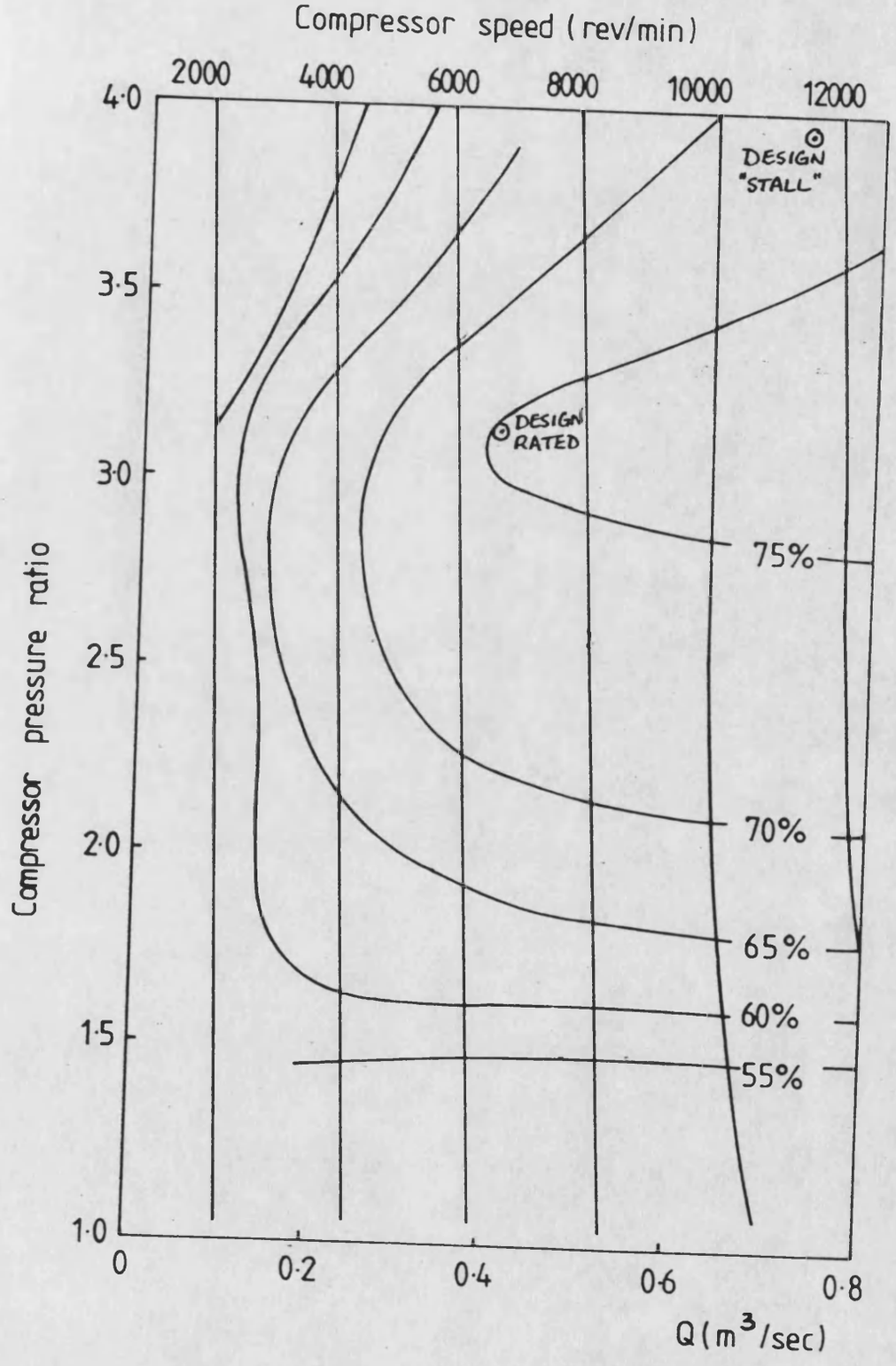

FIG. 2.6 COMPAIR 1200 EFFICIENCY MAP

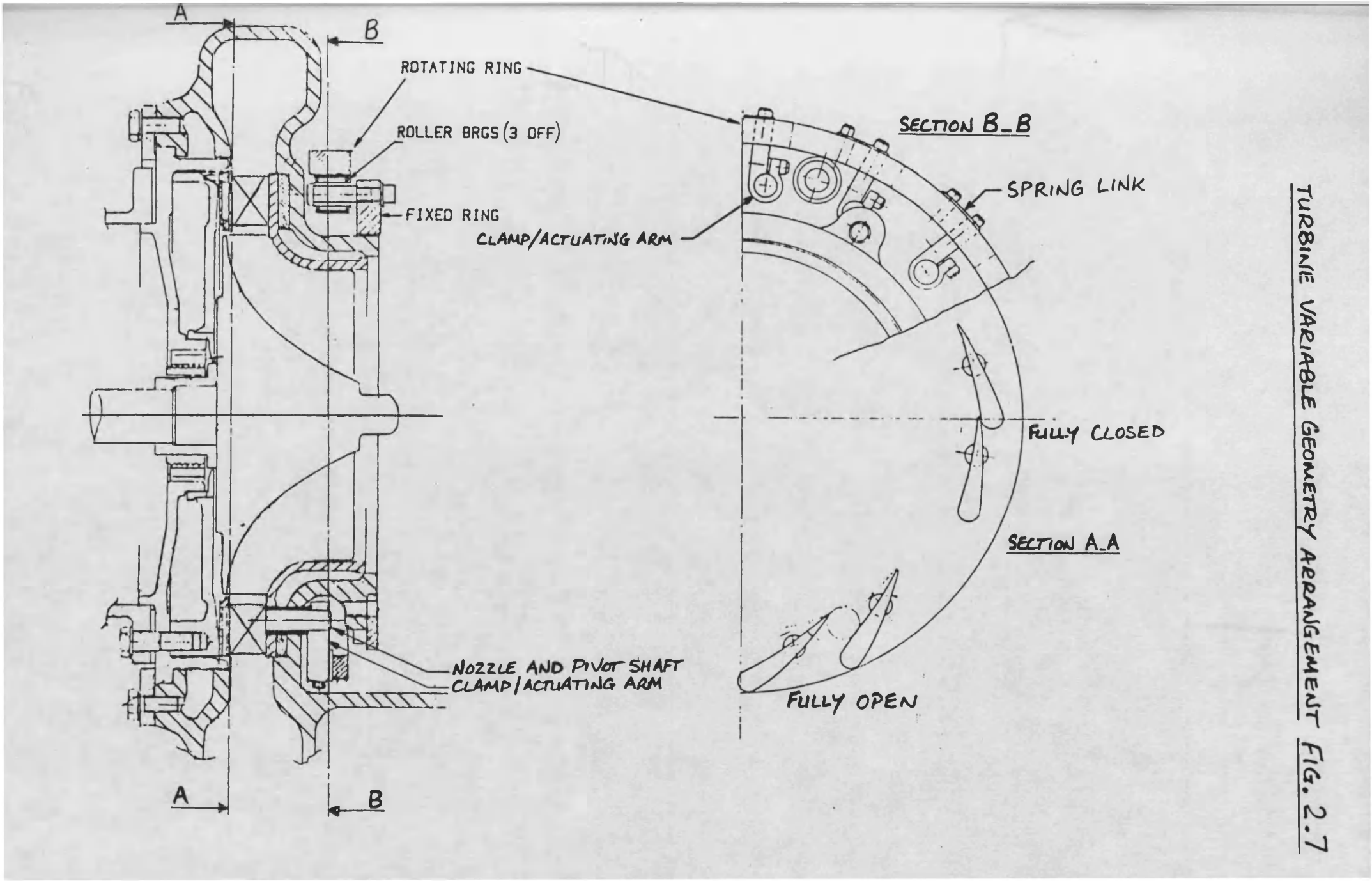

TURBINE VARIABLE GEOMETRY ARRANGEMENT FIG. 2.7

DETAIL OF NOZZLE/ACTUATOR ARRANGEMENT FIG. 2.8

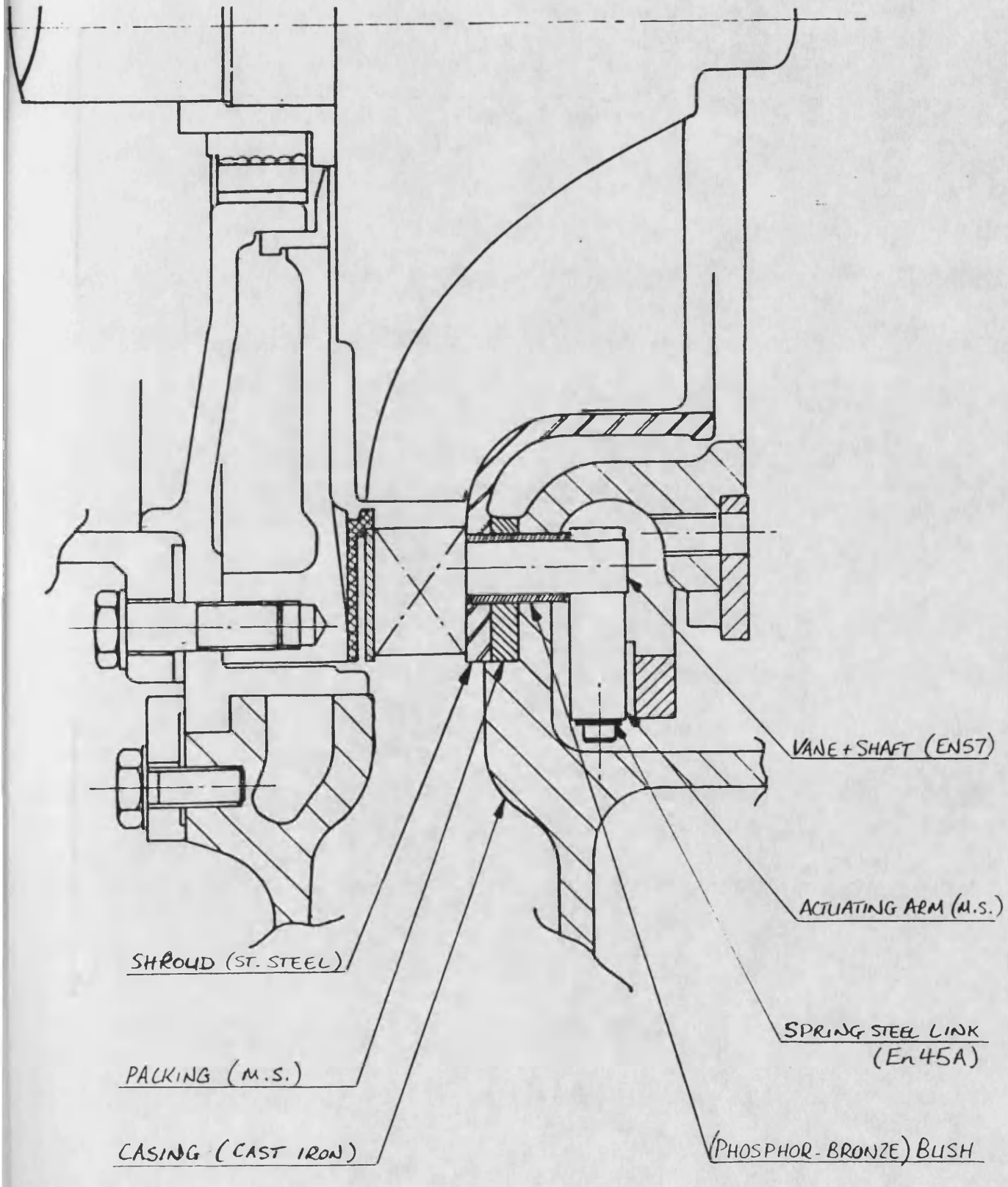

PART-SECTION OF TURBINE

TURBINE NOZZLE BUSHING DESIGNS

FIG. 2.9

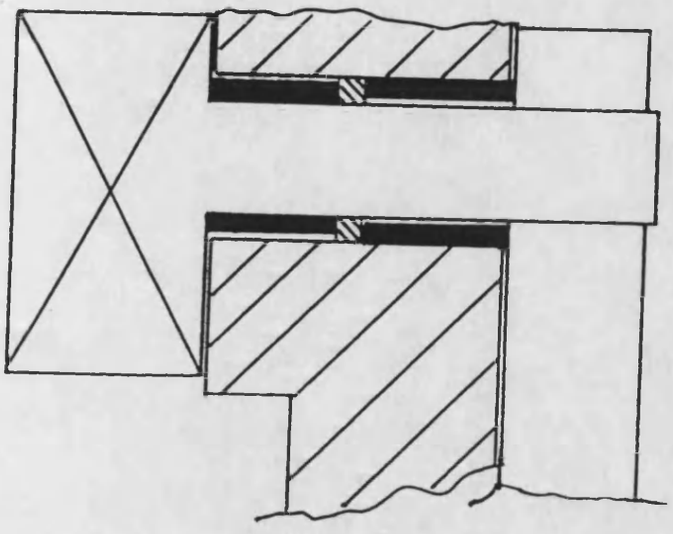

(a) TWO-PIECE PLAIN BUSH

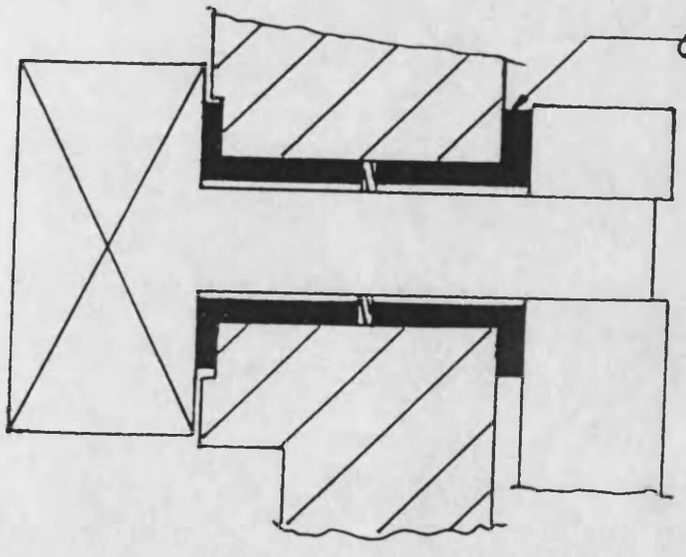

(COUNTERBORE MACHINING ACCESS NOT AVAILABLE ON REAR FACE.)

CLEARANCES SHOWN FOR 'COLD' CONDITION.

(b) TWO-PIECE TOP HAT BUSH

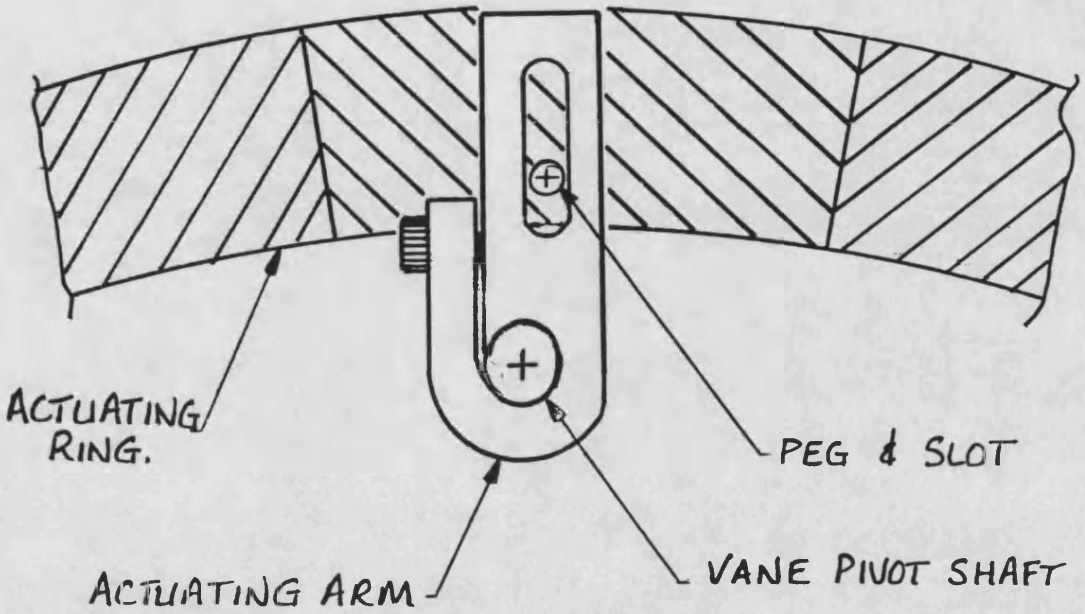

FIG. 2.10 REVISED VG ACTUATING MECHANISM

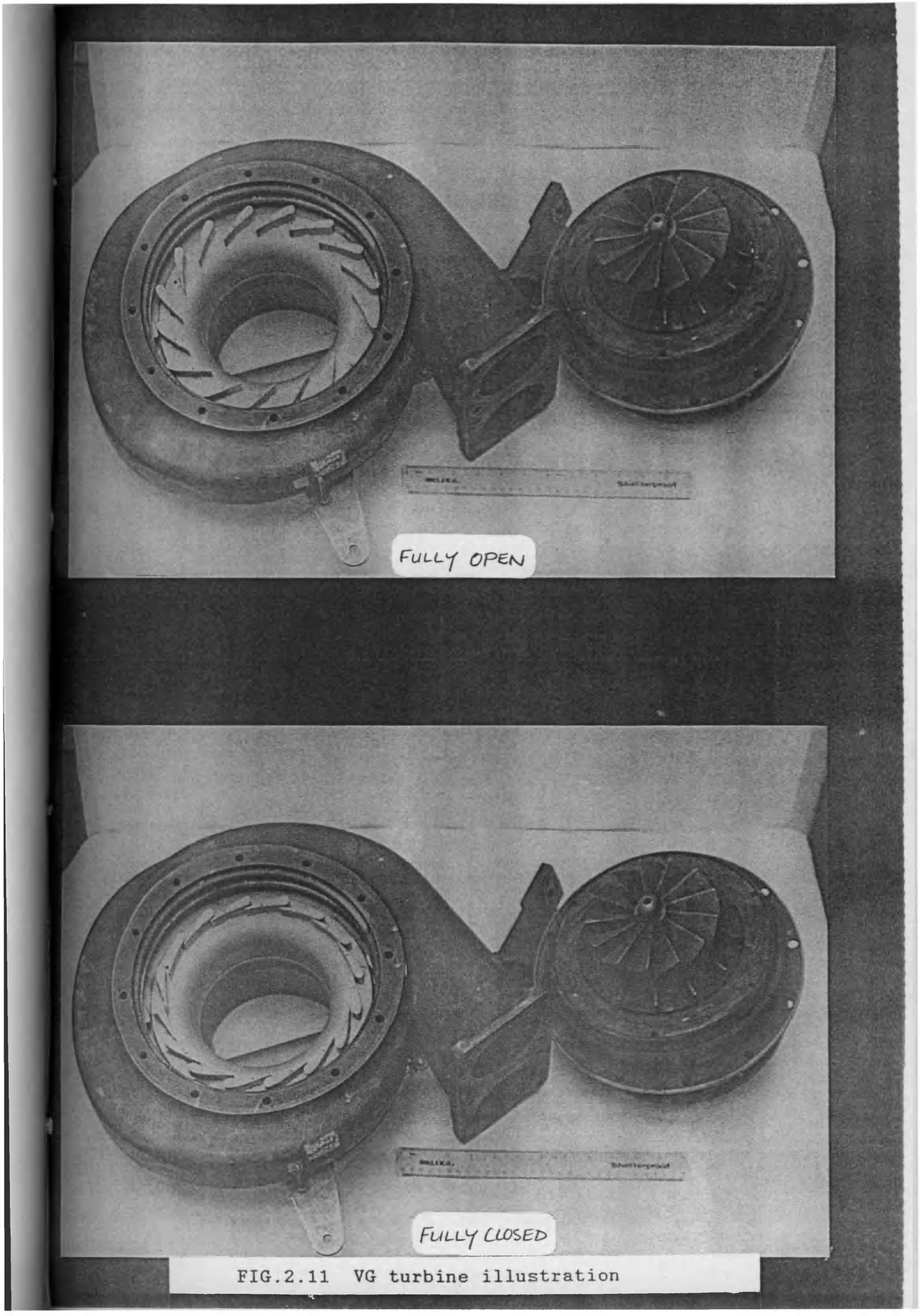

FIG.2.11 VG turbine illustration

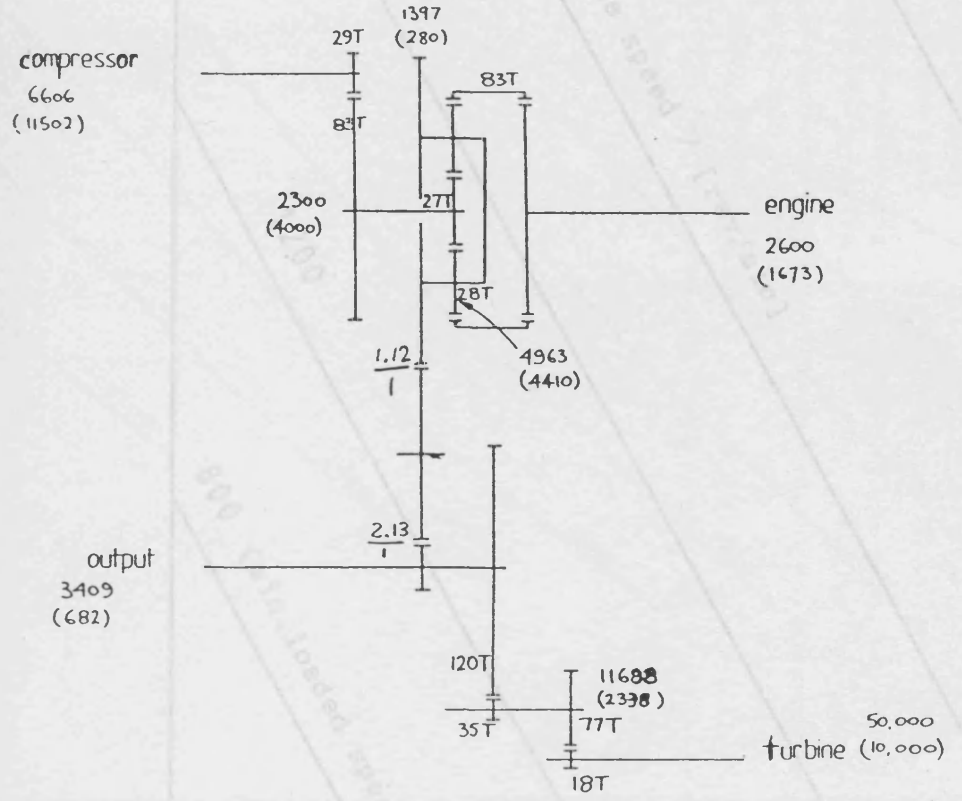

Speeds (RPM) at Rated and (Stall) conditions. T = no. of teeth

FIG 2.12 EPICYCLIC GEAR AND TURBINE GEARTRAIN ARRANGEMENT

FIG. 2.13 52ØDCE component speed relations

NB this shows speed relations imposed by the geartrain;not all regions of this map are thermodynamically attainable.

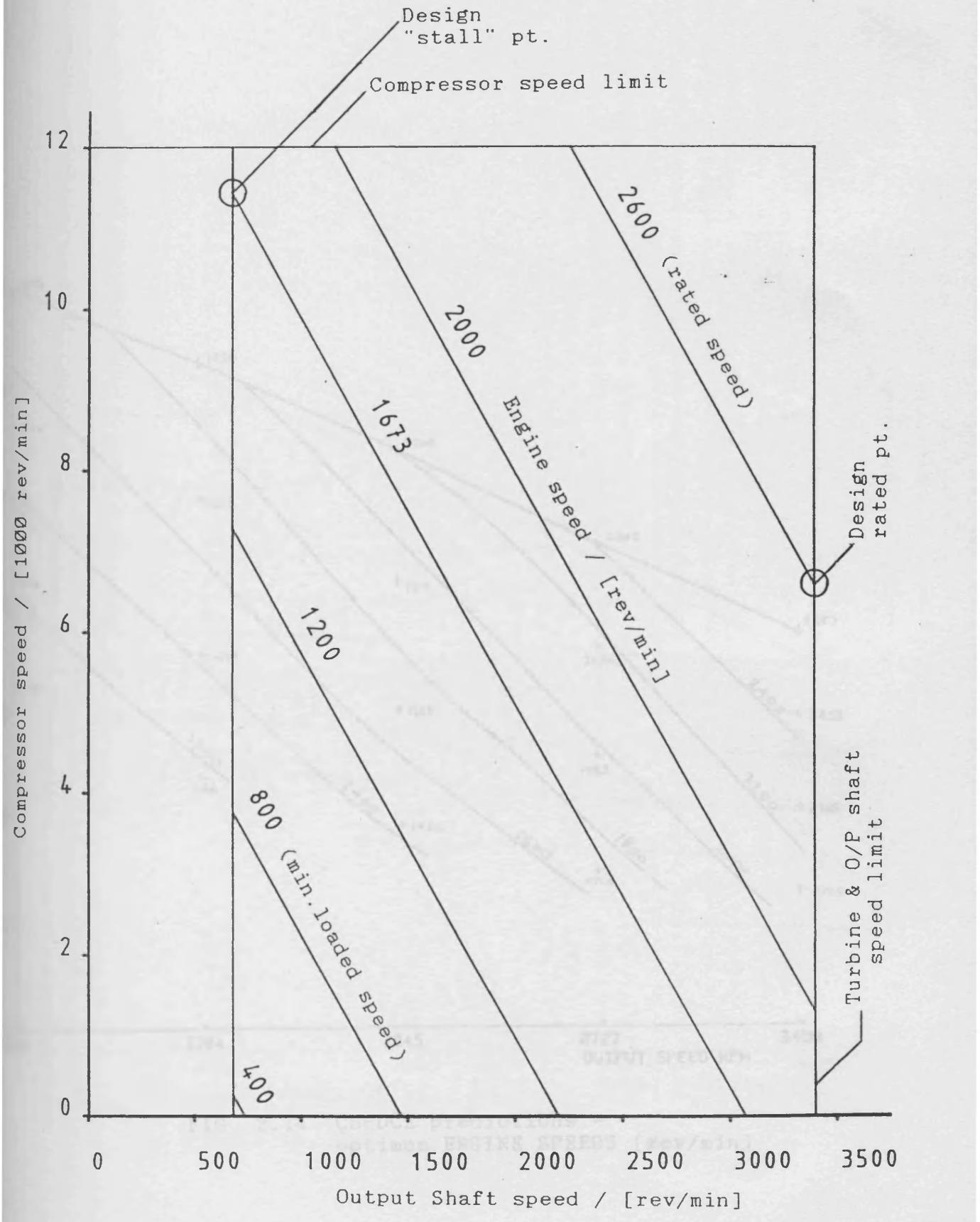

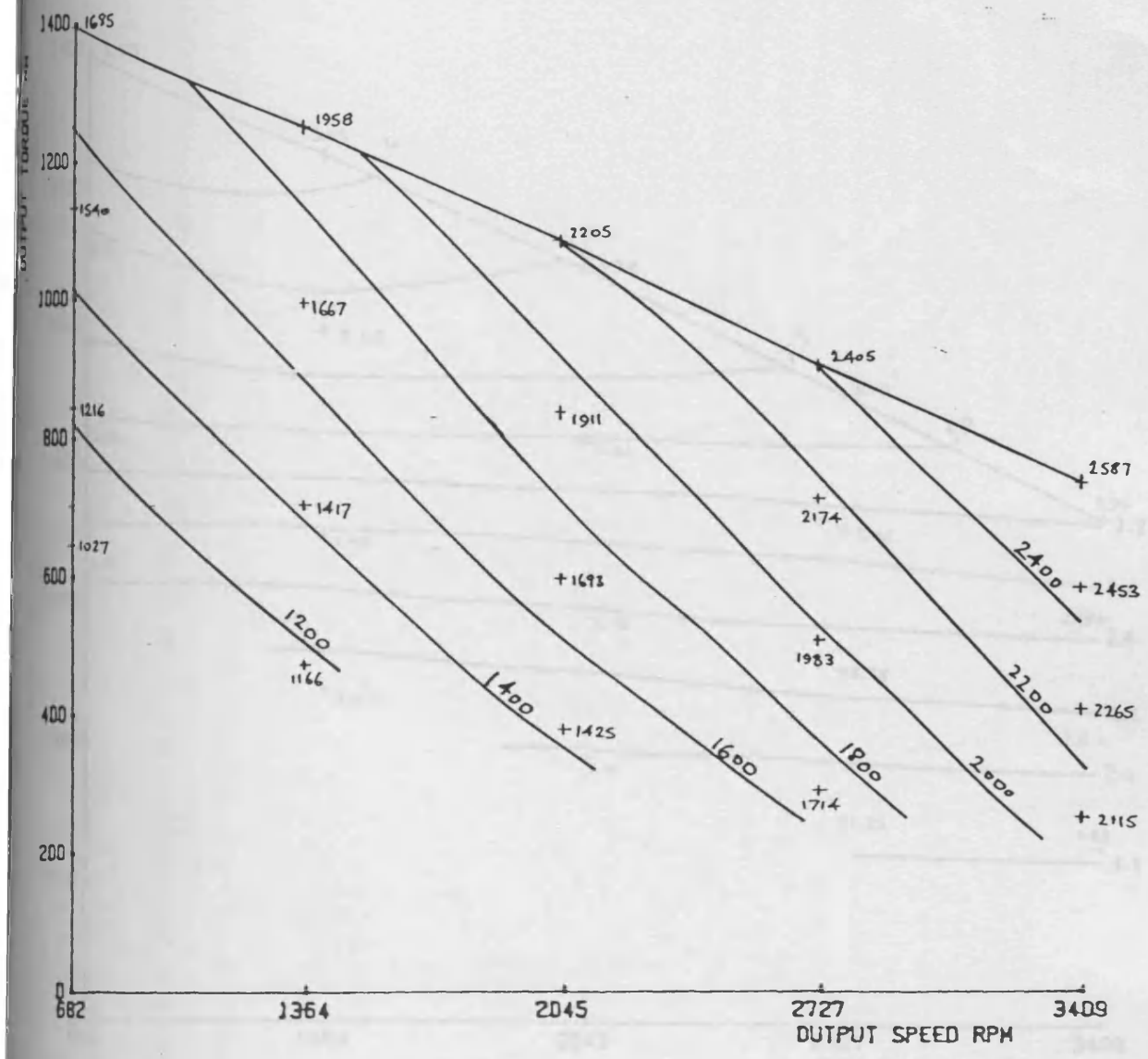

FIG. 2.14 CSPDCE predictions -
optimum ENGINE SPEEDS [rev/min]

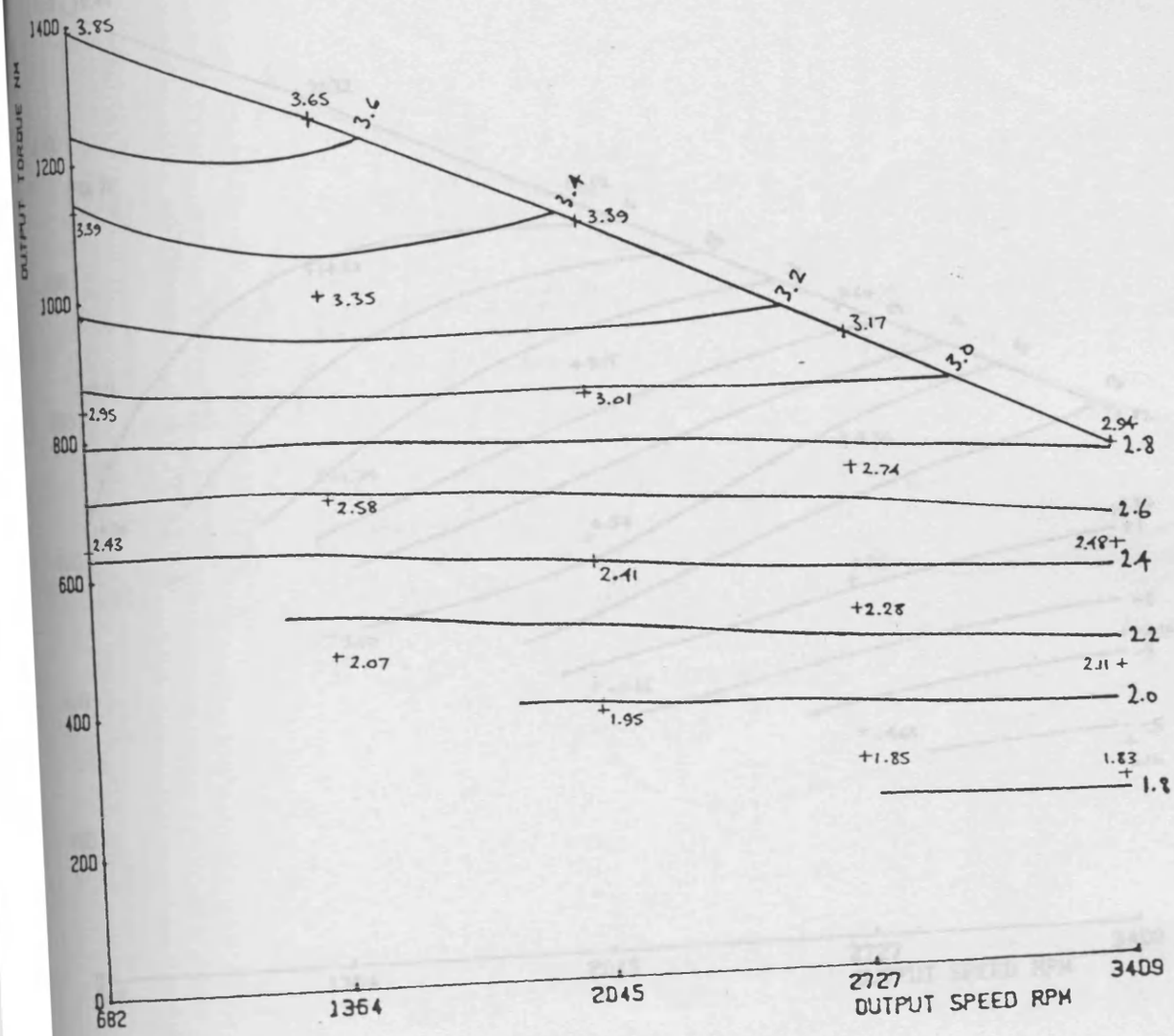

FIG. 2.15 CSPDCE predictions - optimum ENGINE BOOST RATIOS

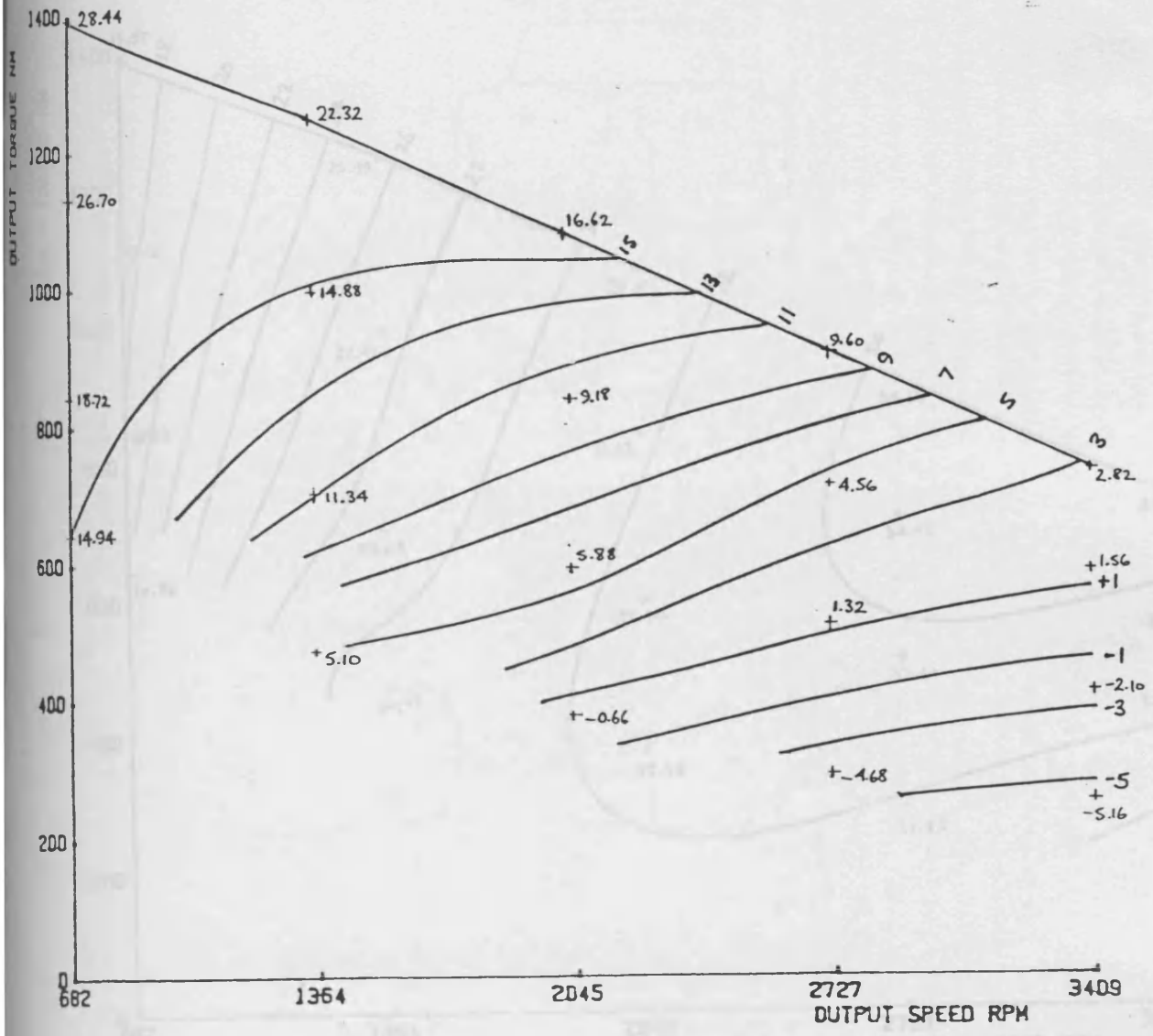

FIG. 2.16 CSPDCE predictions -
optimum BYPASS FLOWS [kg/min]

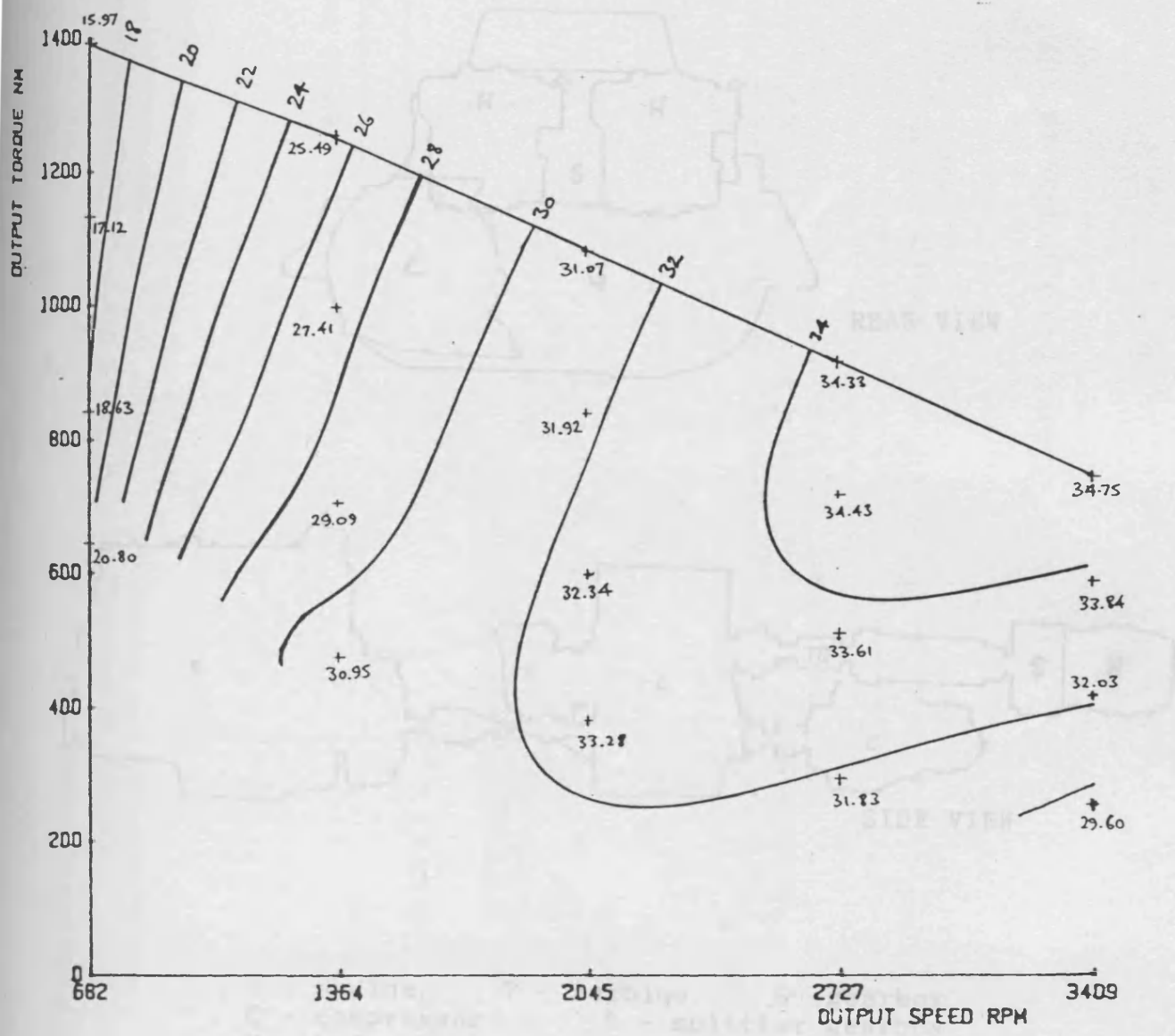

FIG. 2.17 CSPDCE predictions - optimum
O/P SHAFT BRAKE THERMAL EFFICIENCIES [%]

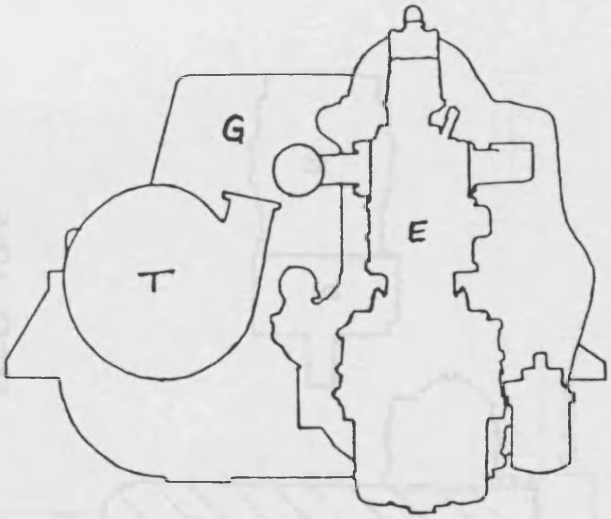

FRONT VIEW

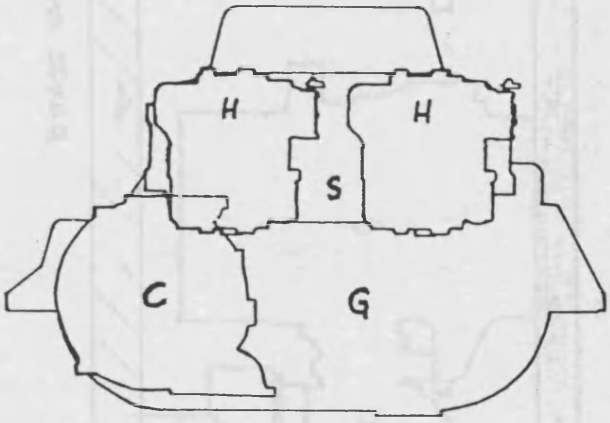

REAR VIEW

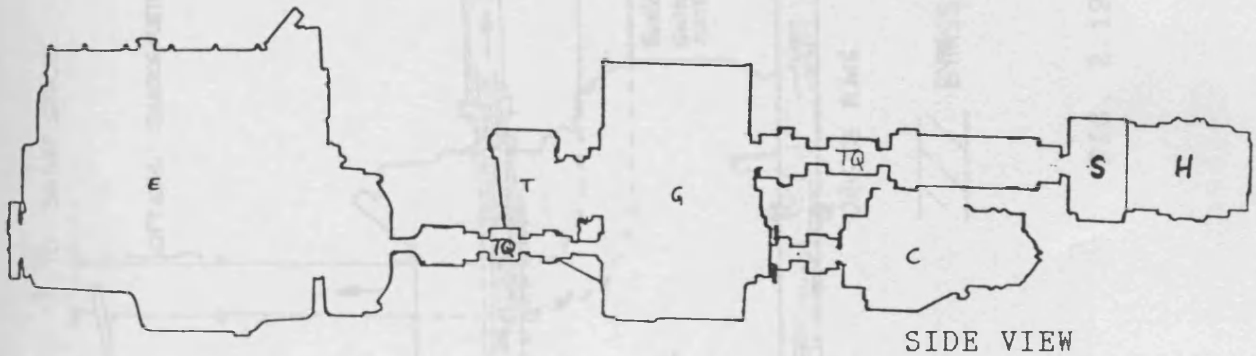

SIDE VIEW

E - engine T - turbine G -gearbox
C - compressor S - splitter gearbox
H - hydrostatic pumps TQ - torquemeters

FIG. 2.18 52ØDCE LAYOUT

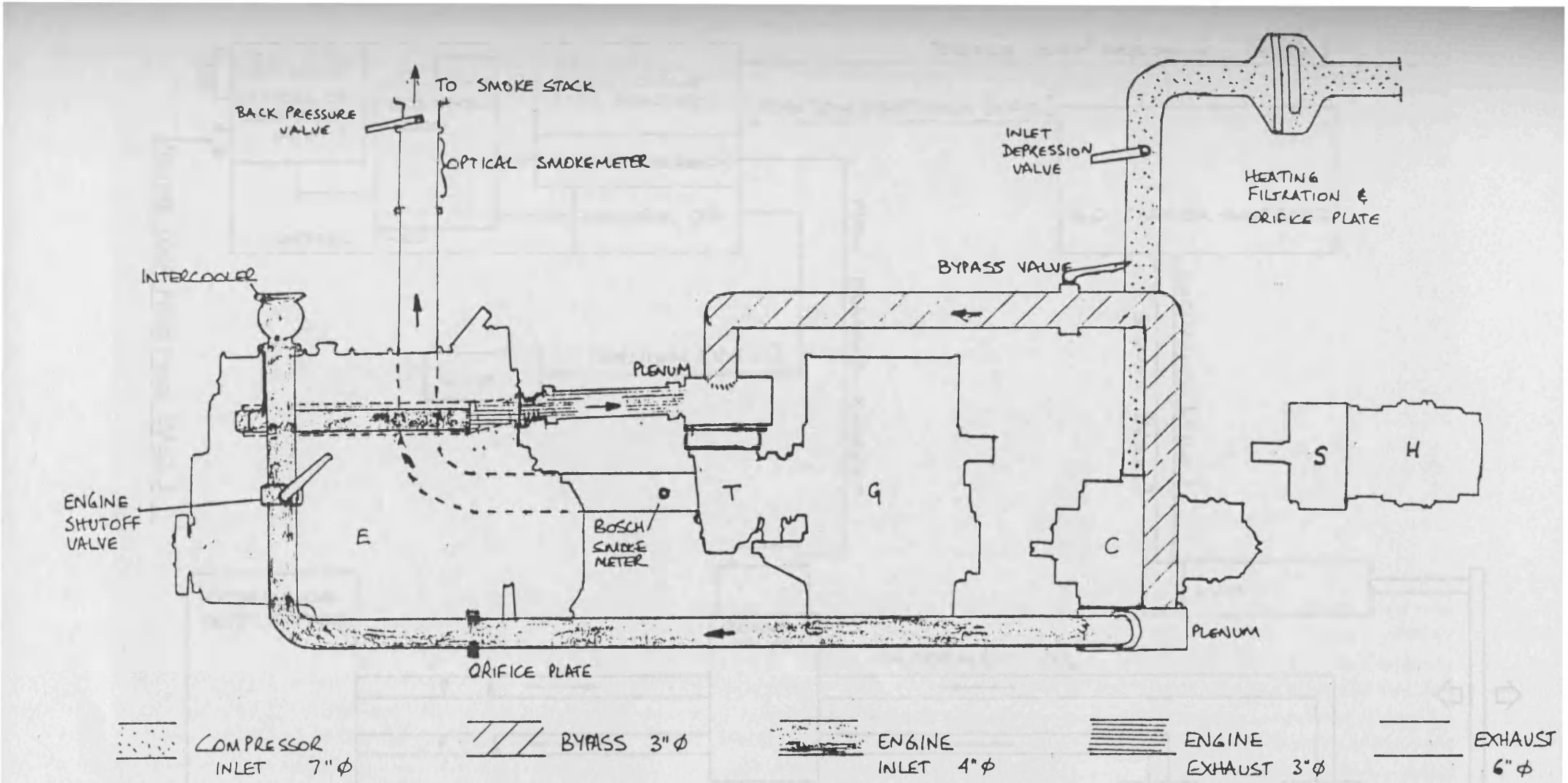

FIG. 2.19 520DCE GAS PIPEWORK LAYOUT

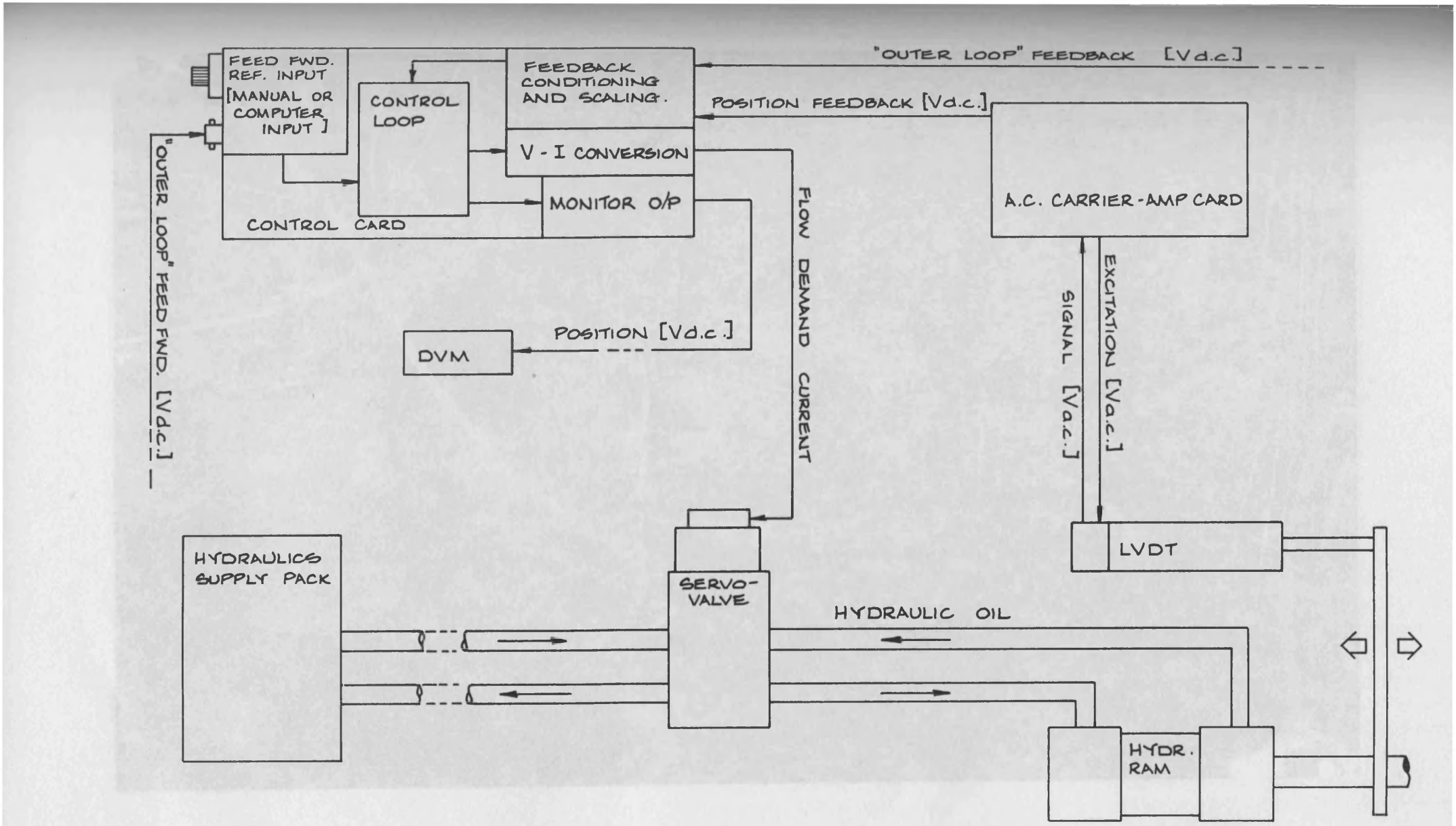

FIG. 2.20 ELECTRO-HYDRAULIC ACTUATOR CIRCUIT - SCHEMATIC.

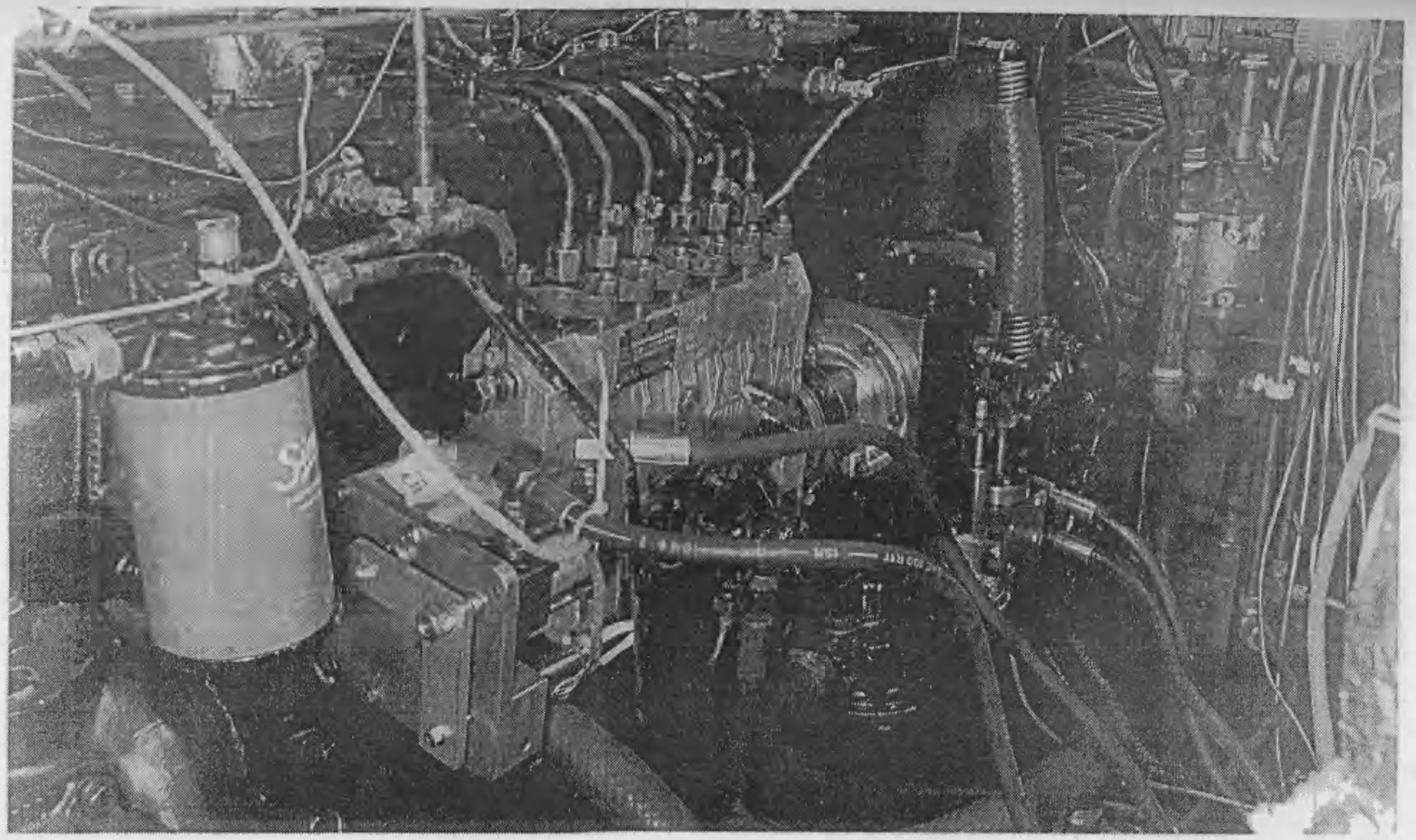

FIG. 2.21 VIEW OF FUEL RACK & INJECTION TIMING ACTUATION ARRANGEMENT

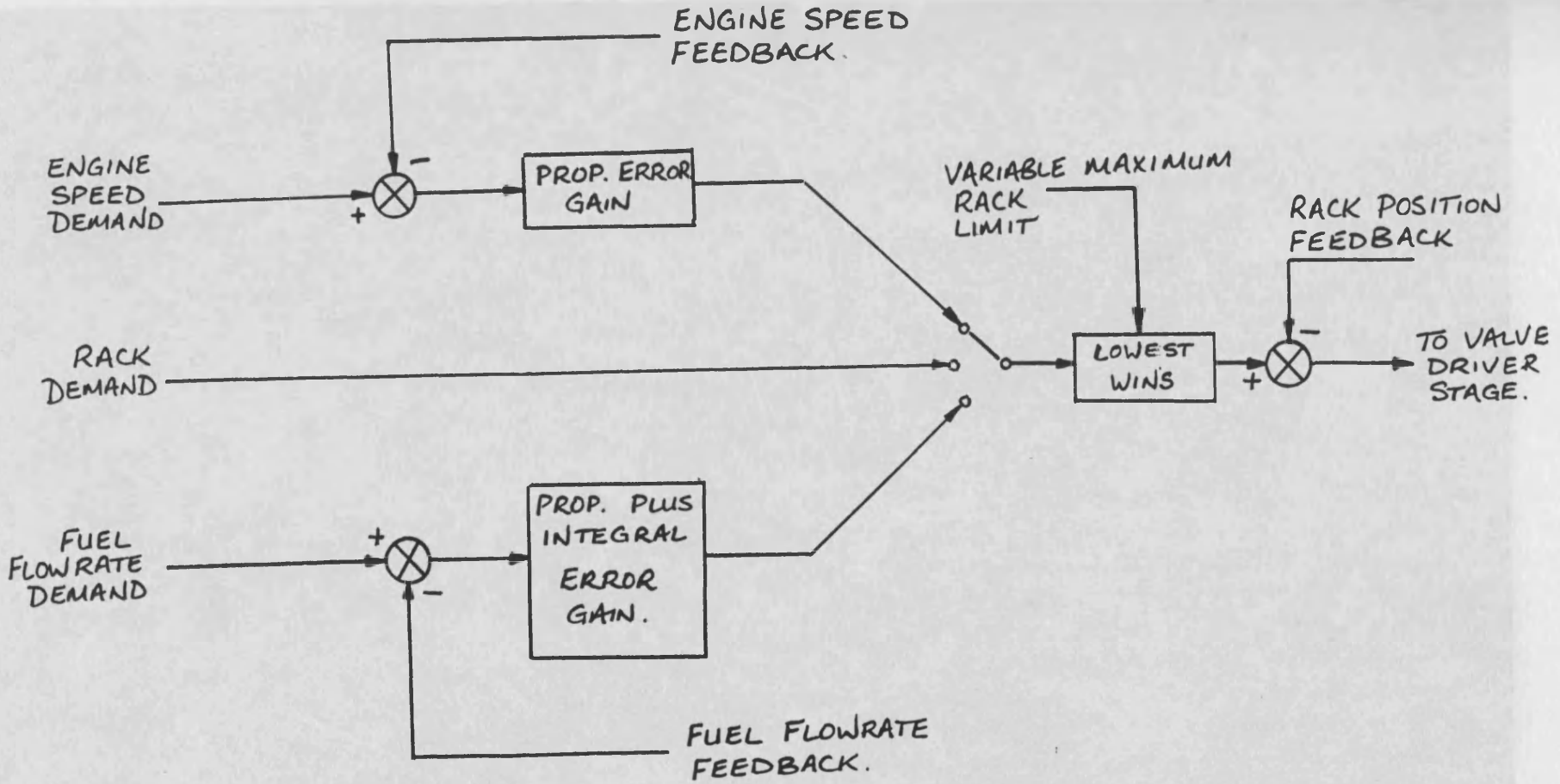

FIG. 2.22 ELECTRONIC GOVERNOR CONTROL

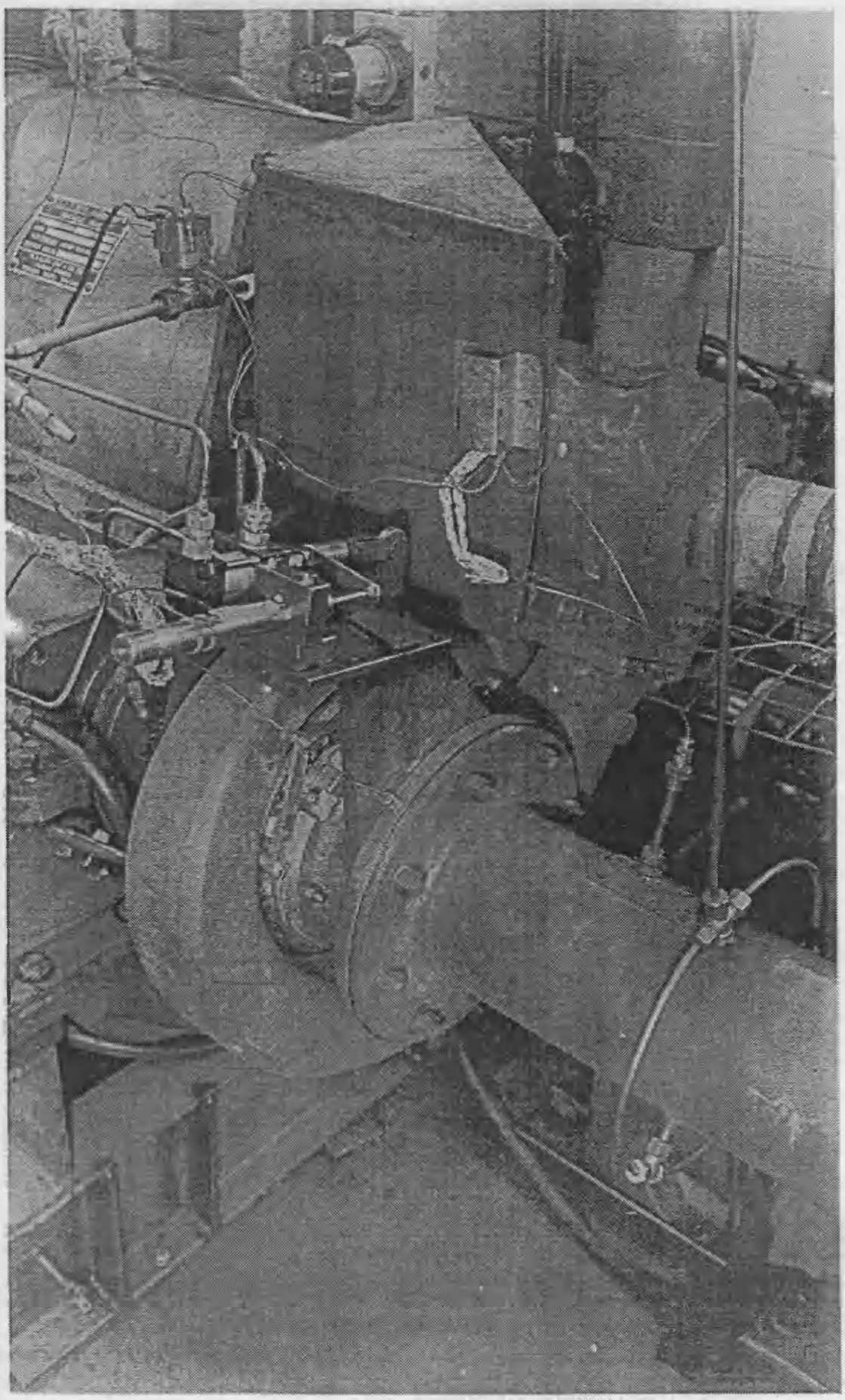

FIG. 2.23 VIEW OF TURBINE V.G. ACTUATION ARRANGEMENT.

FIG. 2.24

ITEM No.	DRAWING No.	DESCRIPTION	No. OFF	MATERIAL	REMARKS

UNIVERSITY OF BATH

SCHOOL OF ENGINEERING — DESIGN GROUP

TOLERANCES	DRAWN	CHECKED
–	J. HALL	
SCALE	DATE	APPROVED
–	16.11.87	

TITLE

TURBINE VARIABLE NOZZLES

POSITIONAL CONTROL CIRCUIT

DRAWING No.

DCE ELECTR.

LATEST ISSUE LETTER

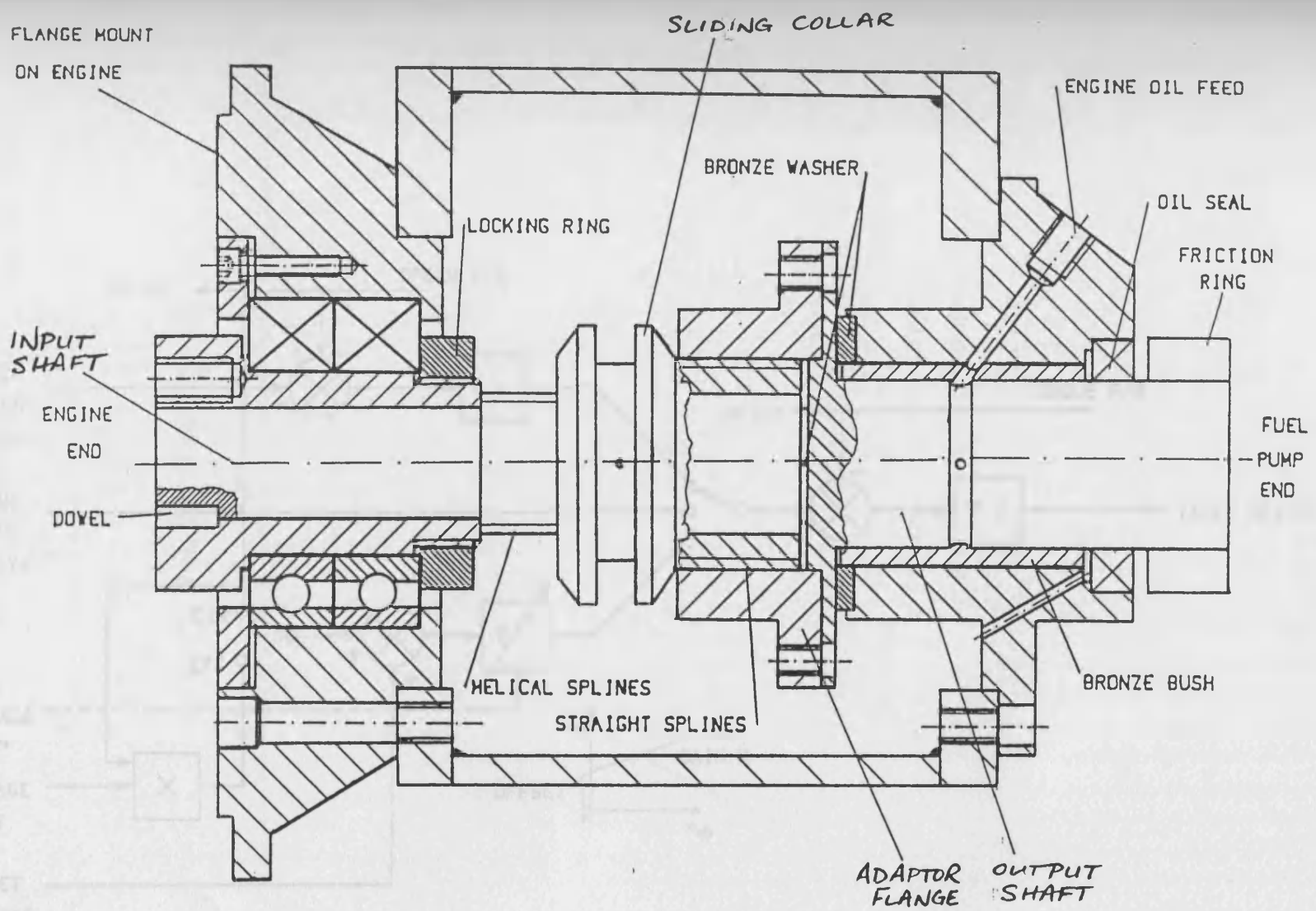

FIG. 2.25 VARIABLE TIMING UNIT

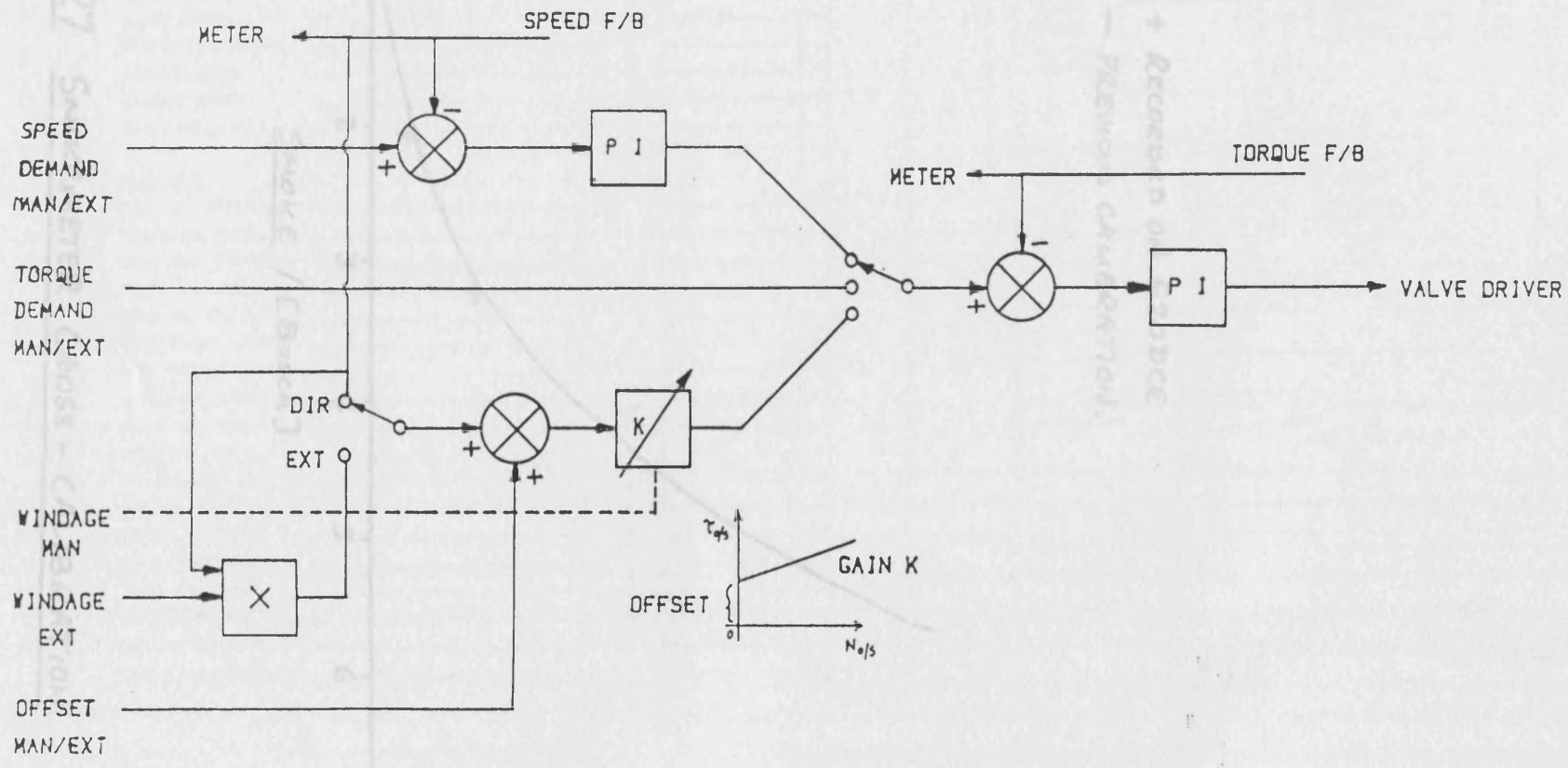

FIG. 2.26 DYNAMOMETER CONTROL.

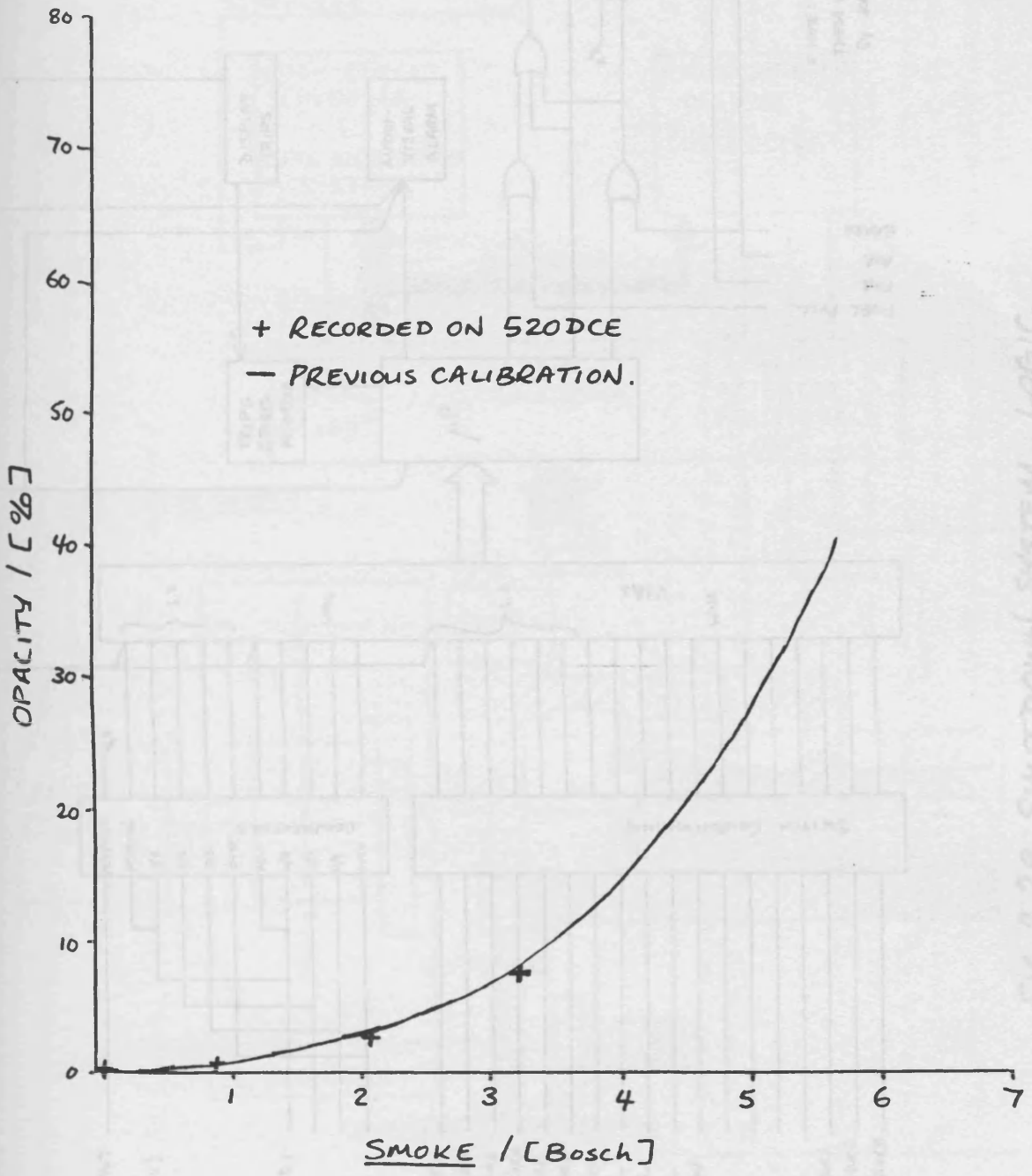

FIG. 2.27 SMOKEMETER CROSS - CALIBRATION

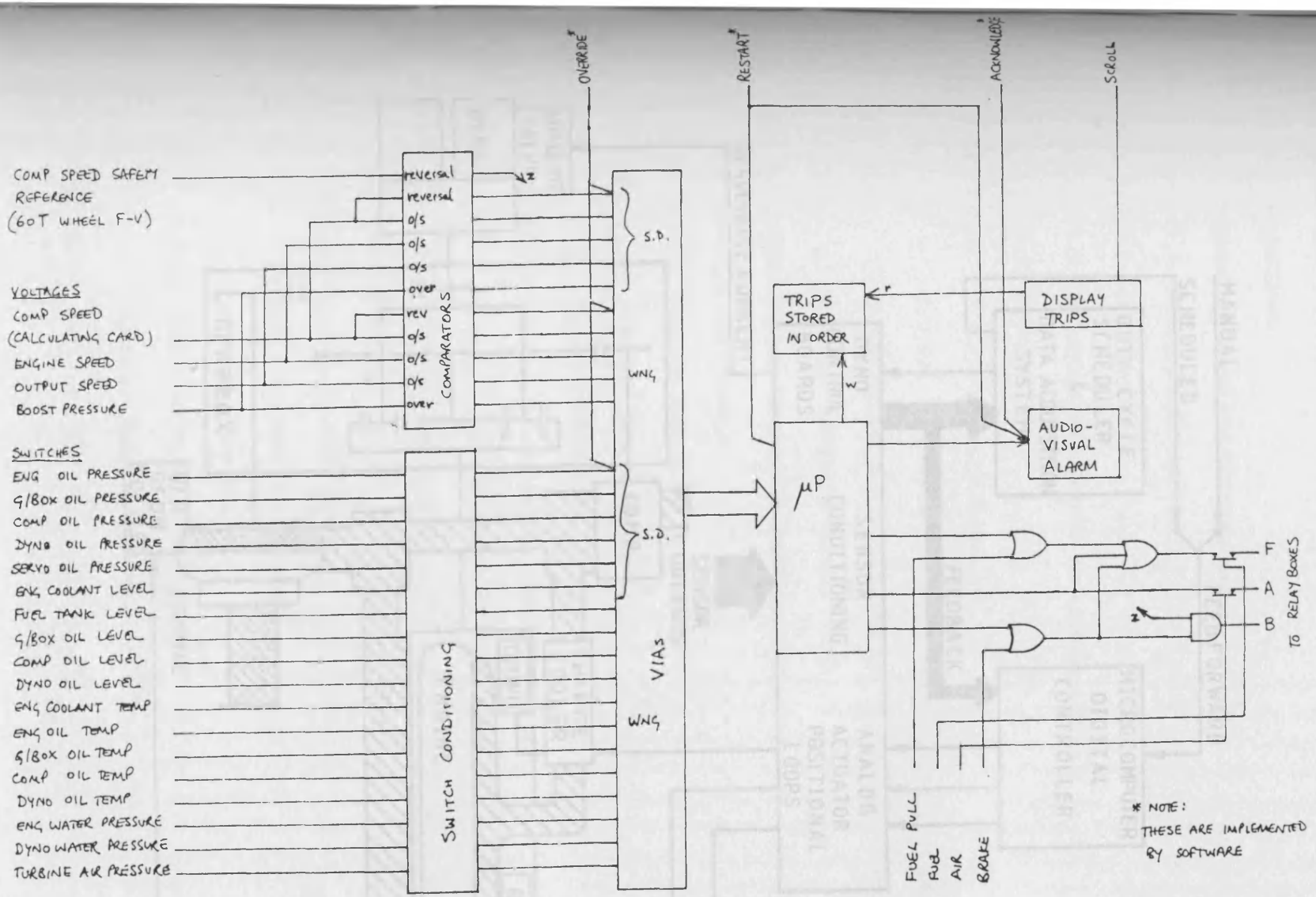

FIG 2.28 SHUTDOWN SYSTEM LOGIC

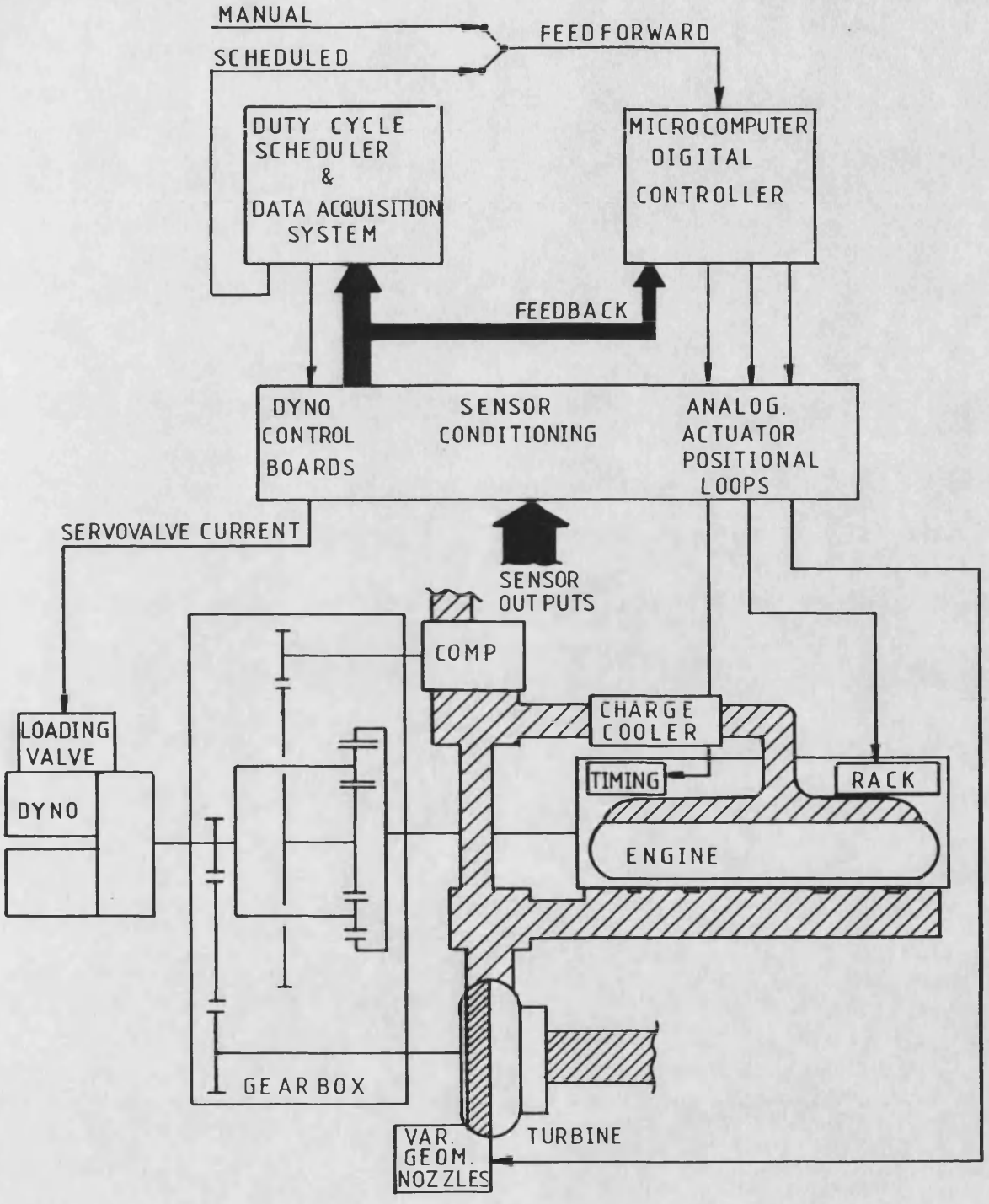

FIG 2.29 LEYLAND 520 DCE TEST INSTALLATION

CHAPTER 3 - CONTENTS

3. STEADY-STATE TESTS

3.1 OBJECTIVES

The primary objective of the steady-state testwork was to provide data on component performance and optimum system performance of the 520DCE, for improved understanding of the DCE and validation of simulation programs.

It was also hoped to demonstrate the operation of a DCE at the relatively high boost ratios and engine settings (by contemporary turbocharged engine standards) required to justify the use of the turbo-compounded DCE system. Previous prototypes had been constrained in this respect by the use of engines having rather low thermal and mechanical limits.

3.2 SYSTEM OPTIMISATION AND MAPPING

3.2.1 Selection/Interaction of Controls

To understand the choice of modes of control adopted for the steady-state test work, it is necessary to appreciate the interaction of the controls and their effect upon the DCE operating condition or "state".

The major decision was the choice of dynamometer and engine control modes. As detailed in the previous chapter, the available modes are :

(i) Dynamometer

Constant load torque, or constant output shaft speed, or windage (load torque increasing with speed).

(ii) Engine

Direct rack control (essentially constant engine torque), or engine speed control, or constant fuel flowrate.

The constant fuel flowrate mode, as previously described uses a PI loop, and in practice has inadequate response and stability for general use. It may be switched in for careful optimisation about a given operating point. This leaves two possible engine control modes and three dynamometer modes. One or both of these modes must give speed stability to the system; the effects of the combinations are summarised below:

	engine mode	dynamometer mode	stability
(i)	speed	torque	stable
(ii)	rack	torque	unstable
(iii)	speed	speed	stable
(iv)	rack	speed	stable
(v)	speed	windage	stable
(vi)	rack	windage	neutrally stable

The reasoning is straightforward : for combination (ii) any difference between the load torque and the output shaft torque implied by the rack setting will cause uncontrolled acceleration/deceleration of the output shaft. For combination (vi) the speeds are loosely controlled by the windage characteristic. It should also be noted that (iii) might lead to hunting if the time constraints of engine and output speed control are similar.

Since it is usual to speed-govern heavy-duty Diesel engines, and the dynamometer response will be fastest with the minimum control action (load torque control is the "innermost" loop in the dynamometer control system Fig 2.26), combination (i) was selected for normal operation.

As described in the previous chapter, the prototype 520DCE has two further control inputs, of turbine VG nozzle position and injection timing. Injection timing has only a second-order effect; it can slightly alter the engine/turbine power split and hence the engine and system efficiencies.

Thus there remain three first-order controls; engine speed and output shaft torque as chosen above, plus VG position. This gives the prototype system three "degrees of freedom", that is to say, three independent states. To define the overall DCE state, the three variables are commonly chosen as controlled parameters (for example component speeds and torque level), but assuming actuator repeatability the control inputs (rack and/or VG position) could equally well be used. The number of possible combinations is large; [43] discusses some examples.

The immediate implication of the above is that at a given output shaft speed and torque, there is only one remaining "degree of freedom" which can be adjusted to optimise the DCE (that is, achieve maximum output shaft thermal efficiency). In other words, a given output shaft condition may be achieved with a range of possible groups of interdependent control settings, engine/compressor speeds, boost pressures and so on, only one of which groups will give maximum system efficiency. The output shaft speed and torque, plus any one independent parameter from the optimum group, would then be an "optimum set", which fully defines the DCE state at a point on the locus of best efficiency.

The second implication is that in designing an automatic control system to schedule the DCE for maximum efficiency, any parameters may be used

to define the "base" for the schedule, provided they and the scheduled parameter form an "optimum set" of three independent variables.

The application of the ability of a flexible "optimum set" of three independent variables fully to define an optimum DCE state is crucial to understanding the steady-state optimisation and control of the DCE.

3.2.2 Test Procedure

During the course of the test programme, three different procedures were used to arrive at optimum steady-state conditions.

(i) Fixed engine speed optimisation

The procedure was to set an engine speed and a load (output shaft) torque, and vary the VG position (initially at a fixed, reasonable, injection timing). This gave a locus of output shaft speeds and corresponding measured output shaft (system) thermal efficiencies (two examples are shown in Fig 3.1). Each locus has a distinct peak at which system efficiency is a maximum for that engine speed and load torque. It is then necessary to prove that this is the maximum achievable efficiency at this output shaft speed and torque for any engine speed. This cannot be proven, but it was shown in preceding simulation results and initial testwork that optimum engine speeds increase almost linearly with output shaft speed at a given output shaft torque (refer back to fig 2.14). It was therefore argued that these "local" optima found at fixed engine speeds were also "global" optima, that is, the best achievable efficiencies at the resulting output shaft speed and torque. Further slight improvements were finally sought by adjusting injection timing at this point.

The advantages of this approach were that (a) engine speed and load torque were both directly set by the control modes chosen above (section 3.2.1), so that little adjustment was required as VG position was varied, and (b) a set of data could be recorded over a range of VG positions at a fixed engine speed - thus facilitating comparison with simulation runs carried out at that time [49].

(ii) Fixed fuel flowrate optimisation

The operation of the fuel flowrate control was described in the previous chapter. With the gross fuel consumption thus fixed, and again using fixed load torque, the VG and injection timing settings which give maximum output shaft speed must also give maximum thermal efficiency. It is therefore possible to find the optimum settings without taking intermediate fuel consumption measurements.

In practice, the control mode is very loose, leading to drift and unrepeatability during the optimisation procedure, and long settling times. This also means that the fuel rack must be switched into engine speed control mode to move between test points and to hold a stable condition for data recording at optimum conditions. For these reasons, few tests were conducted in this mode.

(iii) Fixed output shaft speed

Previous optimisation procedures had output shaft speed as a dependent variable, leading to rather haphazard location of optimum points in the output shaft speed/ torque plane. Finally therefore, optimisation was carried out by using engine speed and load torque control as before, but adjusting both engine speed and

VG position to maintain a desired output shaft speed. One combination of engine speed and VG position would thus be found which gave maximum efficiency at a fixed output shaft speed and torque. Again injection timing was fixed throughout this process, and then adjusted to pick up further small efficiency gains.

Mapping of the limiting torque curve (LTC) required a slightly different approach. The LTC for the DCE is the maximum output torque achievable at a given output shaft speed, within engineering limits, using any possible combination of control settings.

The engineering limits for the 520DCE are :

(i) Maximum component speeds : engine 2600 rev/min, compressor 11500 rev/min.

(ii) Maximum boost pressure : 3.bar gauge at the compressor plenum. Note that owing to the epicyclic and compressor torque/boost relationships (section 2.2.1), this implies a maximum engine loading of approximately 20 bar BMEP.

(iii) Maximum gas temperatures : exhaust manifold 700 deg.C, turbine plenum 650 deg.C.

(iv) Maximum cylinder pressure : 150 bar.

(v) Maximum smoke : 3 Bosch (within BS 141AU).

Limiting torque (LT) at maximum output shaft speed (3409 rev/min) is the rated condition, at minimum speed (682 rev/min) LT is the so-called stall condition.

Because the DCE has the characteristic of decreasing maximum torque with increasing speed, it is possible to approach the LTC "horizontally",

that is, finding the maximum achievable speed at a given torque rather than vice versa. The test procedure was thus :

(i) At a low output shaft speed, set the desired output shaft (load) torque. (A prior knowledge of the approximate LTC position is helpful.)

(ii) Set a VG position.

(iii) Increase engine speed (and thus output speed) until a limit is met (cylinder pressure or exhaust temperature).

(iv) Adjust injection timing to keep within limits (trade off cylinder pressure and exhaust temperature).

(v) Repeat (iii), (iv) until both limits are simultaneously met. Check that the smoke limit is not exceeded, and record the output shaft speed attained.

(vi) Repeat (ii)-(v) with different VG positions (as VG restriction is increased, the boost limit will be met). The overall maximum output shaft speed is a point on the LTC.

All three control inputs (rack, VG, injection timing) are thus significant in mapping the LTC. To obtain the rated and stall conditions, a final "loop" is implemented by the tester, adjusting the load torque until the maximum output shaft speed coincides with the desired speed. In practice the process converges quickly.

3.2.3 Repeatability Checks On Existing Data

Earlier steady-state results had been obtained by Prince [36] before failure of the turbine gear train. Following the rebuild and recommissioning it was advisable to repeat selected tests to ensure that the system performance was unaltered to within acceptable limits.

Repeatability was found to be good, optimum operating conditions and efficiencies agreeing very closely. A typical result is given in table 3.1 and discussed below. The original result was found by fuel flowrate mode optimisation, the repeat results were obtained by setting the same engine speed and freely optimising with the VG, and then timing, controls. Three repeats points are shown, tightly-grouped around the optimum. The output shaft speeds are dependent variables, and differ only fractionally (less than 1 per cent). At the same boost ratio (repeat 2 compared to baseline), optimum timing was found to be identical, and gave identical peak cylinder pressure and exhaust temperatures. Engine brake thermal efficiency was fractionally worse (by 0.7 percentage points) and this was reflected in system thermal efficiency. The true optimum (repeat 1) was found at slightly lower boost than the baseline, but identical system efficiency (28.4 per cent) was obtained.

Given the complexity and component interdependence of the DCE, this level of repeatability was considered acceptable. Discrepancies at the above point may partly be due to ambient changes - cell temperature was increased by 4 deg.C between the baseline and the optimum repeat condition. Other results from [36] were therefore taken to be valid, and were not repeated.

3.2.4 Results

3.2.4.1 Presentation

Results from the differing test phases described above were combined without distinction. Only optimised data are presented here (not the full sets of optimum and non-optimum data recorded for the simulation comparisons in [49]). The tabulated data are too bulky for inclusion,

but are held on file and floppy disks in the Wolfson Laboratory. The results are presented graphically as discussed below.

3.2.4.2 Optimum settings

Optimised values of the system parameters are presented as contours on the output shaft speed/torque map. The important parameters are engine speed (Fig. 3.2), and VG nozzle position (Fig. 3.3) which primarily sets boost pressure (compressor delivery pressure - Fig. 3.4). It should be remembered (from section 3.2.1) that all these parameters are interdependent - specifying any one parameter at a given output shaft speed/torque point implies dependent values for all other parameters. While a whole group of optimum contour plots is presented for analysis, any one plot theoretically defines the 520DCE optimum surface.

Optimum engine speeds (Fig. 3.2) shows the expected trend (compared with CSPDCE predictions given in Fig. 2.14), increasing smoothly with output shaft speed, and reducing with output shaft load. The contour non-linearities approaching stall are a result of the compressor boost pressure limit (Fig. 3.4); optimisation is constrained by this limit and the engine is forced to operate at a higher speed/lighter load (lower boost) condition than that which would give truly maximum system efficiency.

The pattern of optimum VG nozzle positions is unclear (Fig. 3.3). All results were obtained before the VG mechanism redesign described in Chapter 2. It is probable that some results were affected by gradual deterioration of the original VG arrangement; the unclear pattern is compounded by the fact that the turbine operates near to full VG restriction at all optimum conditions, so that the range of interest is

condensed. Repeated results with the revised VG design are discussed in section 3.2.5.

Optimum compressor pressures (Fig. 3.4) increase roughly in proportion to the output shaft torque. This implies either that turbine power always contributes a similar proportion of output power, or that engine/compressor net power dominates. Again there is reasonable agreement with CSPDCE predictions (engine boost ratios - Fig. 2.15).

Optimum bypass flowrates are shown in Fig. 3.5. Generally, the flows are negligible except at low output shaft speed and high load, where they reach of the order of 30 per cent of the compressor flow. The predicted trend (Fig. 2.16) of gradually increasing optimum bypass flow from reverse flow at high speed/light load to significant positive flow near stall was not seen in practice. Evidently maximum efficiency is obtained by increasing VG restriction to minimise the compressor-bypass-turbine air "torque conversion" effect wherever possible. This is to be expected unless very high efficiency compressor and turbine are available; in this case the fixed turbine gear ratio further degrades the "conversion" efficiency. At the low output shaft speed, high load conditions, compressor speed and massflow are high, and increasing VG restriction eventually leads to the compressor boost pressure reaching its limit. It is then necessary to allow increasing bypass flow. The system has reached the limit of epicyclic torque rise (that achieved by allowing engine torque and boost to rise with falling speed) and must now employ the bypass "torque conversion" to achieve further output shaft torque rise. That this effect is seen only in a small region of the 520DCE operating map is due to the fixed turbine gear ratio. With a turbine CVT the bypass "torque conversion" dramatically increases the low speed torque rise.

The engine loads at the optimum settings are shown in Fig. 3.6. The engine torques (and thus BMEPs, as shown) follow the same trend as compressor delivery pressures, since as discussed earlier the two must be nearly in proportion at steady-state. The peak BMEP of 20.7 bar is the limit imposed indirectly by the compressor delivery pressure limit, although the engine was approaching its exhaust temperature and cylinder pressure limits. For given engine torque levels the corresponding engine boost ratios (Fig. 3.7) were below the design levels, owing to high charge cooler pressure losses. The effect of these pressure losses upon system operation is discussed further in the next subsection.

The optimised output shaft brake thermal efficiencies are shown in Fig 3.8. A rather disappointing peak efficiency of 31.8 per cent was achieved, compared to predicted efficiencies of up to 34.8 per cent (Fig. 2.17). The trends are similar from prediction to experiment, except that peak efficiency actually occurs below the rated condition (design point). The component contributions to these efficiencies are discussed below.

3.2.4.3 Component efficiencies

The overall DCE output shaft thermal efficiency is as sensitive as a conventional turbocharged engine/layshaft gearbox powertrain to engine thermal efficiency. It is also very sensitive to compressor and turbine efficiencies since both are geared. In a turbocharged engine, lower component efficiencies will lead to lower achievable boost ratios and a less favourable pumping loop (reduced pressure gradient across the engine). However, with a geared compressor lower efficiencies imply the need to match for higher compressor power consumption at a given boost ratio. Similarly with a geared turbine, lower efficiency obviously

implies a proportional loss in turbine power at a given boost ratio. For the DCE, turbomachinery efficiencies become increasingly important towards the stall point, where compressor and turbine power flows become large, and less of the engine power is transmitted directly to the output shaft.

As with a conventional powertrain, gearbox and ancillary losses (charge cooler and manifold pressure losses for example) also penalise efficiency.

The efficiencies/losses of the components are discussed in turn below:

(i) Engine

Engine brake thermal efficiencies are shown in Fig. 3.9 (on a base of engine speed and load). The maximum recorded efficiency was 41.8 per cent, equivalent to 203 g/kWh. It is irrelevant that these efficiencies do not account for the compressor power consumption incurred in providing boost; for assessment of engine efficiency alone, it is sufficient that the engine be compared to others operating at similar conditions. The relevant conditions are speed, load or air/fuel ratio, and the inlet/exhaust pressures. Comparison data were available from a current automotive turbocharged, charge-cooled DI Diesel with variable injection timing, operating at similar BMEPs. This was a larger engine of 12 litre swept volume (bore x stroke 130 x 150mm, 6 cylinder), so the comparison was made on a mean piston speed (mps) basis. Table 3.2 compares the performance of the 520DCE engine at the rated condition with that of the turbocharged engine at

(a) similar mps and BMEP and

(b) similar mps and air/fuel ratio

The DCE engine operates with a large pressure rise across it, since the exhaust is kept at approximately compressor delivery pressure by the bypass connection, whereas the inlet charge has suffered a pressure drop in the charge cooler. The turbocharged engine has only a small pressure rise across it, associated with a well-matched efficient turbocharger. This is reflected in increased volumetric efficiencies at near-identical inlet manifold temperatures.

The DCE engine has the higher BSFC and smoke at similar BMEPs and air/fuel ratios. The higher BSFC is partly attributable to the adverse pumping loop work, but must also be partly due to mismatching between the air system and the uprated fuel injection equipment, and to the inherent disadvantage of the reduced compression ratio.

The higher smoke of the DCE engine at similar air/fuel ratios indicates poorer combustion, but there may have been slight exhaust gas recirculation (reverse bypass flow) at this condition (the value of -1.3 kg/min recorded is within the bounds of experimental uncertainty in measuring the difference between compressor and engine airflows).

In summary, engine efficiency was good, given the high inlet to exhaust pressure rise imposed upon it. Experimental efficiencies were slightly better (typically 1-3 percentage points) than the CSPDCE predictions, but direct comparison is difficult since boost ratios and speed/torque conditions differ.

(ii) Charge Cooler

The pressure losses between compressor plenum and inlet manifold over the operating range are shown in Fig. 3.10. Since the pipework was sized for very low losses, the values shown are almost entirely attributable to the charge cooler: at rated condition the combined engine orifice plate and estimated pipe friction loss was only 33mbar, compared with an overall loss of 440 mbar as shown in the figure. The compressor plenum pressure at the rated condition was 2.75 bar (absolute), so that the loss was an unreasonably large fraction of the delivered pressure. The manufacturer's given loss at this condition was 103 mbar, which would - if achieved - have given a reasonable overall loss of 136 mbar. In view of the relatively low number of running hours, fouling would not be expected; it may be noted that losses reached the quoted "maximum" 103 mbar at low power conditions which were run very early in the test programme.

These high losses penalise limiting torque curve (LTC) performance, since the engine receives lower boost (and thus lower airflow) at a given torque, implying lower air/fuel ratio and thus an earlier approach to the thermal limit. Part load efficiency is also penalised because the engine operates at a reduced air/fuel ratio for a given torque.

(iii) Compressor

Since compressor power consumption is not measured but is extracted from a map on the basis of pressure ratio and speed, it is not possible to comment upon compressor efficiencies. Having accepted the manufacturer's power data, one must also accept the implied efficiencies, presented in Chapter 2. Nor is it possible to cross-check efficiencies based on manufacturer's data with

isentropic efficiencies based on the measured temperature rise across the compressor, since heat rejection cannot be neglected (the compressor housing is water-cooled). For this reason, calculated "isentropic" efficiencies (based on pressure ratio and temperature rise) produced by DCETAB are considerably higher than the "overall" efficiencies (based on pressure ratio and mapped power consumption).

(iv) Turbine

Measured turbine isentropic efficiencies were generally within the expected range, falling particularly at low speeds. Although the boost pressure/massflow combination is set using VG during the optimisation process, this is guided mainly by the engine/compressor match, not by turbine efficiency.

However, the efficiency values were sometimes erratic. This was thought chiefly to be due to poor inlet temperature measurement. The two turbine plenum thermocouples often gave substantially different readings due to poor mixing of engine exhausts and bypass flows. Inlet enthalpy was calculated as the product of the total mass flow, the mass-averaged (temperature-corrected) specific heat capacity, and the mean of the two temperatures, and was thus an unrealistic estimate.

Further tests to measure turbine power more reliably are discussed in section 3.3.

(v) Gearbox

Gearbox losses were calculated as the net difference between the measured engine and output shaft powers, the mapped compressor powers, and the turbine enthalpy drops. The losses therefore

included turbine bearing and heat rejection losses, and the combined errors in measuring/calculating the other component powers. At light loads the apparent losses became increasingly improbable, exceeding 40 per cent of the output power at some conditions.

Further tests to measure gearbox losses are discussed in section 3.4.

3.2.4.4 Limiting torque curve (LTC)

The LTC was coarsely mapped with a low speed point and the rated point. The low speed point is typical of the conditions expected on the LTC : the engine is operating at maximum BMEP (approximately 20 bar), this limit being imposed directly by the compressor pressure limit (3 bar gauge). The engine speed is as high as possible within the limits of cylinder pressure and exhaust temperature. The design ratio of boost pressure to BMEP was

$$3.0 / 15 = 0.2$$

This was achieved at the compressor plenum, but due to the aforementioned charge cooler losses the ratio at the engine inlet manifold was typically 0.17. As a result the thermal limit was met at an engine power of 245kW (fuel flow 15.7 g/s), slightly below the design power of 266kW. This shortfall in engine power implied a shortfall in exhaust energy available to the turbine. Furthermore, there was a large unaccounted ("gearbox") loss of 37kW, so that the LTC was ultimately well below its predicted level.

Table 3.4 shows two sets of data; one attempting to set to the design point (that is using an engine speed of 2600 rev/min), one at true rated

output power (that is, peak output torque at 3409 rev/min output shaft speed, using whatever engine speed is required). The "design point" case was artificially constrained by the analogue speed governor gains not allowing sufficient rack opening at 2600 rev/min; however, it is clear that rated output power would be obtained at a lower engine speed, particularly since bypass flow was significant at this higher speed. The engine speed contours (Fig. 3.2) and the expected LTC position also implied that this would be the case. Rated output power was achieved with an engine speed of 2438 rev/min. The high charge cooler pressure loss, and insufficient available injection timing advance at this speed, caused the thermal limit to be met at a further reduced engine power of 229kW (fuel flow 14.6 g/s). Again there was also a high "gearbox" loss, so that rated output power was only 190kW, compared to the initial design prediction of 275kW.

3.2.5 Repeat Test With Rebuilt Turbine

As mentioned earlier in this chapter, the results presented so far are with the original turbine VG mechanism, which suffered seizure or partial seizure of some vanes during the test programme. Following the VG mechanism redesign and turbine rebuild, certain test points were repeated to check for any improvements in turbine, and system, performance.

Fig 3.11 shows output shaft thermal efficiencies with the rebuilt turbine; in each case the DCE was re-optimised at the original output shaft speed and torque. Appreciable improvements were seen (the original efficiencies are shown in brackets). Each new optimum was found to occur at a slightly lower engine power and higher turbine power.

It was not considered worthwhile to carry out further re-mapping, chiefly because the original results provided a full and self-consistent set; little insight would be gained by repeating the work with a slightly improved turbine.

3.3 TURBINE PERFORMANCES

As mentioned above, the estimates of turbine power obtained during steady-state mapping of the 520DCE were suspect, firstly because of the uncertainty in calculating turbine inlet enthalpy, and secondly because of the large unaccounted power losses, which were clearly too great to be solely attributable to the gearbox.

3.3.1 Turbine Powers By Difference

To estimate the turbine (and gearbox) powers more reliably, the turbine contribution was removed. The difference between output powers at the same engine/compressor conditions with and without the turbine would give the turbine power by difference.

3.3.1.1 Test arrangement

In order to obtain the same engine/compressor conditions with the VG turbine removed it was necessary to retain control of both engine speed and system swallowing capacity. Simply removing the turbine would constrain the DCE to run along the engine swallowing characteristic, with the bypass necessarily closed.

A spare turbine was fitted with a locked-up bladeless dummy "rotor", and the VG mechanism adapted to meet the existing actuator. This existing electrohydraulic control was set up with a restricted voltage range to suit the altered leverage ratio of the mechanism. Lubricant and air

supplies were blanked off as necessary. Thus remote control of a variable orifice (nominally 0 to 5 sq.in.) was obtained.

With the turbine removed and system exhaust flow control retained it is possible to set exactly the same epicyclic conditions as the original tests points, hence the only difference in the DCE condition is the output shaft torque, which differs by the turbine contribution. The condition may be matched to each original test point as follows :

(i) Set engine speed (electronic governing)

(ii) Set engine torque using the load torque control - with no turbine contribution, output shaft torque is directly proportional to the epicyclic torques. Hence engine and compressor torques (and thus boost) may all be set to the original values.

(iii) Set output shaft speed using the VG "orifice" - this now controls only system massflow, and can have no effect upon boost. Altered massflow implies altered compressor speed - and thus output shaft speed, since the two are interdependent at the fixed engine speed set in (i) above. Thus all shaft speeds are set to their original values.

3.3.1.2 Results

The turbine powers by difference are shown in Fig. 3.12 over the DCE operating range. It should be noted that the turbine was disconnected at the spline coupling (turbine end of the geartrain). If it is assumed that the step-down losses were similar loaded and unloaded, then the figures obtained correctly include the turbine bearing loss and exclude the step-down train loss.

Evidently the turbine performance is poor, the powers being much less than the measured enthalpy drops, which are also shown. The design predicted powers at stall and rated conditions were 52kW and 102kW respectively, but the trends of Fig. 3.12 indicate that these would not be attained, even if the engine and compressor were to achieve their own design conditions.

Turbine losses were estimated to be small. Heat rejection at the maximum inlet temperature was calculated to be about 4 - 6kW; these are chiefly radiative and drop with the fourth power of the casing temperature. The ball bearings remained in excellent condition, so mechanical friction must be low.

The low turbine powers were therefore thought to be due to operation with small VG nozzles angles (near to full restriction). This will lead to edge leakage losses around the nozzles, and incidence losses from nozzle exit to rotor entry. The situation will have been worsened by progressive seizure of the nozzles, such that the flow angles would vary around the nozzle ring. Given that the measured temperatures were all close to stagnation (owing to the use of shrouded thermocouples and low gas velocities in the large diameter pipework) the reasons for the discrepancies between measured powers and enthalpy drops are unclear. The uncertainty in some inlet enthalpy measurements could only be a partial explanation.

It was planned to map the rebuilt turbine fully as a stand-alone unit, to identify the reasons for its poor performance and to note any improvements obtained with the VG nozzles operating correctly.

3.3.2 Turbine Powers By Torque Measurement

Suitable turbine test facilities unfortunately could not be found within the required timescale, despite enquiries to several companies in the gas turbine/turbocharger field. It was therefore decided to proceed with transient testwork, and meanwhile procure a high speed torquemeter, for subsequent incorporation in the prototype. While the turbine data would not be obtained under directly-controlled inlet conditions, nevertheless accurate power and swallowing capacity measurements could be made over the turbine's operating range.

3.3.2.1 Test arrangement

The turbine torquemeter installation was described in Chapter 2. The turbine was tested by operating the DCE over a map of eleven output shaft speed/torque conditions for two turbine VG positions.

An interactive data reduction program, "DTR", was written for the now-available IBM PC-AT compatible microcomputers. A code listing is given in Appendix 1.

3.3.2.2. Results

Measured turbine powers over the DCE operating range, at VG positions of 8.5V and 9.5V are shown in Fig. 3.13(a) and (b) respectively. Where data are missing, this is because the test condition was not achievable at that VG position. (Please note that the positions of the earlier test points are marked only to ease reference back to earlier figures.) Power was slightly increased at the lower restriction (8.5V), but note that since the inlet conditions are not comparable this does not necessarily imply higher turbine efficiency. Turbine efficiencies have not been presented, again because the variation between the two inlet temperature readings made the results unreliable in many cases.

Generally speaking, system efficiencies were higher with the 8.5V position (Fig. 3.13a). It is therefore reasonable to compare these turbine powers with those obtained by difference from the original results (Fig. 3.12), which were at VG settings for best system efficiency.

Although precise comparisons cannot be made since the test points differ, the later results are slightly better overall. It is reasonable to conclude that the powers calculated by difference were reliable, and that turbine efficiency had been slightly impaired by the VG mechanism deterioration. However, turbine performance is still poor, and is the primary cause of the low prototype 520DCE system efficiencies and limiting torque curve performance.

3.4 GEARBOX LOSSES

The oversized Allen Gears epicyclic/layshaft gearbox had been suspected of excessive transmission losses due to friction and/or windage [36]. These losses were estimated in two series of tests.

3.4.1 Losses By Difference

3.4.1.1 Test arrangement

This set of results was obtained simultaneously with the calculation of turbine powers by difference, discussed in section 3.3.1 above. The test arrangement was as described in that section, that is, the turbine contribution was removed, and the DCE set to the earlier optimised epicyclic speed/torque conditions.

With the turbine removed, the gearbox losses at these repeat conditions were known to within the uncertainty of the compressor power data and of

the engine and output torque measurements. Apart from unknown experimental errors in the supplied compressor data, errors arise due to differing inlet conditions and smoothing of the scatter in the supplied data. Furthermore, data were only supplied up to 3.63 pressure ratio; from here to approximately 4.4 pressure ratio experienced in the prototype, the power must be extrapolated.

Thus compressor power may be in error by up to ±5 per cent, perhaps more beyond 3.63 pressure ratio. Engine and output powers were measured to within ±0.5 per cent and ±0.7 per cent respectively (table 2.1).

3.4.1.2. Results

The DCE operating envelope was covered sparsely by ten test points. Gearbox losses by difference are shown in Fig. 3.14. Transmission efficiencies are also given, where

$$\text{Transmission efficiency} = \frac{\text{output power}}{(\text{output power} + \text{gearbox loss})}$$

Towards stall, the loss figures obtained become improbably small, then negative, implying gross errors in the measurement. The shaded region in Fig. 3.14 shows the region where compressor pressure ratio exceeds 3.63 and compressor power is extrapolated from available data. This is also the region of greatest compressor power. It was concluded that compressor power was overestimated in this region by the simple linear extrapolation used in the data reduction program (DCETAB).

Data at lower pressure ratios were considered more reliable. For example, at the point nearest rated power the component powers were measured/calculated to be :

Engine : 176.9 kW

Compressor : 37.9 kW

Output : 128.5 kW

implying a gearbox loss of 10.5 kW (transmission efficiency 92.per cent). Applying the uncertainty limits noted earlier, the errors in these figures were :

Engine : ±0.9 kW

Compressor : ±2.0 kW (estimated)

Output : ±0.9kW

implying a gearbox loss of 10.5 ±3.8 kW (transmission efficiency 90.-95. per cent).

In summary, the gearbox loss results obtained by this method were of poor accuracy at best, and grossly inaccurate at worst.

Removal of the compressor contribution as well as the turbine would reduce the uncertainty in the loss calculation, but since the DCE would then be unable to operate at realistic conditions the results would be of little value. Measurement of compressor torque (by installation of a torquemeter or by mounting the compressor on a trunnion restrained by a load cell) was ruled out by practical difficulties (discussed in [43]). Furthermore, the error accumulation in differing three powers could still give imprecise results. The most promising approach was to infer gearbox losses from heat rejection

3.4.2 Losses By Heat Rejection

The gearbox rejects heat to lubricant, and via the casing to the surroundings. At steady-state, the gearbox heat rejection is equal to the mechanical losses in it. Preliminary calculations showed that the

oil temperature rise across the gearbox would be sufficient for accurate measurement with conventional thermocouples, and that heat rejection to oil would dominate over surface convective/radiative losses, allowing simplifications to be made in calculating the latter without serious loss of accuracy.

3.4.2.1 Test arrangement

The gearbox lubrication circuit is shown in Fig. 3.15. The oil is pumped through a cooler and filter to a manifold block, which directs it to the gearbox and the turbine, or to the dynamometer (Rigby) splitter box, or directly to the pump pick-up line. By selection of orifice sizes and bypass valve setting, the oil pressure is set to the required 30psi and each component receives its required flowrate. A common sump is used.

The following data were required :

(i) Oil Temperatures

The oil temperature could reliably be measured at three places in the circuit, (shown in Fig. 3.15):

T_1 - supply to all components (near manifold block)

T_2 - sump

T_3 - return from dynamometer splitter box

K-type Cr-Al thermocouples were used. T_1 and T_3 were measured to 0.1 deg.C resolution, the difference T_1-T_2 was measured to 0.025 deg. C resolution by a differential amplifier. The thermocouples were "matched" by mounting them isothermally and adjusting absolute temperature readings to identical values before testing.

(ii) Oil Flowrates

Volume flowrates were measured for each line in the circuit-at normal operating pressures and temperatures - before the tests began. The temperature was achieved by pre-conditioning runs, the pressure by a gate valve on the measuring outlet. Mass flows (shown in Fig. 3.15) were based on an oil density of 0.870 kg/m^3 at normal operating temperature.

(iii) Oil Specific Heat Capacity

Data over the required temperature range were obtained from the manufacturer (BP Energol THHT32).

(iv) Surface/Air Temperatures

Measured by hand-held thermometer.

(v) Other Data

For convection/radiation calculations, the gearbox was characterised as a series of vertical and inclined planes. Emissivity was assumed perfect (ε=1). Preliminary calculations (based on the guidelines of [50]) indicated laminar flow convection.

The test procedure was to set the DCE to the required condition, and record differential temperatures over time. When these had stabilised (typically 40-60 minutes), a full set of temperature readings (oil circuit, gearbox surfaces and surroundings) was taken.

3.4.2.2 Results

The results were calculated by hand, using equations from [50]. A set of sample data and calculations may be found in [43]. Owing to the hazards involved in taking temperature measurements within the cell, and the long testing times required, only a limited number of results were

obtained, shown in Fig. 3.16 (corresponding transmission efficiencies are also shown).

Comparing these figures and those obtained by difference (Fig. 3.14), there is good agreement in the high speed region (90-93 per cent transmission efficiencies by difference, 91-94 per cent by heat rejection). At these conditions the losses by difference had been considered fully reliable (compressor power was interpolated and relatively small), so the agreement between the results is reassuring. At the low speed/high load point the heat rejection result seems plausible, with a transmission efficiency of 88 per cent, whereas the results by difference in this region were clearly incorrect.

A full and more systematic mapping of all shaft speed/torque combinations (rather than operating at optimum conditions) would be required for a complete understanding of the sources of the losses. However, these limited data indicate that transmission efficiencies are of the order of 88-94 per cent over the operating range, possibly falling with increasing compressor geartrain speed and load (moving towards stall). There must always be an efficiency penalty associated with the compressor and turbine geartrains which are an integral part of the DCE. Therefore it would be unrealistic to expect a correctly-sized gearbox to achieve efficiencies more than a few percentage points higher than those achieved in the prototype.

CHAPTER 3 LIST OF FIGURES

CHAPTER 3 LIST OF TABLES

REPEATABILITY CHECK - TYPICAL RESULTS TABLE 3.1

	repeat 1	repeat 2	repeat 3	baseline
Engine				
Nom Speed RPM	1250.00	1250.00	1250.00	1250.00
Ave Speed RPM	1248.96	1251.21	1252.17	1249.00
Torque Nm	1025.85	1073.16	1059.31	1066.82
Power kW	134.17	140.61	138.90	139.53
Boost ratio	2.99	3.12	3.09	3.13
bmep bar	15.71	16.44	16.22	16.34
Cyl Pr bar	117.56	136.96	120.86	137.35
DynInj degBTDC	8.84	12.16	7.51	12.21
Inj Duratn deg	22.93	24.02	22.08	21.20
Fuel Flow g/s	7.92	8.13	8.20	7.93
Fuel/Shot mg	126.88	129.95	131.02	126.98
Th Effy %	39.77	40.63	39.77	41.33
Air Flow kg/m	14.65	15.22	14.54	15.17
Vol Effy %	89.52	89.88	86.39	90.20
Air/Fuel	30.83	31.21	29.55	31.89
InlMan Pr barg	1.97	2.10	2.06	2.12
ExhMan Pr barg	2.13	2.29	2.25	2.37
Inl Man Temp C	50.10	53.00	51.90	58.10
Exh Man Temp1C	520.00	508.00	525.00	509.00
Exh Man Temp2C	516.00	513.00	531.00	510.00
Compressor				
Nom Speed RPM	3954.00	3888.00	3914.00	3910.00
Ave Speed RPM	3964.54	3887.84	3937.81	3909.30
Torque map Nm	113.60	121.98	119.92	124.14
Power map kw	47.16	49.66	49.45	50.82
Isen Effy TS %	74.87	74.85	74.40	74.77
Overall Effy %	62.84	60.13	60.94	54.73
Mass orif kg/m	13.74	12.98	13.18	13.49
Mass map kg/m	14.95	14.38	14.60	14.76
Press Ratio	3.20	3.34	3.31	3.37
InletDep mbarg	15.47	14.14	14.53	15.02
Outlet Pr barg	2.13	2.27	2.23	2.31
Inlet Temp C	27.00	28.60	29.60	23.50
Outlet Temp C	184.00	193.00	194.00	187.00
Turbine				
Nom Speed RPM	21589.82	21824.49	21736.49	21736.49
Ave Speed RPM	21561.18	21857.40	21729.78	21731.81
Wheel Torq Nm	13.28	12.29	12.78	12.44
Enthalpy kW	29.98	28.14	29.09	28.31
Isen Effy %	63.48	59.29	60.90	55.03
Noz Angle V	9.30	9.48	9.31	9.32
Massflow kg/m	14.22	13.47	13.67	13.97
Press Ratio	3.07	3.23	3.19	3.26
Inlet Pr barg	2.08	2.24	2.20	2.28
Back Pr mbarg	10.31	10.16	9.82	11.00
Inl Temp1 C	490.00	489.00	505.00	484.00
Inl Temp2 C	496.00	494.00	510.00	487.00
Outlet Temp C	380.00	383.00	394.00	378.00
Output				
Intercooler kW	33.03	35.88	34.79	32.92
Intclr dp mbar	159.29	169.29	169.29	186.62
Inj setting V	2.95	4.78	2.86	3.00
Byp Flow kg/m	.29	.83	.05	1.67
Smoke	.00	.00	.00	.00
Nom Speed RPM	1472.00	1488.00	1482.00	1482.00
Ave Speed RPM	1470.04	1490.24	1481.54	1481.65
Torque Nm	621.54	622.43	623.48	617.89
Power kW	95.68	97.13	96.73	95.87
Th Effy %	28.36	28.06	27.70	28.40
sfc g/kWh	298.13	301.31	305.30	297.77
Gbox Losses kW	28.59	28.81	29.32	21.15
X	.00	.00	.00	.00

TABLE 3.2

ENGINE PERFORMANCE COMPARISON

	Leyland 520DCE engine performance at DCE rated power	Comparison engine : 12l.6cyl.TCA DI Diesel		
		(a) at same BMEP	(b) at same AFR	
mps [m/s]	9.8	9.9	9.0	9.9(1)
BMEP [bar]	13.7	13.7	17.3	18.0
Boost [bar gauge](2)	1.31	1.49	1.56	1.8
Air/fuel Ratio	25.0	28.5	25.0	25.0
Inlet man. temp. [^{o}C]	52	52	53	53
δp [bar] (3)	0.468	0.160	0.120	0.20
δp /Boost [%]	36	11	8	11
η vol [%]	90	93	95	94
BSFC [g/kWh]	231	218	214	c.225
T exhaust [^{o}C]	700	630	725	740
Smoke [Bosch]	3.0	0.9	1.5	1.3

Notes : (1) Data at 9.9 m/s mean piston speed; 25.0 AFR is extrapolated; engine was turbocharger speed-limited

(2) Boost = inlet manifold pressure

(3) δp = mean exh. manifold pres. - mean inlet manifold pres.

LOW SPEED LTC POINT TEST DATA TABLE 3.3

Engine			
Nom Speed	RPM	1785.00	
Ave Speed	RPM	1780.21	
Torque	Nm	1313.85	
Power	kW	244.93	
Boost ratio		3.60	
bmep	bar	20.12	
Cyl Pr	bar	153.56	(limit 150bar)
DynInj	degBTDC	20.72	
Inj Duratn	deg	35.46	
Fuel Flow	g/s	15.69	
Fuel/Shot	mg	176.36	
Th Effy	%	36.65	
Air Flow	kg/m	23.96	
Vol Effy	%	87.10	
Air/Fuel		25.44	
InlMan Pr	barg	2.62	
ExhMan Pr	barg	2.81	
Inl Man Temp	C	62.20	
Exh Man Temp1	C	690.00	(limit 700deg.C)
Exh Man Temp2	C	705.00	
Compressor			
Nom Speed	RPM	8642.00	
Ave Speed	RPM	8650.63	
Torque map	Nm	155.92	
Power map	kw	141.24	
Isen Effy TS	%	80.24	
Overall Effy	%	63.67	
Mass orif	kg/m	33.24	
Mass map	kg/m	34.42	
Press Ratio		4.37	
InletDep	mbarg	97.73	
Outlet Pr	barg	2.97	
Inlet Temp	C	24.30	
Outlet Temp	C	217.00	
Turbine			
Nom Speed	RPM	21633.82	
Ave Speed	RPM	21523.88	
Wheel Torq	Nm	34.86	
Enthalpy	kW	78.61	
Isen Effy	%	54.48	
Noz Angle	V	8.60	
Massflow	kg/m	34.18	
Press Ratio		3.52	
Inlet Pr	barg	2.71	
Back Pr	mbarg	47.44	
Inl Temp1	C	557.00	
Inl Temp2	C	590.00	
Outlet Temp	C	454.00	
Output			
Intercooler	kW	62.44	
Intclr dp	mbar	351.91	
Inj setting	V	3.30	
Byp Flow	kg/m	10.46	
Smoke		2.40	
Nom Speed	RPM	1475.00	
Ave Speed	RPM	1467.50	
Torque	Nm	996.85	
Power	kW	153.19	
Th Effy	%	22.92	
sfc	g/kWh	368.91	
Gbox Losses	kW	37.42	

EXPERIMENTAL "DESIGN POINT" AND RATED CONDITIONS DATA TABLE 3.4

		"design"	rated	
Engine				
Nom Speed	RPM	2600.00	2435.00	
Ave Speed	RPM	2595.10	2437.77	
Torque	Nm	773.07	896.63	
Power	kW	210.09	228.89	
Boost ratio		1.98	2.35	
bmep	bar	11.84	13.73	
Cyl Pr	bar	111.51	135.25	
DynInj	degBTDC	16.50	19.74	
Inj Duratn	deg	28.96	31.44	
Fuel Flow	g/s	13.60	14.64	
Fuel/Shot	mg	104.85	120.12	
Th Effy	%	36.27	36.72	
Air Flow	kg/m	19.98	21.90	
Vol Effy	%	89.74	90.01	
Air/Fuel		24.47	24.93	
InlMan Pr	barg	.95	1.30	
ExhMan Pr	barg	1.28	1.77	
Inl Man Temp	C	45.80	52.30	
Exh Man Temp1	C	675.00	682.00	
Exh Man Temp2	C	695.00	701.00	(limit)
Compressor				
Nom Speed	RPM	6520.00	5156.00	
Ave Speed	RPM	6621.61	5212.13	
Torque map	Nm	89.20	100.59	
Power map	kw	61.85	54.90	
Isen Effy TS	%	82.92	78.53	
Overall Effy	%	64.83	65.69	
Mass orif	kg/m	6.94	19.99	
Mass map	kg/m	26.79	20.58	
Press Ratio		2.55	2.90	
InletDep	mbarg	57.75	32.07	
Outlet Pr	barg	1.35	1.74	
Inlet Temp	C	18.50	21.30	
Outlet Temp	C	126.00	154.00	
Turbine				
Nom Speed	RPM	49999.80	49999.80	
Ave Speed	RPM	49760.04	49837.73	
Wheel Torq	Nm	12.81	12.11	
Enthalpy	kW	66.67	63.23	
Isen Effy	%	96.09	87.19	
Noz Angle	V	6.20	9.00	
Massflow	kg/m	27.61	20.88	
Press Ratio		2.07	2.60	
Inlet Pr	barg	1.21	1.70	
Back Pr	mbarg	87.81	62.86	
Inl Temp1	C	510.00	667.00	
Inl Temp2	C	556.00	673.00	
Outlet Temp	C	407.00	509.00	
Output				
Intercooler	kW	26.97	37.49	
Intclr dp	mbar	403.89	438.55	
Inj setting	V	8.80	10.00	(max.timing advance)
Byp Flow	kg/m	6.81	1.32	
Smoke		1.70	3.00	(limit)
Nom Speed	RPM	3409.00	3409.00	
Ave Speed	RPM	3392.65	3397.95	
Torque	Nm	484.93	533.95	
Power	kW	172.28	189.99	
Th Effy	%	29.74	30.48	
sfc	g/kWh	284.29	277.41	
Gbox Losses	kW	46.97	60.06	

FIXED ENGINE SPEED : 1700 rev/min
O/S LOAD TORQUE : (a) 400 Nm
(b) 200 Nm

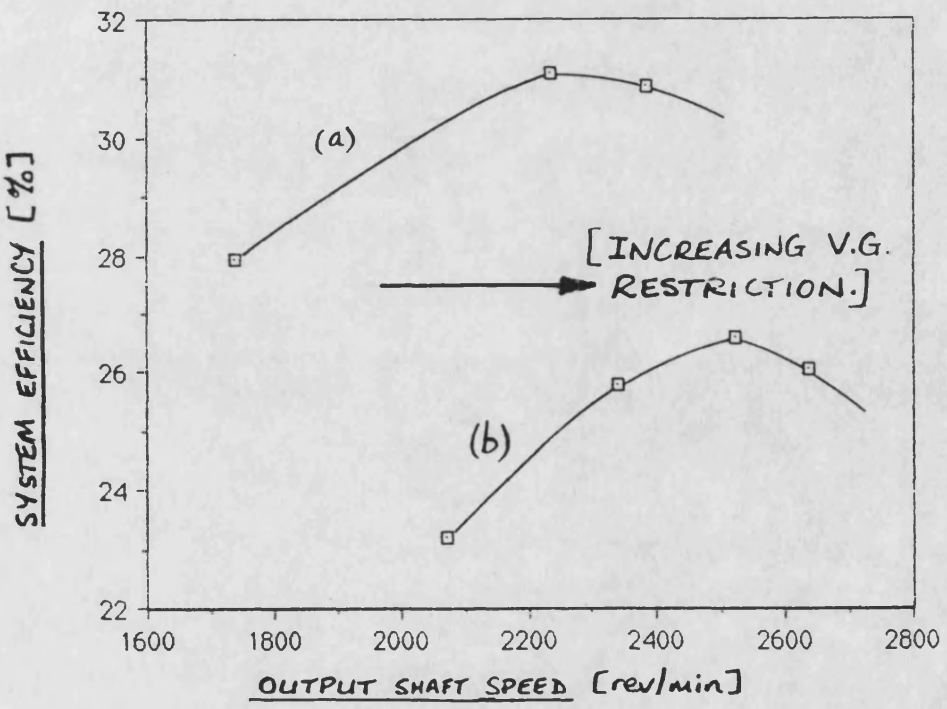

FIG. 3.1 LOCUS OF OUTPUT SHAFT SPEED AND EFFICIENCY AT FIXED ENGINE SPEED AND LOAD TORQUE (2 TYPICAL RESULTS).

OPTIMUM ENGINE SPEEDS

Fig. 3.2

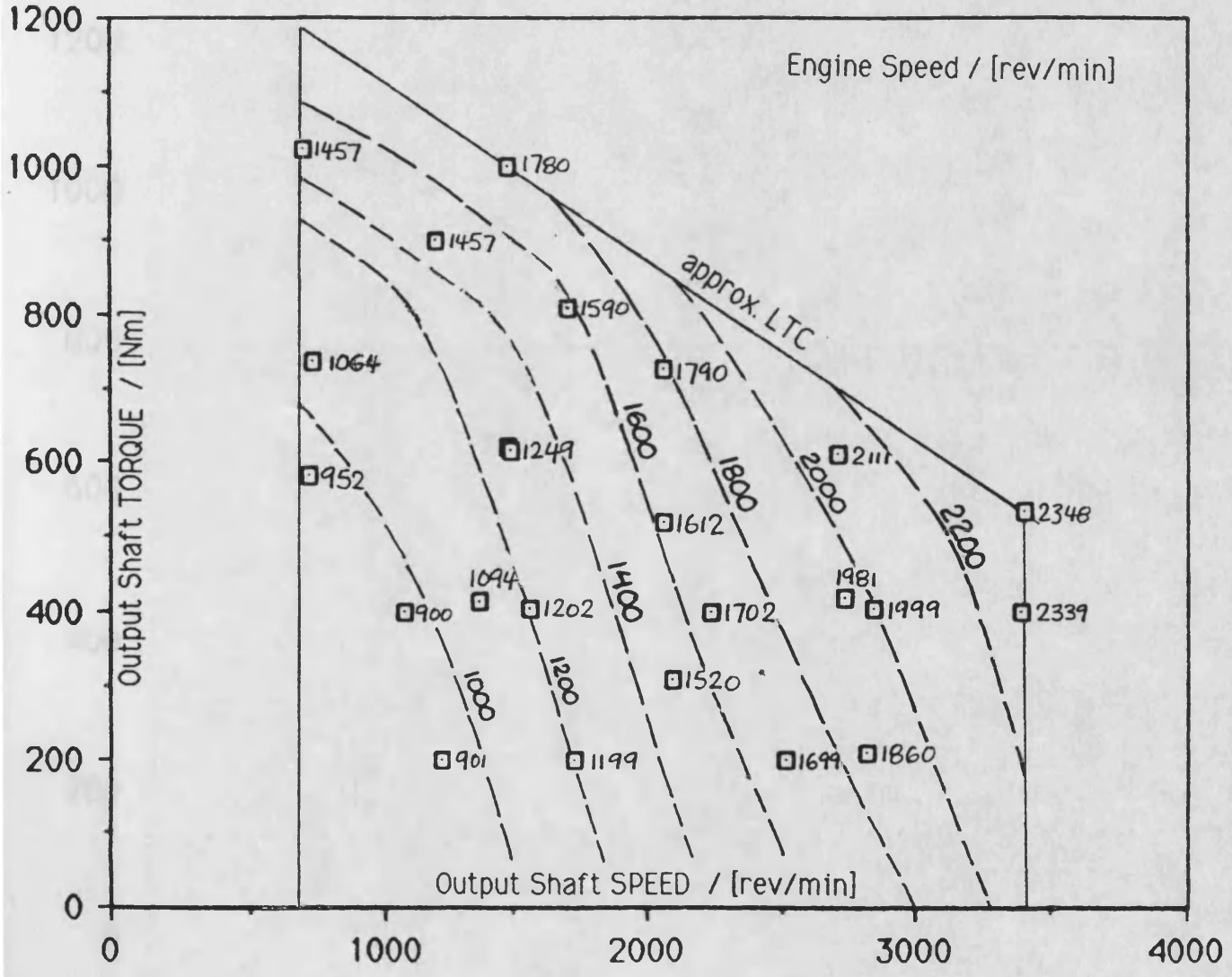

notes: rated output shaft speed 3409 rev/min
minimum output shaft speed 682 rev/min
LTC = limiting torque curve.

OPTIMUM TURBINE NOZZLE SETTINGS Fig. 3.3

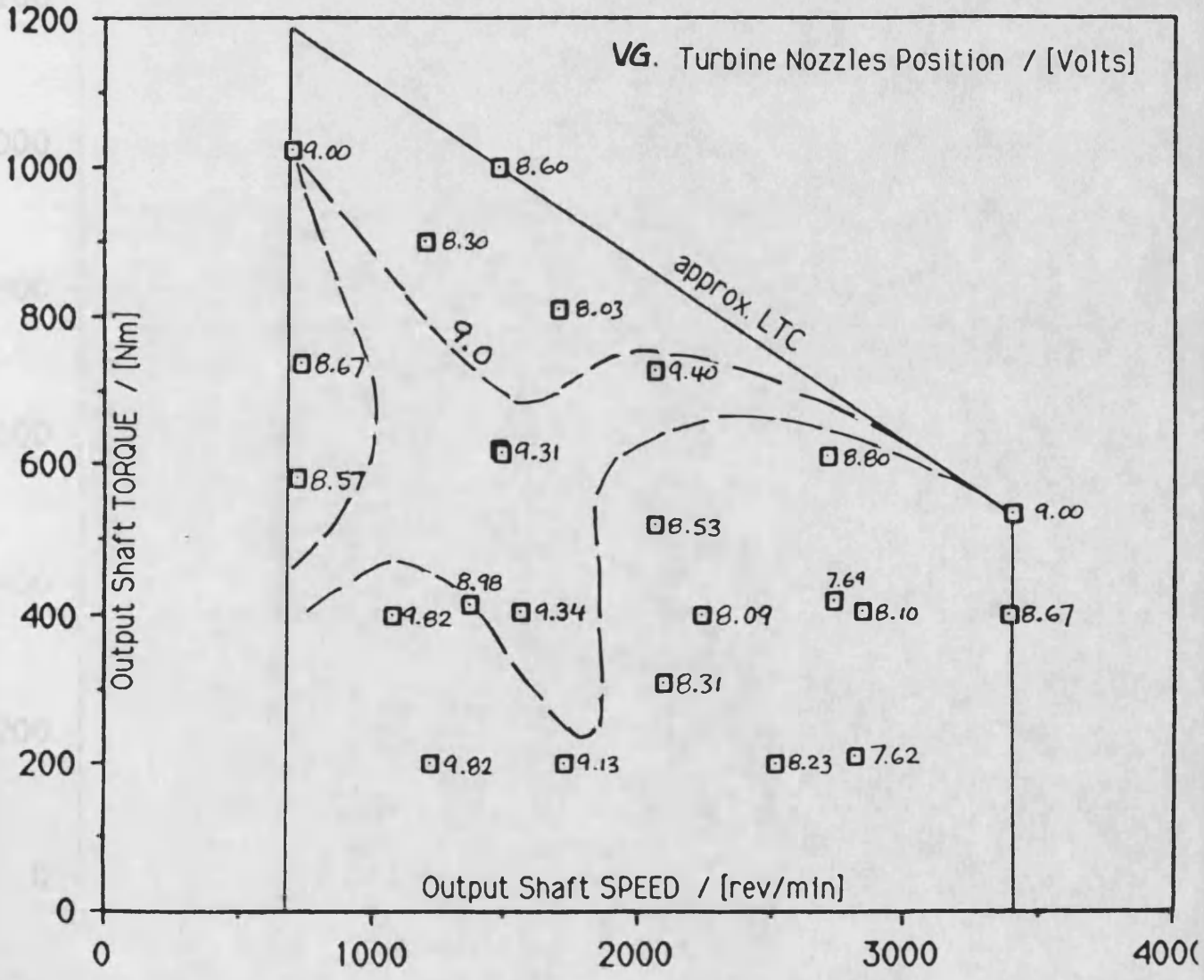

notes: rated output shaft speed 3409 rev/min
minimum output shaft speed 682 rev/min
LTC = limiting torque curve.

OPTIMUM COMPRESSOR DELIVERY PRESSURES

Fig. 3.4

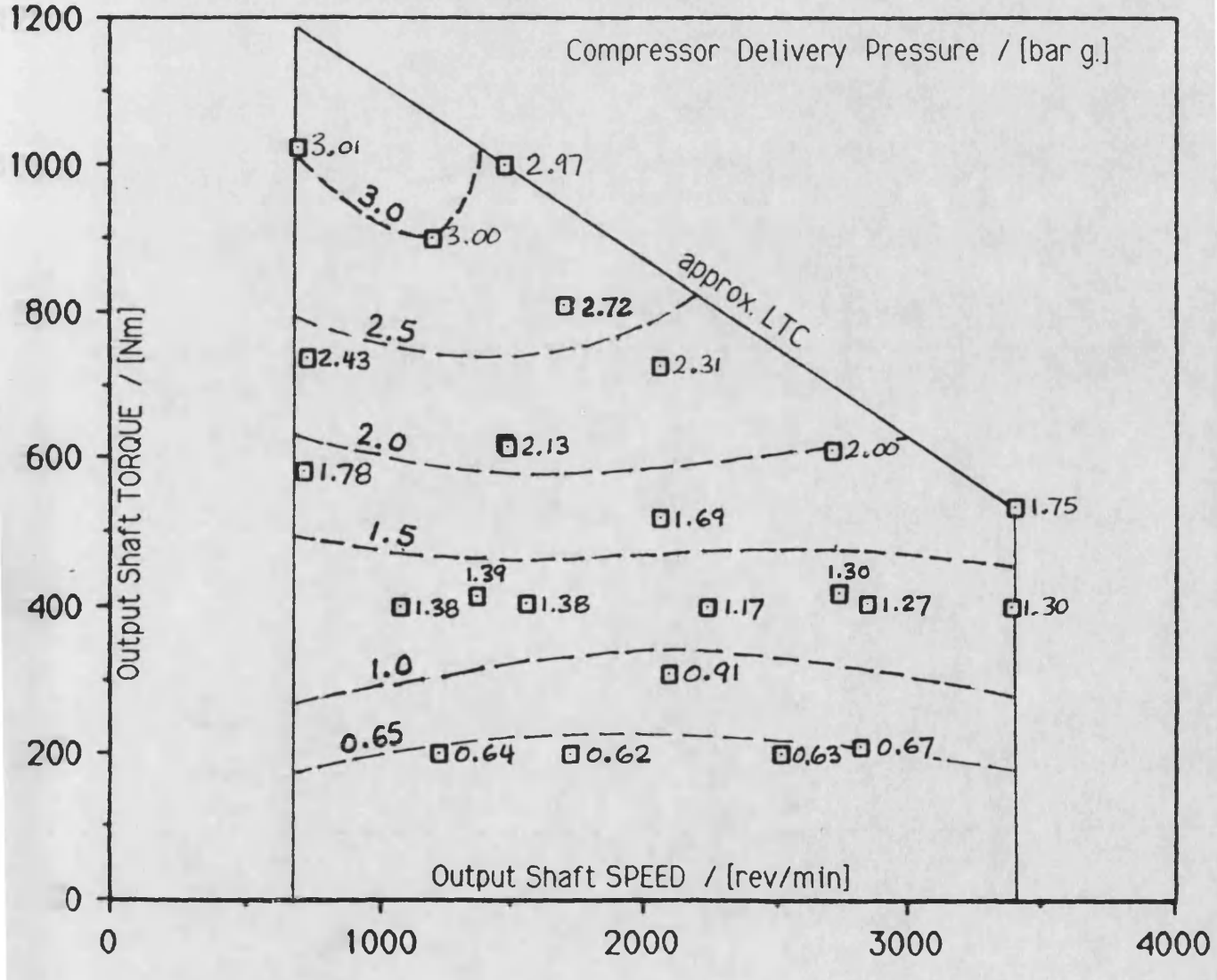

notes: max. compressor delivery pres. 3.0 bar gauge
rated output shaft speed 3409 rev/min
minimum output shaft speed 682 rev/min
LTC = limiting torque curve.

OPTIMUM BYPASS FLOWRATES

Fig. 3.5

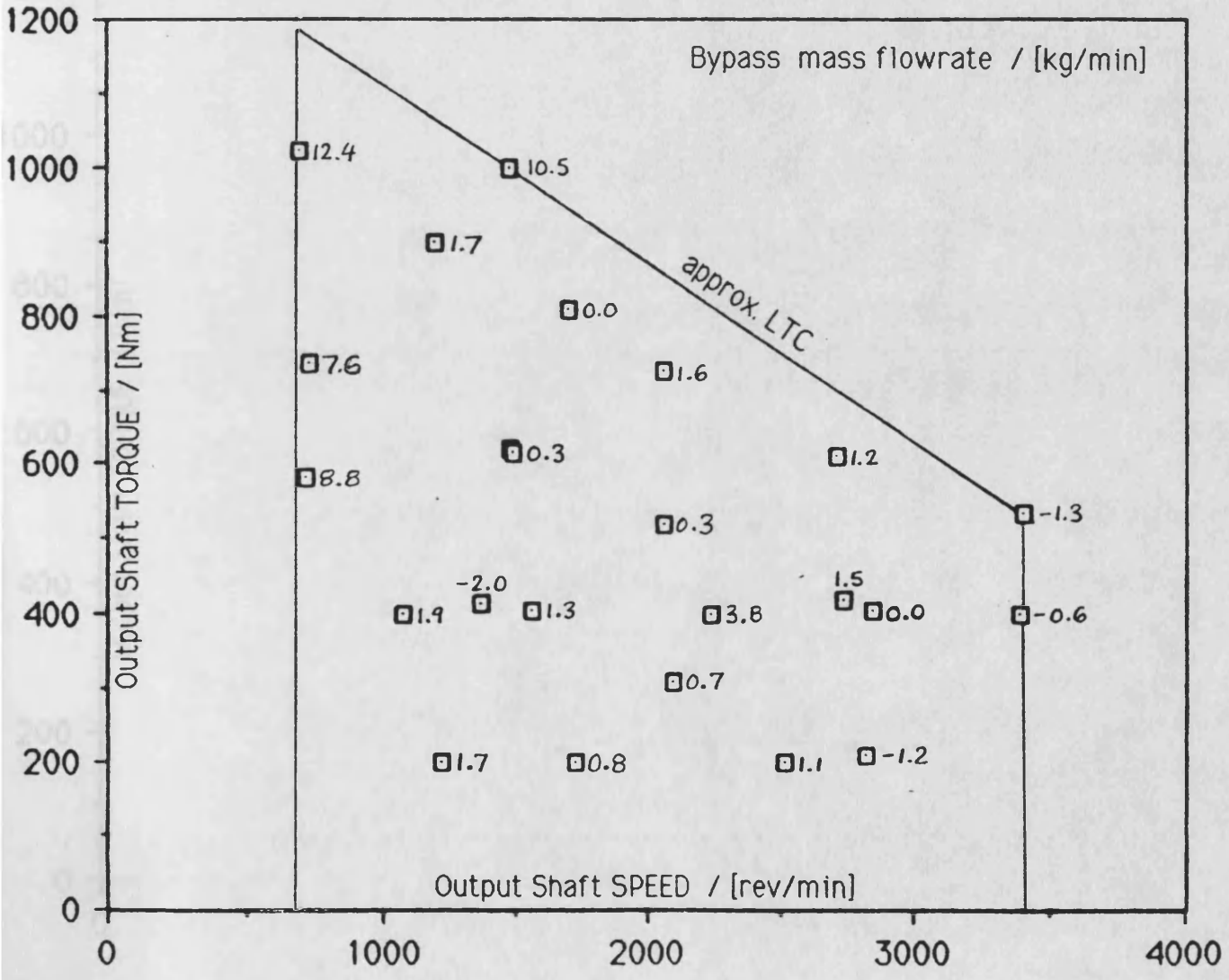

notes: rated output shaft speed 3409 rev/min
minimum output shaft speed 682 rev/min
LTC = limiting torque curve.

OPTIMUM ENGINE BMEPs

Fig. 3.6

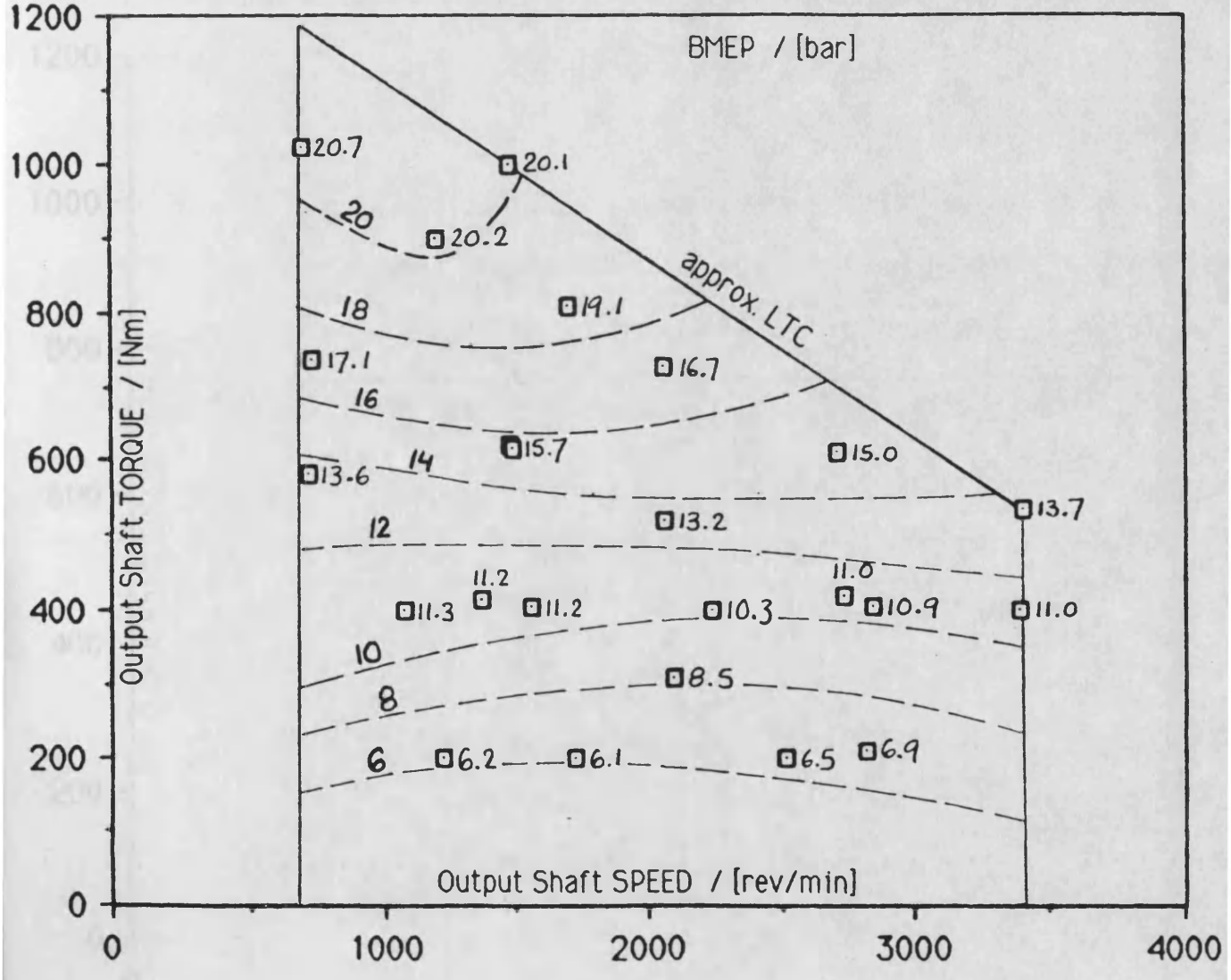

notes: rated output shaft speed 3409 rev/min
minimum output shaft speed 682 rev/min
LTC = limiting torque curve.

OPTIMUM ENGINE BOOST PRESSURE RATIOS

Fig. 3.7

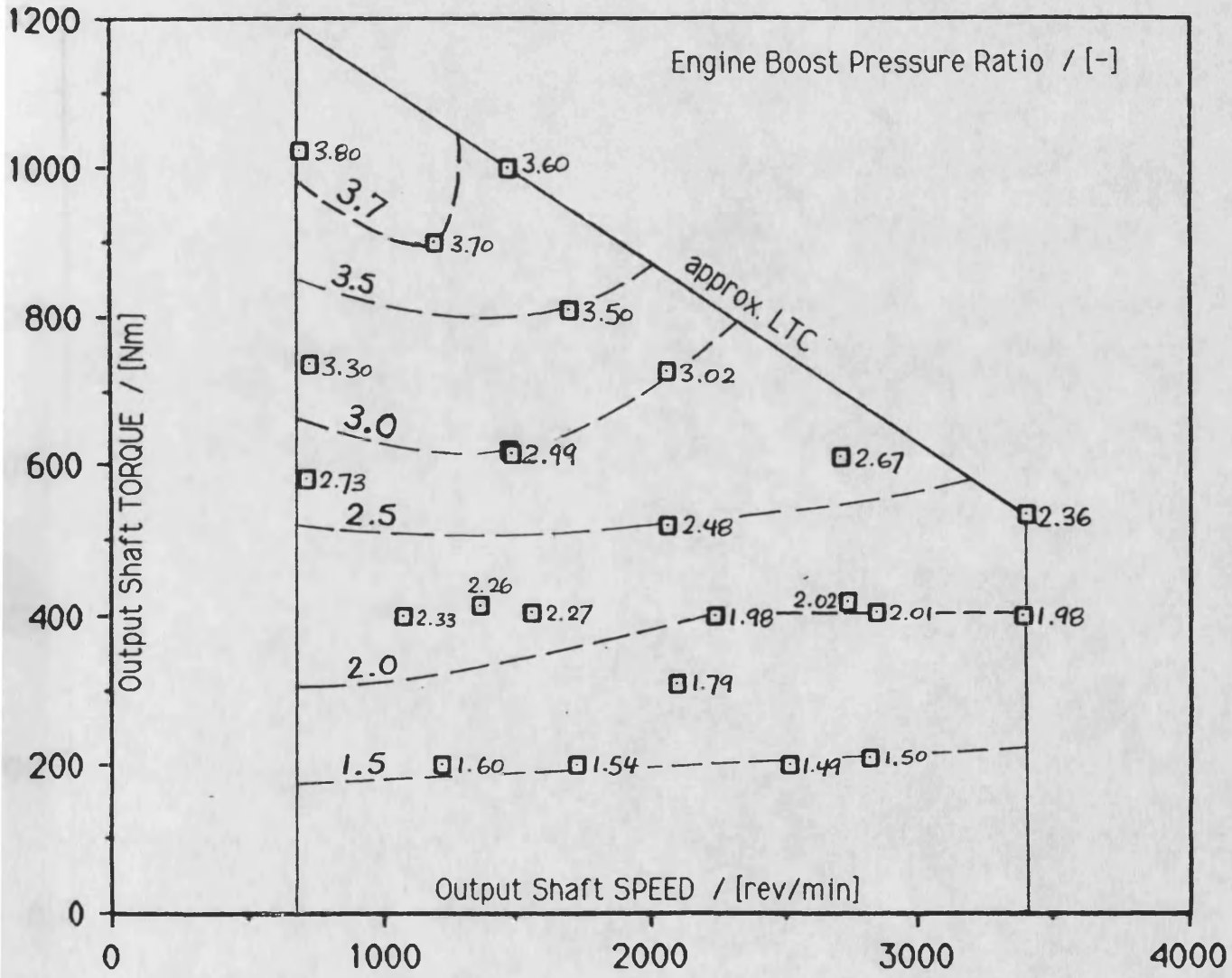

notes: rated output shaft speed 3409 rev/min
minimum output shaft speed 682 rev/min
LTC = limiting torque curve.

OPTIMISED OUTPUT SHAFT BRAKE THERMAL EFFICIENCIES

Fig. 3.8

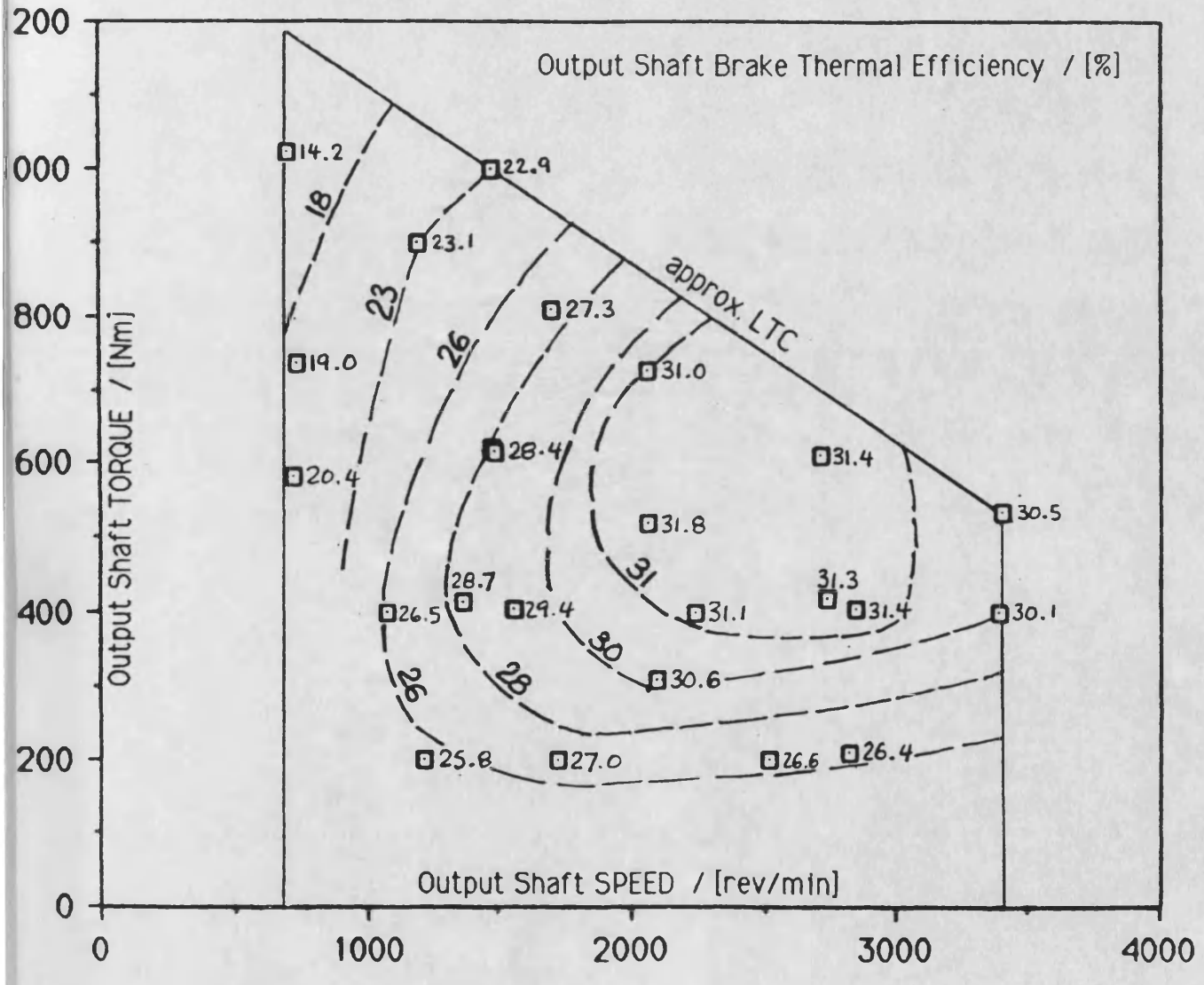

notes: rated output shaft speed 3409 rev/min
minimum output shaft speed 682 rev/min
LTC = limiting torque curve.

ENGINE BRAKE THERMAL EFFICIENCIES

Fig. 3.9

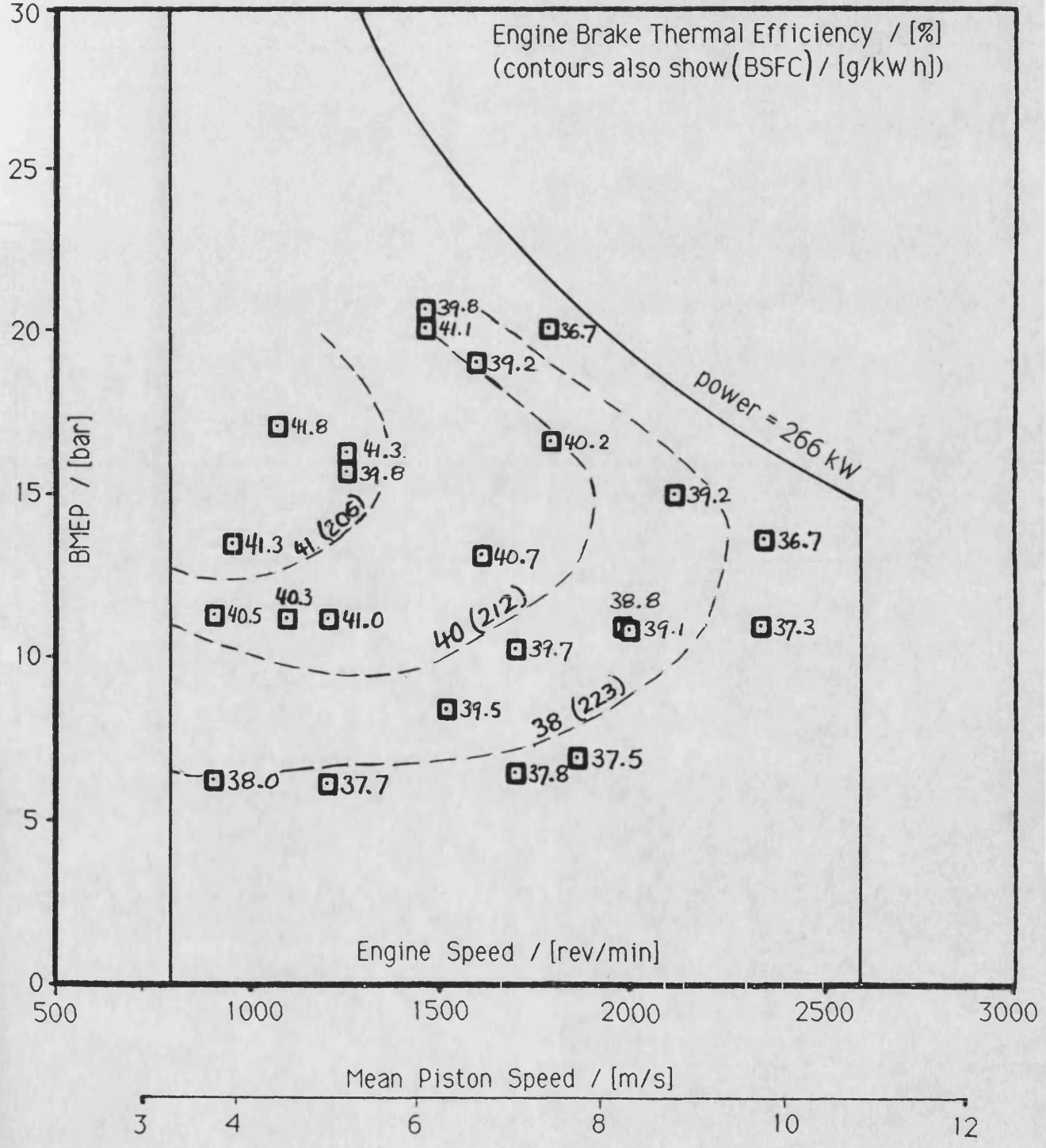

notes: rated engine speed 2600 rev/min
minimum loaded speed 800 rev/min
design maximum power 266 kW

CHARGECOOLER PRESSURE LOSSES. FIG. 3.10

FROM EXPERIMENTAL DATA - VARIATION WITH MASS FLOWRATE AND INLET PRESSURE SHOWN.

TYPE: SERCK AM111/JFL 30.

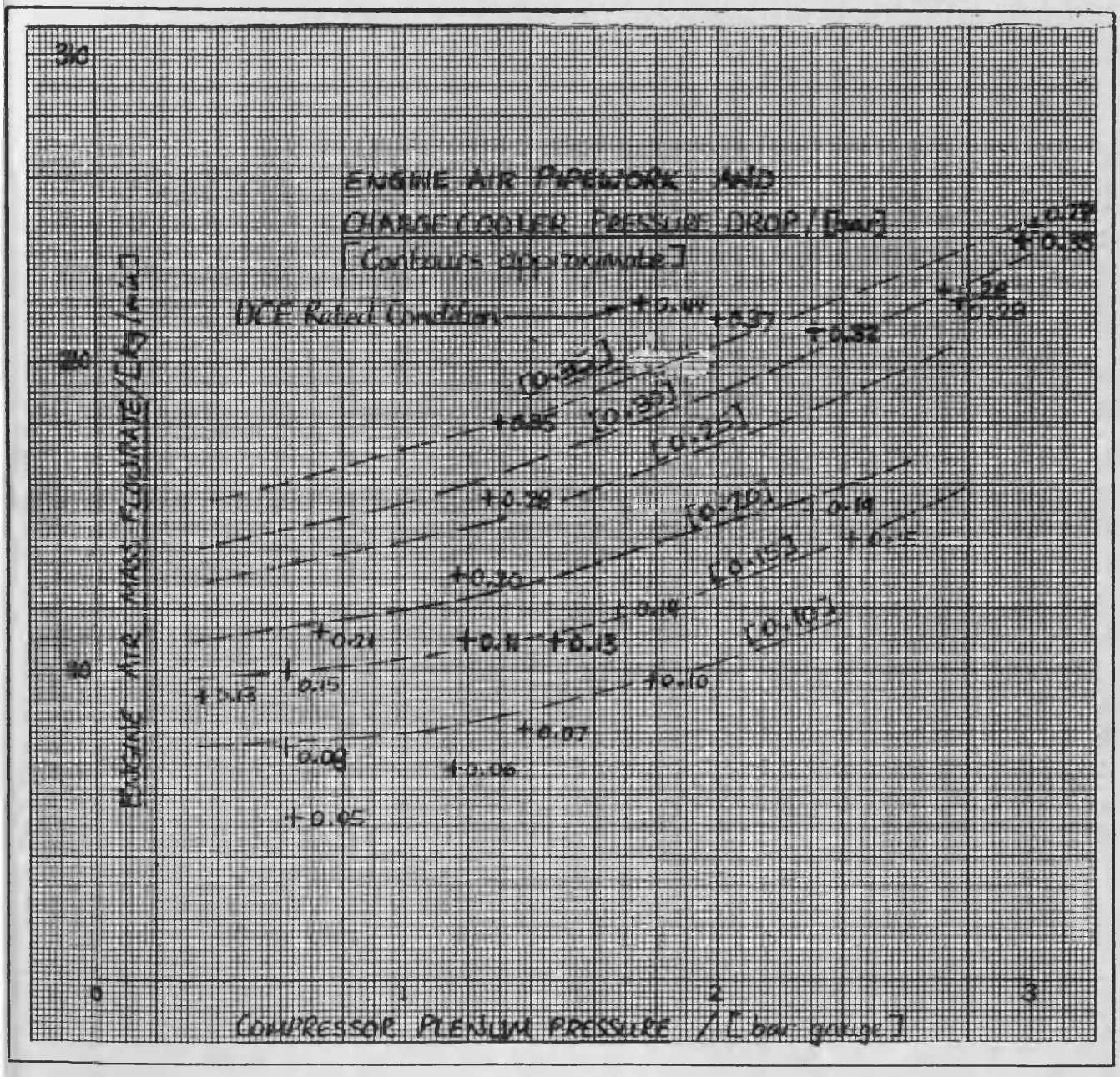

OPTIMISED OUTPUT SHAFT THERMAL EFFICIENCIES
WITH REBUILT VG TURBINE

FIG. 3.11

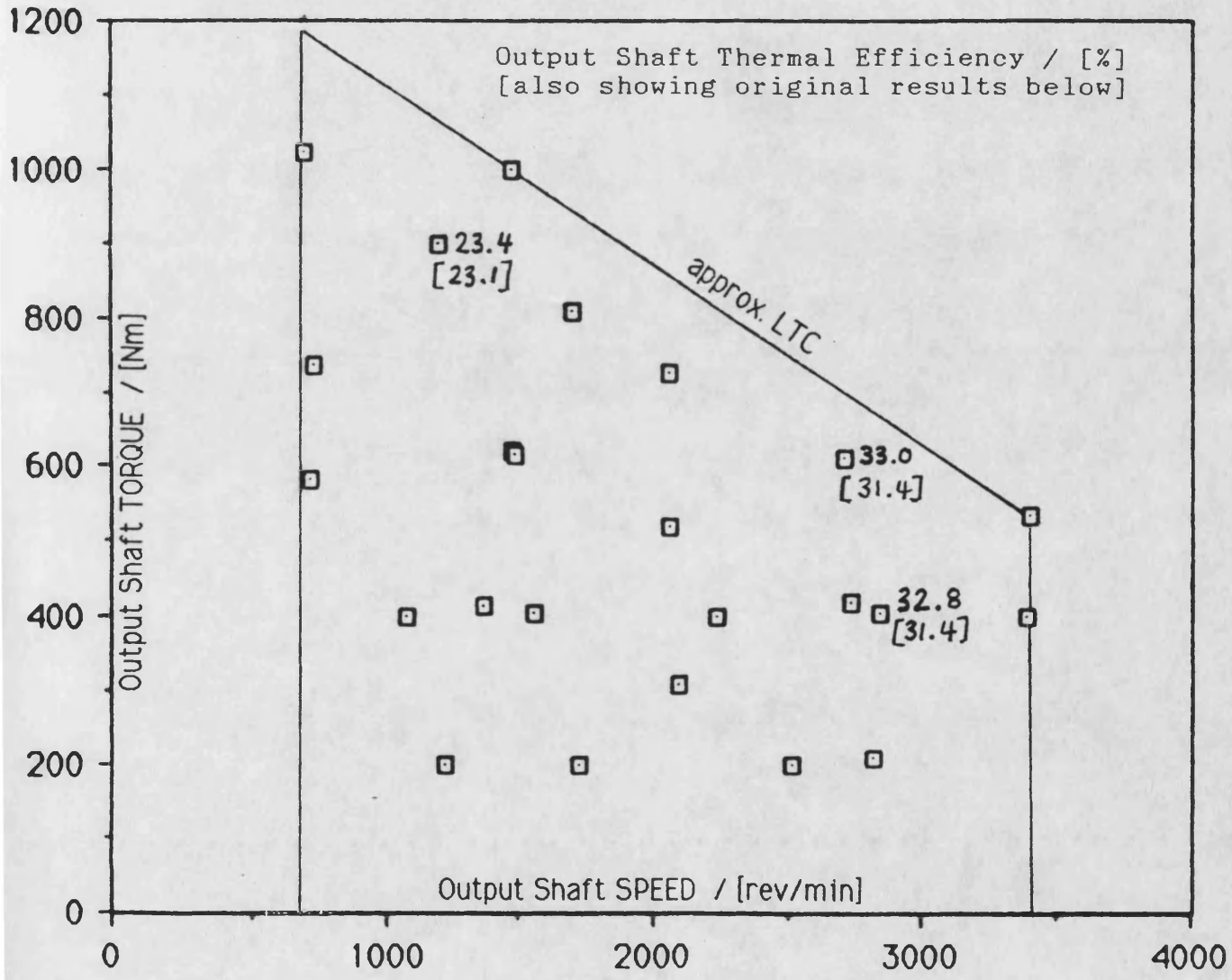

notes: rated output shaft speed 3409 rev/min
minimum output shaft speed 682 rev/min
LTC = limiting torque curve.

TURBINE POWERS (by difference) FIG. 3.12

(also showing measured Enthalpy drops across turbine)

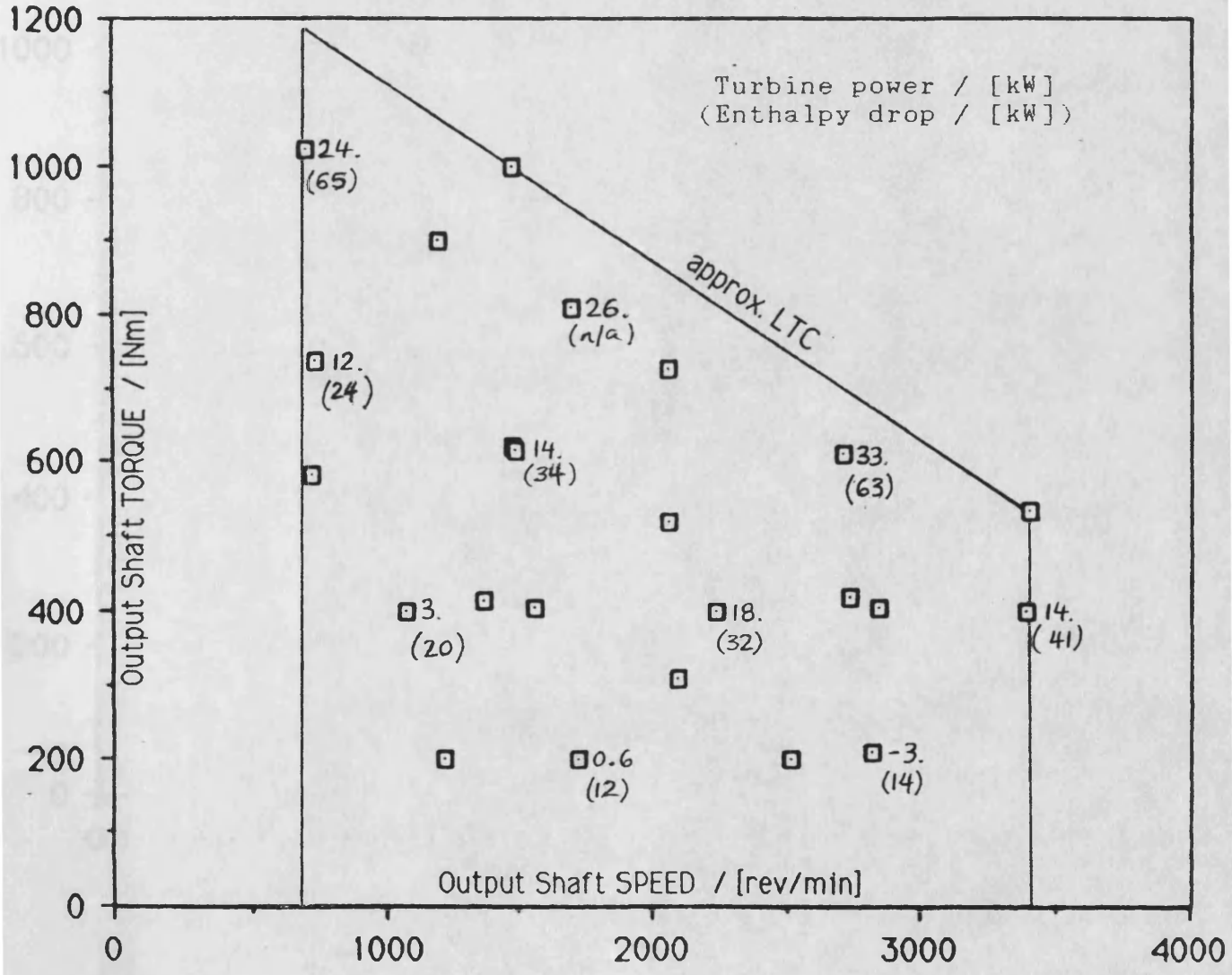

notes: rated output shaft speed 3409 rev/min
minimum output shaft speed 682 rev/min
LTC = limiting torque curve.

TURBINE POWERS (torquemeter) FIG. 3.13a

(a) VG position 8.5 V

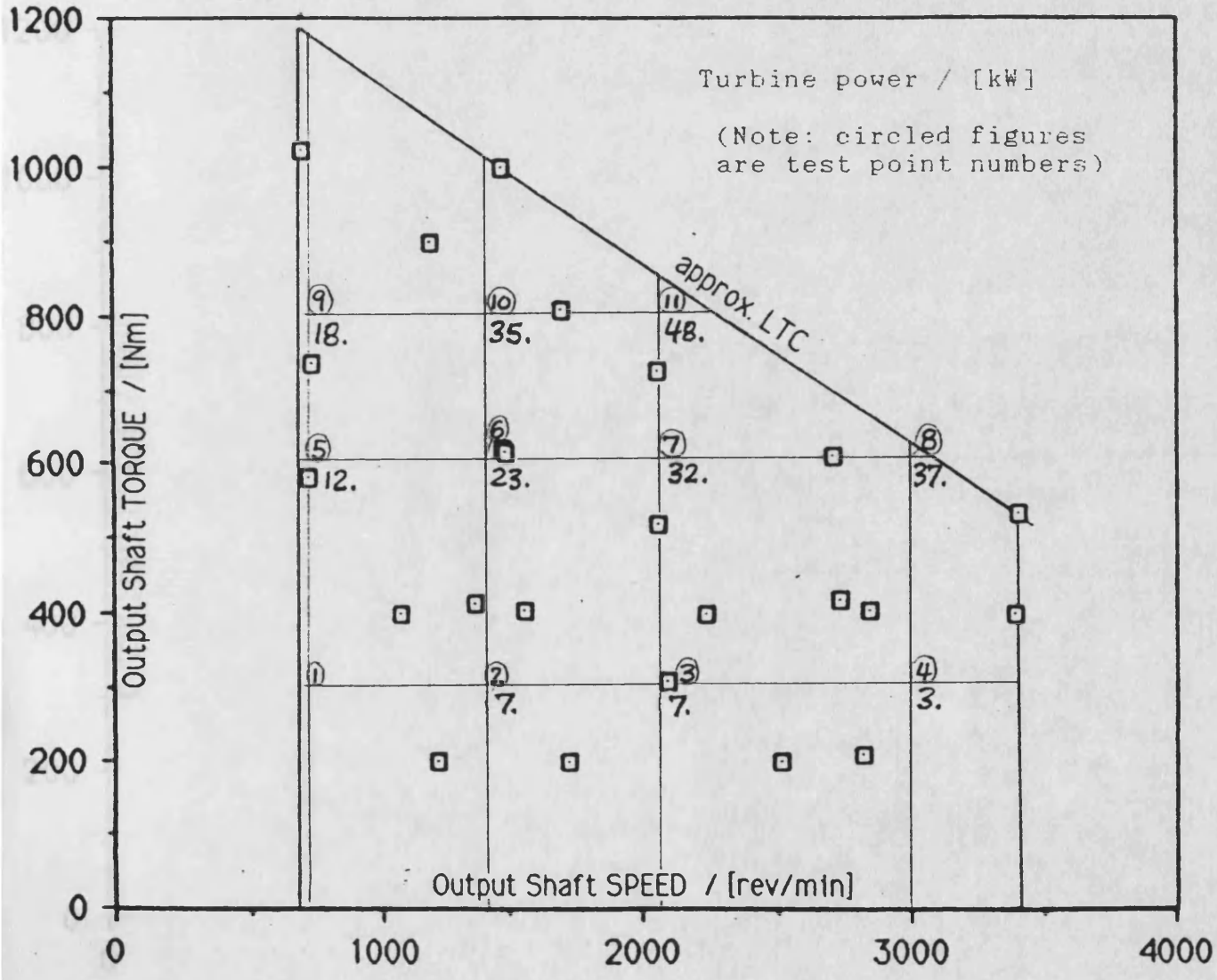

notes: rated output shaft speed 3409 rev/min
minimum output shaft speed 682 rev/min
LTC = limiting torque curve.

TURBINE POWERS (torquemeter) FIG. 3.13b

(b) VG position 9.5 V

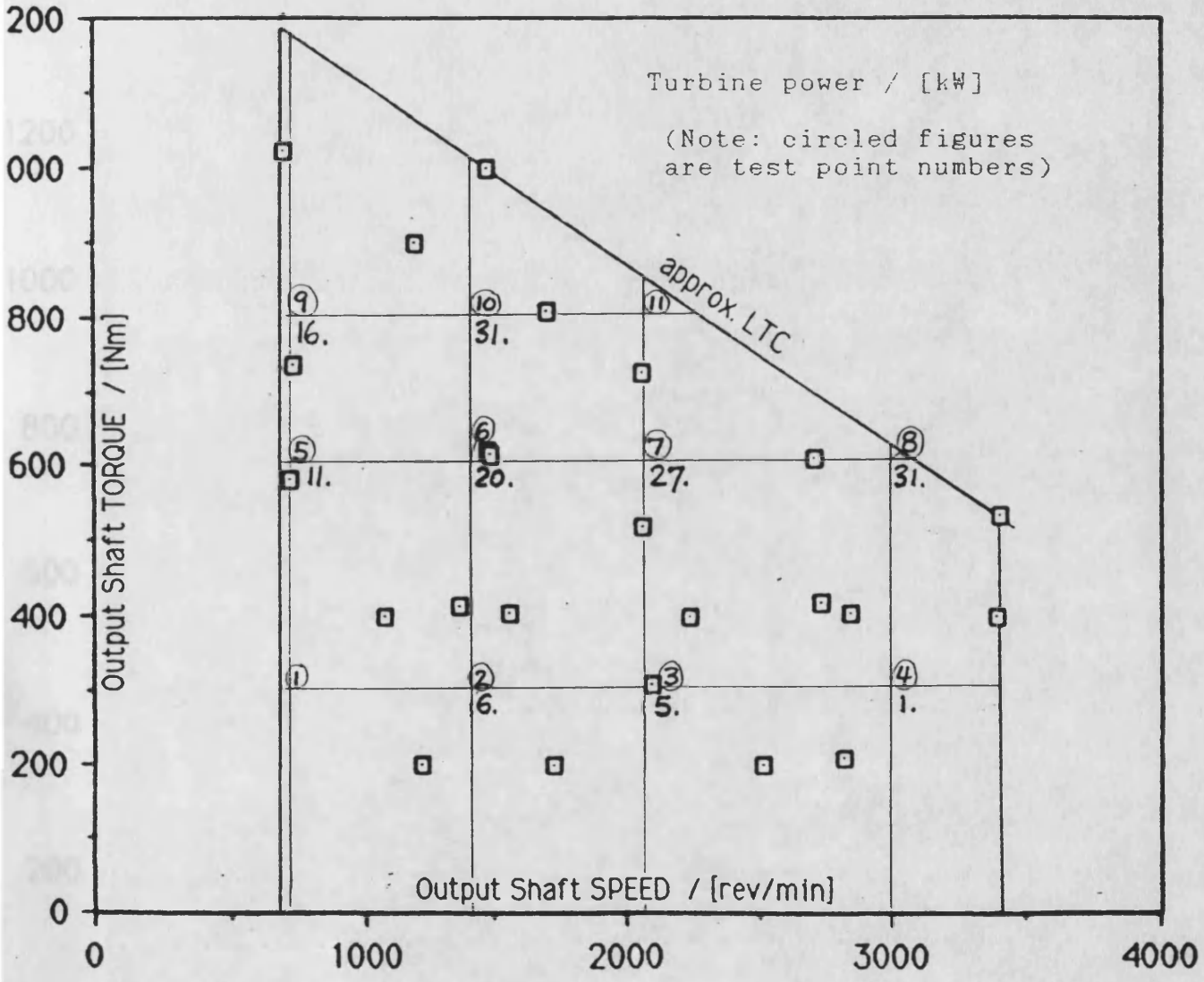

notes: rated output shaft speed 3409 rev/min
minimum output shaft speed 682 rev/min
LTC = limiting torque curve.

GEARBOX LOSSES AT OPTIMUM CONDITIONS
(calculated by net power difference)

FIG. 3.14

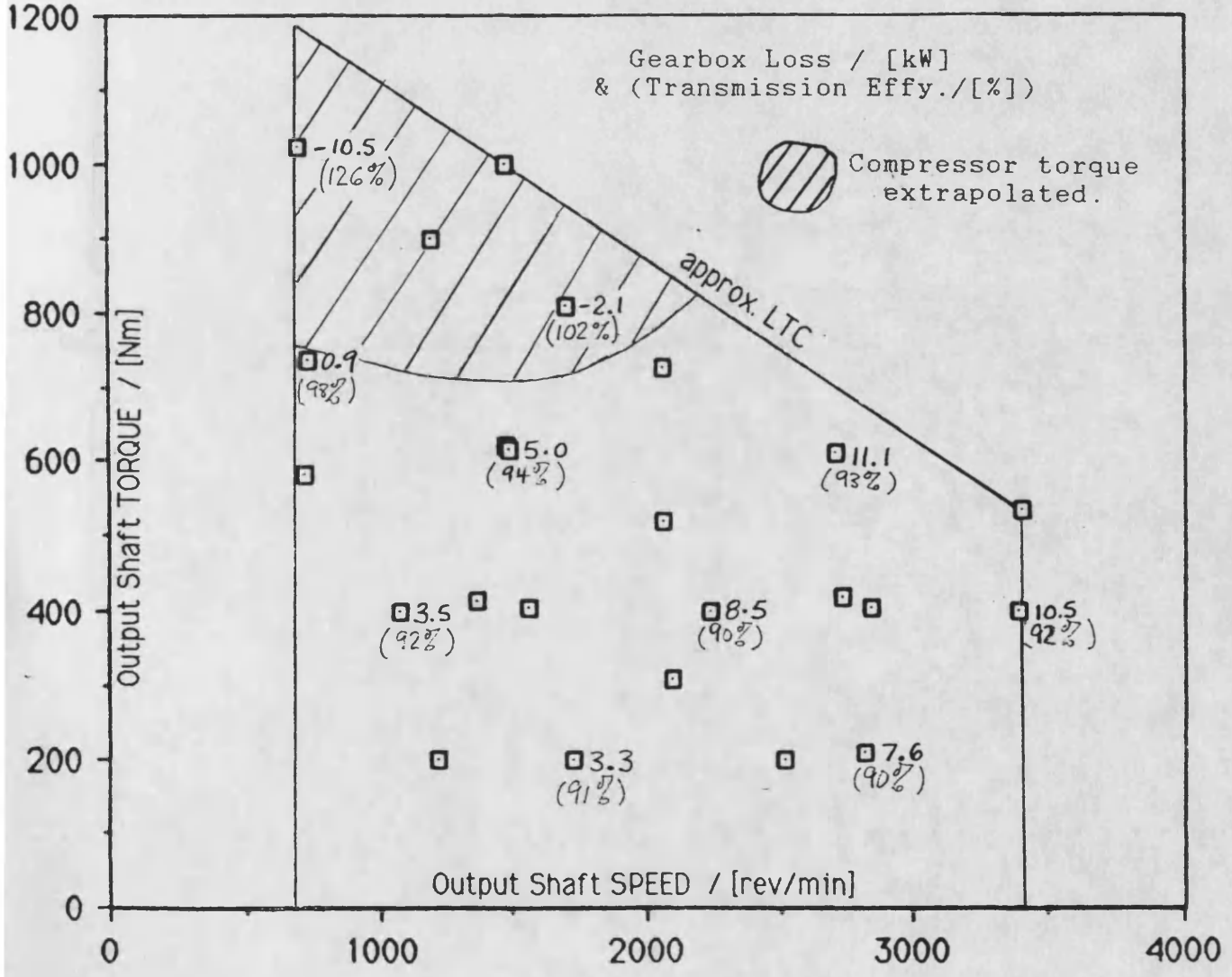

notes: rated output shaft speed 3409 rev/min
minimum output shaft speed 682 rev/min
LTC = limiting torque curve.

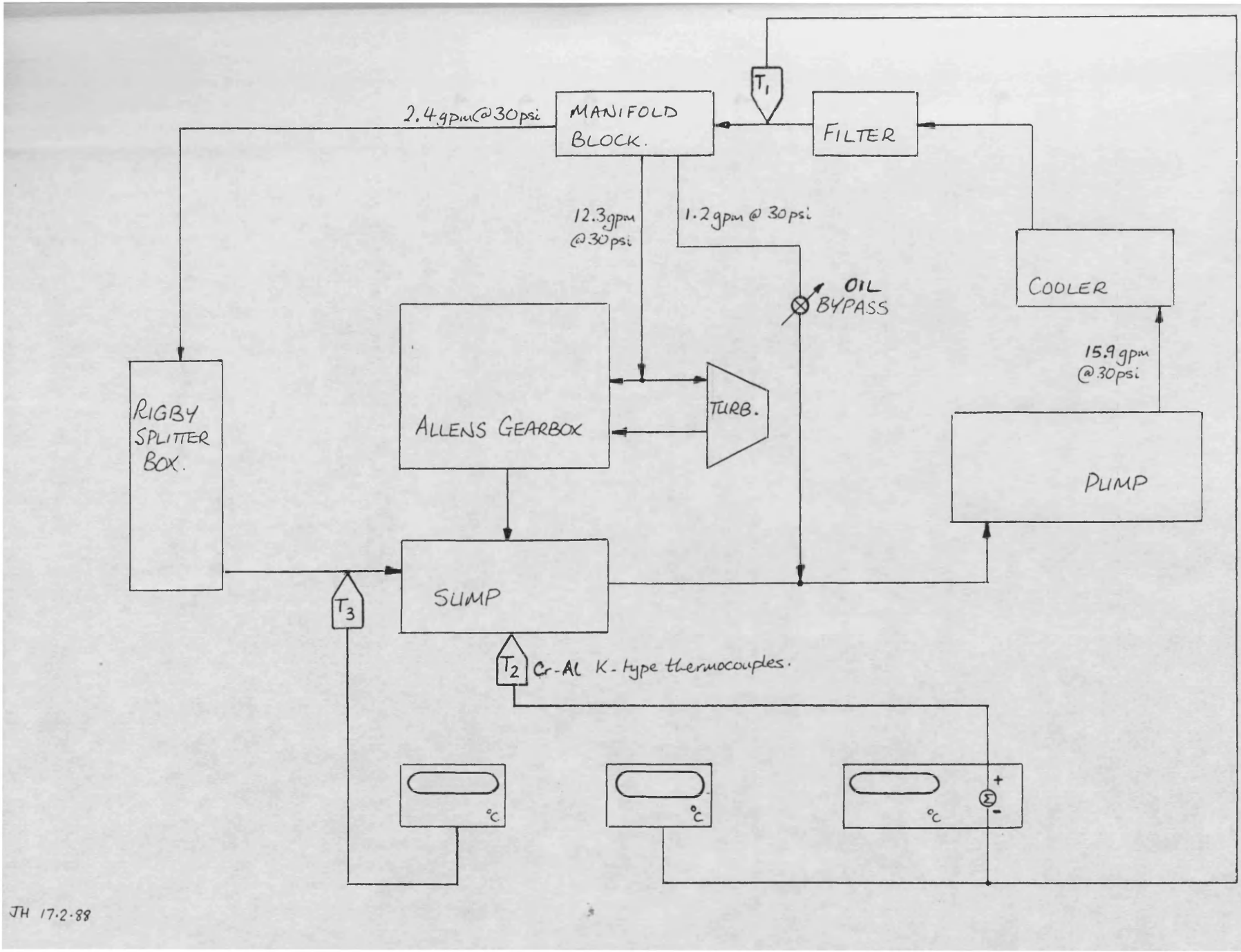

JH 17.2.88

GEARBOX/TURBINE LUBRICATION CIRCUIT

FIG. 3.15

4. TRANSIENT TESTS

4.1 INTRODUCTION AND OBJECTIVES

4.2 MICROCOMPUTER-BASED CONTROLLER

4.2.1 System requirements and selection

4.2.2 Hardware description

4.2.3 Software description

4.3 CONTROL PROGRAM

4.3.1 Structure

4.3.2 Control loops

4.3.3 Safety/signal error checking

4.3.4 Using the control program

4.4 COMMISSIONING

4.4.1 Hardware tests

4.4.2 Software tests / steady state checks

4.5 TRANSIENT TEST PROCEDURE

4.6 RESULTS

4.7 VEHICLE SIMULATION

4.7.1 Background

4.7.2 Possible approaches

4.7.3 System trials

4. TRANSIENT TESTS

4.1 INTRODUCTION AND OBJECTIVES

The stated objectives of steady state testing of the prototype were to provide data for simulation purposes and to demonstrate operation of a DCE at representative ratings. The resulting 52ØDCE prototype described in chapter 2 had relatively large component/shaft inertiae and pipework volumes. For this reason, and also because it had become clear that the prototype steady state performance was well below its design targets, the prototype was not expected to demonstrate the full transient response potential of the design. Furthermore, since the prototype did not incorporate the turbine CVT which would be a necessary feature of a production DCE, experimental transient results would be of little intrinsic value.

Thus the objective of the transient testwork was purely to provide data for validation or improvement of the simulations, so that transient predictions for a DCE with CVT might be treated with confidence.

The writer developed and used a simple dynamic simulation, "SIMDCE", to be described in the next chapter. A major part of the simulation work was the design of DCE control systems by interactive use of the dynamic simulation. The experimental work described in this chapter was thus carried out in parallel with simulation work described in chapter 7, and the early sections of the present chapter cover the implementation of a control system designed and initially tested by simulation.

Because of this interaction between transient testing and simulation, many of the experimental results have been reserved for chapter 7,

where they can be compared to predictions without causing repetition.

4.2 MICROCOMPUTER-BASED CONTROLLER

4.2.1 System requirements and selection

Even the simplest automatic control system for the DCE would require a microprocessor base, since setpoint scheduling is required. In a research prototype, the obvious choice is a microcomputer-based system, which enables changes to schedules or control loops to be made purely in software, and for which commercially-developed hardware and operating systems are available off-the-shelf.

The required system was thus a microcomputer supporting readily-available analog interfacing cards (compatible with the Ø-1ØV d.c. bi-polar signals employed in the 52ØDCE installation), and programmable in a high level language. The simulation work had set a target controller rate of 2ØØ Hz; that is, the system must sample all required feedback signals, compute the control inputs, and output the analog signals (with all necessary error and safety checks) within 5 msec.

The DEC LSI11/23 microcomputer then used for the simulation work was first considered. This had originally been specified for setpoint scheduling of analog control loops ("supervisory control") in variable geometry turbocharged engine research [11,37,51]. The analog interface cards (8 channel 12 bit multiplexed Analog/Digital Converter -ADC- and 4 channel 12 bit Digital/Analog Converter -DAC) were adequate for the proposed DCE work, and the software was convenient to use - the above supervisory program had been written in FORTRAN with a short assembly code routine to drive the ADC.

To ascertain whether this system would be sufficiently fast, without having first to develop the code, a "benchmark" test was set having the same number and type of computation and logic statements as the control system to be implemented (that is, as many as the simulation's control subroutine). This speed test program was thus computationally equivalent to the control loops of the (as yet unwritten) controller. By timing a large number of iterations of the sequence of statements, the achievable controller rate could be calculated. The above neglects time for signal error checking and ADC plus DAC conversions, which were obviously not required in the simulation. To allow for this, the target rate for the speed test was set at 300 Hz rather than 200 Hz.

Programs coded in FORTRAN, first using floating point computations, then integer (16 bit) only, achieved 52 Hz and 120 Hz respectively. Re - coding in assembler (again giving 16 bit accuracy) increased the speed to 820 Hz. However, the development in assembler of correctly structured code for the control program (rather than the disconnected simple statements of the speed test program) would be tedious and error prone; a high-level language was preferable.

Given the rapid increases in the computational power of "professional" microcomputers since the design of the LSI11/23, a current machine could easily exceed the speed target using a high-level language; therefore a new system was purchased.

4.2.2 Hardware description

The chosen system was a Dell 200 (80286 PC AT -compatible; switchable 6.5/8.3/12.5 MHz clock rate) with 80287-8 maths co-processor and MS-DOS operating system. The reasons for the choice of this machine were:

(i) Performance/cost - PC-compatible machines are manufactured for a broad and competetive market rather than being specialised equipment.

(ii) Standardisation - PC-compatibles were increasingly being used at Bath, therefore technical support would be good and any software developed would readily be portable to other machines within the School. In particular, the transient data acquisition system, which forms part of the test installation described in chapter 2, was also PC based. It was a major advantage, when using the two machines together during testing, that both used the same operating system.

(iii) Availability of analog interfaces - suitable PC-bus cards were available from several manufacturers. The chosen cards were:

(a) ADC : Blue Chip Technology AIP-24

24 channel (4 multiplexed converters) 12 bit selectable bipolar / unipolar input, range 0 to +/- 10.24 V.

(b) DAC : Blue Chip Technology AOP-8

8 channel 12 bit unipolar output, range 0 to 10.24 V.

Details of the installation of these cards into the Dell 200 may be found in the logbook held with the machine. Ribbon cables link the cards to a remote connection box, which has BNC terminals for connection with analog instrumentation, as shown schematically in fig.4.1.

4.2.3 Software description

A further advantage of using a PC-compatible machine was the wide range of available languages. While Fortran is the most widely used high-level language in engineering applications, the writer decided to use C in this case. C allows the development of well-structured programs at an equally high level to FORTRAN (which are thus easily readable), and gives fast executing code. C is becoming increasingly popular in real-time applications as a structured and self-contained language (unlike FORTRAN, library functions are themselves written in C rather than a lower level code), replacing assembler.

Two complementary packages were purchased; Microsoft "QuickC" (for rapid program development, but with limited library functions and compiler options) and Microsoft "C5.1" (full library functions and compiler optimisation supported).

To decide which variable type to use for control computations, and which C environment to use (QuickC or C5.1), the speed test (target rate 300 Hz) was again applied.

Using QuickC the speed test program ran at:

Floating point	260 Hz
Integer (16 bit)	3300 Hz
Integer (32 bit)	1250 Hz.

With compiler optimisation in C5.1 (making maximum use of the 80287 co-processor for example), the speeds were:

Floating point	450 Hz
Integer (16 bit)	5000 Hz.

Therefore, any variable type could be used. Given that the analog

interfaces are limited to 12 bit precision, 16 bit integer computations should be sufficiently precise, since the number of operations (and thus the error build-up) on any one variable is not great. In fact, the long integer (32 bit) type was used, giving more than adequate precision and speed.

4.3 CONTROL PROGRAM

4.3.1 Structure (fig.4.2)

The control program, "AMI", was structured to have a main segment having access to five functions, each of which is independent of the others. A listing of the code is given in appendix 2. The tasks of the main segment and each of the functions are described in turn below. The program is written entirely in C, including the ADC and DAC driver routines, using the Microsoft C5.1 environment.

(i) Main segment

The tasks carried out in the main segment are the input of data from disk file (control gains and schedules), interaction with the operator (putting instructions to the screen, and accepting keyboard commands), and computation of the control inputs, along with the associated signal scaling and error checking.

(ii) get(chan)

This function reads a given ADC channel. The code in appendix 2 is well commented and self-explanatory. The bit codes required to start the conversion and to check it is complete, and the position of the 12 data

bits within the 2 input bytes, are explained in [52].

(iii) put(outvar,outch)

This function puts the contents of variable outvar to DAC channel outch, first converting the given decimal integer to a 12 bit binary number, then splitting this into 2 bytes according to [53]. Again the code is self-explanatory.

(iv) pull(array,spd,fuel)

This function returns a scheduled setpoint from the given array (either of compressor speed or injection timing). The schedules are mapped onto bases of output shaft speed and fuelling, using a matrix of 54 points (figs.4.3 and 4.4). Two-dimensional linear interpolation is used. As shown in the code listing, care is taken with scaling to ensure that the integer quantities remain large, to prevent quantisation errors in the interpolation.

(v) offset(nos,fuel)

This function returns a VG position offset as a function of output shaft speed and fuelling.

(vi) racklm(neng)

The absolute fuelling limit was constructed as a piece-wise function of engine speed. At low speeds fuelling is limited to prevent 20 bar BMEP being exceeded. At higher speeds maximum BMEP must be reduced to prevent the 266 kW design power limit being exceeded, so the fuelling limit is gradually reduced. This function is self-explanatory from the listing in appendix 2.

4.3.2 Control loops

As explained in the introduction to this chapter, the control loops to be implemented in AMI were exactly those developed by dynamic simulation. At this point then, the control loops and scheduling will be only briefly listed; a full discussion of their development is given in chapter 7. The control loops are shown schematically in fig.4.5 (the simulation counterpart to this is shown in fig.7.6).

(i) Fuel rack

The fuel rack is used for engine speed control, with proportional error gain. The single demand input to the microcomputer is interpreted as an engine speed demand. This input is normally set manually by the operator, but during a transient test it is set by input from the data acquisition computer, which is used to run the transient from a pre-set data file. Fuelling is constrained by the fuelling limit curve, by a fuel/boost ratio control (smoke-limiting), and by fuelling cutback if output shaft speed exceeds the rated speed. In addition, a further control (not used in the simulation) reduces fuelling if exhaust temperature exceeds its limit.

(ii) Turbine VG

Under steady state conditions VG is used to control compressor speed to scheduled values. Under transient conditions VG controls boost to improve response. The discrete switch between the two modes is made on the basis of controlled rack position demand (in effect the error between demanded and actual engine speeds). As indicated at the start

of this section, the principles of the controller are explained fully in chapter 7. In both modes proportional error gains are used; to achieve the necessary precision of control, the resulting control inputs are superposed onto near-optimum VG position offsets.

(iii) Injection timing

Static injection timing is set according to a steady state schedule, under both steady state and transient conditions.

4.3.3 Safety/signal error checking

Since the computational speed of the machine was much higher than required, it was possible to include all necessary safety and signal error checks, even in the most speed-critical parts of the program.

The test installation monitoring and shutdown system remains active at all times; the aim of the checks within the controller is to "catch" problems before the shutdown system is invoked.

To simplify the program design, all "failures" (apparent signal loss or component speeds out of safe range) cause the DCE to be automatically dropped to a "fast Idle" mode, as listed below:

(i) Engine speed demand equivalent to 1400 rev/min (the operator demand input is ignored)
(ii) Fixed VG position demand of 5 V
(iii) Fixed timing position demand of 6 V.

At the same time a screen message explains why the switch to Idle mode was made, and the current options (shutdown or transfer back to manual

control). Idle mode may also be selected by the operator at any time, by a single keystroke.

If the engine speed feedback signal is lost, the Idle mode speed demand is replaced by a low rack position demand, causing a gentle but positive shutdown.

Only one measureable parameter, cylinder pressure, is not checked by the control software and/or the monitoring and shutdown system. While it would be possible to install a peak hold circuit, triggered and sampled by the control software, excessive cylinder pressures are very unlikely to occur under computer control. Acceptable cylinder pressures always obtain when the DCE is operated according to its steady state schedules. Under transient conditions boost is generally lower at a given fuelling than at steady state, thus cylinder pressure is unlikely to be greater. Finally, in the event of timing actuator problems, the servovalve and the mechanism are biased to retard, giving lower cylinder pressures.

For test purposes with the DCE not running, the operator is given the option of disabling signal error checking. Thus the correct operation of individual control loops and scheduling can be verified without having to simulate the full set of feedback signals.

4.3.4 Using the control program

With the DCE under manual control, the controller is run by typing "ami" in the D:\CONTROL subdirectory. From this point the operator is given full instructions on the use and capabilities of the controller,

by screen messages. The main stages are listed below.

(i) A sequence of 6 blocks of information introduces the control system, and allows the operator to disable signal error checking for program development or validation purposes.

(ii) Interactive instructions are given for bumpless transfer to computer control.

(iii) A set of 4 blocks of information is held permanently on the screen whilst under computer control. These include instructions for transfer to Idle mode and manual control (transfer to manual control must always be via Idle mode - this simplifies the process).

(iv) On transfer to Idle mode, further operator information is held on the screen.

(v) On selecting the option to transfer back to manual control, a block of instructions is given for bumpless transfer.

(vi) The program is then stopped. To transfer back to computer control, the program must be re-run.

4.4 COMMISSIONING

4.4.1 Hardware tests

The main hardware to be tested were the ADC and DAC cards and the BNC connection box. To facilitate this a test program "TESTIO" was written, allowing the user to read test signals at any chosed BNC input channel and send any value to any chosen BNC output channel.

These preliminary checks proved valuable; intermittent faults with the ADC card (replaced by the manufacturer), and unreliable DAC operation at very low binary outputs were identified. The DAC fault (giving random voltage outputs for binary inputs corresponding to less than 4 mV) was overcome simply by not demanding less than 4 mV. Fortunately none of the actuators need be set to Ø V during normal operation. For the VG and timing actuators, Ø V corresponds to fully open and fully retarded settings respectively, which are not required; for the rack actuator, zero fuelling is obtained anywhere below 3 V.

4.4.2 Software tests / steady state checks

Firstly, the correct operation of each control loop, fuelling cutback and signal error check was verified using calibrated signal inputs.

The DCE was then run under computer control to check that it was being held to its steady state scheduled setpoints, and that these did not give excessive cylinder pressure or exhaust temperature (with the automatic cutback disabled) on the limiting torque curve (LTC).

Fig.4.6 shows the engine speeds obtaining under computer control,

superposed upon the original optimum contours. The agreement is quite good; discrepancies are chiefly due to the approximations made in creating regular schedules (evenly-spaced points) from irregular test points, and in then interpolating from these schedules.

Fig.4.7 shows exhaust temperatures and cylinder pressures near the LTC. Slight timing schedule changes were subsequently made near the LTC to reduce cylinder pressure (which is not monitored by the controller) at the expense of exhaust temperature (which is controlled by fuelling cutback).

Fig.4.8 shows output shaft thermal efficiencies superposed on the original optimum contours. From these limited data it seems that efficiency has improved despite operating slightly off the scheduled optimum settings. This is due to the improvements in turbine efficiency with the VG mechanism rebuild, as discussed in chapter 3; that is, the comparison is not really valid. Nevertheless these results indicated that the steady state controls were functioning reas.onably well. It should be remembered that the purpose of the controller was to enable testing of transient response and comparison with the simulation results. Steady state control was strictly only needed to give representative start and end conditions for a transient test.

4.5 TRANSIENT TEST PROCEDURE

A transient test procedure was devised to promote repeatability of the results. As described in chapter 2, most of the test installation parameters are controlled in closed loop, the major exception being compressor inlet air temperature. For transient tests this was brought to 25 +/- 2 deg.C at the start of each test simply by opening the external cell doors as required. Experience shows that transient emissions (only exhaust smoke opacity was measured in this case) may vary with pre-conditioning of the engine. In particular, any build-up of leaked oil at light loads will be burned off during a transient, giving a smoke level which will generally be unrepeatable. In the 520DCE, slight oil leakage occurs from the compressor bearings to the rotors at low pressure ratios.

The following procedure was therefore used:

(i) Run at the initial condition for the transient for 10 minutes, adjusting the inlet air temperature to the required range during this time.
(ii) Run the transient
(iii) Return to the initial condition
(iv) Repeat (i) - (iii).

Three or four runs were conducted for each test; the first was discarded as it might have unrepeatable oil "burn-off" in the smoke data.

The transient was scheduled by the data acquisition computer (the layout was shown in fig.2.29). With the control computer active, there

are only two inputs to the rig, namely operator demand and load torque. Each is scheduled from a data file set up using the Labtech Notebook software (chapter 2). The start of each file includes an 18 second "plateau" at the initial condition during which time the operator demand and load torque demand are switched from manual to computer input. The end of each file leaves the computer inputs fixed at their final values, for the switch back to manual demand input.

4.6 RESULTS

As stressed in the introduction to this chapter, discussion of transient performance has mainly been reserved for chapter 7, where experimental and simulated data can be compared and discussed together.

The results presented here are a repeatability check, and an experimental investigation into the effects of smoke-limiting fuel restriction upon response.

Fig.4.9 shows five transient responses superimposed. These were recorded on two separate days; initial conditioning runs were excluded. Repeatability was very good, including that of smoke opacity. Compressor and turbine pressures are similar; the circles on the figure attempt to distinguish the two groups. It will be noted that the torque signals were noisy. The data were recorded at 10 Hz, so it was thought that the oscillations seen might be aliases of higher frequency oscillations. Using a high frequency digital storage 'scope two main vibration peaks were found in the engine torque signal: at engine firing frequency and at a rather variable low frequency of the order of

10 Hz, possibly associated with the Holset flywheel coupling. The output shaft torque signal had only one major peak, at the engine firing frequency. It should be pointed out that the turbine torques shown are not measured but are calculated in the data reduction software on the basis of measured engine and output torques, inertia torques and assumed losses [48]. Thus the large oscillations shown effectively result from differencing two oscillating signals.

Fig.4.10 shows the same transient test as above, for a run without pre-conditioning (in fact the first run after starting and warming-up the DCE). The increased smoke opacity is clearly evident, although no other parameters differ significantly from fig.4.9 (note that the torque scales differ between fig.4.9 and 4.10).

Figs.4.11 and 4.12 show responses with and without smoke-limiting respectively. The smoke-limited response has a minimum air/fuel ratio (AFR) of approximately 28., with peak smoke opacity of 20 per cent (equivalent to approximately 4.4 Bosch), a typical acceptable figure for truck Diesels. Peak output shaft speed is reached in 8.0 seconds in this particular transient. It must be noted however, that AFR falls only gradually to its minimum value. As indicated in section 4.3.2, smoke limiting is effected by imposing a maximum fuelling/boost ratio. There is a non-linear relationship between engine boost pressure and engine airflow, in other words at a given fuelling/boost ratio the resulting AFR will vary with the engine condition. If this non-linearity were taken into account in the smoke-limiting control, or if direct AFR control were used (in practice requiring a mass airflow sensor rather than pressure sensor), then response could be improved whilst maintaining the same minimum AFR.

With the smoke-limiting disabled, minimum AFR falls to approximately 21., with peak opacity 57 per cent (about 6. Bosch). Acceleration time is reduced to approximately 5.1 seconds.

This improvement in response is much greater than would be expected for a turbocharged engine. The reason for this is that in the DCE, engine/compressor acc eleration is directly dependent upon the excess of engine over compressor power. More severe smoke-limiting reduces the amount of fuel injected for a given boost pressure, and thus reduces the achievable engine torque at a given compressor torque. The ratio of powers thus decreases almost linearly, but the margin of engine over compressor power decreases much more quickly. The implications of this are discussed further in chapter 7.

4.7 VEHICLE SIMULATION

4.7.1 Background

Because the DCE is an integrated engine-transmission, comparison of its transient response with that of "competitive" turbocharged Diesel engines is difficult. Turbocharged engine tests commonly involve torque steps at constant engine speed, or free engine acceleration, but the DCE covers a much wider speed and torque range, so direct comparisons cannot be drawn with DCE output shaft torque steps or acceleration responses.

The approach adopted in recent theoretical comparisons between DCE and turbocharged engine / stepped transmission systems [39,54] was to

compare vehicle acceleration and route performance. Experimental vehicle simulation had also been carried out at Bath on a turbocharged engine, using analogue circuitry to simulate inertia and fixed road loads [37,51]. It was decided to investigate experimental vehicle simulation for the DCE prototype, using microcomputer-based inertia / road load simulation.

It was pointed out earlier that the prototype lacks a turbine CVT, and thus does not have the full torque characteristic required for automotive applications. While this would limit the value of any results obtained, it was considered worthwhile to investigate possible techniques.

4.7.2 Possible approaches

There are two possible approaches to vehicle simulation:

(i) Scheduling output shaft speed and torque setpoints according to data obtained from a heavy-duty truck operating under typical conditions. An example of this is the U.S. Federal Register emissions certification test cycle [1], which translates vehicle data into an engine speed / torque drive cycle for a given engine. This is rather inflexible for general research purposes. One difficulty for the DCE is the need to schedule output shaft speed and torque; clearly only one of these may be set by the dynamometer, the other must be set by the DCE controller. The DCE controller described earlier in this chapter sets output shaft speed indirectly (the operator demand relates to engine speed), therefore a revised control scheme or additional outer loop would be required.

(ii) Real-time simulation of vehicle inertia and tractive effort. The DCE must be matched to the hypothetical vehicle. This may be a complex process, considering the maximum vehicle speed, gradeability and fuel efficiency under "cruise" conditions, but basically leads to the choice of rear axle ratio. Given this choice, and typical data for the vehicle (mass, wheel/axle inertia, aerodynamic and tyre drag, rear axle efficiency and so on), then it is possible to calculate the load torque equivalent to vehicle tractive effort for any output shaft speed, and inertia torques due to output shaft acceleration / deceleration.

This approach can be implemented in two ways:

(a) Output shaft (load) torque control

The tractive effort torque τ_{te}, and the inertia torque τ_i may be calculated:

$$\tau_{te} = \text{fnc}\ (N_{o/s}, \text{vehicle parameters}) \qquad (4.1)$$

$$\tau_i = J_{ref} \frac{d(N_{o/s})}{dt} \qquad (4.2)$$

where $N_{o/s}$ = o/p shaft speed

J_{ref} = simulated vehicle inertia, referred to the o/p shaft.

Then the sum of these

$$\tau_l = \tau_{te} + \tau_i \qquad (4.3)$$

at any instant is the load torque setpoint.

(b) Output shaft speed control

The difference between the measured output shaft torque τ_m and the calculated tractive effort torque τ_{te} causes acceleration of the output shaft:

$$\frac{d(N_{o/s})}{dt} = \frac{\tau_m - \tau_{te}}{J_{ref}} \qquad (4.4)$$

Integrating this equation gives:

$$N_{o/s}\Big]_{T2} - N_{o/s}\Big]_{T1} = \int_{T1}^{T2} \frac{\tau_m - \tau_{te}}{J_{ref}} .dt \qquad (4.5a)$$

or, in difference form:

$$N_{o/s}\Big]_{k+\Delta t} = N_{o/s}\Big]_{k} + \left[\frac{\tau_m - \tau_{te}}{J_{ref}}\right]_k . \Delta t \qquad (4.5b)$$

Hence output shaft speed control may be used for vehicle simulation, where the setpoint is continually updated using the above relation.

The latter method (b) was used in [37]. Because the setpoint is calculated by integration (eqn 4.5) rather than by differentiation (eqn 4.2) of the measured signal, the latter approach should be more robust. As the referred inertia increases, the latter approach becomes increasingly preferable. Unfortunately, this approach requires output

shaft speed control, not implemented on the DCE prototype. Therefore the former approach (a) was explored.

4.7.3 System trials

The most convenient way to implement the vehicle simulation was to make use of the general purpose PID control loops available in the data acquisition system's Labtech Notebook software [47]. Clearly it was possible to use the derivative term for inertia simulation (using output shaft speed as the error signal). It was also possible, making a simplification, to use the proportional term to simulate the tractive effort torque, as described below.

For a powertrain of the 520DCE rating, installation in a 32 t truck would be reasonable. Using typical truck data already obtained for SIMDCE (chapter 5), and simplistically choosing a rear axle ratio to give a vehicle speed of 110 km/h at the rated output shaft speed, the referred inertia was calculated as 282 kgm^2 (the physical dynamometer inertia was insignificant, but should be taken into account when a small referred inertia is to be simulated). A tractive effort curve (fig.4.13) was also calculated, for a level road. The linear approximation shown in fig.4.13 enables the proportional term to be used to simulate this tractive effort. The error involved, in the speed range of interest, is up to 20 per cent; however, under the accelerating conditions which are of most interest, inertia torques dominate and the error becomes small.

Initial trials at a sample rate of 100 Hz showed major instabilities caused by noise on the output shaft signal; this causes small

perturbations on the differentiated signal, which are then amplified by the high simulated inertia (high derivative gain). A typical trace is shown in fig.4.14. Increasing the sample rate would only increase the frequency of the oscillations; filtering the output shaft speed signal was ineffective in the face of the very high loop gain.

Clearly the alternative approach, of using output shaft speed control with setpoints updated by numerical integration, should be adopted. Because output shaft speed control was not implemented on the prototype, this experimental work was not pursued further. Theoretical investigations of fixed output shaft speed responses, and consideration of vehicle/route performance, are covered in chapter 7.

LIST OF FIGURES

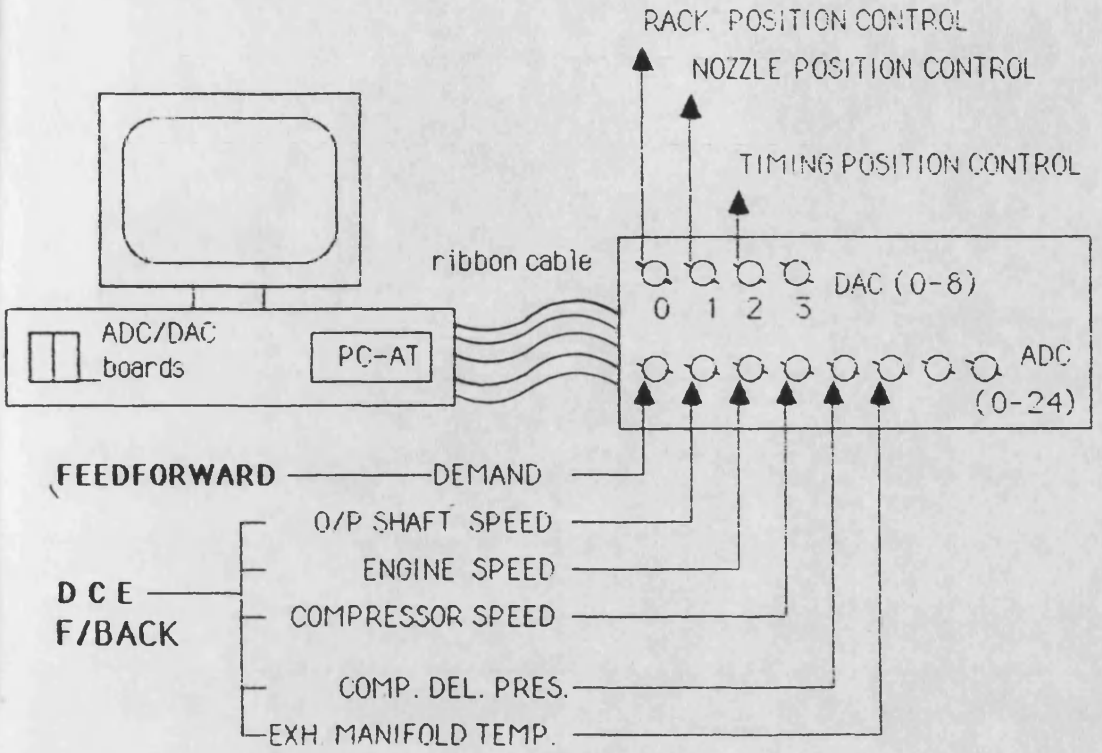

SIGNAL	PURPOSE
demand	single "driver" input
o/p shaft speed	scheduling and turbine overspeed limiting
engine speed	control loop feedback
comp. speed	control loop feedback
comp. del. pres.	smoke and maximum boost limiting
exh. man. temp.	active maximum fuelling control

FIG.4.1 MICROCOMPUTER CONTROLLER HARDWARE

CONTROL PROGRAM STRUCTURE FIG. 4.2

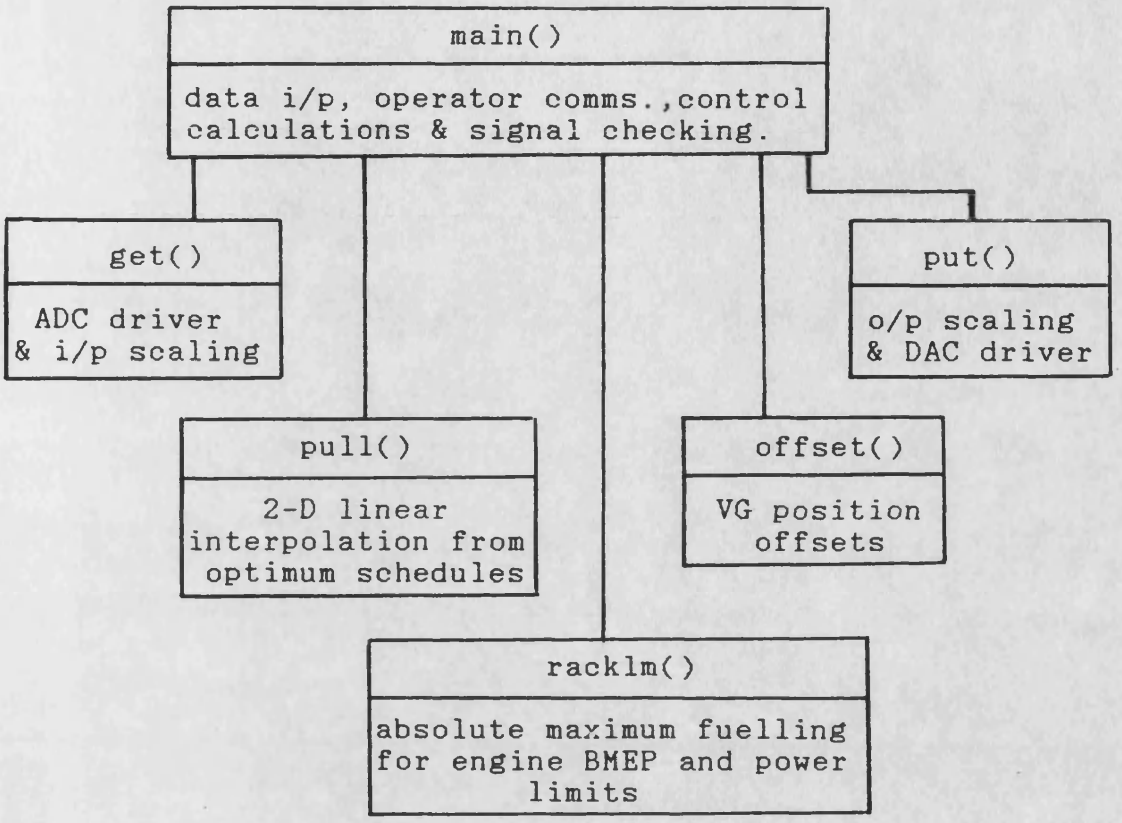

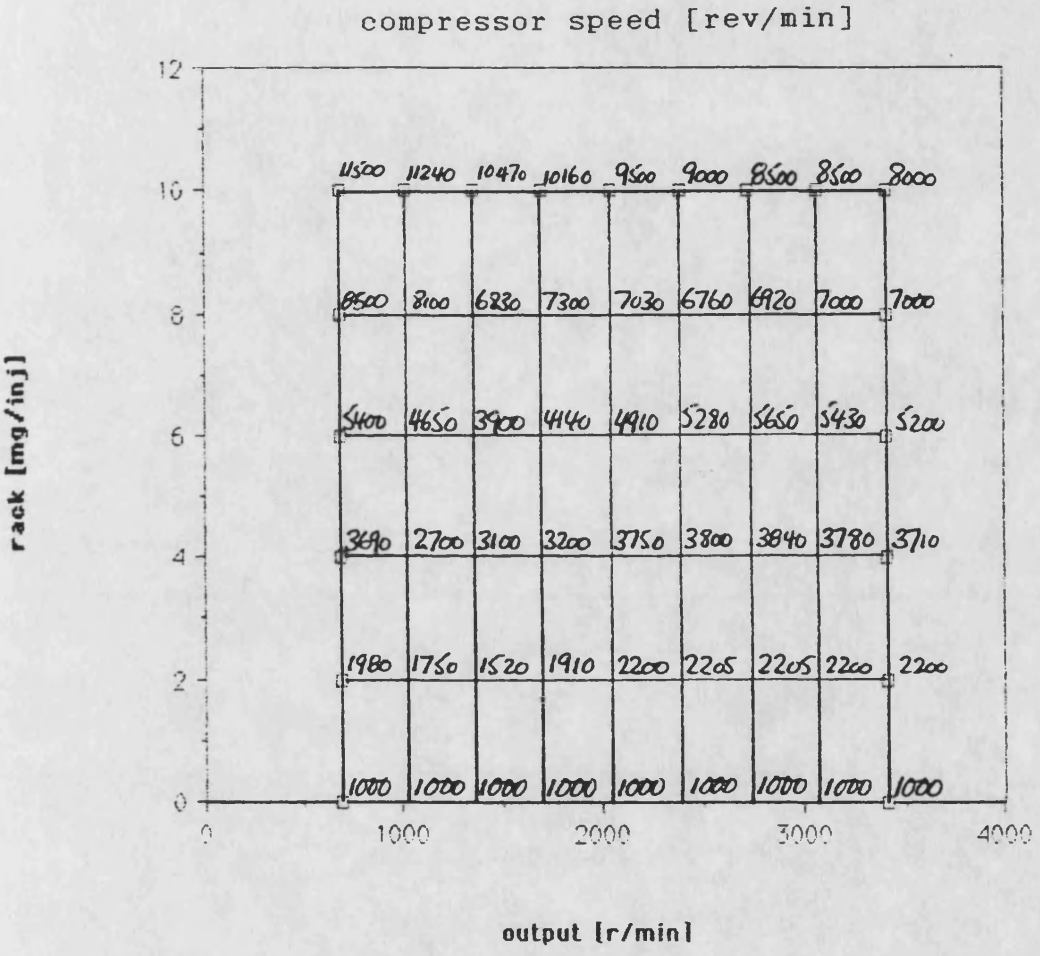

FIG. 4.3 COMPRESSOR SPEED SCHEDULE

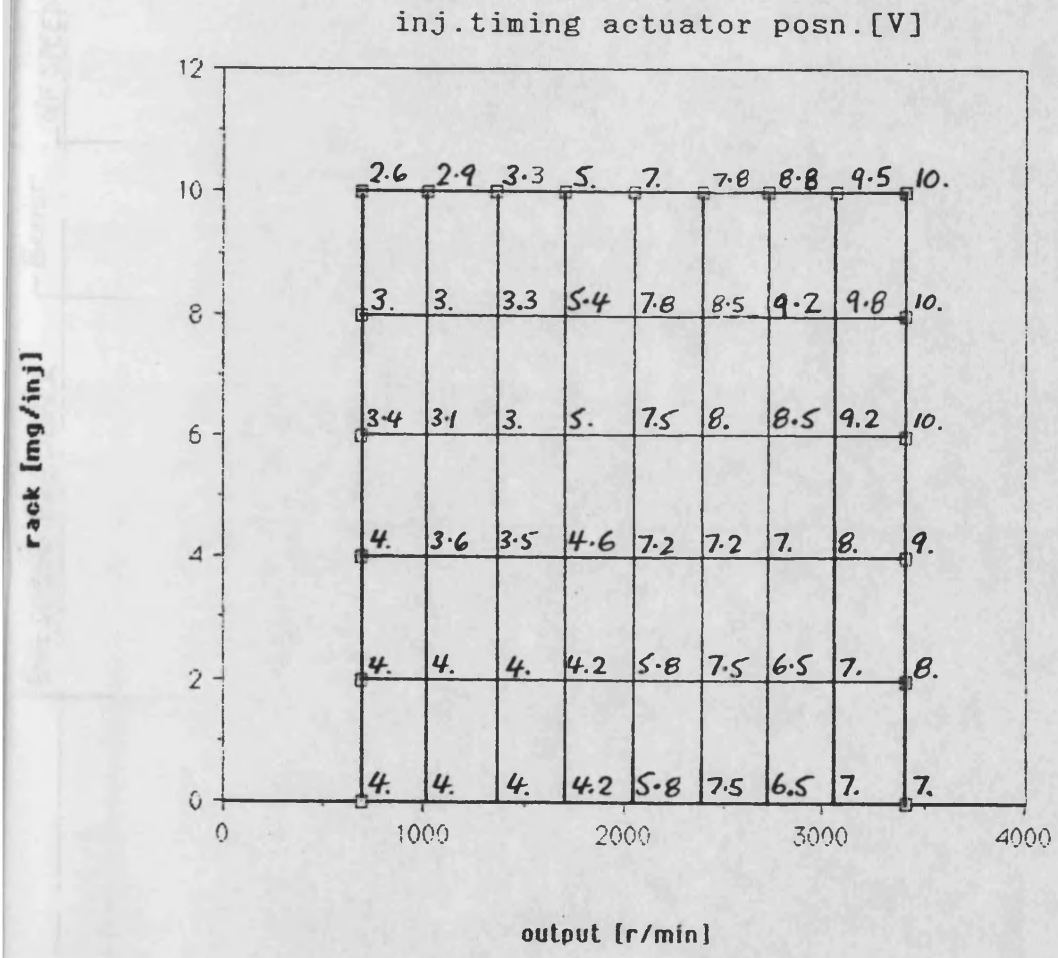

FIG. 4.4 STATIC INJECTION TIMING SCHEDULE

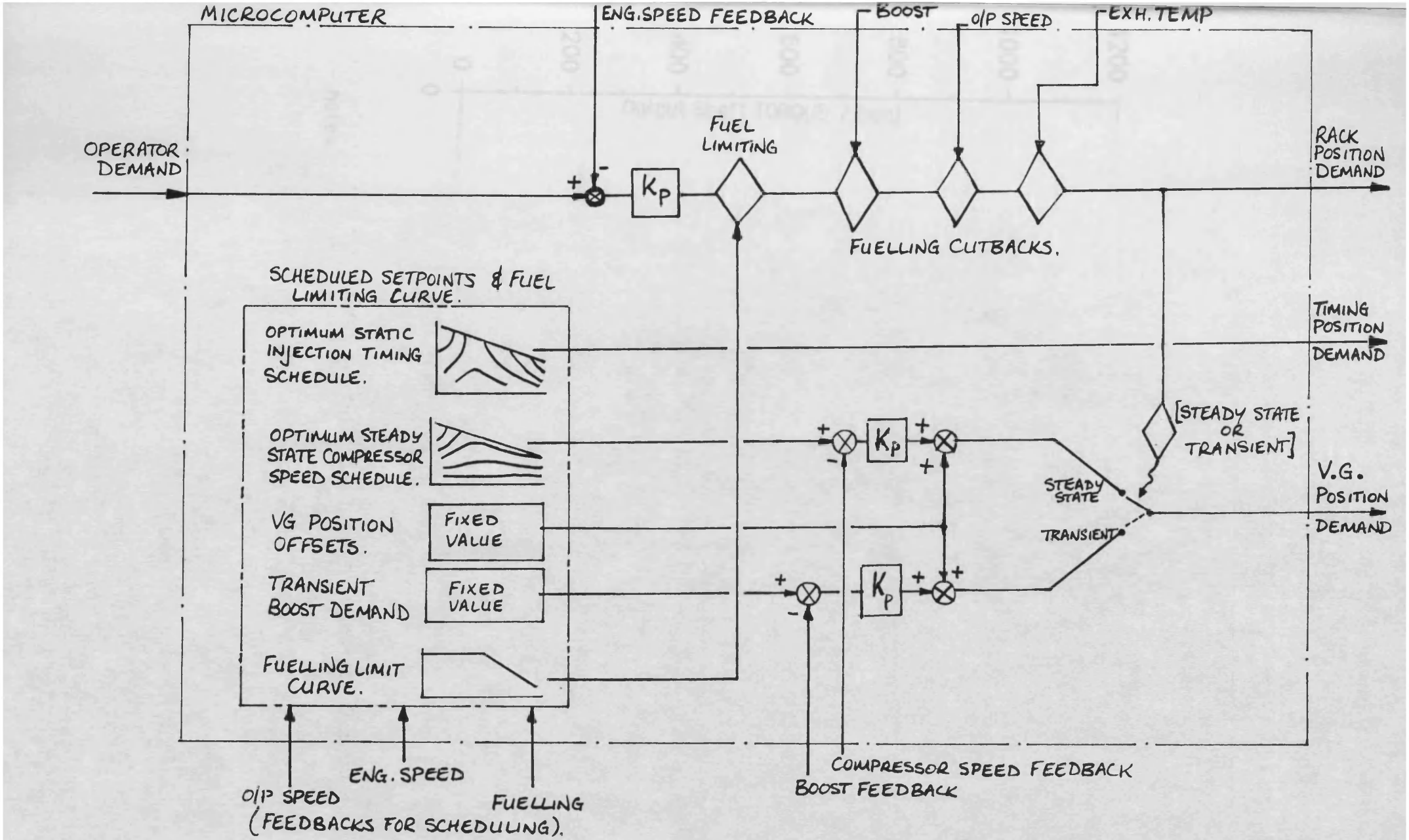

FIG. 4.5 CONTROL LOOPS SCHEMATIC

FIG. 4.6 ENGINE SPEEDS UNDER COMPUTER CONTROL

Note: underlined figures show values under computer control, superposed on original optimum data.

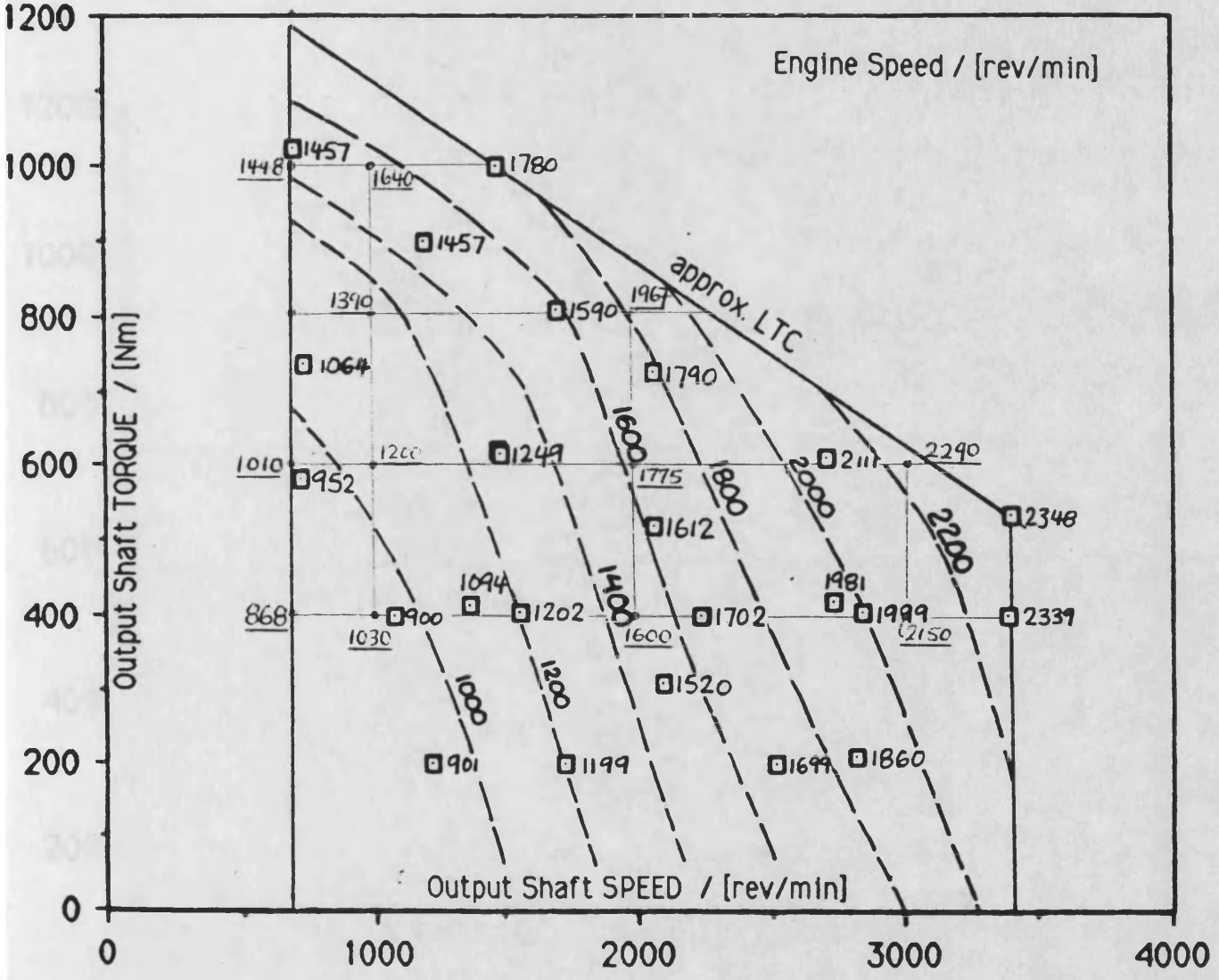

notes: rated output shaft speed 3409 rev/min
minimum output shaft speed 682 rev/min
LTC = limiting torque curve.

FIG. 4.7 LIMITING CONDITIONS UNDER COMPUTER CONTROL

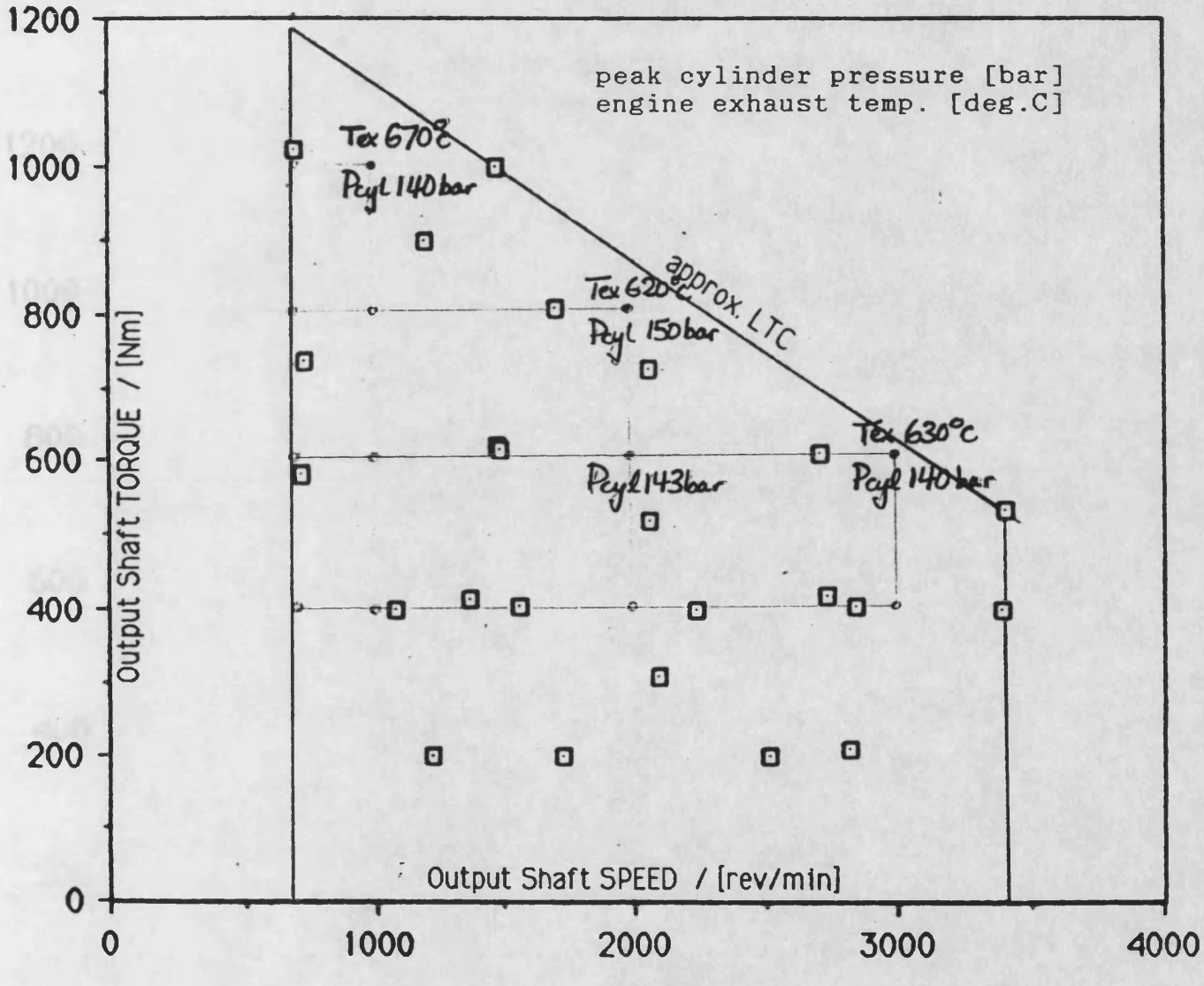

notes: rated output shaft speed 3409 rev/min
minimum output shaft speed 682 rev/min
LTC = limiting torque curve.

FIG. 4.8 OUTPUT SHAFT THERMAL EFFICIENCIES
UNDER COMPUTER CONTROL

Note: underlined figures show values under computer control, superposed on original optimum data.

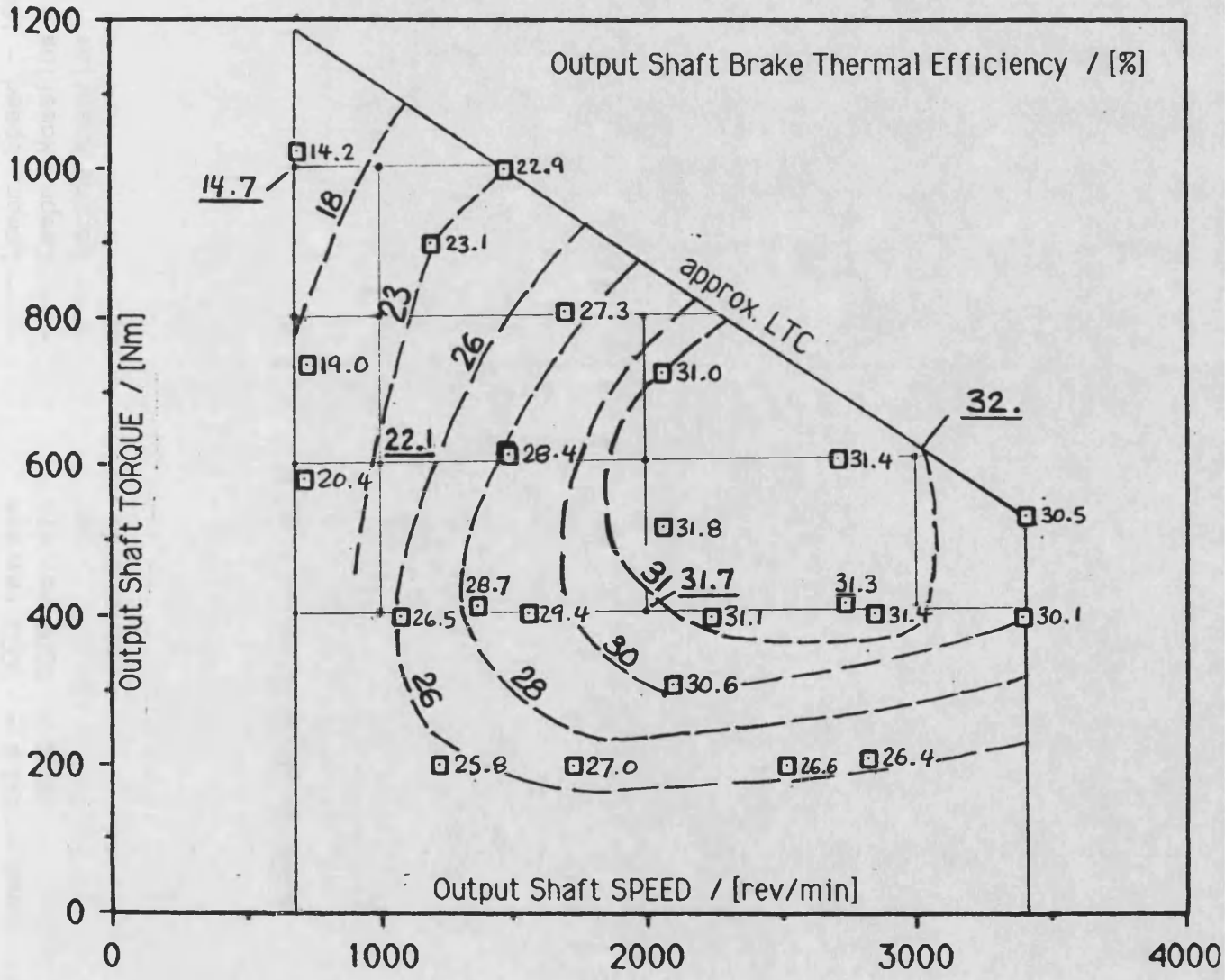

notes: rated output shaft speed 3409 rev/min
minimum output shaft speed 682 rev/min
LTC = limiting torque curve.

DCE transient tests - Repeatability check
5-10V dem. step at 500Nm
FILES: DEMST5, DEMST6, DEMST7, DEMST8, DEMST9

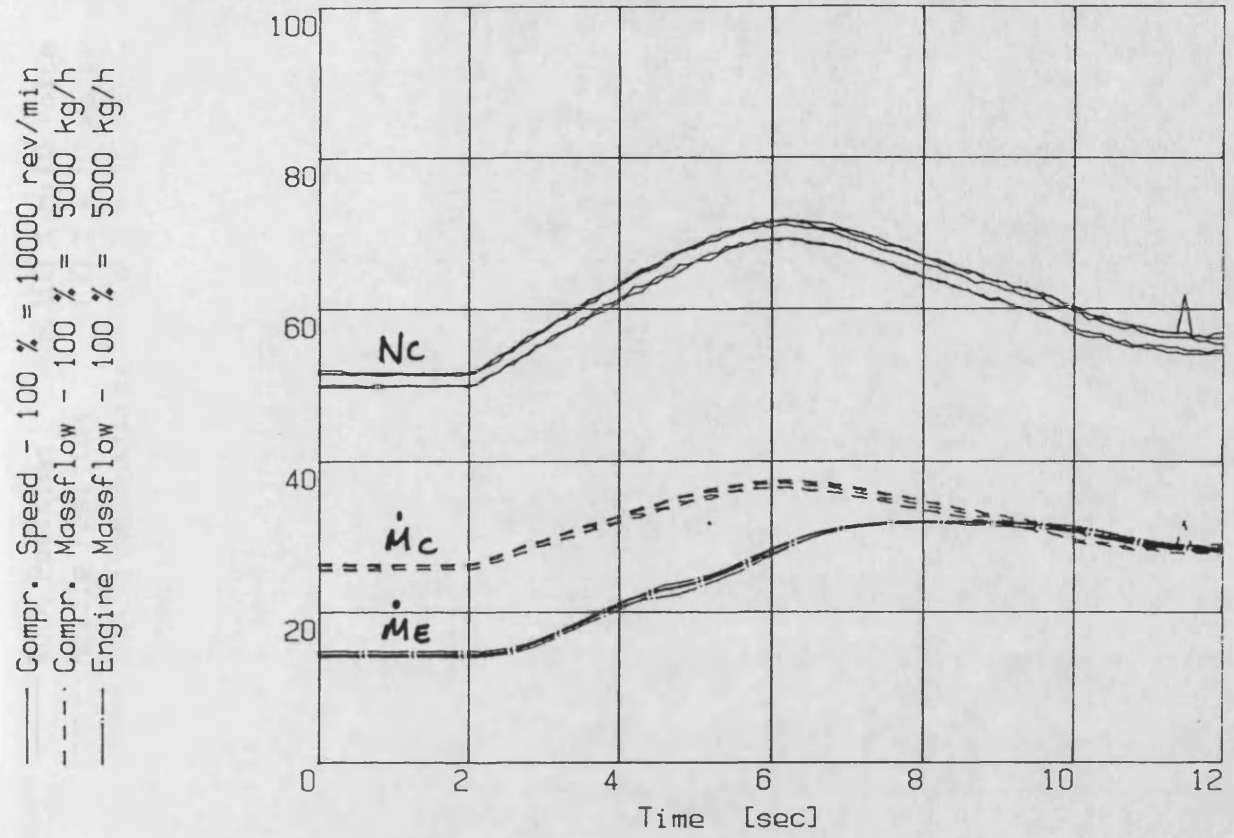

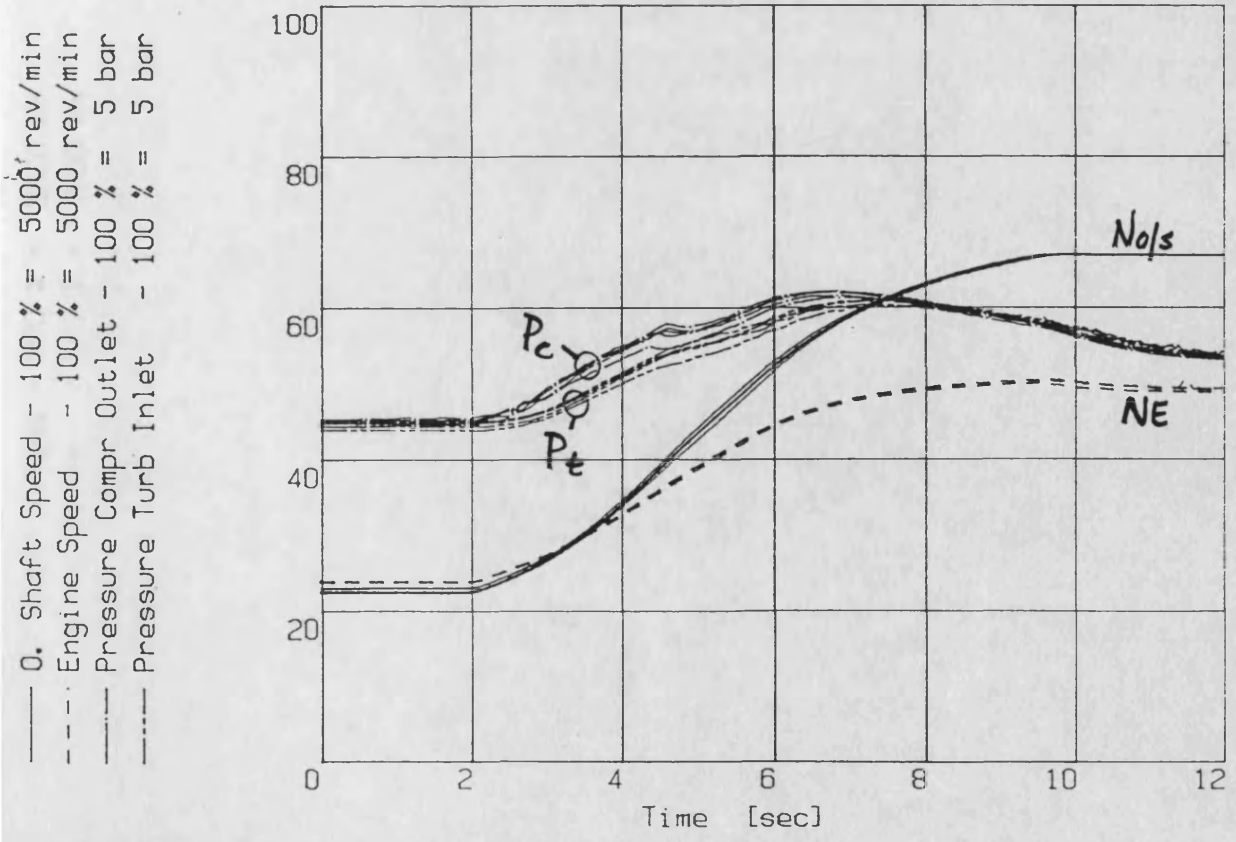

FIG. 4.9a REPEATABILITY CHECK

DCE transient tests - Repeatability check
5-10V dem. step at 500Nm
FILES: DEMST5, DEMST6, DEMST7, DEMST8, DEMST9

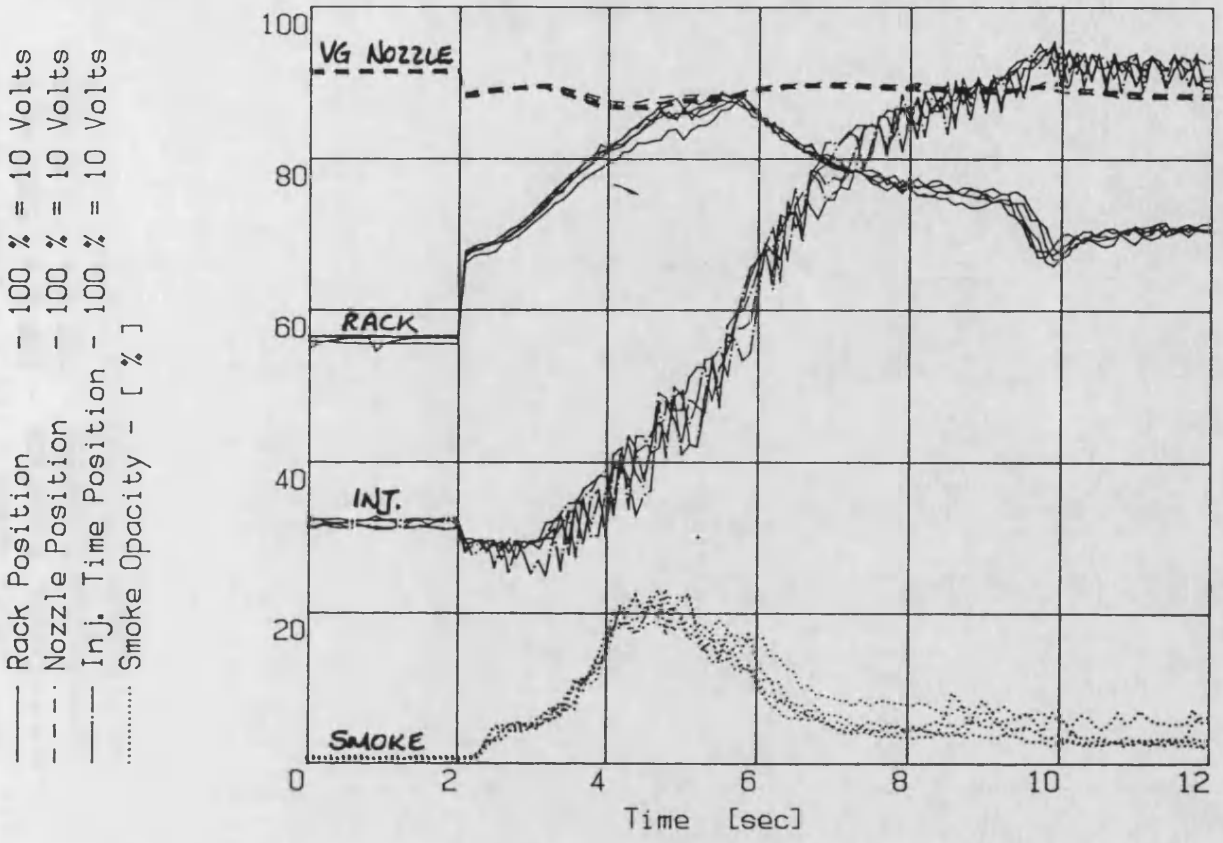

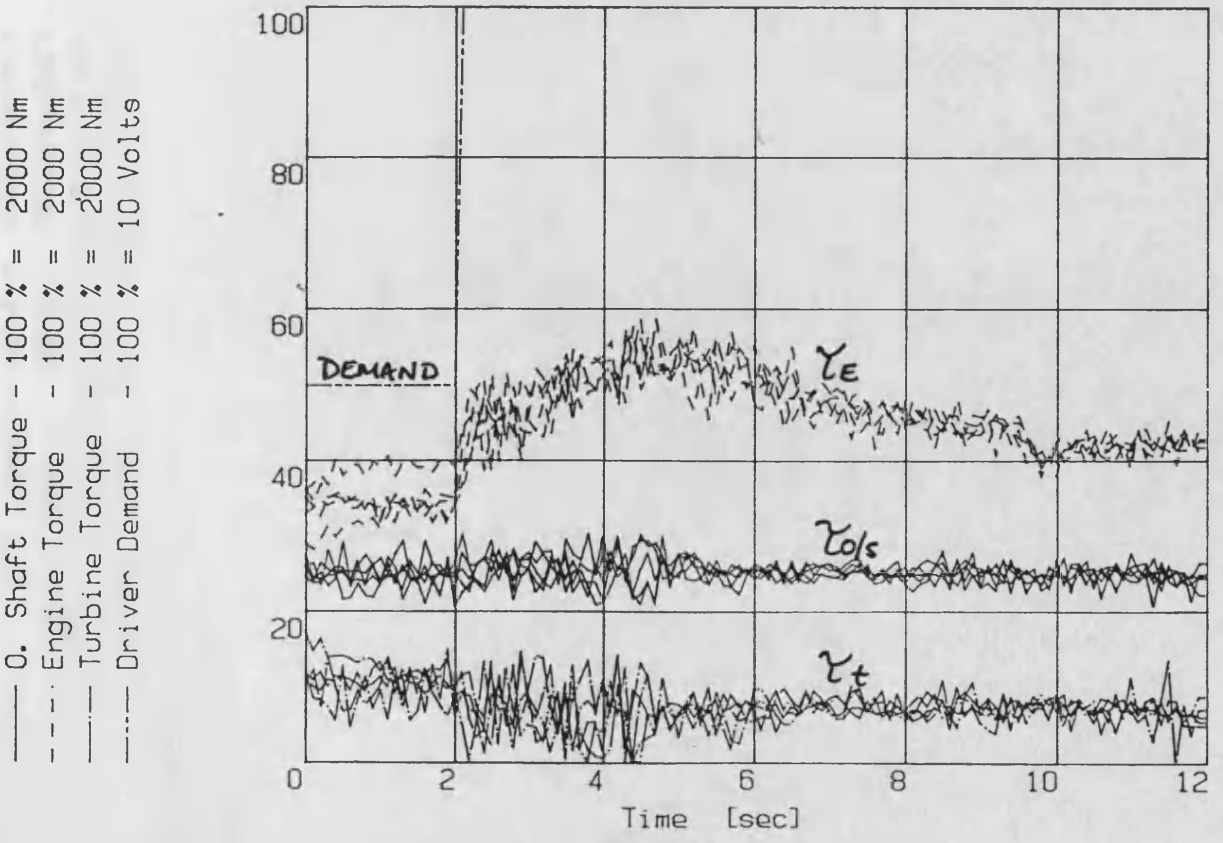

FIG. 4.9b REPEATABILITY CHECK

"DCe transient tests"
"5-10V dem. step at 500Nm"
INPUT FILE : c:\nb\demst3

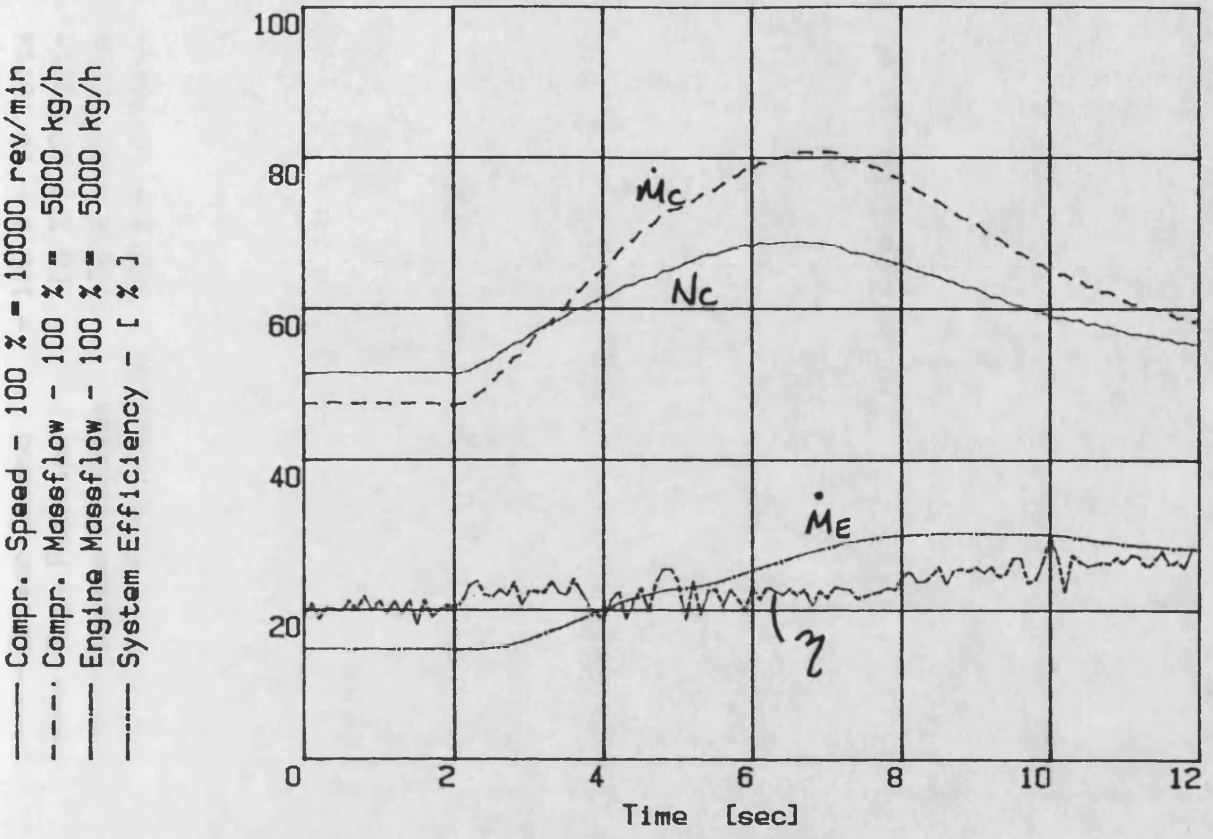

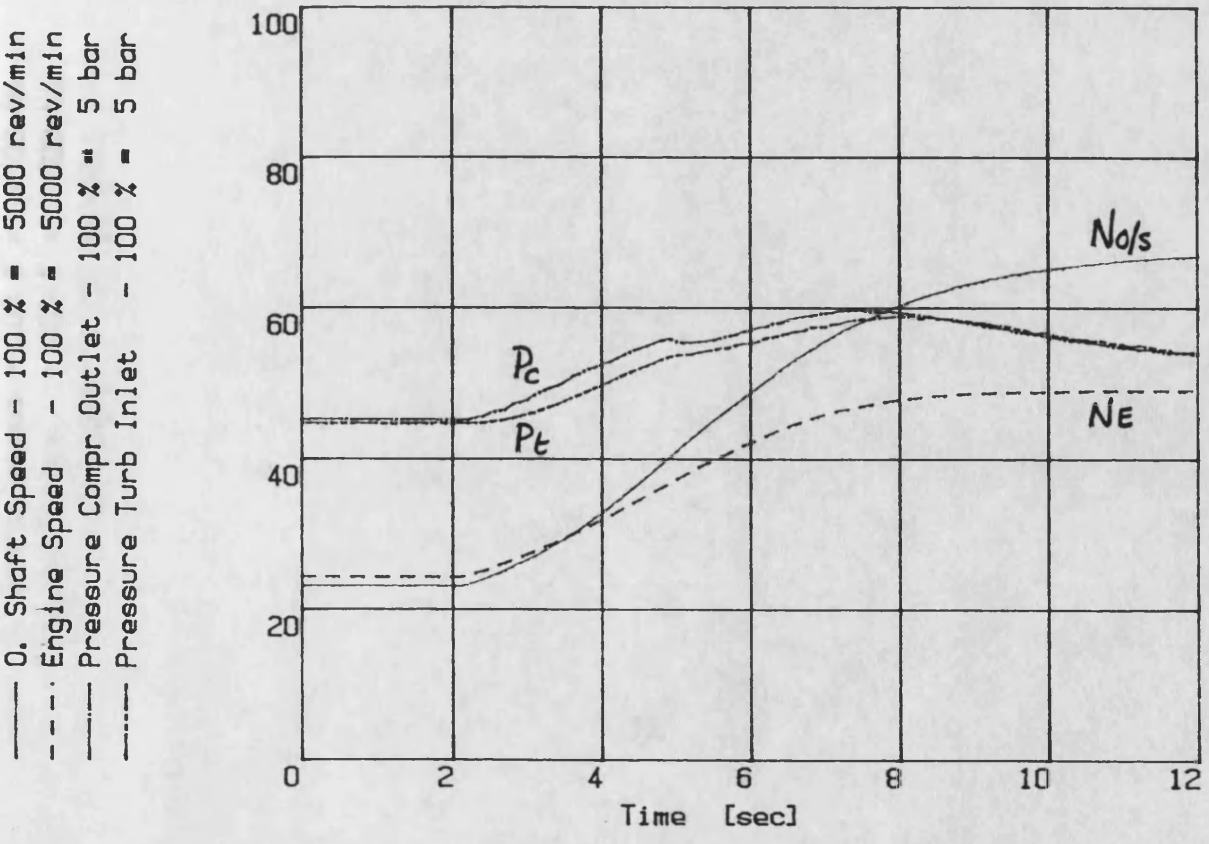

FIG. 4.10a UNCONDITIONED RUN

"DCE transient tests"
"5-10V dem. step at 500Nm"
INPUT FILE : C:\NB\DEMST3

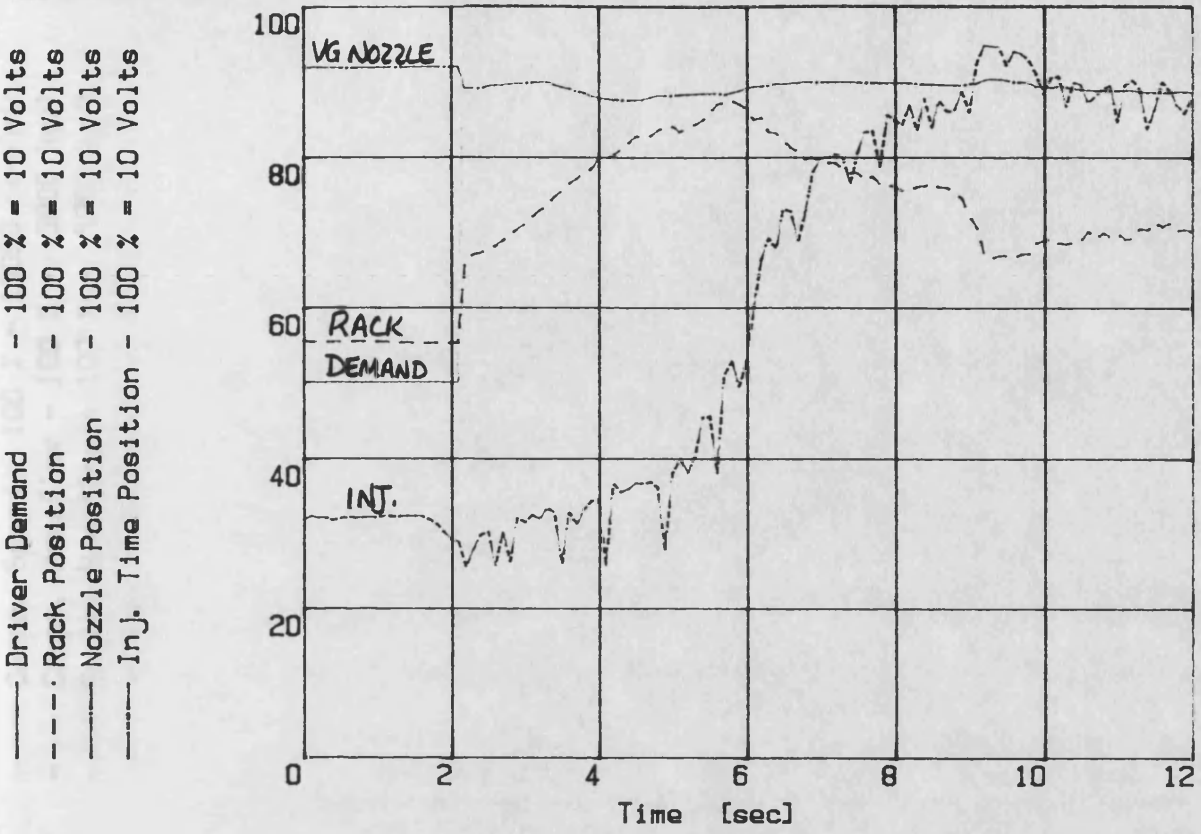

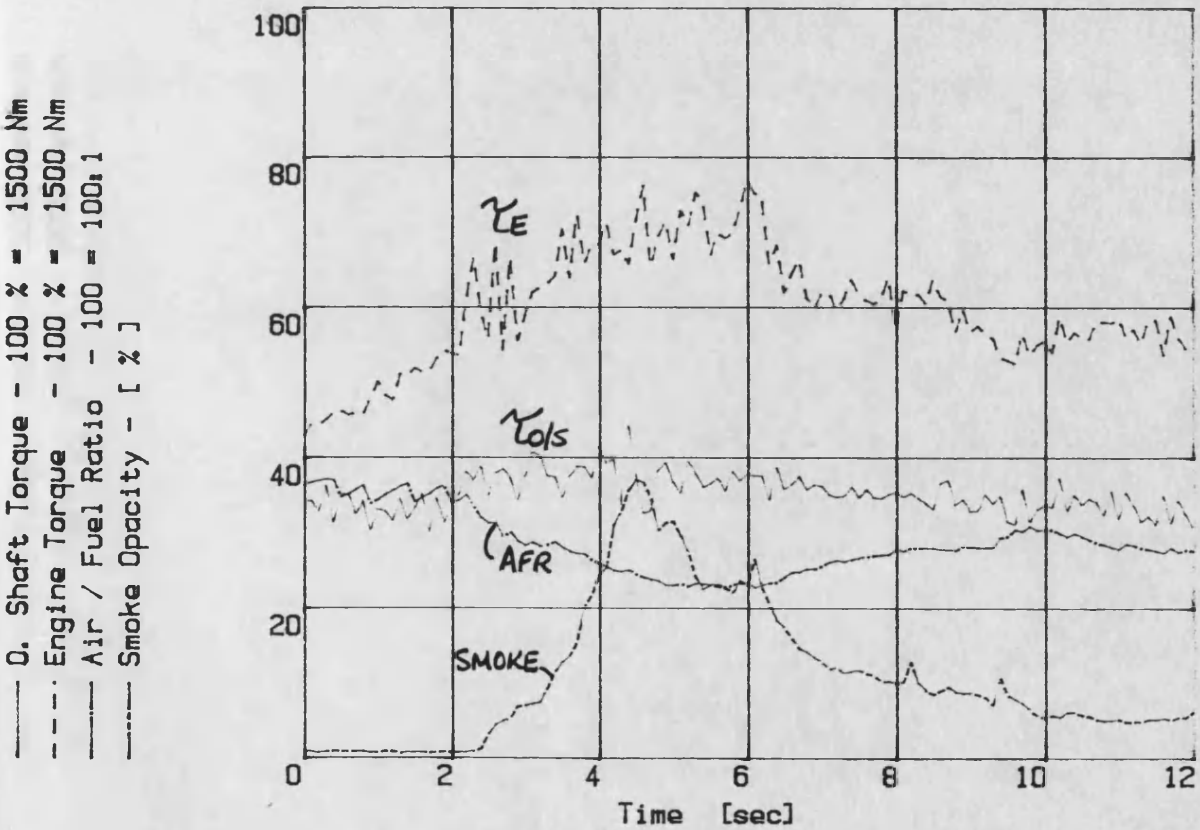

FIG. 4.10b UNCONDITIONED RUN

"DCE transient tests"
"5-10V dem.step at 500Nm"
INPUT FILE : demst8

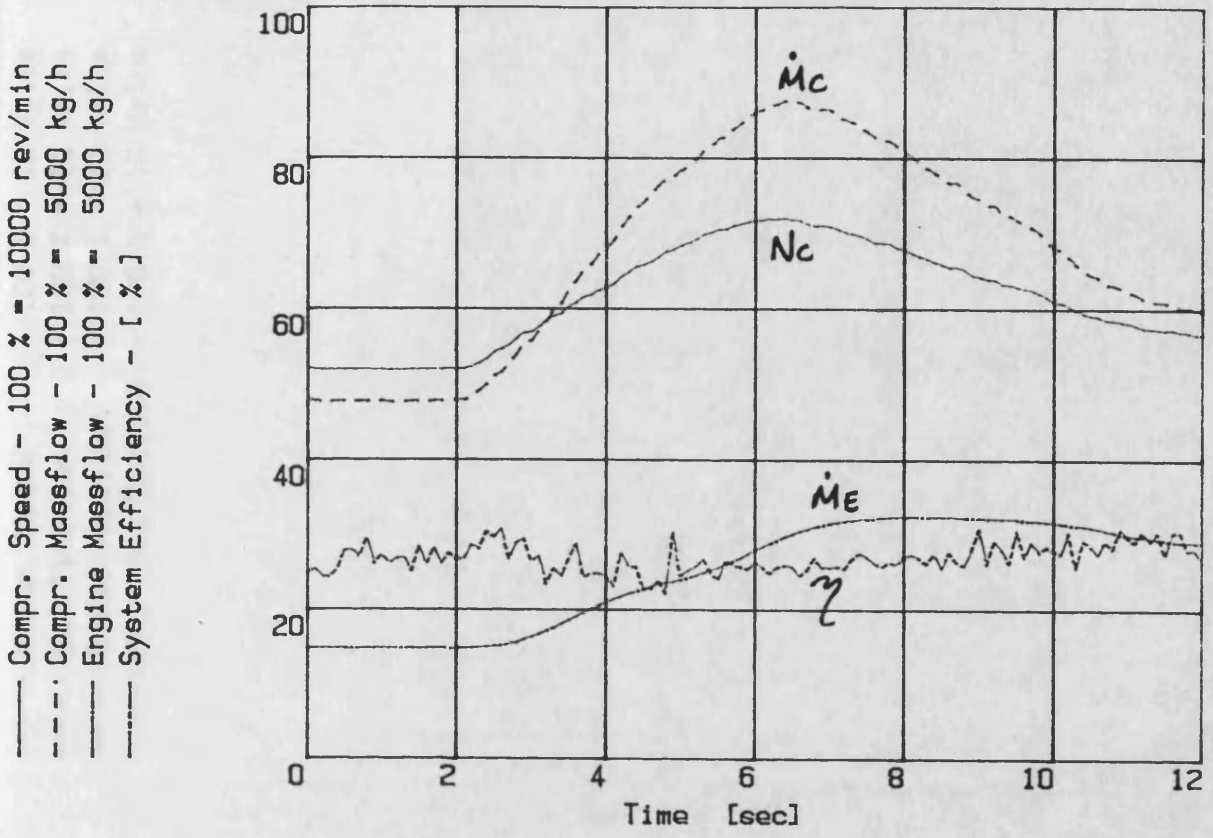

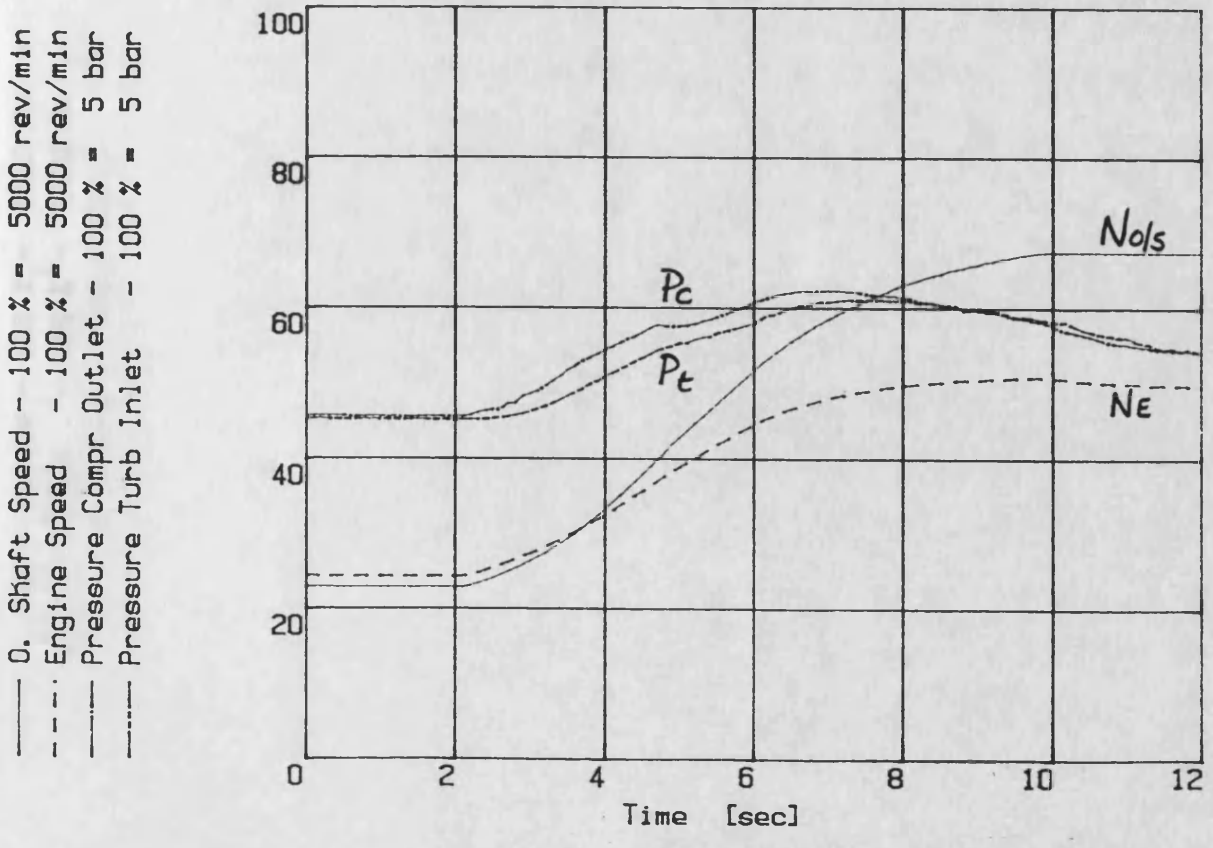

FIG. 4.11a ACCELERATION WITH SMOKE-LIMITING

"DCE transient tests"
"5-10V dem. step at 500Nm"
INPUT FILE : demst8

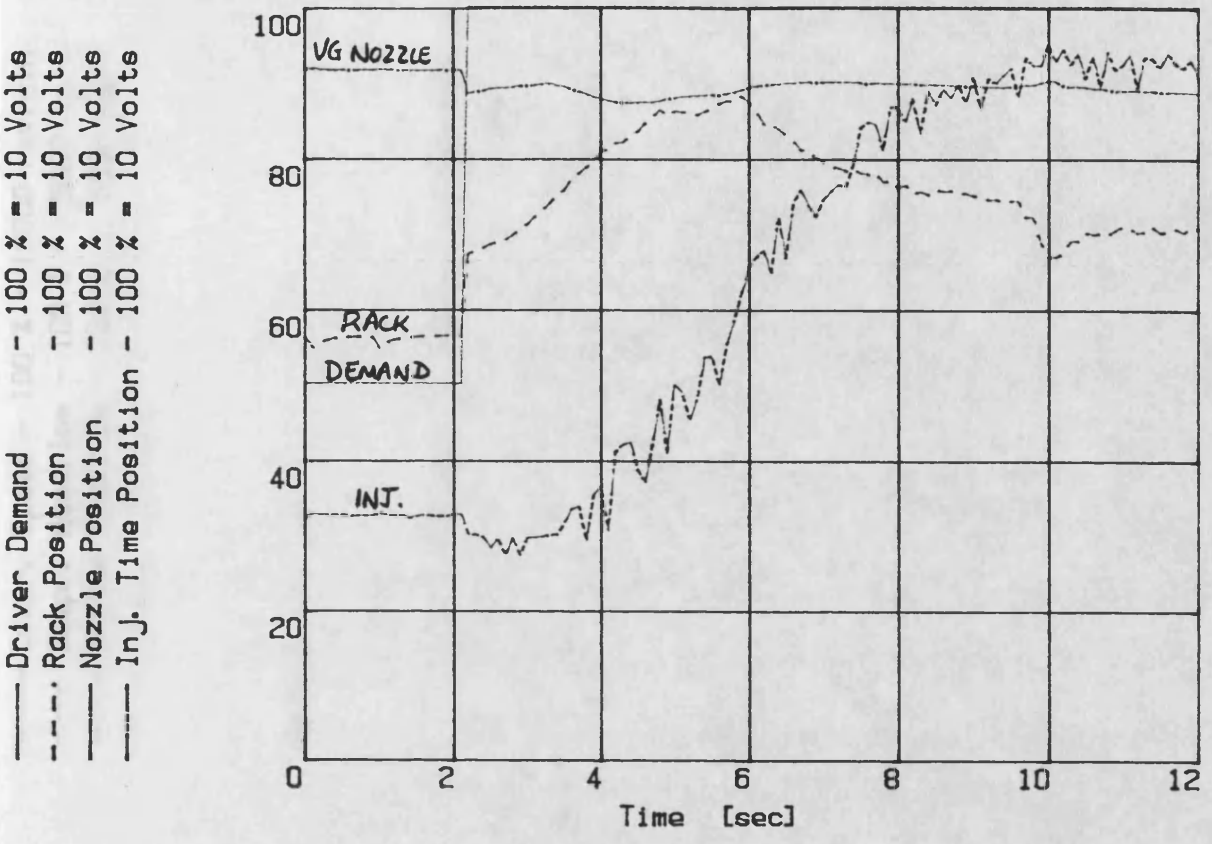

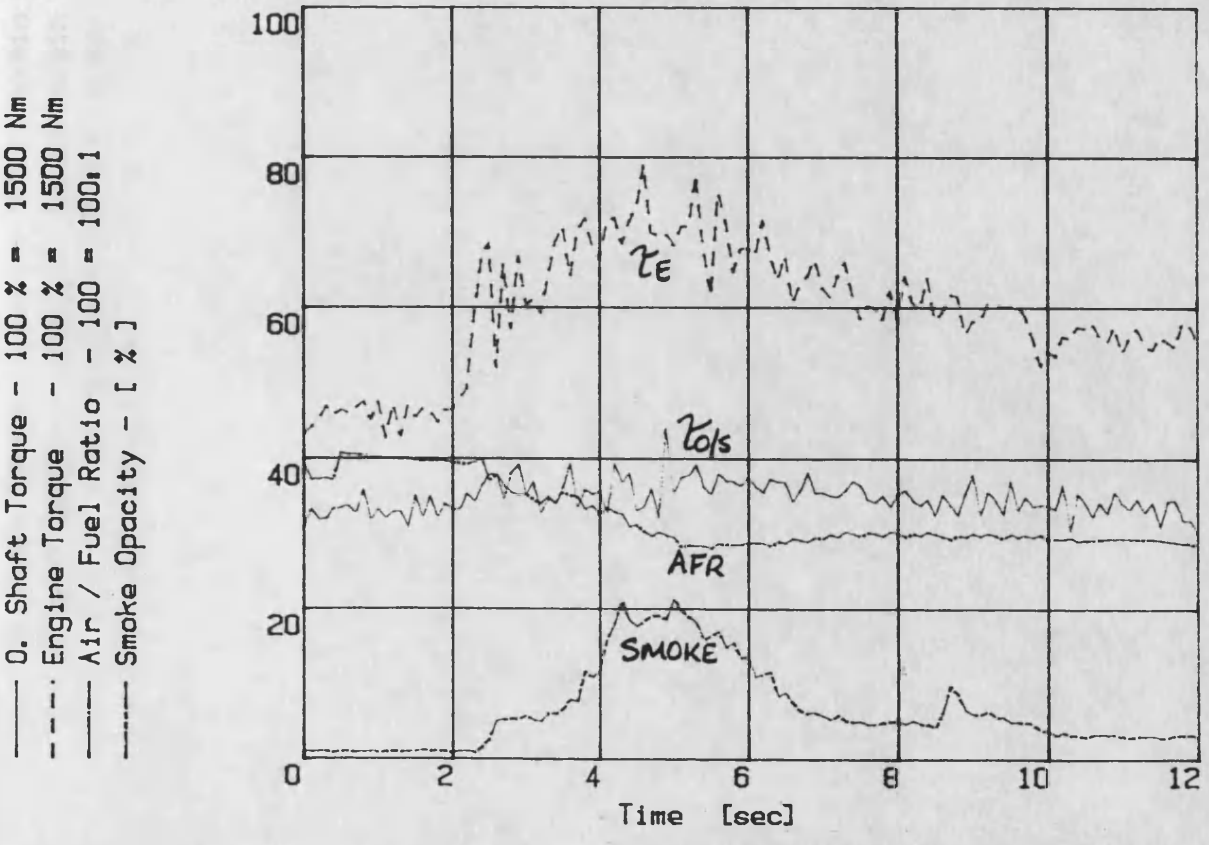

FIG. 4.11b ACCELERATION WITH SMOKE-LIMITING

"DCE transient tests"
"5-10V dem.step at 500Nm"
INPUT FILE : dst11

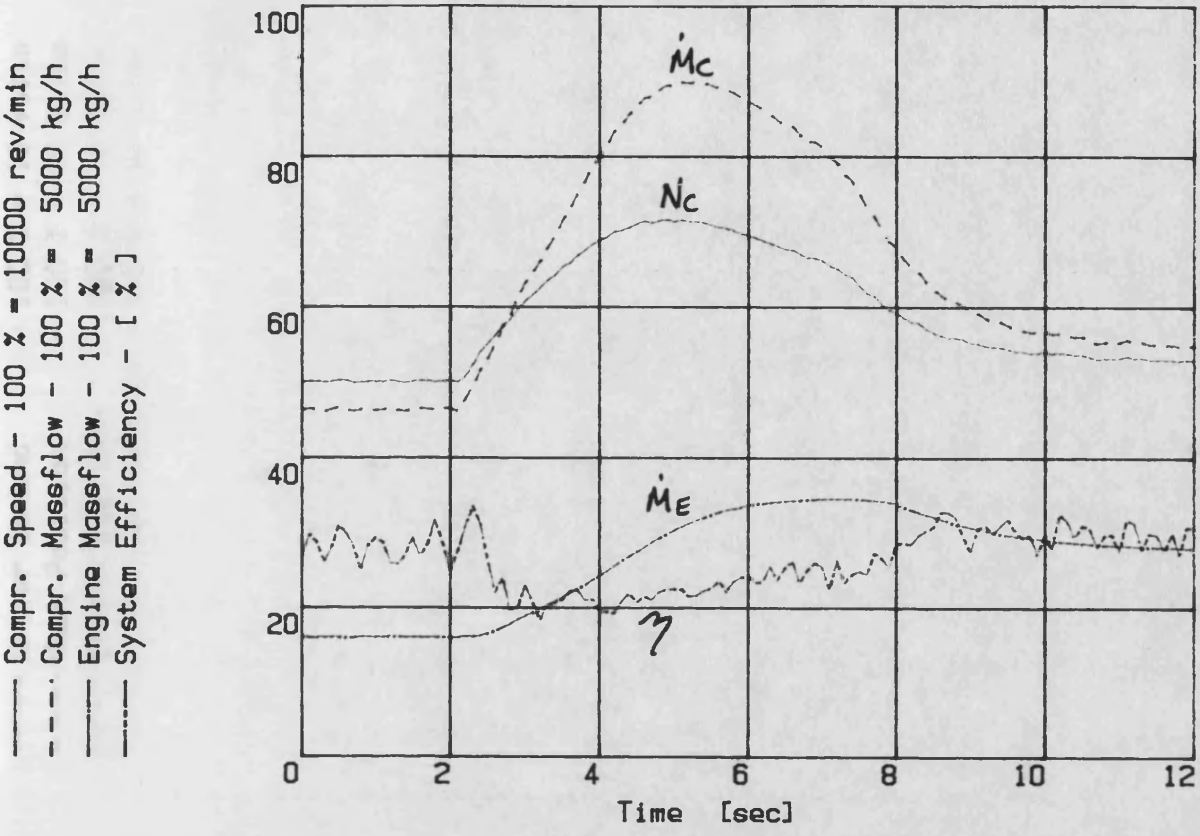

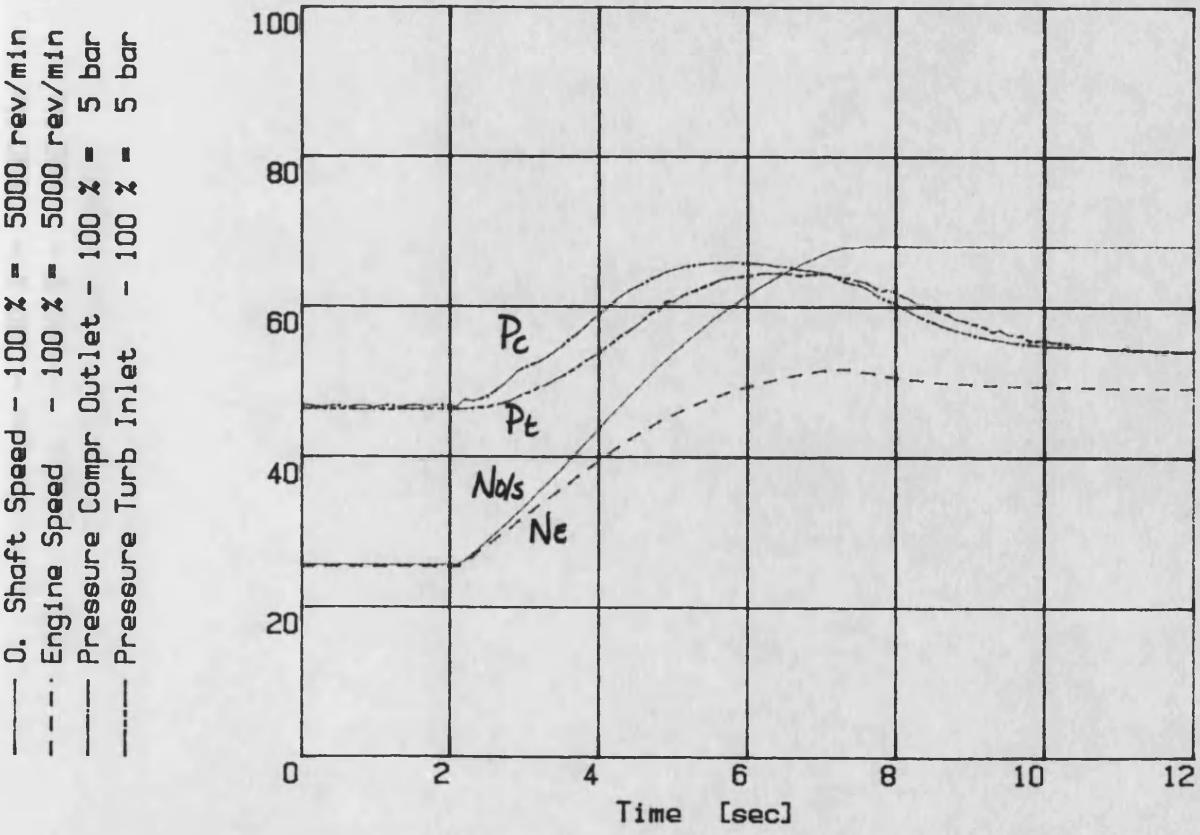

FIG. 4.12a ACCELERATION WITHOUT SMOKE-LIMITING

"DCE transient tests"
"5-10V dem. step at 500Nm"
INPUT FILE : dst11

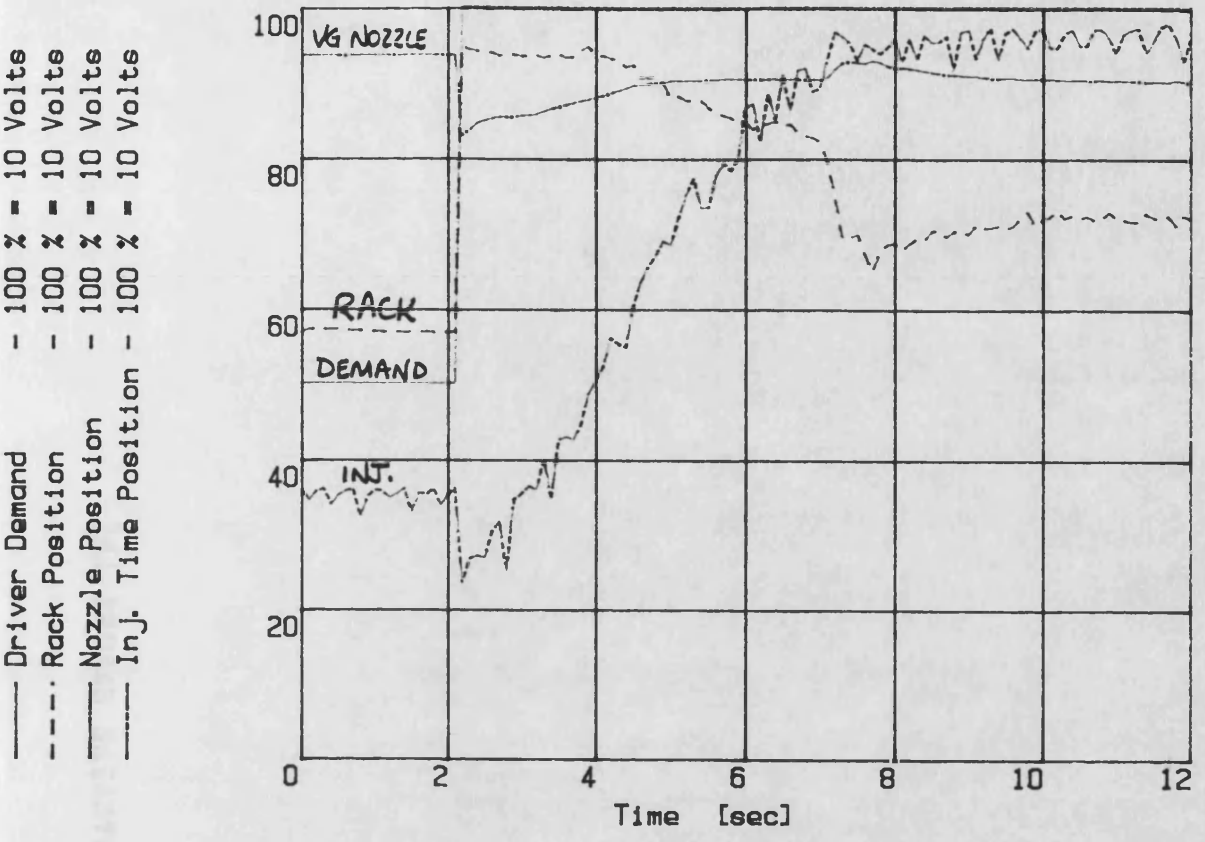

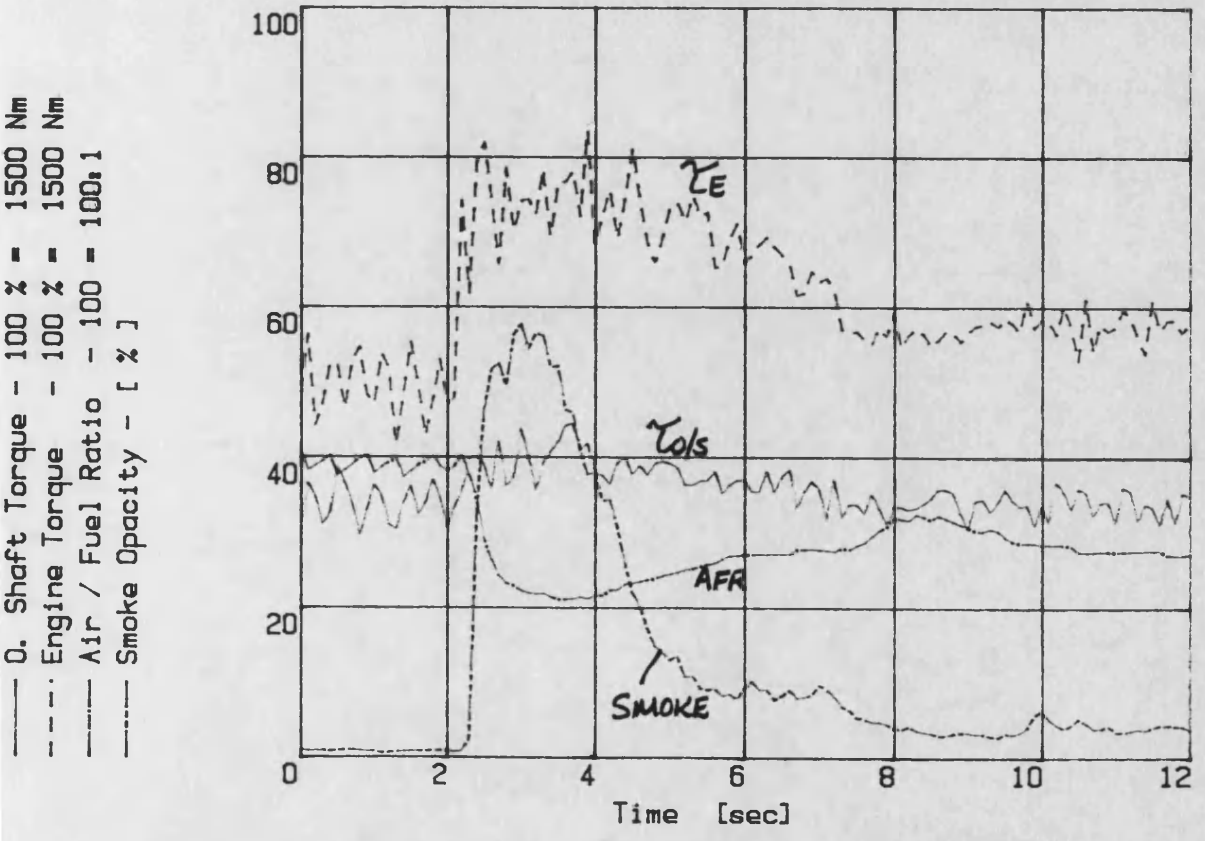

FIG. 4.12b ACCELERATION WITHOUT SMOKE-LIMITING

FIG. 4.13 TRACTIVE EFFORT CURVE

typical 32tonne truck, gearing for vehicle speed 11Økm\h at 34Ø9r/min

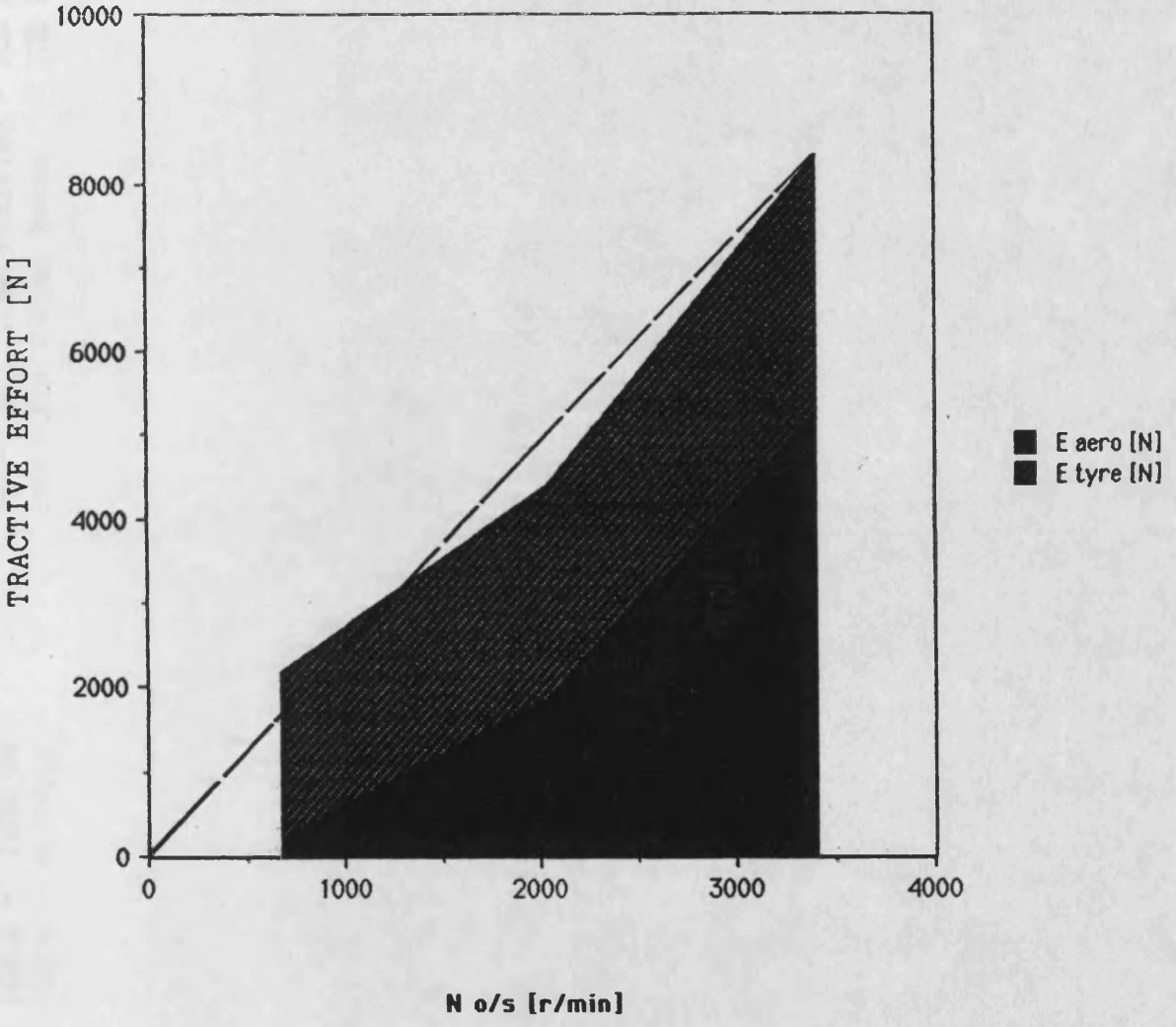

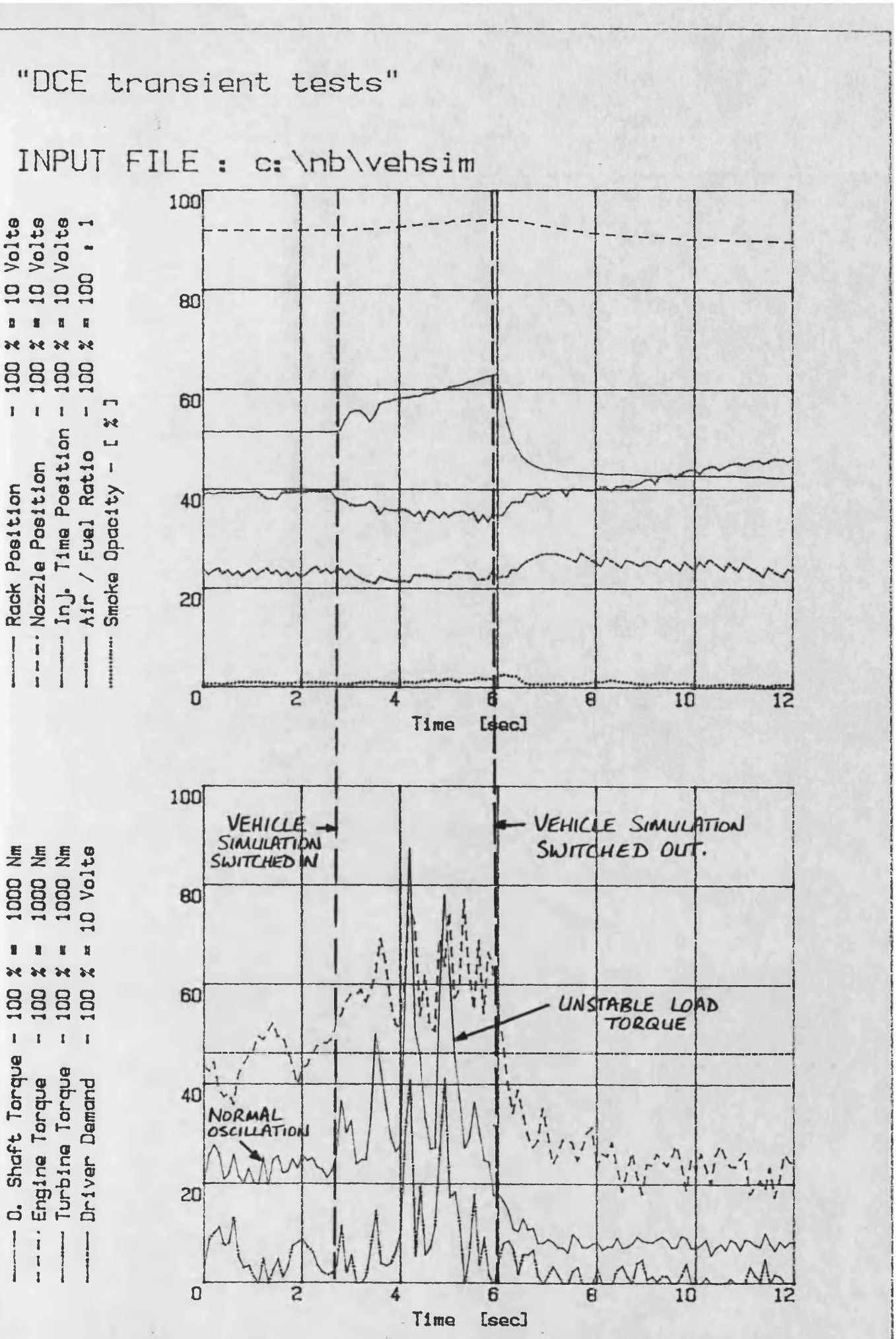

FIG. 4.14 INSTABILITIES WITH VEHICLE SIMULATION

5. DYNAMIC SIMULATION

5.1 Simulation in engine/powertrain design

5.2 Dynamic simulation of the DCE

5.2.1 Introduction

5.2.2 SIMDCE - specification

5.2.3 Hardware/language selection

5.2.4 SIMDCE structure

5.2.5 Main program ("DCECON")

5.2.6 Numerical integration - EULER1

5.2.7 DCE dynamic model - DCECSB/C/E

5.2.8 Controller models - CTRLRA/.../K

5.2.9 Extremal routines - OPTICA/B

5.2.10 Setpoint scheduling - GETSET

5.2.11 Interpolation routines - RITRPS

5.2.12 Vehicle simulation - VEHICL

5.2.13 Output routines - WRITOP/PROUT/PLOT1/2

5.2.14 Using SIMDCE

5. DYNAMIC SIMULATION

5.1 SIMULATION IN ENGINE/POWERTRAIN DESIGN

The importance of computer-based component design and system modelling in engine/powertrain engineering is due to :

(i) The increasing performance per unit cost of computing facilities, and the development of effective modelling techniques.

(ii) The increasing cost of prototype development, and demand for reduced lead times despite generally increasing powertrain complexity.

A complex powertrain such as the DCE therefore relies heavily on system simulation to investigate alternative designs and component selection/matching. Simulation and prototype development should be a feedback process, with prototype results leading to software validation or improvement, leading to more successful prototype design. In commercial terms the simulation must be sufficiently valid at the pre-production prototype stage for design targets (performance, system and component efficiencies, thermal/mechanical loadings etc.) to be met at the first pass, without the need for a second design/build/test iteration.

Several simulation programs have been developed for the DCE, in line with the range of general Diesel engine/systems modelling techniques used at Bath. Their complexity varies from idealisation of the engine cycle to degree-by-degree filling and emptying models, and from a thermodynamic/gas dynamics turbine model to interpolation from steady-state turbomachinery maps.

Predictions from a number of these DCE models are presented in this thesis for comparison with experimental steady-state and transient data. The scope of each model is therefore outlined below.

(i) "CSPDCE" and "CSPDCETRAN"

These are, respectively, steady-state and transient prediction programs with an engine model based on "CSP", a degree by degree filling and emptying model validated for conventional turbocharged engines. The compressor is modelled from a steady-state map. The turbine is modelled by routine TURBW4/TURBWB, a one-dimensional steady flow, adiabatic, model of nozzleless or variable geometry nozzled radial inflow turbines [55]. The epicyclic geartrain model is based on a compound epicyclic model [56], and includes viscous and tooth friction losses. However, the loss coefficients of [56] were matched to one gearbox (Leyland pneumocyclic) and therefore simulation of other gearboxes strictly requires appropriate validated coefficients.

(ii) "DCE3"

Similar to "CSPDCE", but using a simplified 10 point engine cycle model with diagram factor, this simulation was used to check the correlation between early experimental results and system predictions reported in [49].

(iii) "SPICEDCE"

This most recent steady-state and transient DCE simulation is a particular case of the SPICE (Simulation Program for Internal Combustion Engines) general engine/transmission simulation package. The model is set up as a series of pro-forma control volumes, flow paths and shaft junctions, and is run on a crank angle basis. Thus the engine is modelled as a control volume

varying with crank angle, and poppet valves similarly are modelled as flow paths with characteristics varying with crank angle. The compressor and turbine are treated as flow paths characterised by steady-state maps. Where a postulated turbine is to be modelled, the map may be generated by routine TURBW4 mentioned above. A filling and emptying method is used. The epicyclic gear is a particular case of 3-shaft interconnection, handled in the SPICE software by a loss-free 3 dimensional matrix formulation of Newton's second law.

SPICE is detailed in [57]. Development and extensive use to model a DCE based on the Cummins L10 Diesel are described in [58].

5.2 DYNAMIC SIMULATION OF THE DCE

5.2.1 Introduction

The writer's particular interest in simulation was to test and develop control strategies and designs before implementation on the prototype DCE. This required a simulation with the following attributes:

(i) Accurate modelling of dynamic response, matched to the prototype, and incorporating any significant dynamics justifiably ignored in more theoretical predictions, e.g. actuator dynamics.

(ii) Accessible and easily-modified control system models, e.g. separate subroutines linked with the dynamics model.

(iii) Robustness to extreme transients, including simulation of unstable behaviour which may be experienced with ill-tuned controls.

(iv) Simulation setpoint inputs should be analogous to prototype setpoint inputs. As noted in the earlier discussion of steady-state results, existing simulations specify a steady-state

setpoint in terms of fixed parameters (e.g. fuel flowrate, output speed and nozzle angle in the case of CSPDCE) which are at odds with practical prototype setpoint inputs, thus making direct comparisons convenient.

(v) The ability to simulate transient cycles, rather than simple load or demand steps, is required. Vehicle behaviour is of interest, so driveline and road condition models should be incorporated.

(vi) Short run times are always desirable, particularly for this quite interactive application.

A new dynamic simulation package, SIMDCE, was developed to meet the above requirements.

5.2.2 SIMDCE - Specification

Given the general aims of the simulation listed above, a brief functional specification for the software was written. This specification was intended to encompass all possible uses of the simulation, and anticipate future changes and extensions so that these could be made in a tidy and structured way.

It should be noted that at this early stage the author anticipated possible involvement with research on a turbocharged heavy-duty Diesel (Leyland TL11) with V.G. turbocharger and electronic fuelling/injection timing control. Performance development and conventional control studies had been carried out [11], [51], [59], but further work on optimization for operation on variable quality fuels and with charge air temperature control was proposed. At that stage multivariable control ideas had not been pursued. The ability to interchange dynamic models was therefore important. Multivariable optimization methods and their application to the DCE and TL11 are discussed in Chapter 6.

The functional specification is outlined in Appendix (3). SIMDCE meets this specification for the DCE case.

5.2.3 Hardware/Language Selection

A DEC LSI11/23 microcomputer was available in Wolfson laboratory, having been purchased in 1981 and used for setpoint scheduling of the VG TL11 engine in steady-state and transient testing. The LSI11/23 is a 16 bit machine, in this case having hardware floating point arithmetic and 256 kbytes of virtual RAM. Importantly, it was specified with a multi-function card including an RS232 serial interface, suitable for communication with available HP7470A plotters. Having been used for this earlier control design work, it was clearly suitable for the present work.

The LSI11/23 uses PDP11 software. Two high level languages were available; BASIC and FORTRAN. Owing to the age of the machine the latter was FORTRAN IV. However, since F.IV is a subset of later versions, this was an acceptable choice.

Unfortunately, on attempting to recommission the machine, the operating system disk was found to be corrupted, with no backup disk available. A single-user operating system environment was assembled from the original disks supplied by DEC, and no further problems were encountered.

Later in the project an IBM PC-AT compatible microcomputer was purchased for the implementation of microcomputer-based control on the DCE prototype. This faster machine was required due to the increased level of control handled within the computer compared with the V.G. TL11

supervisory controller, as discussed in Chapter 4. It was sensible to take advantage of the increased speed and memory size (plus better editing facilities and system support) for the simulation. All SIMDCE code was therefore transferred via RS232 to the PC-AT. As indicated above, FORTRAN IV is a subset of later FORTRAN standards (in this case Microsoft FORTRAN version 4.1), so the conversion was straightforward.

All SIMDCE code listings in this thesis are as run on PC-AT compatibles.

5.2.4. SIMDCE Structure

The final structure of SIMDCE is shown in figure 5.1. The main change from the proposed structure discussed in Appendix (3) is that the control subroutine (CTRLR) is called directly by the dynamic model ("DCECS-") and the external algorithm ("OPTIC") is in turn a subroutine of the controller. Each can still be replaced independently with no changes required to the others.

Each part of SIMDCE is discussed in turn below. The code is listed in Appendix (4).

5.2.5 Main Program ("DCECON")

A flowchart for DCECON is shown in Fig. 5.2. After initialising arrays for the dynamic model states, scheduled control setpoints, etc., data files are read from disk. These are : - "dcemod.dat", which contains steady-state maps of DCE components, coefficients for linearised correlations used in the dynamic model and other system data.

-"Scheds.dat", which contains linearised schedules of control setpoints for steady-state operation. Again the meaning of these schedules is

arbitrary and depends upon their interpretation by the control subroutine currently in use. Typically they contain boost pressures or compressor speeds and static injection timings for minimum BSFC, and turbine gear ratios to simulate fixed gearing or a CVT. Additional data informs the scheduling subroutine ("GETSET") of the dimensions and scaling of the maps, so that coarser or finer scheduling may be used without modifying the program code.

-"modes.dat", which specifies the "duty cycle". A sequence of up to 20 demand/load conditions may be simulated. If a dynamometer simulation is selected, each "mode" is specified by one feedforward demand, the dynamometer load torque, and the run time in that mode. For a vehicle simulation the mode is specified by the feed forward demand, road gradient, distance in that mode, and servicebraking effort applied. Twenty modes was a limitation imposed by memory size constraints on the LSI11/23 - using PC-ATs the number may be extended if required.

The program branches if a vehicle simulation is selected and reads "truck.dat", which contains the necessary data on the vehicle mass, referred inertia, overall gearing, drag factors etc., then calls "VEHICL" to obtain an engine/transmission output shaft load torque equivalent to the road load for the current mode. Examples of the above data files are given in Appendix (4).

The dynamic model is then run in the first mode until the states have stabilised to within pre-set limits on rates of change. Clearly the stability of output shaft speed for the DCE model depends on the load inertia being modelled, so the convergence limit is adjusted accordingly. On convergence the current operating condition is written

to the data record array, and simulation proceeds through the first mode and on through the specified duty cycle. Again the program branches according to the selection of dynamometer or vehicle simulation. In each case the numerical integration routine (and thus dynamic model) are called at each timestep and the simulation passes through the duty cycle as time accumulates. In the vehicle case, "VEHICL" is called at each timestep to compute the driveshaft load torque, and the distance covered is computed on the basis of mean wheel speed over the timestep, to determine when each mode is completed.

At completion of the run, or on filling of the data record array, "PROUT" is called to generate an output data file, and "PLOT1", "PLOT2" are called to generate two standard plot files which may be output directly to an HP7470A plotter.

5.2.6 Numerical Integration - EULER1

The dynamic models are of state-space type, that is the system is reduced to a set of first order differential equations. The state variables are updated at each timestep by numerical integration of their rates of change. A predictor-corrector technique is used. This is reasonably light on computation and seems to work stably. The convergence limits are relaxed by geometric progression after a certain number of iterations. However, when instability occurs this is generally a valid result of the modelled system's behaviour rather than a fault with the method.

5.2.7 DCE Dynamic Model - DCECSB/C/E

Three basic dynamic models of the DCE have been written for use in SIMDCE, denoted B, C, E. Several other versions exist but differ in minor ways only. These three versions will be discussed in turn.

(i) DCECSB

As discussed earlier in this thesis, the fundamental operating condition (state) of the prototype DCE can be defined by three independent state variables. These are generally best chosen as two epicyclic speeds and one torque or boost pressure, but any independent combination is valid. Thus, with some sacrifice in the accuracy of pressure dynamics predictions, a single control volume (implying a single dynamic boost pressure) may be used, and a suitable dynamic model set up with only three dynamic states. The many other related states (for example engine speed, engine inlet pressure, dynamic torques) may be computed using steady flow pressure difference calculations, and steady-state relationships with due allowance for inertia effects. In earlier DCE research, Howard [37] had recognised this, and had written a simple single-volume model. Although the Leyland 520DCE prototype had not been completed at that time, the model had been matched to a more comprehensive simulation (DCETRAN) and used the same compressor and turbine models, which were applicable to the 520DCE. This earlier model was an excellent starting point from which to develop DCECSB. The following is a description of the final model, in order of computation, indicating how the model was matched to available steady-state data. The gas dynamics model uses a simple form of filling and emptying calculation, on a time rather than crank angle basis. This is illustrated in fig. 5.3.

Compressor

Compressor speed and delivery pressure are known from the previous timestep. Volume flow (FAD) and compressor load torque are obtained from schedules based on steady-state experimental data

obtained from CompAir (the unit is an ex-prototype) and used in DCETRAN. Since the real work is known and the isentropic outlet temperature and work may be calculated, the actual outlet temperature may be calculated. The ideal temperature rise at unity pressure ratio is made slightly non-zero to make the simulation robust to extreme transient conditions.

Charge Cooler

The charge air compressor is thermostatically controlled to approximately 323K. Transient excursions are neglected for simplicity, modelling of the closed-loop heat exchanger - thermostatic feedback dynamics would be complex. A first-order combination of constant air temperature, and constant coolant temperature plus fixed effectiveness might give a better model. The experimentally-obtained pressure losses were significant, as discussed in Chapter 3, and a simple correlation was used to represent these in the model.

Engine

a) Air and fuel flow :

As indicated above, the model runs on a time rather than crank angle basis, and uses a single control volume. The engine is thus treated simply as a steady flow path, and cyclic variations in manifold flows and pressures are neglected. Constant volumetric efficiency is assumed to give volume flow, then massflow may be calculated from charge cooler outlet conditions. The rack actuator dynamics were found in experimental investigations to be significant, and a 2nd order response of rack position to rack position demand is modelled (i.e. using two coupled first order

states-rack position and rack velocity). This is discussed in Appendix (5). Fuelling is obtained from fuel pump calibration tests. Transient testing and modelling was complicated by two pump rebuilds which altered the fuelling characteristic.

b) Torque corrections for Air/Fuel Ratio:

Air/fuel ratio (AFR) is calculated on the basis of clean airflow only, that is using the lower of engine and compressor mass airflows to discount exhaust gases recirculating through the bypass. The AFR is used to scale indicated engine efficiency according to air availability, so inert gases must not be included. Some published data [59], [60] of the effect of AFR on engine efficiency is shown in figure 5.4, together with the correlation used in DCECSB based on limited 520DCE experimental data at low AFRs. A quadratic correlation is used in [61]; however, in this case a very detailed schedule of torque as a function of fuelling and speed was used, and the correlation was applied only below a very low AFR of 18. Apart from requiring extensive experimental mapping (90 points, including motoring conditions in the above case), this latter approach would seem to be poor for a dynamic simulation, since the effect upon torque of differing transient and steady-state AFRs at a given fuelling is not modelled.

To predict the basic torque value to which the AFR-based correlation is applied, two simple approaches are possible. For production engines which may be comprehensively mapped, a schedule of torque as a function of speed and fuelling may be set up [60], [61], [62]. In practice linearised regressions were obtained from the schedules in two of the above references. This second method

is used in DCECSB; IMEP is taken to be proportional to fuelling. This is of course to assume constant ISFC. Figure 5.5 compares the correlation with early experimental data and with CSPDCE predictions, showing that reasonable predictions will be made.

c) dynamic torque delay:

The simple quasi-static model of the engine neglects both cyclic torque variations and pure time delays in torque response to fuelling changes (due to discrete injection). In [60] a similar torque model is run on a crank angle basis and the predicted IMEP was used to scale one of a stored set of "typical" cylinder pressure : crank angle curves. The gas pressure torque and piston/rod torque for each cylinder at the current crank angle were then calculated and added vectorially, to give an overall instantaneous indicated torque. It was nevertheless necessary to choose at what point in the cycle a new fuelling level is taken to change the predicted IMEP. The (computationally costly) generation of individual cylinder torques was presumably enforced because the engine was a V8 with uneven firing intervals. For the DCE, given the evenly-firing IL6 configuration, only the effect of pure injection time delay on torque response was modelled. While this short lag is insignificant to transient response, time delays may affect the behaviour of control systems. It is possible to formulate a difference equation for torque production with a delay (outlined in Appendix (6)), but it would again be necessary to determine the delay. In practice, multi-cylinder engines respond more smoothly: DCECSB uses a familiar [63] first order lag approximation to model torque delay. This is implemented as a difference equation in the engine model, as explained in Appendix (6).

d) Other factors:

Engine friction is modelled as a fixed torque plus a speed-dependent torque. Fortunately, experimental friction data for a conventional turbocharged Leyland 520 was available in [56], and the model is matched to this.

Finally, the effect of injection timing on efficiency is modelled, primarily for use in testing extremal (self-optimising) control algorithms (Chapter 6). No data were available for the Leyland 520, but a representative empirical correlation was formed from data of a 12 litre 6 cyl. TC/A DI Diesel operating at similar BMEPs to the DCE. From DCE experimental data a reasonable correlation was found between static injection timing set by the controller and dynamic timing (Start of Needle Lift-SNL) as shown in figure 5.6. Please note the false zeroes in Figure 5.6; the scatter is chiefly a speed effect, as fuel line pressure dynamics do not change in proportion to engine speed. From the TC/A engine, ignition delay (time basis) was plotted against torque for all speeds (figure 5.7a) and then for individual speeds (figure 5.7b). An approximate correlation of ignition delay with speed and load was thus found. The two above correlations give start of combustion (SOC) timing. The TC/A engine timing swings showed that optimum SOC was always about 0.7 ms BTDC and that the loss of efficiency with time deviation from this optimum was similar over the operating range. Thus a final empirical expression was obtained for the variation in efficiency with SOC timing, as shown in the code listing (Appendix (4)). This gives a representative non-linear model. Although the timing actuator has comparable dynamics to the rack and VG nozzle actuators, the former were

neglected to save computation, since timing has only a secondary effect on the DCE operating condition.

The temperature rise across the engine is calculated from the heat loss to exhaust. This is assumed to be a fixed fraction of the current engine work, i.e. effectively assuming fixed thermal efficiency and fixed percentage heat rejection to exhaust. At low fuellings, isentropic compression is used to give a nominal minimum value of temperature rise.

Bypass

The bypass mass flowrate is the difference of compressor and engine massflows. Gas conditions are taken to be either those at compressor outlet or those in the control volume, depending on the flow direction. The differential pressure across the bypass is inferred from the flow velocity and density (Darcy's method) [64]:

$$\Delta p_{byp} = \rho_{byp} \cdot v_{byp}^2 \cdot k_{byp}$$

Where the friction factor kbyp was chosen to match differential pressures as far as possible with experimental data. Variable bypass closure is modelled , but the single volume model would obviously not hold if the bypass were fully closed, so a nominal minimum flow area is imposed. Valve dynamics are represented by an arbitrary slew rate limit - the prototype's bypass valve was not remotely controlled.

Turbine

As indicated earlier, the turbine model is based on that used by DCETRAN, which was in turn generated by routine TURBWB. The

turbine had not been experimentally mapped at any significant pressure ratios. An initial non-dimensional massflow (NDMF) is calculated either as a fixed value for pressure ratios above choking or as a scheduled function of non-dimensional speed if unchoked. This NDMF is then scaled by the VG nozzle angle. As discussed in Chapter 2, TURBWB predicted a turndown ratio of about 9 in choked NDMF over the VG range (nozzle angles from 30^{o} to 50^{o}), so the accuracy of this scaling is very important. As experimental data became available, predicted and experimental massflows were matched by altering the relation between the measured nozzle actuator position and the nozzle angle used in the model. The nozzle actuator dynamics are again modelled as a 2nd order response (see Appendix (5)).

Turbine thermodynamic work is assumed identical to enthalpy change, i.e. heat rejection is neglected. The pressure ratio comes from the control volume pressure (as shown in figure 5.3 the volume is taken to be at the turbine end of the bypass) and an assumed back pressure. The isentropic efficiency used to calculate the enthalpy change is based on a chosen peak efficiency and an efficiency reduction away from optimum blade speed ratio. The reduction is based on data which had been obtained using TURBW4, as shown in figure 5.8.

Turbine dynamic torque (i.e. after accounting for inertia torque) is calculated such that if a turbine CVT is simulated - by changing the turbine gear schedule - then the inertias are correctly referred. That is, the CVT will appear to be at the low speed end of the turbine reduction train.

Volume Dynamics

The rate of change of pressure in the control volume is obtained from the perfect gas equation

$$P_{vol} \cdot V_{vol} = M_{vol} R T_{vol} \qquad (5.1)$$

$$\dot{P}_{vol} V_{vol} = R(\dot{M}_{vol} \cdot T_{vol} + M_{vol} \dot{T}_{vol})$$

the rate of change of mass $\dot{M}vol$ stored being simply

$$\dot{M}_{vol} = \dot{M}_{comp} + \dot{M}_{fuel} - \dot{M}_{turb}$$

The rate of change of temperature $\dot{T}vol$ is obtained from the energy equation for a quasi-steady open system. Heat transfer is neglected, and K.E. is neglected since the prototype manifolds and plenums are large. Thus :

$$\frac{d(Mu)_{vol}}{dt} = \sum_{i=\text{all paths}} \frac{d(M_i) h_i}{dt}$$

or using mean C_v, C_p for all flows,

$$C_v \frac{d(MT)_{vol}}{dt} = C_p \sum_{i=\text{all paths}} \frac{d(M_i) T_i}{dt} \qquad (5.2)$$

$$\text{ie } C_v(M_{vol} \cdot \dot{T}_{vol} + \dot{M}_{vol} \cdot T_{vol}) = C_p(\dot{M}_{eng\,exh} \cdot T_{eng\,exh} + \dot{M}_{byp} \cdot T_{byp} - \dot{M}_{turb} T_{vol}).$$

$$\text{or } \dot{T}_{vol} = [\gamma(\dot{M}_{e.exh} \cdot T_{e.exh} + \dot{M}_{byp} \cdot T_{byp} - \dot{M}_{turb} \cdot T_{vol}) - \dot{M}_{vol} \cdot T_{vol}] / M_{vol} \qquad (5.2a)$$

To minimise the number of dynamic states the volume temperature Tvol is not numerically integrated from $\dot{T}vol$, but is calculated by assuming perfect mixing of flows entering the volume.

Torque and Inertia Dynamics

The annulus torque is the dynamic engine torque :

$$\tau_{ann} = \tau_{eng} - J_{ann} \cdot \dot{W}eng \qquad 5.4$$

where J_{ann} is the total inertia referred to the annulus, including engine, annulus and engine coupling. Compressor and planet carrier torques are obtained from the epicyclic/step-up gear ratios, using fixed gear efficiencies. These are somewhat nominal since it was difficult to identify individual losses from available overall gearbox loss data. Thus :

$$\tau_{sun} = \eta_{comp.train} \cdot \tau_{ann} / CGR \qquad 5.5$$

where the compressor gear ratio CGR includes the epicyclic and step-up ratios. Note that this implies that the sun torque τ_{sun} is referred to the compressor speed. The input torque to the planet carrier, τ_{pci} is given by :

$$\tau_{pci} = \tau_{ann} / OGR \qquad 5.6$$

where the input gear ratio again includes both epicyclic and step-up ratios. The dynamic planet carrier torque, available at the output shaft, is given by

$$\tau_{pco} = \eta_{pc\ train} \cdot (\tau_{pci} - J_{pc} \cdot \dot{W}o/s) \qquad 5.7$$

where J_{pc} includes only referred planet carrier and idler inertiae, not load inertia.

The developed output shaft torque is the sum of the dynamic planet carrier and referred turbine torques :

$$\tau_{o/s} = \tau_{pc} + \tau_{turb.} \qquad 5.8$$

To summarise, the compressor load torque, τ_{comp}, was calculated as a function of the compressor pressure ratio and speed. The load torque, τ_{load}, was either set directly in the duty cycle or

calculated from vehicle conditions. The developed torques to meet these loads are respectively τ_{sun} (equ. 5.5) and $\tau_{o/s}$ (equ. 5.8). The shaft accelerations are thus :

$$\dot{\omega}_{comp} = (\tau_{sun} - \tau_{comp}) / J_{comp} \quad 5.9$$

$$\dot{\omega}_{o/s} = (\tau_{o/s} - \tau_{load}) / J_{o/s} \quad 5.10$$

Where Jo/s is the referred load (dynamometer or vehicle) inertia, and Jcomp is the total compressor drive train inertia referred to the compressor shaft.

Using the epicyclic speed relations, again with the appropriate step-up ratios, the engine acceleration $\dot{W}_{eng}$ is calculated as a dependent variable :

$$\dot{W}_{eng} = (\dot{W}_{comp}/CGR) + (\dot{W}_{o/s} / OGR) \quad 5.11$$

The engine acceleration so obtained is used to initiate the inertia dynamics calculations from equ. 5.4 at the next timestep.

(ii) DCECSC

This is the second of the three different DCE system models mentioned at the start of section 5.2.7. Its purpose, and differences from the basic model DCECSB, are discussed below.

For automotive applications the behaviour of a powertrain under "power-off" conditions, i.e. whilst coasting or providing engine braking, is of considerable interest. The 520DCE prototype (as modelled in DCECSB) is not configured to operate effectively under these conditions. DCECSC incorporates an over running compressor clutch (sprag) model. The use of this model is discussed in chapter 7.5. DCECSC is based on DCECSB, using an extra dynamic state for separate compressor and compressor drive train dynamics.

As for DCECSB, all compressor dynamic calculations are referred to the compressor shaft. In this case two states ("Ncomp" and "Ncdrv" in the code - see listing in Appendix (4)) are used to represent respectively the compressor speed, and the sunwheel speed referred to the compressor shaft. This implies that the sprag is fitted at the high speed end of the train, but for modelling purposes this is unimportant since the compressor inertia dominates the gear train (being 96% of the total in the 520 DCE).

Engagement/disengagement of the sprag clutch is modelled as follows :

Step 1 Assume the sprag is disengaged, and calculate compressor and drive train accelerations independently. Compressor speed (Ncomp) and drive speed (Ncdrv) are states available from the last numerical integration.

Step 2 The sprag will transmit power (engaged) only if Ncomp $\leq$ Ncdrv and $\dot{N}$comp $<$ $\dot{N}$cdrv.

Otherwise the compressor is over running (disengaged).

Step 3 If the sprag is disengaged the accelerations from step 1 apply. If it is engaged then impose speed compatibility - set the two states equal; and impose acceleration compatibility - recalculate $\dot{N}$cdrv with compressor load torque and inertia present, then set $\dot{N}$comp equal to $\dot{N}$cdrv.

The remainder of the model is identical to DCECSB.

(iii) DCECSE

This is the third and final DCE model mentioned above. It uses a two-volume model of the air system, for the reasons described below:

Modelling of power-off conditions, discussed in Chapter 7.5, indicated the importance of bypass flow control. Furthermore, some form of compressor bypass was required to enable the engine to operate with the compressor stopped. A two control volume model was therefore written, since the system would now have two unknown bypass pipe flows. This is illustrated in Fig. 5.9. Note that to reduce the complexity of a practical system, flow valves are proposed, operated naturally by pressure gradients to allow primarily undirectional flow.

Flow through compressor and engine bypasses is dependent upon the differential pressures and the current flow areas. The flap valves give 0 to 100% bypass closure. The direction of flap valve movement (opening or closing) is set by the direction of pressure gradient. The valves are assumed to move in the appropriate direction at a chosen maximum slewrate regardless of the magnitude of the pressure gradient. This gives a simple but realistically "damped" model.

The individual volume dynamics calculations are similar for both volumes to those used in DCECSB. The program listing (appendix (4)) is well commented, so the equations are not repeated here.

As indicated above, there are two unknown bypass pipe flows, connected to the compressor side control volume. Thus the quasi-steady state calculation of bypass flow used in DCECSB cannot be used. All component and bypass flows are independently dynamically calculated. Use of a poor or ill-matched pipe flow model would give poor predicted pressures in the control volumes.

By running the simulation to steady state the predicted massflows should be compatible at a realistic differential pressure between the control volumes. This differential pressure is available from steady-state tests for validation if we take compressor and turbine plenum pressure to be analogous to control volume pressures.

Two methods were considered to model the bypass flows. Initially an orifice analogy was considered, since in this case partial bypass closure (effectively a variable-area orifice) was of interest. Secondly, a simpler pipe friction model was evaluated.

The orifice analogy is commonly used for port/valve modelling in engine simulation. This assumes negligible inlet velocity c.f. orifice velocity. For the steady 1D case, and assuming there is no expansion downstream of the orifice, it may be shown [64] that

$$\dot{m} = C_d A_{orif} p_1 \sqrt{\left\{ \left(\frac{2\gamma}{\gamma-1} \cdot \frac{1}{RT_1} \left[\left(\frac{p_2}{p_1} \right)^{2/\gamma} - \left(\frac{p_2}{p_1} \right)^{\frac{\gamma+1}{\gamma}} \right] \right\}} \quad (5.12)$$

where 1,2 are the upstream and downstream conditions respectively. The discharge coefficient was included for matching to experimental data. Table 5.1 shows the Cd required to match equ. 5.12 to steady-state data (with bypass wide open) over the operating range. Matching is somewhat unreliable due to the low differential pressures usually encountered, which also imply poor experimental flow measurement accuracy discussed in Chapter 3. Poor predictions, that is the need for low Cd's, might also be expected since in practice the engine bypass when wide open is a constant area pipe with bends and sharp-edged junctions. With increasing bypass closure the model might be more applicable.

The simpler alternative was to invert Darcy's method used in DCECSB, giving :

$$\dot{m}_{byp} = K_{byp} \cdot A_{byp} \cdot \sqrt{\Delta p_{byp} \cdot \rho} \qquad (5.13)$$

where K_{byp} is the reciprocal of a friction factor. Again the K_{byp} required to match steady-state experimental and predicted flows (wide open bypass) are shown in Table 5.1. The range of K_{byp} and Cd required is similar for these conditions.

The latter method was adopted (less computation) and gave reasonable results with a fixed mean K_{byp}.

All other aspects of DCECSE are identical to DCECSB.

5.2.8 Controller models - CTRLRa/.../K

The function of all versions of the controller subroutine is similar. Using a single feedforward demand, scheduled setpoints, and other DCE parameters as required, the controller generates inputs to the rack, nozzle and timing actuators in the dynamic model. Additional inputs such as bypass valve or turbine CVT ratio settings may also be generated. The model and controller may be run with differing timesteps to simulate a digital controller's discrete time operation.

The subroutine is replaced to investigate alternative control strategies or control design techniques. It may also be replaced by software to carry out system identification. Rather than describe each version here, individual subroutines are introduced with their corresponding results in Chapter 7 and 8.

5.2.9 Extremal routines - OPTICA/B

As mentioned earlier, the simulation was to be used to evaluate self-

optimising (extremal) setpoint controllers. Extremal routines may therefore be called by the main controller subroutine (see program structure in fig 5.1). The theory and implementation of extremal methods is discussed in Chapter 6.

5.2.10 Setpoint scheduling - GETSET

At steady-state, the control subroutine is generally required to control the DCE model to run at optimum output shaft efficiency. This condition is specified by scheduling the "free" states of the DCE to their optimum values at the current operating point. The routine can handle up to 3 schedules, with flexibility in selecting the two variables on which the schedules are based and the scheduled variable. An example would be to schedule compressor speed and injection timing for best efficiency on a base of o/p shaft speed and torque, and to schedule turbine CVT ratio on the same base to model the fixed gearing using the prototype. Setpoints are interpolated from the 2 dimensional schedules using routine RITRP2, outlined below.

5.2.11 Interpolation routines - RITRPS

RITRPS comprises 1 and 2-dimensional linear interpolation functions.

5.2.12 Vehicle simulation - VEHICL

In both dynamometer and vehicle simulations the dynamic model is given a driveshaft load torque. As shown in the DCECON flowchart (fig 5.2), in a vehicle simulation this torque is calculated by VEHICL using data about the vehicle (data file truck-dat) and about the road conditions (gradient and service braking effort) in the duty cycle.

The vehicle is modelled as a rigid load. Complex driveline (propshaft/axle/wheel and tyre) dynamics would be important when

evaluating driveline-engine-controller interactions for a production vehicle. For the current work on a research prototype with a variety of potential applications, the rigid load model is a sensible basic case. Driveline dynamics would be included in the dynamic model rather than VEHICL since this does not communicate with the numerical integration routine.

As discussed in Chapter 2, in a vehicle installation the gap between driveshaft "stall" speed (20% of rated speed in the 520DCE) and zero speed would be bridged by a torque converter with bypass ("lock-up") clutch. Torque converters are proprietary devices; their torque/speed and efficiency characteristics may be empirically modelled using manufacturers' data. Typical data for a high torque ratio device suitable for the 520DCE is shown in fig. 5.10.

Service (i.e. wheel) braking is modelled simply as an additional tractive effort. Driver braking is not easy to model; different combinations of service braking and engine braking (downchanges or exhaust braking, or a particular control strategy for the DCE) may be used and the amount of braking done on a given route depends on driving technique. Thus the modelling of driving technique is very important when simulating vehicle route performance [65]. An acceptable approach might be to interpret the "braking" input as a maximum vehicle speed on each route segment, and apply full engine braking plus proportional service braking with excess vehicle speed. Some chosen engine braking strategy must be incorporated in the controller model if this condition is to be simulated.

The tractive effort calculations are clearly presented in the listing (appendix (4)). Aerodynamic drag is modelled as in [65]. Tyre drag is

based on SAE recommendations. A summary of drag correlations is given in [66]. Typical heavy-duty truck aerodynamic data were taken from [25]; tyre data were obtained from Michelin.

The output shaft inertia equivalent to a given vehicle mass is obtained by considering stored kinetic energy. That is, given the driving axle ratio and the tyre rolling radius (which gives the vehicle speed for a given shaft speed), the kinetic energy of an equivalent inertia will be identical to that of the vehicle.

5.2.13 Output routines - WRITOP/PROUT/PLOT1/2

Writop is called at each recording interval to update a single data array. If this array becomes full before the simulation is completed, the simulation is halted and output files are produced as normal. PROUT creates a disk file from this array in a readable format. PLOT1/PLOT2 create a pair of pro forma plot files with automatic scaling, suitable for output to HP7470A plotters. The plot routines were developed by T.Rolle to the author's specification, to facilitate comparison with similar experimental transient data plots, and superseded a stand-alone plotting program written by the author for the LSI11/23. Listings may be found in [48].

5.2.14 Using SIMDCE

SIMDCE may be run on any PC-AT compatible machine. Input data files must be prepared as mentioned above (refer to examples in appendix (4)). Existing or new controller subroutines or dynamic models may be incorporated by altering batch file SIM.BAT (appendix (4)) and re-linking. The program is run by typing "DCECON". The HP7470A handshaking and output of the plot files is done by running batch file INI.BAT (appendix (4))

LIST OF FIGURES

TABLE 5.1

a) BYPASS MODEL - ORIFICE ANALOGY

Model $$\dot{m}_{byp} = C_d \cdot A_{byp} \cdot p_1 \cdot \sqrt{\left\{\left(\frac{2\gamma}{\gamma-1}\right)\frac{1}{RT_1}\left[\left(\frac{p_2}{p_1}\right)^{2/\gamma} - \left(\frac{p_2}{p_1}\right)^{\frac{\gamma+1}{\gamma}}\right]\right\}}$$

Test pt No.	Tcomp outlet [°C]	Pcomp outlet [barg]	Pturb. inlet [barg]	engine bypass Δp [bar]	measured $\dot{M}$byp [Kg/min]	predicted $\dot{M}$byp if Cd = 1 [Kg/min]	red'd Cd for Match
22	84	0.63	0.62	0.01	1.13	16.6	.07
17	131	1.38	1.37	0.01	1.93	18.7	.10
3	155	1.68	1.10	0.58	17.27	132.0	.13

b) BYPASS MODEL - Darcy's Method

Model $$\dot{m}_{byp} = k_{byp} \cdot A_{byp} \cdot \sqrt{\Delta p_{byp} \cdot \rho_{byp}}$$

Test pt No.	Tcomp outlet [°C]	Pcomp outlet [barg]	Pturb. inlet [barg]	engine bypass Δp [bar]	measured $\dot{M}$byp [Kg/min]	predicted $\dot{M}$byp if Kbyp=1 [Kg/min]	req'd Cd for Match
22	84	0.63	0.62	0.01	1.13	0.199	5.7
17	131	1.38	1.37	0.01	1.93	0.226	8.5
3	155	1.68	1.10	0.58	17.27	1.78	9.7

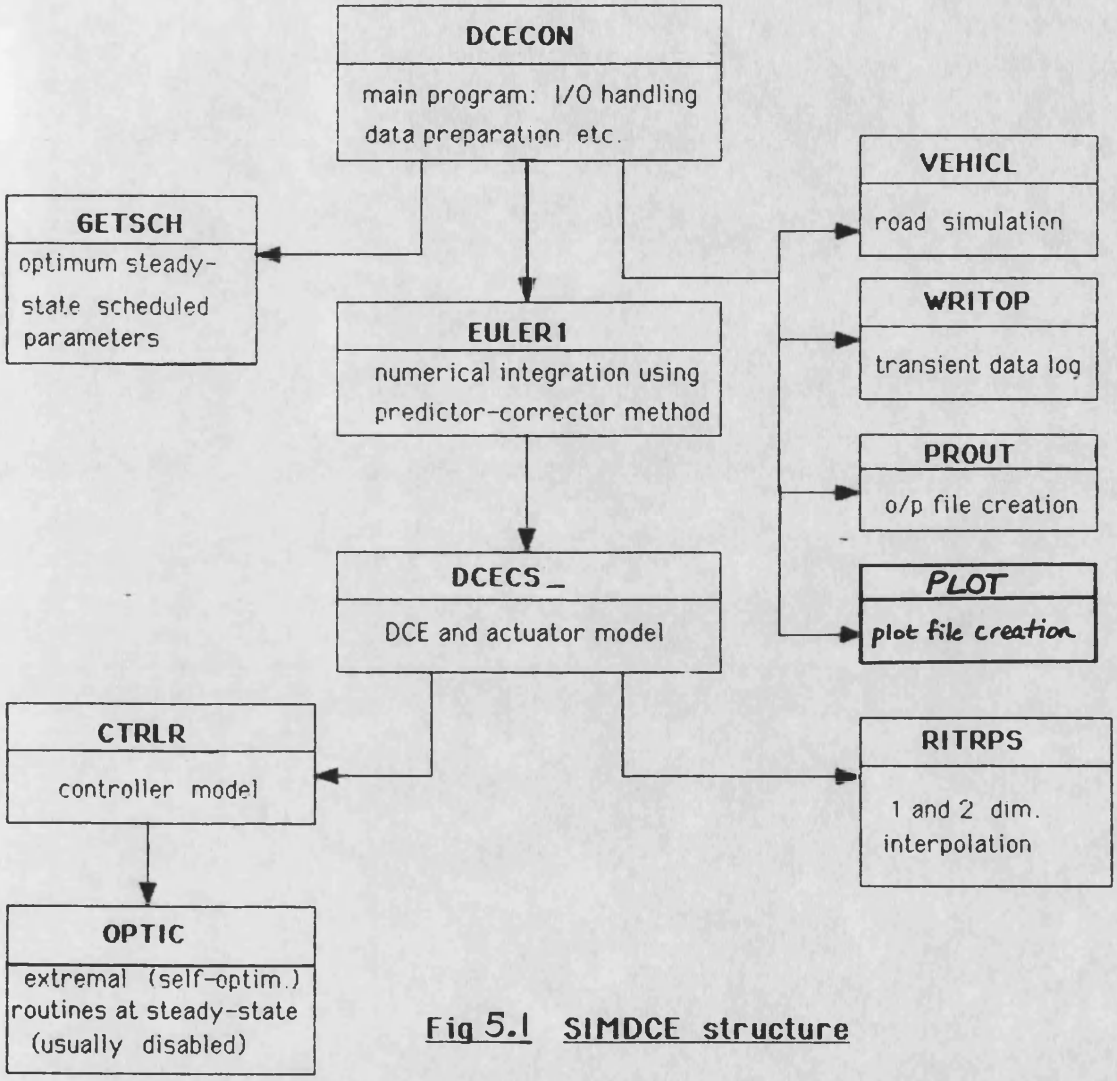

Fig 5.1 SIMDCE structure

DCECON FLOWCHART

SHEET 1 OF 2.

PLEASE NOTE : SOME MINOR CALCULATIONS AND ALL ERROR-HANDLING LOOPS HAVE BEEN OMITTED FOR CLARITY.

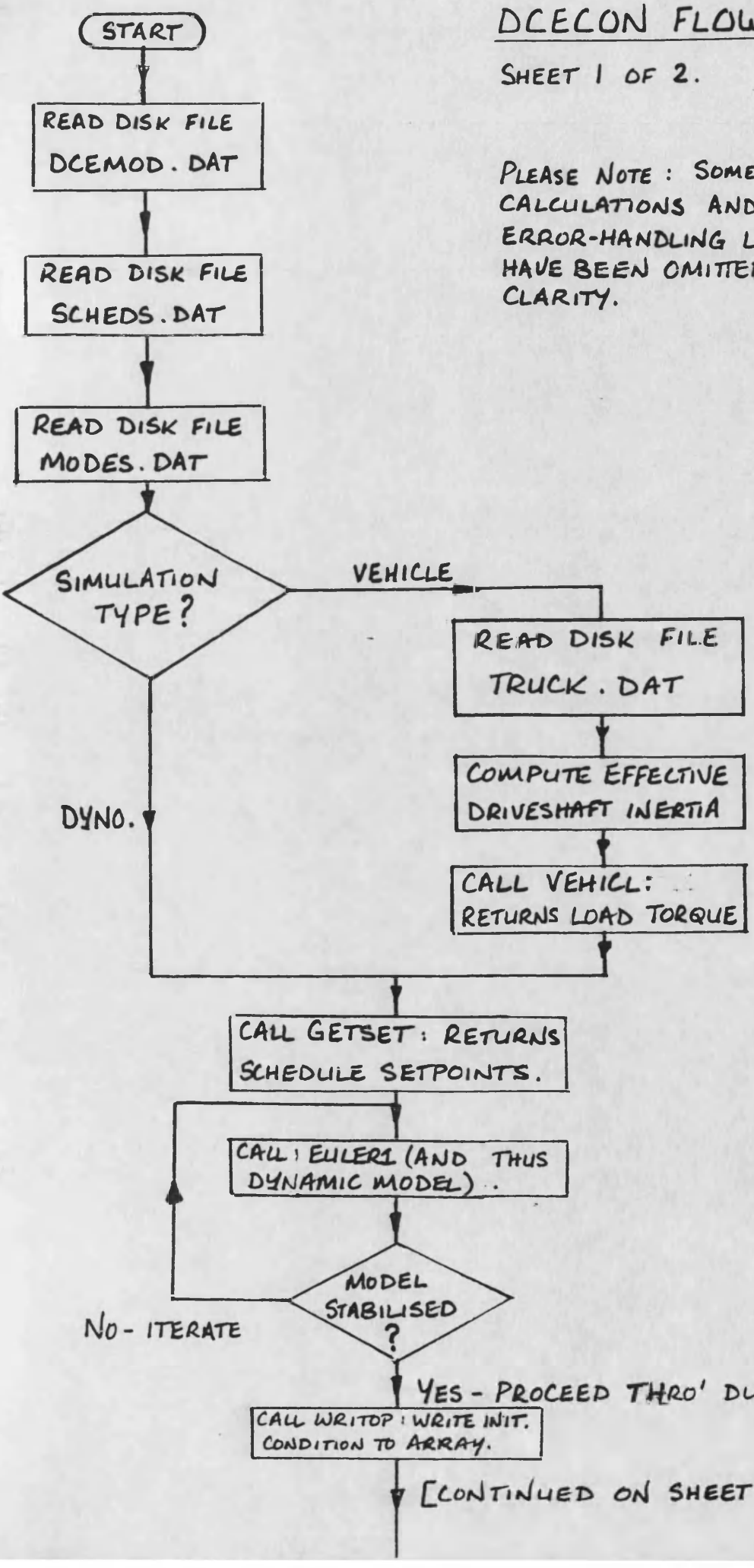

FIG. 5.2

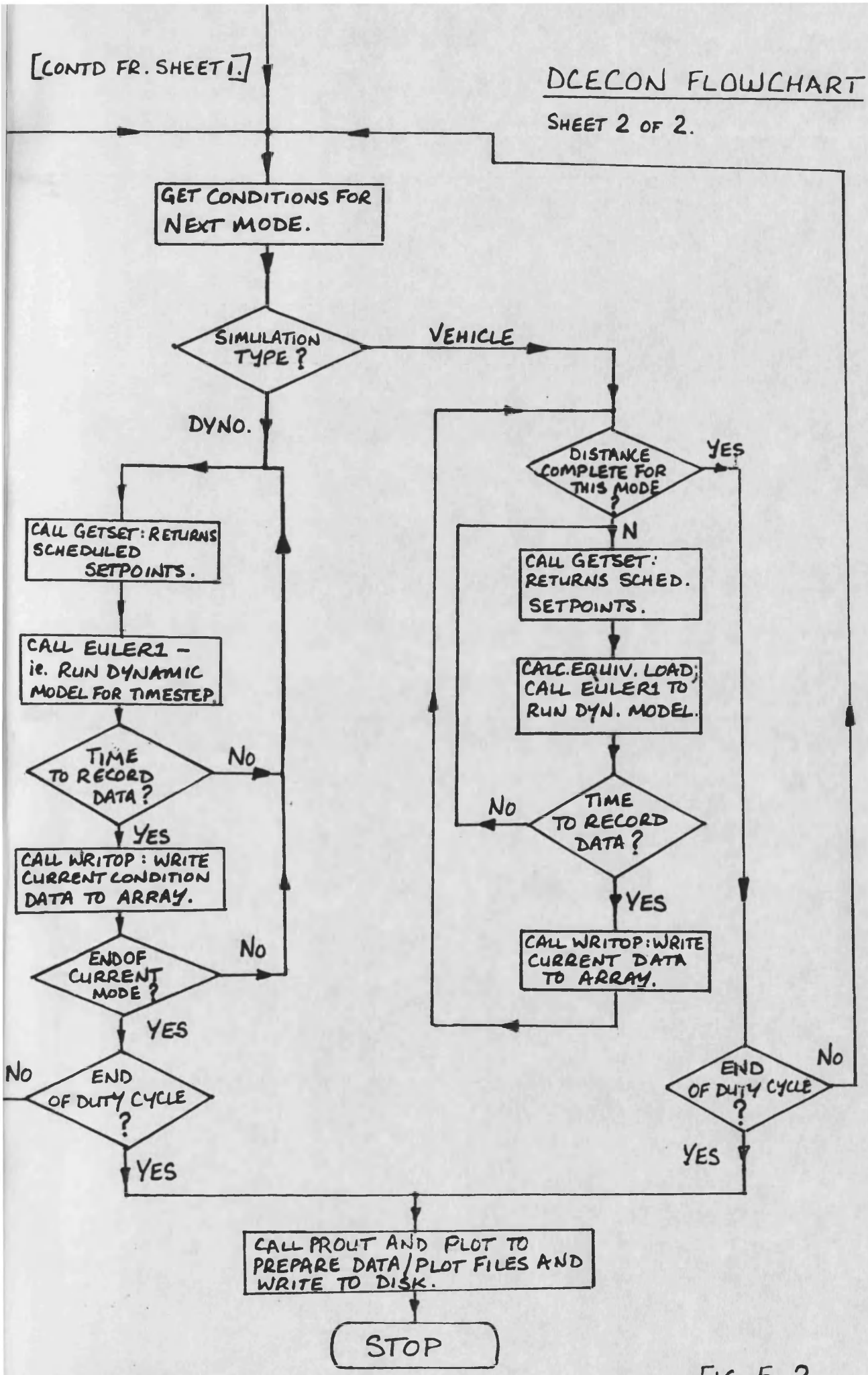
[CONTD FR. SHEET 1.]
DCECON FLOWCHART
SHEET 2 OF 2.
GET CONDITIONS FOR NEXT MODE.
SIMULATION TYPE ?
VEHICLE
DYNO.
DISTANCE COMPLETE FOR THIS MODE ?
YES
N
CALL GETSET: RETURNS SCHEDULED SETPOINTS.
CALL EULER1 - ie. RUN DYNAMIC MODEL FOR TIMESTEP.
TIME TO RECORD DATA ?
No
YES
CALL WRITOP : WRITE CURRENT CONDITION DATA TO ARRAY.
ENDOF CURRENT MODE ?
No
YES
No
END OF DUTY CYCLE ?
YES
CALL GETSET: RETURNS SCHED. SETPOINTS.
CALC.EQUIV. LOAD; CALL EULER1 TO RUN DYN. MODEL.
No
TIME TO RECORD DATA ?
YES
CALL WRITOP: WRITE CURRENT DATA TO ARRAY.
No
END OF DUTY CYCLE ?
YES
CALL PROUT AND PLOT TO PREPARE DATA/PLOT FILES AND WRITE TO DISK.
STOP

FIG. 5.2

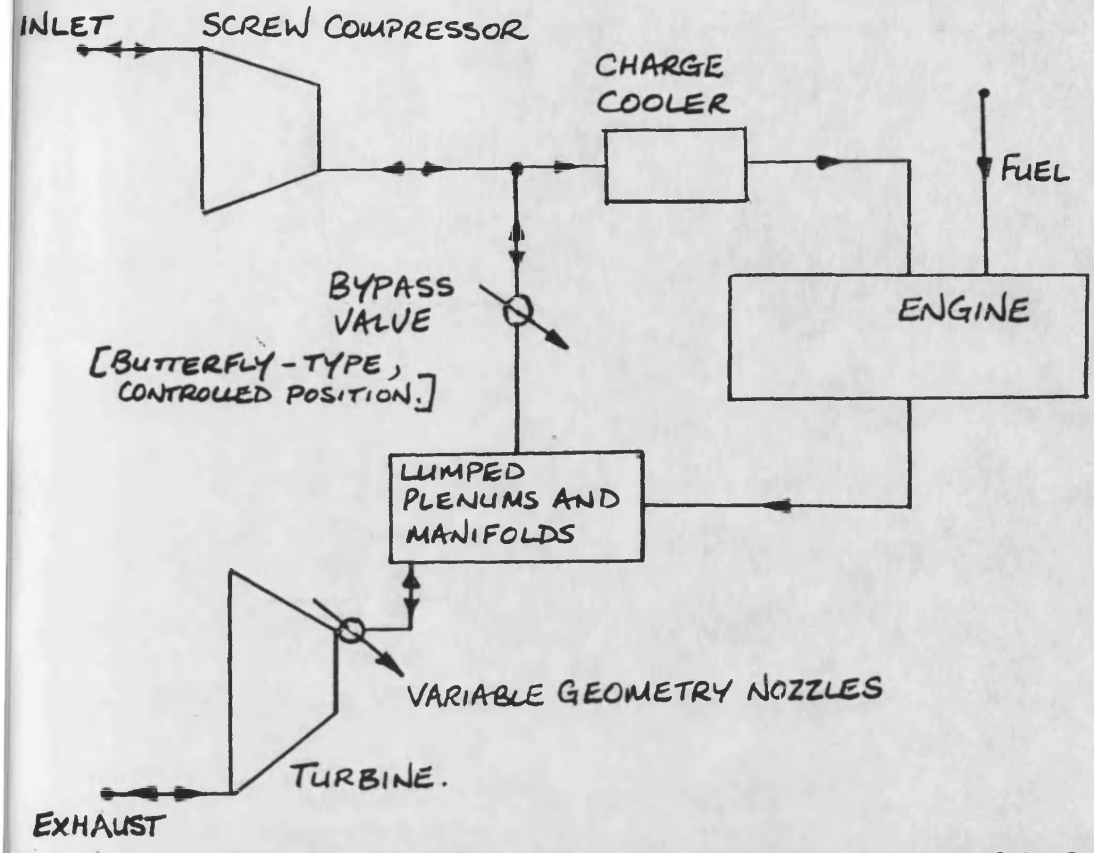

a) GAS FLOWS : ARROWS SHOW POSSIBLE FLOW DIRECTIONS AS MODELLED.

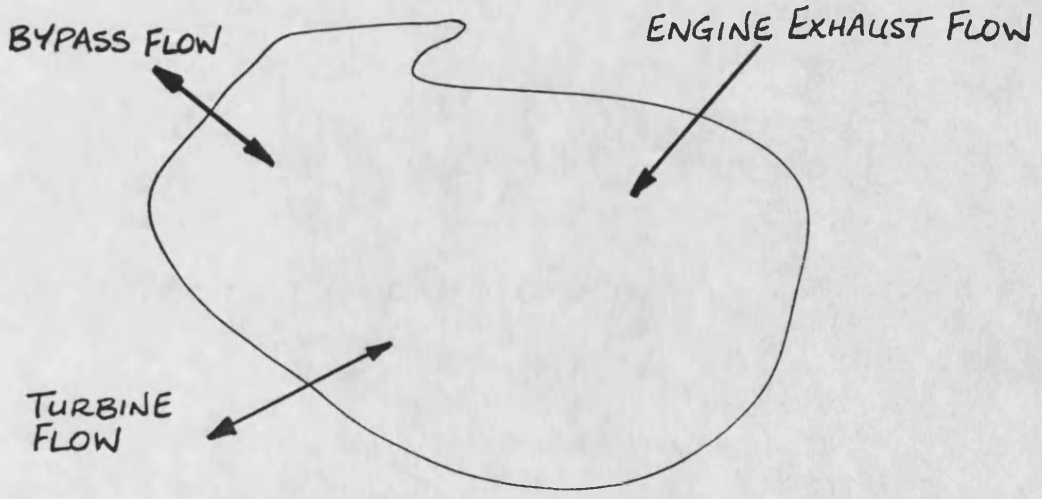

b) VISUALISATION OF SINGLE CONTROL VOLUME

FIG. 5.3 DCECSB GAS DYNAMICS MODEL

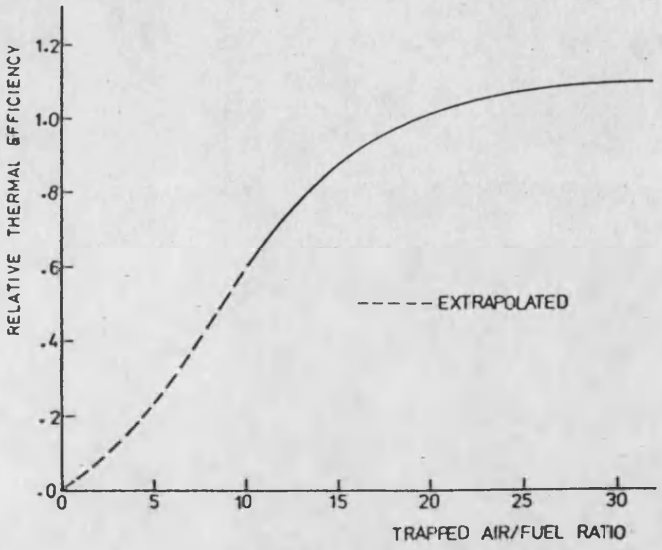

a) SIMULATED RELATIVE IMEP/FUELLING [REF. 59]
(RUSTON 6APC MEDIUM SPEED 4 STR. DIESEL)

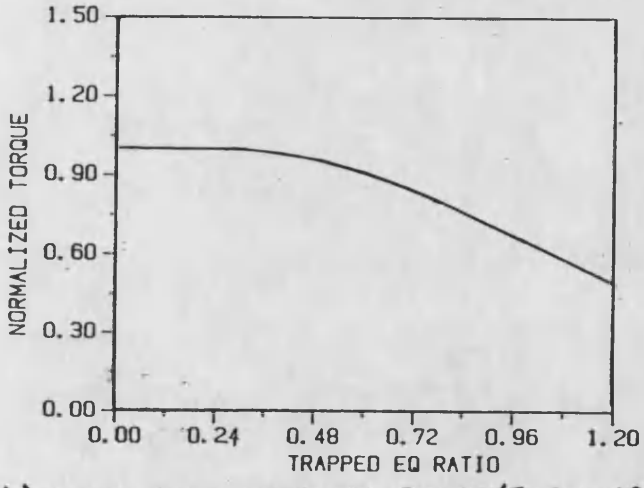

b) SIMULATED RELATIVE BMEP/FUELLING [REF. 60]
(DETROIT DIESEL HEAVY-DUTY 2 STROKE.)

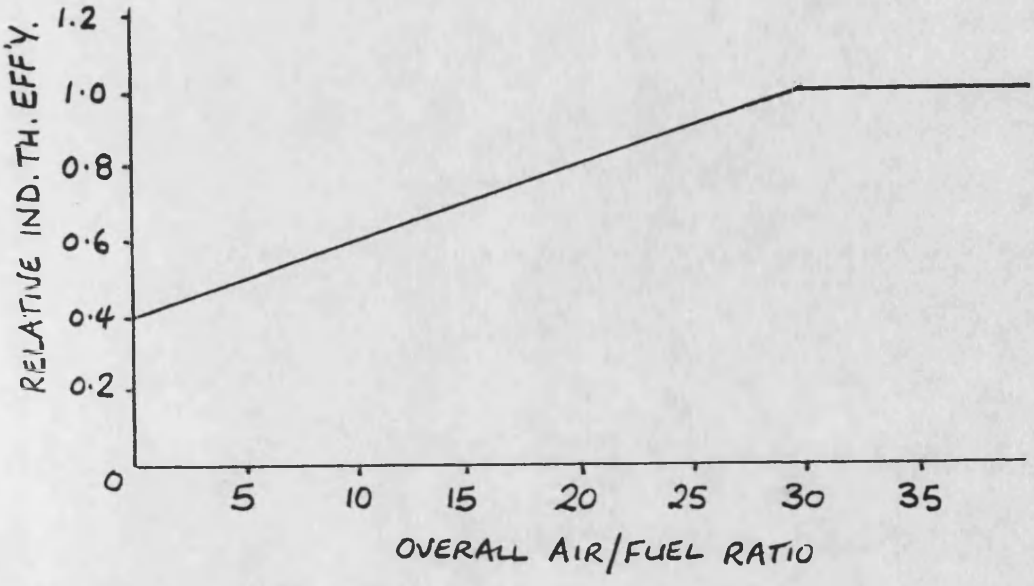

c) LEYLAND 520 DCE EXPERIMENTAL ENGINE DATA

FIG 5.4 EFFECT OF AFR UPON ENGINE THERMAL EFFICIENCY

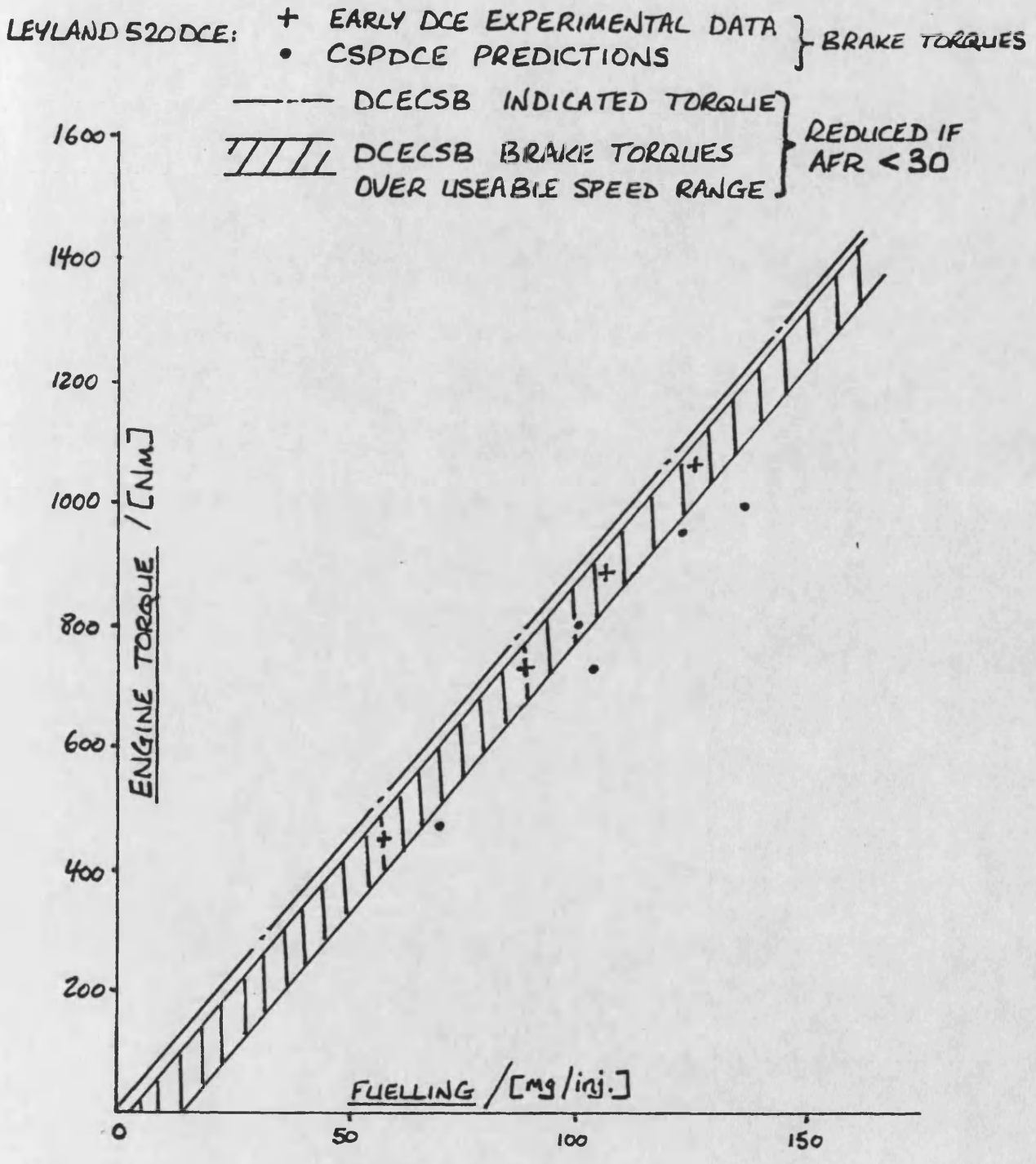

FIG. 5.5 TORQUE/FUELLING CORRELATIONS

DCE STATIC - DYNAMIC INJECTION TIMING CORRELATION

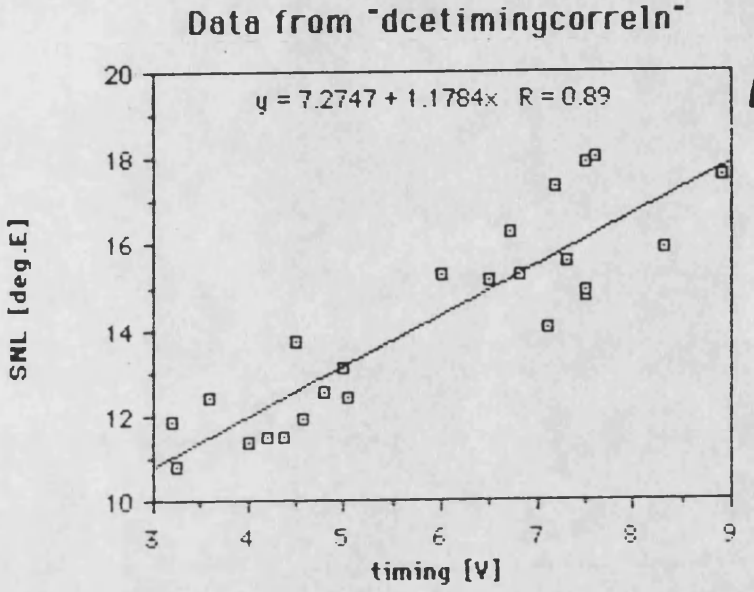

[EXPERIMENTAL DATA]

[PLEASE NOTE FALSE ZEROES]

NOTE: CONVERSION FROM CRANK DEGREES TO TIME [ms] IS:

$$\frac{t}{\theta}\ [ms/^{\circ}cr.] = \frac{166.6}{N\ [rev/min]}$$

$$\text{ie}\quad \frac{t}{[ms]} = \frac{[rev/min]}{N} \cdot 166.6 \cdot \frac{\theta}{[deg.cr.]}$$

$$t = 166.67 \cdot \frac{\theta}{N}$$

FIG. 5.6

EMPIRICAL IGNITION DELAY CORRELATION

12 l 6cyl T/A DI diesel, (swirl port).

(a) MEAN SLOPE FOR ALL SPEEDS

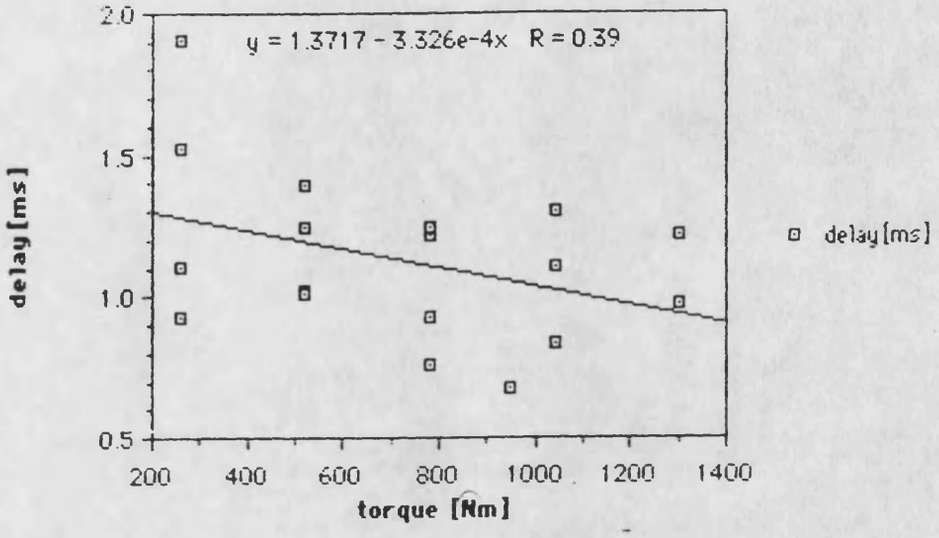

(b) SHOWING VARIATION WITH SPEED

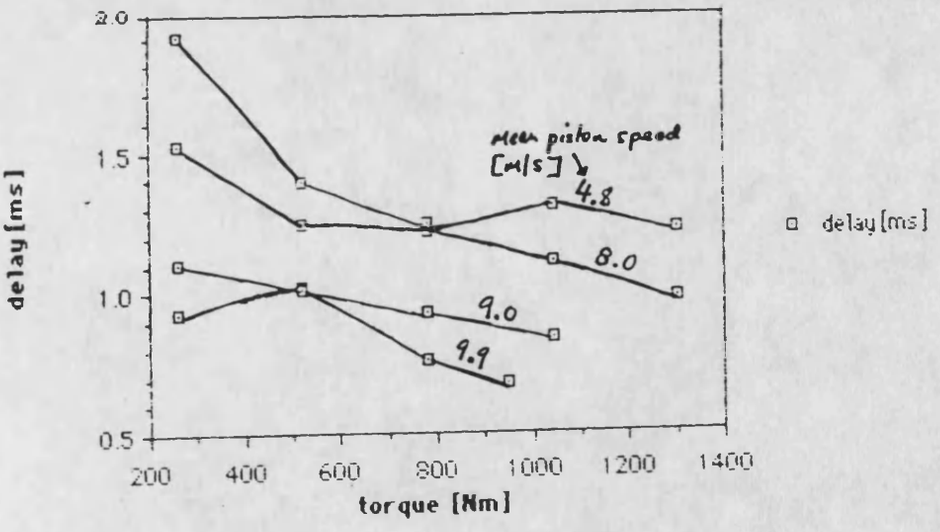

OVERALL CORRELATION:

$$\frac{\text{DELAY}}{[ms]} = 10^{-4}\left(2.2\times10^{-3} - 5.8\,\frac{N_{engine}}{[rev/min]} - 3.3\,\frac{\tau_{engine}}{[Nm]}\right)$$

FIG. 5.7

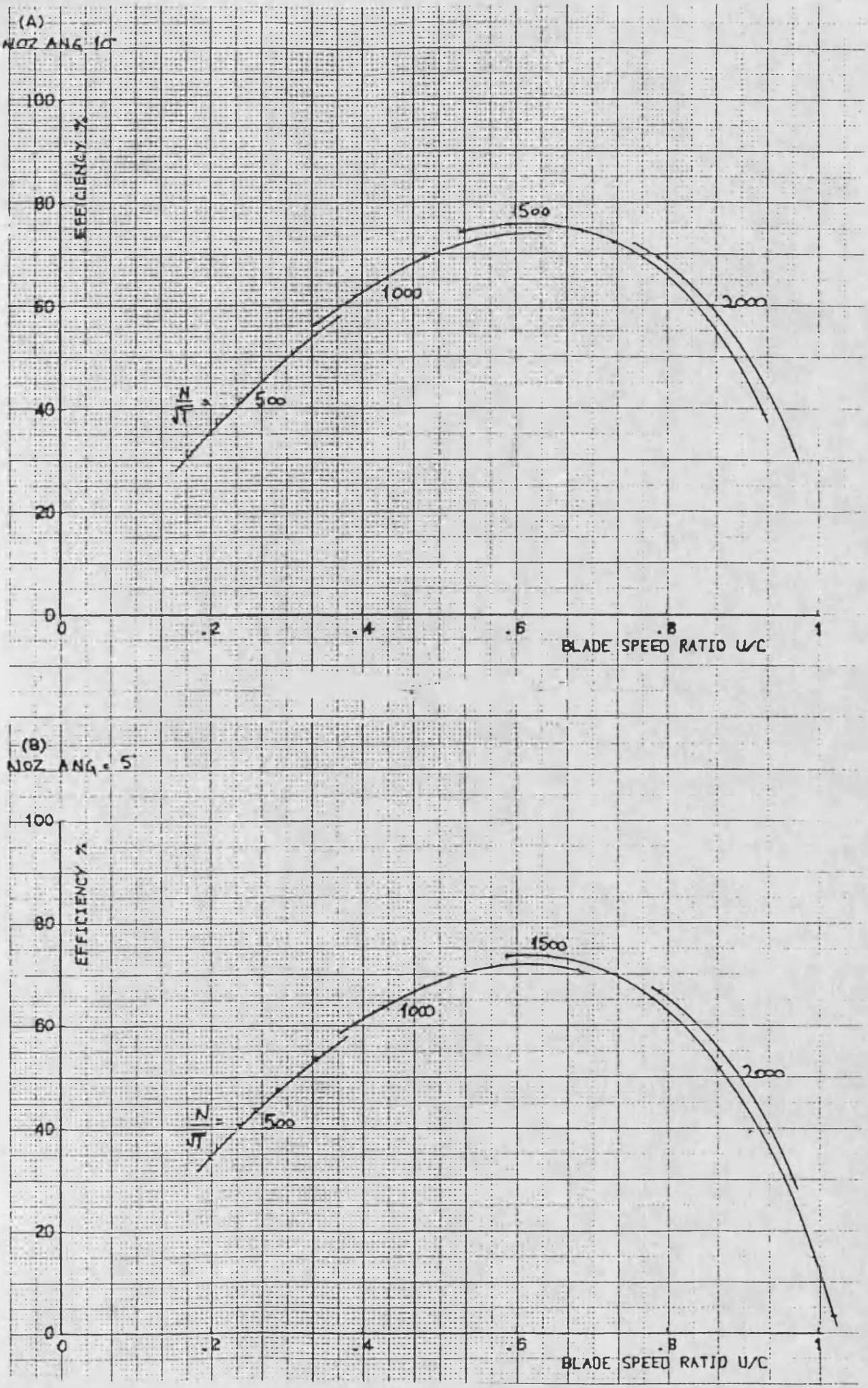

FIG. 5.8 PREDICTED TURBINE EFFICIENCIES

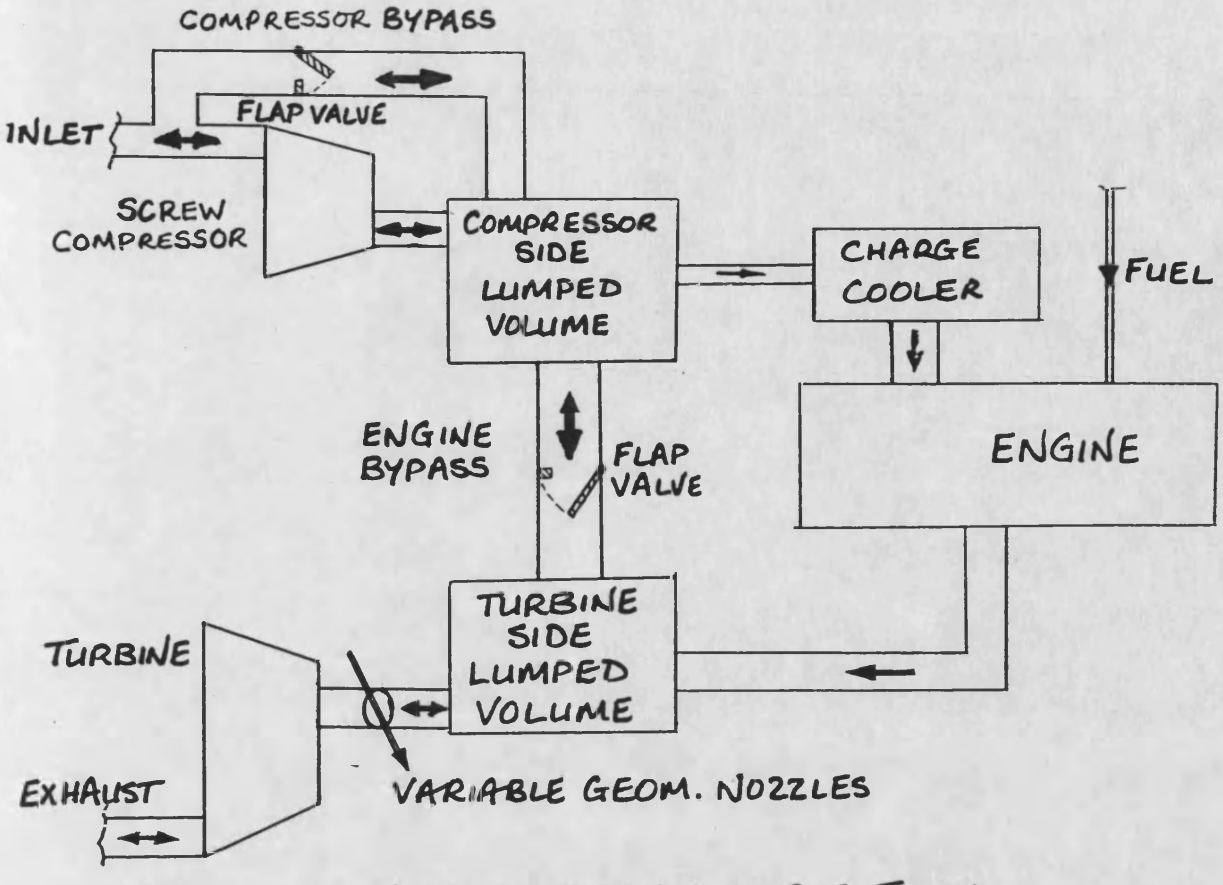

a) GAS FLOWS: ARROWS SHOW POSSIBLE FLOW DIRECTIONS AS MODELLED.

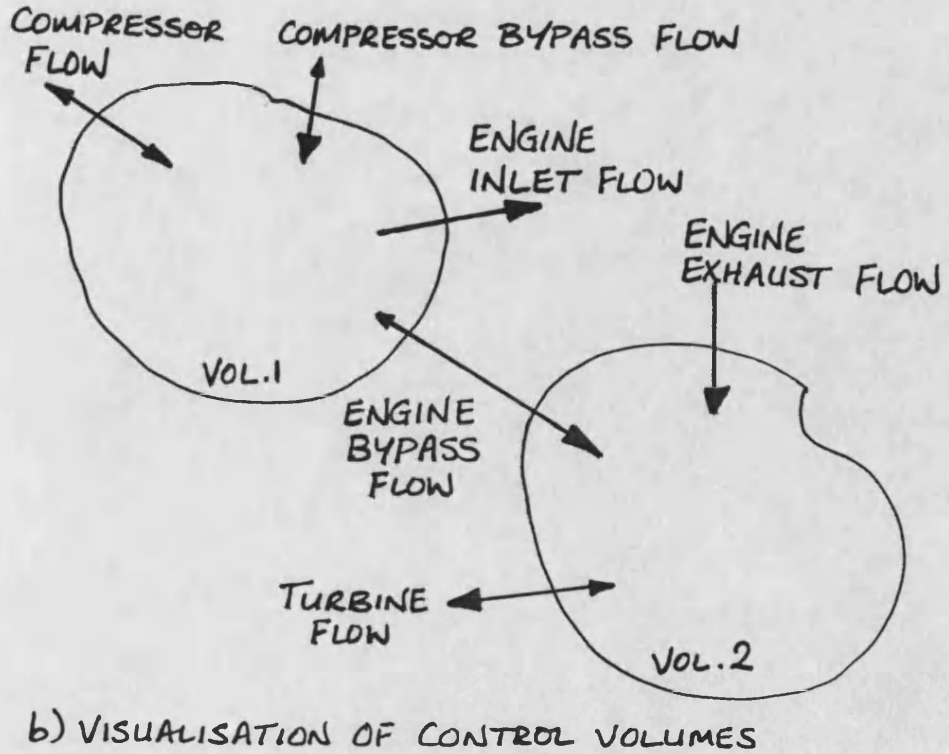

b) VISUALISATION OF CONTROL VOLUMES

FIG. 5.9 DCECSE GAS DYNAMICS MODEL

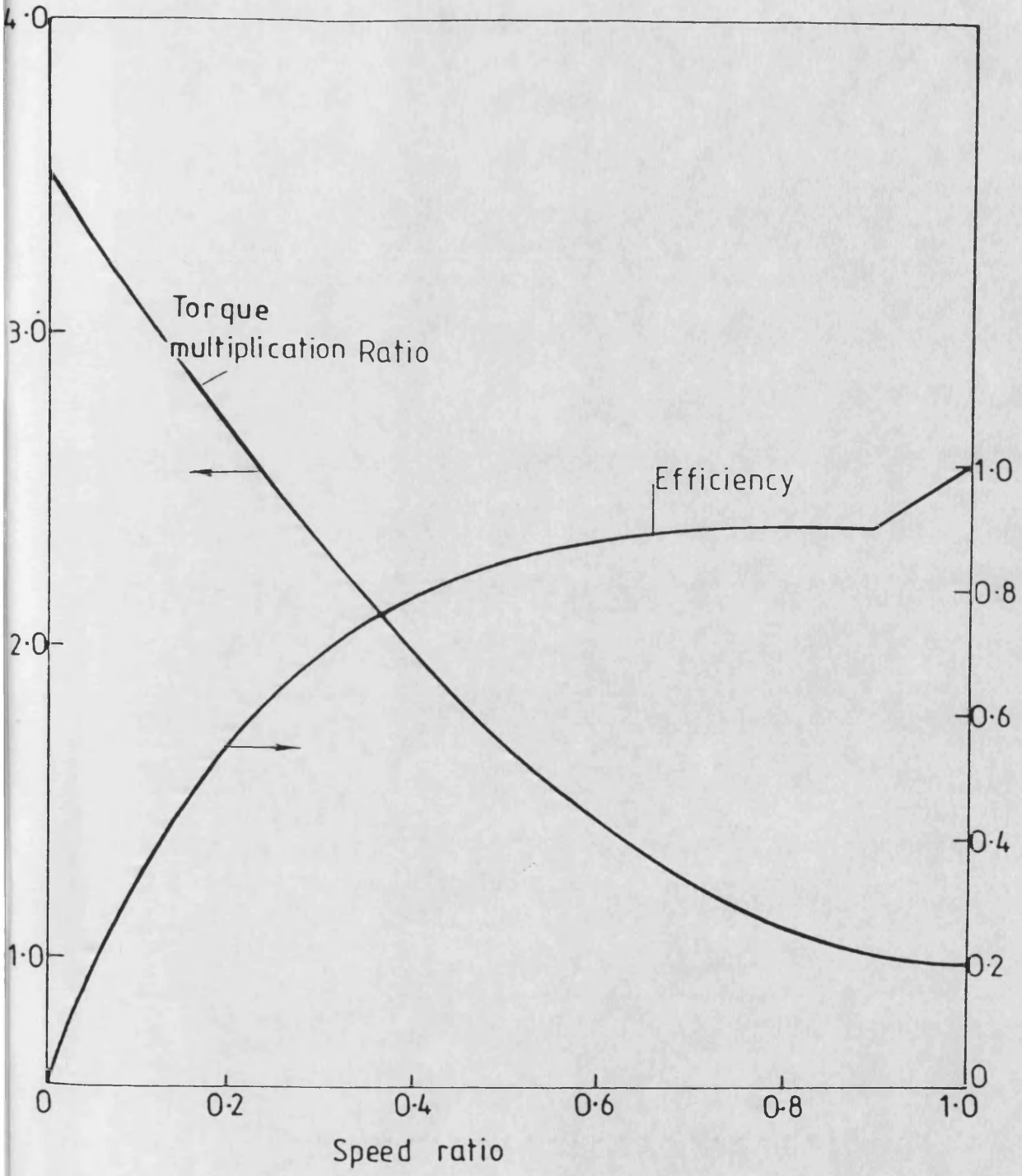

Fig. 5.10 torque converter characteristics

6. OPTIMISATION TECHNIQUES

6.1 Introduction

6.2 Optimisation of steady-state BSFC

6.2.1 General approach

6.2.2 Alternative extremal algorithms

6.2.2.1 Adaptive step size random search

6.2.2.2 Combinatorial heuristic method

6.2.2.3 Hooke-Jeeves pattern search method

6.2.2.4 Simplex method

6.2.2.5 Hill-climbing search

6.2.2.6 Gradient-based methods

6.2.3 Summary of extremal algorithms

6.2.4 Evaluation of two preferred methods by simulation

6.2.5 Practical implementation

6. OPTIMISATION TECHNIQUES

6.1 INTRODUCTION

The gradually increasing operational flexibility of Diesel engines was noted in chapter 1. At the time of writing, fuel injection equipment (FIE) with fixed characteristics, and fixed geometry turbocharging systems, still predominate, even on premium engines. However, controllable systems will inevitably be adopted to meet legislative and market pressures.

In the automotive field the primary considerations in steady state operation are fuel economy and emissions, with the further task of providing high torque backup over as wide a speed range as possible. These aims may more easily be met if the engine can be actively "re-matched" over the operating range. For conventional turbocharged engines flexibility may be introduced in the form of variable geometry (VG) turbocharging and electronic FIE. The latter may provide control of injection rate as well as timing. This becomes increasingly important as engine ratings increase, to preserve good fuel/air mixing over a wide range of fuellings. In addition, variable charge cooling has been employed by several manufacturers.

In summary, Diesel engines for automotive (as well as marine, rail and other traction) duties may have several controllable parameters susceptible to optimisation over the operating range. In chapter 1 the possible use of various electronically-controlled transmissions was also noted. The optimisation process might initially be carried out at the development stage to provide control schedules for production engines. Looking further ahead the optimisation could be automated as part of an

engine management system and carried out continuously in service. To develop such a self-optimising ("extremal") controller, optimisation methods must first be evaluated. This chapter discusses the application of extremal control methods to two multivariable powertrains; the DCE and a VG turbocharged heavy-duty Diesel engine.

As described in chapter 2, the 520DCE has two "primary" controls (that is, affecting component speeds, torques and so on), namely rack position and turbine VG setting, and one "secondary" control (affecting only secondary parameters such as efficiency and emissions), namely injection timing. Complete DCE schemes might incorporate further controls such as variable turbine gear ratio or bypass air restriction.

The VG turbocharged Diesel was a Leyland TL11, 11.2 litre, 6 cylinder, 4 stroke engine. This had been installed for VG turbocharger research as reported in [11,37], with electrohydraulic VG control plus fuelling and injection timing controls similar to those used on the 520DCE. The interest in extremal control for this engine was as part of a research project investigating operation on variable quality fuels in marine applications. This project, under the direction of Prof.FJ Wallace and Dr.SJ Charlton, was part of a major programme of fuel rating and engine performance/durability studies managed by Lloyds Register of Shipping. The writer was involved only in the initial stages, where work on extremal control was relevant to both this project and DCE research.

The TL11 had additionally been fitted with charge air temperature (CAT) control for the above project. This comprised cooling by external circuit (pond) water and heating by electric resistive elements. A proprietary (Eurotherm) self-tuning PID controller was used to handle the differing

dynamics of the cooling/heating processes.

Thus the TL11 had a single primary control, namely rack position, and three secondary controls, namely turbine VG, CAT and injection timing.

At this point it should be noted that the broad term "multivariable optimisation" may be sub-divided into distinct classes requiring different approaches:

	INPUTS		OUTPUTS/STATES OF INTEREST
(i)	many	---------->	one
(ii)	one	---------->	many
(iii)	many	---------->	many

For class (i) the single objective can be stated simply as either a value or the achievable extremum, using some combination of the multiple inputs. For classes (ii) and (iii) the optimum state must be defined in some formal way, typically using a cost function. For example, in [67] optimal control theory was applied to a marine Diesel with a single control (rack), where speed regulation, fuel efficiency and other operating parameters (affecting durability) were all of interest. In this case one might choose to define the state as

$$x = [N,p,T]$$

where N denotes engine speed

p boost pressure

T exhaust temperature;

with the desired state

$$x_{\emptyset} = [N,p,T]_{\emptyset}$$

corresponding to the desired speed plus desireable boost pressure and exhaust temperature levels for good combustion and durability; and with

an output η_e (shaft thermal efficiency). The rack control input may be denoted u.

The cost function could then be formulated as

$$J(t_1,t_2)=1/2\int_{t_1}^{t_2}\{[x_\phi - x]^T.Q.[x_\phi - x] + u.k_1.u + k_2.(1-\eta_e)\}\,dt \qquad (6.1)$$

where Q, k_1, k_2 are used to weight the importance of the states, the control level and the output, and where (t_1, t_2) is the time interval of interest. In practice eqn.6.1 would be formulated in discrete-time with time interval from zero (the present) to some future time (horizon). The optimal solution to eqn.6.1 is obtained by Linear Quadratic (LQ) control methods, as covered in numerous texts (see for example [68]). The solution over some future time period requires some form of linear state space model to predict state x and output η_e for any control input u.

The application of optimal methods to multivariable transient control of the 520DCE is covered in chapter 8. However, for steady state operation, and for the purposes of the current projects, both the DCE and TL11 were in class (i) as defined above. In either case the objective of the extremal controller would purely be minimum brake specific fuel consumption (BSFC), achieved by optimisation of multiple inputs and subject only to the usual engineering constraints of thermal and mechanical loading, component speeds, and smoke.

6.2 OPTIMISATION OF STEADY STATE BSFC

6.2.1 General approach

For generality, optimisation of three input variables was considered. As discussed above the TL11 has three secondary control inputs, and complete DCE schemes may have several primary/secondary

inputs. In mathematical terms we are concerned with single-criterion minimisation subject to fixed constraints:

$$\text{minimise} \quad f$$

$$\text{subject to} \quad \alpha_l < \alpha < \alpha_h$$

$$\beta_l < \beta < \beta_h$$

$$\gamma_l < \gamma < \gamma_h$$

$$\text{and} \quad p < p_m, \; T_i < T_{im}, \; N_i < N_{im}, \; S < S_m$$

where the single criterion f is BSFC, α, β, γ are control inputs (subscripts l and h denote the low and high bounds of their ranges) and p_m, T_{im}, N_{im}, S_m are constraints on cylinder pressure, gas temperature(s), component speed(s) and smoke.

Where possible those inputs considered together in the optimisation process should have similar levels of importance. Relatively unimportant controls would be "swamped" and might confuse and delay optimisation of the important controls.

The most fundamental decision to be made was whether to use model-based or heuristic methods.

(i) Model-based approach:

For a worthwhile model-based approach very accurate BSFC predictions would be required over the operating range of the engine and the control inputs. Two model types may be considered:

(a) Phenomenological - that is, conventional engine simulation based on understanding of the processes involved.

(b) Identified - that is, simplified (often linear) equations treating the engine as a "black box", where the equation parameters are experimentally identified. (Again the use of identified models formed

part of the DCE transient control studies, described in chapter 8).
It is questionable whether conventional engine simulation could in general achieve the required accuracy. BSFC prediction is of course highly dependent upon modelling of heat release, a very difficult task. A semi-empirical technique is commonly used, matching simplified heat release functions to experimental data. This clearly becomes an unsatisfactory approach where controls are being used chiefly to modify the heat release characteristic. Furthermore, to use this type of model in an adaptive controller would require high computing power, unless extremal control were employed only during long periods of steady state operation.

The identified linearised model, being highly simplified, cannot be sufficiently accurate if used with fixed parameters. The parameters must be identified adaptively by perturbing the control inputs and measuring, in this case, BSFC. This gives a localised linear model, which is inherently limited since BSFC is generally an extremal function. While this approach is feasible, it is apparent that the perturbations applied for identification could instead be used directly in an heuristic search for minimum BSFC.

(ii) Heuristic approach:

In view of the above, only heuristic methods were considered. Forthcoming work by other researchers on the TL11 rig will attempt to achieve real-time modelling for condition monitoring [69], but this is still in the future. Alternative heuristic extremal algorithms are reviewed below.

6.2.2 Alternative extremal algorithms

6.2.2.1 Adaptive step size random search (ASSRS) [70]

The principles of this method as applied to this three-input (α , β , γ) single-output (f) problem are:

(i) Generate a random unit vector $\underline{d}$ in the 3-dimensional space.

(ii) Use this vector to map from the current operating condition, denoted $\underline{x}_0 = (\alpha_0, \beta_0, \gamma_0)$ to a trial condition $\underline{x}_1 = \underline{x}_0 + k.\underline{d}$

(iii) If $\underline{x}_1$ is within constraints and $f_1 < f_0$ (i.e. BSFC is reduced), a trial vector is set:

$$\underline{x}_y = \underline{x}_0 + k_s.(\underline{x}_1 - \underline{x}_0) \quad \text{where } k_s > 1$$

k_s is a step size increase ("success") factor used to build upon a successful move.

Otherwise, k is decreased by a "failure" factor:

$$k = k_f . k, \quad \text{where } k_f < 1$$

(iv) If $\underline{x}_y$ is within constraints and $f_y < f_0$, set $k = k_s . k$ and $\underline{x}_1 = \underline{x}_y$. Again this capitalises upon previous successful moves.

Otherwise, increment a failure counter and return to step (i).

(v) Check for termination. Ideally this would be when f becomes close to some pre-selected minimum. In practice the ideal is unknown, and in this case the variability of the system (continual minor changes in operating condition, and engine unrepeatability) precludes termination even at nominal steady state. A practical extremal controller would cycle through (i)-(iv) continually.

The above is a simplified summary of the method. Checking for the constraints and for consistently-failing trial vectors adds complexity.

The method has been briefly tested by simulation (described later), and the subroutine listing (subroutine "OPTICa" in Appendix 4) shows the method more fully.

In [7Ø] it is stated that the ASSRS method works best in the initial stages. In practical applications an extremal controller would probably start from an operating condition set by a scheduling controller. Since these schedules would be at least near-optimal, the performance of the extremal controller in the final stages could be of more significance. Clearly the increasing "success" step size ([7Ø] suggests k_s =1.618, k_f =Ø.618) with approach to the optimum will cause overshoot. Choice of k_s less than unity would reduce overshoot, but this contradicts the principle of the method.

An extremal controller which causes large swings around the optimum point is of little value in this application, where it would operate continuously and the true objective is really minimum gross fuel consumption over some duty cycle rather than an instantaneous approach to minimum BSFC.

6.2.2.2 Combinatorial heuristic method [71]

As before, the method is described as it would be applied to this problem. In principle a semi-random search is carried out, one variable at a time:

(i) Take the current BSFC to be the minimum,

fmin = fØ

For each variable (α, β, γ) in turn, carry out the following process:

(ii) Optimise the i^{th} variable, with others fixed:

(a) Select q additional values of the i^{th} variable which give f

< f_{min} (a trial-and-error process). If this is not possible, restart with $(i+1)^{th}$ variable.

(b) Choose the best of the above, and set

$$y_{min} = f \text{ at this condition.}$$

This is a temporary baseline.

(c) Look-ahead search to the next variable. For each of the q values above, conduct a random search for q values of the next variable which give $f < y_{min}$. Select the best of these; the value of the i^{th} variable at this point is taken to be the optimum.

(d) If $i < 3$, repeat from (ii)(a) above with the $(i+1)^{th}$ variable.

(iii) Perform a random search in the 3rd variable to find minimum f, holding the other variables at their optima from above. The result is the new base point $x_{\emptyset}$ and the procedure is repeated from (i).

The choice of $3 < q < 5$ is suggested in [71], which is a compromise between considering sufficient possible settings and completing the process in a reasonable time. Clearly this would be a lengthy process. The random search phases seem inefficient, especially near the optimum where improved settings will be hard to find. A random jump phase may be useful where multiple local optima exist, but in practice BSFC tends to present a smooth curve to a single global optimum.

6.2.2.3 Hooke-Jeeves pattern search method [71,72]

This is a combination of single-variable exploratory moves with pattern (acceleration) moves regulated by some heuristic method.

(i) Exploratory moves - with a chosen step size, each variable in turn is simply stepped once from its starting position. If f does not

decrease, the variable is stepped back to the opposite side of the base point. If f does not decrease here the variable is returned to the base, and the next variable is explored. When all the variables have been explored, this is the new base point $\underline{x}_{\emptyset}$.

(ii) Pattern move - step along the same vector as the exploratory step to a new "pattern" point $\underline{x}_p$. If $f_p < f_{\emptyset}$ then $\underline{x}_p$ is accepted as a new base point. Otherwise the pattern move is retracted and an exploratory move is made.

(iii) Repeat (i) and (ii) - when the exploratory move no longer finds lower f, the step size is reduced (a factor of Ø.1 is suggested in [72]) and the process continues. An additional "pattern exploitation" move is suggested in [71] using expanding steps after successful pattern moves (compare with ASSRS algorithm). However, as noted in [73], as the function surface becomes less regular the pattern moves become less successful and the method degenerates into a sequence of purely exploratory moves.

An extension of the Hooke-Jeeves method is proposed in [73], using a quadratic objective. The argument is that near the optimum most non-linear functions tend to a quadratic form. The proposed method requires algebraic manipulation, and becomes impractical for this application.

6.2.2.4 Simplex method [74]

A set of (n+1) mutually equidistant points in n-dimensional space is known as a "regular simplex". In this three-dimensional case the simplex is thus a tetrahedron. Reference [74] suggests the use of an irregular simplex to search a space, manipulated by reflection and expansion/contraction to close in upon optimum settings (coordinates in the space). The procedure is lengthy to describe, but is summarised below

(again for the three input case):

(i) Choose 4 points $\underline{x}_i = (\alpha_i, \beta_i, \gamma_i)$, i=1,...,4 and measure each f_i (BSFC).

(ii) Measure the highest, second highest and lowest f_i; denoted

f_h, f_g, f_l respectively.

(iii) Find the centroid of all points except $\underline{x}_h$. Denote this $\underline{x}_\emptyset$ and measure $f_\emptyset$.

(iv) Try to move away from $\underline{x}_h$ (highest BSFC is the worst case): reflect $\underline{x}_h$ in $\underline{x}_\emptyset$ to find a new point $\underline{x}_r$, and measure f_r. A reflection scale factor k_r may be applied:

$$\underline{x}_r = (1 + k_r).\underline{x}_\emptyset - k_r.\underline{x}_h$$

(v) Compare f_r with f_l:

- If $f_r < f_l$ this is a good direction to move in. Make an expansion in this direction to $\underline{x}_e$, where

$$\underline{x}_e = k_e.\underline{x}_r + (1 - k_e).\underline{x}_\emptyset$$

and k_e is an expansion factor. Then if $f_e < f_l$ replace $\underline{x}_h$ by $\underline{x}_e$ and repeat the process from (ii) above. However, if $f_e > f_l$ abandon $\underline{x}_e$ (have overshot).

- If $f_r > f_l$ but $f_r < f_g$, $\underline{x}_r$ is a partial improvement. Replace $\underline{x}_h$ by $\underline{x}_r$ and repeat from (ii).

- If $f_r > f_g$, f_r continue to step (vi) below.

(vi) Compare f_r with f_h:

-If $f_r > f_h$ a contraction (factor k_c) is required to close in upon the optimum. Otherwise continue with $\underline{x}_h$ replaced by $\underline{x}_r$. Thus:

either $\underline{x}_c = (1 - k_c).\underline{x}_\emptyset + k_c.\underline{x}_h$ (if $f_r > f_h$)

or $\underline{x}_c = (1 - k_c).\underline{x}_\emptyset + k_c.\underline{x}_r$ (if $f_r < f_h$)

(vii) compare f_c and f_h:

- If $f_c < f_h$ replace $\underline{x}_h$ by $\underline{x}_c$ and continue from (ii) above
- If $f_c > f_h$ we have failed to find a new point $\underline{x}$ for which $f < f_h$; continue to step (viii).

(viii) Reduce simplex size - halve the distance of each apex from the current minimum point $\underline{x}_l$, and continue from (ii).

Factors $k_r = 1.$, $k_c = 0.5$, $k_e = 2.$ are recommended in [74].
The systematic nature of the method is appealing; it involves no random steps and only three simple mapping moves (reflection, expansion, contraction). At each step the simplex is distorted and then "reforms" somewhat around an improved setting.

6.2.2.5 Hill-climbing search

This is the simplest form of sequential search method. Some extremal-seeking strategy is applied to single variables in turn. In manual optimisation a trial-and-error search is modulated by experience. For automatic use the following strategy was devised:

(i) Step one control input a preset distance. If f (BSFC) is reduced, repeat the step (no expansion, to reduce overshoot). When f is increased, halve the step size and reverse the direction. Repeat until the step size reaches some preset minimum.

(ii) Reset to the original step size, hold previous control inputs at their optimum settings and repeat (i) above for the next variable. When the final variable has been optimised, continue from the first variable. The minimum step size may be allowed to diminish if time permits. The method takes the form of a binary search commonly used in database file searching, successive approximation digital converters, etc.

Where one variable has a dominant effect it may be searched first, down to a small step size. If the variables have equal effect,the minimum step size may be kept large initially to encourage cycling through the variables, then reduced to approach the optimum more closely.

6.2.2.6 Gradient-based methods [71]

These include Cauchy's method, Marquadt's method and Newton's method. Cauchy's method employs the first derivative of f with respect to the control vector $\underline{x}$. The principle is simply to proceed in the direction of steepest descent until the minimum is found. At the minimum the gradient is of course zero, implying that the method will slow down and inherently works least well close to the optimum.

Both Marquadt's method and Newton's method employ the second derivative, giving better performance near to the optimum.

However, any derivative of BSFC (particularly w.r.t. several variables) imposes extra computation and requires several exploratory moves to measure the derivative. Therefore these methods become impractical.

6.2.3 Summary of extremal algorithms

Five heuristic algorithms have been outlined. Gradient-based methods have been discounted because of the exploratory effort required to measure the derivatives. Three of these algorithms (combinatorial heuristic, Hooke-Jeeves and binary step hill-climbing methods) are "sequential" - each variable is explored in turn. The adaptive step size random search (ASSRS) and the simplex method are "parallel" - all variables are altered (in general to different extents) simultaneously.

Where the relative effects of the control inputs are similar or are unknown a priori it would seem that parallel methods are preferable, since no decision need be made on the searching order. The control moves are made freely in all dimensions and will inherently be "pulled" towards optimisation of the dominant control inputs. However, the sequential binary step hill-climbing (BSHC) method may accommodate this situation by the use of an initially large minimum step size, as discussed earlier.

No mention has been made of the effect upon the various methods of the control input constraints listed in section 6.2.1. These constraints (actuator positions and engineering limits) will undoubtedly be met, and must not degrade the performance of a chosen algorithm.

The application of one parallel (ASSRS) and one sequential (BSHC) method to the DCE was investigated by dynamic simulation, as described in the following section.

Other researchers involved with the TL11-based variable quality fuels project applied a simplex method, as reported in [75]. In this case control input constraints were dealt with by a penalty-function method. If the new simplex point violated the input constraints then the BSFC returned to the algorithm was artificially increased from the value at the constrained point.

6.2.4 Evaluation of two preferred extremal methods by simulation

The adaptive step size random search (ASSRS) and binary step hill-climbing (BSHC) algorithms were applied to the DCE dynamic simulation

SIMDCE (chapter 5). As matched to the 52ØDCE, the control inputs were fuel rack, turbine VG and injection timing actuator positions. The controller subroutine modelled simple engine speed governing by proportional rack control. The VG and timing positions were set by the extremal algorithm.

(i) ASSRS - "OPTICa"

The extremal algorithm was incorporated as subroutine "OPTICa" (program heirarchy was shown in fig.5.1). The code listing is included in appendix 4 and the flowchart is shown in fig.6.1. As shown, the subroutine operates only at steady state (specified in the simulation in terms of shaft accelerations). At this stage actuator dynamics had not been modelled, but realistic slewrate limits were imposed. Where a control is slewrate-limited the ASSRS algorithm is suspended until the move is complete. Additionally, since this is a dynamic simulation the DCE must be allowed to stabilise from the effect of the control move before BSFC is evaluated. An alternative, in the simulation and in practice, is to evaluate BSFC repeatedly until it stabilises. If the required control positions exceed the Ø-1ØV actuator limits these are constrained, and the BSFC at the constrained positions is used without modification.

Two load inertiae (1 and 3Ø kg m^2) were investigated, at two feedforward (engine speed) demand and load torque conditions:

(i) demand 4.5V (45%), load 4ØØNm

(ii) demand 9. V (9Ø%), load 8ØØNm

(the 52ØDCE stall torque is approximately 12ØØNm)

After initial runs only the low inertia case was used, as the effects will be similar, merely requiring longer stabilisation times with higher

inertia. It should be noted that since VG setting has a primary effect upon the DCE, VG control moves will affect output shaft speed and other major parameters as well as BSFC. It was also recognised that the simultaneous optimisation of VG and timing was not ideal since their effect upon BSFC differs significantly. However, since the algorithm steps both inputs in parallel, no time is wasted.

The base step size of the algorithm was gradually reduced by trial-and-error. The step size expansion with successful moves led (as expected) only to overshoot. Finally a contracting success step size was used to improve "homing-in", recognising that the algorithm would then only be effective if initiated close to the optimum. The best results are shown in figs.6.2-6.5. These are for the 9V/800Nm condition. Fig.6.2 shows the pattern of successive trial moves over a 5 second period.Data were recorded only every 20 timesteps due to memory size constraints, so not all the moves are shown. VG nozzle angle is shown - larger values correspond to less restriction. The resulting changes in output shaft brake thermal efficiency (BTE) are shown in figs.6.3 and 6.4. There is no pattern of improvement, just small oscillations about a mean. Fig.6.5 shows the resulting fuelling variations as the engine speed controller counteracts the effect of VG moves upon the operating condition. Similar variations in epicyclic torques and boost pressures occurred as a result. This would be noticed as "hunting", although the amplitudes are low (+/- 1% about the mean value). Although the algorithm had been modified in the "success" step expansion phase, this would not account for the unstable reversals of control move direction, and this must be attributed to the random step element of the algorithm.

(ii) BSHC - "OPTICb"

The second algorithm to be tested was implemented in the same way, and evaluated at the same conditions, as the ASSRS algorithm above. Again, a listing of the code for OPTICb is given in appendix 4. A flowchart for the subroutine is shown in fig.6.6 and may be interpreted with reference to the code listing. In this case actuator constraints can be incorporated seamlessly into the algorithm. If the controlled variable step exceeds the constraints (which can only happen as part of a successful move pattern) then worsened BSFC is flagged and the binary search "converges" in the region of this final step. If no improvement is found (that is, BSFC is improving beyond the actuator limits) then the routine naturally proceeds to the next variable.

In the DCE case, VG nozzle position was taken as the first variable, and a base step size of Ø.2V (VG range is Ø-1ØV) was used. Typical results, for the 9V/8ØØNm condition, are shown in figs.6.7-6.11. The changes in control settings are shown in fig.6.7. The nozzles are progressively closed - figs.6.8 and 6.9 show output shaft BTE increasing steadily. The peaks occur chiefly because the engine/compressor deceleration dynamic torques increase the instantaneous output shaft torque. The plateaux occur because BTE has settled before the DCE is considered stable, the stabilisation check being done on the dynamic state variables rather than the BTE for simulation purposes. The execution time of the algorithm could therefore be reduced if BTE were used to determine "stability".

In the 5 second interval shown, the algorithm does not reach a peak in BTE, and thus does not move on to alter injection timing. The reason is that in systematically moving the nozzles in one sense (more restriction) the DCE condition slowly changes. In this case the epicyclic torques

increase (engine fuelling is shown in fig.6.10) and the output shaft - being under constant load- accelerates (fig.6.11). The DCE is not being optimised at one output shaft condition, but is being moved across the operating envelope at 800Nm towards the speed at which the BTE is highest for 9V (90%) demand. This may in certain cases not lead to a true optimum, for reasons which were discussed in chapter 3. However, the speed control loop could be chosen to operate on output shaft speed for optimisation at a fixed output shaft condition as required. The above effect was masked for the ASSRS algorithm by the frequent reversal of the control moves.

Of the two algorithms tested, the BSHC method was superior in this application. However, as noted above, a parallel method (simplex) was applied by other researchers to the optimisation of three secondary control inputs on the TL11. This generally worked well, although problems were reported where input constraints were frequently encountered [76].

In summary, parallel and sequential methods are available which achieve successful automatic optimisation under simulation and laboratory conditions. It is worth re-iterating that if input constraints will frequently be encountered then the method adopted must handle this efficiently. The following section considers the use of extremal controllers under "real world" conditions.

6.2.5 Practical implementation

The practical implementation of an extremal controller must take into account:

(i) System and sensor costs - The hardware cost will be directly

related to the required speed of optimisation and the required sensor accuracies. Alternative algorithms may be more or less robust to sensor inaccuracies or noise - this may be investigated by experimental trials or by simulation with realistic noise introduced. It should be borne in mind that the engine will require some time to stabilise - this defines the upper limit on worthwhile computational speed.

High unit cost engines (marine, generation or special applications) can of course support higher hardware costs than automotive engines. Higher power output engines derive greater financial savings from a given efficiency improvement, thus, for example, large generating plant commonly incorporates expensive in-line torquemeters for efficiency monitoring.

(ii) Operating trends - the ability of a given extremal controller to achieve significant fuel savings depends upon the proportion of time spent at steady state. In generation and marine applications this may be large. In automotive applications the operating condition may be sufficiently stable for optimisation only rarely, even in long-distance haulage. Fig.6.12 shows the U.S. F.T.P. "Los Angeles Freeway" heavy-duty Diesel drive cycle for a 12 litre turbocharged engine. If "steady state" is defined for example as (numerically):

$$-N_s < N < N_s$$

$$-\dot{\tau}_s < \dot{\tau} < \dot{\tau}_s$$

where N_s = (high idle speed - idle speed)/100

and $\dot{\tau}_s = \dot{\tau}_{peak}/100$

that is, where speed and torque changes are negligibly small, then steady state obtains for only 10 per cent of the cycle time. Of this, approximately half is engine idling, where fuel consumption is very low.

While other long-haul routes may be more favourable, the applicability of direct BSFC-optimising controllers to truck Diesel engines is questionable. Even for marine engines, external disturbances such as rough seas may preclude automatic optimisation [75].

(iii) Initiation point - the benefits achievable by an extremal controller, without major unknown system changes (for example the unmonitored variation of fuel quality, or component fouling), are dependent upon the optimality of the initial settings. For accurately-scheduled control systems the benefits will be small. However, if the system characteristics change in some unprogrammed way the potential benefits are greater.

LIST OF FIGURES

OPTICa.FOR FLOWCHART

FIG. 6.1

Adaptive Step Size Random Search Optimiser.

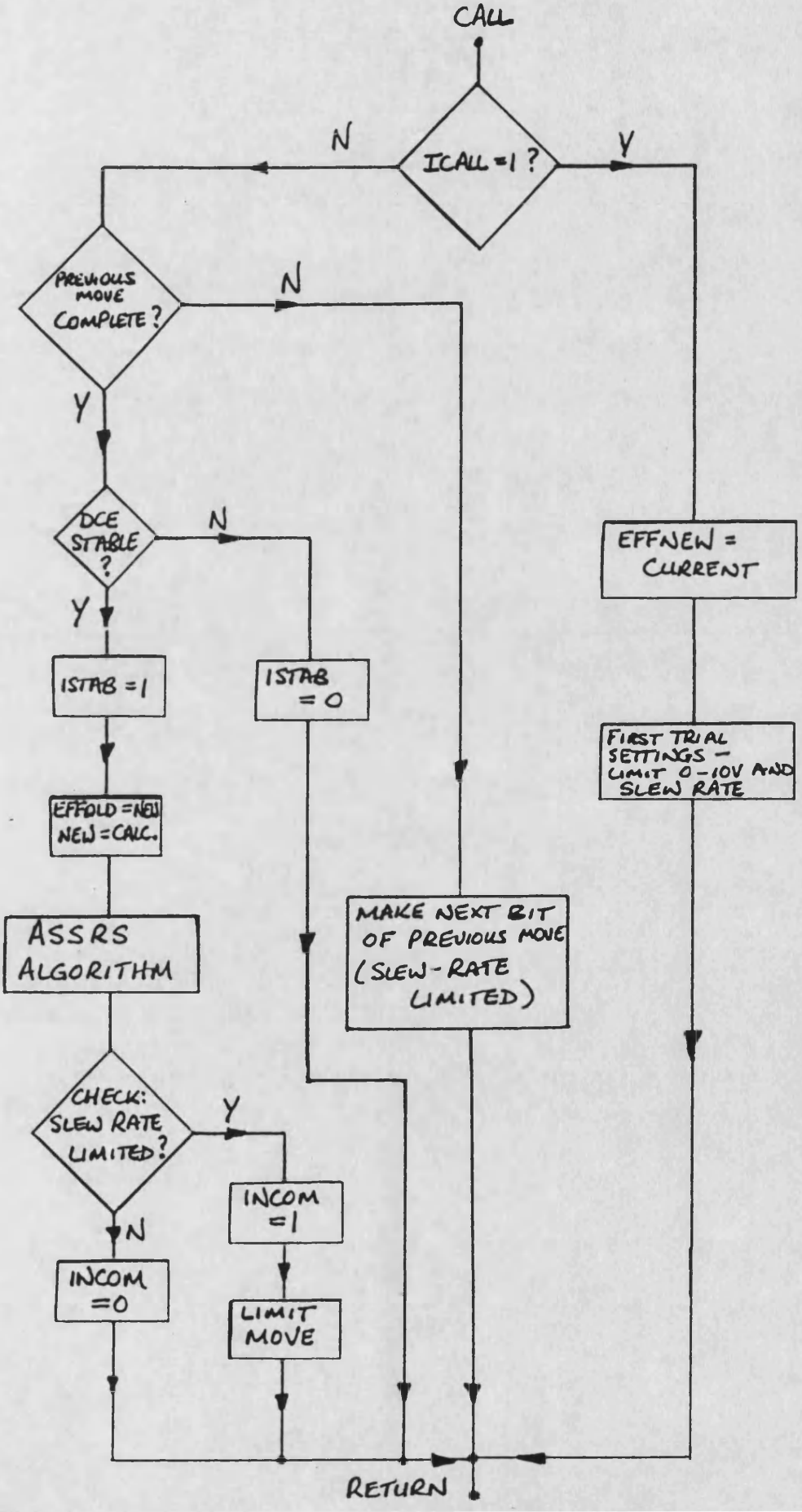

ASSRS ALGORITHM: CONTROL MOVES

Demand 9.0V (90%)
Load 800 Nm
Base step size 0.2V, contracting "success" step size
NB data shown every 0.2s, not every move.

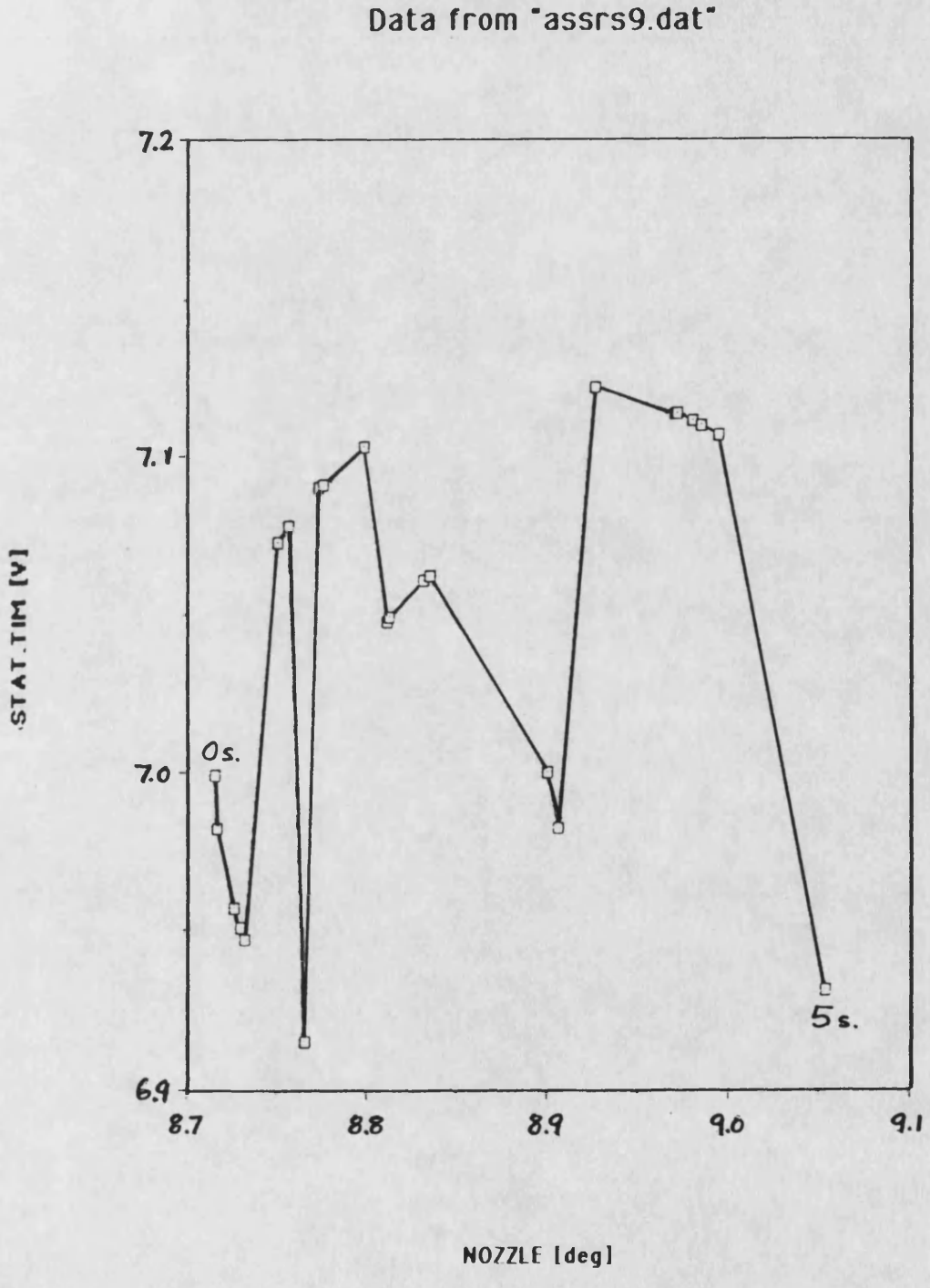

FIG. 6.2

ASSRS ALGORITHM: BTE CHANGES

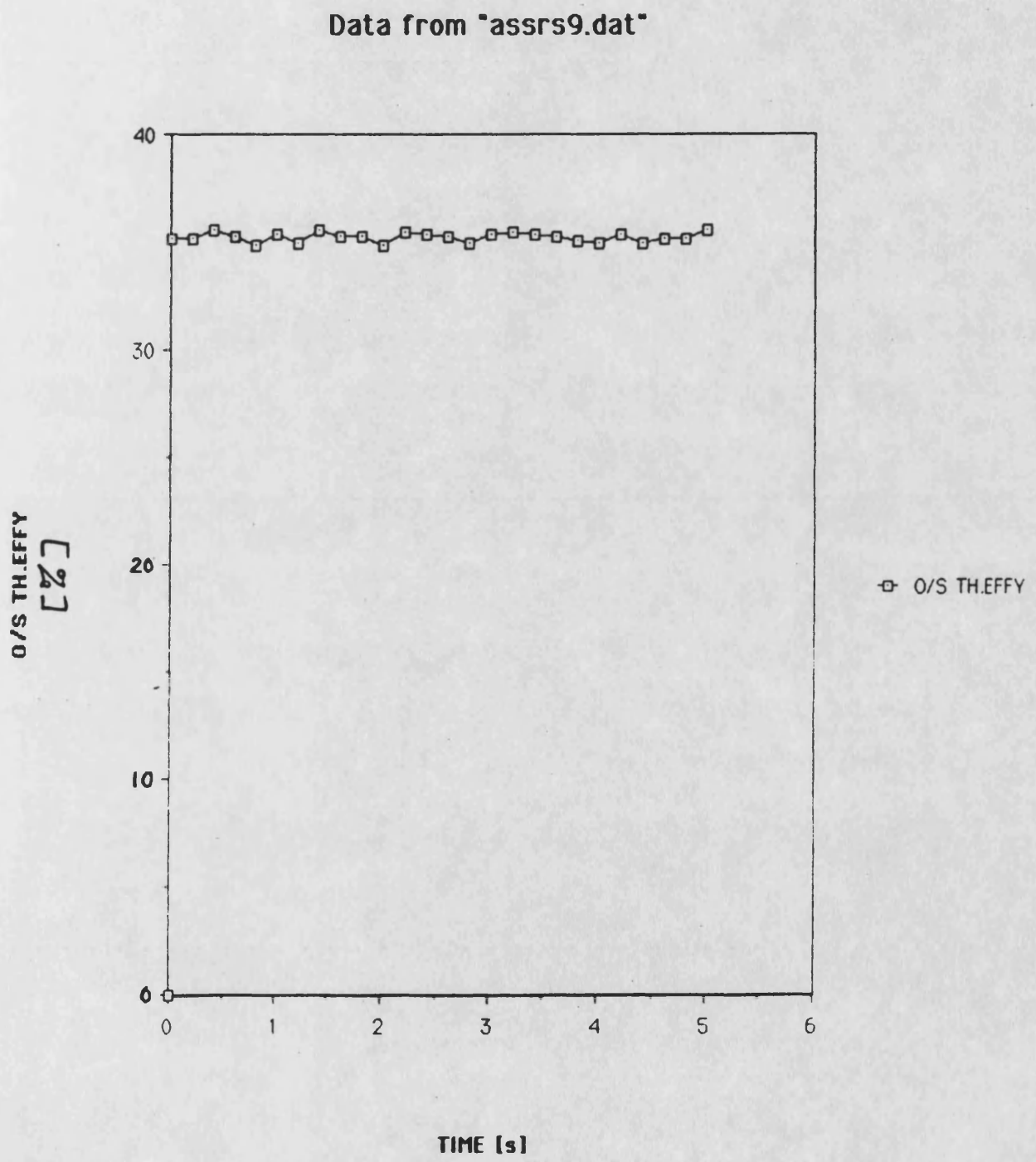

FIG. 6.3

ASSRS ALGORITHM : BTE CHANGES - DETAIL

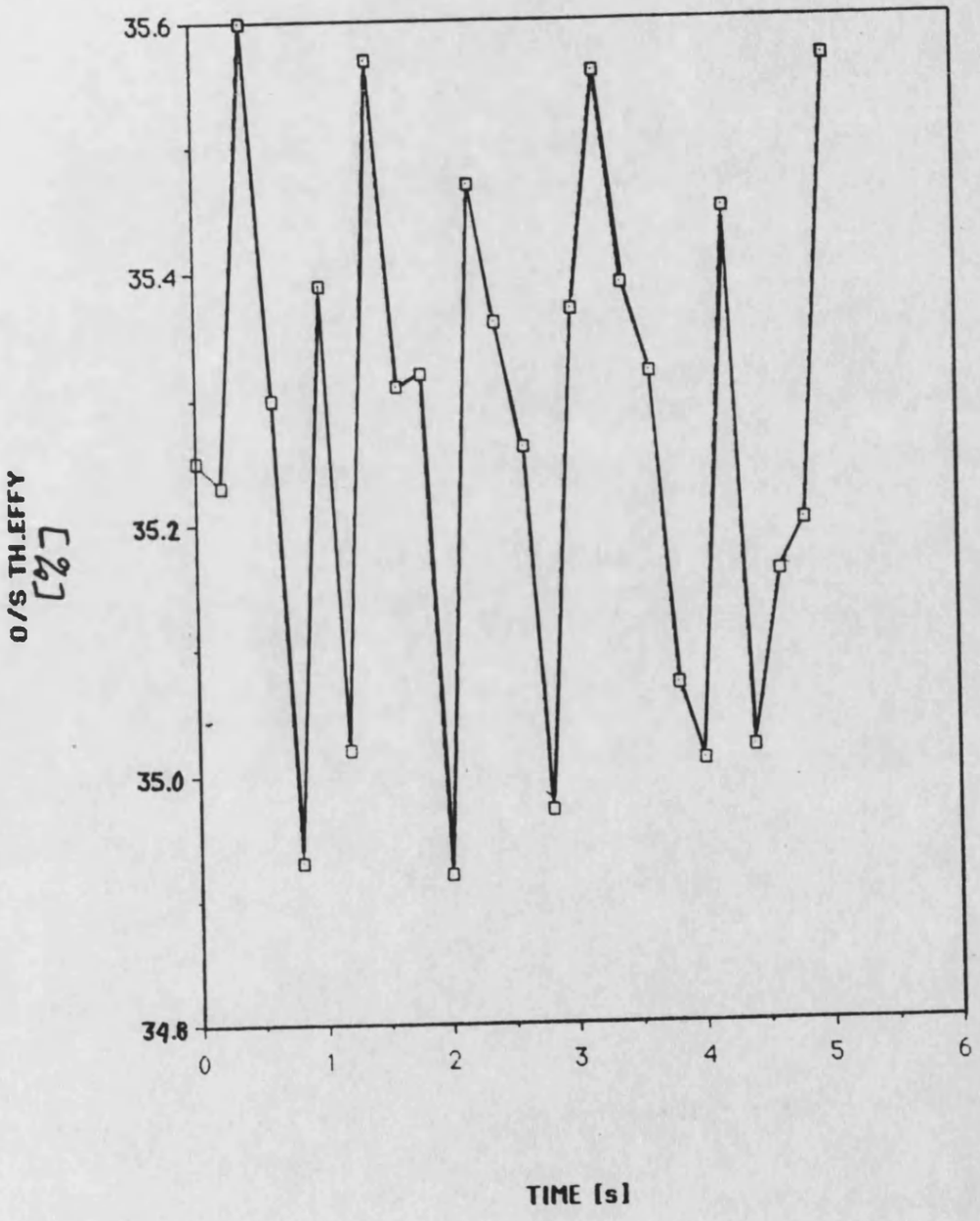

FIG. 6.4

ASSRS ALGORITHM : ENGINE FUELLING RESPONSE

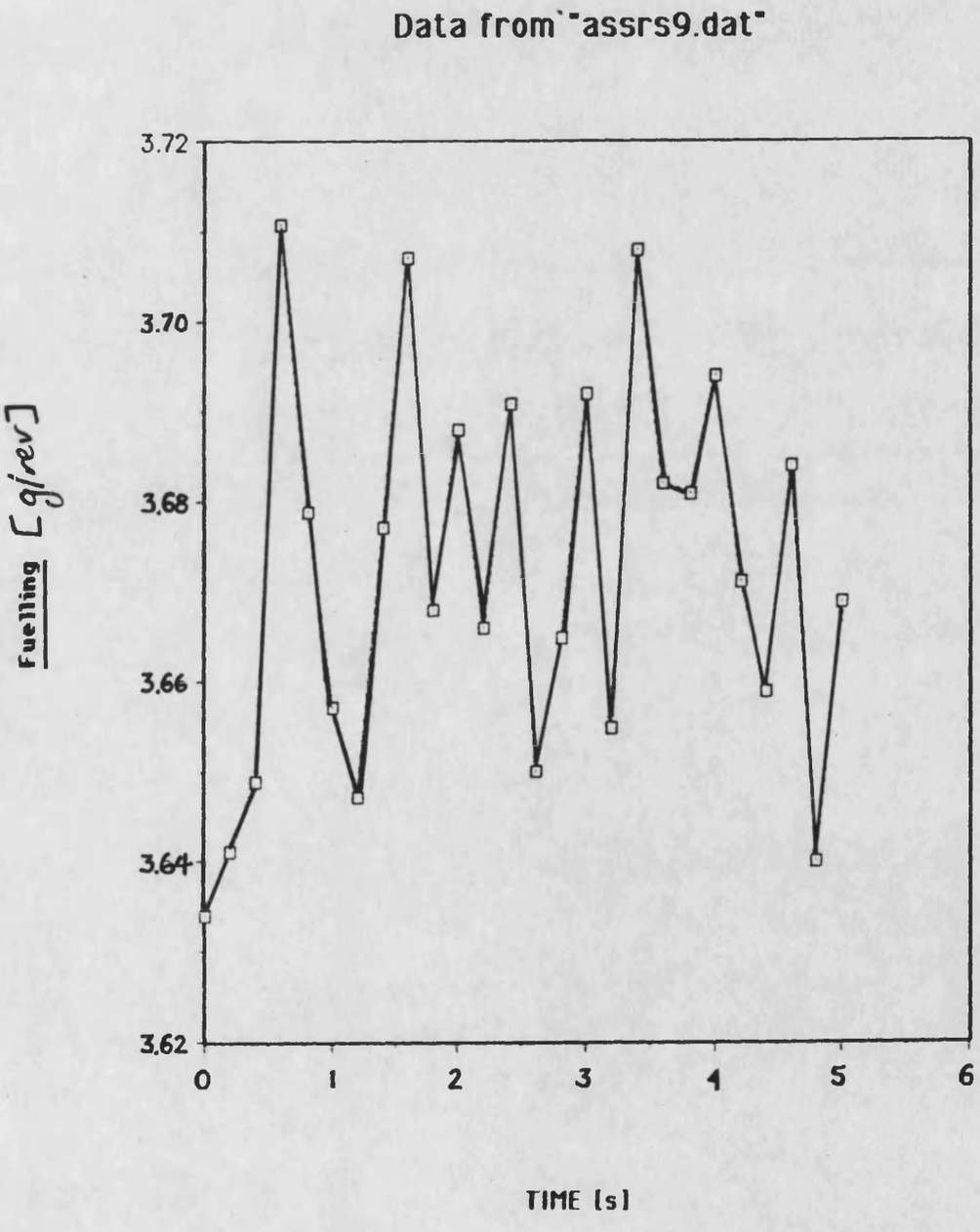

FIG. 6.5

OPTICB.FOR FLOWCHART

FIG. 6.6

Binary step hill-climbing optimiser.

(NUMBERS ARE CORRESPONDING POINTS IN FORTRAN CODE)

Note:
KB - base step size
KC - current step size
KR - step size reduction factor (0.5).

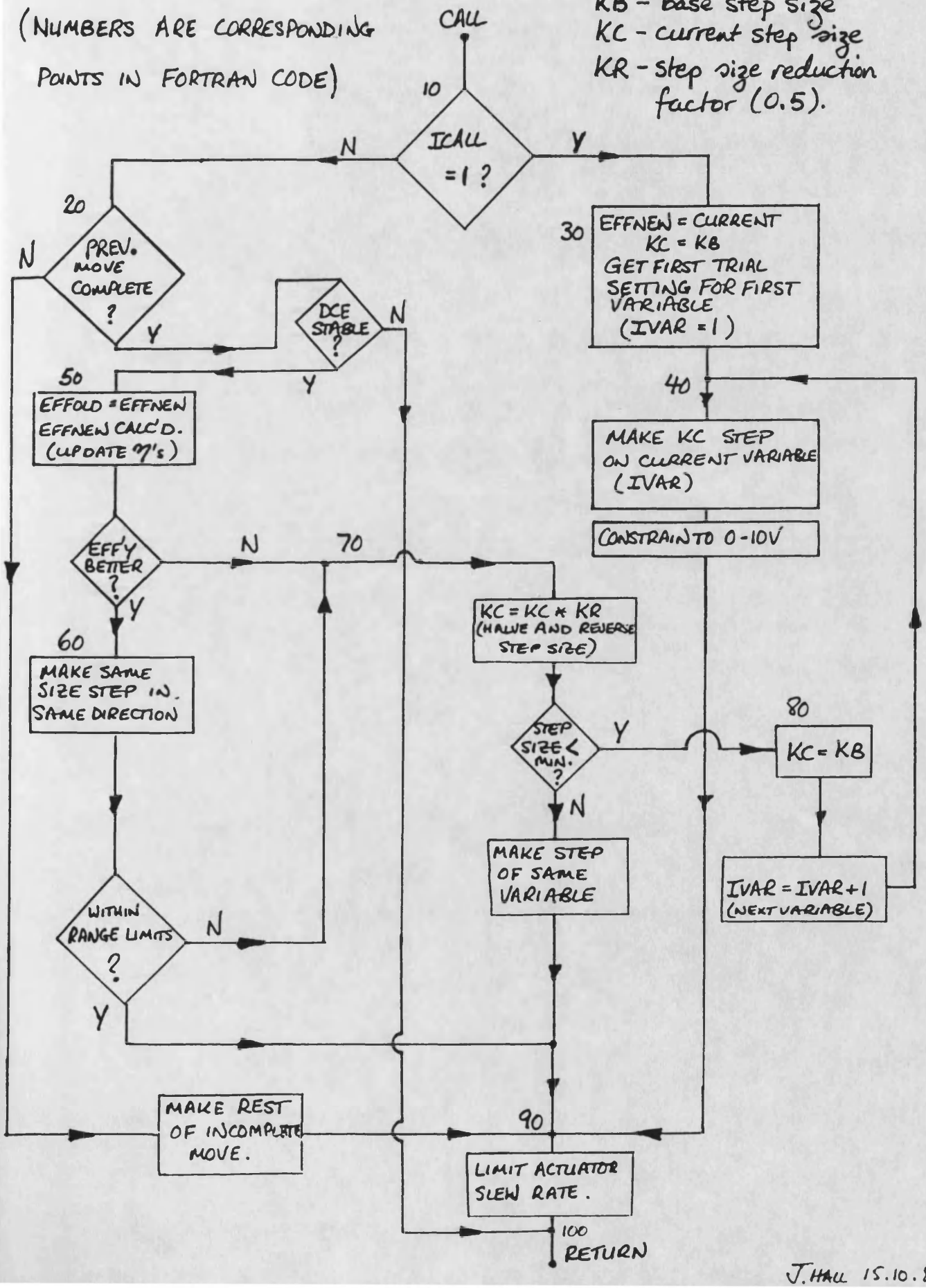

J. HALL 15.10.87

BSHC ALGORITHM : CONTROL MOVES

NOZZLE ANGLE STEPS AS SHOWN.
TIMING HELD AT 7V STATIC.

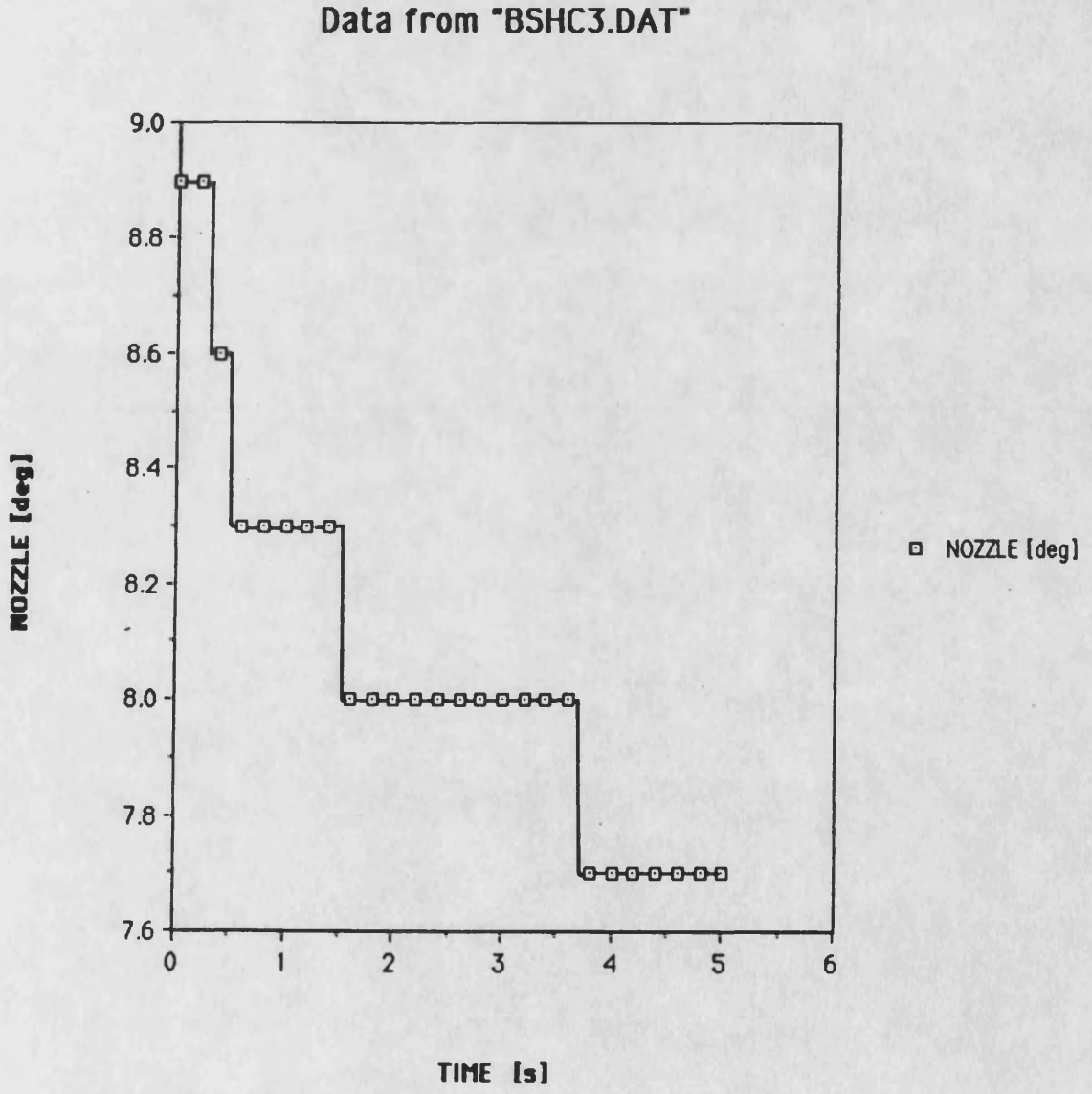

FIG. 6.7

BSHC ALGORITHM : BTE CHANGES

Demand 9.0V (90%)
Load 800 Nm
Base step-size 0.2V
Results show data at 0.2s intervals only.

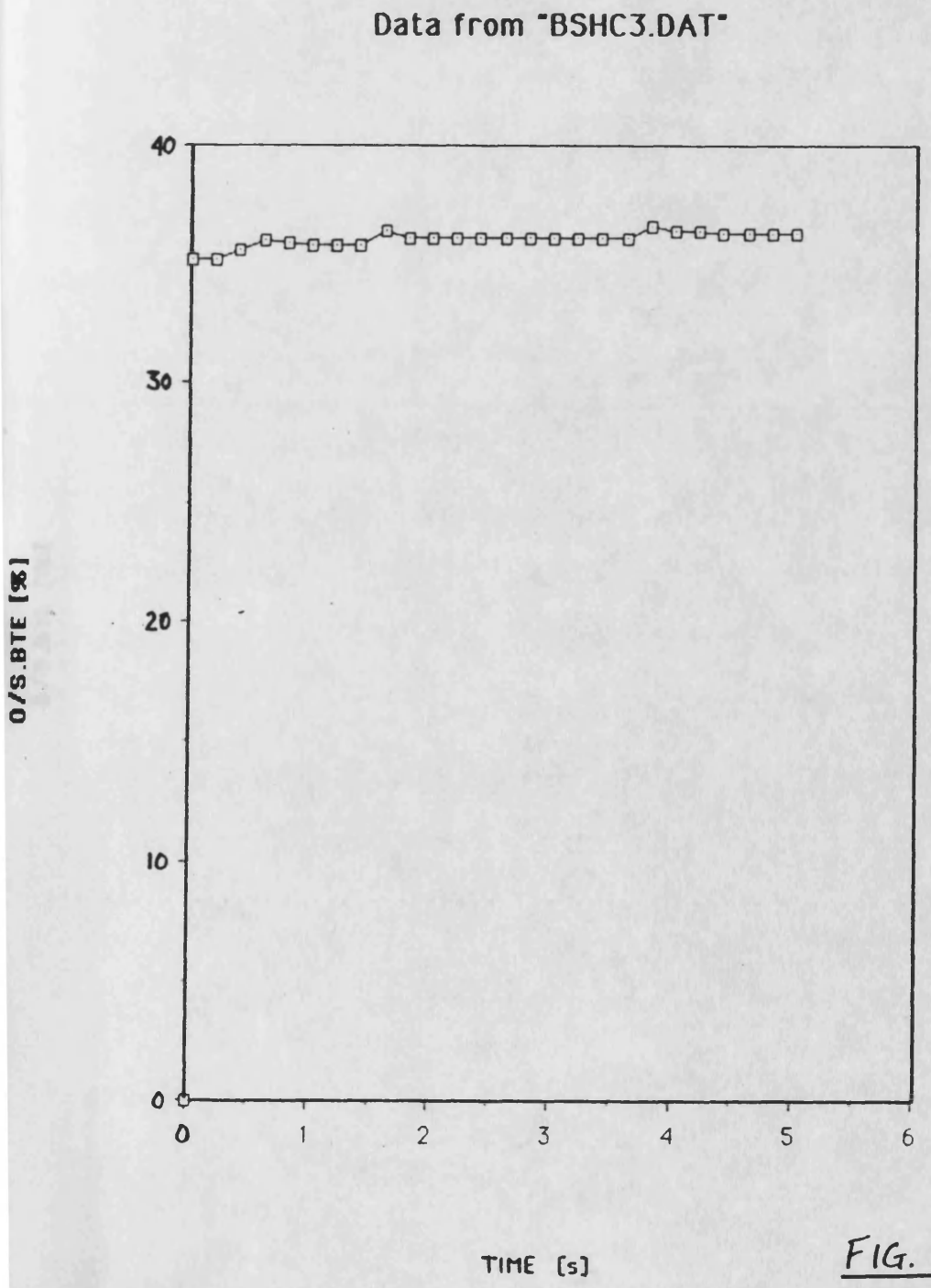

FIG. 6.8

BSHC ALGORITHM : BTE CHANGES - DETAIL

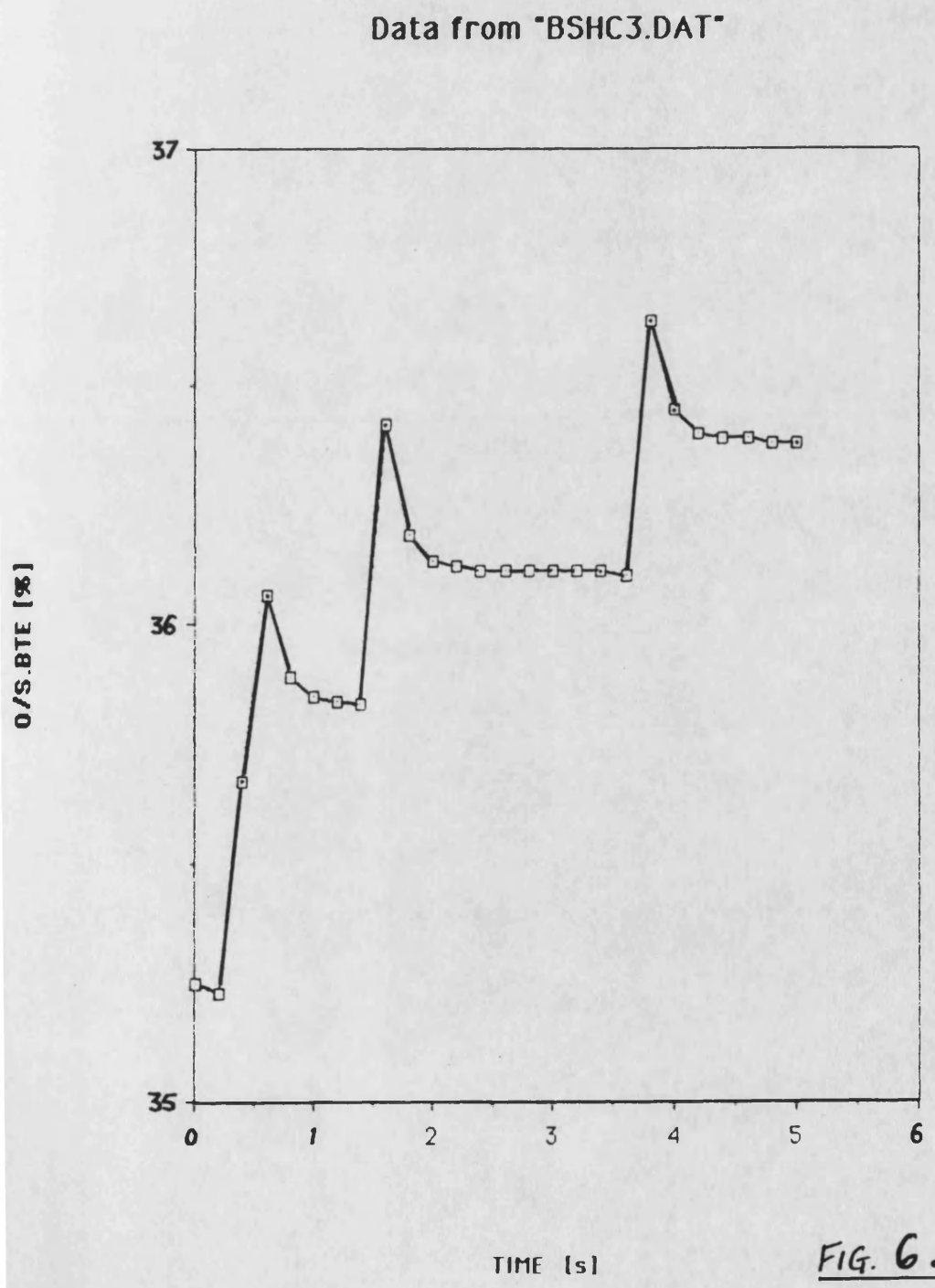

FIG. 6.9

BSHC ALGORITHM : ENGINE FUELLING RESPONSE

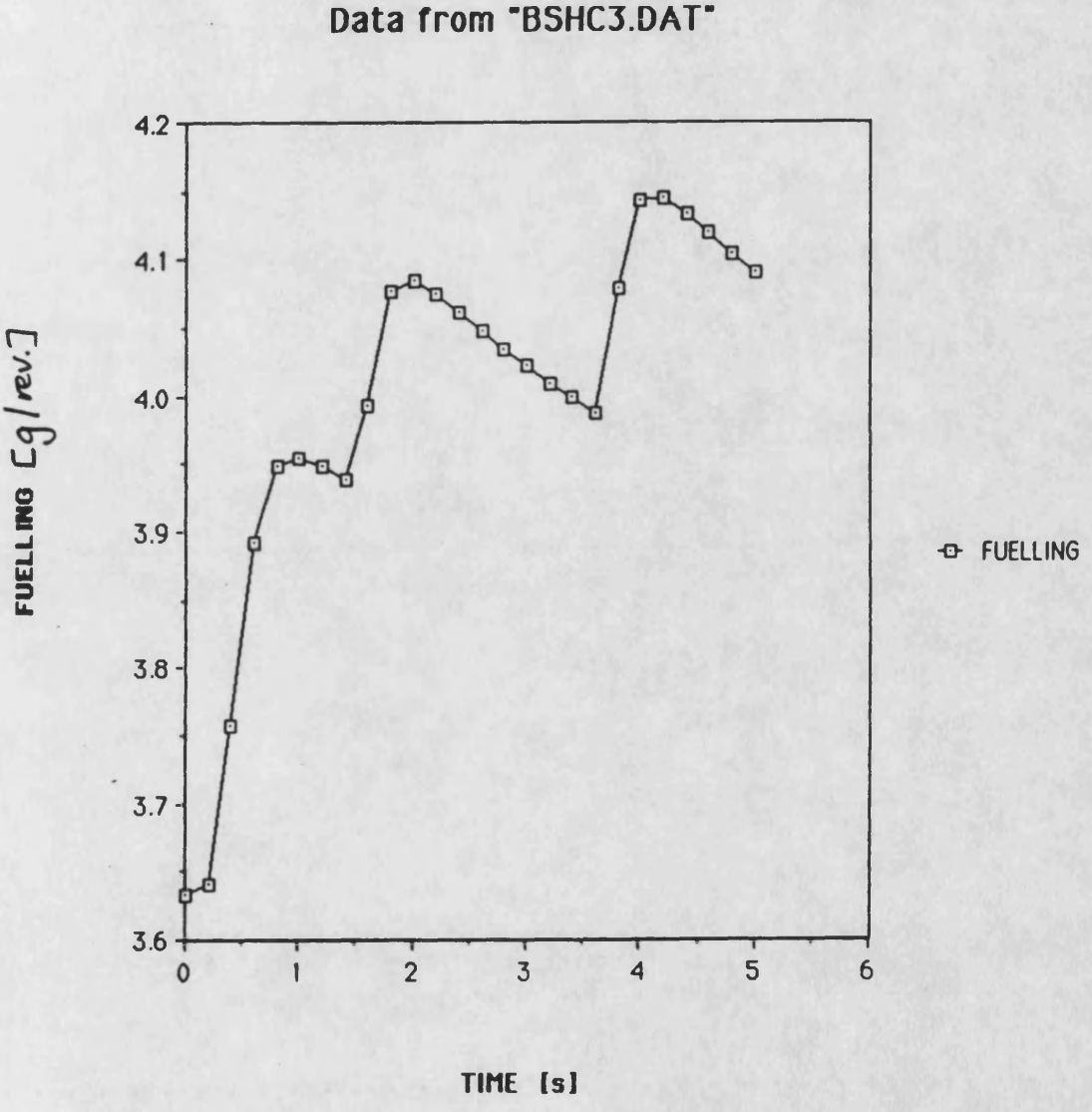

FIG. 6.10

BSHC ALGORITHM : OUTPUT SHAFT SPEED RESPONSE

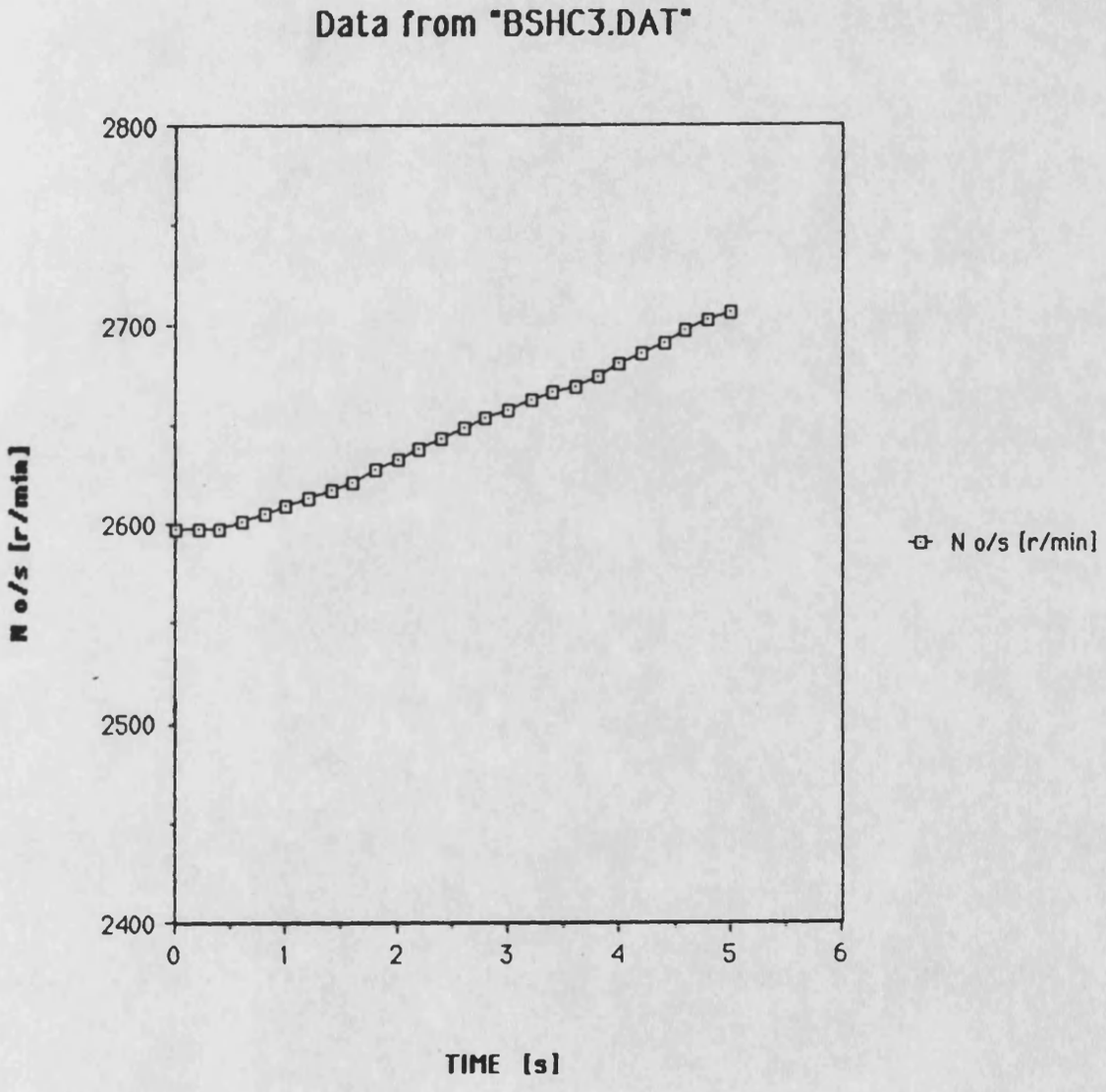

FIG. 6.11

U.S. FTP Los Angeles Freeway Drive Cycle

(12 litre Heavy-Duty Diesel)

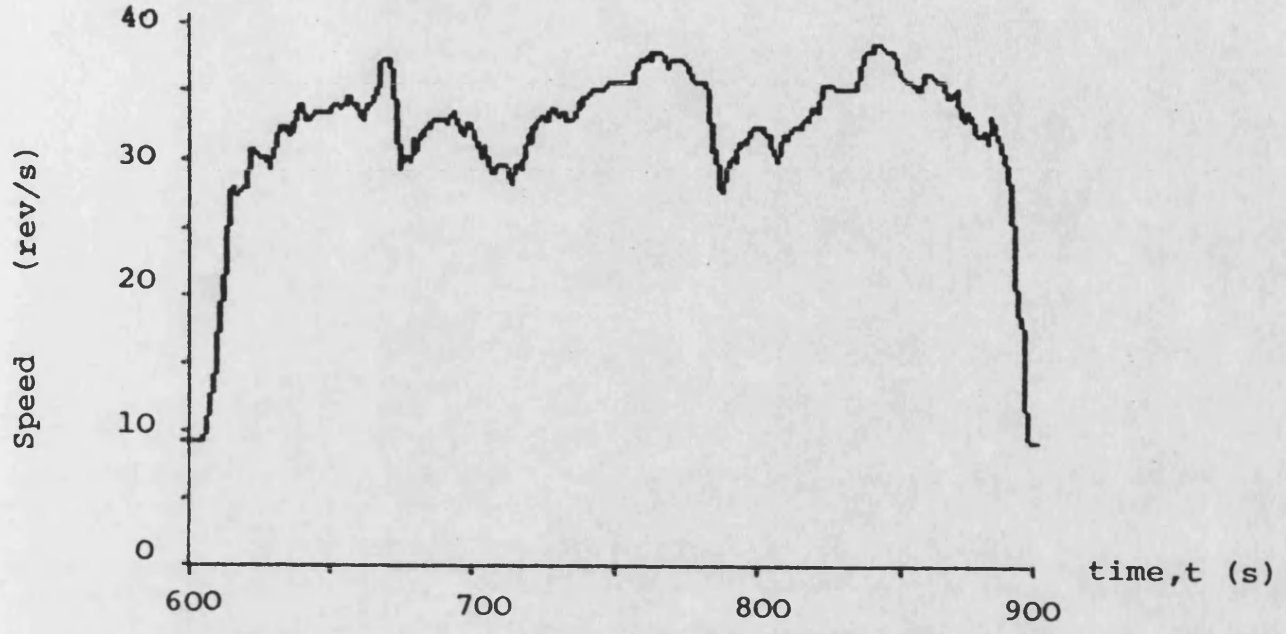

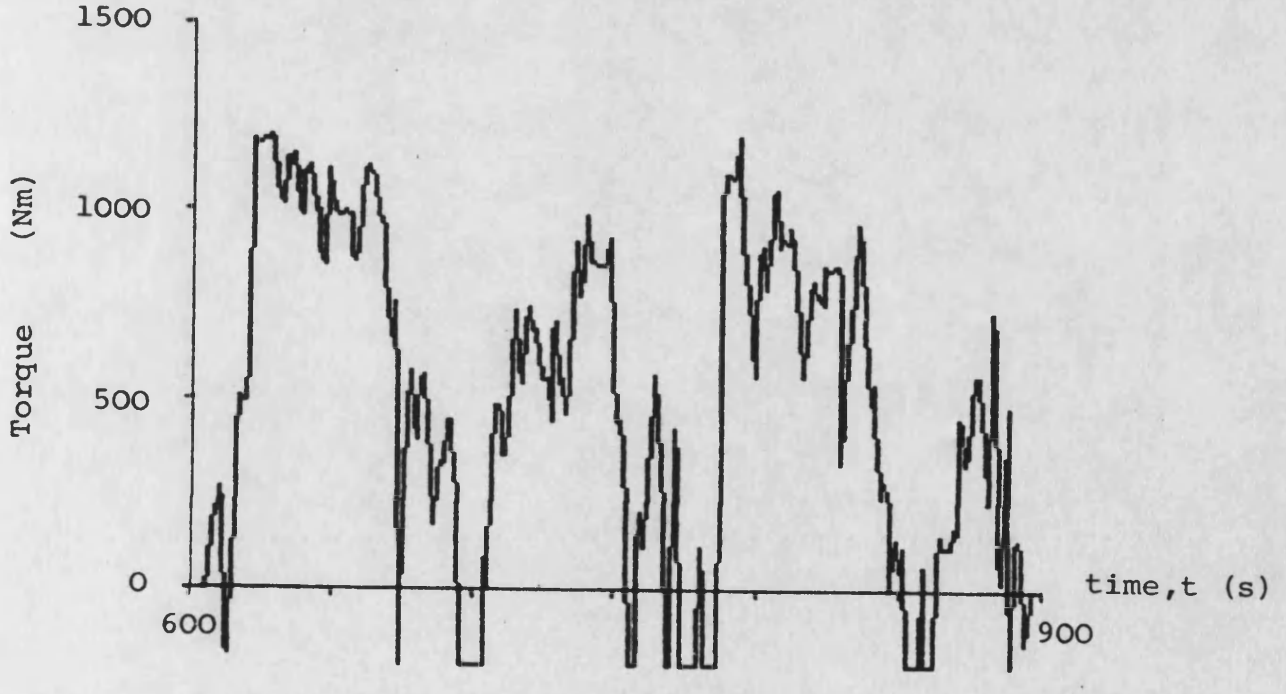

FIG. 6.12

7. CONTROLLER DEVELOPMENT AND TRANSIENT SIMULATIONS

7.1 Introduction

7.2 DCE control design

7.2.1 Control strategies

7.2.2 Controller C1

7.2.3 Controller C2

7.2.4 Digital implementation

7.3 Experimental / simulated transient comparisons

7.3.1 Initial comparisons

7.3.2 Engine torque model revisions

7.3.3 Turbine swallowing capacity revisions

7.3.4 Other conditions

7.4 Parametric study

7.4.1 Introduction

7.4.2 Maximum fuelling/boost ratio

7.4.3 System volumes

7.4.4 Turbine swallowing capacity

7.4.5 Turbine CVT

7.4.6 Driver output shaft speed demand

7.4.7 Transient boost pressure

7.4.8 Transient bypass restriction

7.4.9 Parametric study - conclusions

7.5 Low driver demand operation

7.6 VG turbocharged engine comparisons

7. CONTROLLER DEVELOPMENT AND TRANSIENT SIMULATIONS

7.1 INTRODUCTION

This chapter is concerned firstly with the selection of control strategies for the DCE, and the development of control designs to implement these strategies effectively. Secondly, the resulting simulated transient performance of the DCE over a range of possible dynamometer and vehicle condition is discussed. Comparisons between experimental and simulated transient responses are made at this point, to indicate the validity of these predictions. Finally a brief parametric study is discussed, chiefly concerned with modifications for a practical vehicle application.

The DCE presents a potentially difficult control task. The responses of the main operating variables (component speeds, torques, boost pressure and so on) to the control inputs are likely to be quite non-linear, and to vary with operating point (non-stationary). This is true of conventional engines, but may be worse in the DCE case owing to the increased number of components, and associated speed, torque and gas flow interactions. The control inputs are also strongly non-linear in as much as they may be limited to much less than desired levels. For example fuelling (rack control input) is almost invariably constrained due to inadequate boost during transients. Furthermore, as discussed in Chapter 2, the DCE exhibits significant cross-coupling between the effects of the two primary control inputs, fuel rack and turbine VG position.

Three practical approaches to controller design are possible :

(i) Select the form of the control loops qualitatively, and tune and test the controller systematically.

(ii) Identify the response of each controlled parameter to each control input to obtain some form of linearised model (continuous transfer function, state-space or discrete input-output form). Design compensators using established techniques such as pole placements or Bode plots, or "optimal" (cost-function based) methods. This will include compensation for multivariable cross-coupling effects where these are significant.

(iii) Establish the general form of the responses, and carry out identification and compensator design for each control loop in real time; that is implement adaptive control.

In each case it is possible to use a dynamic simulation to develop the controller, without the difficulties and potential damage involved in working directly on the DCE prototype. The simulation must model the non-linear DCE dynamics accurately, and must also model any significant actuator dynamics. "SIMDCE" (Chapter 5) was developed for this purpose.

The application of approach (ii) to an automotive gas turbine is described in [22, 23]. The two-shaft gas turbine in automotive applications is closely analogous to DCE in that the control inputs (gas generator fuelling and free turbine nozzle angle) have cross-coupled effects upon the major operating parameters (gas generator speed, free turbine inlet temperatures and speed). Continuous transfer functions were obtained from a dynamic model [22]. Having selected suitable control strategies (that is, the desired input-output couplings), multivariable precompensators were designed to diminish cross-coupling, using the Inverse Nyquist Array (INA) technique [77]. However, the individual loop compensation was developed quantitatively using the simulation [23]. Large reductions in transient response lag were

achieved with the multivariable control system. This could largely be attributed to the insight into suitable strategies - particularly the use of free turbine nozzle angle during transients - obtained from the system identification study, rather than multivariable design techniques per se.

At the start of the DCE control work reported here, there was of course considerable existing knowledge about suitable control strategies. These strategies were summarised in [32, 37], and are the basis of the current work.

Because of the aforementioned DCE and control input non-linearities (which were similarly encountered in the referred gas turbine study, demanding local linearisation), and because the DCE responses to the control inputs were qualitatively understood from experimental work it was decided initially to adopt an heuristic approach to the control design (approach (i) mentioned above). That is, control terms would be introduced and tuned as necessary in the dynamic simulation, to achieve the desired control accuracy, stability and dynamic response over the DCE operating range. This approach necessarily is restricted to single-input, single-output (SISO) loops. A multivariable controller would be extremely difficult to tune heuristically. Furthermore, it was decided to use the general concept of proportional integral-derivative (PID) control, since the effect of each term is readily understood. Manually-tuned PID controllers are widely used for straightforward applications in all fields of control. Relatively inexpensive microprocessor-based PID controllers are now available in which the tuning heuristic is carried out automatically, and often continuously (adaptive control).

It should be noted at this point that all control designs were to be digitally implemented using a microcomputer, hence control design complexity would not be restricted.

Control designs based on identified system models, and incorporating multivariable compensation, are covered in Chapter 8.

7.2 DCE CONTROL DESIGN

7.2.1 Control Strategies

The objectives of the DCE controller are quite simple : at steady-state fuel efficiency should be maximised, in transients output shaft torque response should be maximised. In all situations the controller must accept a single feedforward demand (hereafter termed "driver demand") and generate all necessary DCE control inputs according to current (feedback) operating conditions. In principle only output shaft torque - and thus output shaft speed - need to be controlled stably, since everything else is "transparent" to the driver. In practice unstable operation of, for example, boost, and high control effort in the actuators, would be unacceptable for reasons of durability and subjective driver "feel".

In conventional heavy-duty Diesels, driver demand is commonly interpreted as an engine speed demand, and fuelling is varied in proportion to the error between demanded (feedforward) and feedback speeds (all speed governing). Of course, the corresponding driveshaft speed - and vehicle speed - depends upon the selected transmission ratio. The driver effects an intelligent closed loop around vehicle speed and moderates the speed demand accordingly. The DCE situation is very similar - if fuel rack is used to control engine speed, then output

shaft speed at, say, a fixed turbine VG setting, will vary continuously ("droop") with load. Again the driver would naturally compensate for this droop by altering the driver demand. The use of fuel rack to control output shaft speed directly is feasible, but it will be demonstrated later that the choice is somewhat arbitrary because of the "driver feedback", and that the implied open-loop control of engine speed is less satisfactory than open-loop control of output shaft speed. Thus the rack control input was used to control engine speed, and driver demand was taken to be engine demand.

The effect of turbine VG upon the remaining DCE parameters ("states") was discussed with reference to experimental optimization in Chapter 3. The VG control input has the following tasks [78]:

(i) At steady-state, with engine speed set by the driver demand, and output shaft torque level set by the (extraneous) load, the VG restriction must set the remaining independent state (compressor speed or output shaft speed or a boost pressure) to achieve best thermal efficiency. Open-loop VG position scheduling was ruled out because of potential VG mechanism unrepeatability as result of fouling, wear or inaccurate calibration. In a production context, manufacturing tolerances would be a further reason.

(ii) During a transient the epicyclic torque and boost relationships no longer hold. The VG control may thus be used to set any boost pressure irrespective of torque. The chosen boost pressure will determine the development of individual component speeds and torques in a given transient. As stated above the objective is stable, rapid output shaft torque response, for acceleration or load acceptance.

Alternative controller designs are discussed in sections 7.2.2 and 7.2.3 below :

7.2.2 Controller C1. (fig 7.2)

The first stage of each controller design is to specify how the VG control is to be scheduled for optimum steady-state thermal efficiency. It had been proposed [32] that the DCE could be held on the optimum surface by scheduling boost pressure. However, this can be shown to be incompatible with the practical need to map the schedule onto a base of output shaft speed versus fuelling (rack position), which requires only a speed and position sensor; rather than the obvious output shaft speed versus output shaft torque basis, which requires a speed and torque sensor. The argument is as follows : at steady-state, engine torque is broadly proportional to fuelling. Compressor torque is proportional to engine torque due to the epicyclic gearing, and with the positive displacement compressor boost pressure is nearly proportional to torque. Thus fuelling and boost are practically proportional at steady-state, irrespective of VG setting.

To set the basic DCE condition, three independent states are required, as explained in Chapter 2. These may be any two epicyclic speeds, and either an epicyclic torque or a boost pressure. Having chosen output shaft speed and fuelling (implying the epicyclic torque level) as the indices of the schedule, the scheduled variable must be either compressor or engine speed. Although engine speed is already being controlled by the rack input, it would be valid to schedule engine speed as the feedforward to the VG control loop: the VG would have the effect of "pulling" the schedule across, that is output shaft speed would change until the current optimum engine speed coincided with the actual

engine speed. Scheduling compressor speed was the more obvious choice for C1, but it should be noted that an additional speed sensor (or at least computation of compressor speed from sensed engine and output shaft speeds) is incurred. The schedule (based on experimental data) is shown in fig. 7.1.

The variety of possible scheduling arrangements may appear daunting, but the concept of three independent states can be used to show that the selection is nominal and may be made freely on the basis of convenience or sensor costs.

A schematic of C1 is shown in fig. 7.2. The engine speed control loop (top of figure) uses proportional compensation only (Kprop.), giving droop with load as in a conventional allspeed govenor. Choice of Kprop and the driver demand scaling (Kscale) was therefore based on mechanical governor rules: a typical choice of about 8% governor run-out, that is high idle speed relative to reated speed (2600 rev/min), implied a maximum speed demand of 2800 rev/min. Zero to full driver demand corresponds to 0-10 Volts in the prototype and the simulation. Kscale was thus chosen to be

$$\frac{\text{max. speed demand}}{\text{max. driver demand}} = \frac{2800 \text{ [rev/min]}}{10 \text{ [Volts]}}$$

and Kprop was therefore the ratio of maximum rack position at rated speed (based on experimental data) to maximum speed error at rated speed:

$$\frac{7.5 \text{ [Volts]}}{(2800 - 2600) \text{ [rev/min]}}$$

The use of compressor speed rather than boost pressure control removes any closed-loop limitation on the boost level reached at steady-state or

in transitions between transient and steady-state control. Therefore an additional loop was added to prevent boost exceeding the 4 bar engineering limit.

It was found extremely difficult to control compressor speed accurately whilst the use of the nozzle VG was restricted by boost-limiting. Ideally the boost-limiting control would :

(i) Not interfere with steady-state scheduling action below the 4 bar boost limit

(ii) Close to 4 bar, act quickly to prevent this limit being exceeded.

The final control terms, as shown in fig. 7.2, were proportional plus integral (PI) control of compressor speed error and proportional plus derivative (PD) control of "boost relief". Importantly, the latter proportional term was switched out below 3.9 bar to enable steady-state compressor speed control to work unhindered. The derivative term was used to give "velocity feedback" to damp the response. The compressor speed integral term was zeroed during major transients to prevent saturation.

As discussed in section 7.2.1 above, the VG control objective in transients is to achieve the best combination of boost and air flow developments for fast transient response.

Since the engine is the "prime mover", delivering both output shaft power and power to the compressor for increased boost and air delivery, maximum fuelling is incontrovertibly required. To limit smoke, a minimum engine air/fuel ratio (AFR) must be observed. In common with mechanical fuel pumps (aneroid limiter), C1 uses fuelling/boost ratio

(FBR) in lieu of AFR. Thus transient boost must be at least sufficient to allow full fuelling without exceeding the chosen FBR limit. However, given that the DCE components have been matched correctly, the achievable boost pressure is always greater than that required for smoke control. The decision must therefore be made whether to control for operation at the smoke limit, or with the higher boost.

Higher boost will reduce the acceleration of the engine-compressor combination, and transmit a higher torque directly through the planet carrier to the output shaft. Alternatively, if the engine and compressor are allowed to accelerate more freely (smoke-limiting boost only), the engine will be able to generate more power. Furthermore, it must always be remembered that the turbine contribution is important, and that the boost/airflow trade-off will affect turbine energy utilisation. The optimum boost level was therefore not clear-cut. Controller C1 used the minimum (smoke-limiting) transient boost. The effect of a higher boost level was subsequently investigated, as described later in this chapter.

It should be stressed that the required transient boost pressure must be calculated on the basis of the desired fuelling rather than the actual (smoke-limiting) fuelling.

The controller was tuned by investigating the response to two "standard" major transients:

(i) Driver demand step : 5-10V (1400-2800 rev/min) driver demand at 500 Nm load torque (fig. 7.3).

(II) Load step : 400-1400 Nm load step at 10V (2800 rev/min) driver demand, with low and high output shaft inertiae (fig. 7.4).

The fundamental problem encountered was that sufficiently high control gains to control compressor speed and maximum boost tightly led to oscillation, and to hunting between these two controls.

The finalised control terms and gains are shown in table 7.1. Three transient responses are presented for C1; the driver demand step and load step above, plus a combined step:

4.5V (1260 rev/min) driver demand, 800 Nm load torque to
9V (2520 rev/min) driver demand, 1600 Nm load torque (fig. 7.5)

All are with the estimated dynamometer inertia of 30 Kgm^2. The parameters of most interest are output shaft speed (the ultimate measure of the response), the VG nozzle control position and resulting compressor speed and delivery pressure.

Fig. 7.3 shows the driver demand step. It should be noted that the data is shown only in 0.5 sec. intervals, owing to memory size constraints. Compressor speed and boost responses are quite smooth. Output shaft speed levels off at approximately the rated speed of 3400 rev/min, due to automatic fuelling reduction (turbine over-speed limiting as shown in fig. 7.2). The most important response is the VG control position : the response is poor in that full restriction is not used despite the inadequate boost at the start of the transient. This is due to the rather low gains required for stability, and to the addition of steady-state and transient VG control inputs to form the net VG input.

Fig. 7.4 shows the load step. Output shaft speed falls from the initial limiting speed as the very high load is applied. Since engine speed is controlled and roughly fixed, the differentially-driven compressor

increases speed. Although turbine swallowing capacity will increase somewhat as its speed falls (fixed gearing to the output shaft), the increase in compressor air delivery far outweighs this and boost rises rapidly. This is the inherent DCE characteristic, giving good load acceptance even with a fixed geometry turbine. In fact it is seen that the VG response is oscillatory as boost approaches the 4 bar limit. As noted earlier, the proportional term in the boost-limiting control is switched out below 3.9 bar to avoid interference with steady-state compressor speed control, and this severe non-linearity makes tuning difficult.

Fig. 7.5 shows the combined step; again as boost rises rapidly with compressor speed, VG restriction first reduces, then becomes oscillatory as the boost limit is approached.

In summary, while C1 gave quite smooth engine speed, output shaft speed and boost responses, keeping within engineering limits, the VG control inputs were frequently oscillatory. Furthermore, the combination of steady-state and transient objective control inputs was detrimental to both, and required the use of velocity feedback for acceptable transient boost control. The large number of control terms implied a major tuning effort, and it seemed likely that re-tuning would be necessary if C1 were implemented on the 520DCE. A simpler, more robust controller was required, though using similar strategies.

7.2.3 Controller C2 (fig. 7.6)

It may be noted from experimental results (Chapter 2) that optimum VG position is usually near full closure (typically 80-95% closure). Although open-loop VG position scheduling was ruled out earlier, it was

possible to combine position scheduling with closed-loop proportional control of compressor speed and/or boost pressure. The advantages are twofold - firstly, the removal of the integral term, and secondly the ability to reduce the proportional term in all VG control loops - both of which may improve stability.

In addition, a discrete switch is made between steady-state (compressor speed) control and transient (boost) control, rather than combining the two inputs. Again this is made possible by the use of position offsets plus reduced gains, which enables smoother transitions to be made. The most effective transient indicator was considered to be rack position. Given the engine speed control loop, rack will increase with increase of demand and/or load. The switchover is made at a predetermined level, in this case maximum rack (before smoke-limiting rack reduction is applied). In minor transients, where the required rack position is less than this the DCE will follow the optimum thermal efficiency surface, which seems reasonable. A schematic of C2 is shown in fig. 7.6. It will be noted that the problematic maximum boost control has been deleted; with the more accurate offset-plus-proportional steady-state control it was found that boost implicity remained below 4 bar. The finalised control gains are shown in table 7.2 - VG control gains are reduced by a factor of at least ten compared with C1. A program listing for C2 is given in Appendix (4).

Driver demand, load and combined step responses are shown in figs. 7.7, 7.8 and 7.9 respectively. These are directly comparable to the C1 responses, figs. 7.3 - 7.5. In the driver demand step (fig. 7.7) boost rises more quickly than for C1, with a corresponding improvement in output shaft speed response. The discrete switch back to steady-state

control at approximately 7.5 seconds causes a slight "kick" in boost pressure - the slight dip in output shaft speed at this point is a result of fuelling cutback to prevent overspeeding. The load step and combined step responses (figs. 7.8, 7.9) are similar; both exhibit smooth VG control, with corresponding smooth compressor speed and boost increases. As indicated earlier, boost settles below the 4 bar limit as an implicit result of accurate scheduling control. The system does not return to steady-state control because the greatly increased load in both cases depresses engine speed for below the demanded level.

The following conclusions may be drawn from this comparison of C1 and C2:

(i) C1 gives oscillatory VG nozzle control, particularly for transients involving load steps. This is chiefly a result of the need to operate usually near maximum turbine restriction, requiring high control gains for acceptably tight control. This was overcome in the C2 design by incorporating scheduled VG position offsets.

(ii) C2 gave slightly better output shaft speed response than C1 in each transient case. The difference was greatest for the driver demand step, being attributable to the more rapid boost rise allowing more rapid fuelling increase. This is in turn a result of the discrete switch to transient control, rather than combining steady-state and transient control inputs. The discrete switch back to steady-state control led to a "kick" in boost pressure. With a representative vehicle inertia this may be acceptable; otherwise steady-state and transient control inputs could be combined with weighting according to desired rack position.

It was decided that C2 was acceptable for implementation on the 520DCE prototype. Since the controller was to be implemented into a microcomputer, it was first necessary to investigate the discrete-time behaviour of C2.

7.2.4 Digital implementation

The controller development described in the preceding sections assumed analogue control. In simulation terms this means that the controller subroutine was called at the same time intervals as the dynamic model subroutine. To simulate discrete-time (digital) control, the controller subroutine was run asychronously from the model.

Techniques for the direct design of digital controllers are discussed in Chapter 8. At this stage the task was to convert an existing analogue design. Given a general analogue PID controller of the form

$$\frac{U(s)}{E(s)} = k_p + \frac{k_i}{s} + k_d.s \qquad (7.1)$$

where u, e are the control input and the output error respectively and s denotes the laplace operator, it is evident that the integral and derivative terms would have to be based on discrete calculations.

Formal "discretisation" methods are explained in [68, 79]. First the analogue expression (7.1) is converted to a discrete "equivalent" using one of several accepted rules (the same rules are used in direct digital design and are described in Chapter 8), and assuming some fixed controller sample interval. The resulting expression has the form:

$$\frac{U(z)}{E(z)} = fnc.(z) \qquad (7.2)$$

where Z is the discrete-time operator, Z^{-1} denoting a time delay of one sample interval. This is then expressed as a difference equation of the form

$$u_i = fnc(e_i, e_{i-1}, \ldots, u_i, u_{i-1}, u_{i-2}, \ldots) \qquad (7.3)$$

where the subscripts i, i-1... denote current and past sample instants. Again the step from (7.2 to (7.3) may follow different rules, giving difference levels of robustness and simplicity [79].

The use of VG position offsets in controller C2 enabled all control loops to use only proportional terms. In this case the digital control consisted simply of calculating the loop errors at each sample instant. Fig. 7.10 shows load step responses for C2 operating continuously and at two (low) frequencies. Generous initial condition convergence limits were set in the simulation for the digital cases, and this resulted in higher initial output shaft torques than for the analogue case. When this is taken into account there is a general deterioration in torque response with reducing controller rate. Similarly, air/fuel ratio becomes gradually less well controlled. It should be stressed that these frequencies are low, and could easily be exceeded by an economic commercial microprocessor-based system. The engine frequency ranges up to 130Hz, and rack position is thus "sampled" at this rate. However, the rack and VG actuator closed-loop dynamics are relatively slow, both falling to negligible amplitude response before 50Hz (details in appendix 5). The deterioration in performance at 50Hz controller rate was thought to be mainly due to the intersample changes in boost pressure. Again the data were recorded at 0.5 second intervals due to memory limits, so that the variations seen are unfortunately only aliases of the true oscillations. From a quantitative assessment of response with higher sample rates, a target rate of 200Hz was set. The implementation of a microcomputer-based digital controller on the 520DCE was described in Chapter 4.

7.3 EXPERIMENTAL/SIMULATED TRANSIENT COMPARISONS

7.3.1 Initial comparisons

Experimental transient testing of the 520DCE was described in Chapter 4. The point has already been made that the primary objective of the 520DCE was to provide experimental data to validate and improve DCE modelling. For this reason extensive experimental transient data are presented here with comparable predictions, rather than in Chapter 4.

In this section, comparisons are first made between initial transient test results and preceding simulated responses. The reasons for discrepancies are identified, and improved predictions are presented having made the necessary changes to the model.

Transient testing concentrated on simple driver demand and load steps as used for the preceding simulation work.

Driver demand steps : 5-10V (again interpreted as 1400-2800 rev/min engine speed) driver demand at 500Nm load were run using the microprocessor implementation of controller C2, with the transient strategy disabled for simplicity. A typical experimental response is shown in fig. 7.11 (repeatability was very good as discussed in Chapter 4). The corresponding simulated result is shown in fig. 7.12. One change had been made to the simulation at this stage; maximum fuelling limits (nominally to prevent engine operation beyond 20bar BMEP or 266kW, the design limits) were introduced as used in the microcomputer controller, replacing earlier less precise limits. Overall, there is a very good correlation, the experimental response being slightly slower, output shaft speed reaching maximum speed in approximately 9 seconds compared to the predicted 8 seconds. It is difficult to discuss the

response of individual parameters, owing to their interaction. If one considers fuel rack response, its rise to a peak at 5 seconds is constrained by boost pressure (smoke-limiting control); from there to approximately 7.5 seconds the absolute limit is reduced with increasing engine speed (nominal 266 kW limit). Rack response thus depends upon boost and engine speed response. These however, depend upon excess engine torque available for engine/compressor acceleration at a given rack position, as well as the precise turbine swallowing capacity at the controlled VG position.

The only significant discrepancy was in output shaft torque. This was due to a simplification made in the simulation, where the load inertia and the DCE planet carrier, output shaft step-up and turbine train inertiae were lumped into a single output shaft inertia. The predicted dynamic output torque would thus be at some conceptual point in the DCE gearbox rather than at the physical output shaft. For high load inertia the difference is negligible. However, in this case the load (dynamometer) inertia is very low, and the difference becomes significant. The model was subsequently altered to model output shaft step-up, turbine plus gear train, and load inertiae separately (as described in Chapter 5).

7.3.2 Engine torque model revisions

A limited sensitivity analysis was carried out to investigate the effect of engine torque modelling errors upon overall response. The major parameters in predicting the engine torque margin available for acceleration are :

(i) The maximum fuelling/boost ratio (FBR) allowed by the control

system. In the limit as FBR is reduced the engine can no longer support the compressor load at all conditions, so the DCE becomes inoperable. For the 520DCE this occurs at approximately

$$FBR = \frac{\text{Maximum allowed rack position [V]}}{\text{Current compressor delivery pressure [bar]}} = 2.1 \qquad (7.4)$$

Figs. 7.13 and 7.14 show the aforementioned driver demand step responses with FBR = 2.35 and 3 V/bar respectively. Similar results were obtained experimentally as discussed in Chapter 4. From the point of view of simulation, lower FBR reduces the available acceleration torque margin, and the predicted response therefore becomes increasingly sensitive to errors in the absolute engine torque prediction.

(ii) The engine torque prediction. The model is described in Chapter 5; the primary factors are a linearised correlation between fuelling and indicated torque, from which friction torque is deducted according to a second correlation. The result is scaled non-linearly with low air/fuel ratio (AFR), that is, reflecting deteriorating thermal efficiency.

All three effects may be significant. The first two correlations could be based quite confidently upon steady-state data, but the modelled effect of transient low air/fuel ratio was more tentative. Figs. 7.15 and 7.16 show driver demand step responses, respectively with and without AFR-based efficiency reduction. The differences in response are substantial. It is clear that accurate correlations for all three of the above factors are necessary for this simple engine model to be reliable.

7.3.3 Turbine swallowing capacity model revisions

The above comparisons were made without the transient control strategy. When this was reintroduced, much greater discrepancies between experimental and simulated responses were seen. As reported in Chapter 4, only slight improvements in response were achieved experimentally, whereas significant improvements had been predicted. Since the only difference was in turbine VG control (more restriction being used by the transient strategy to increase boost), it was clear that the error lay in incorrectly modelled turbine swallowing capacities. In particular, the model underestimated swallowing capacities at full VG restriction (VG position 10 Volts), and thus overestimated the increase of boost pressure under this condition. Some error at the nominally fully-closed position was to be expected - since the restriction will be very sensitive to exact sychronisation of the individual nozzle vanes, and to vane leakage - although the general correlation over most of the VG range was quite good. A series of DCE experimental tests (Chapter 3) were therefore run solely to map turbine swallowing capacity, paying particular attention to VG positions at, and near to, maximum restriction. The simulated responses with this revised correlation were in reasonable agreement. Figs. 7.17 and 7.18 show comparable predicted and experimental responses respectively for the 5-10V driver demand step at 500 Nm load, with transient control strategy in use. The obvious importance of VG restriction to transient response is discussed further in the parametric study later in this chapter.

7.3.4 Other conditions

Although the above driver demand step is a highly informative transient since it involves both torque/boost and speed dynamics, matching for other transients was investigated. Fig. 7.19 shows experimental speeds

and boost responses to a step in driver demand from 7-10V (1960-2800 rev/min) at a fixed load of 700Nm. At this high initial power level there is little available excess torque for acceleration so that output shaft speed rises slowly. At 12 seconds acceleration has practically finished, the DCE now operating on the limiting torque curve at approximately 2630 rev/min/700Nm. The simulated responses (fig. 7.20) are similar, but output shaft speed rises too quickly. Again slight errors in engine torque prediction lead to a disproportionate error in the predicted acceleration margin.

Fig. 7.21 shows experimental responses to a step in load torque from 400-800Nm at a constant 10V (2800 rev/min) driver demand. The initial output shaft speed is 3400 rev/min, fuelling being limited to prevent overspeeding. As the load is applied output shaft speed falls. Load acceptance is achieved by the differential compressor acceleration and thus boost increase, which allows increased fuelling and also generates increased turbine torque. The predicted response (fig. 7.22) is much "sharper"; output shaft speed falls to a similar level but does so more quickly and thus recovers more quickly also as compressor speed (and thus massflow and boost) have been driven up more quickly. In view of the much better predictions achieved for the driver demand steps, these differences were unexpected. It is thought that the gentler experimental response was mainly a result of slow loading system response. The experimentally-measured parameter denoted "output shaft torque" is the dynamic output shaft torque which is identical to the applied load torque. Thus in fig. 7.21(b) it can be seen that load torque rises only gradually to the new value of 800Nm, in approximately 1.5 seconds, whereas the simulated load step was applied instantaneously.

7.4 PARAMETRIC STUDY

7.4.1 Introduction

Having used the dynamic simulation SIMDCE to develop a prototype DCE controller, and refined SIMDCE (chiefly in respect of engine and turbine swallowing capacity prediction) in the light of subsequent transient test results, SIMDCE was then used to investigate how the transient performance of the 520DCE might be improved for a practical vehicle installation, while retaining the main component characteristics and efficiencies achieved by the 520DCE prototype. The major changes would therefore be

(i) the incorporation of a turbine CVT

(ii) reduced air system volumes (manifolds and plenums)

(iii) reduced turbine swallowing capacity (by re-sized turbine or increased VG turndown range).

(iv) the ability to operate within smoke limits at higher fuelling/compressor delivery pressure - either by reduction of charge cooler pressure drops, which were excessive in the prototype, or by improved combustion system matching.

In addition, modified control schemes were assessed in comparison to controller C2, namely:

(i) The interpretation of driver demand as an output shaft speed, rather than engine speed, demand.

(ii) The use of maximum boost demand under transient conditions, rather than the lower value required to enable full fuelling.

(iii) The use of transient engine bypass restriction for more rapid boost increase.

Each of the above modifications is discussed in turn below.

7.4.2 Maximum fuelling/boost ratio (fig. 7.23)

The influence of fuelling/boost ratio (FBR) upon transient response was indicated in section 7.3 above and in the discussion of experimental responses (Chapter 4). Figs 7.13 and 7.14 show the improvement in driver demand step response for an increase in maximum FBR from 2.35 to 3.V/bar (where FBR is defined by equ. 7.4). Figs. 7.22 and 7.23 show comparable load step responses, again for FBRs of 2.35 and 3.V/bar respectively. In this case there is a remarkable improvement with much reduced output speed drop (Fig. 7.23a) and recovery to final speed in approximately 3 seconds. Minimum air/fuel ratio is reduced from 29. to 23., a perfectly acceptable figure for a well-matched engine. However, it should be noted that both cases used steady-state control only. Given increased turndown in turbine swallowing capacity, transient VG control would give a useful boost increase such that full fuelling would be enabled more quickly in both FBR cases. The influence of the FBR limit would then be diminished.

7.4.3 System volumes (figs. 7.24 and 7.25)

The 520DCE prototype uses a large volume exhaust manifold and turbine plenum for constant pressure turbine operation. Furthermore, owing to the elongated layout, air pipework volumes are also large. The total system volume is approximately 80 litres. For a vehicle installation this would be substantially reduced, although the need to mix exhaust and bypass air flows adequately to preserve turbine efficiency might demand a greater volume than used in comparable turbocharged engines. Modelling smaller volumes in SIMDCE would not reflect improvements in turbine energy utilisation (the model is too simple) but would indicate any improvements in boost response due to volume filling, and any resulting control instabilities.

A driver demand step (5-10V at 500Nm load) was simulated, with a high FBR limit, for control volumes of 2 and 200 litres. The respective speeds and boost responses are shown in figs. 7.24 and 7.25. There is only a slight variation over this very wide volume range. The gross response is dominated by inertia dynamics (compressor acceleration) and turbine outflow, owing to the generally high flowrates involved. Detailed design for effective engine scavenging and turbine efficiency would of course be important for a production DCE; a complex model with wave action, and experimental development, would then be required.

7.4.4 Turbine swallowing capacity (figs. 7.26 and 7.27)

The point has been made in preceding sections that the DCE boost response is simply dependent upon compressor acceleration (system inflow) and turbine swallowing capacity (system outflow), and that the 520DCE prototype had inadequate VG turbine restriction. The importance of transient VG restriction is dependent upon the DCE operating condition. If a transient is initiated from a condition of high bypass flow then the greater VG restriction will enable faster conversion of this flow into boost pressure. However, if the transient begins at a condition of zero bypass flow then engine/compressor acceleration is required to raise boost, and excessive VG restriction will only lead to reverse bypass flow and performance detriment. Experimental steady-state (optimised settings) bypass flowrates were discussed in Chapter 2; over most of the operating range these are very small, and in fact significant bypass flows only occur at low output speeds/high boost pressures, which are already adequate for full fuelling. Transient VG restriction (and transient boost and torque response in general) should therefore be assessed with caution, considering a range of initial conditions.

Fig. 7.26 shows a 5-10V driver demand step/500Nm load response with experimentally-matched turbine swallowing capacities. A high load inertia was simulated (equivalent to a 32 tonne truck) but with a fixed load for simplicity. Despite transient VG closure, boost takes 3 seconds to reach the required level for full fuelling, rising in line with compressor speed. Output shaft torque rises gradually to 1250Nm at 6 seconds.

Fig. 2.27 shows the corresponding result with increased restriction. The closed turbine massflow at full restriction (VG position 10 Volts) was reduced by half. It should first be noted that this allowed tighter steady-state control, such that the initial boost pressure and output shaft speed were higher. Nevertheless, the sharp increase in boost and torque is clear, and λ_{full} fuelling was reached after 0.7 seconds. However, later in the transient, output shaft torque was greater in the baseline case. This was due partly to the DCE torque-speed characteristics (maximum torque reducing with higher speed), but mainly to higher referred turbine torque (fig. 7.26b compared to fig. 7.27b). The turbine produces greater power under the lower torque/higher massflow conditions which result from the experimentally matched turbine restriction. These results were for the fixed turbine gear ratio case; with a CVT the turbine conditions would have increased importance, since its contribution would be a greater fraction of the total output shaft torque.

It is apparent that the optimum transient boost level is not obvious, so that the transient boost strategy used in controller C2 could be improved upon. This is investigated further in section 7.4.7.

7.4.5 Turbine CVT

As discussed in Chapter 2, the preferred DCE scheme, as adopted for the 520DCE design, incorporates a continuously-variable transmission (CVT) between turbine and output shaft to optimum turbine performance over the operating range. The 520DCE prototype did not incorporate the turbine CVT; this reduces the design stall conditions from :

Engine : 1673 rev/min, 20bar BMEP (229kW)

Compressor : 11500 rev/min, 3.95 pressure ratio (173kW absorption)

Turbine : 46500 rev/min, 3.95 pressure ratio (156kW)

Output shaft : 682 rev/min, 2718 Nm (194kW)

(turbine step-down ratio - including CVT = 68.2)

to:

Engine : as above

Compressor : as above

Turbine : 10000 rev/min, 3.95 pressure ratio (52kW)

Output shaft : 682 rev/min, 1400 Nm (100kW)

(turbine step-down ratio fixed at 14.66)

That is, stall torque is approximately halved (as is output shaft efficiency, since engine conditions - implying fuel flow - are the same). This reduction in turbine power affects not only the overall transient response capability, but also boost response directly : at a given output shaft load an increased turbine contribution implies a reduced epicyclic load, and thus an increase margin of epicyclic torque for engine/compressor acceleration.

By introducing a CVT model, while retaining the realistic increases in turbine VG restriction and maximum fuelling/boost ratio discussed earlier, substantially validated transient response predictions could be

made for a fully-configured 520DCE. These would be comparable to initial design prediction for the 520DCE [32] and predictions for the L10DCE [80] - which is very similar in concept and component ratings to the 520DCE design - but would objectively incorporate demonstrated component efficiencies and dynamics.

For simplicity, CVT ratios were scheduled such that the turbine would always operate at the rated speed of 50000 rev/min. This gives a close approximation to the predicted optimum ratios of [32] over the important medium and high output shaft torque range. Also, a fixed CVT efficiency of 90 per cent was assumed.

A step from low to maximum driver (engine speed) demand near output shaft stall speed was simulated, in line with data available from [32, 80]. This data had been obtained using DCETRAN, described in Chapter 5. Output shaft speed was held fixed by specifying a very large inertia. For both the 520DCE and the L10DCE, stall speed is one-fifth of rated speed. In each case the fundamental transient VG control strategy was to provide just sufficient boost to maintain acceptable air/fuel ratios at maximum fuelling.

Boost response (fig. 7.28a) was excellent in all cases. This is because the initial bypass flow (not shown) was high; the boost rise can be generated by VG restriction rather than compressor acceleration, without causing bypass recirculation. The 520DCE DCETRAN response shows a transition to steady-state control at 1.6 seconds, since engine speed had reached the required levels for the control schedules used.

Air/fuel ratio (AFR) responses (fig. 7.28b) are similar for the two 520DCE cases, with a limit of approximately 20.5. The less sharp 520DCE SIMDCE response is due to the inclusion of rack dynamics. After 1.6 seconds the 520DCE DCETRAN AFR increases in line with the boost increase to steady-state conditions. The predicted L10DCE AFR is always higher than that of the 520DCE SIMDCE case, despite similar boost pressures. The reasons for this are threefold:

(i) The 52DCE SIMDCE boost is quoted before the charge cooler, which imposes a pressure drop.

(ii) The L10 has inherently better breathing characteristics than the Leyland 520, since it employs a quiescent rather than high swirl combustion system.

(iii) Later in the transient the L10DCE operates at lower BMEP (controlled by the scheduled fuelling limit curve).

Engine torque response (shown as BMEP to correct for larger capacity of the L10) is shown in fig. 7.28c. The two 520DCE responses are similar; BMEP rises almost instantaneously to the limit of approximately 20 bar, and substantially remains at this level. The L10DCE rises equally rapidly to its slightly high peak of approximately 21 bar BMEP, then declines along the fuelling curve as engine speed rises. The 520DCE fuelling limit does not reduce at the engine speeds encountered in this transient.

The output shaft power responses (fig. 7.28d) are of greatest importance. Here the 520DCE SIMDCE response is markedly inferior. For example at 0.25 seconds there is a 32kW deficit compared to the 520DCE DCETRAN prediction. Of this, 14kW is attributable to the lag in engine speed response, (fig. 7.28e). This initial 0.1 second lag corresponds

to the initial engine torque response (fig. 7.28c) which, as mentioned above, is due to the inclusion of the prototype rack actuator dynamics. In a production engine, which might use digital (pulsewidth-modulated) injection, the engine torque delay would be reduced approximately to that shown by the DCETRAN predictions. The remaining deficit throughout the transient must be attributable to the higher gear losses and lower turbine efficiency modelled in SIMDCE. It may also be partly due to the fixed 50000 rev/min turbine speed causing lower turbine efficiencies in the early part of the response.

Towards the end of the transient, 520DCE SIMDCE and L10DCE output powers are similar, where the engine powers are similar (520DCE engine power 249kW at 2.75 seconds, L10DCE engine power 236kW) and turbine speeds (not shown) are similar. The final output power of the 520DCE DCETRAN predictions is 213kW; this is greater than the design stall power (194kW) stated earlier, and indicates mismatch between this model and the steady-state model.

The output shaft speed responses (fig. 7.28f) confirm that the responses were at reasonably comparable speeds, the L10DCE response being at slightly above stall speed.

To summarise, extrapolations from a validated transient 520DCE model in SIMDCE to one with turbine CVT and increased VG range have shown similar boost and engine power responses to those predicted by DCETRAN for the 520DCE and L10DCE. However, output shaft power response was significantly poorer, though this would be improved if more complete CVT ratio scheduling were modelled. The 520DCE DCETRAN output power predictions were optimistic, finally exceeding the design stall power by approximately 10 per cent.

7.4.6 Driver output shaft speed demand (figs. 7.29 and 7.30)

This is the first of three sections discussing modified control schemes for the DCE with fixed turbine gear ratio. In the earlier (7.2.1) considering control strategies it was stated that the interpretation of driver demand was somewhat arbitrary; while it should be taken to be a speed demand for reasons of stability, either engine speed or output shaft speed could be used. Engine speed demand was chosen for controller C2.

The effects of this choice were examined for simple transients. The loop gains for the now proposed output shaft speed control were chosen in the same way as the gains for C2. Maximum driver demand (10 Volts) was interpreted as an output shaft speed demand of 3500 rev/min (rated speed 3409 rev/min), giving the feedforward scaling, and the output shaft speed error at rated speed should lead to the rated engine fuelling, giving the droop again. VG control, fuelling/boost ratio and maximum fuelling limits were identical to those used in C2. It was still necessary to monitor engine speed and increase fuelling to maintain the maximum engine speed at light loads. Maximum engine speed was not explicitly controlled; adherence to steady-state schedules, and transient boost control gives inherent engine speed control.

A load step (500-1000Nm) at part (7 Volts or 70 per cent) driver demand showed the differences between engine and output speed demand most clearly. The responses are shown in figs. 7.29 and 7.30 for engine and output speed demand respectively. The initial conditions were identical for the two cases. In each case there is a short delay before transient control is invoked, corresponding to the time for the controlled speed to be depressed by the increased load. Boost then

rises rapidly to the required value of 2.85 bar (giving a minimum AFR of approximately 20 at full fuelling). Boost continues to rise thereafter as compressor speed rises, the VG control being too loose to maintain just 2.85 bar.

The responses for the two cases are virtually identical over the first 4 seconds. It should be noted that for engine speed demand the setpoint is :

70 per cent of 2800 rev/min = 1960 rev/min

whereas for output shaft speed demand the setpoint is :

70 per cent of 3500 rev/min = 2450 rev/min

At 4 seconds, engine speed has recovered to within droop range of the setpoint, so for the engine speed demand case there is a transition back to steady-state control. The VG nozzles are closed (fig. 7.29b) bringing compressor speed and boost (fig. 7.29a) to their optimum steady-state values. Output shaft speed stabilises at 1645 rev/min (compared to the initial speed of 2340 rev/min). In contrast, for the output shaft speed demand case, fig. 7.30, output shaft speed is far below the setpoint so that transient control continues. Consequently, engine speed rises above its initial level and output shaft speed continues to recover. Fig. 7.31 shows this latter case over an extended time. After 12 seconds the DCE has recovered as far as possible, and is operating at the highest output shaft speed, (approximately 2150 rev/min) at which it can achieve 1000Nm in transient control mode. The engine is naturally operating at a much higher speed (2230 rev/min) than the corresponding engine speed demand setpoint (1960 rev/min), and at maximum fuelling.

So output shaft speed demand gave load step recovery to a much higher speed than engine speed demand. However, as indicated earlier, in a vehicle application the driver would naturally set 100% demand on sensing the initial deceleration. In the engine speed demand case this would give recovery to the 2150 rev/min/1000Nm point above (since ultimately the available power is the same). In the output shaft speed demand case this extra demand would have no effect.

In effect, the use of engine speed control rather than direct output shaft speed control gives greater droop, with more progressive and predictable response to the driver's input. The writer therefore favours engine speed control for general automotive-type applications.

7.4.7 Transient boost pressure (figs. 7.29 and 7.32)

Controller C2 used a transient boost level which was required to allow full fuelling with acceptable AFR. It has been noted that because of the complex trade-off between transient boost pressure and system massflow for maximum system power (particularly the turbine contribution), this may not always be the best choice. In this section, two simple transient responses, using C2 with a transient demand for maximum boost (that is, 4 bar), are compared with earlier results for C2 with the "required" boost demand.

Fig. 7.32 shows the maximum boost scheme response to at 500-1000Nm load step at 70 per cent driver (engine speed) demand. The comparable required boost response was shown in fig. 7.29. For the maximum boost scheme the VG nozzles remain fully closed (10 Volts) through the transient (fig. 7.32b), with the desired increase in boost (fig. 7.32a compared with fig. 7.29a). However, this causes much reduced compressor

massflow, with resulting reduced turbine torque. Output shaft torque (fig. 7.32b) thus fails to reach 1000Nm, resulting in continuing engine and output shaft deceleration (fig. 7.32a) over the 6 second duration of the run. The load must be supported eventually, since the boost setpoint is consistent with high torque/low speed steady-state operation, but the final speeds will be low.

Fig. 7.33 shows the maximum boost scheme response to a 50-100% driver demand step at 500 Nm load with high load inertia. The comparable required boost response was shown in fig. 7.27. The initial more rapid boost rise of the maximum boost scheme allows slightly faster fuelling increase, and improves engine torque throughout the transient due to efficiency gains with higher air/fuel ratios. Initial output torque response (fig. 7.33b) is noticeably better than for the required boost scheme (fig. 7.27b). However, after 3 seconds the advantage reverses as the required boost scheme benefits from increasing turbine torque (compressor-turbine "torque conversion" effect).

Some progressive combination of the two boost setpoints would give the best overall response, but in long transients the lower boost scheme alone would be adequate.

Given a finalised DCE design, and an application (for example heavy-duty automotive use, where transient response with high load inertia is most important), the transient boost for best output torque response could be mapped over the operating range by transient simulation. The transient boost feedforward could then be scheduled (rather than a fixed value) in the same way as optimum steady-state boost or compressor speed feedforward is scheduled currently.

7.4.8 Transient bypass restriction

An engine bypass control valve has been incorporated in all DCE schemes, derived from early schemes in which a normally-closed compressor air path was opened to a second "stall" torque at high compressor speeds. With the bypass wide open compressor delivery pressure and turbine inlet pressure are similar at steady-state, and the engine thus has similar inlet and exhaust pressures (in the 520DCE prototype there is always a pressure rise across the engine owing to significant charge cooler losses). With bypass restriction some degree of independence can be achieved; the compressor can be made to operate at a higher pressure ratio than the turbine, with a positive engine pressure gradient. At steady-state it should be remembered that at high and moderate loads optimum system efficiency is generally found at low bypass flows (because the compressor-turbine "torque conversion" is inefficient), so that bypass restriction is ineffective. At higher loads and lower speeds this torque conversion is necessary (otherwise the output torque rise cannot greatly exceed the limited engine torque rise), so that the use of bypass restriction would increasingly be constrained with higher loads. In practice the reduction in engine pumping work with bypass restriction may be offset by turbine efficiency reduction at the lower pressure ratio incurred; simulation studies have found that maximum steady-state efficiencies were achieved with wide-open bypass.

For transient use the bypass valve potentially could give improved boost response, particularly where turbine VG restriction is limited. Turbine torque rise should not seriously be reduced since system massflow is governed by compressor delivery pressure (which largely determines compressor acceleration), which would be - as before - that required at maximum fuelling. Thus a controller model was written in which a bypass

valve (with realistic slew rate limit) was used to control transient boost, while turbine VG was used exclusively to control steady-state conditions with wide-open bypass.

It was found necessary to use very low control gains to avoid generating excessive boost under high initial bypass flow conditions. To achieve safe, fast boost response over the operating range would probably require some form of gain scheduling (possibly based on relative compressor and engine speeds). There was also interaction between bypass valve and VG control effects during transients; it would however, be possible to set a fixed VG position under transient conditions. It was concluded that the use of the VG nozzles (with adequate restriction) alone for both steady-state and transient control would be more effective, and of course simpler, than use of VG and bypass valve. If the use of a fixed geometry turbine were to be considered, the transient use of a variable bypass should be re-evaluated.

7.4.9 Parametric study - conclusions

The SIMDCE parametric study showed that DCE transient response is most strongly dependent upon

(i) the maximum fuelling/boost ratio allowed (equivalent to the minimum air/fuel ratio allowed)

(ii) the range of turbine VG restriction available

The former could be improved (relative to the 520DCE prototype) by reduction of charge cooler pressure losses - giving increased inlet manifold pressure at a given compressor delivery pressure, or by combustion system development to reduce smoke at a given air/fuel ratio. The latter is dependent upon turbine sizing and VG design.

The relative importance of these parameters varies with operating condition. Where there is significant bypass flow, VG restriction is important to "convert" this flow to boost; boost then rises rapidly, enabling full fuelling to be used almost immediately at any fuelling/boost limit. Conversely, where bypass flow is small, boost and torque rise requires engine compressor acceleration; a higher fuelling/boost limit gives greater acceleration torque margin.

Air/exhaust system volume was found to have negligible effect upon boost response over a range of practical volumes. The system would therefore by developed for engine scavenging, bypass/exhaust flow mixing and turbine efficiency. A combination of a pulse converter exhaust manifold with a relatively large exhaust/bypass air mixing volume would seem to be preferable; this is a matter of detailed development.

The use of variable bypass closure during transient, was problematic owing to the variation in its effect over the DCE operating range. The use of turbine VG alone, (given adequate restriction) is preferred. For schemes using a fixed geometry turbine, the use of transient variable bypass closure should be re-evaluated.

With postulated increases in VG restriction and the fuelling/boost limit, and with a turbine CVT model incorporated, SIMDCE predicted transient boost, engine torque and engine responses similar to those predicted by DCETRAN. Output shaft torque response, however, was significantly poorer than that anticipated from the DCETRAN predicitions. This was due to the inclusion of actual prototype component efficiencies and pressure losses, but the picture may have been worsened by the use of non-optimum CVT ratios in SIMDCE.

Finally, it was demonstrated that the choice of engine speed or output shaft speed as the parameter related to the driver demand was nominal, but that engine speed demand gave more progressive behaviour. It was also found that the optimum transient boost pressure was a function of the operating condition and should ultimately be scheduled rather than fixed.

7.5 LOW DRIVER DEMAND OPERATION

DCE modelling has mainly been concerned with optimum steady-state conditions and transients involving increasing power output. This section is concerned with the behaviour of the DCE when driver demand is reduced, typically to zero. In vehicle applications this may occur under loaded conditions (for example, deceleration on a level road) or under motoring conditions (descending a hill). The DCE response will vary according to these load conditions, and according to the load inertia. The provision of engine braking is discussed at the end of this section, but first it is necessary to investigate whether the DCE can operate at zero driver demand (i.e. idling engine speed demand).

Fig 7.34 shows the predicted 520DCE response to a simultaneous reduction of driver demand to zero and change from loading to motoring torque at the drive shaft. A low load inertia was modelled to "condense" the response. The transient begins at 2 seconds; DCE braking torque (mainly engine motoring torque) is insufficient, so that engine and output shaft speeds rise and compressor speed falls (fig. 7.34a). At this particular condition compressor massflow falls to zero, thus the engine exhaust gases are entirely recirculated to engine inlet. This is clearly unacceptable since the engine could not subsequently generate power.

Investigation of the zero driver demand behaviour with a compressor freewheeling clutch (sprag) and with the engine bypass closed against reverse flow led to the final scheme shown in fig. 5.9a (the simulation model - DCECSE - used was described in Chapter 5). The DCE would incorporate a flap-type engine bypass valve, which self-closes when flow reverses. In addition a compressor bypass would be provided; this would allow the engine to self-aspirate with the compressor stopped, but would self-close when compressor delivery pressure exceeds ambient pressure. Compressor reversal would be prevented either by the sprag, or preferably by a brake-for reasons discussed later.

Fig. 7.35 shows the zero driver demand, motoring driveshaft torque, response with the above modifications (this is comparable to fig. 7.34, noting the altered output shaft and engine speed axes scaling). Boost pressure at the compressor outlet (fig. 7.35a) rises initially as the engine bypass valve closes, then falls as compressor massflow falls below engine massflow. At approximately 3 seconds boost falls below the ambient level, remaining at approximately 0.95 bar due to the opening compressor bypass. Turbine inlet pressure rises, being dependent only upon engine massflow and turbine swallowing capacity. It should be noted that compressor massflow is considerably less than engine massflow at this zero demand condition. If the driver demand were increased the engine would operate naturally-aspirated (and thus with limited torque) until the compressor had been accelerated; boost and torque build-up would be slow.

The need to provide engine braking in automotive applications was mentioned above. With conventional engines this braking effort is provided by engine friction and pumping work, increased in some cases by

an exhaust restrictor ("exhaust brake") which usually takes the form of a manually-operated butterfly or guillotine valve. Engine braking is maximised by selecting gears to give a high engine speed at a given road speed. In the DCE the floating epicyclic train causes the compressor to decelerate and the engine speed to fall with respect to the output shaft speed under reverse torque conditions. Thus the engine is "underdriven" and braking effort is reduced.

If a compressor brake, rather than sprag, is used, this effect is minimised. However, the maximum achievable DCE engine braking, incorporating an exhaust braking strategy, was investigated in [81] and considered inadequate. It was concluded that, as in the DDE [29], the torque convertor (which is an integral part of the transmission system) should also be used as a hydraulic retarder. The combination of engine braking and hydraulic retarder was expected to give acceptable deceleration.

7.6 VG TURBOCHARGED ENGINE COMPARISONS (figs. 7.36-7.39)

This Chapter has compared the transient responses of the 520DCE with alternative control schemes, and compared the responses of a postulated "improved prototype" 520DCE with the original 520DCE design predictions and with predictions for the Cummins L10DCE. In this final section a set of fixed speed responses for the 520DCE are presented which may be compared with responses for alternative powertrains. These responses were predicted using the SIMDCE model matched to 520DCE experimental data, but with increased VG restriction, and allowing a minimum air/fuel ratio of approximately 20.

It is common practice when evaluating the transient response of conventional engines to conduct zero to maximum fuelling steps at a series of fixed driveshaft (that is, engine shaft) speeds. The equivalent tests for the DCE are zero to maximum driver demand steps at a series of fixed output shaft speeds. Figs. 7.36 - 7.38 show the DCE responses at output shaft speeds of 682 rev/min (stall), 2046 rev/min (mid-speed) and 3409 rev/min (rated). The compressor and engine bypass valving arrangement discussed in the previous section was retained to enable operation to zero driver demand. At stall speed (fig. 7.36) zero driver demand led to engine operation in the idle speed range. Thus the initial condition (transient starts at 0 seconds) is at approximately 600Nm engine torque and 1.9 bar boost. It should also be noted that compressor massflow greatly exceeds engine massflow (fig. 7.36b). Thus boost rise is obtained by VG closure, reaching the required level within 0.5 seconds, and engine and output torques rise quickly.

At midspeed and rated speed (fig. 7.37 and 7.38) the initial conditions (transient starts at 2 seconds in these cases) are truly at zero fuelling. Engine and output torques are negative (engine motoring torque), boost pressures are 1.bar (compressor bypass open) and compressor flow is less than engine flow. The transient boost responses are therefore poor in both cases, being dependent upon engine - compressor acceleration. There is an immediate engine torque step from braking to the naturally-aspirated limit, followed by a delay until the compressor massflow matches engine massflow (and the compressor bypass closes), then slow torque rise in line with boost pressure.

Comprehensive vehicle simulation comparisons between the Cummins L10DCE and a similarly-rated turbocharged L10 with stepped transmission [58]

did not show response problems which might be expected from these two latter transients. It would therefore seem that these extreme transients, while enabling a quantitative comparison to be made between alternative engine systems, do not reflect realistic vehicle operation.

An alternative comparison was made between the 520DCE and an 11.2 litre VG turbocharged Diesel for which fixed speed transient results were available. The VG T/C engine rated power was similar to that achieved by the 520DCE prototype; its salient features were [77]:

ENGINE : Leyland TL11\11a 6 cylinder D.I. Diesel
bore x stroke 127 x 146 mm
swept volume 11.2 litres, compression ratio 15.75
max.BMEP 13 bar at 1350 rev/min
rated power 191kW at 2300 rev/min

FIE : CAV Majormec in-line pump, electrohydraulically-controlled. Static timing 22^{o}cr. BTDC $\pm$ 10^{o}cr.

TURBOCHARGER : Holset mk.IIb prototype nozzled single entry turbine, with variable nozzle area.
Moment of inertia .244 x 10^{-3} kgm^2

The VG T/C engine responses were steps to full fuelling at fixed speed starting at approximately 200Nm load torque. Since the 520DCE without turbine CVT has similar peak torque to the larger VG T/C engine, the 520DCE responses were simulated on the same basis, that is, steps to full driver demand from an initial demand which gave 200Nm output shaft torque, with fixed output shaft speed.

Two comparisons were made, at 52 and 78 per cent of the rated driveshaft speeds (figs. 7.39a and b respectively). Peak torque speed for the VG T/C engine was 59 per cent of rated speed, so it was realistic to expect good transient performance at the 52 per cent speed. VG T/C engine data were also available at 35 per cent of rated speed, but since this equates to only 800 rev/min it was of little practical interest.

It should be noted immediately that whereas the 520DCE was subject to smoke-limiting (minimum air/fuel ratio was approximately 22 in these runs), the VG T/C engine had run without restriction to accelerate differences between VG and fixed geometry behaviour. Thus VG T/C rack and torque rise very quickly. However, the 520DCE achieves equally fast boost response, and can generate full boost rapidly at the lower speed where the VG T/C engine boost is still slowly rising at 3 seconds. The 520DCE would therefore develop the greater torque if smoke-limiting fuel restriction were applied to both engines (note : the tight DCE boost control was achieved by a more advanced control design which will be described in Chapter 8; the VG T/C engine used an optimised PID-type boost control system for steady-state efficiency and transient response).

At both speeds the 520DCE turbine is operating with full VG restriction at the initial steady-state condition to attempt to reach the scheduled optimum setpoint. The transient boost rise is thus entirely due to the accelerating engine compressor. As noted earlier, tolerance of a lower air/fuel ratio would therefore improve the boost response further. In addition, bypass flows (not shown) were significant, so that further increases in VG restriction would also be effective.

To summarise, in this limited comparison the 520DCE demonstrated better boost response than a similarly-rated VG T/C engine (both having optimised control system). The VG T/C engine showed poor boost build-up near the peak torque speed; with smoke-limiting, transient torque would thus be penalised. As the peak boost ratio of premium turbocharged engines increases, the shortfall between steady-state and transient torque will become increasingly significant.

It is dangerous to draw conclusions from limited data; as the earlier zero-maximum driver demand steps showed, transient response is highly dependent upon initial conditions. Comparisons between DCE systems and other powertrains should ultimately be made on the basis of results over typical duty cycles for a given application.

TABLE 7.1

CONTROLLER C1 - CONTROL TERMS AND GAINS

Parameter	Control Input	Control Terms	Gain
Engine Speed (1)	Rack	P	.0375 [V/rev/min]
Compressor Speed (2)	VG nozzles	P	.004 [V/rev/min]
		I	.01 [V/rev]
Fuelling/boost ratio	Rack	cut off at maximum f/b ratio	
	VG nozzles	P	10. [V/bar]
		D	0.2 [V/bar/s]
Maximum boost (3)	VG nozzles	P	5. [V/bar]
		D	0.2 [V/bar/s]
o/p shaft overspeed (4)	Rack	P	0.03 [V/rev/min]
Injection timing	Timing	positional only	

P - proportional

I - Integral

D - derivative

Notes (1) control of error between demanded engine speed (scaled driver demand) and actual engine speed.

(2) control of error between optimum and actual compressor speeds

(3) proportional term is switched in above 3.9 bar; the boost limit is 4 bar. Derivative term is velocity feedback

(4) output shaft overspeed (above the 3409 rev/min rated speed) also implies turbine overspeed. Fuelling is cut back with excess speed.

TABLE 7.2

CONTROLLER C2 - CONTROL TERMS AND GAINS

Parameter	Control Input	Control Terms	Gain
Engine Speed	Rack	P	.0375 [V/rev/min]
Compressor Speed	VG nozzles	SO + P	.0002 [V/rev/min]
Fuelling/boost ratio	Rack	cut-off at maximum f/b ratio	
	VG nozzles	SO + P	1. [V/bar]
o/p shaft overspeed	Rack	P	0.03 [V/rev/min]
Injection timing	Timing	positional only	

P - proportional

SO - scheduled offsets

CHAPTER 7 LIST OF FIGURES

CHAPTER 7 LIST OF TABLES

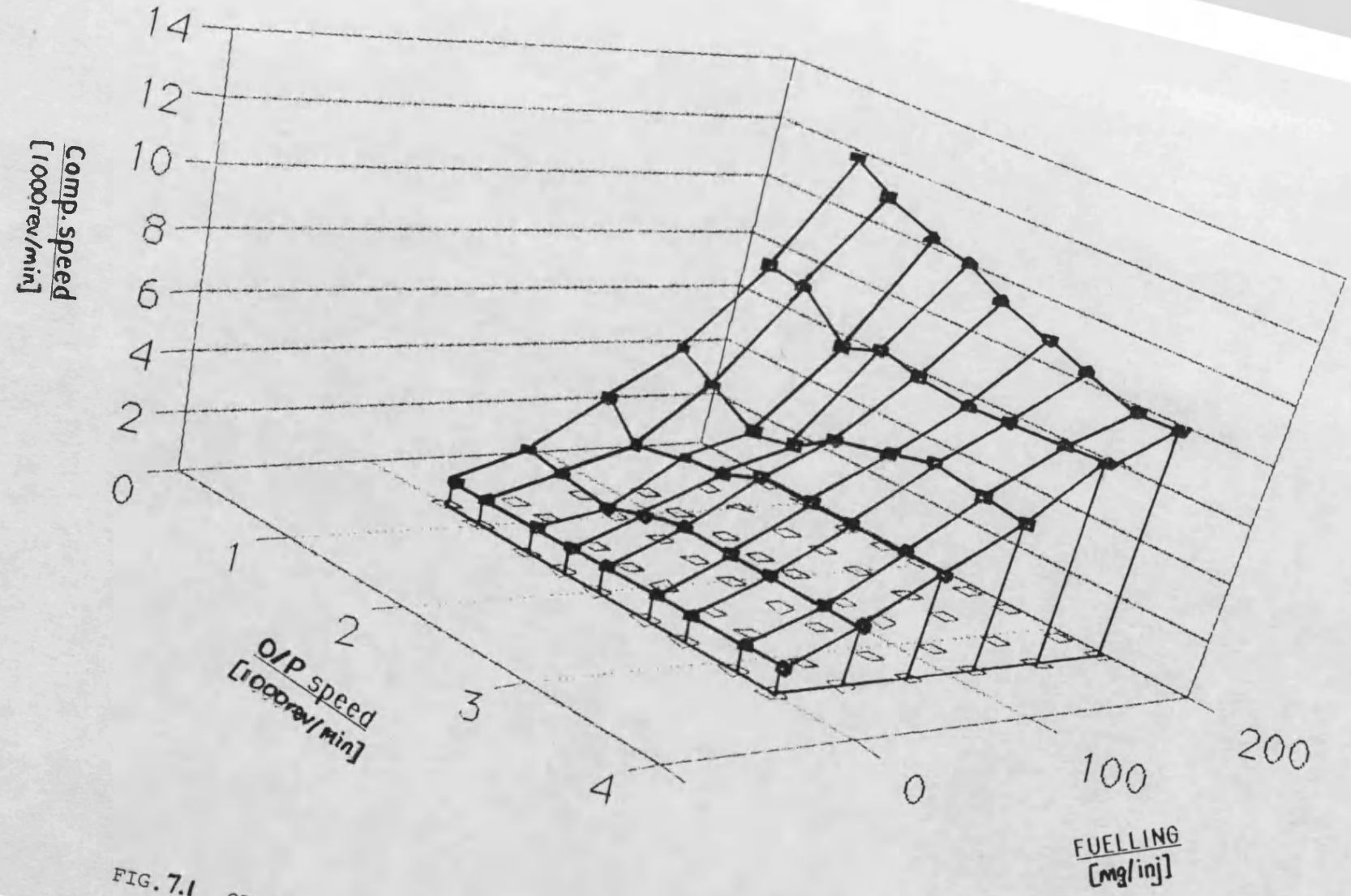

FIG. 7.1 OPTIMUM COMPRESSOR SPEEDS

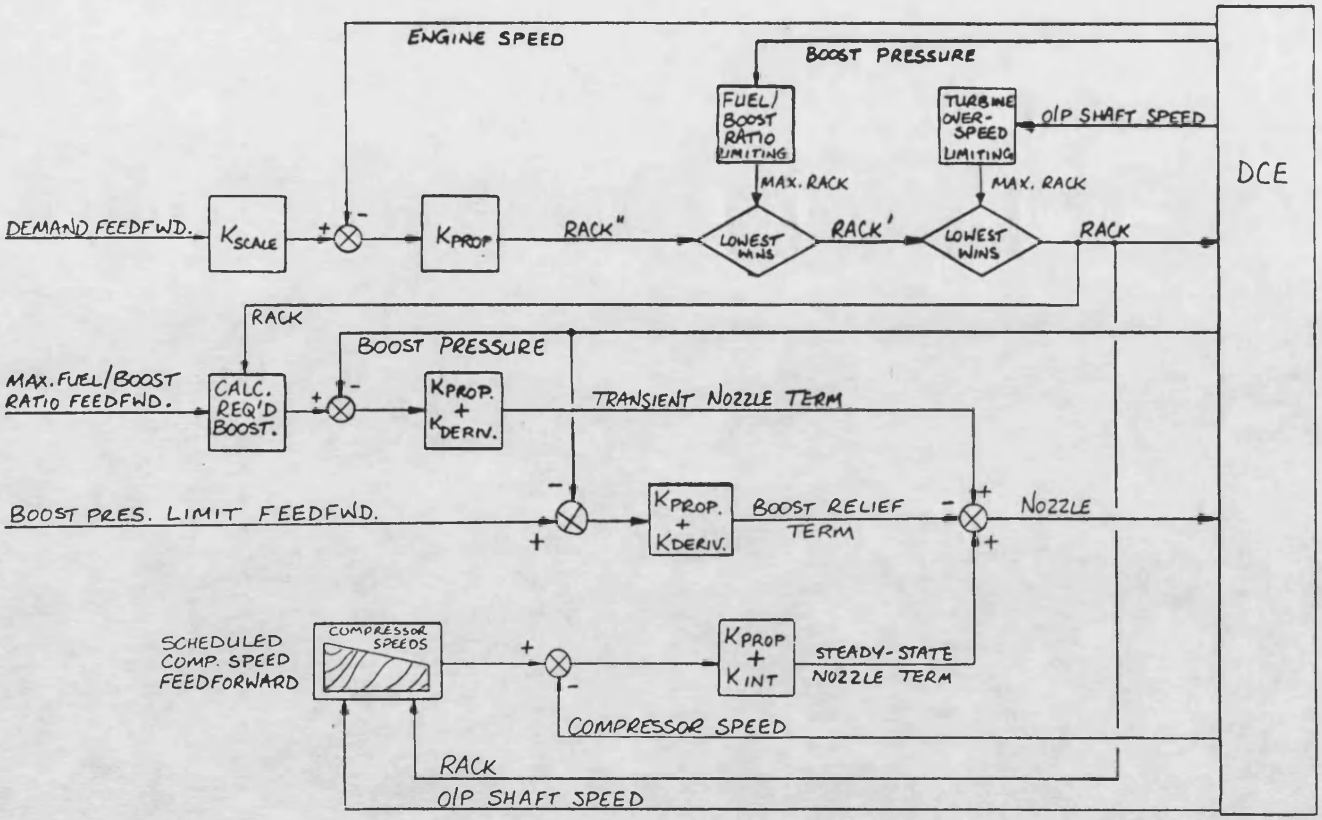

FIG. **7.2** CONTROLLER SCHEMATIC - C1

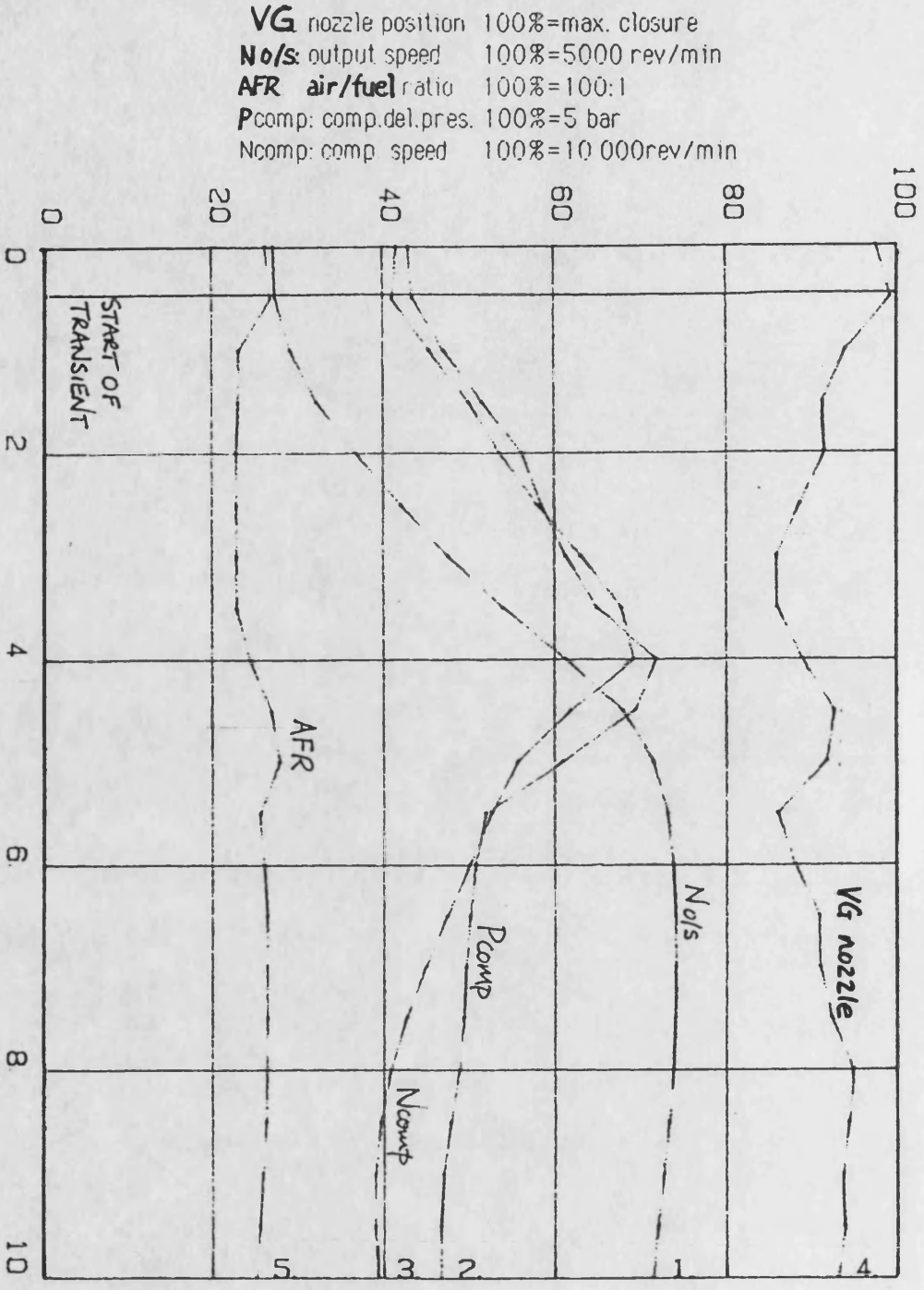

FIG. 7.3 DRIVER DEMAND STEP: C1

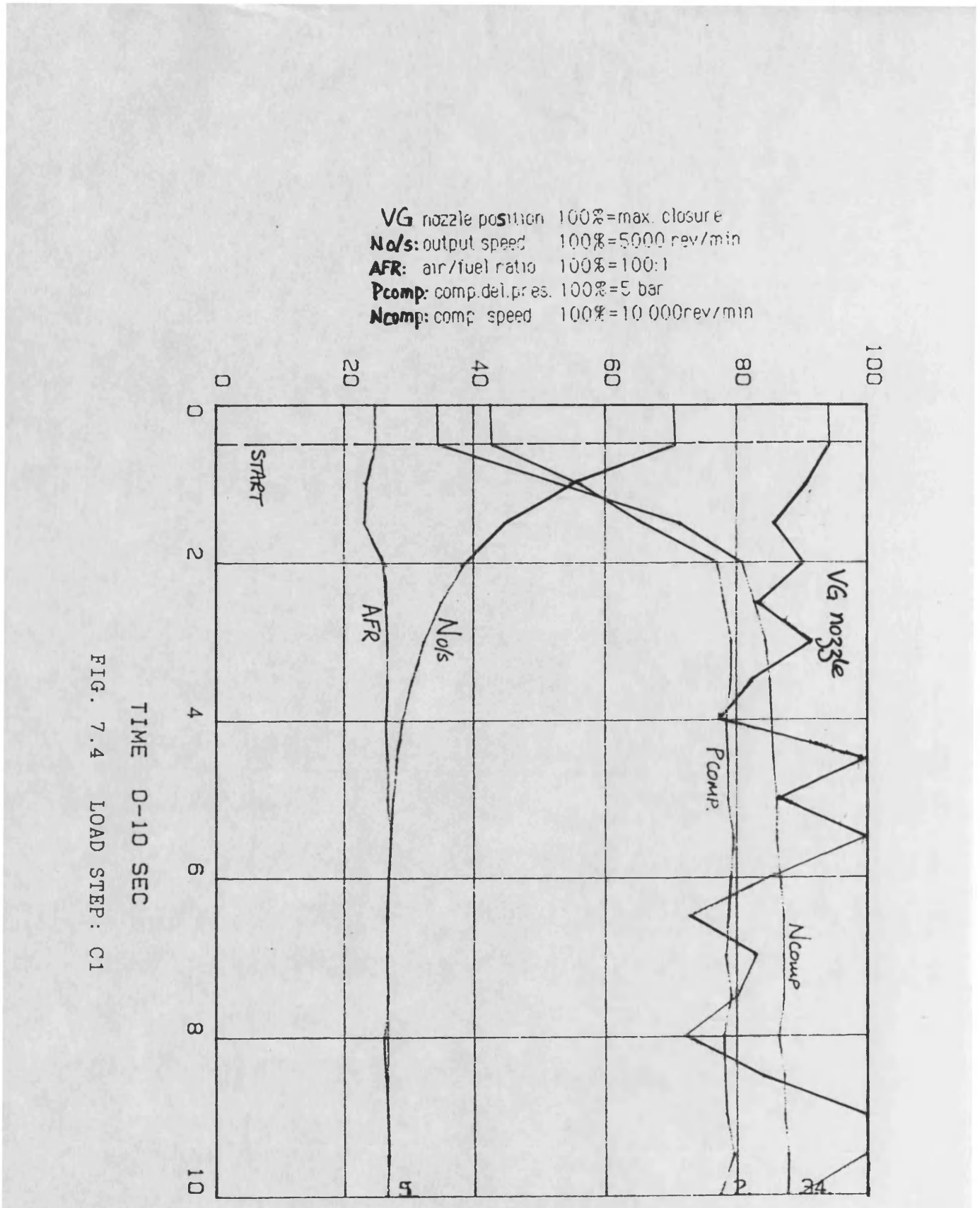

FIG. 7.4 LOAD STEP: C1

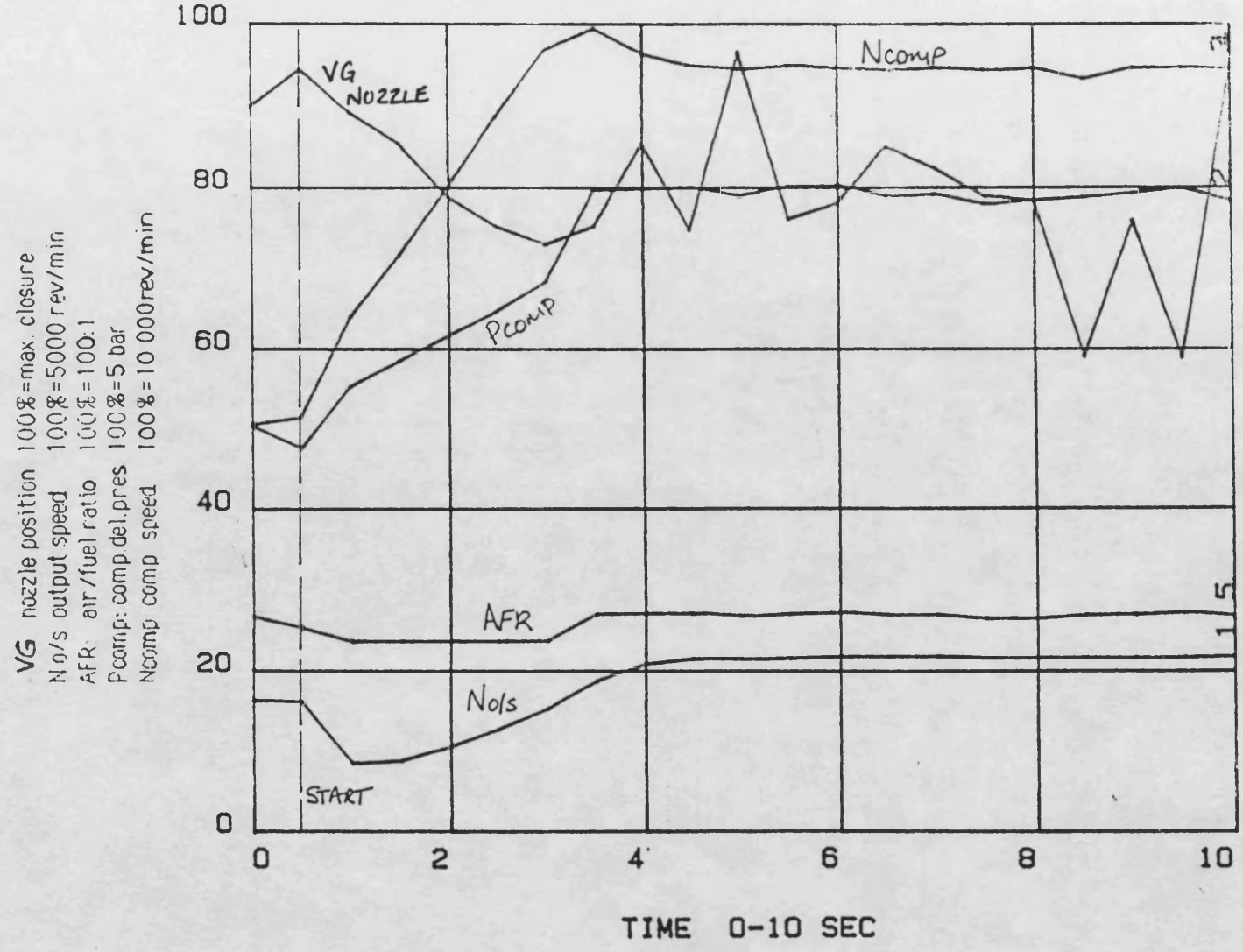

FIG. 7.5 COMBINED STEP: C1

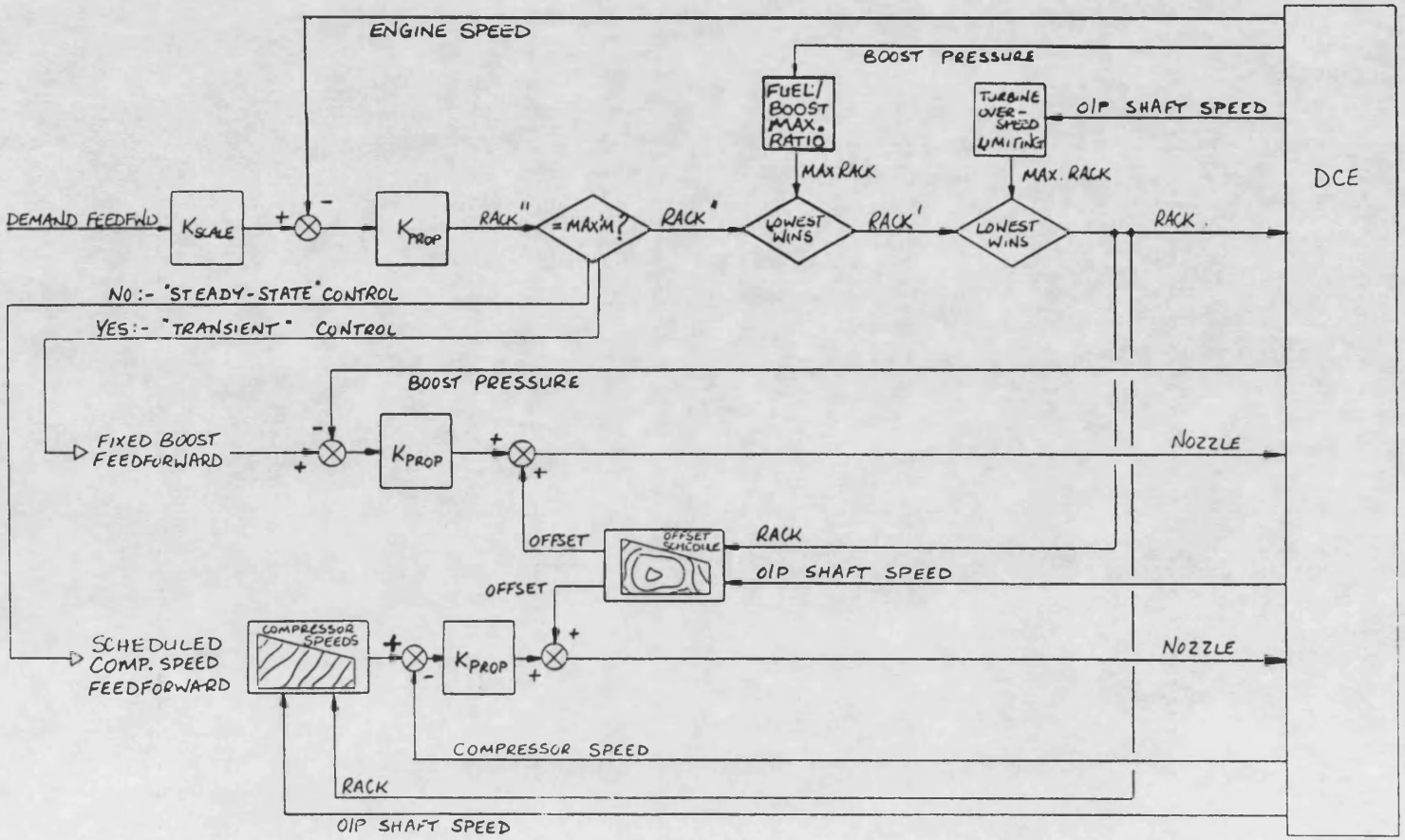

FIG. 7.6 CONTROLLER SCHEMATIC - C2

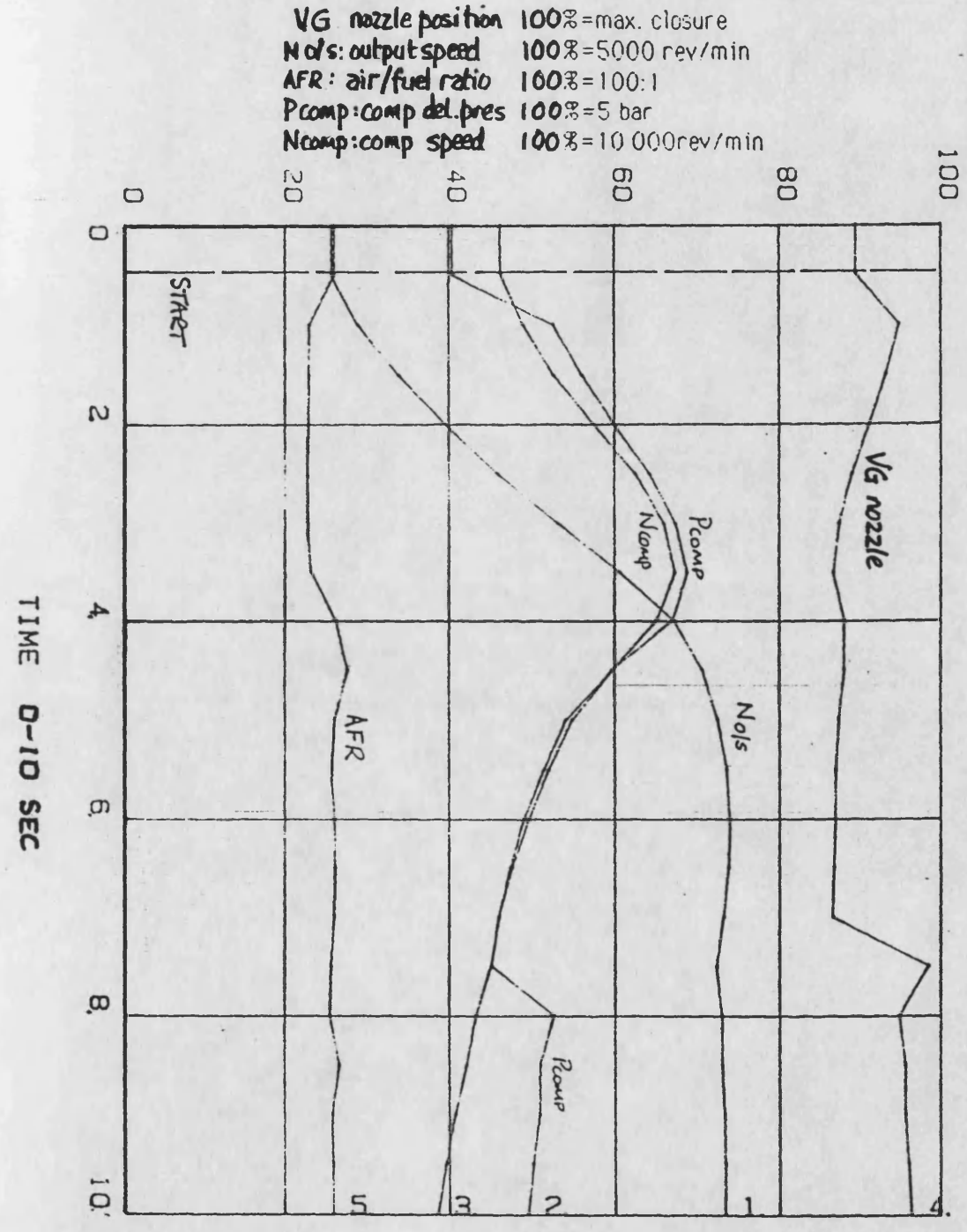
VG nozzle position 100% = max. closure
N o/s: output speed 100% = 5000 rev/min
AFR: air/fuel ratio 100% = 100:1
Pcomp: comp del. pres 100% = 5 bar
Ncomp: comp speed 100% = 10 000 rev/min
0
20
40
60
80
100
START
VG nozzle
Ncomp
Pcomp
N o/s
AFR
Pcomp
1
2
3
4
5
0
2
4
6
8
10
TIME 0-10 SEC

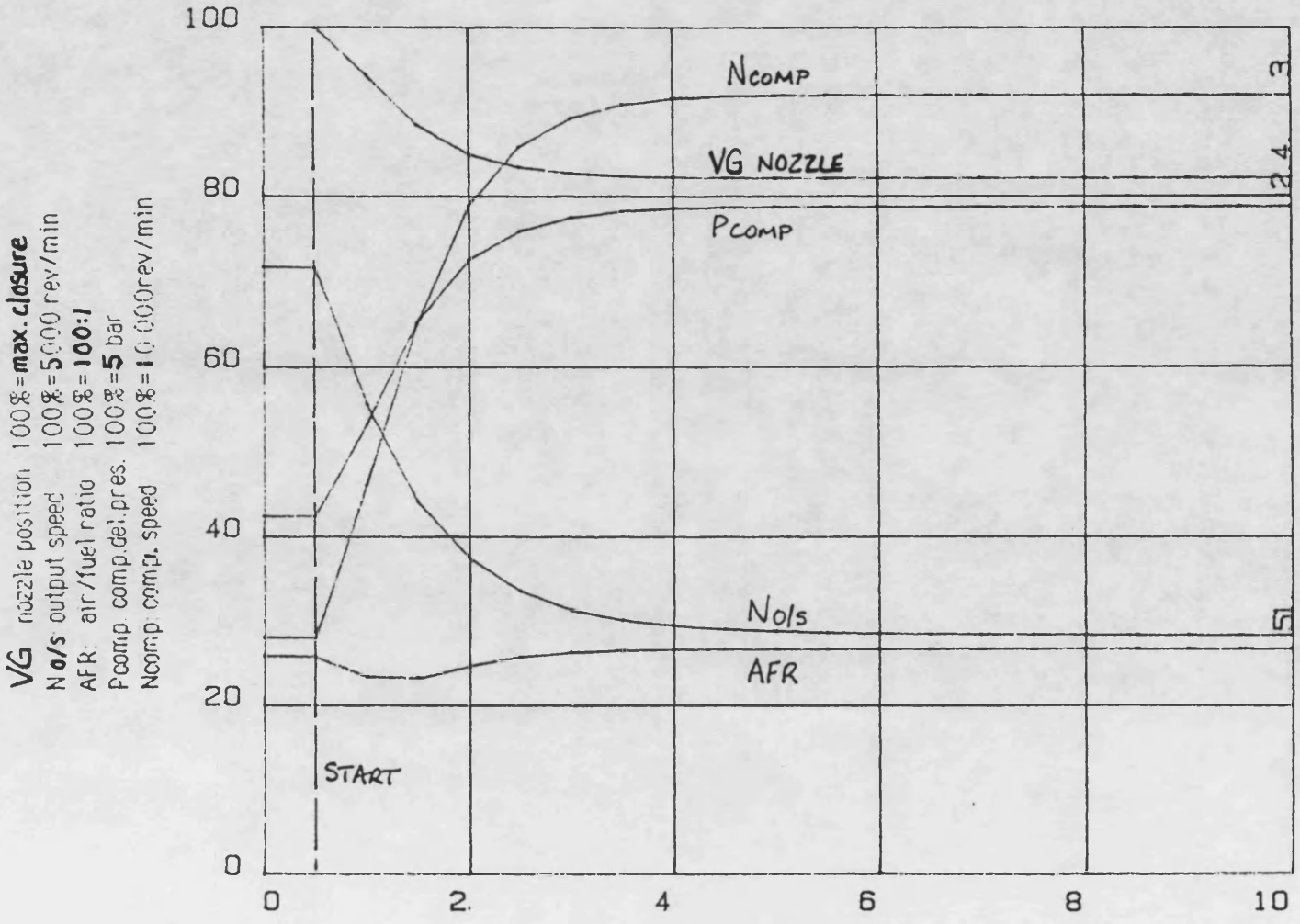

FIG. 7.8 LOAD STEP: C2

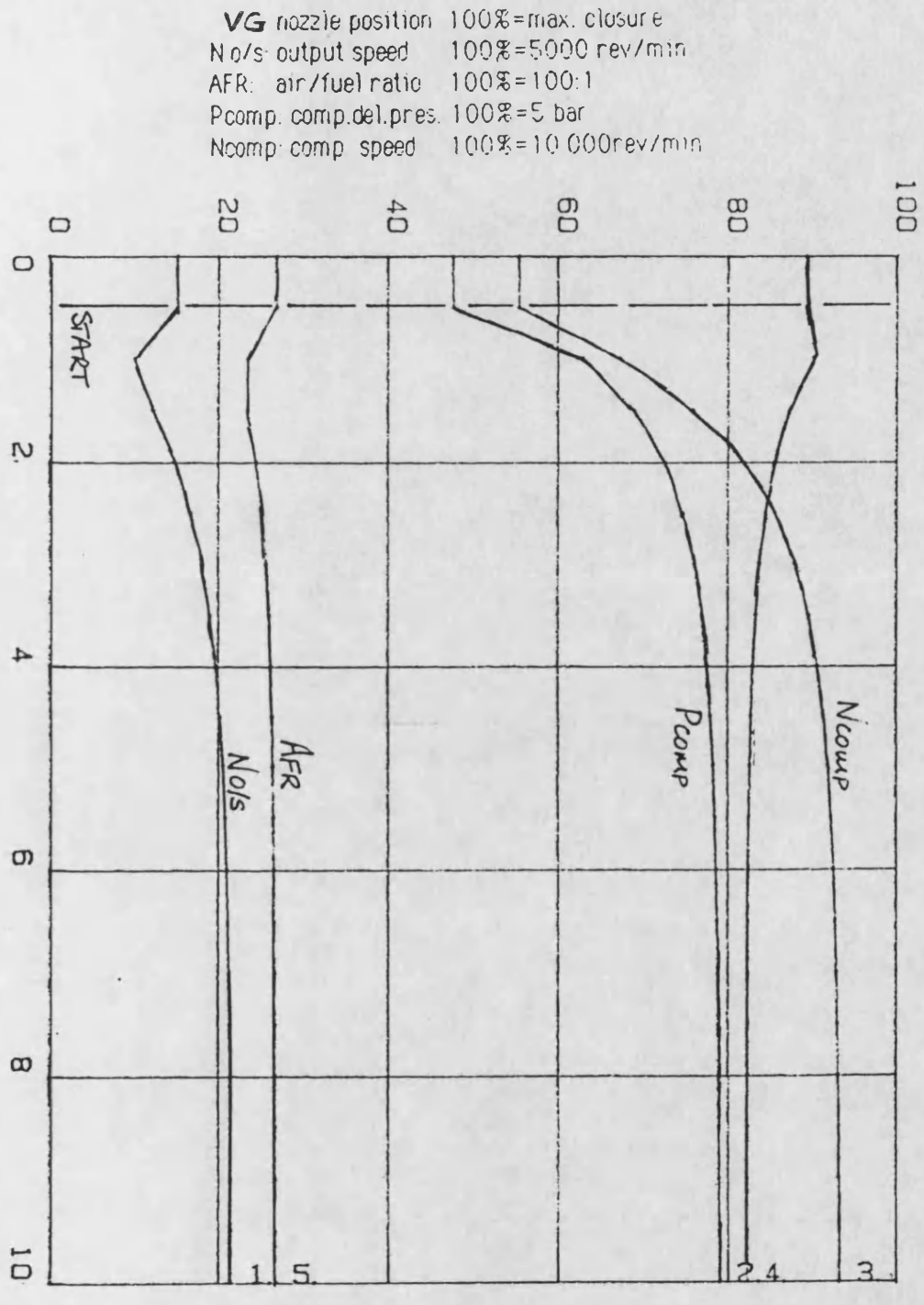

FIG. 7.9 COMBINED STEP: C2

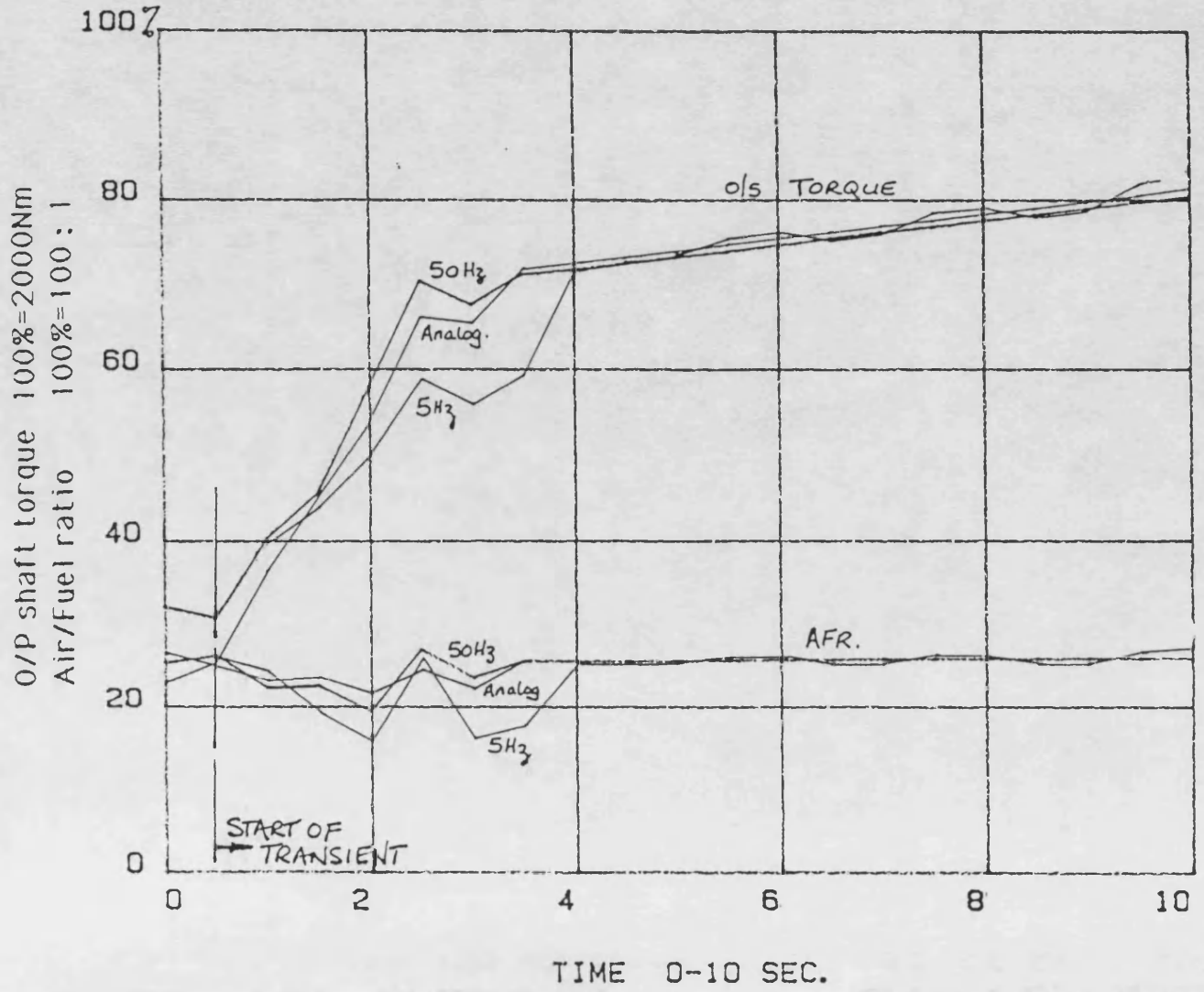

FIG. 7.10 LOAD STEP: C2, DIGITAL CONTROL

DCE transient tests
5-10V dem. step at 500Nm
INPUT FILE : DEMST1

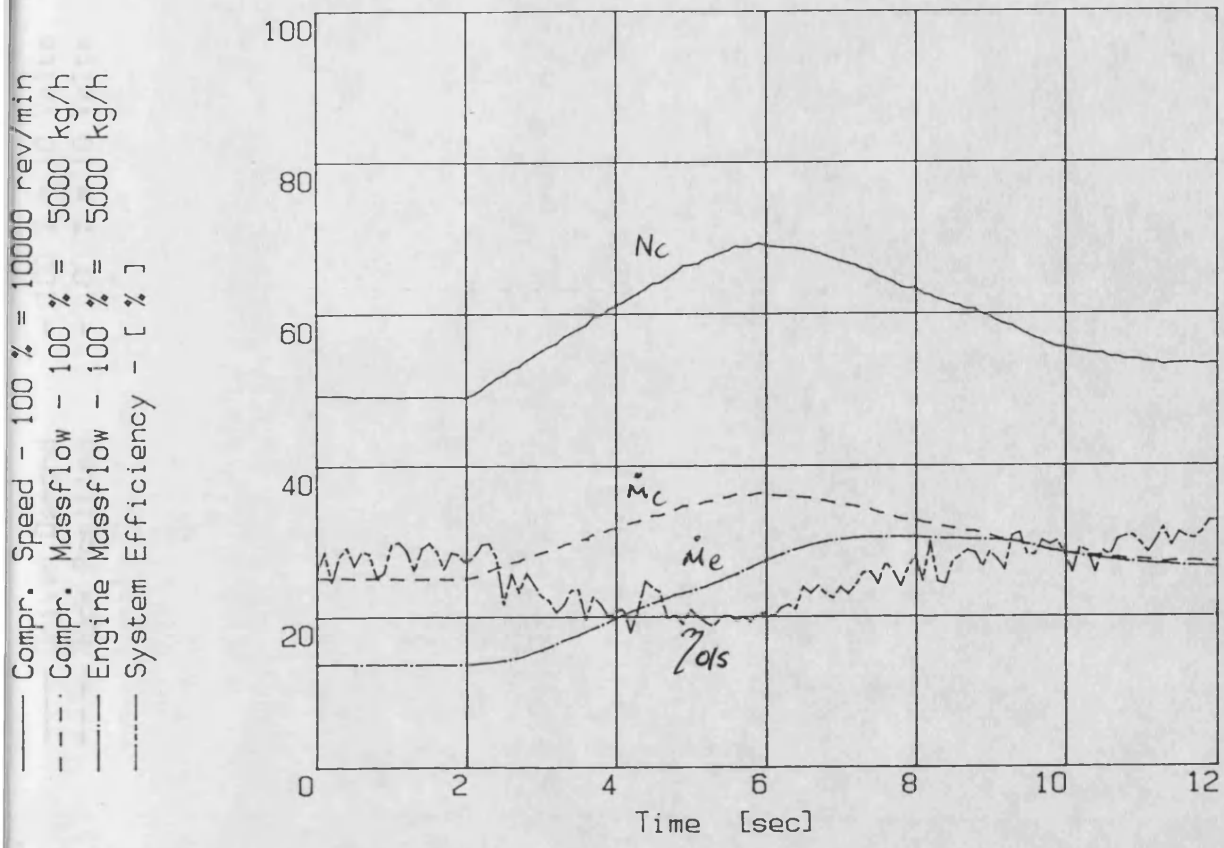

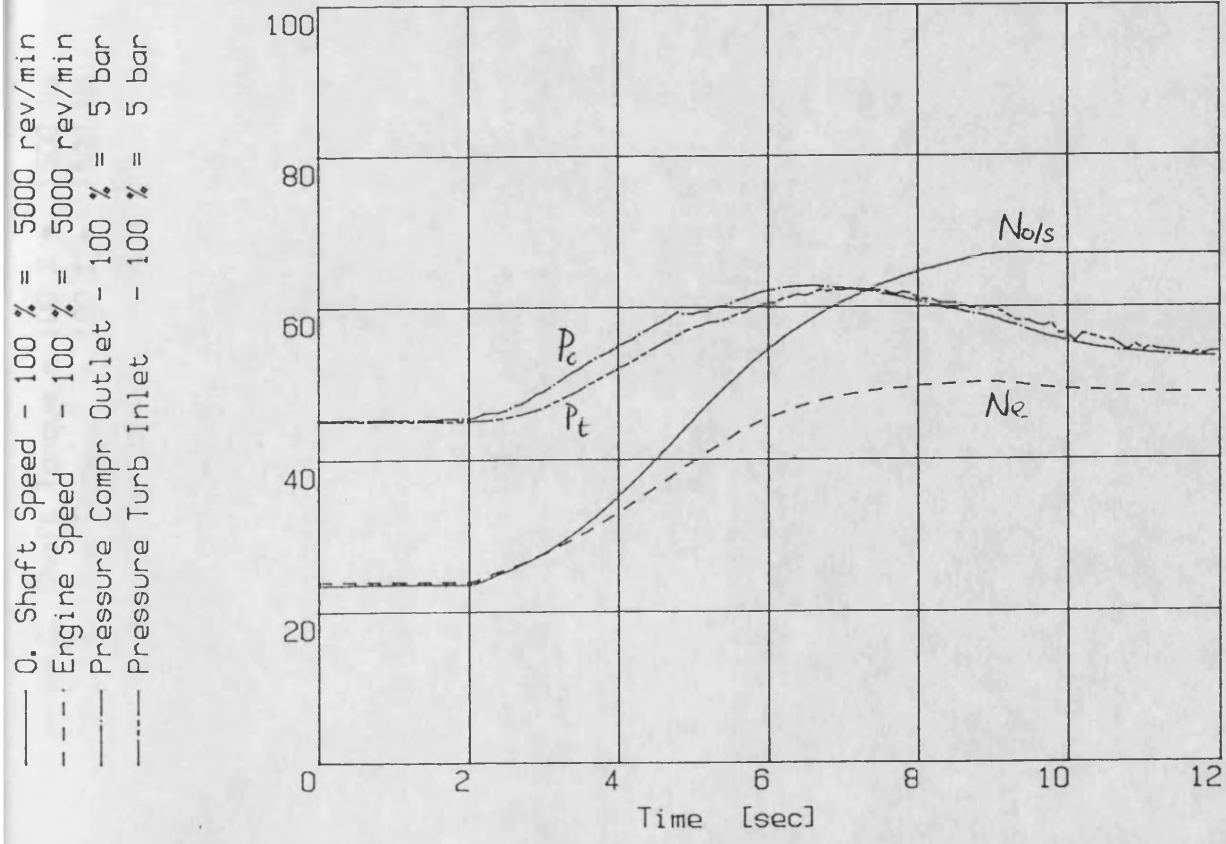

FIG. 7.11(a) EXPERIMENTAL DRIVER DEM.STEP RESPONSE

"DCe transient tests"
"5-10V dem. step at 500Nm"
INPUT FILE : DEMST1

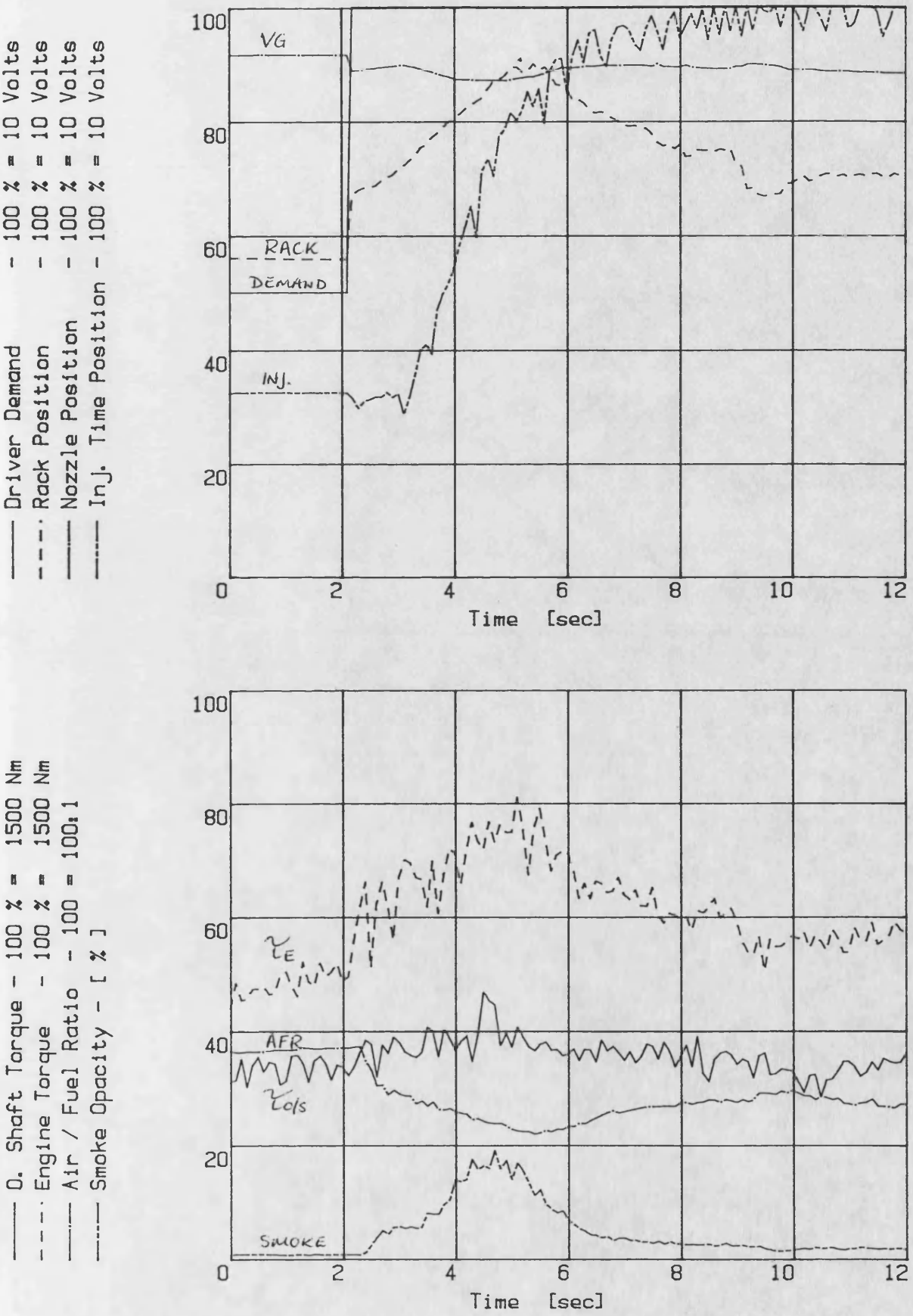

FIG. 7.11(b) EXPERIMENTAL DRIVER DEM.STEP RESPONSE

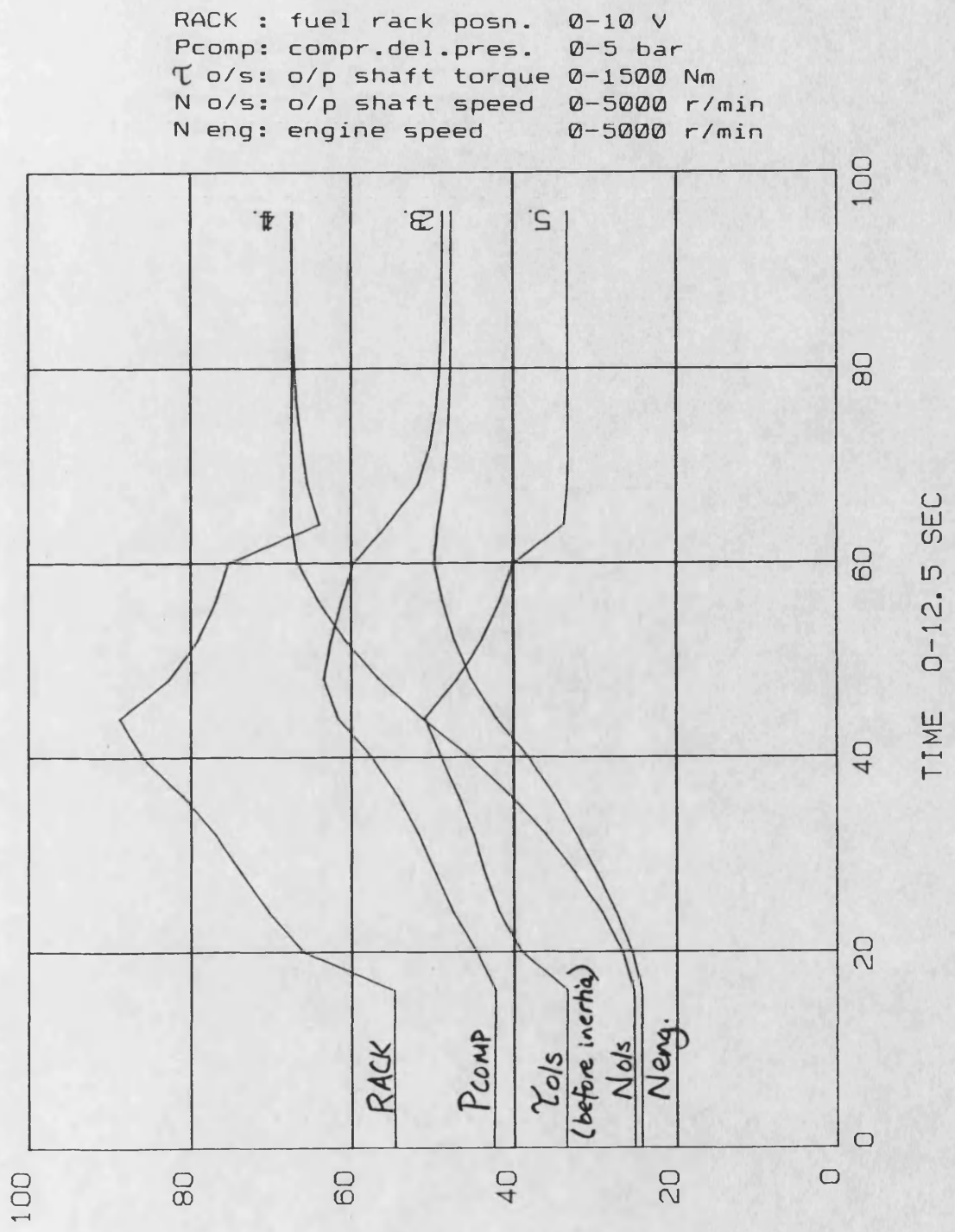

FIG. 7.12 PREDICTED DRIVER DEMAND STEP RESPONSE

RACK: fuel rack posn. Ø-10V
Pcomp: compr.del.pres Ø-5bar
N o/s: o/p shaft speed Ø-5000r/min
AFR : air/fuel ratio Ø-100

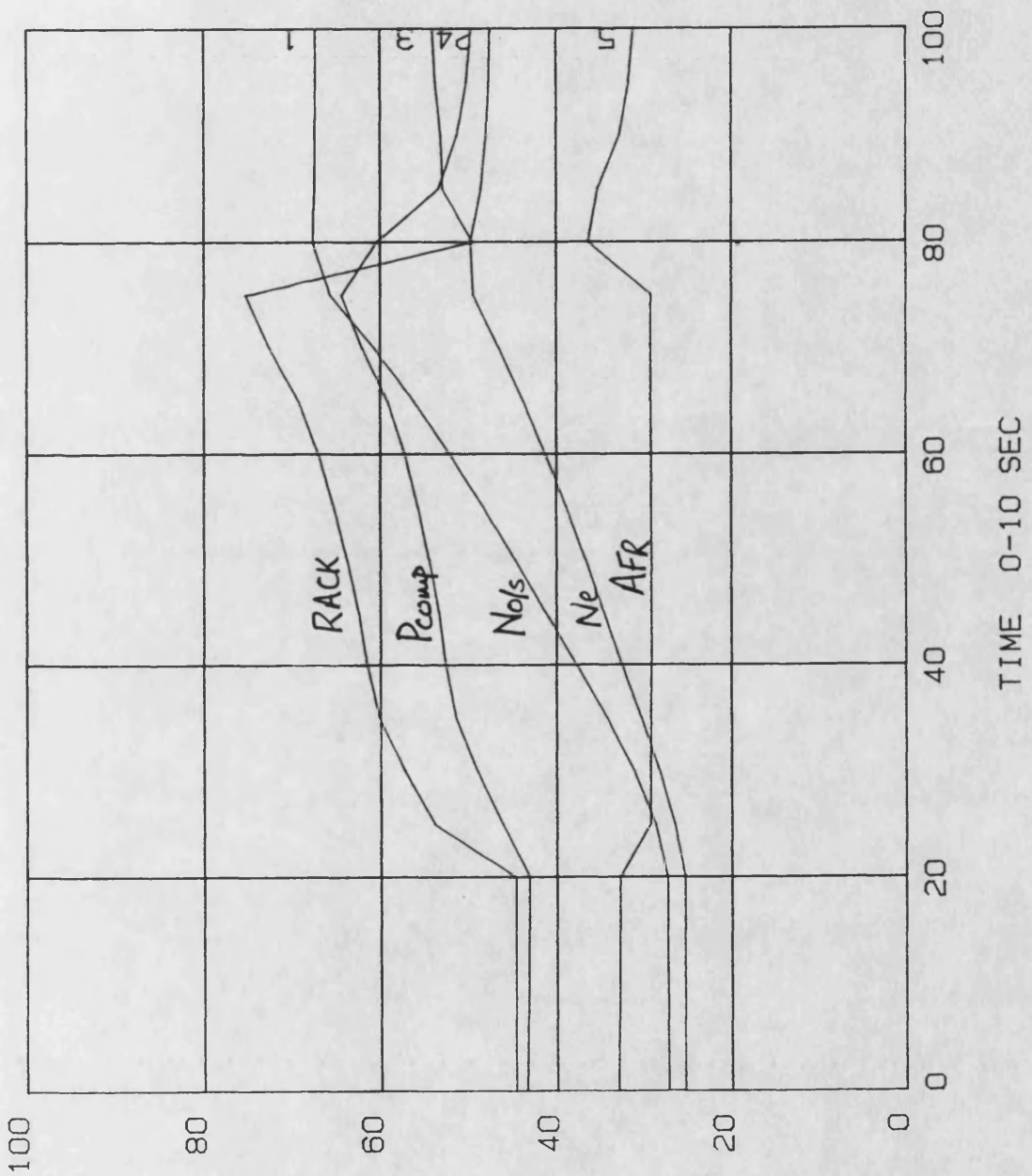

FIG. 7.13 PREDICTED DRIVER DEM.STEP: FUEL/BOOST LIM.2.4 V/bar

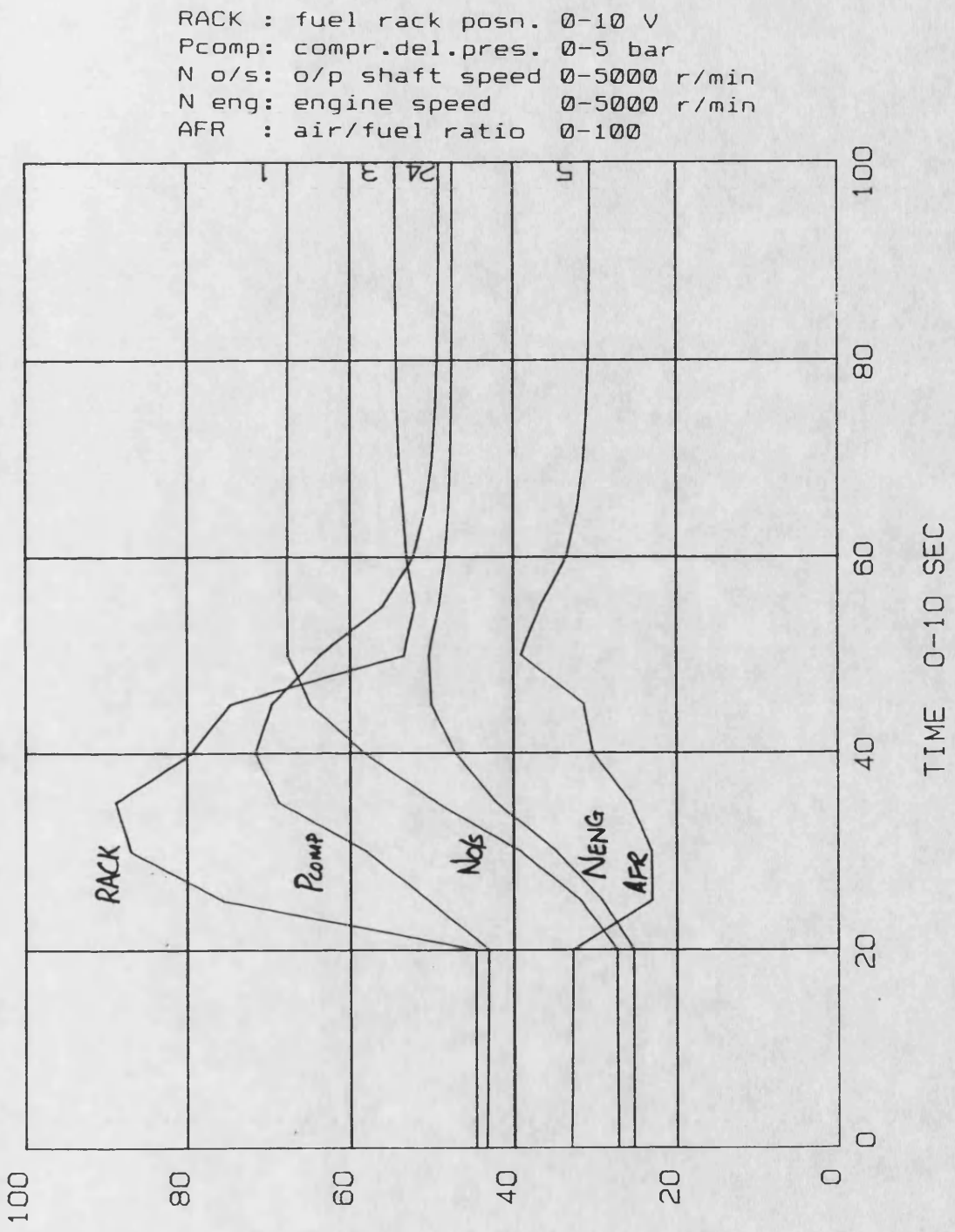

FIG. 7.14 PREDICTED DRIVER DEM.STEP: FUEL/BOOST LIMIT 3. V/bar

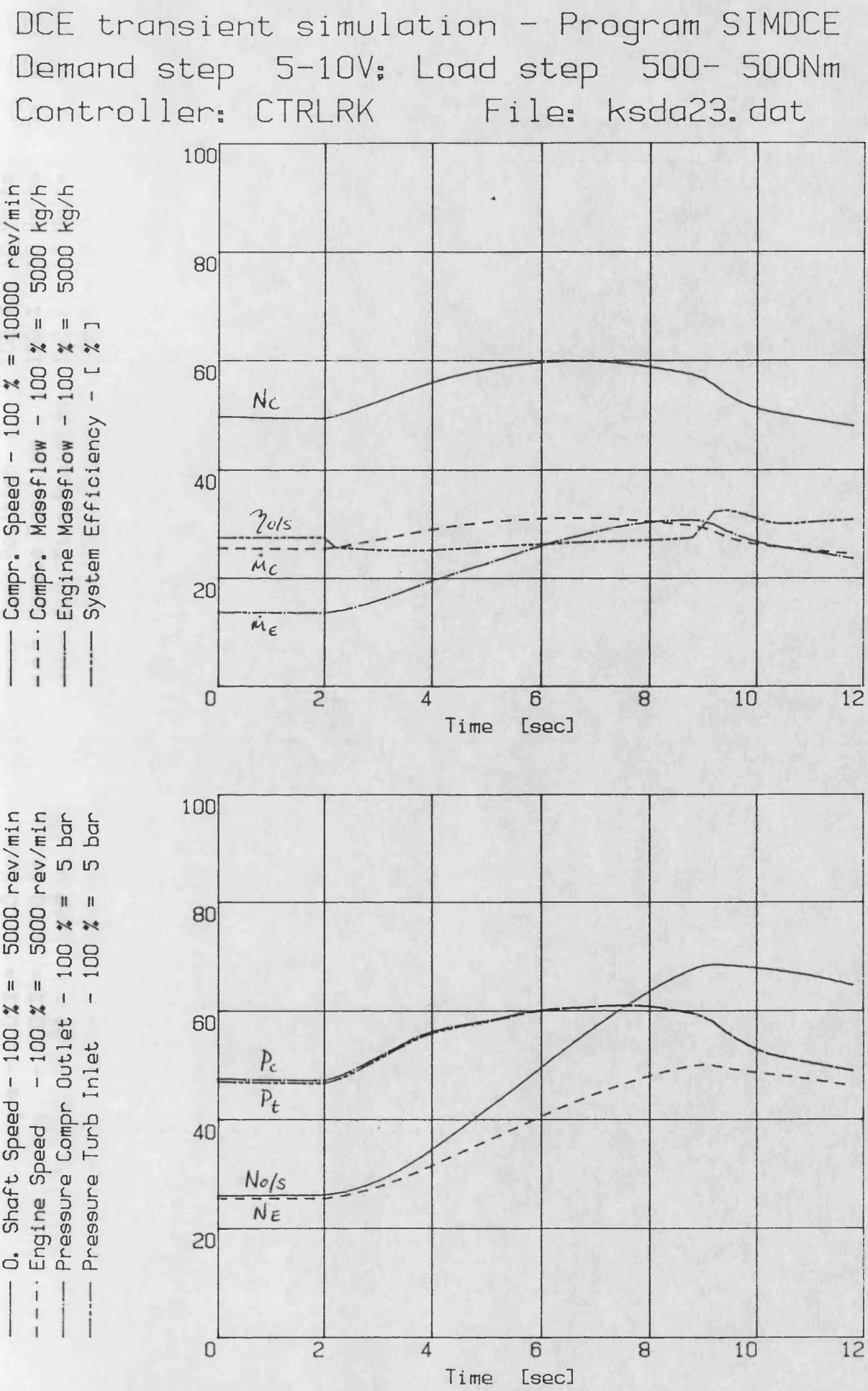

FIG. 7.15a PREDICTED DRIVER DEMAND STEP: ENGINE EFFICIENCY DETERIORATION WITH LOW AIR/FUEL RATIO

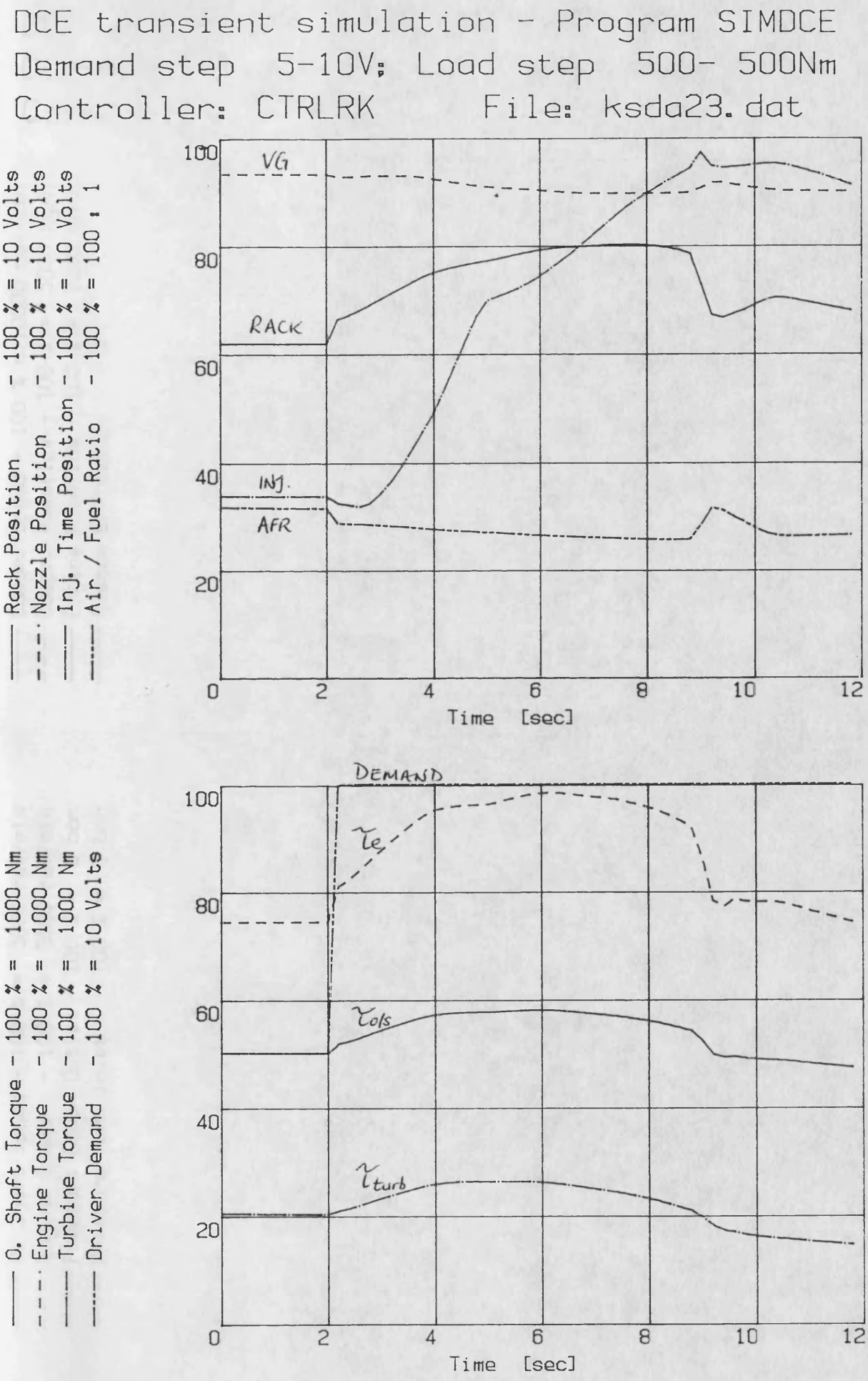

FIG. 7.15b PREDICTED DRIVER DEMAND STEP: ENGINE EFFICIENCY DETERIORATION WITH LOW AIR/FUEL RATIO

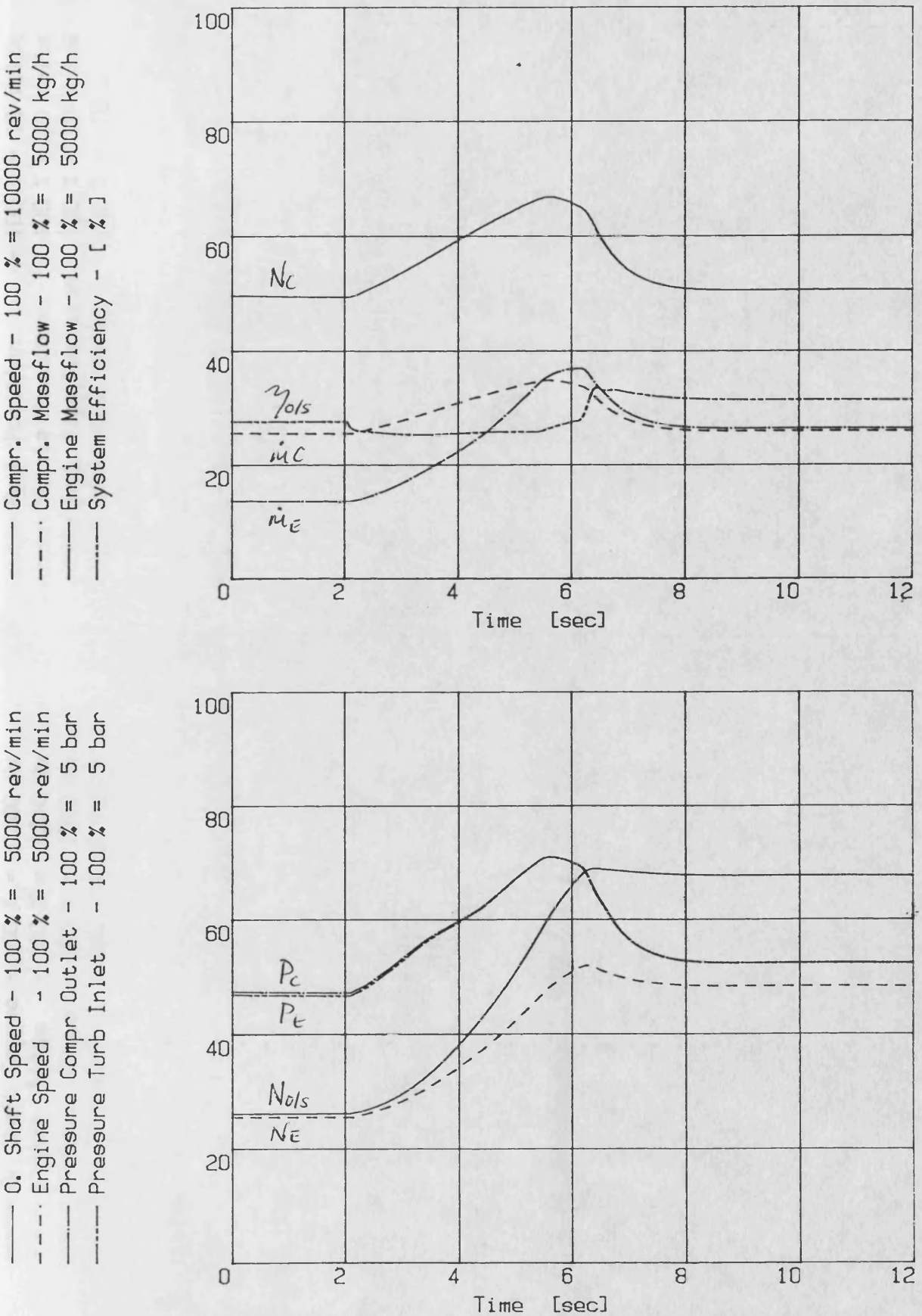

FIG. 7.16a PREDICTED DRIVER DEMAND STEP: NO ENGINE EFFICIENCY DETERIORATION WITH LOW AFR.

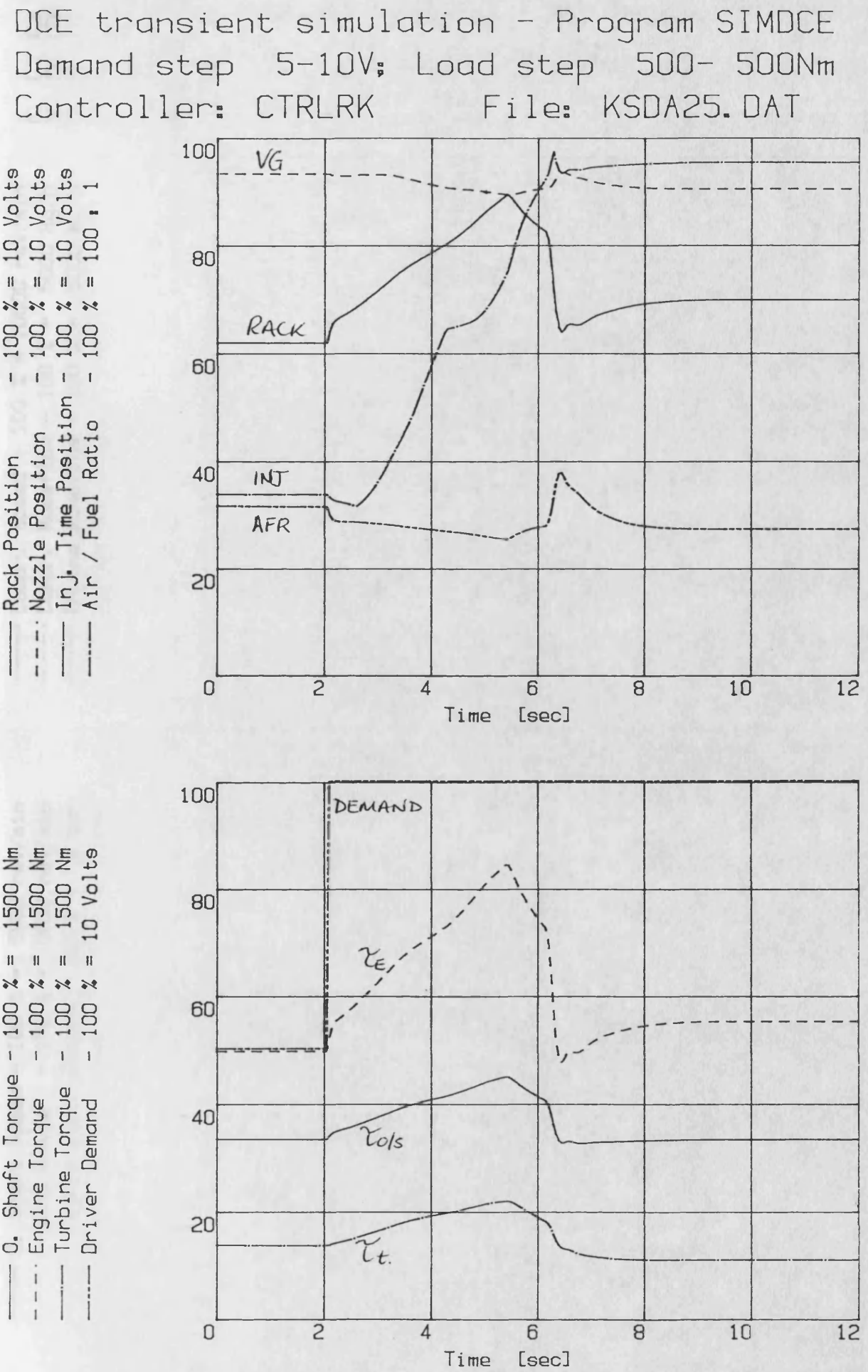

FIG. 7.16b PREDICTED DRIVER DEMAND STEP: NO ENGINE EFFICIENCY DETERIORATION WITH LOW AFR.

DCE transient simulation - SIMDCE 130389
Demand step 5-10V; Load 500Nm . ddsa1.dat
exptal-matched turb.swall.cap.

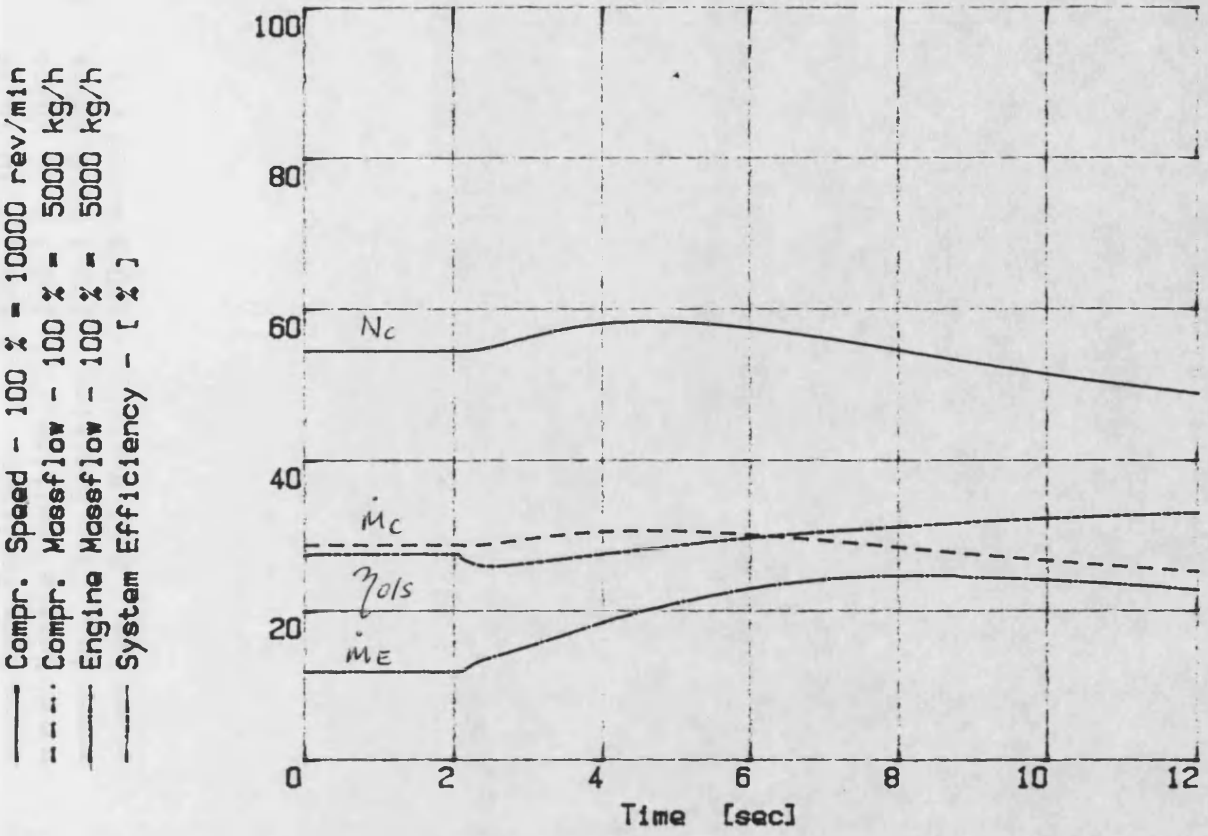

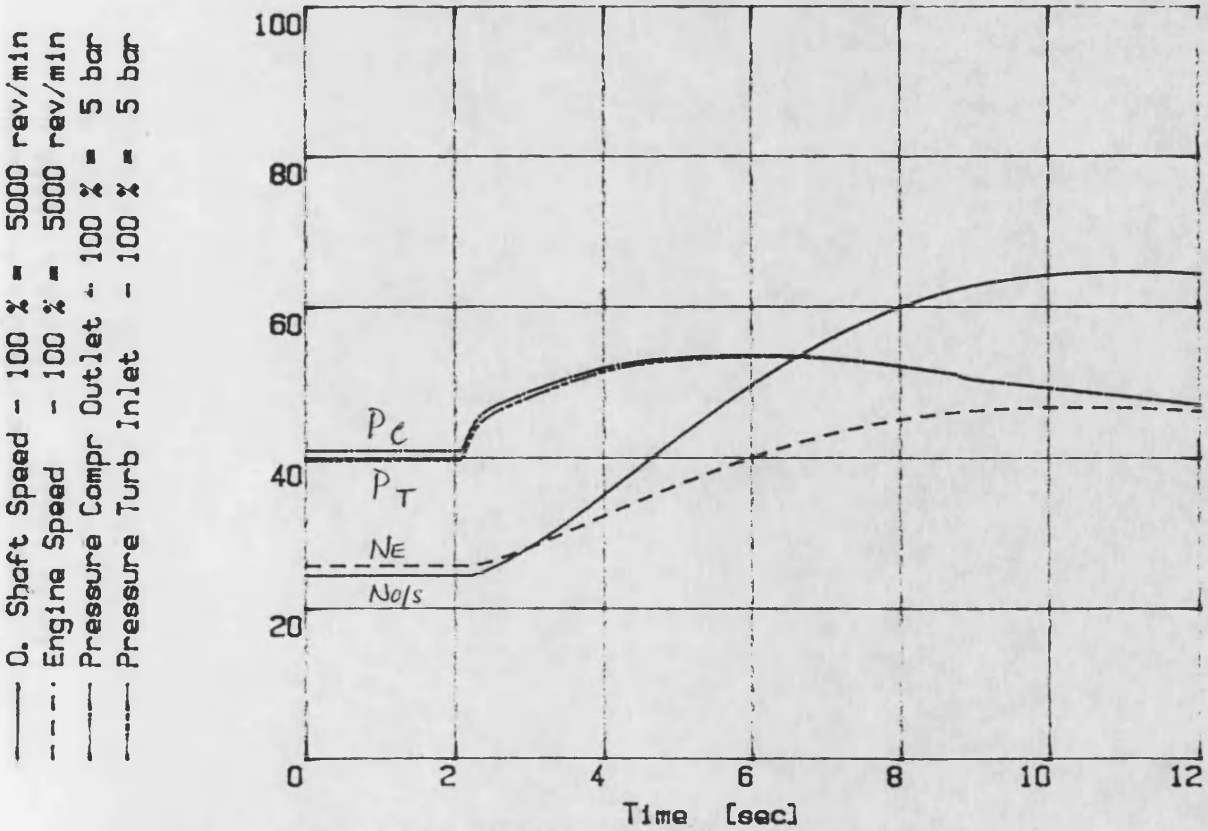

FIG. 7.17a PRED.DEM.STEP,TRANSIENT CTRL.
(matched swallowing capacity)

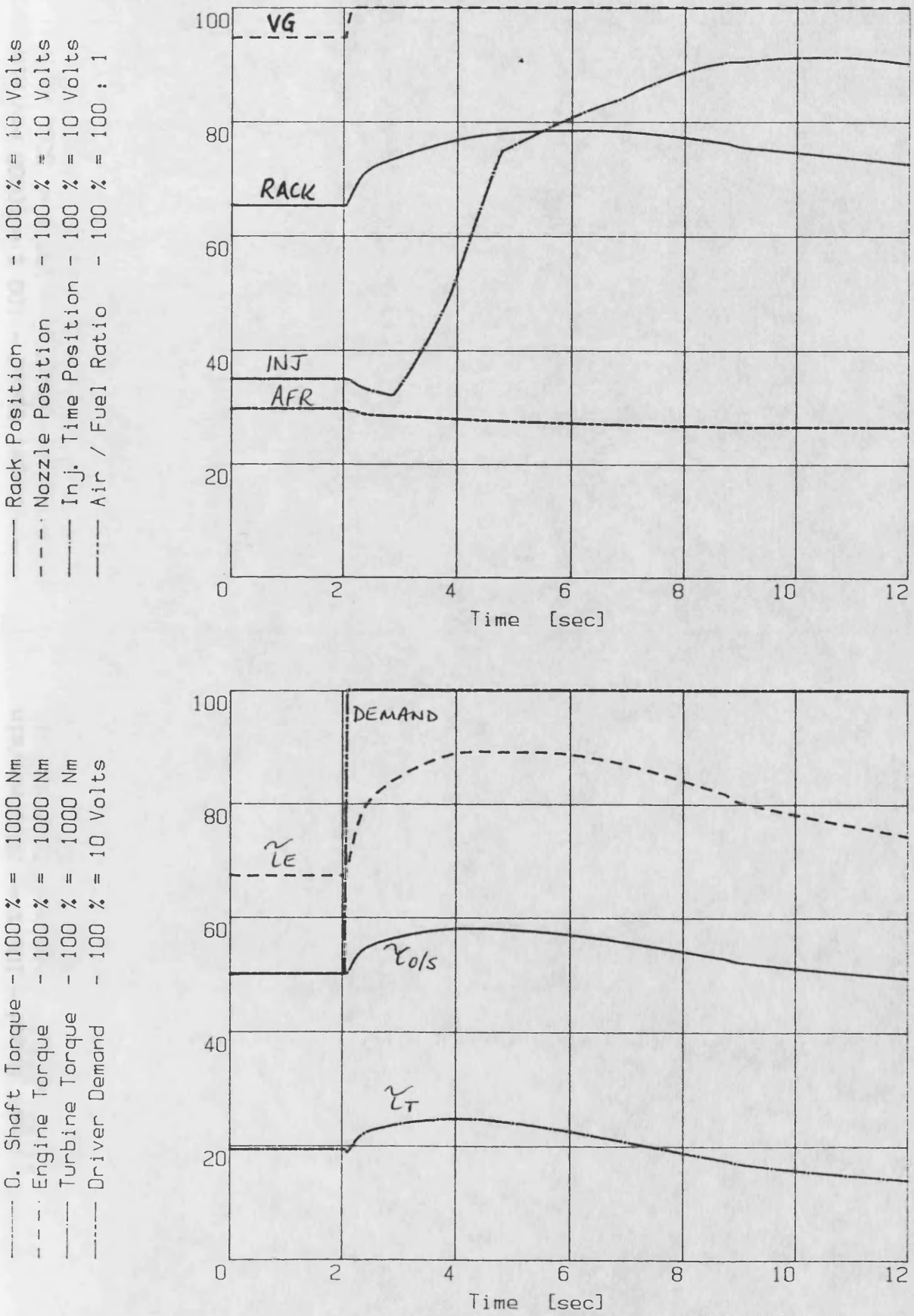

FIG. 7.17b PRED.DEM.STEP,TRANSIENT CTRL.
(matched swallowing capacity)

"DCE TRANSIENT TESTS"
"5-10V dem. step at 500Nm"
INPUT FILE : a:\dsta4.

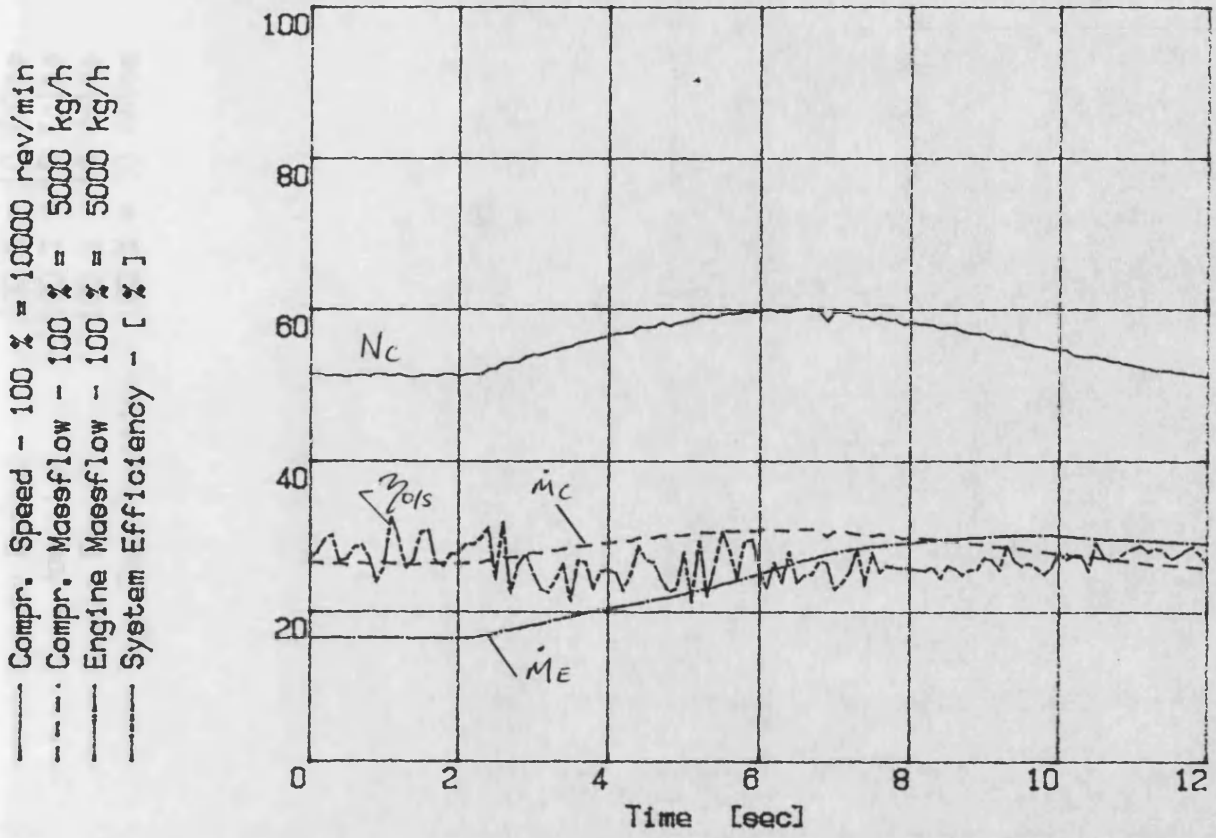

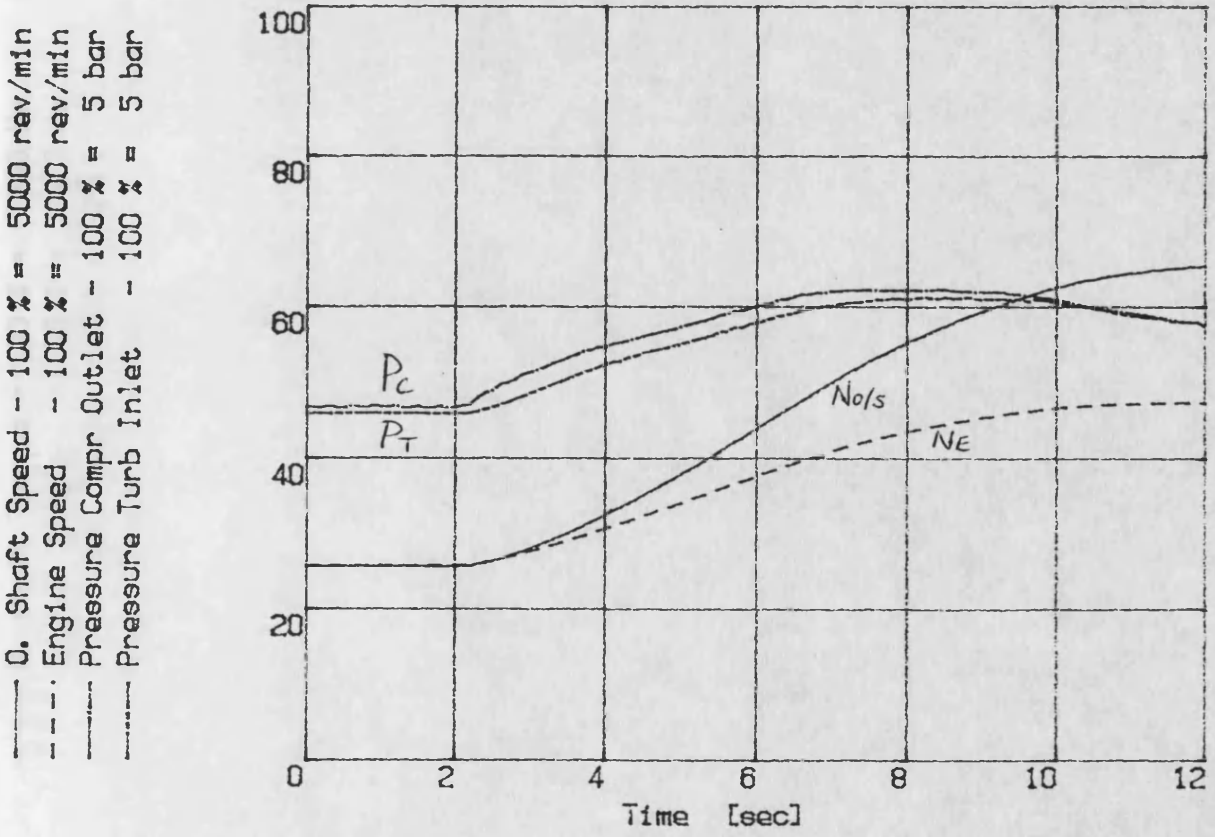

FIG. 7.18a EXPTAL DEM.STEP,TRANSIENT CTRL.

"DCE TRANSIENT TESTS"
"5-10V dem. step at 500Nm"
INPUT FILE : a:\dsta4.

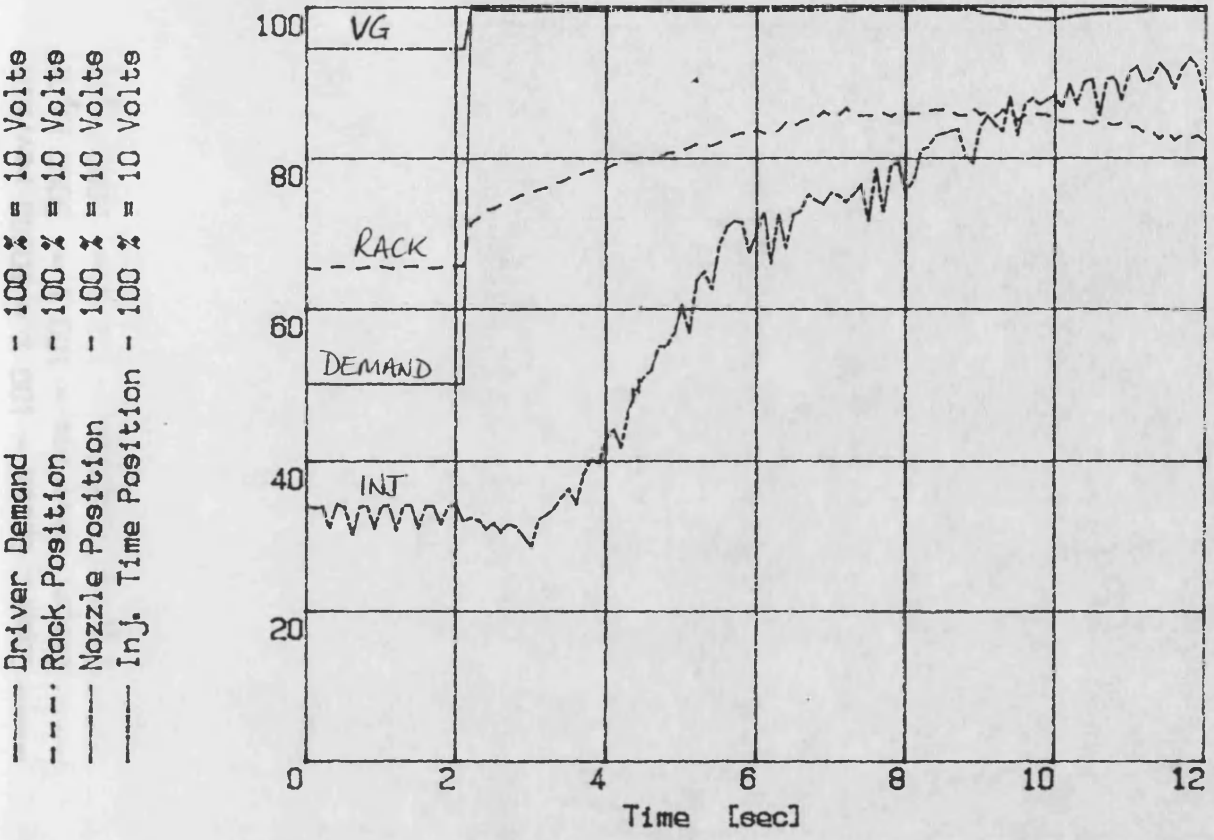

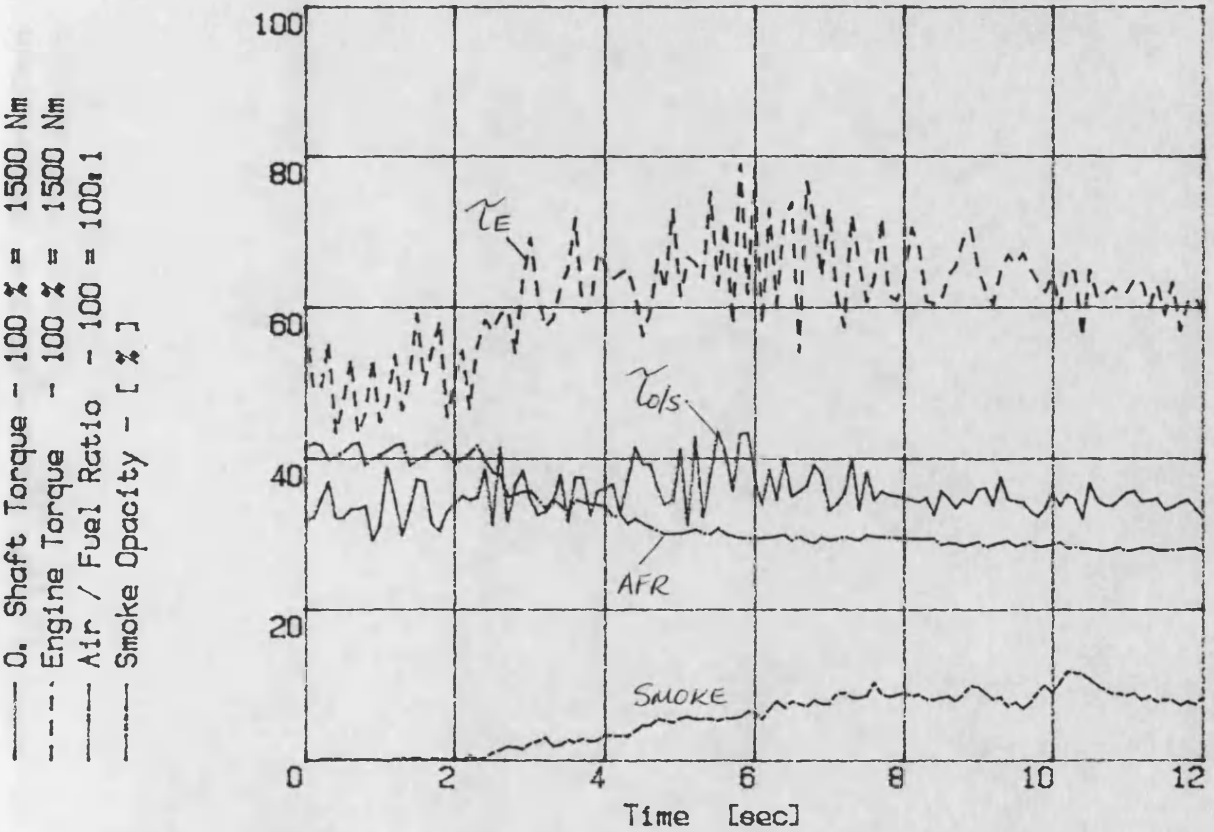

FIG. 7.18b EXPTAL DEM.STEP,TRANSIENT CTRL.

"DCE TRANSIENT TESTS"
"7-10V dem.step at 700Nm"
INPUT FILE : dstb

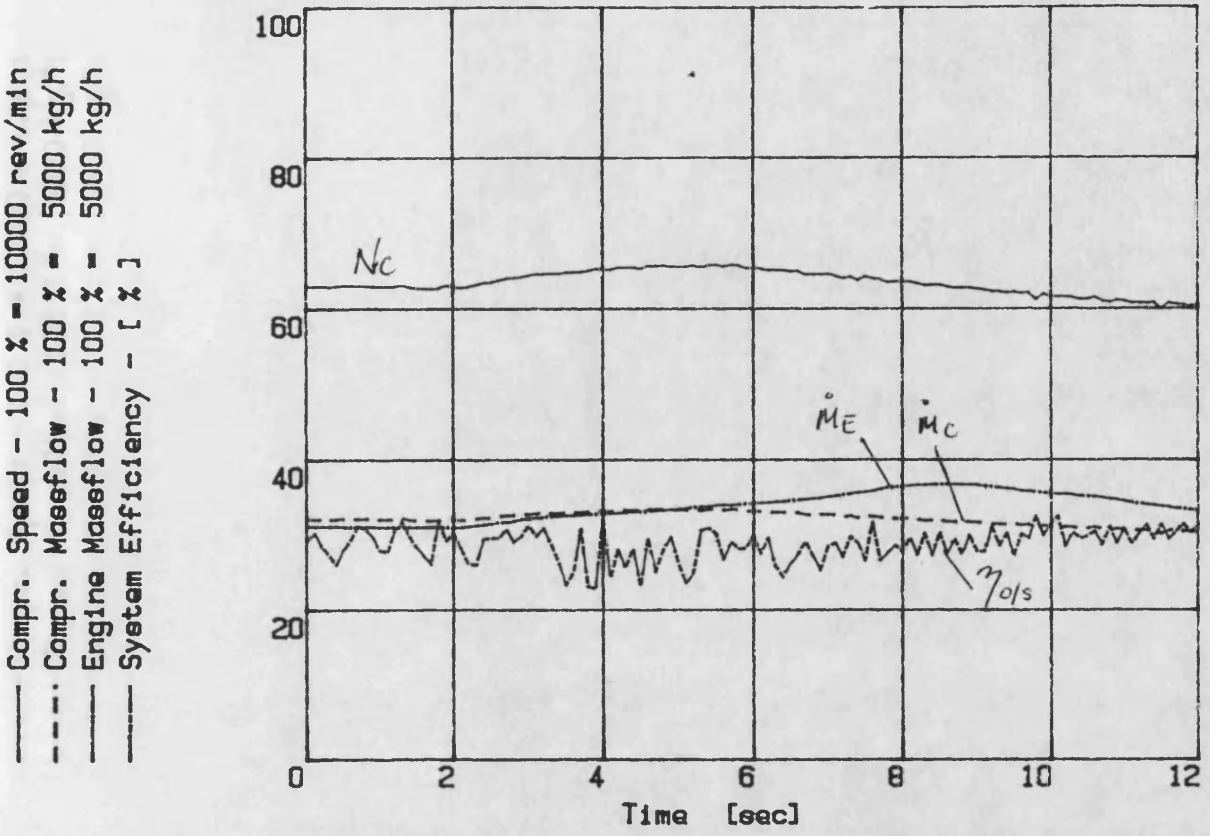

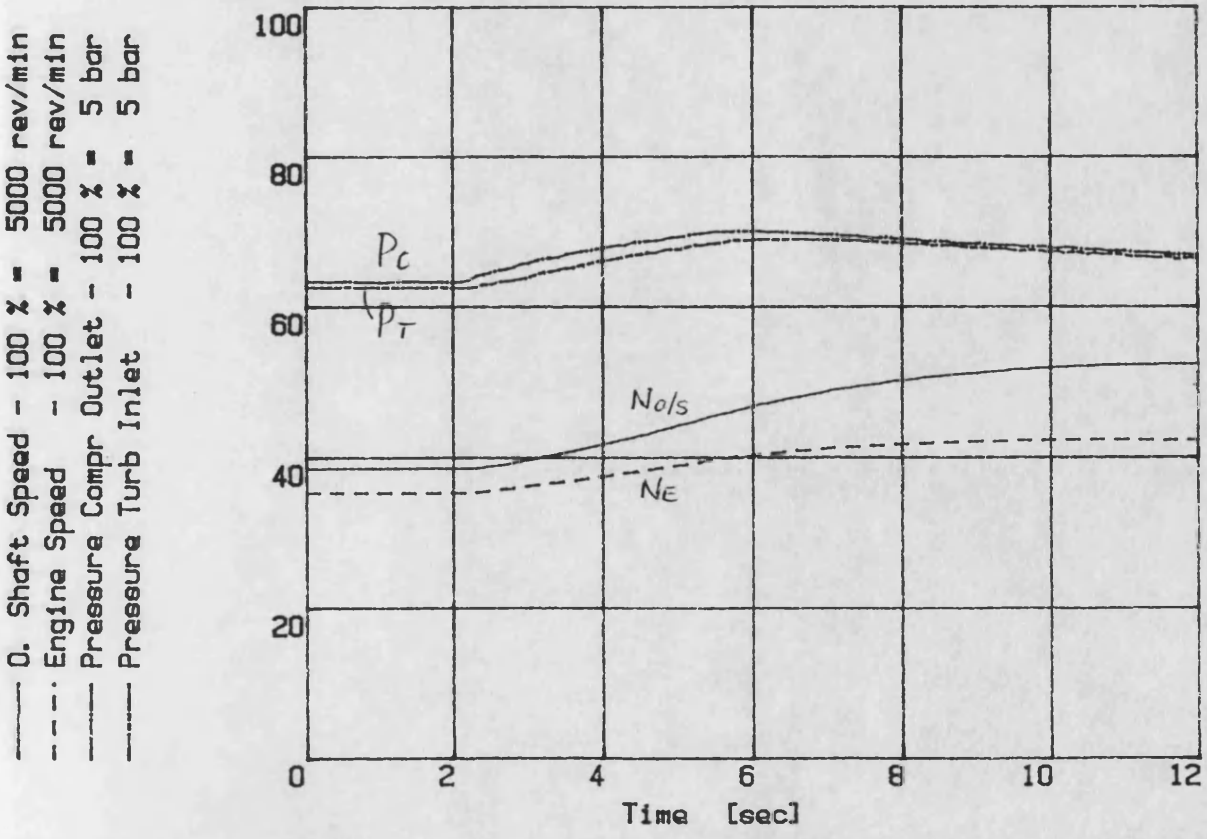

FIG. 7.19 EXPTAL 7-10V DEM.STEP/700Nm RESPONSE, TRANSIENT CONTROL

DCE transient simulation - Program SIMDCE
Demand step 7-10V; Load step 700- 700Nm
File: KSDB20.DAT

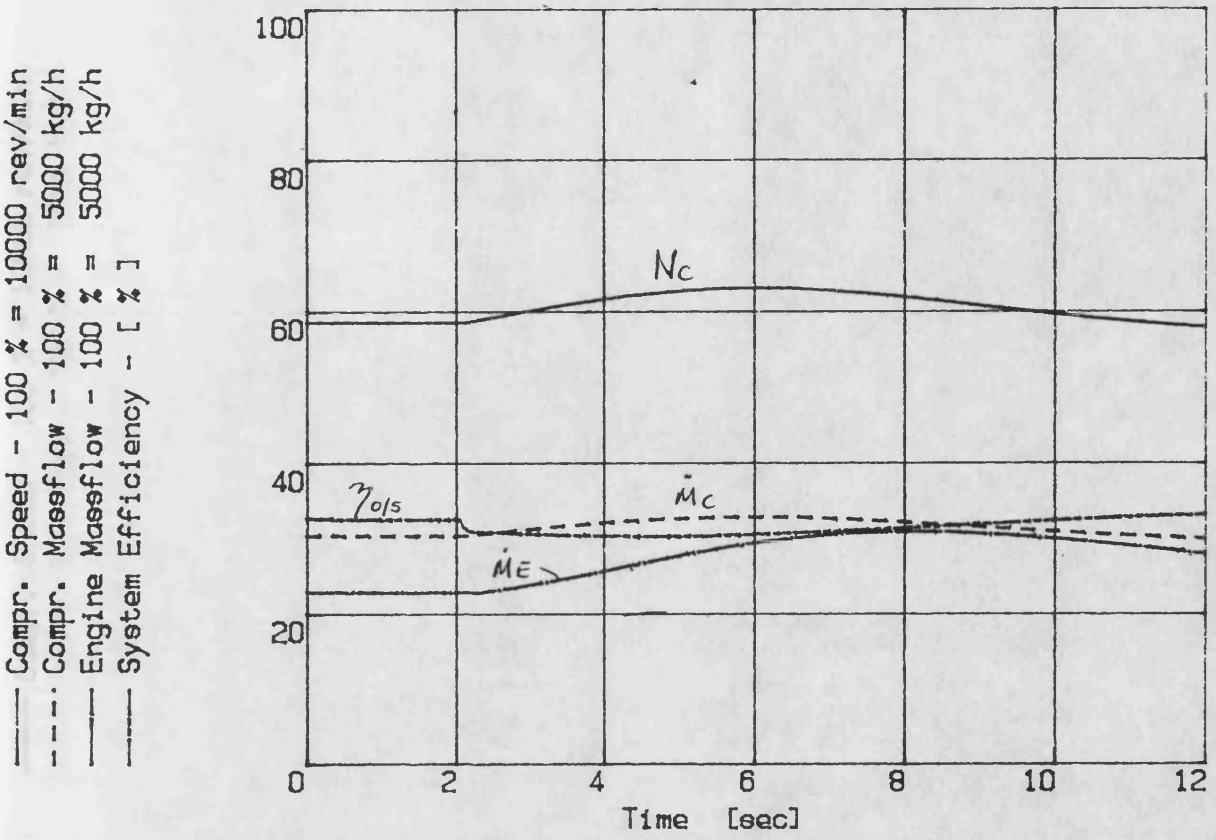

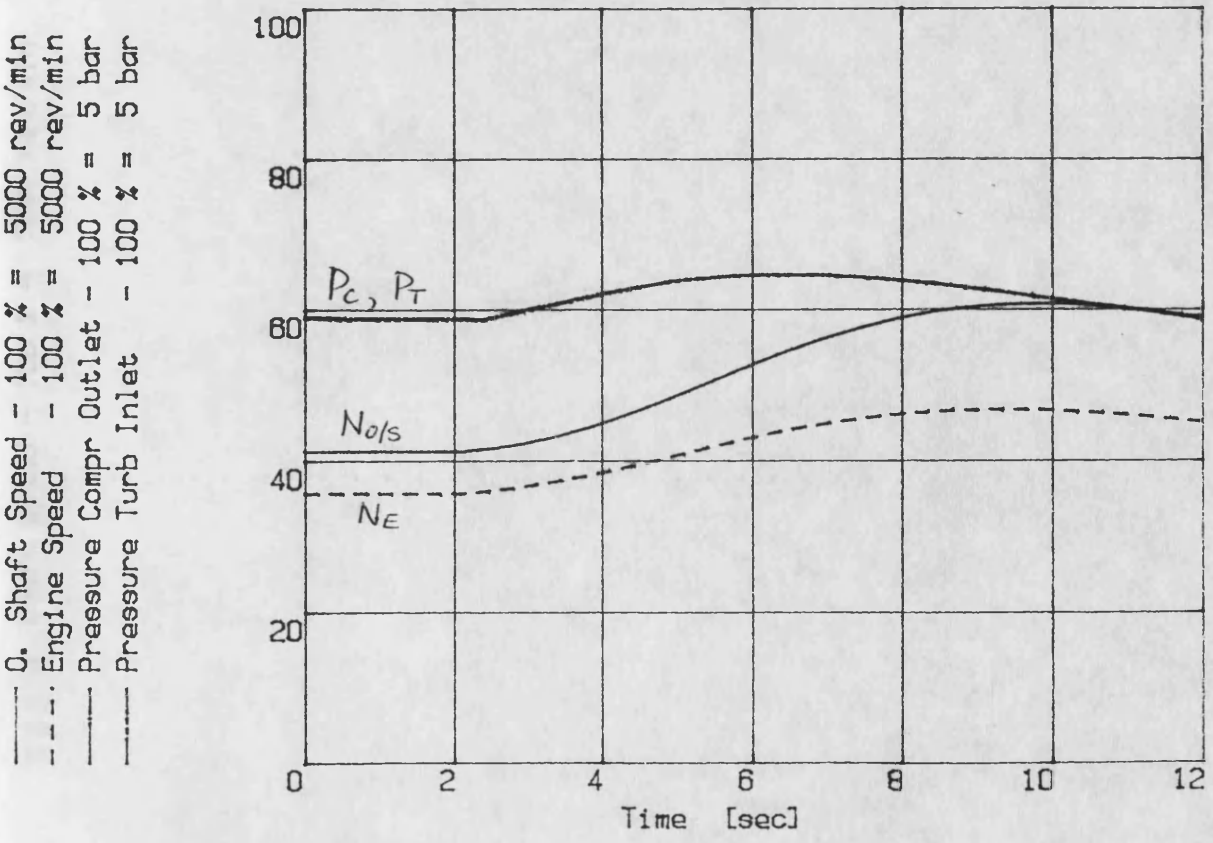

FIG. 7.20 PRED. 7-10V DEM.STEP/700Nm RESPONSE, TRANSIENT CONTROL

"DCE TRANSIENT TESTS"
"400-800Nm load step at 10V demand.
INPUT FILE : a:\lstal.

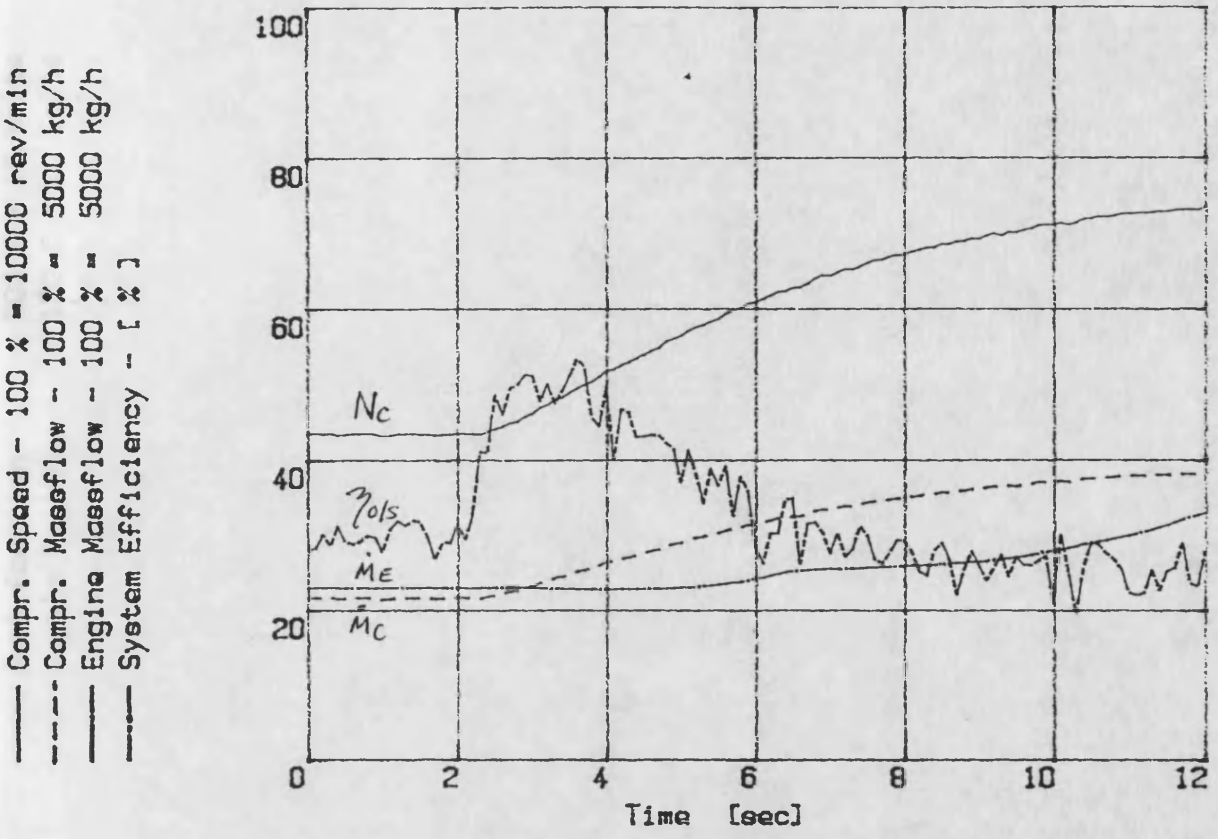

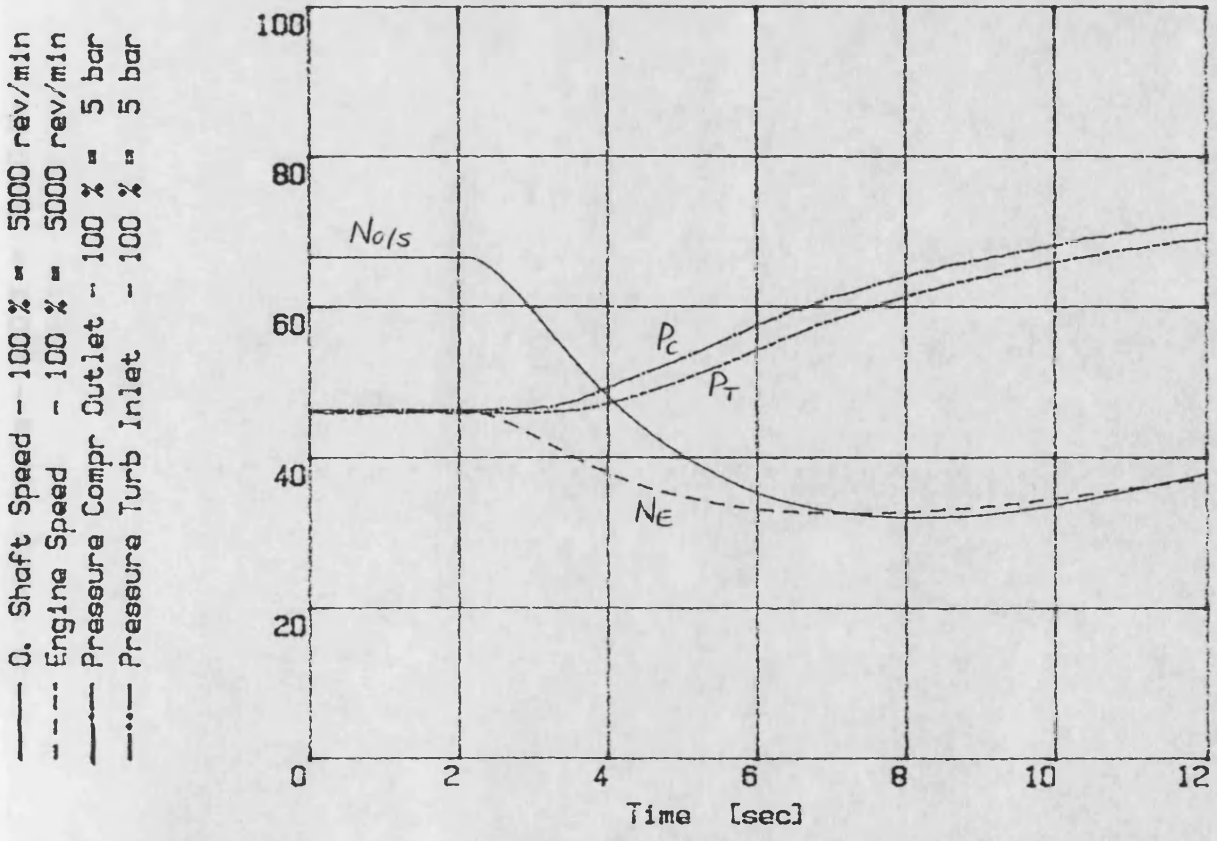

FIG. 7.21a EXPTAL 400-800Nm LOAD STEP RESPONSE

"DCE TRANSIENT TESTS"
"400-800Nm load step at 10V dem.
INPUT FILE : a:\lsta1.

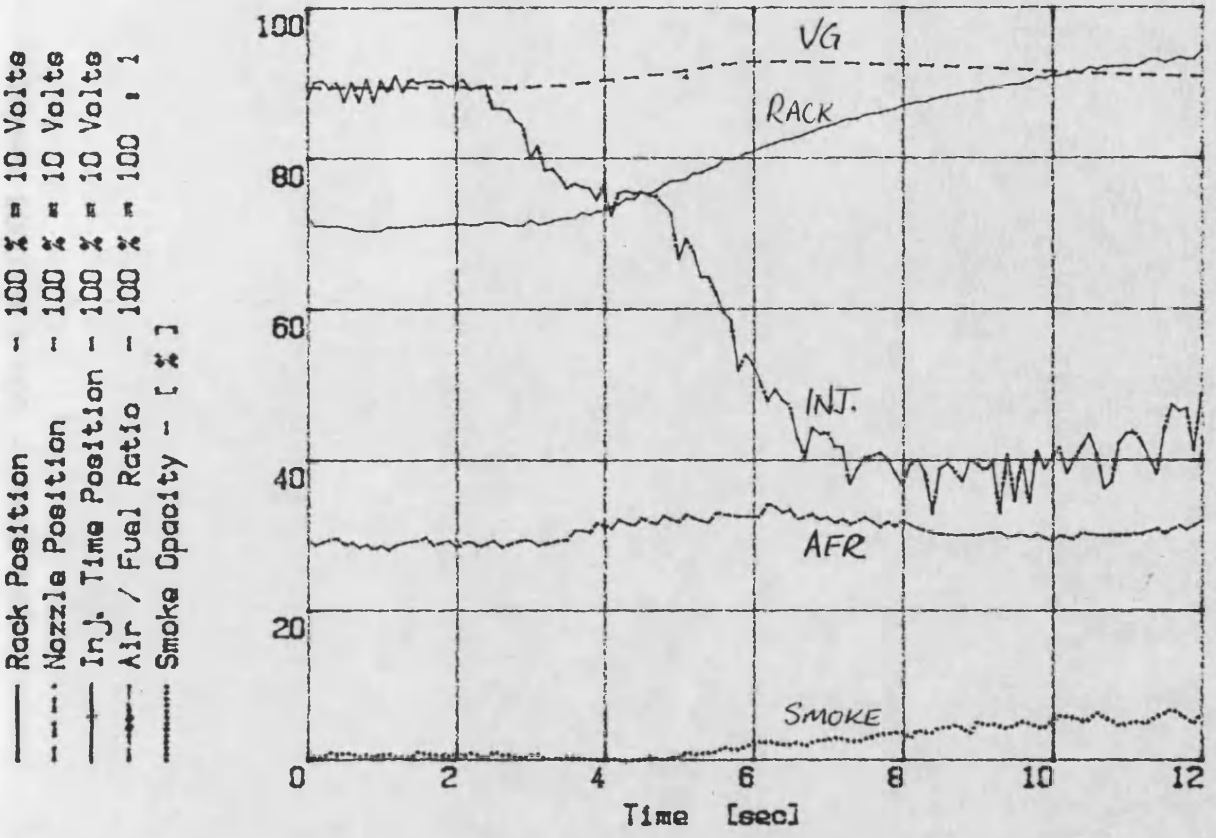

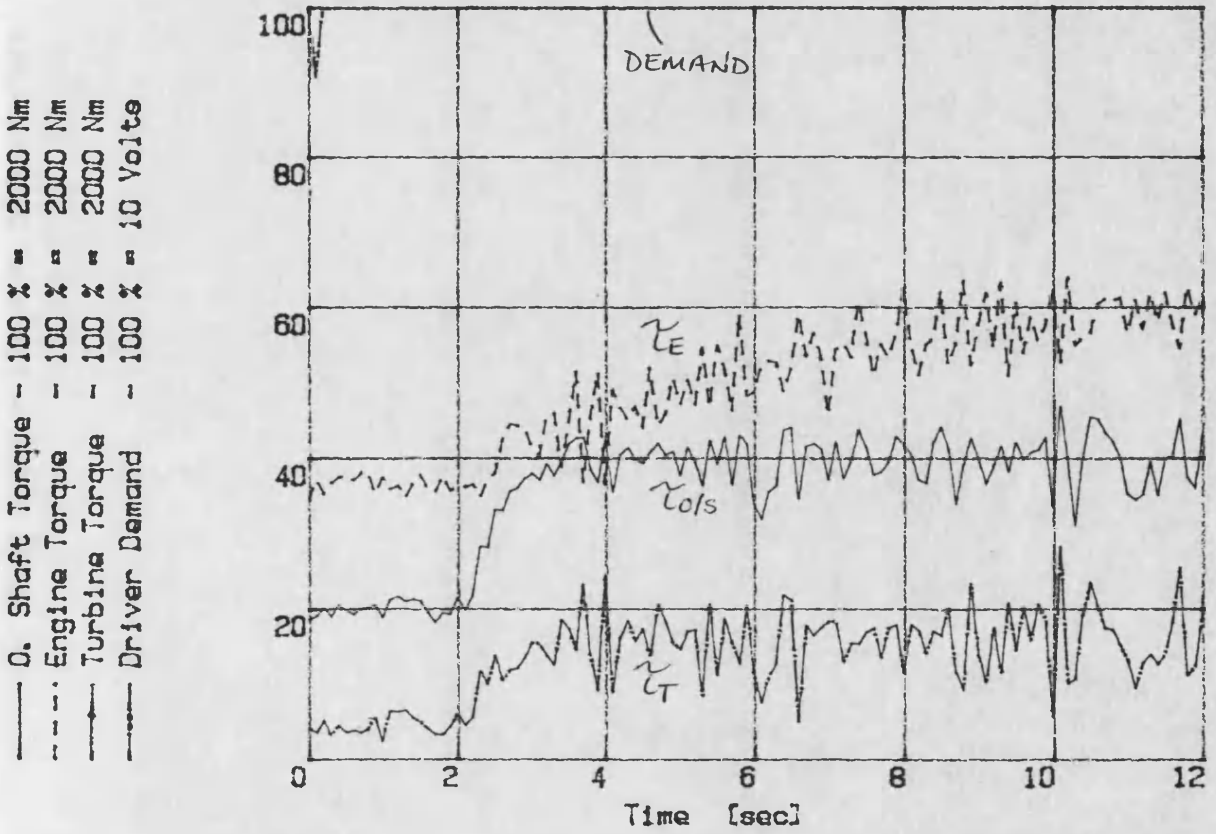

FIG. 7.21b EXPTAL 400-800Nm LOAD STEP RESPONSE

DCE transient simulation - Program SIMDCE
Demand step 10-10V; Load step 400- 800Nm
Controller: CTRLRK

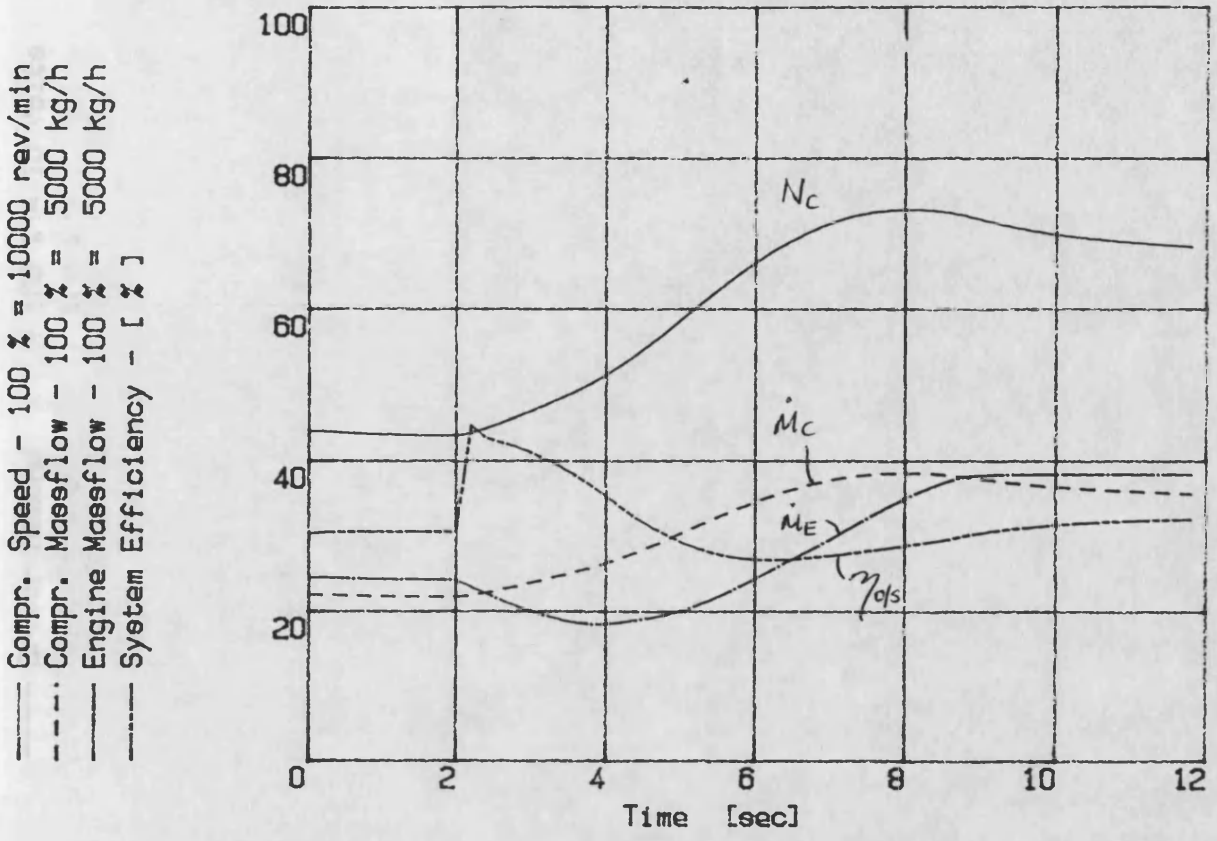

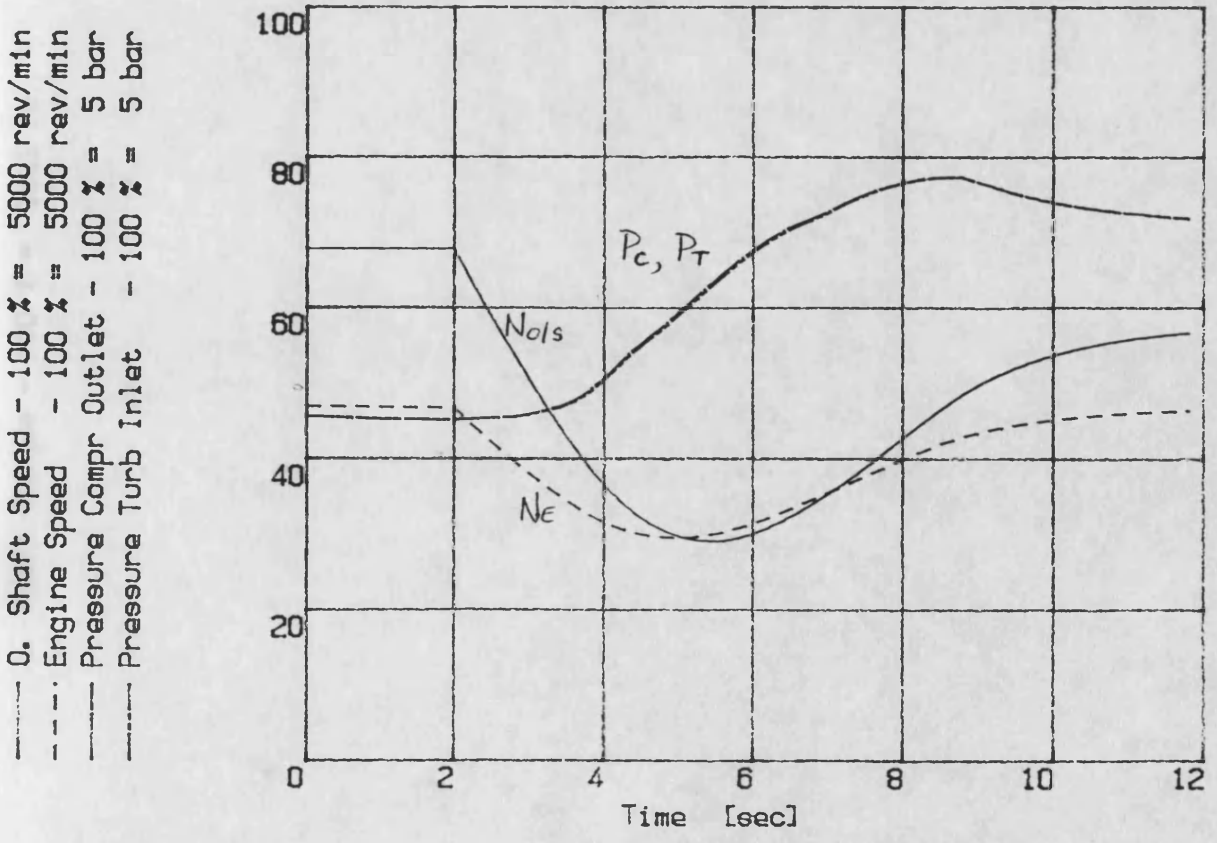

FIG. 7.22a PREDICTED 400-800Nm LOAD STEP RESPONSE

DCE transient simulation - Program SIMDCE
Demand step 10-10V; Load step 400- 800Nm
Controller: CTRLRK

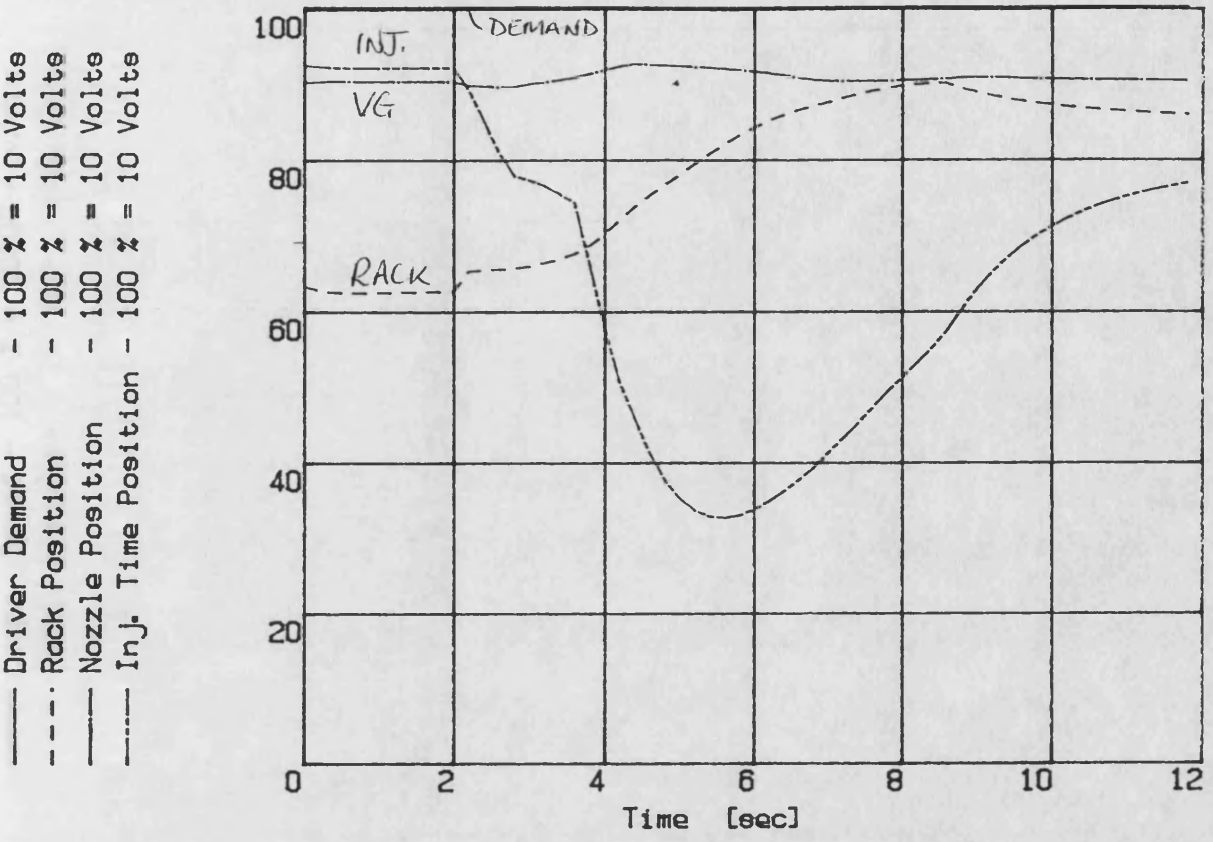

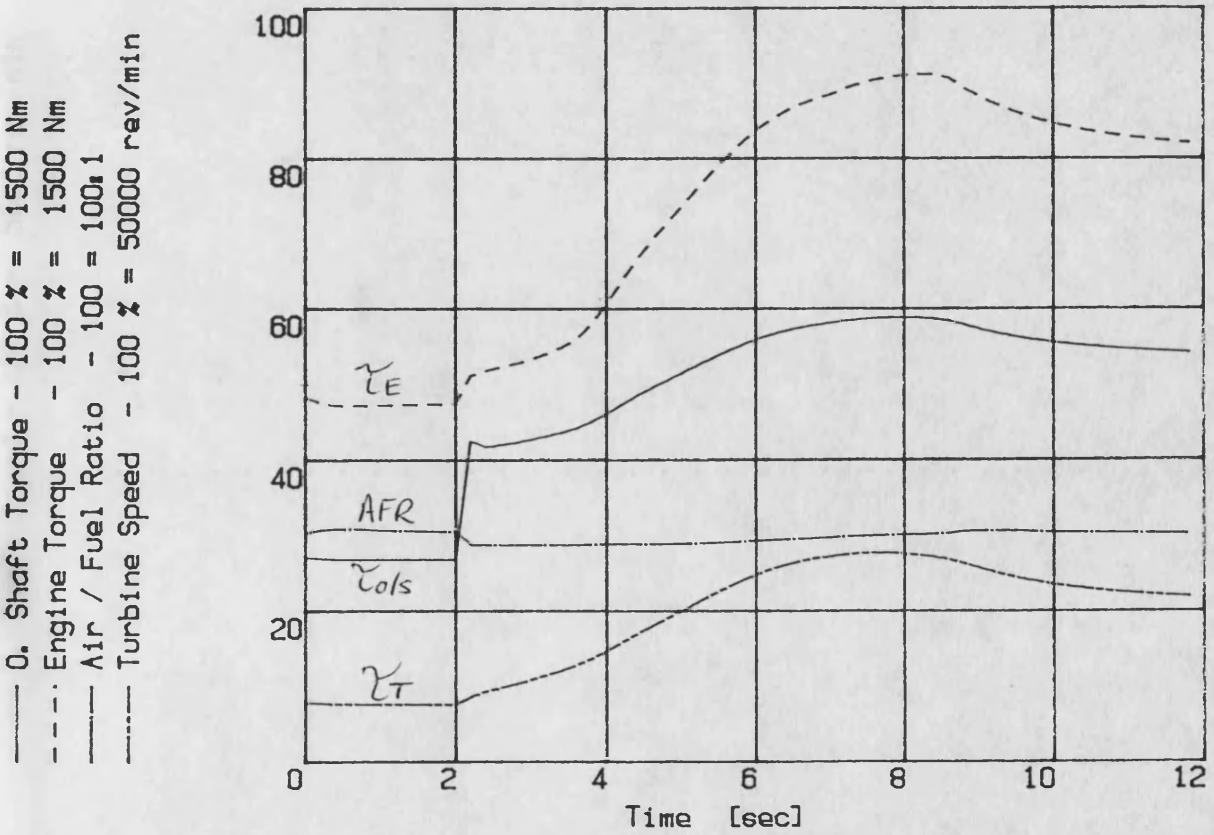

FIG. 7.22b PREDICTED 400-800Nm LOAD STEP RESPONSE

DCE transient simulation - Program SIMDCE
Demand step 10-10V; Load step 400- 800Nm
Controller: CTRLRK

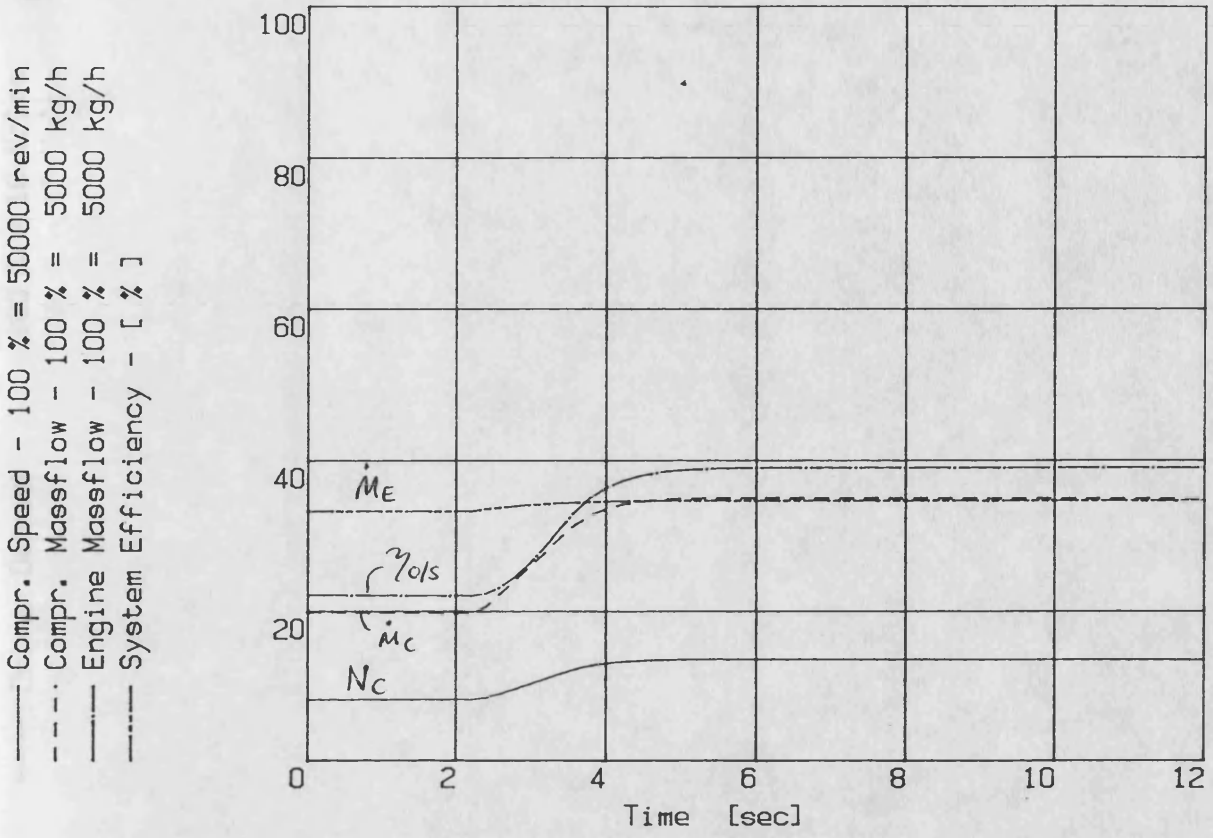

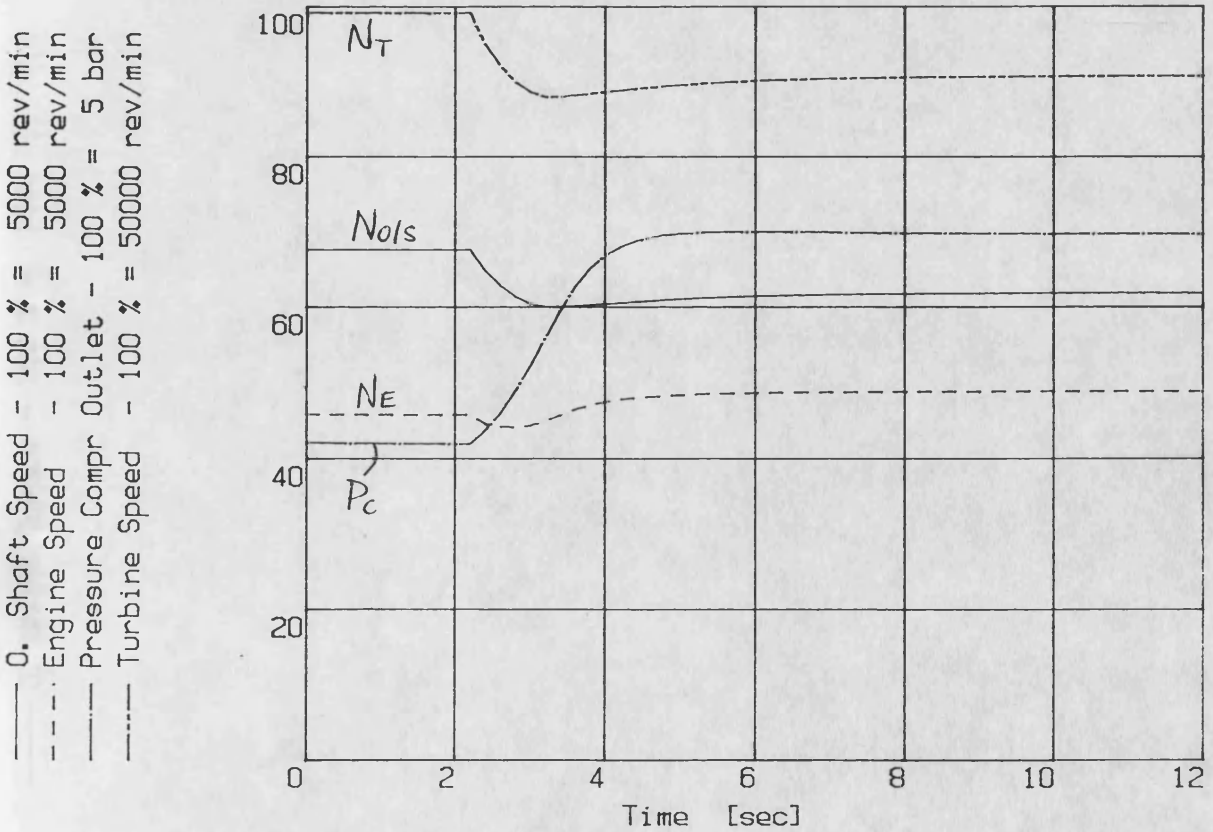

FIG. 7.23a PREDICTED 400-800Nm LOAD STEP RESPONSE
increased fuel/boost limit

DCE transient simulation - Program SIMDCE
Demand step 10-10V; Load step 400- 800Nm
Controller: CTRLRK

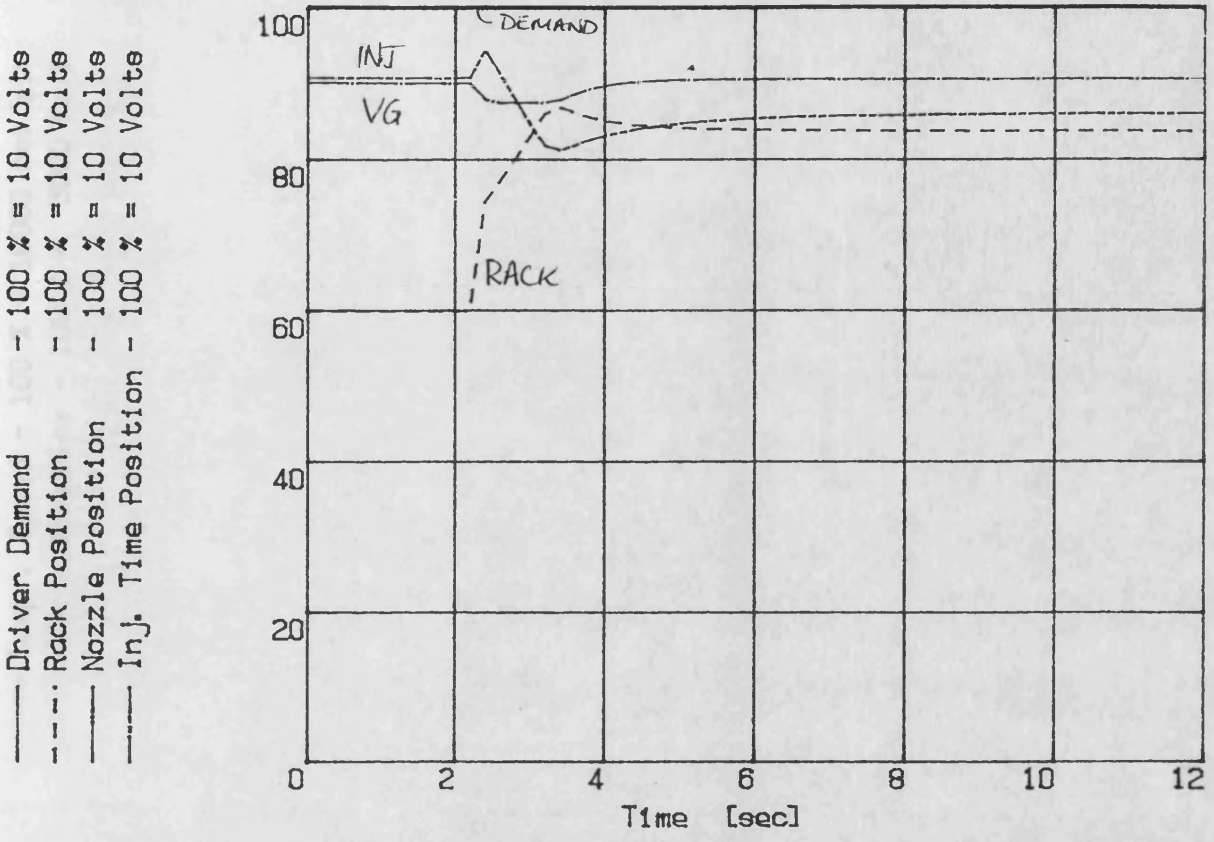

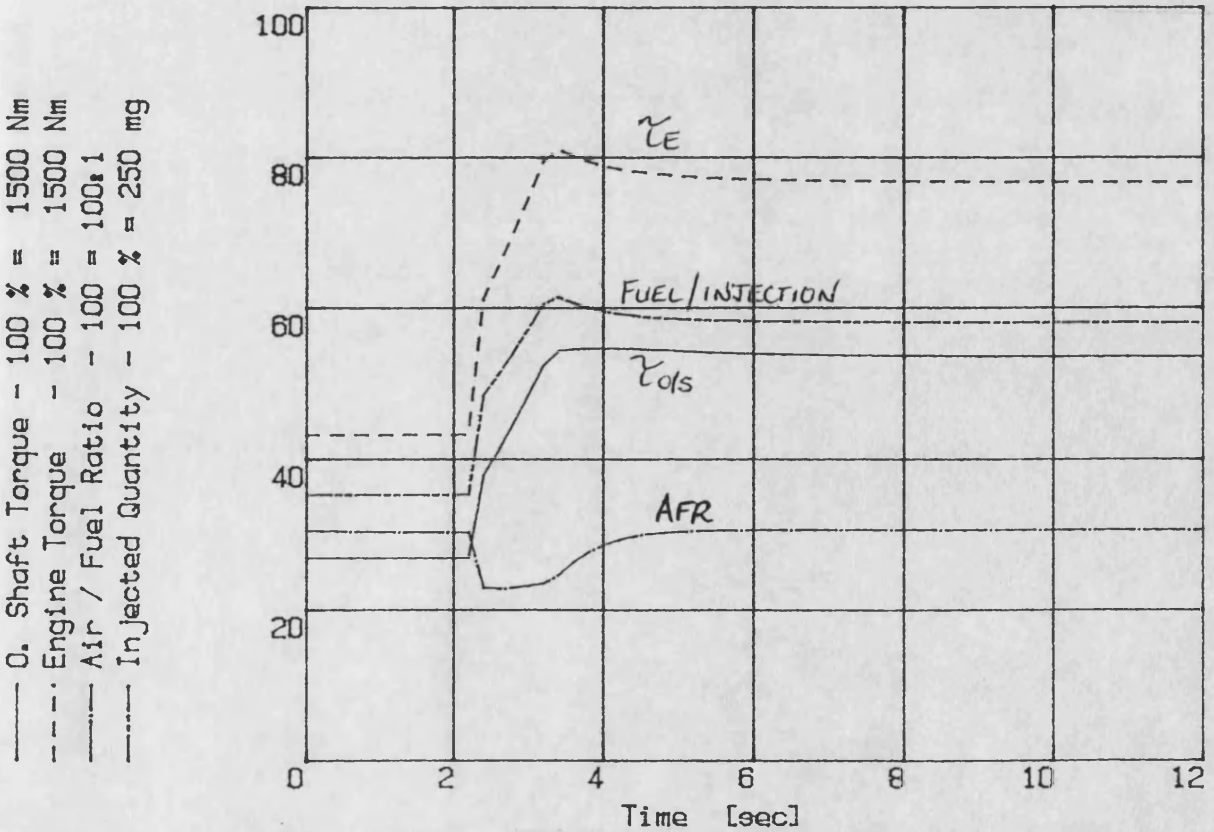

FIG. 7.23b **PRED.** 400-800Nm LOAD STEP RESPONSE
increased fuel/boost limit

DCE transient simulation - Program SIMDCE
Demand step 5-10V; Load step 500- 500Nm
Controller: CTRLRK

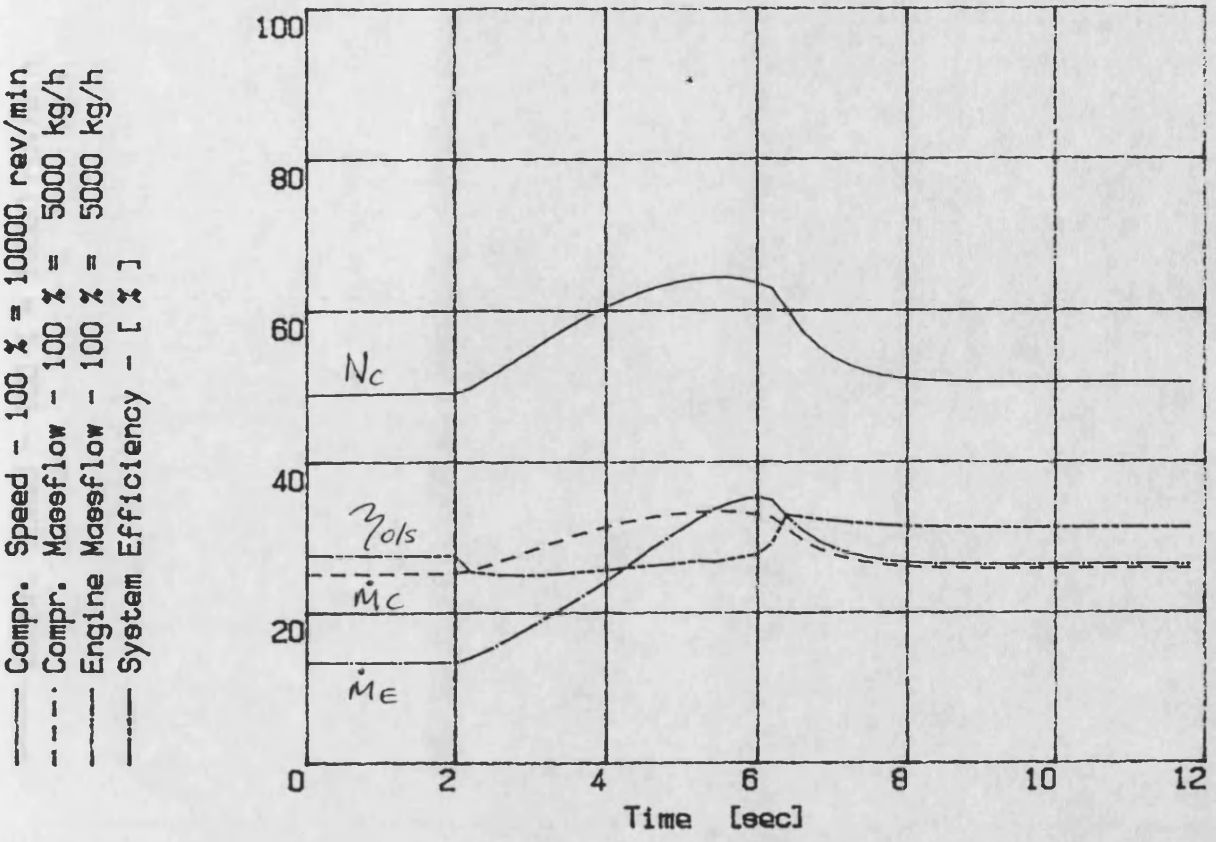

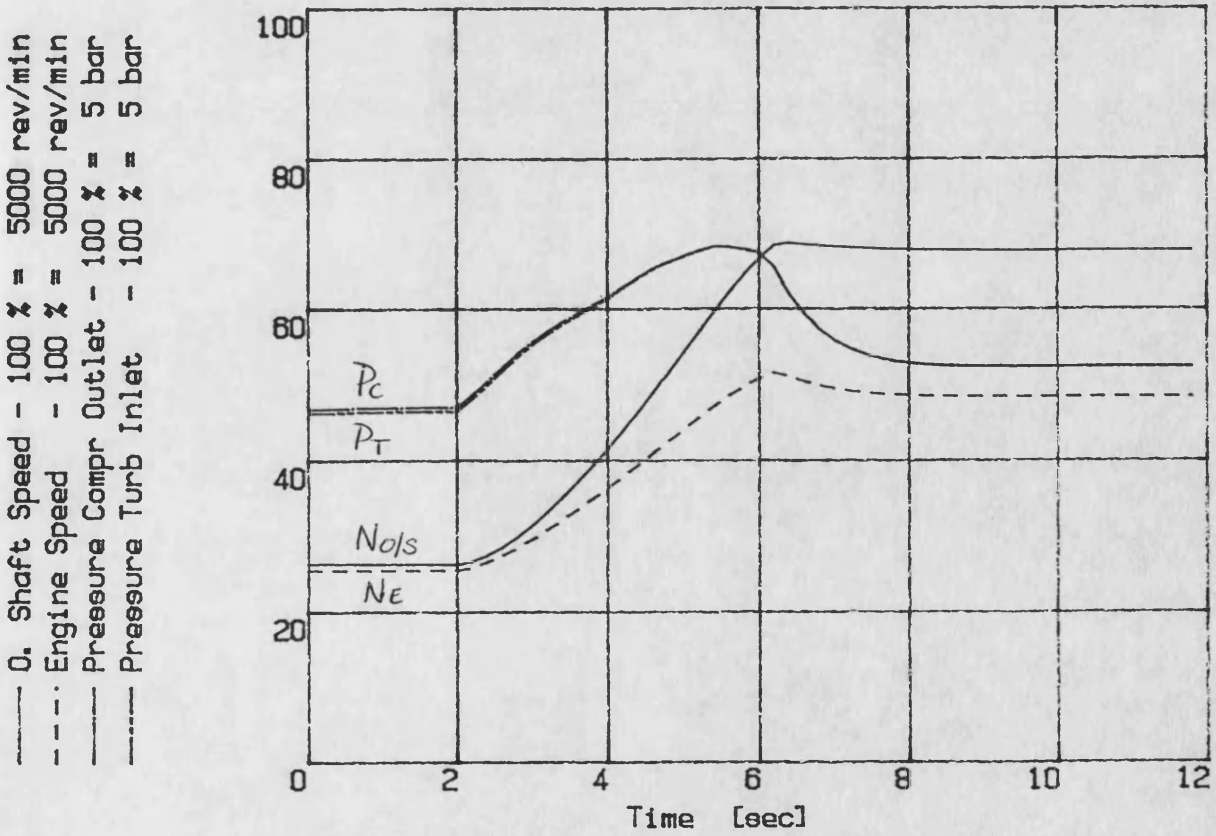

FIG. 7.24 PRED. DEM.STEP RESPONSE,2 ltr CTRL.VOL.

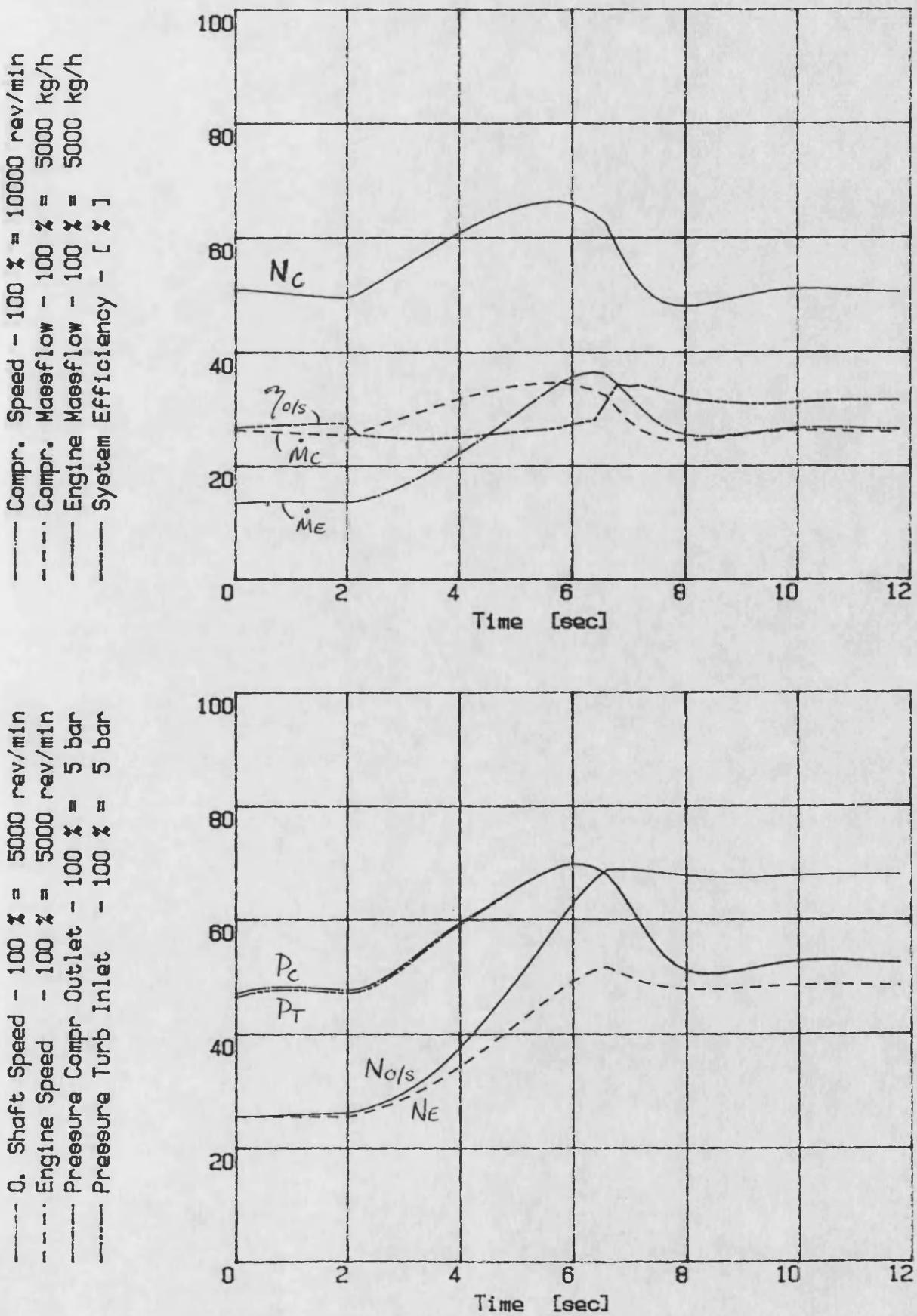

FIG. 7.25 PRED. DEM.STEP RESPONSE,200 ltr CTRL.VOL.

DCE transient simulation - SIMDCE 210289
Demand step 5-10V; Load step 500- 500Nm
Controller: CTLRK2 File: TDSA5.DAT

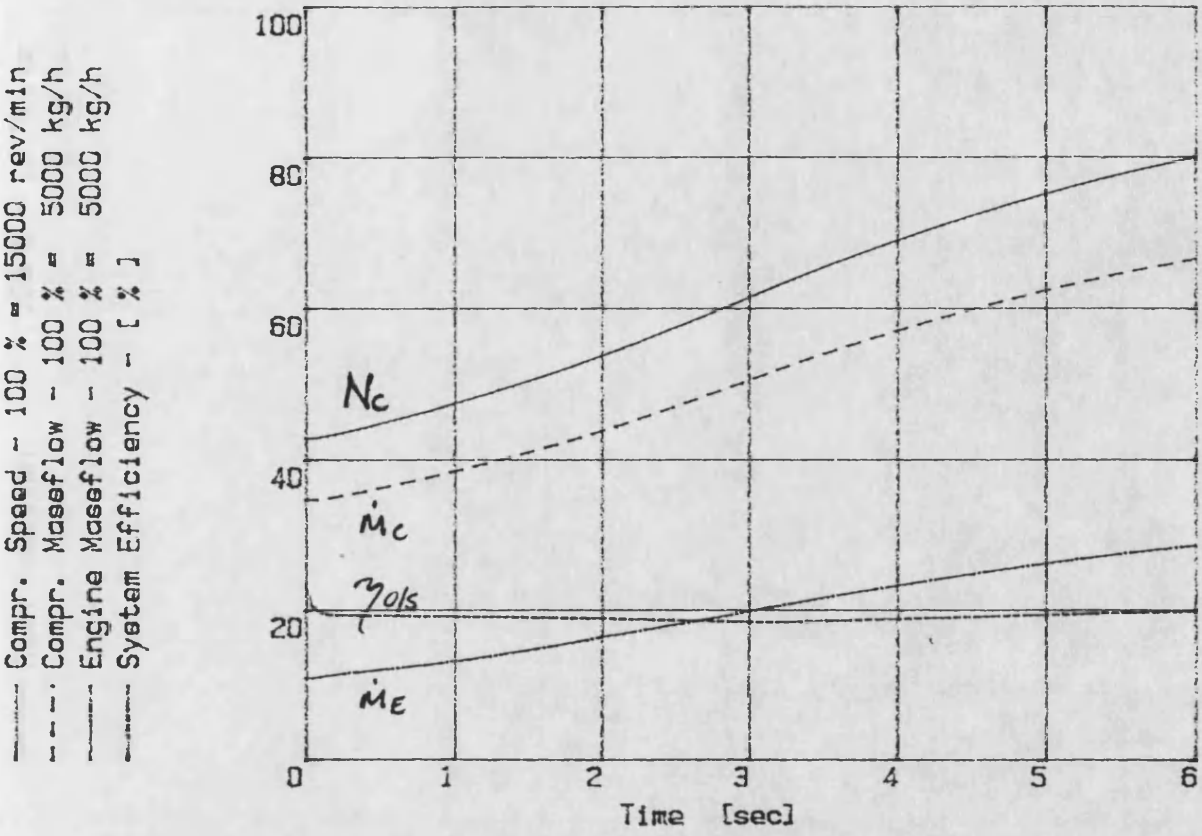

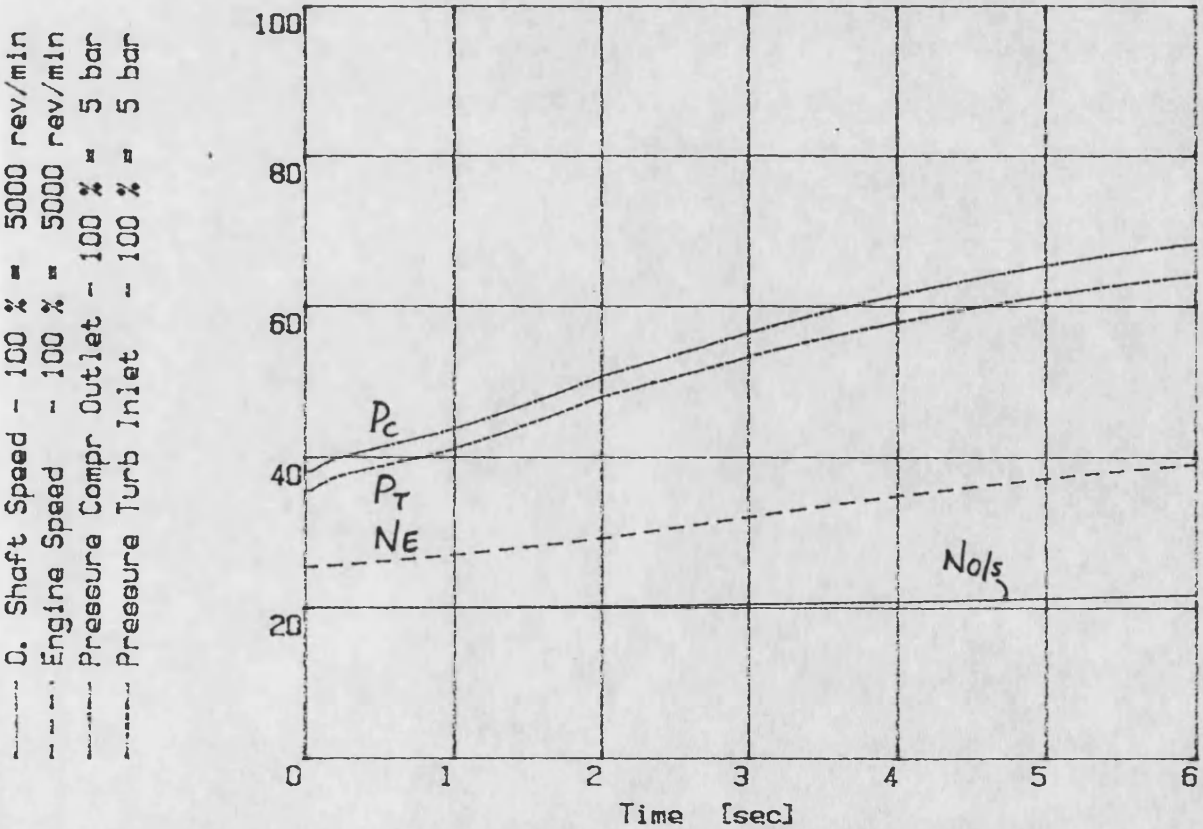

FIG.7.26a PRED.DEM.STEP;HIGH LOAD INERTIA,
(expt-matched VG restriction)

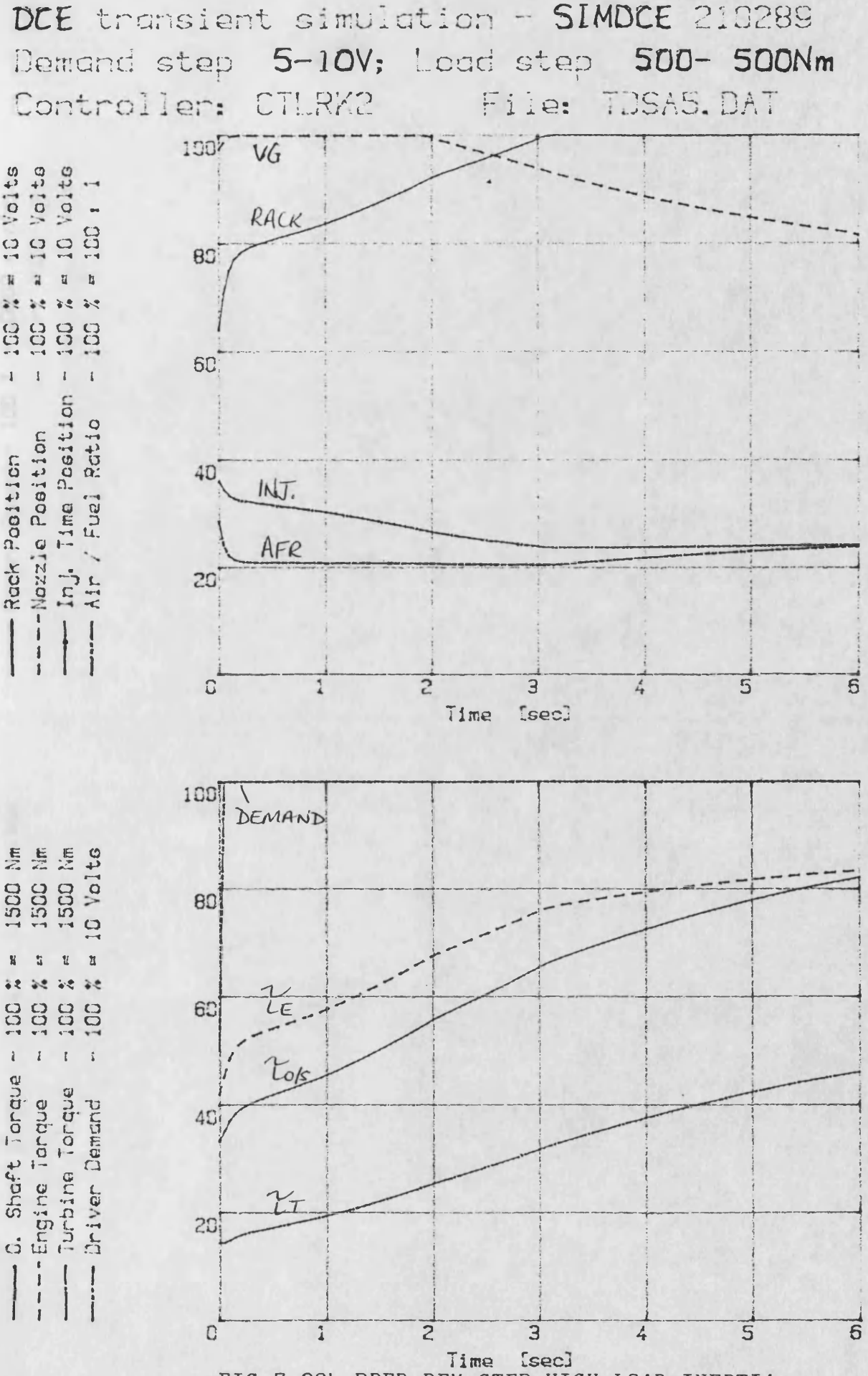

FIG.7.26b PRED.DEM.STEP;HIGH LOAD INERTIA,
(expt-matched VG restriction)

DCE transient simulation - SIMDCE 170289
Demand step 5-10V; Load step 500- 500Nm
CTLRK2: low AFR File: tdsa2.dat

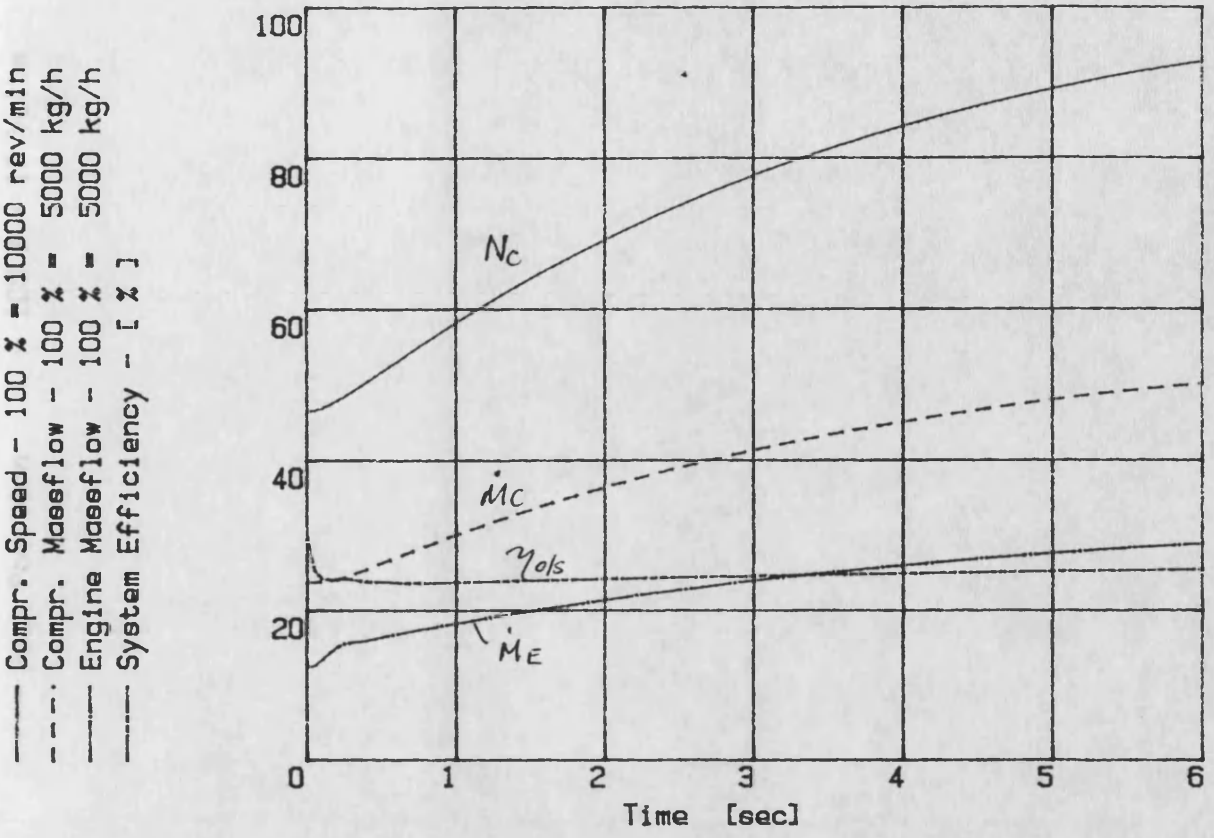

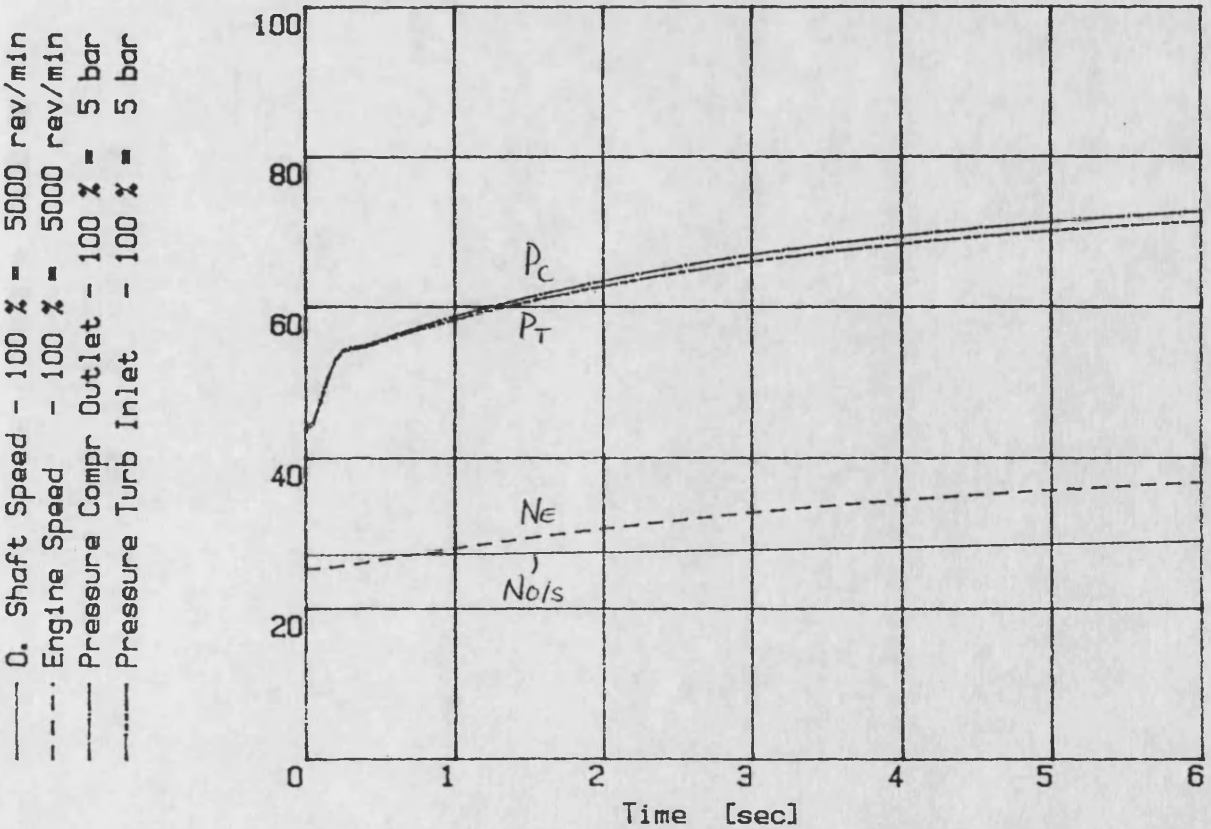

FIG.7.27a PRED.DEM.STEP;HIGH LOAD INERTIA,
(increased VG restriction)

DCE transient simulation - SIMDCE 170289
Demand step 5-10V; Load step 500- 500Nm
low AFR File: tdsa2.dat

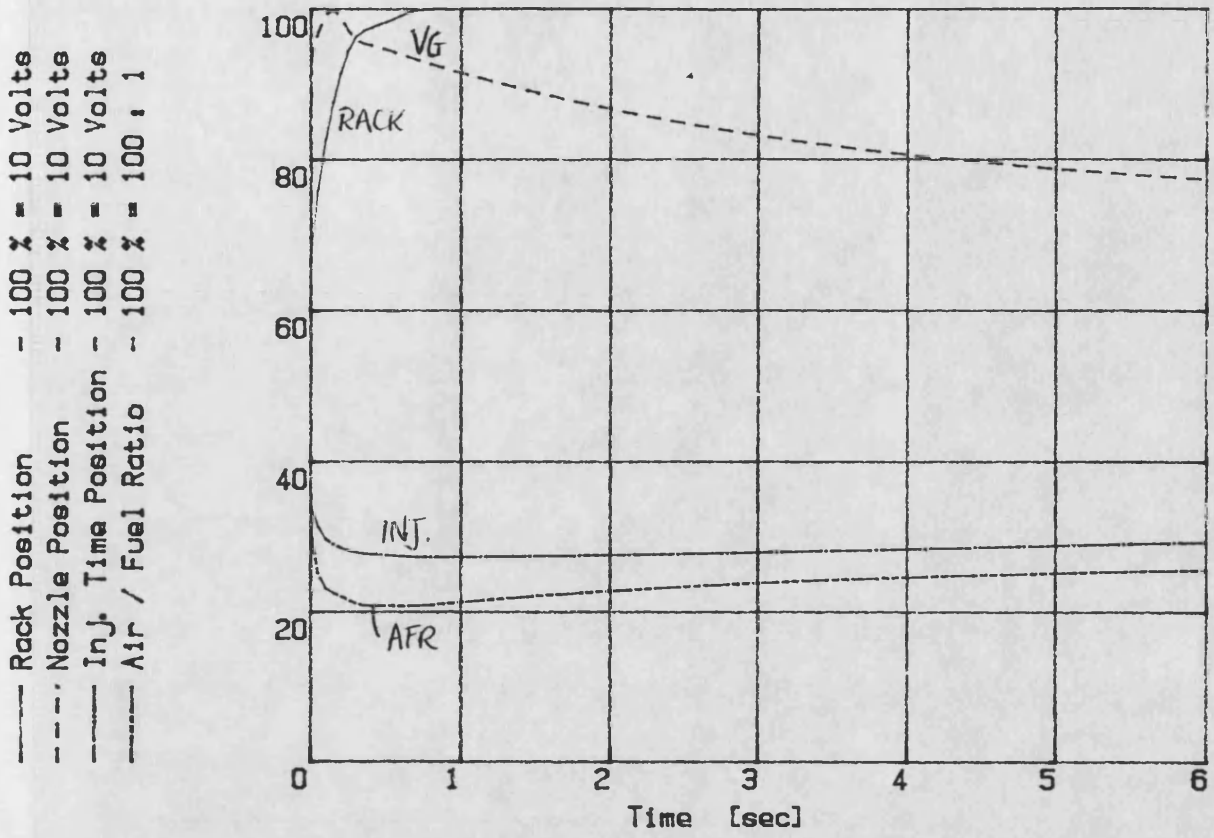

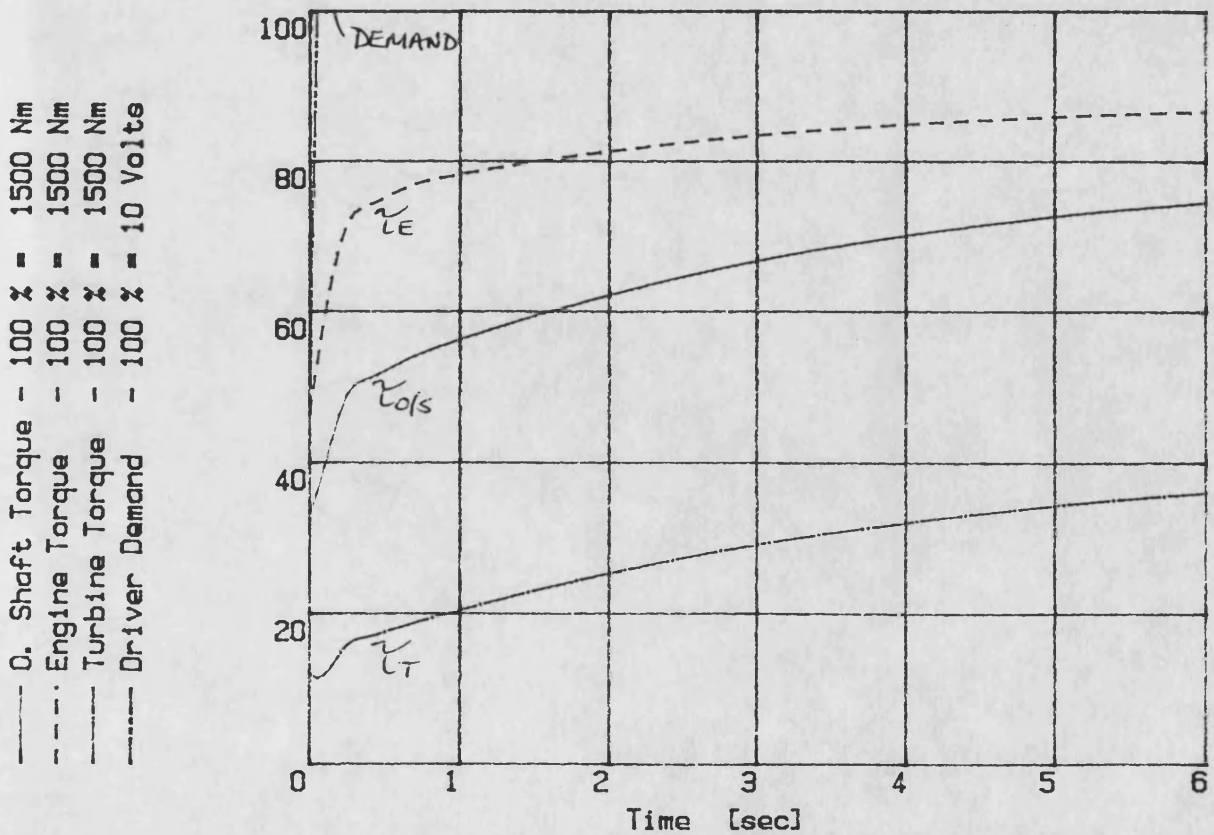

FIG.7.27b PRED.DEM.STEP;HIGH LOAD INERTIA,
(increased VG restriction)

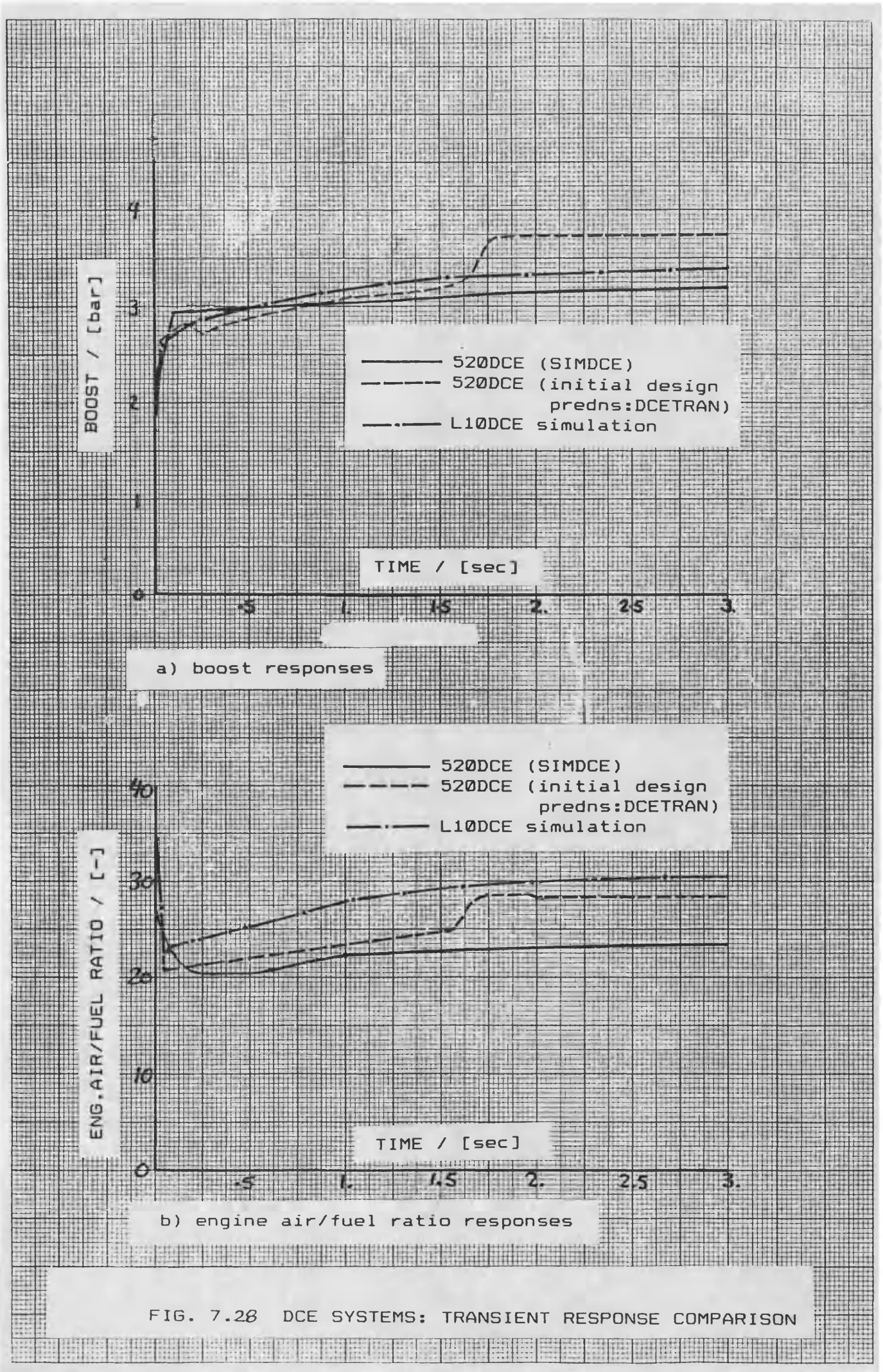

FIG. 7.28 DCE SYSTEMS: TRANSIENT RESPONSE COMPARISON

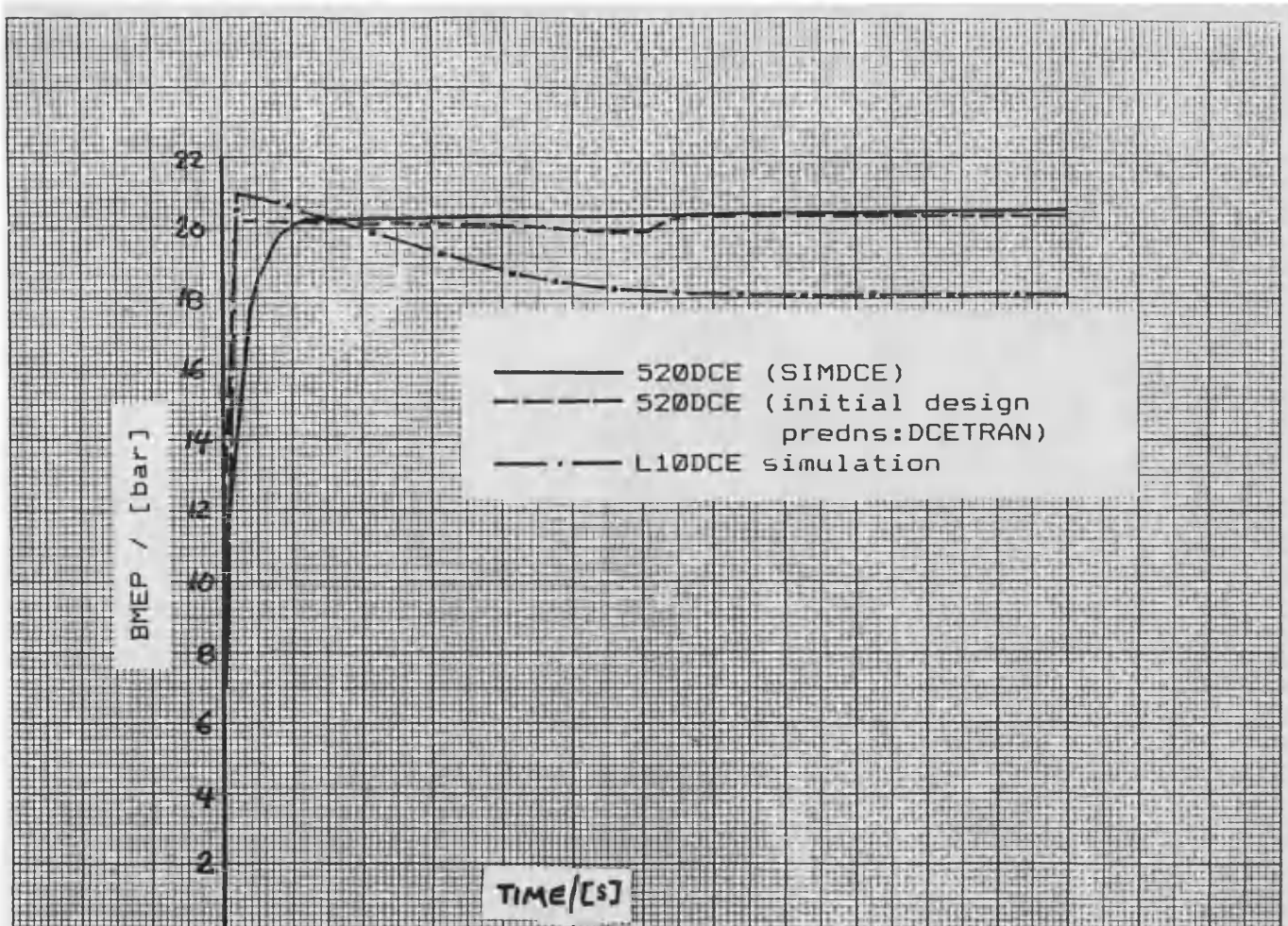

c) engine torque (BMEP) responses

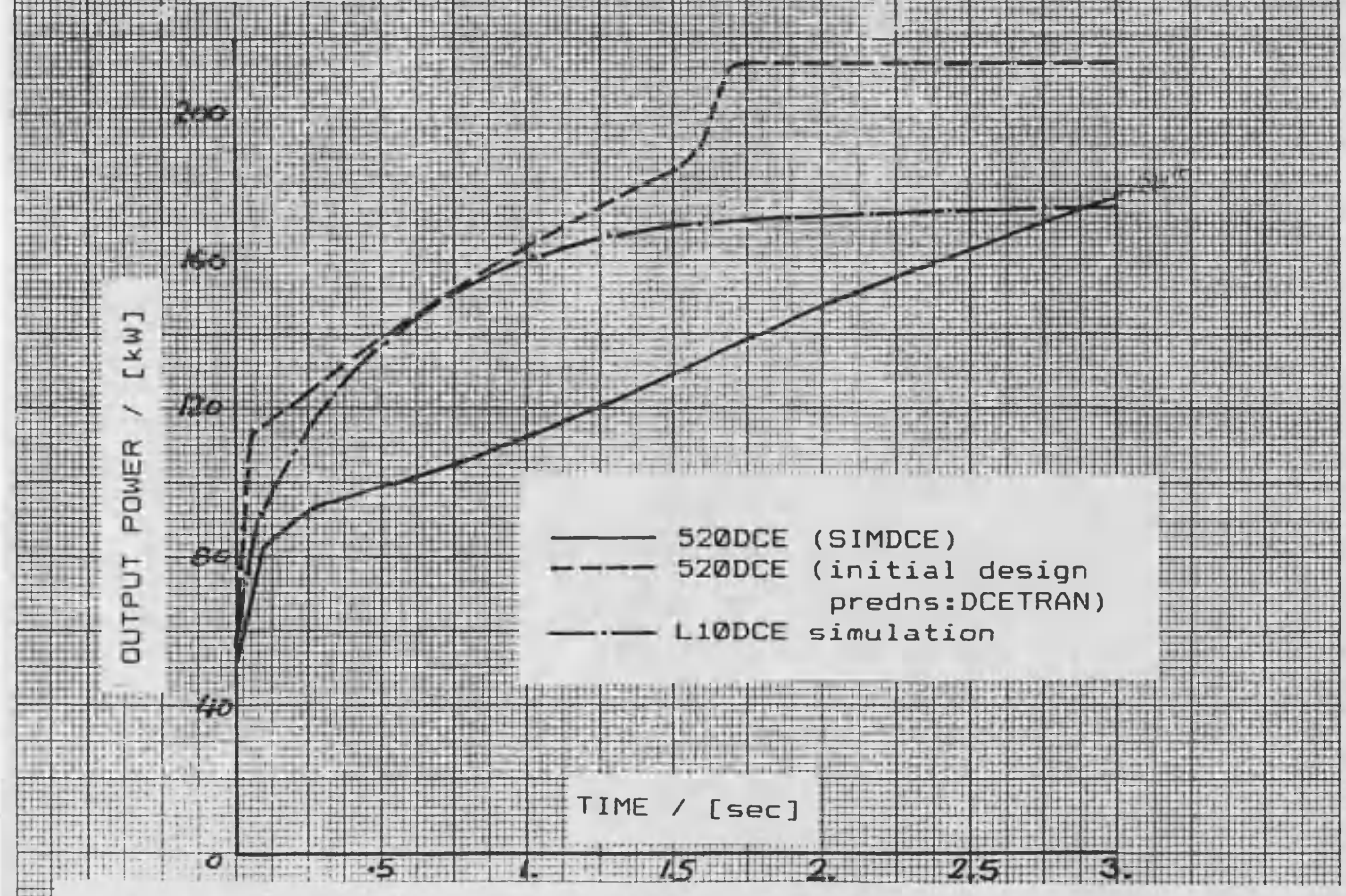

d) output shaft power responses

FIG. 7.28 DCE SYSTEMS: TRANSIENT RESPONSE COMPARISON

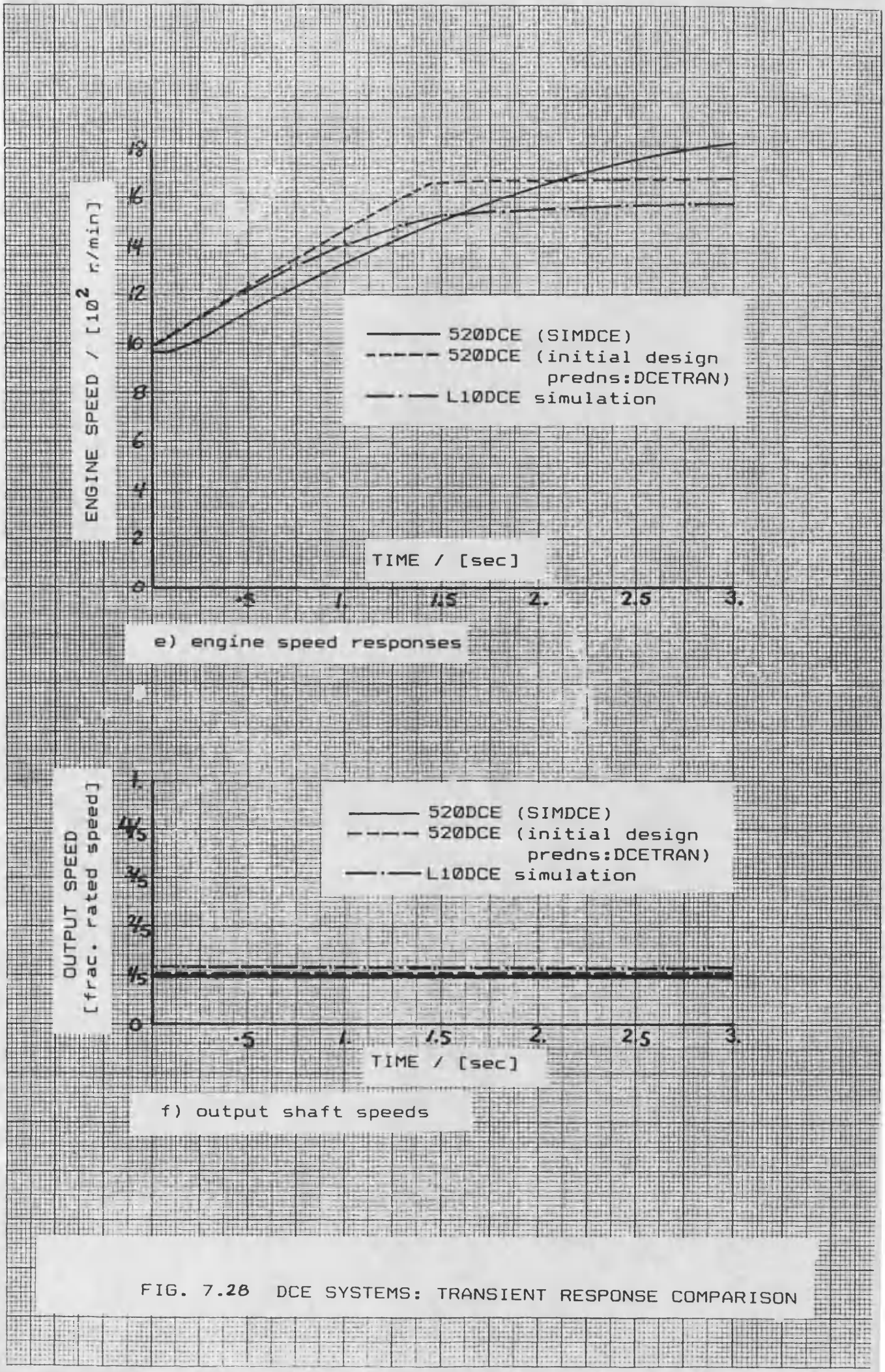

FIG. 7.28 DCE SYSTEMS: TRANSIENT RESPONSE COMPARISON

DCE transient simulation - SIMDCE 170289
Demand step 7- 7V; Load step 500-1000Nm
CTLRK2: low AFR File: LSB2.DAT

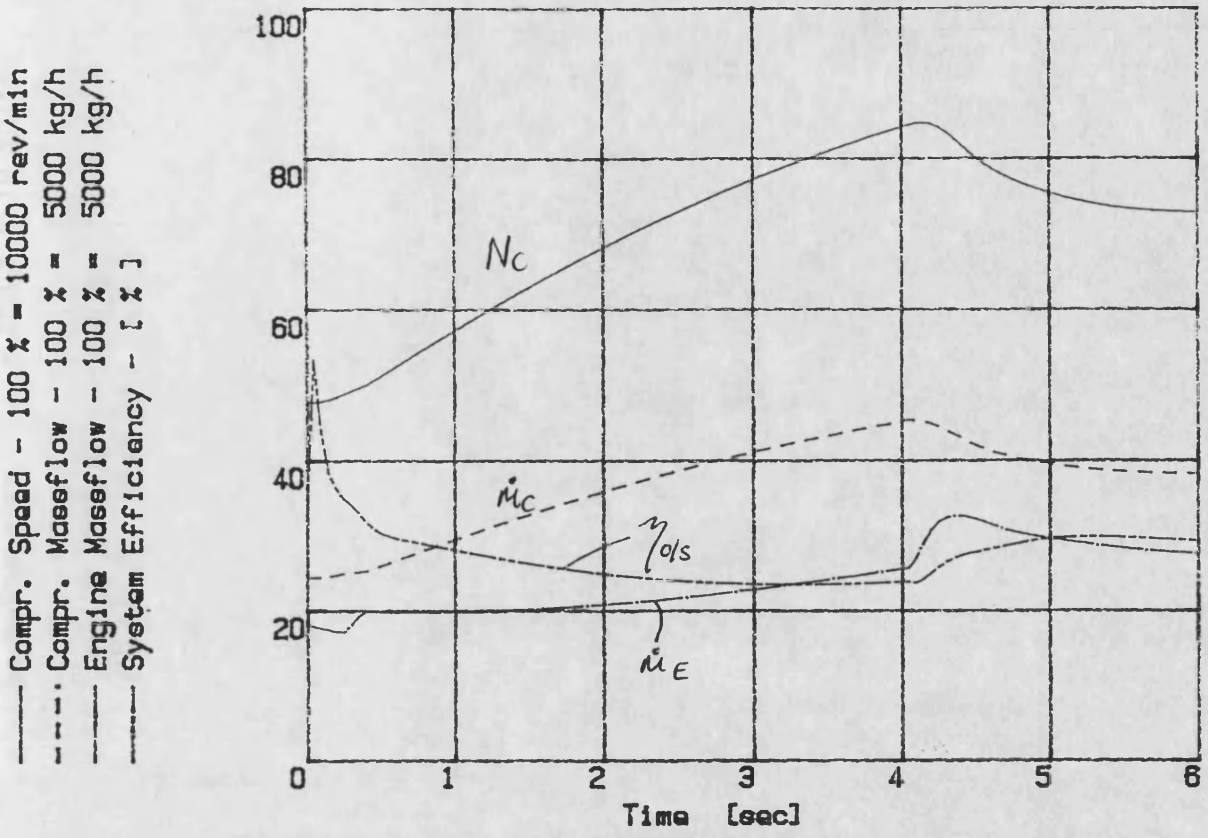

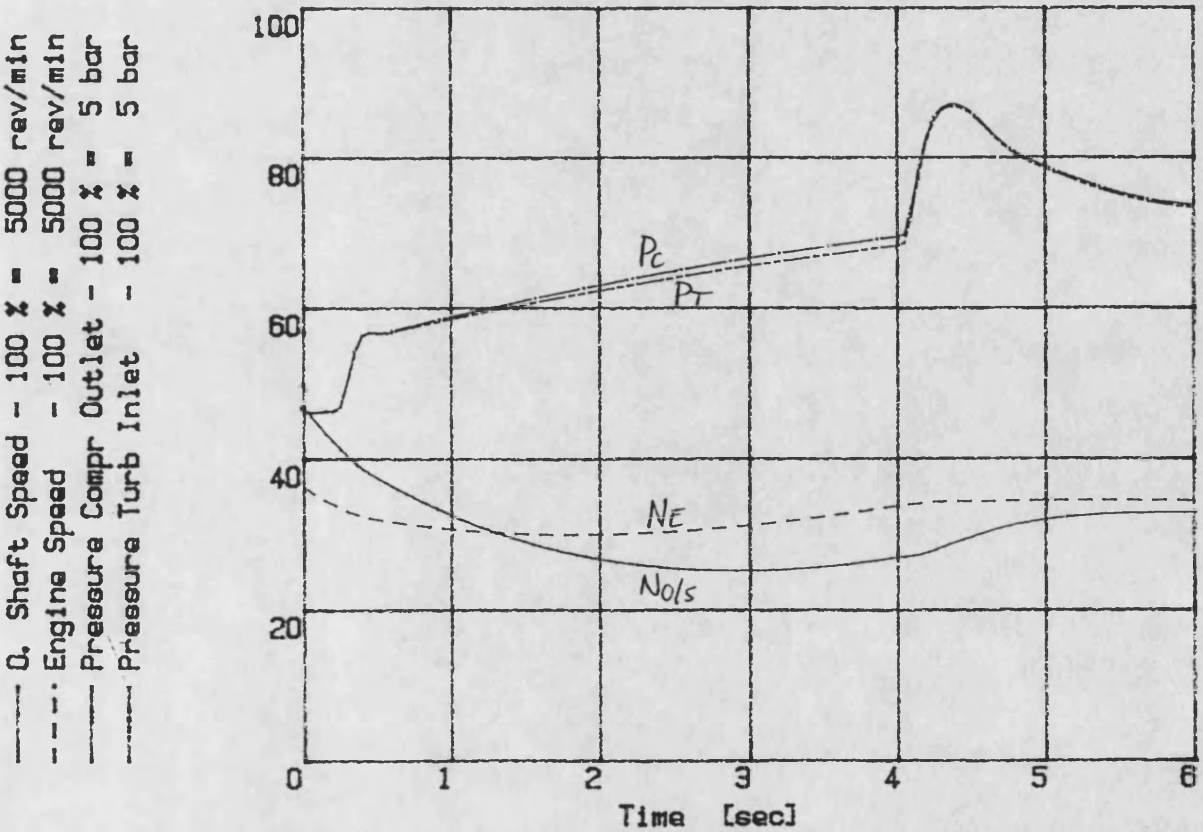

FIG. 7.29a LOAD STEP:ENGINE SPEED DEMAND

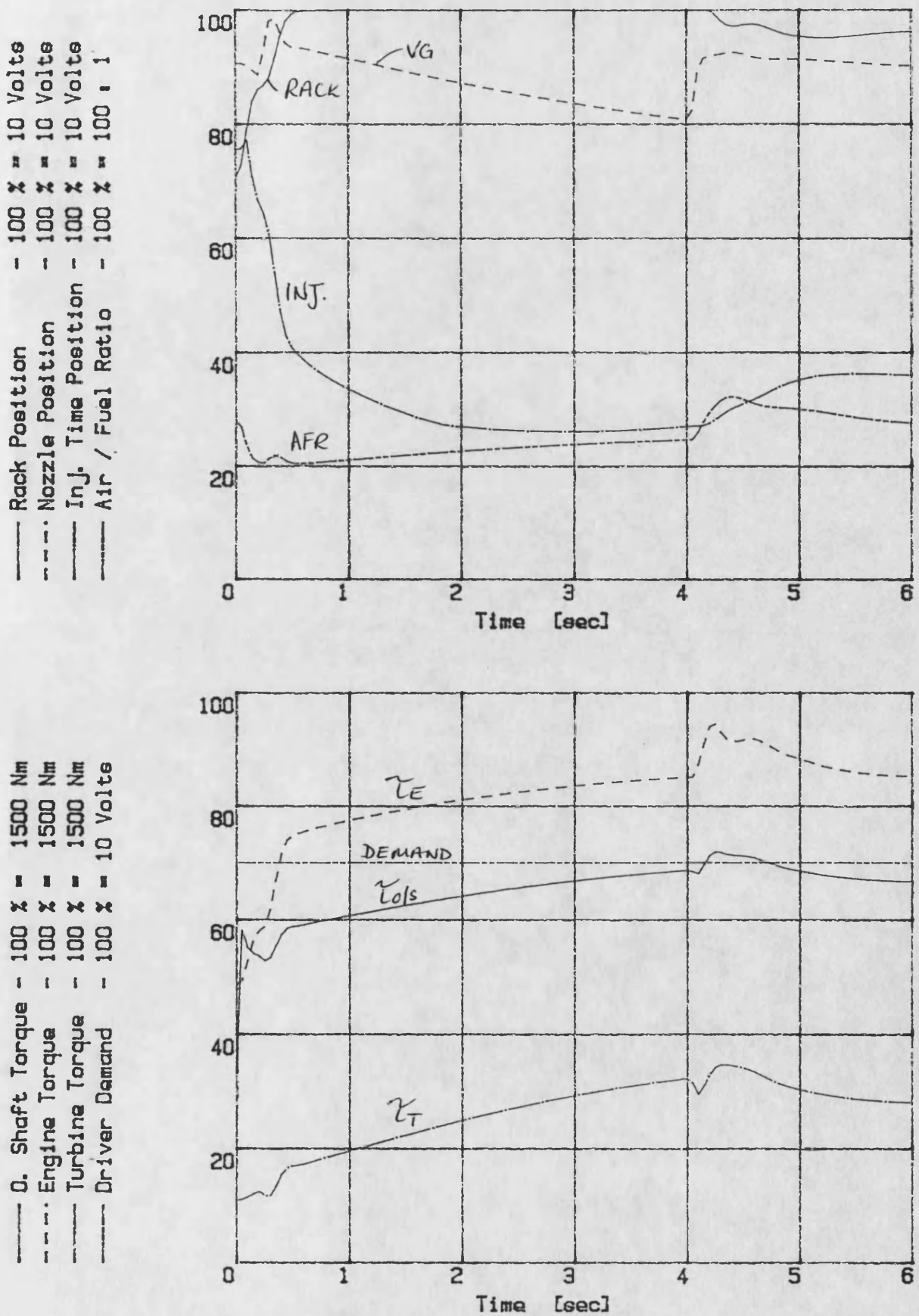

FIG. 7.29b LOAD STEP:ENGINE SPEED DEMAND

DCE transient simulation - SIMDCE 210289
Demand 7V, Load step 500-1000Nm
Controller: CTLRM File: lsb3.dat

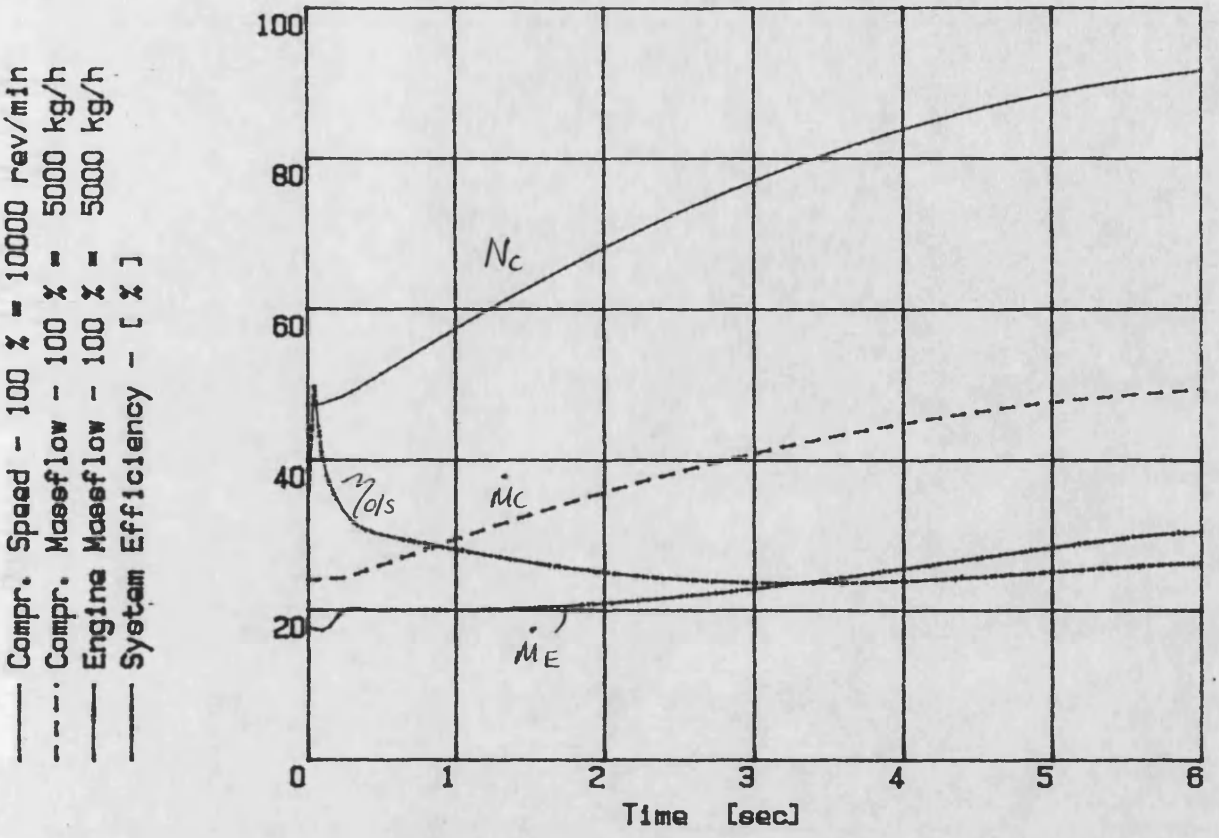

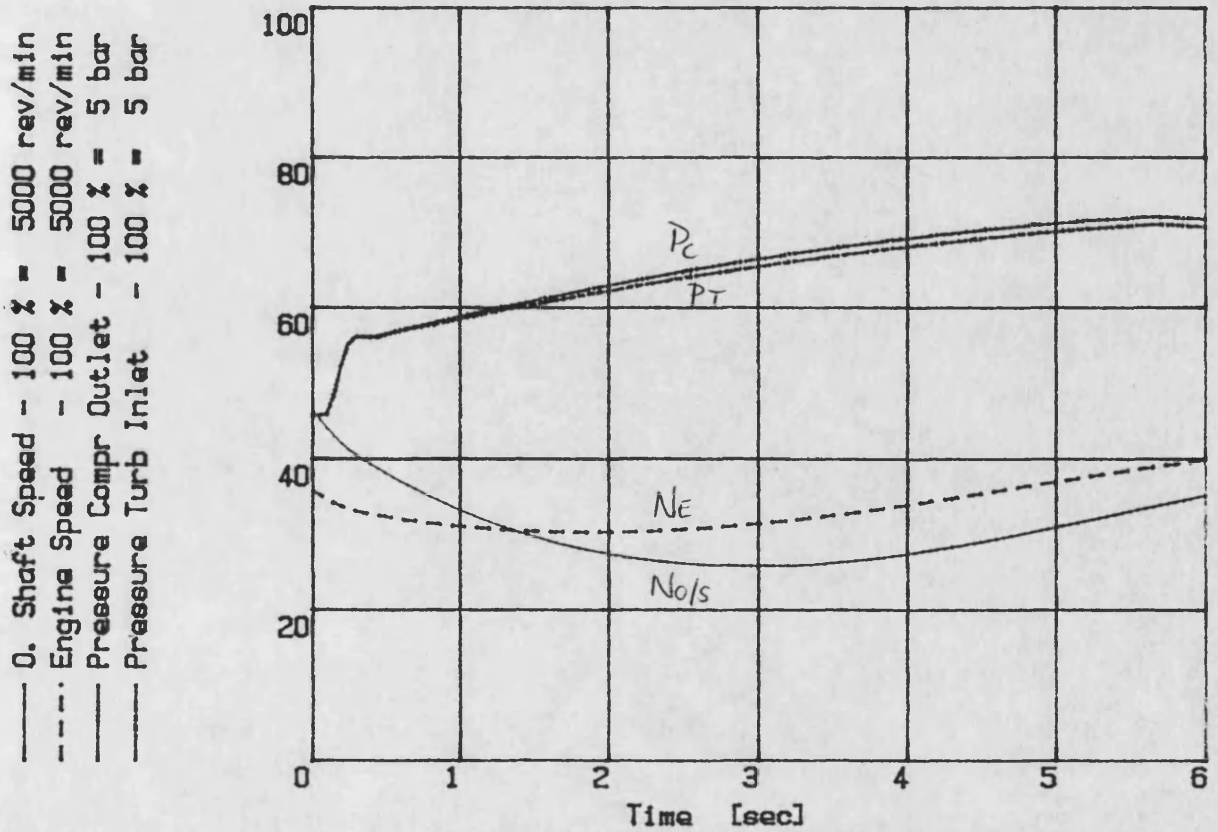

FIG. 7.30a LOAD STEP:O/P SHAFT SPEED DEMAND

DCE transient simulation - Program SIMDCE
Demand 7V, Load step 500-1000Nm
Controller: CTLRM File: lsb3.dat

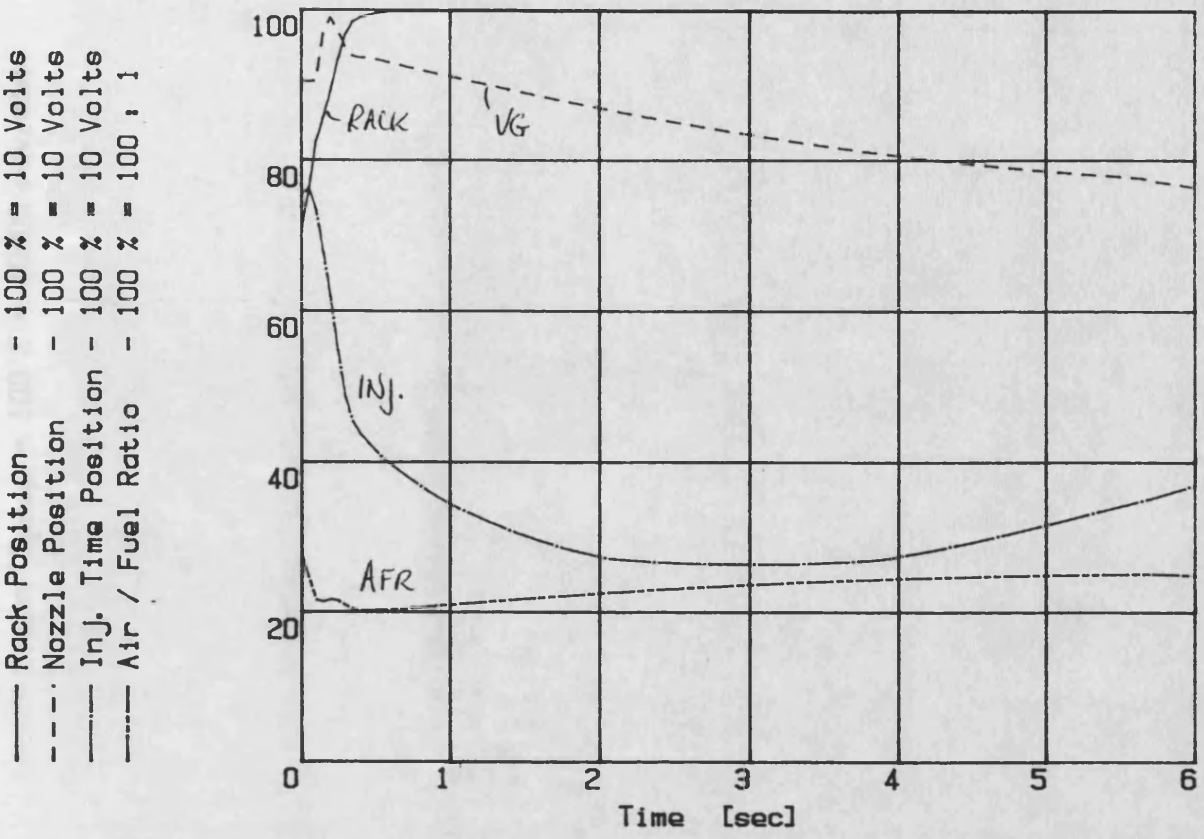

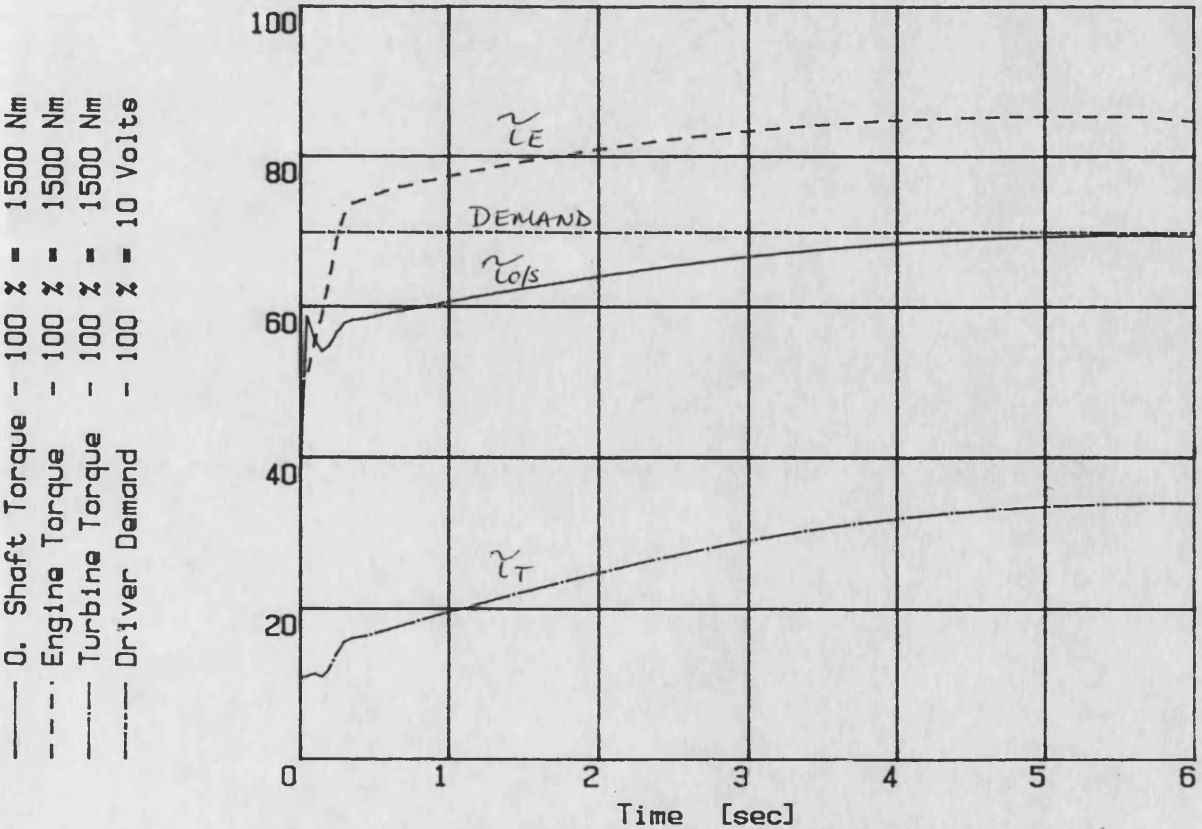

FIG. 7.30b LOAD STEP:O/P SHAFT SPEED DEMAND

DCE transient simulation - SIMDCE 220289
Demand 7V; Load step 500-1000Nm
Controller: CTLRM File: lsb5.dat

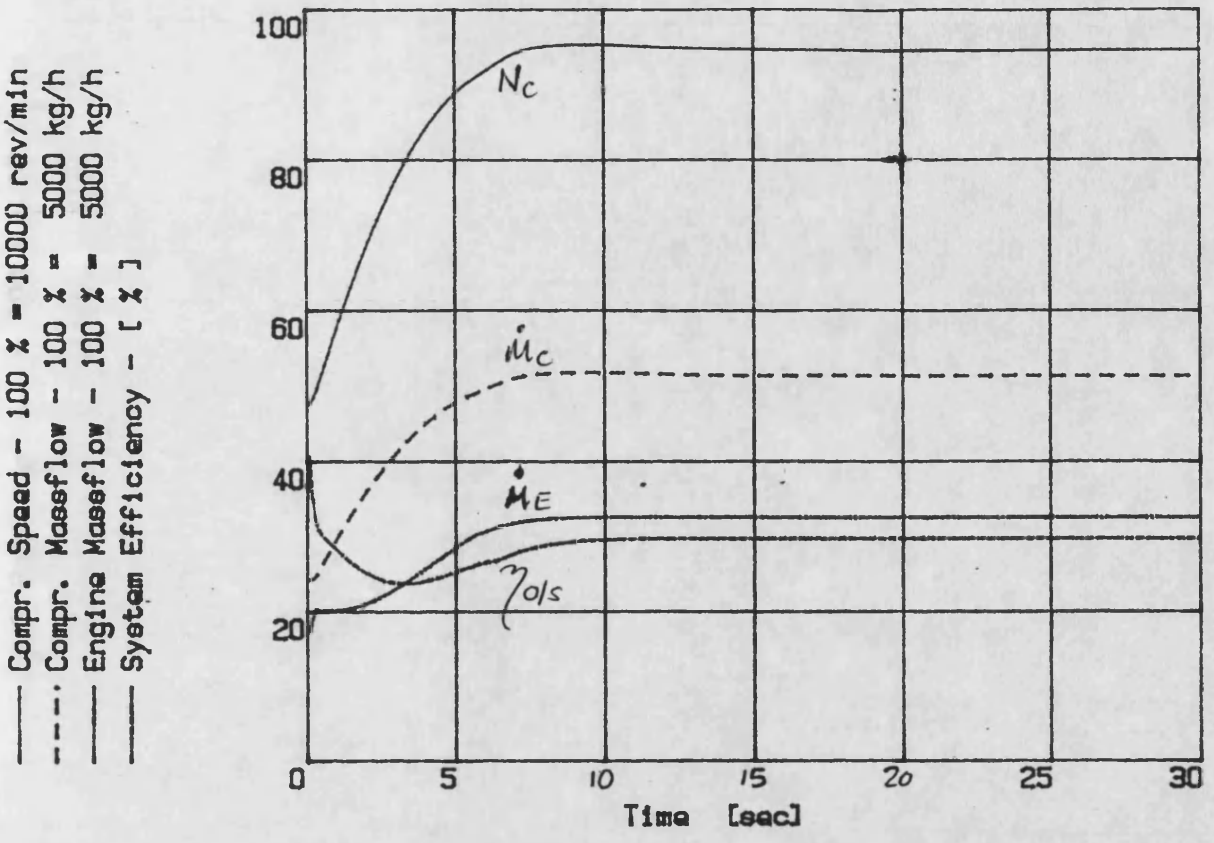

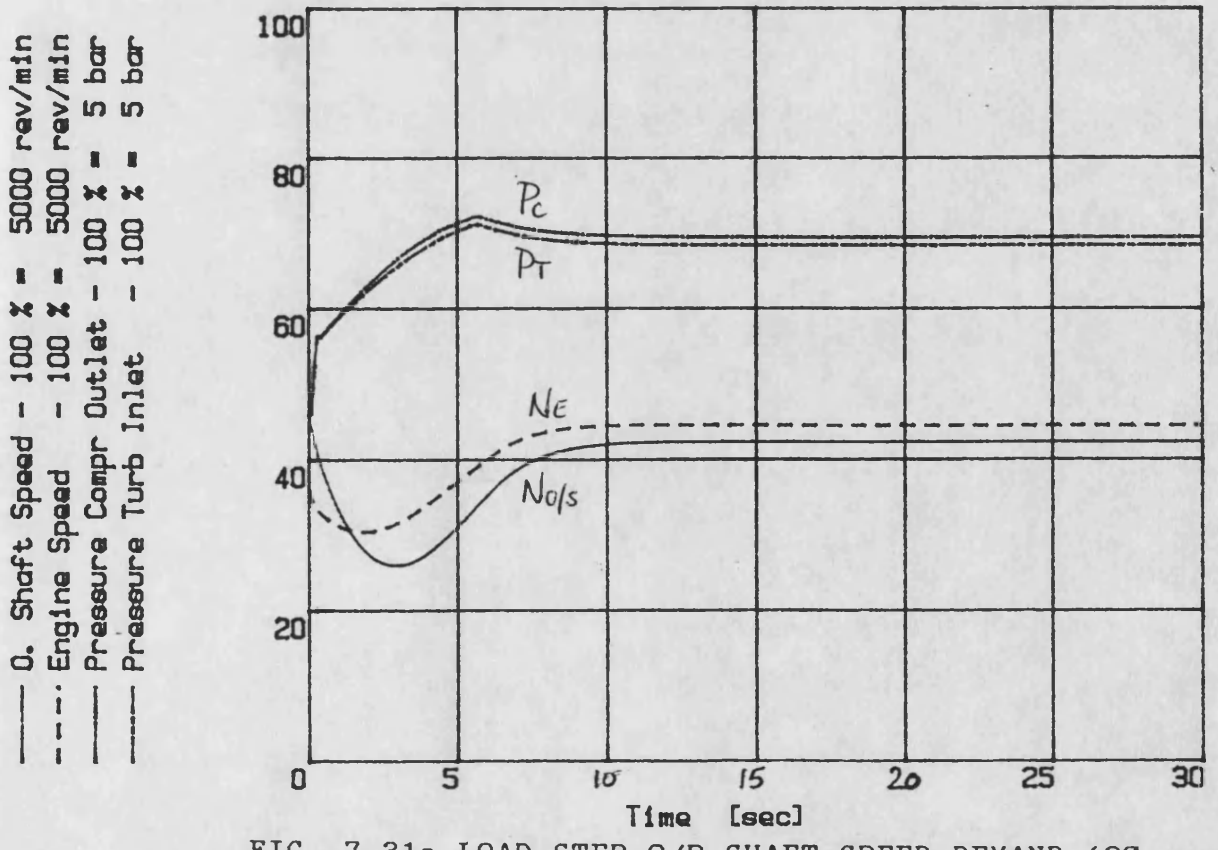

FIG. 7.31a LOAD STEP:O/P SHAFT SPEED DEMAND (30 sec.)

DCE transient simulation - SIMDCE 220289
Demand 7V; Load step 500-1000Nm
Controller: CTLRM File: lsb5.dat

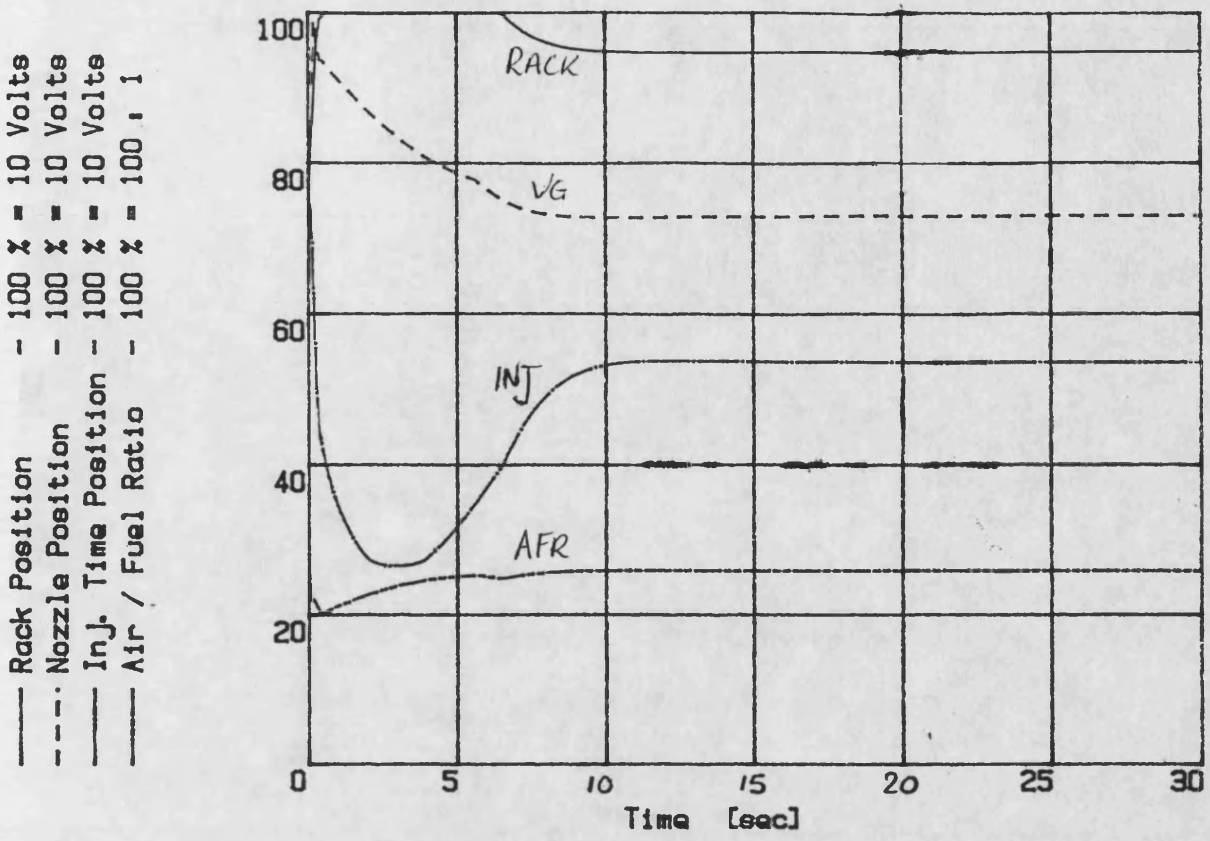

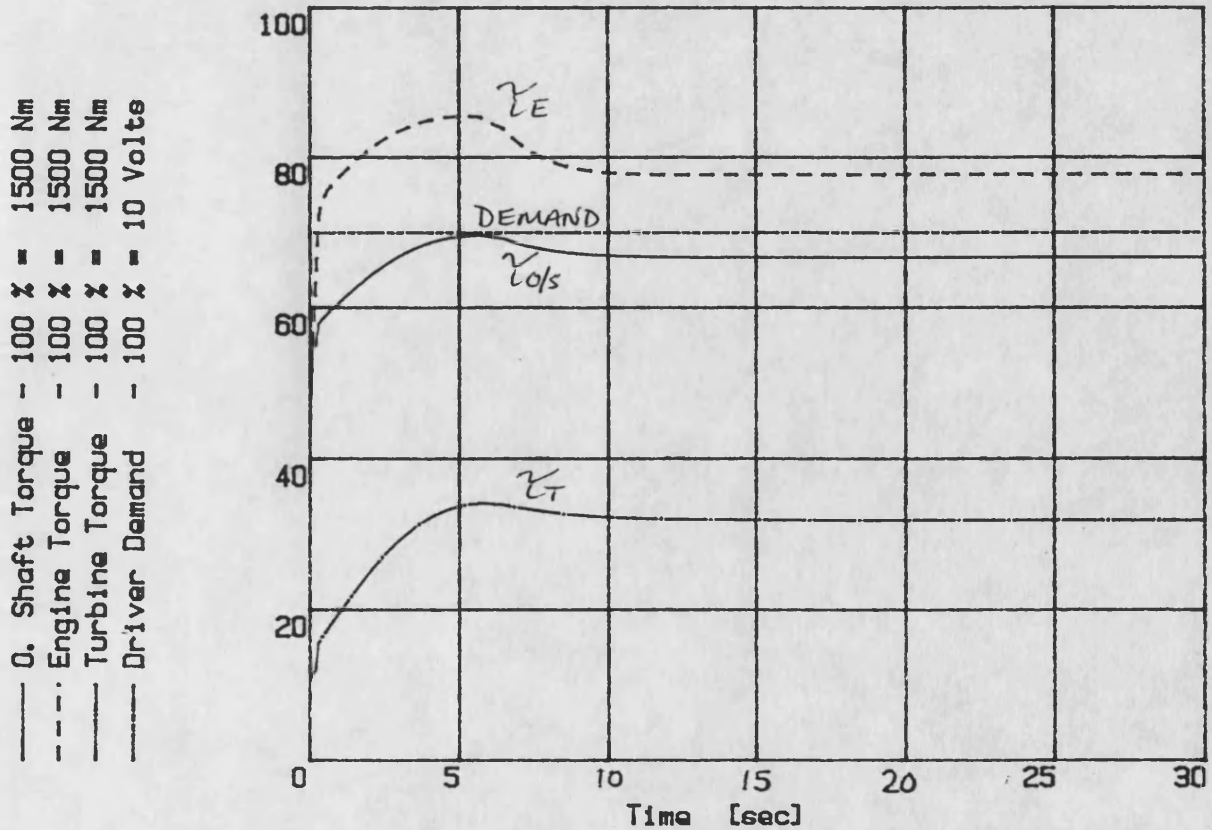

FIG. 7.31b LOAD STEP:O/P SHAFT SPEED DEMAND (30 sec.)

DCE transient simulation - SIMDCE 170289
Demand step 7- 7V; Load step 500-1000Nm
CTLRK3: low AFR File: lsb1.dat

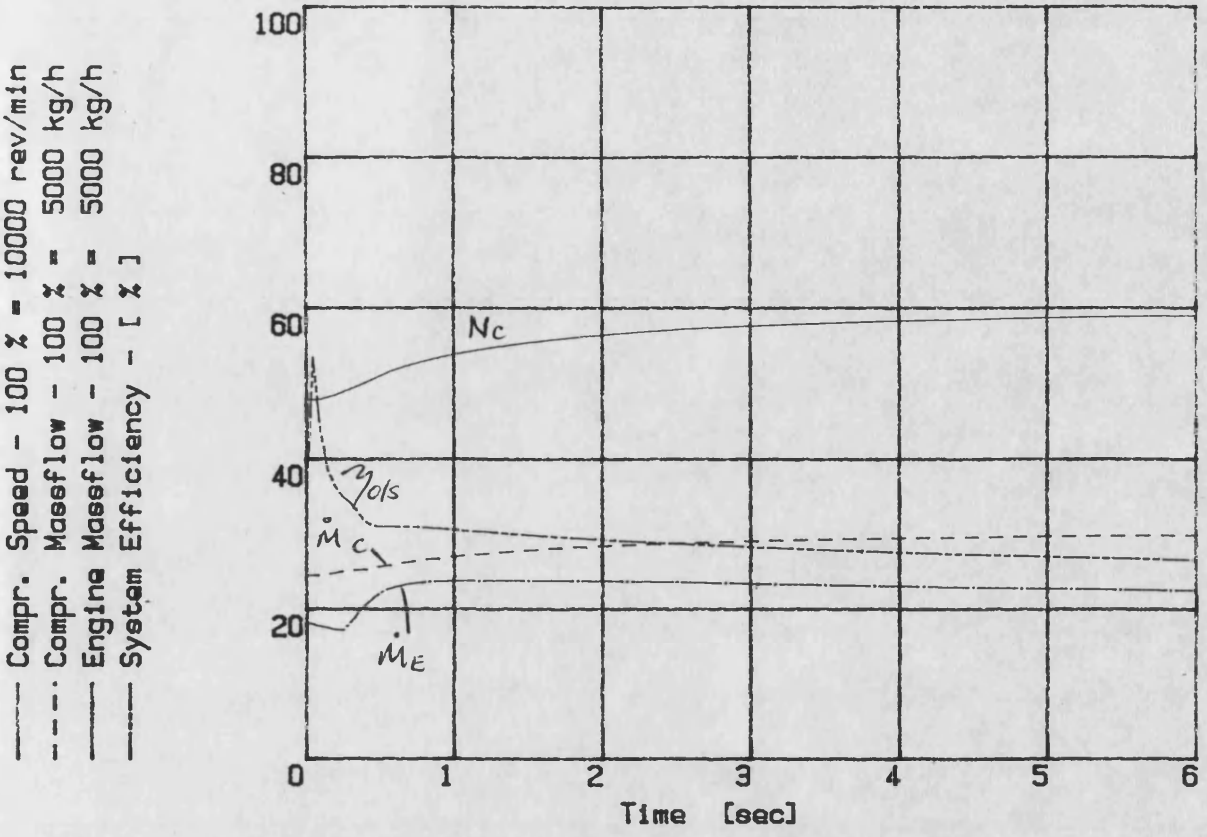

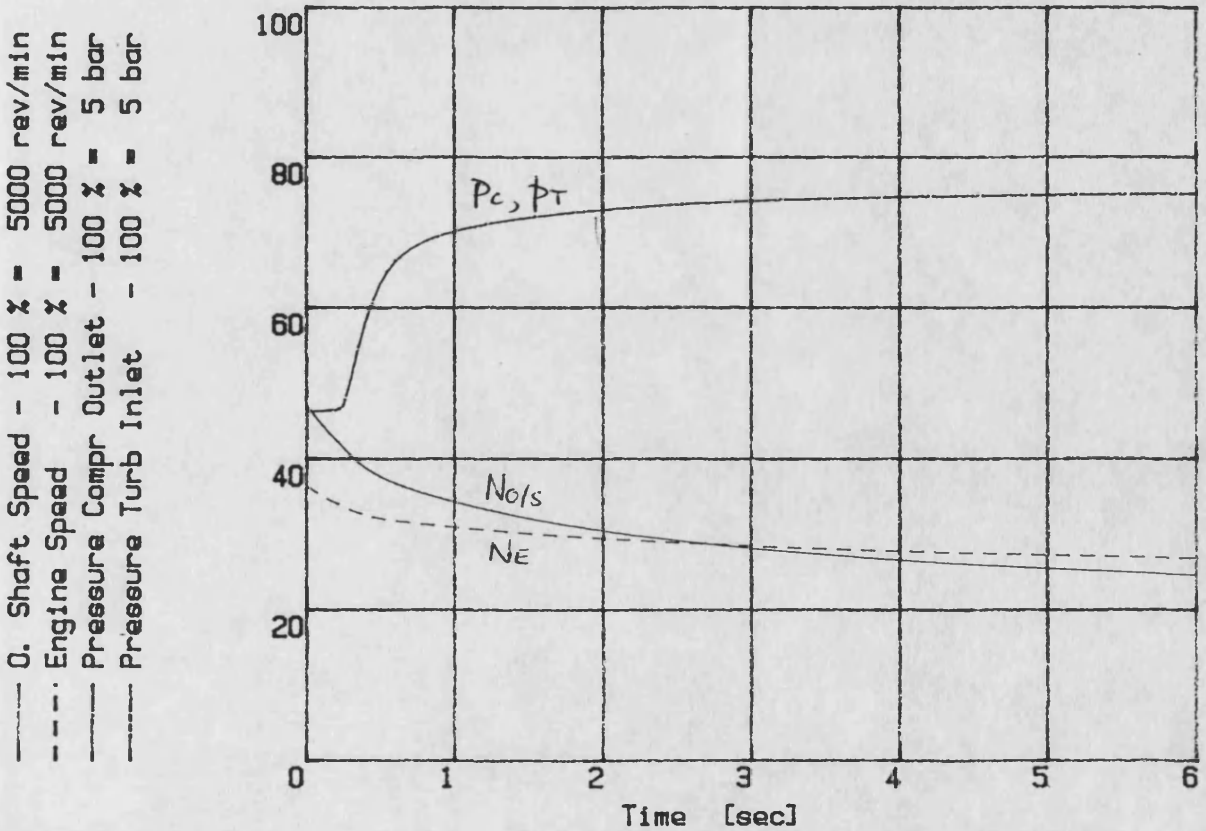

FIG. 7.32a LOAD STEP: MAX.TRANSIENT BOOST

DCE transient simulation - SIMDCE 170289
Demand step 7- 7V; Load step 500-1000Nm
CTLRK3: low AFR File: lsb1.dat

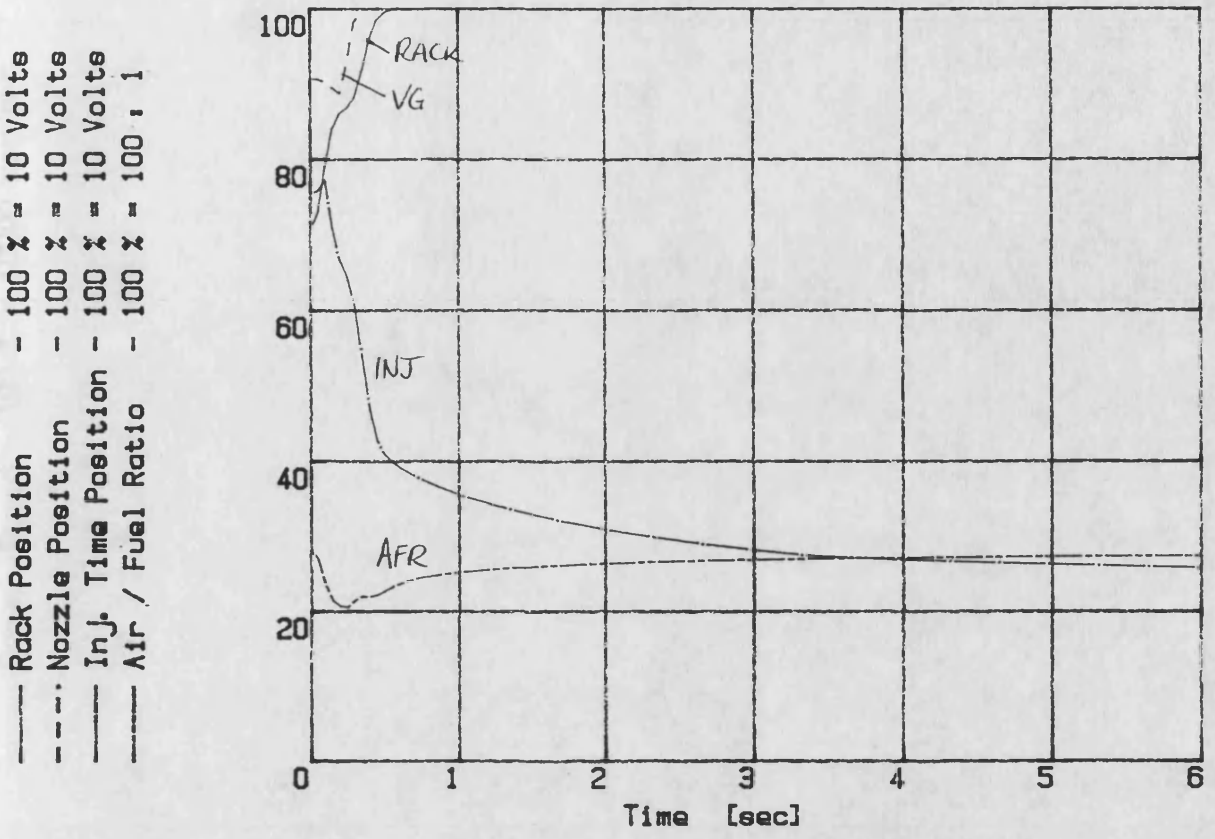

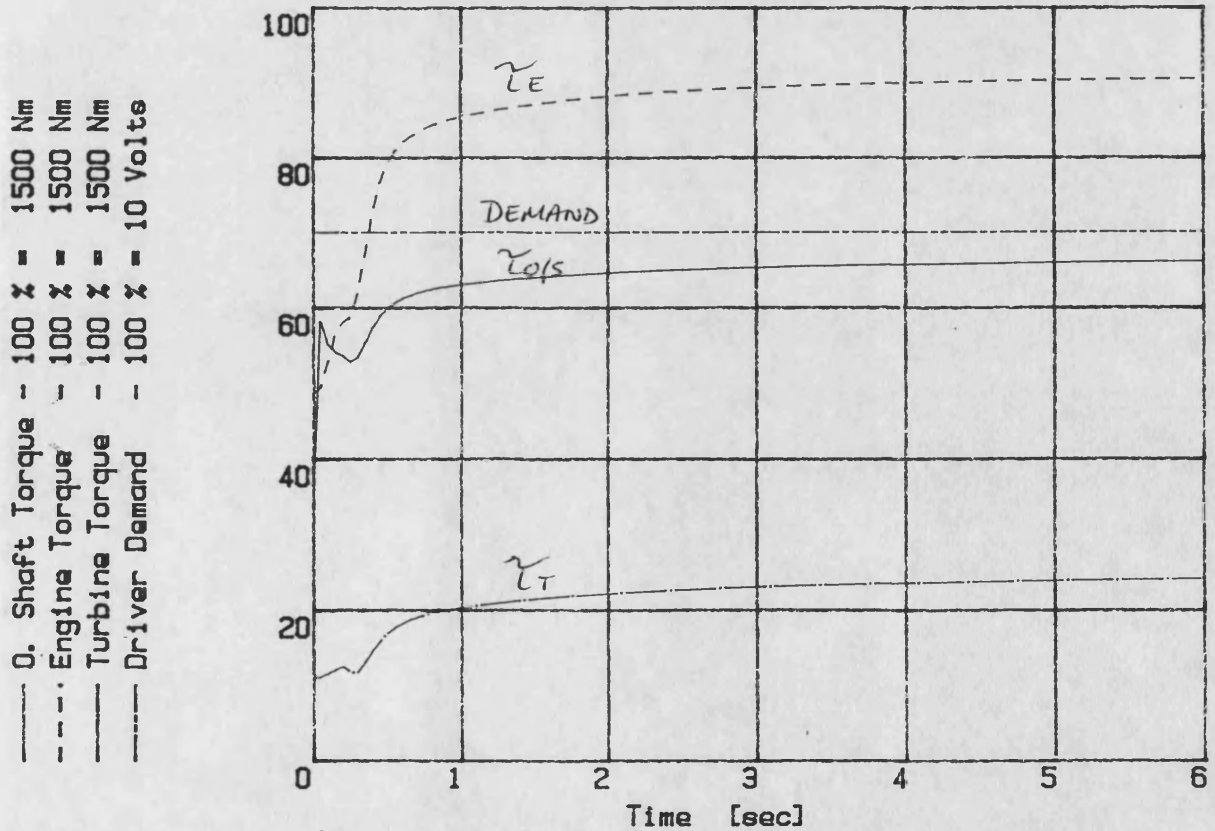

FIG. 7.32b LOAD STEP: MAX.TRANSIENT BOOST

DCE transient simulation - SIMDCE 170289
Demand step 5-10V; Load step 500- 500Nm
CTLRK3: low AFR File: tdsa3.dat

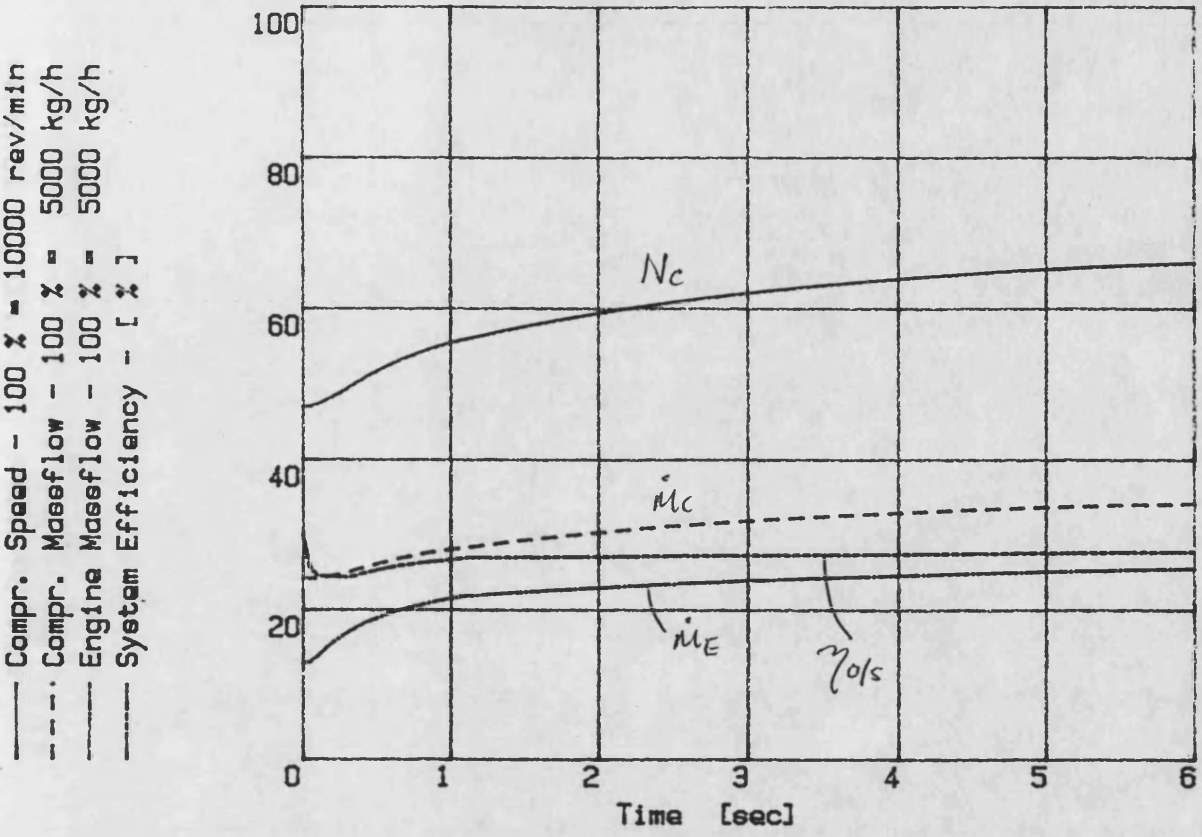

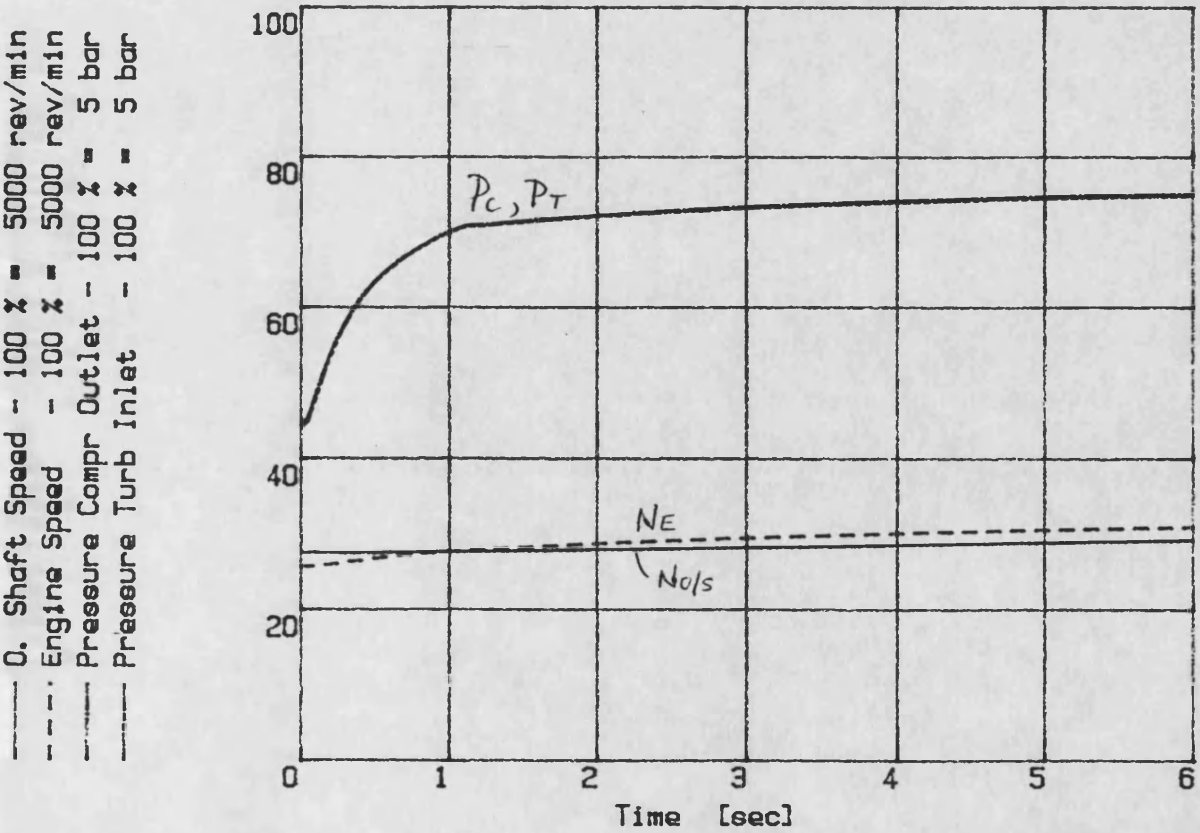

FIG. 7.33a DEMAND STEP: MAX.TRANSIENT BOOST

DCE transient simulation - SIMDCE 170289
Demand step 5-10V; Load step 500- 500Nm
CTLRK3: low AFR File: tdsa3.dat

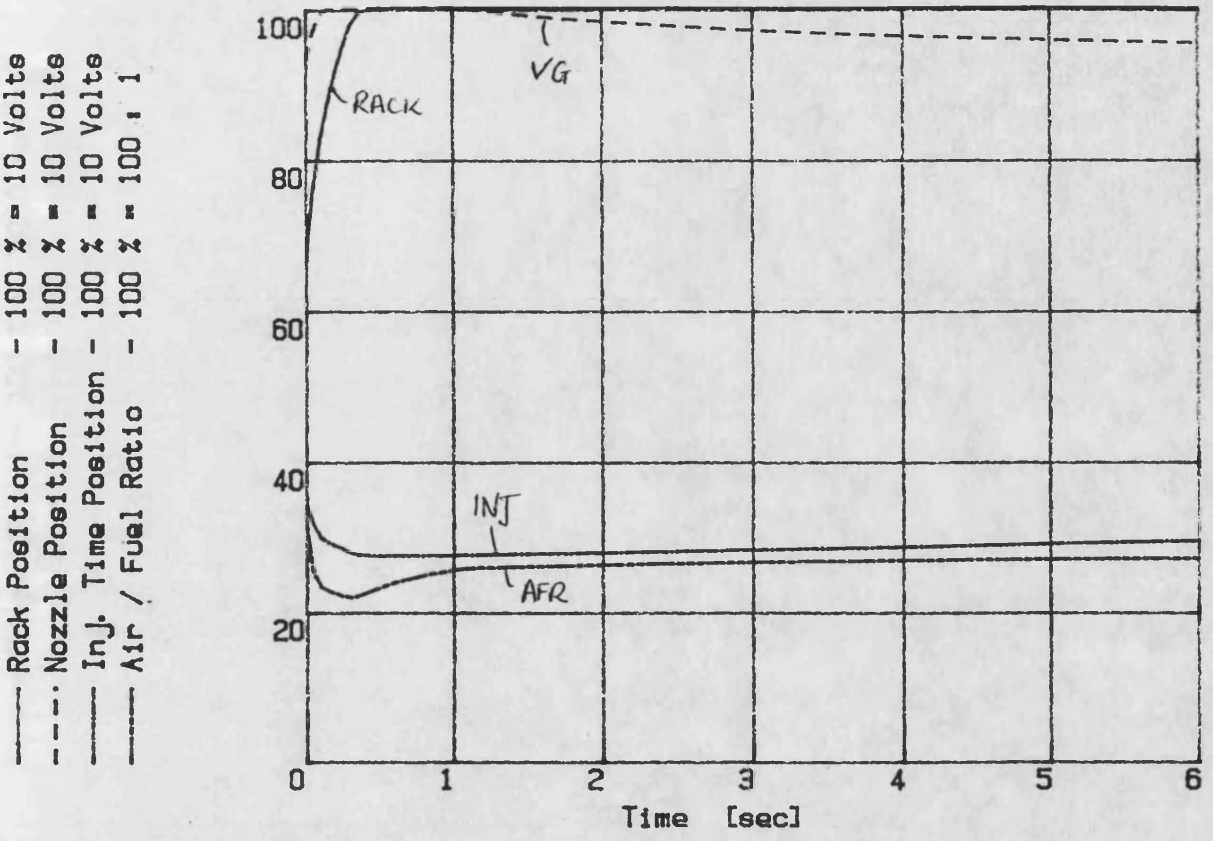

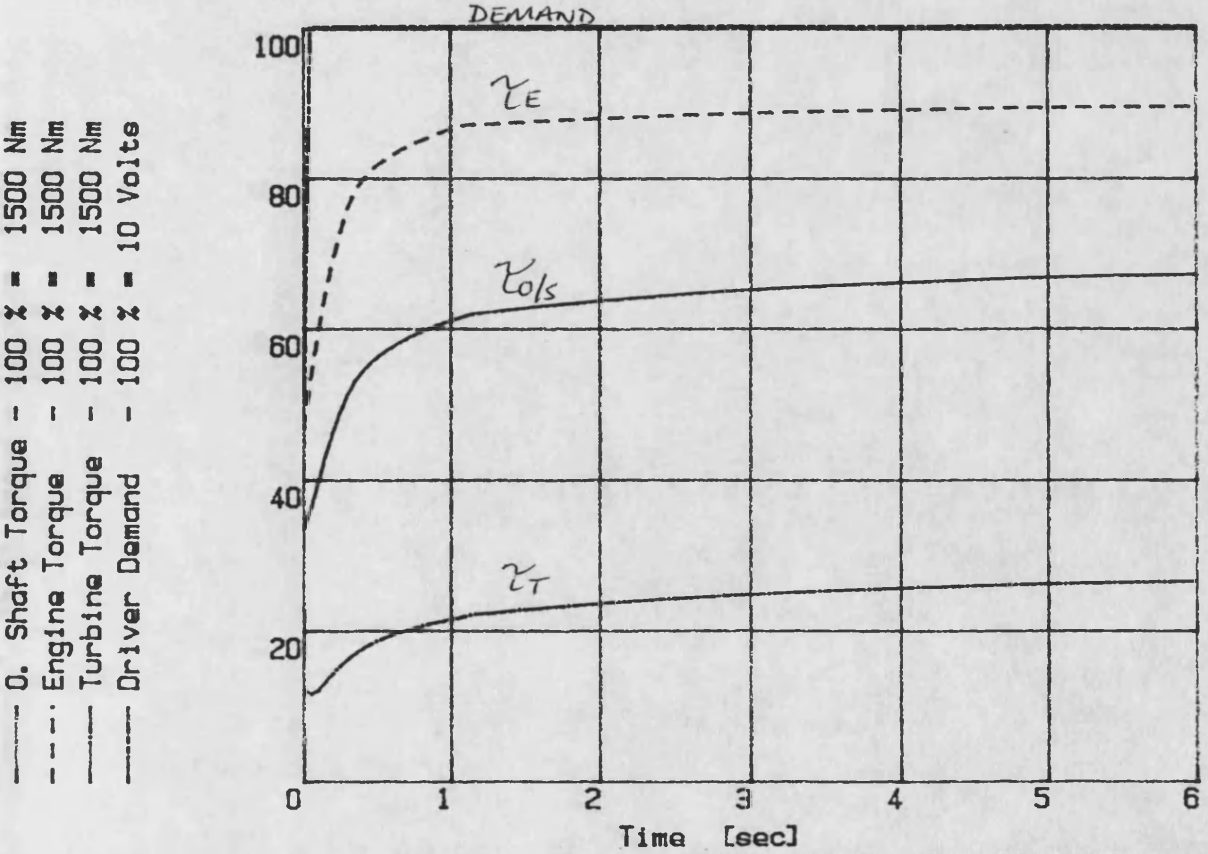

FIG. 7.33b DEMAND STEP: MAX.TRANSIENT BOOST

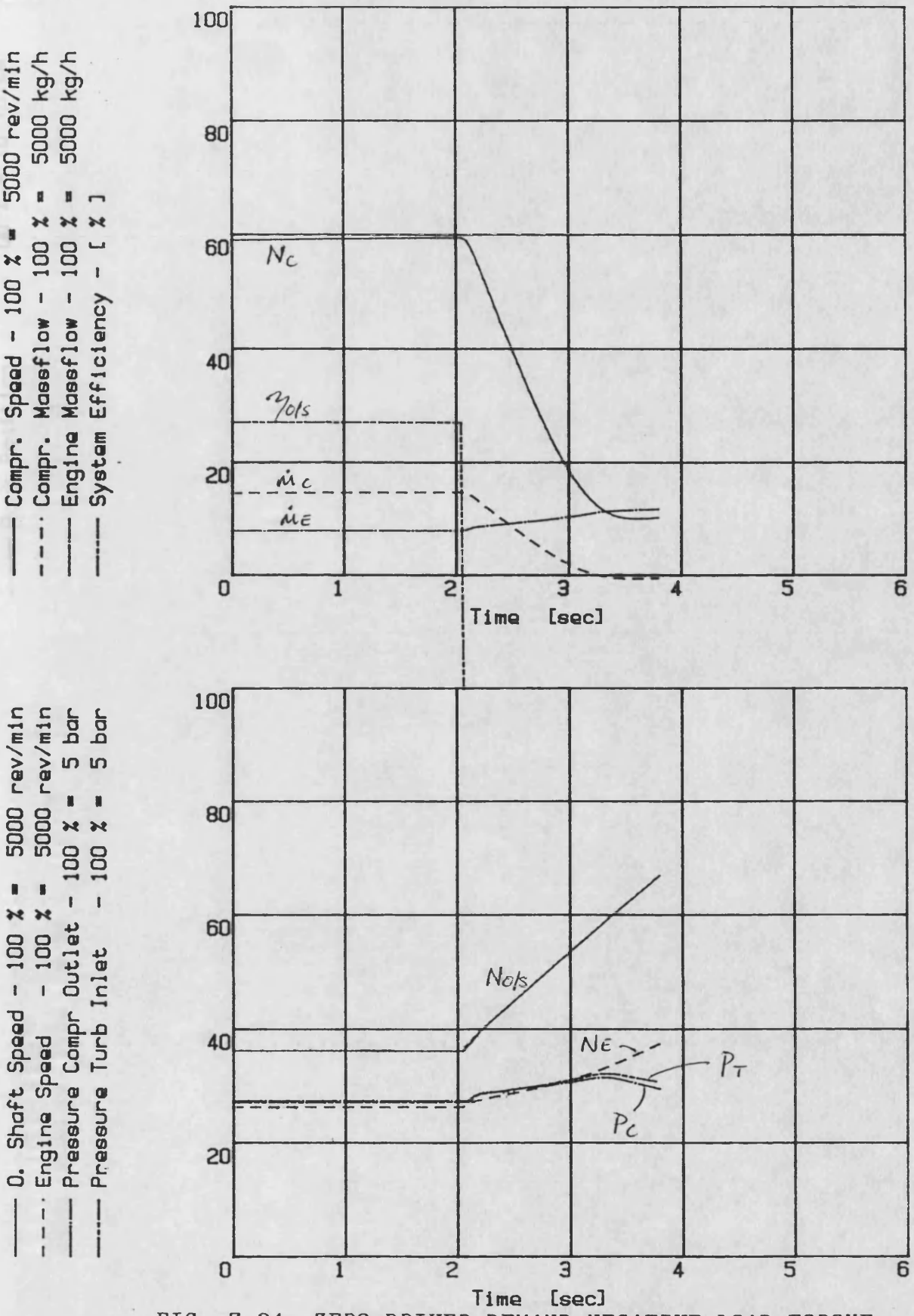

FIG. 7.34a ZERO DRIVER DEMAND, NEGATIVE LOAD TORQUE

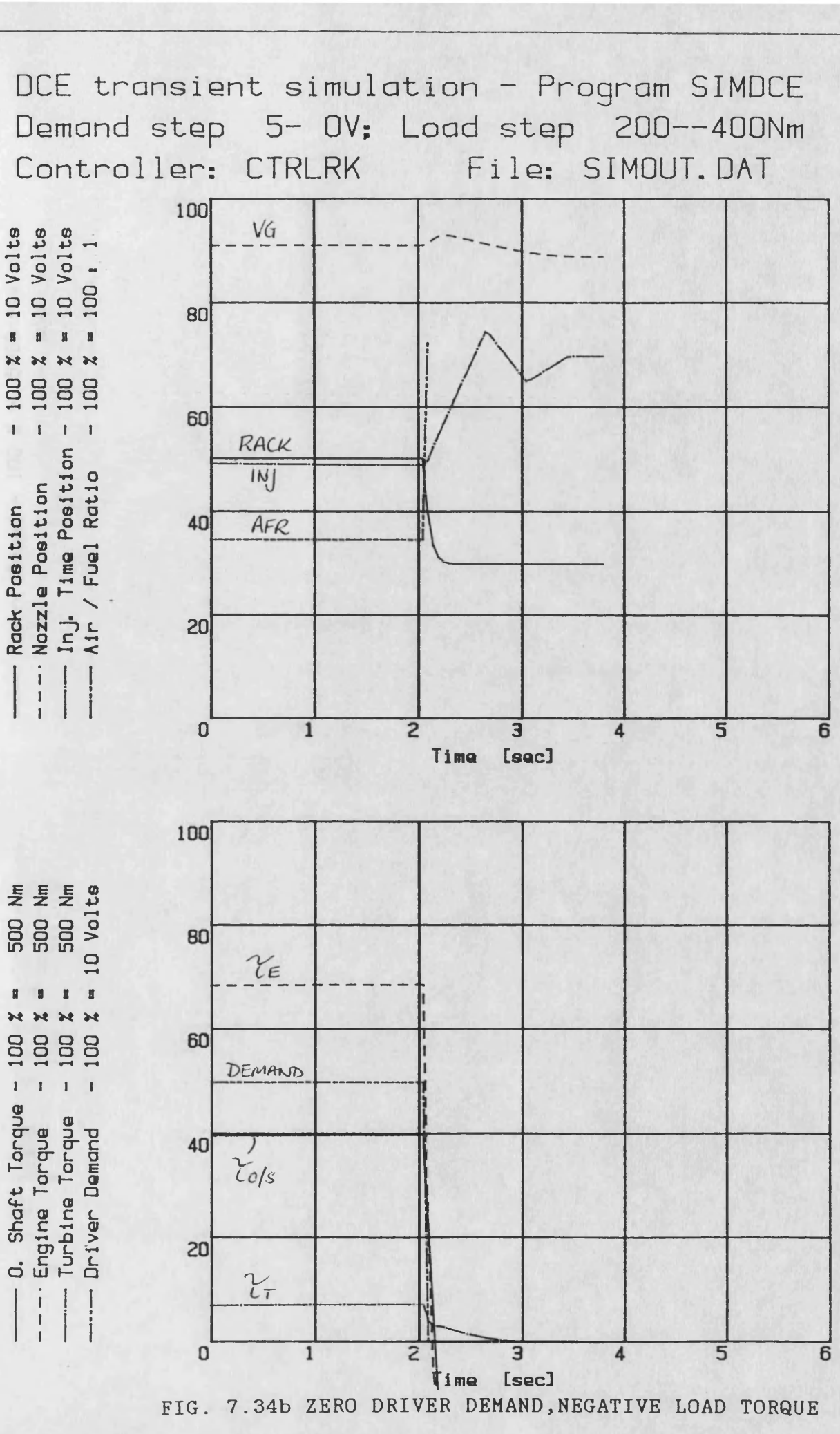

FIG. 7.34b ZERO DRIVER DEMAND,NEGATIVE LOAD TORQUE

DCE transient simulation - SIMDCE 210389
Demand step 5b OV; Load step 200b-400Nm
CTLRK2; 2 vol.model File: ora17.dat

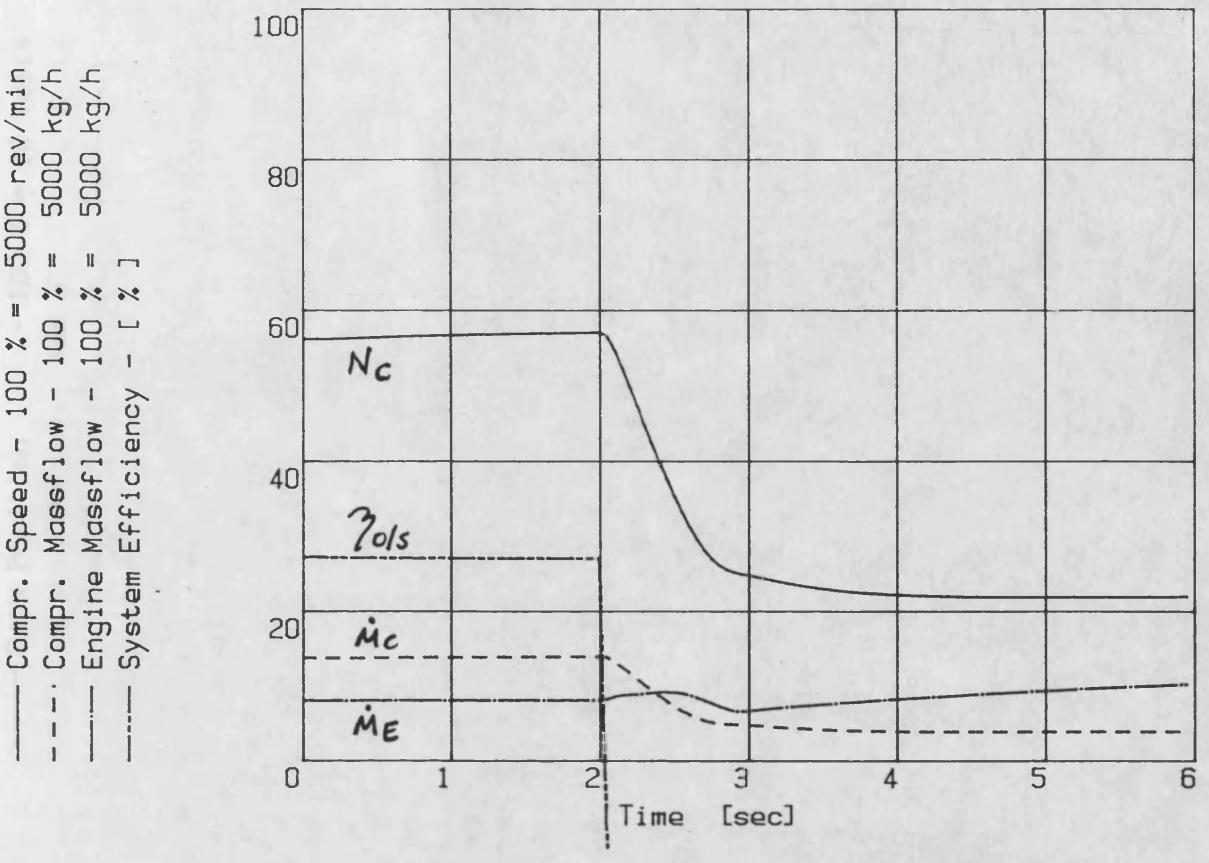

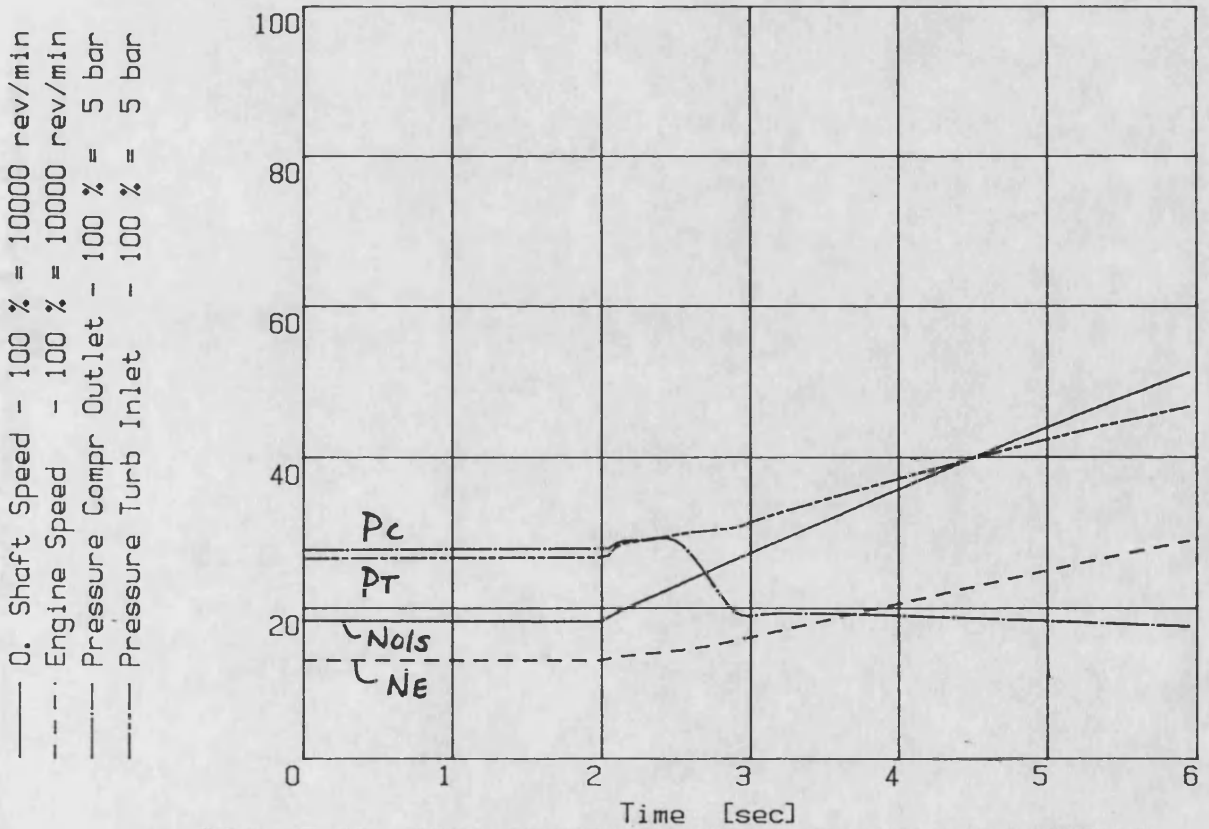

FIG. 7.35a ZERO DRIVER DEMAND, NEGATIVE LOAD TORQUE
(compr. & engine bypass control)

DCE transient simulation - SIMDCE 210389
Demand step 5 to 0V; Load step 200 to -400Nm
CTLRK2: 2 vol. model File: ora17.dat

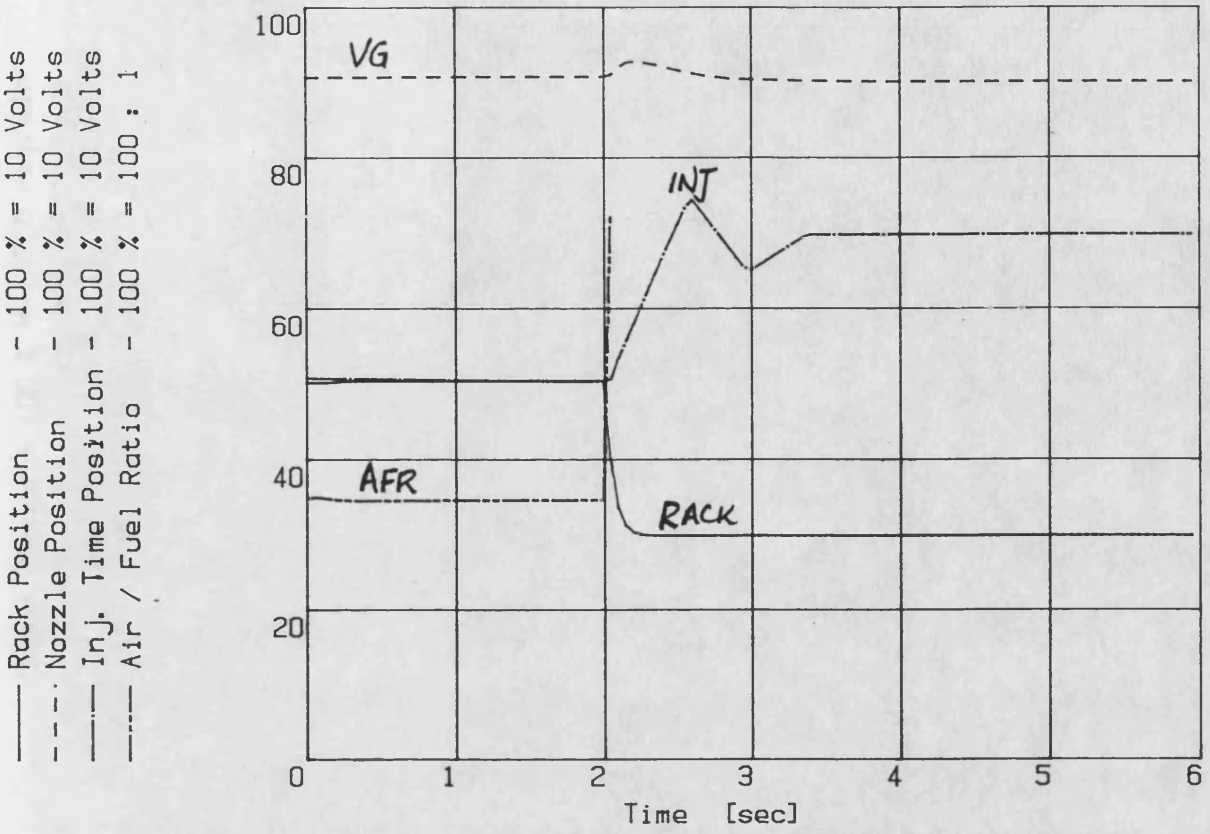

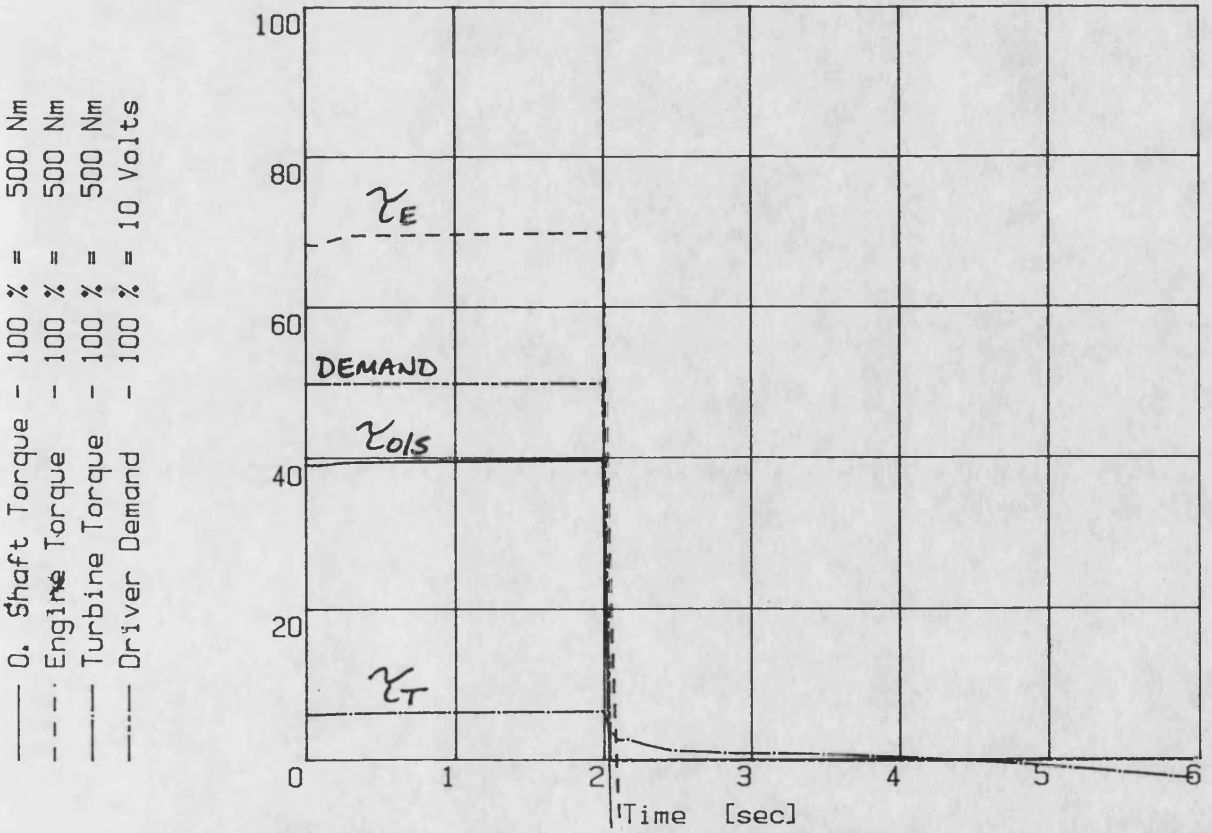

FIG. 7.35b ZERO DRIVER DEMAND, NEGATIVE LOAD TORQUE
(compr. & engine bypass control)

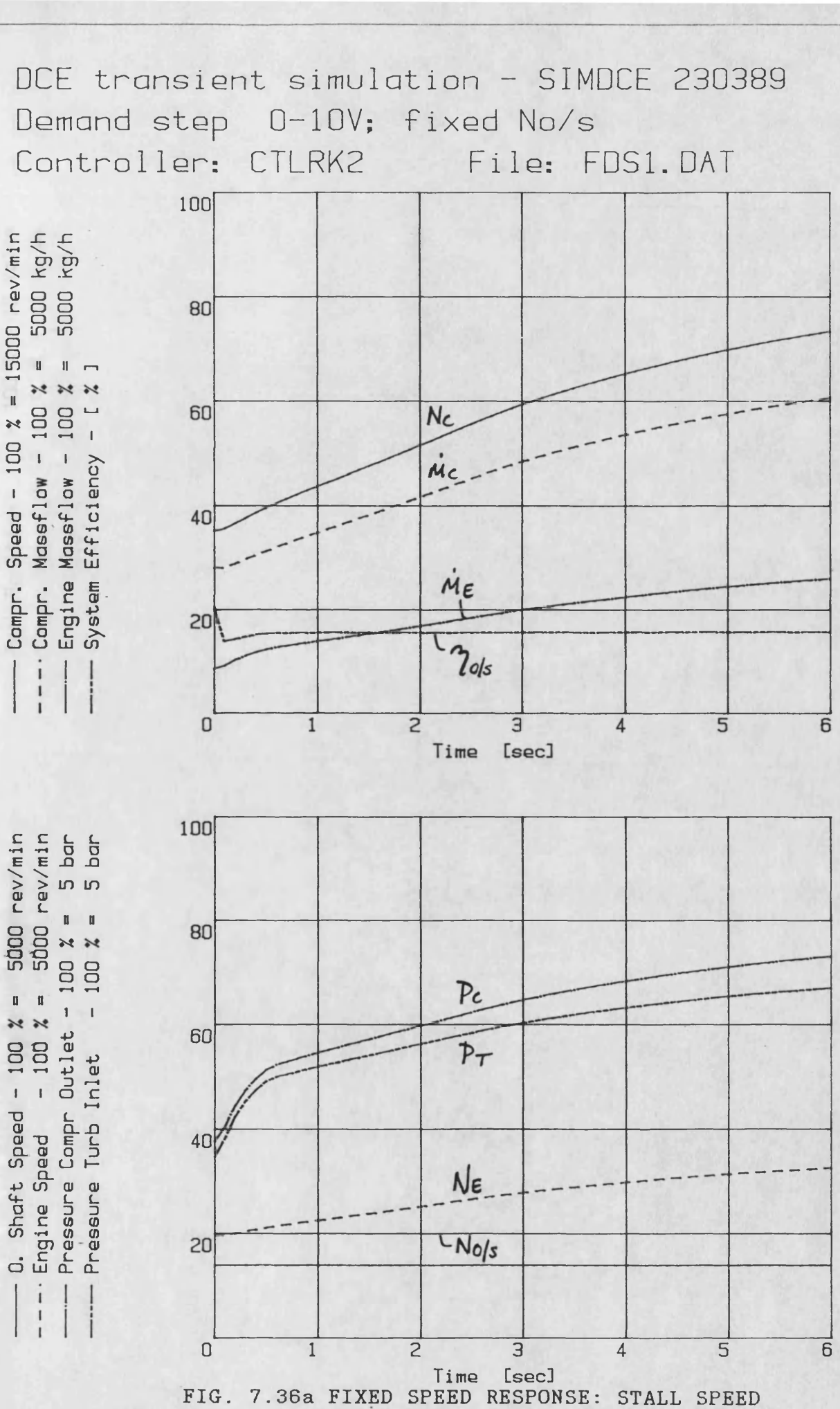

FIG. 7.36a FIXED SPEED RESPONSE: STALL SPEED

DCE transient simulation - SIMDCE 230389
Demand step 0-10V; fixed No/s
Controller: CTLRK2 File: FDS1.DAT

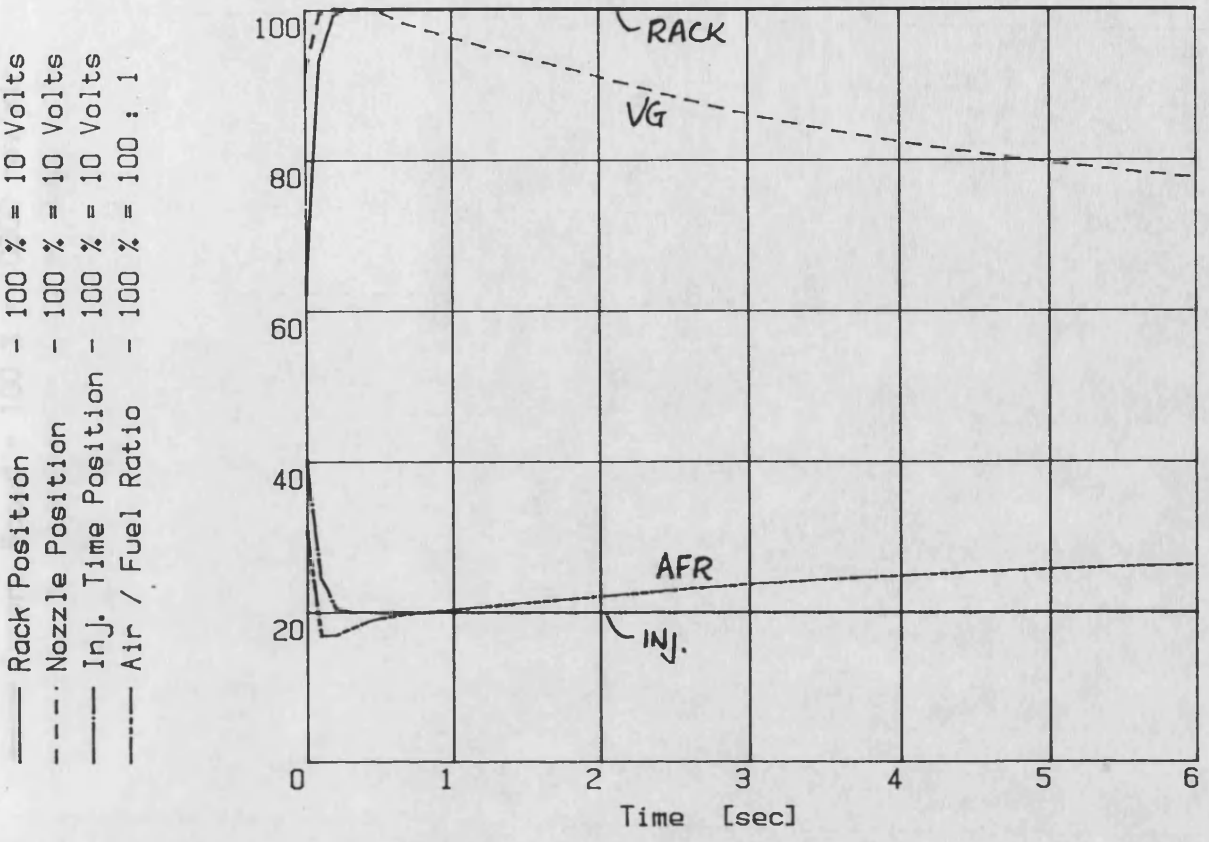

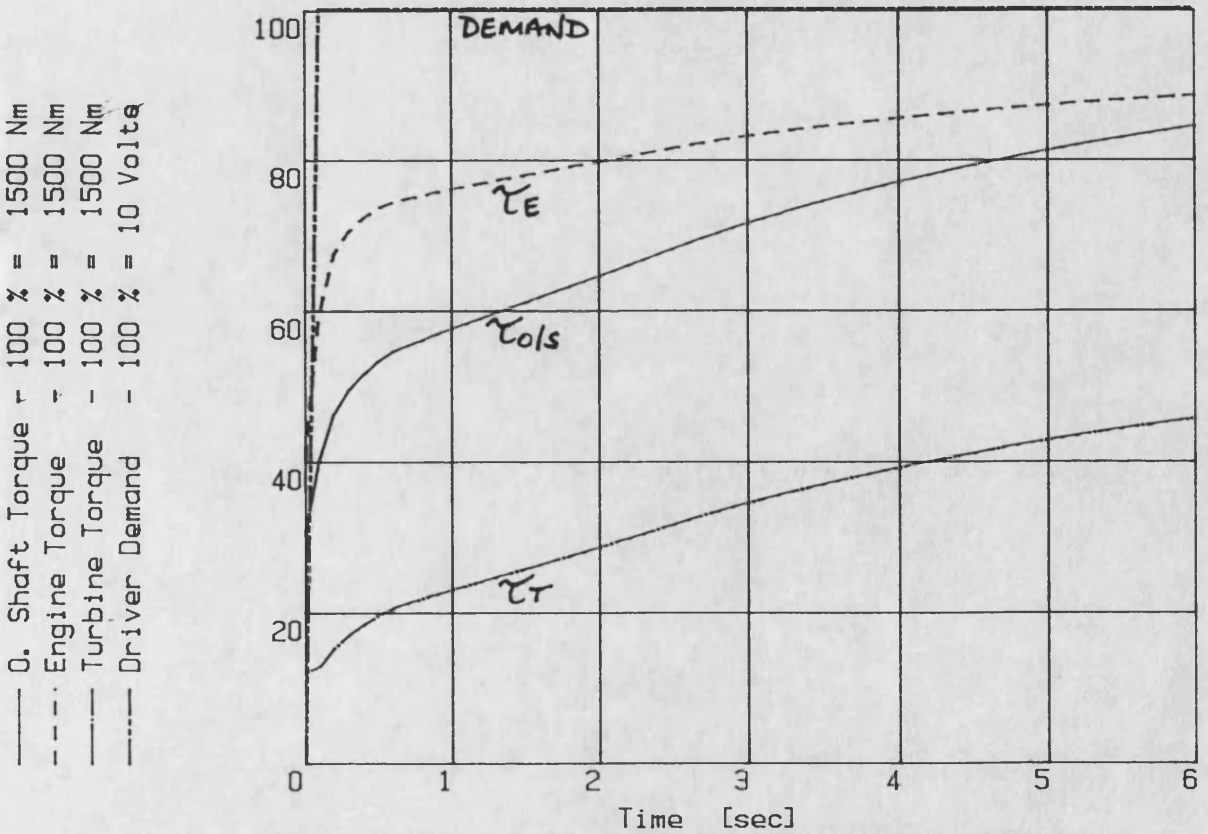

FIG. 7.36b FIXED SPEED RESPONSE: STALL SPEED

DCE transient simulation - SIMDCE 230389
Demand step 0-10V at mid-speed
Controller: CTLRK2 File: FDS2.DAT

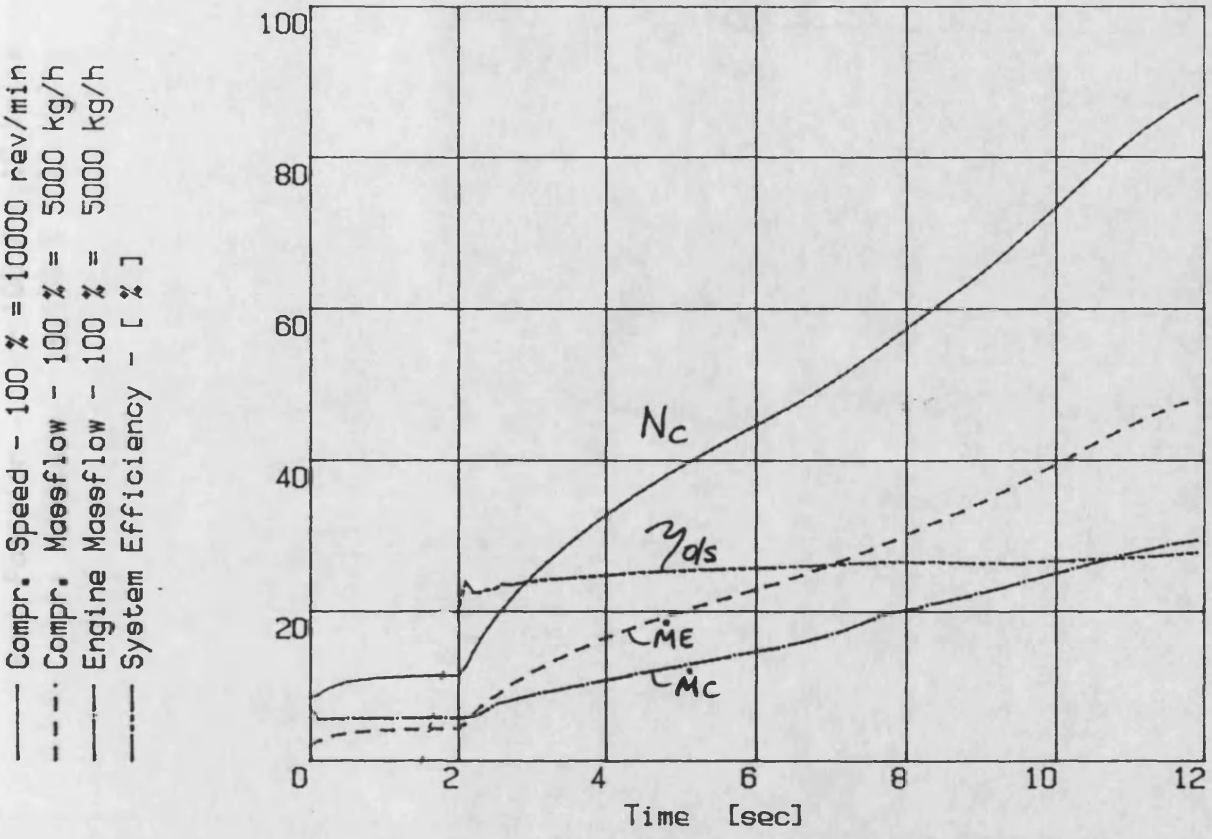

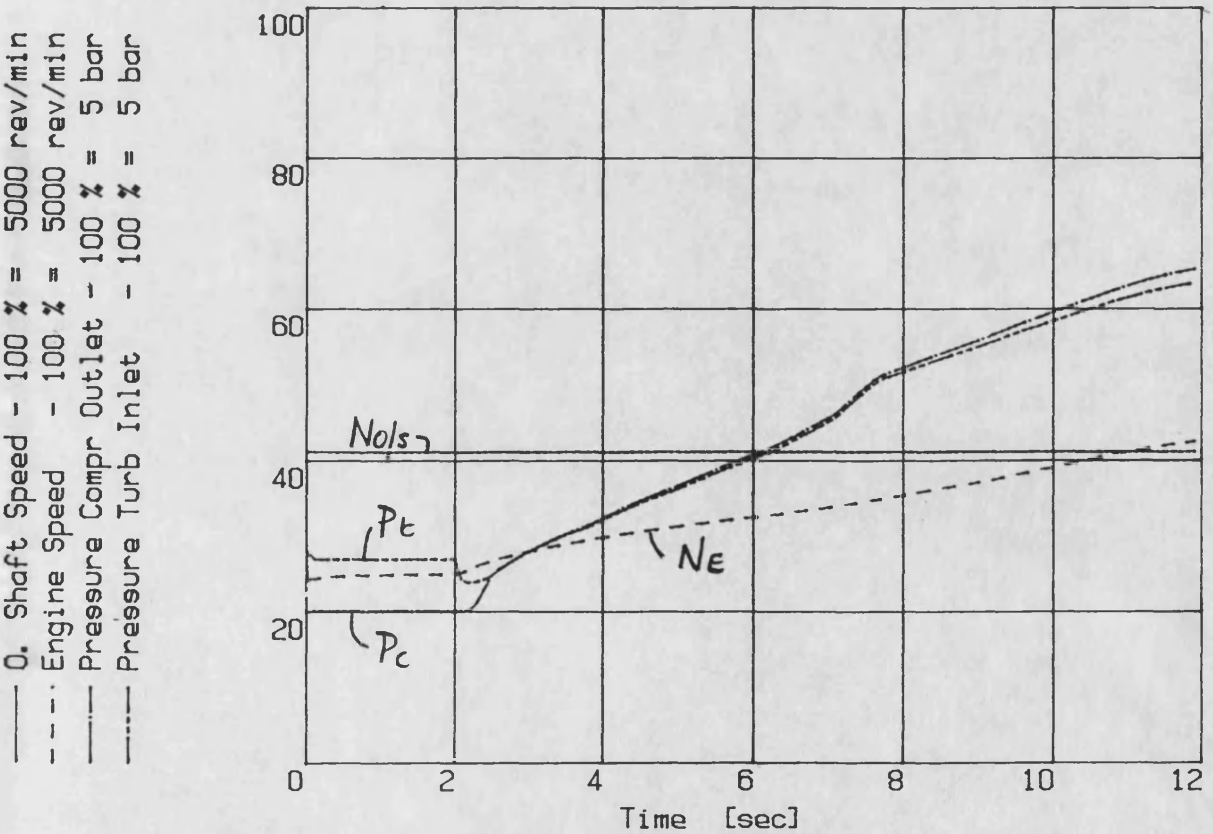

FIG. 7.37a FIXED SPEED RESPONSE: MID-SPEED

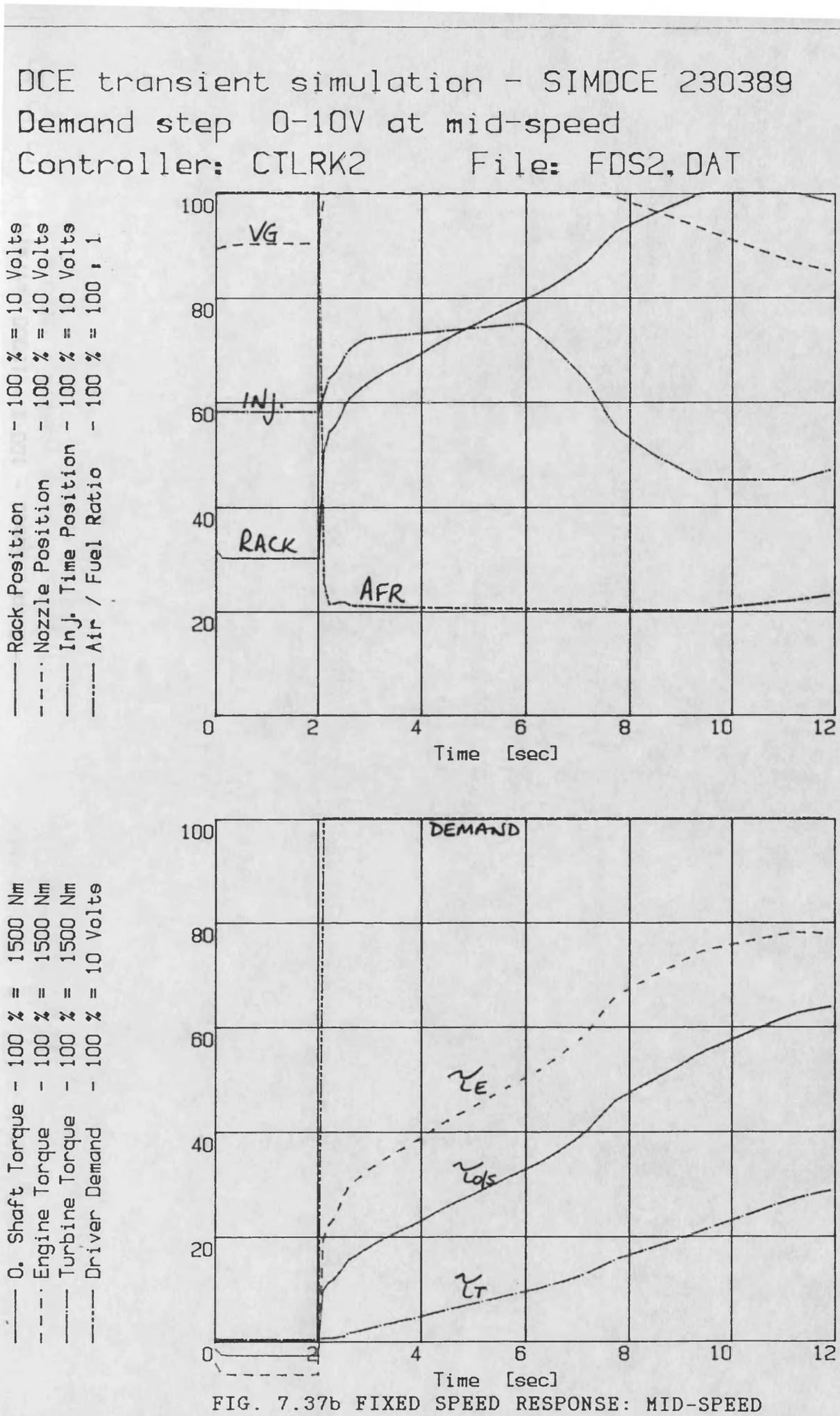

FIG. 7.37b FIXED SPEED RESPONSE: MID-SPEED

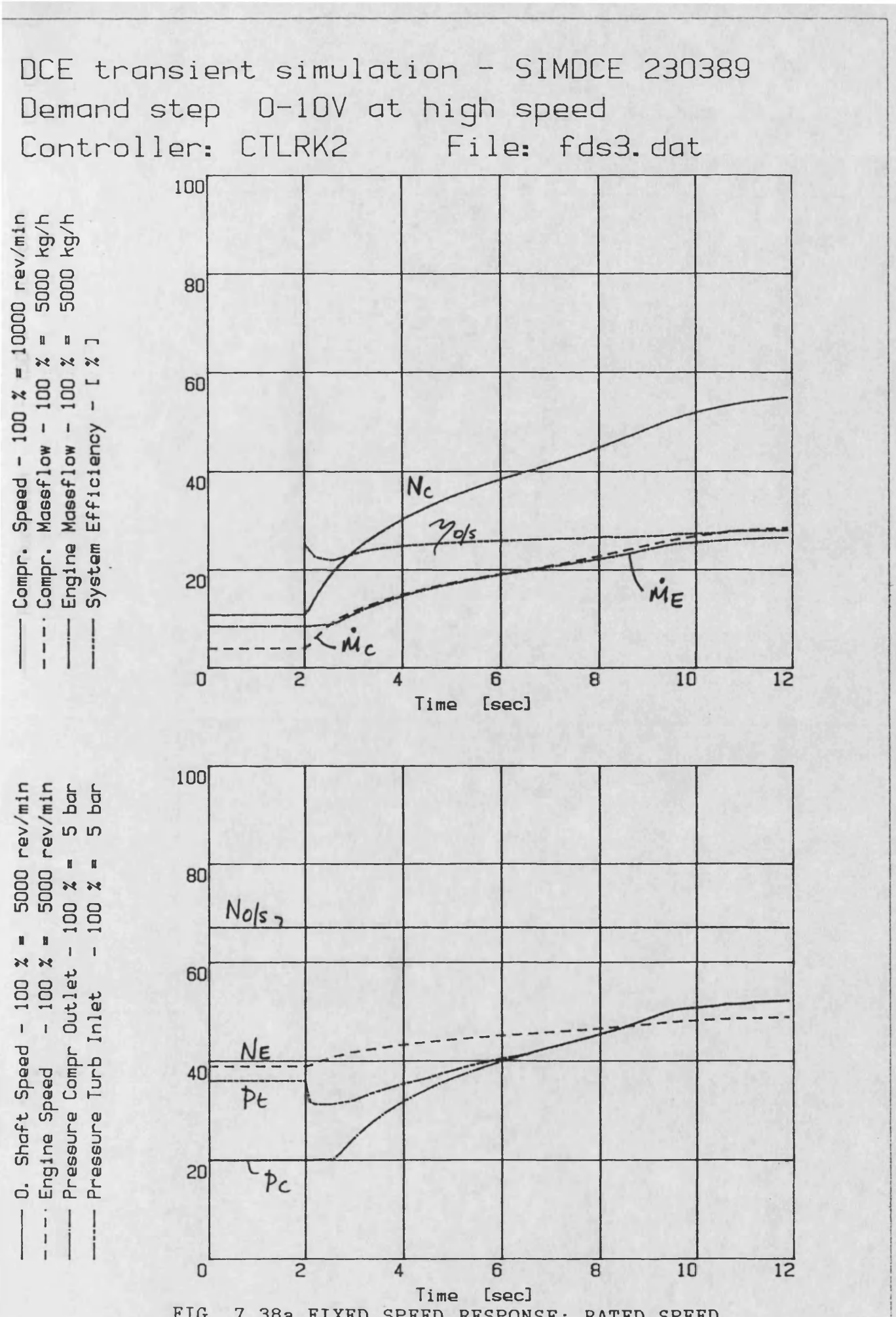

FIG. 7.38a FIXED SPEED RESPONSE: RATED SPEED

DCE transient simulation - SIMDCE 230389
Demand step 0-10V at high speed
Controller: CTLRK2 File: fds3.dat

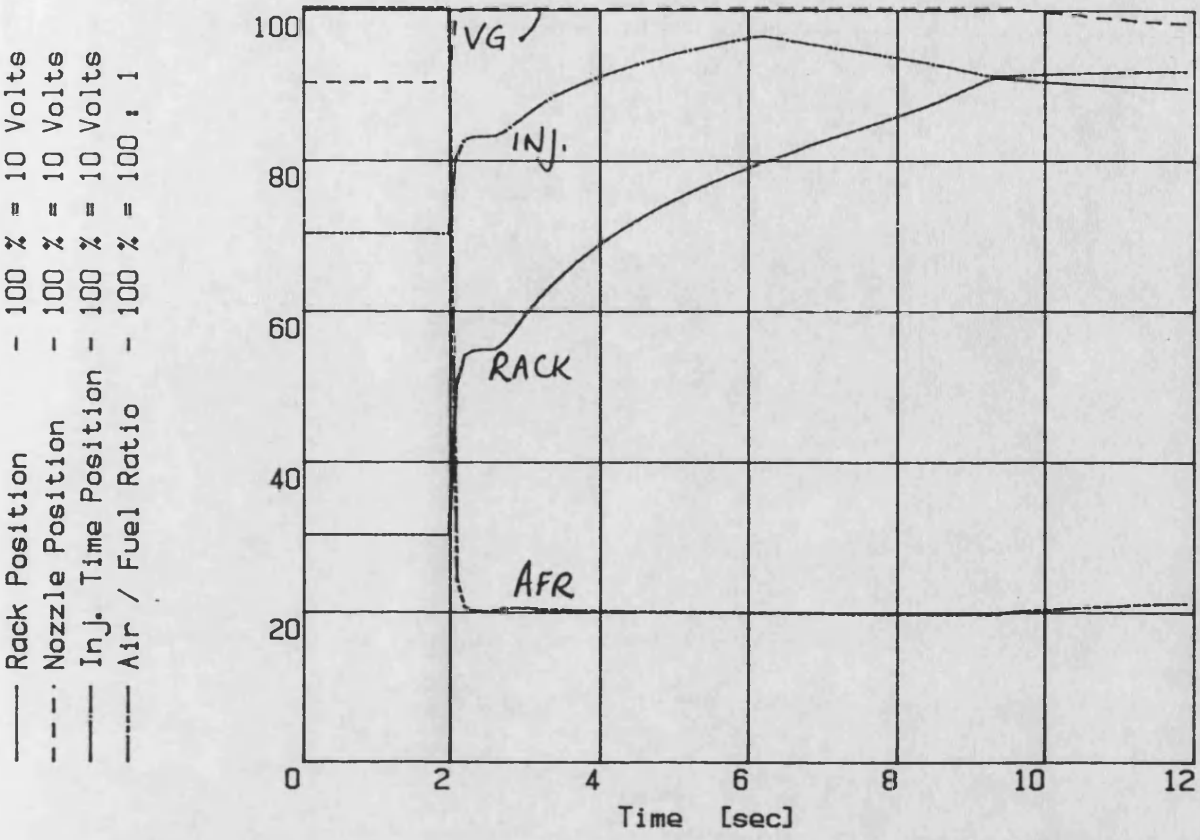

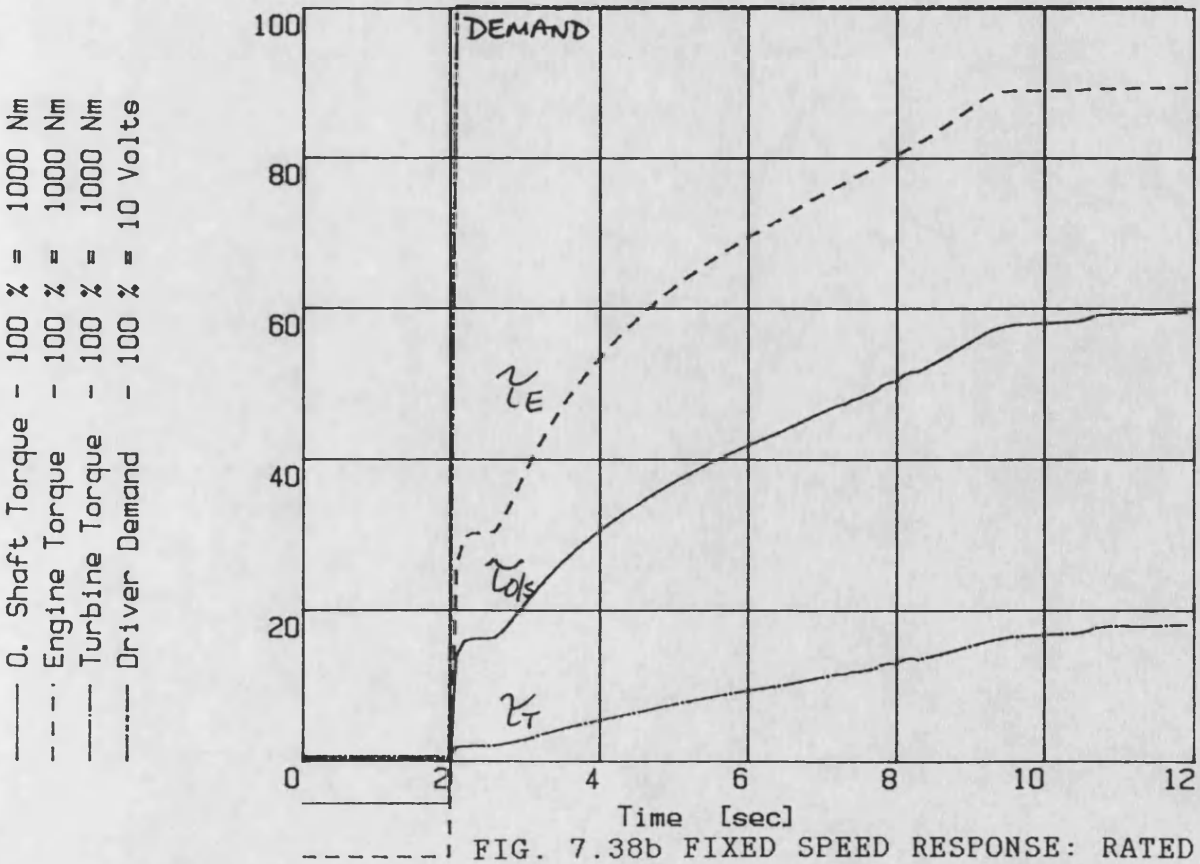

FIG. 7.38b FIXED SPEED RESPONSE: RATED SPEED

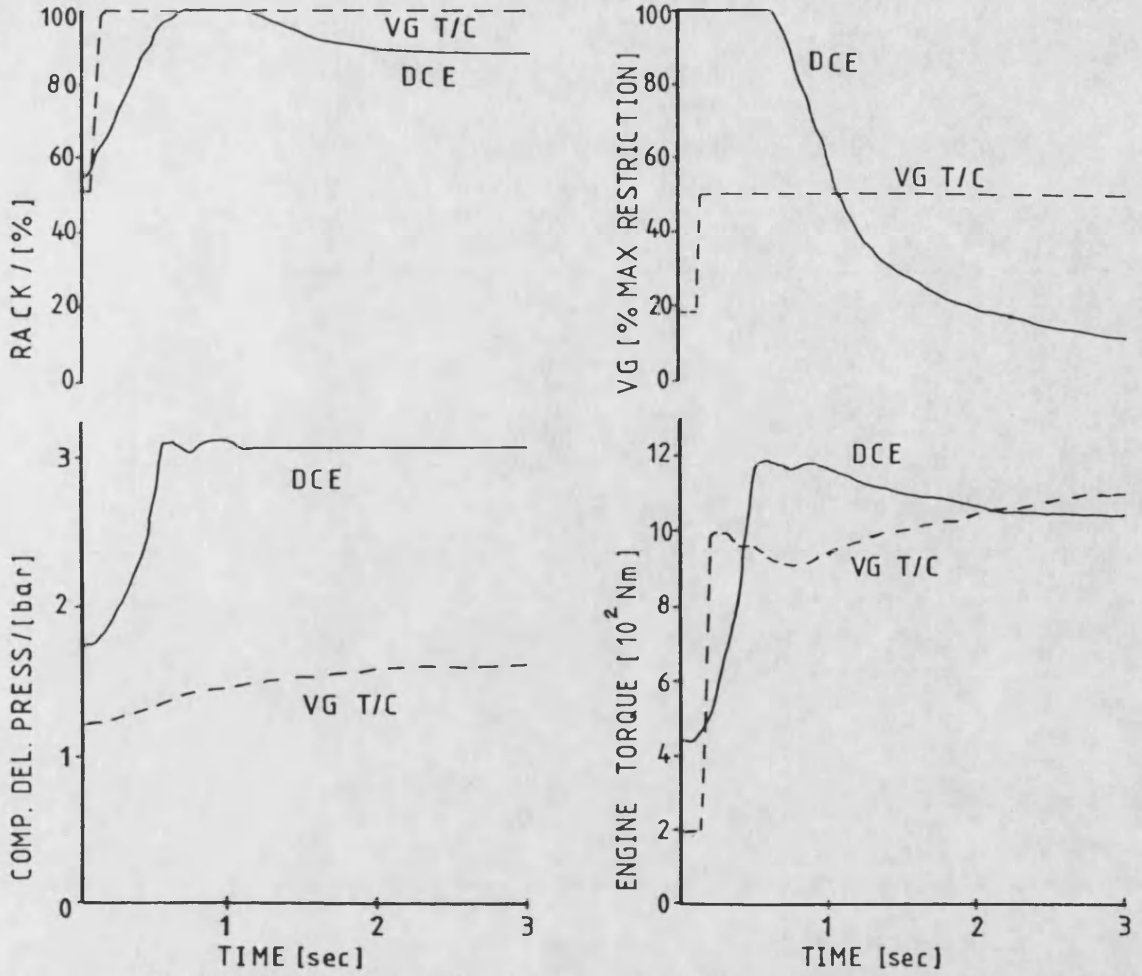

FIG. 7.39(a) DEMAND STEP AT FIXED 52% RATED SPEED

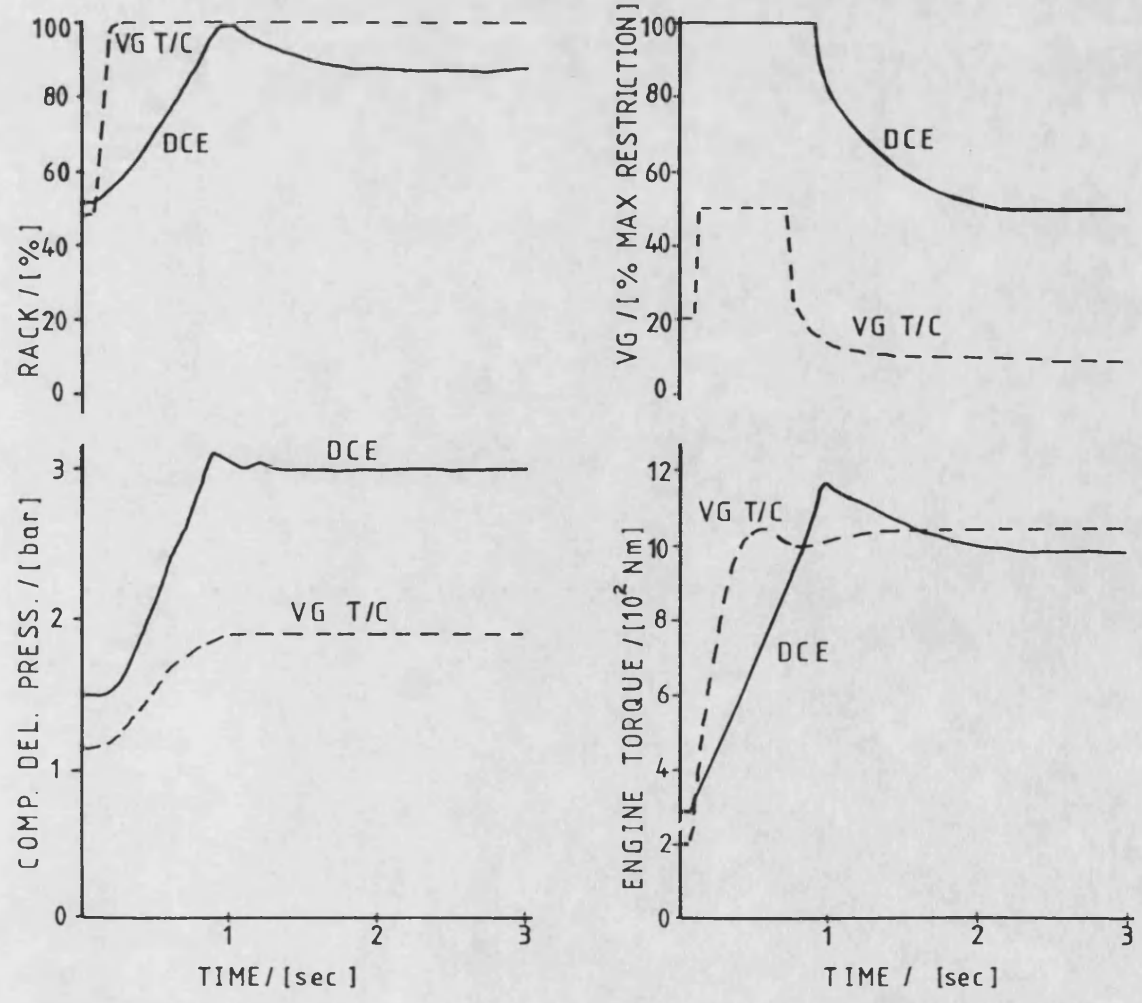

FIG. 7.39(b) DEMAND STEP AT FIXED 78% RATED SPEED.

8. ADVANCED CONTROL TECHNIQUES

8.1 Introduction

8.2 Theoretical background

8.2.1 System models

8.2.2 Identification techniques

8.2.3 State space control design

8.2.4 Input - output models control design

8.2.5 Model selection for DCE work

8.3 DCE identification

8.3.1 Method and implementation

8.3.1.1 General approach

8.3.1.2 Recursive least squares method

8.3.1.3 Implementation and validation

8.3.2 DCE results

8.3.2.1 VG nozzle - boost model

8.3.2.2 Multivariable model

8.4 Parametric DCE control designs

8.4.1 Deadbeat boost control

8.4.2 LRPC: boost control

8.4.3 Multivariable LRPC

8.4.3.1 Rack : engine speed LRPC

8.4.3.2 Dual SISO LRPC

8.4.3.3 Multivariable (decoupling) LRPC

8.5 Practical applications of optimal control

8. ADVANCED CONTROL TECHNIQUES

8.1 INTRODUCTION

The previous chapter described the development of a proportional-integral-derivative (PID) type controller for the 520DCE, and the resulting predicted performance of the 520DCE. The microcomputer-based implementation of the controller in the 520DCE prototype, and experimental results, were discussed in Chapter 4. Following this demonstration of a successful conventional control system, more advanced techniques were investigated. The main goals were to provide a systematic approach to DCE control system design, and to discover what improvements could be achieved by taking into account the multivariable nature of the DCE.

As stated previously, any control system would be implemented digitally. Systematic design methods would therefore involve parametric system models (that is, model equations in terms of a finite number of variables with quantitative coefficients) rather than the use of graphical methods such as Bode or Nyquist plots, or root locus diagrams. If a systematic control design method could successfully be applied to the 520DCE then this could lead to a set of design rules for future DCE controllers, which previously had been developed in a rather ad hoc fashion. A systematic design method has the further advantage that it may be automated to some extent, and be carried out in real time (assuming adequate computing power), giving adaptive control. This would be useful where system dynamics change with time or operating condition ("non-stationary"); in such cases a fixed control design would have to be conservative in its control actions, giving stability at the expense of performance at some conditions. It was anticipated that the

520DCE dynamics would be significantly non-stationary. This was apparent whilst developing the PID-type controller by simulation, and is well-known for Diesel engine systems [59, 82, 83].

It had long been realised that the DCE is a multivariable system, with appreciable cross-coupling between the effects of the important control inputs (fuel rack and turbine VG). However, the severity of the cross-coupling had not previously been quantified. It was thought that controller performance might be improved by identifying these dynamics and compensating for them. It was also noted that identification might give insight into alternative control strategies; in automotive gas turbine control studies mentioned earlier [22, 23], identification tests had led to the unexpected choice of power turbine nozzle angle as the primary input to control gas generator speed.

The first part of this chapter gives a brief introduction to alternative parametric system models and identification methods, indicating the reasons for the choice of models used in the work reported here. Control design methods applicable to the different models are also reviewed. The implementation of identification routines within the 520DCE dynamic simulation is then described, and the resulting identified models are discussed. Finally alternative control designs based on the models are described, and simulated 520DCE transient responses are compared with those employing the PID-type control system.

8.2 THEORETICAL BACKGROUND

8.2.1 System Models

Parametric system models may be grouped into two classes, namely state space forms and input-output forms. These two groups will be discussed

in turn below; however, it should be noted that there is an equivalence between two parametric models describing a given system, and the link between the groups will be indicated. It should be stressed that the following descriptions apply to linear stationary (that is, fixed coefficients) systems. Furthermore, only the discrete-time case will be considered, as required for digital control system design.

(i) State space forms

The current condition or state of the system is expressed as a (linear, stationary) combination of the state at the previous discrete time, the current inputs, and noise or disturbance inputs:

$$\underline{x}_{k+1} = \underline{\Phi}\,\underline{x}_k + \underline{\Gamma}\,\underline{u}_k + \underline{\Gamma}_1\,\underline{\xi}_k \qquad (8.1)$$

where $\underline{x}$ are the system states

$\underline{u}$ are control inputs

$\underline{\xi}$ are noise or disturbance inputs

k, k+1 denote successive discrete time instants

For a system with n states and m inputs the system matrices have dimensions

$\underline{\Phi}$ [n x n]

$\underline{\Gamma}$ [n x m]

$\underline{\Gamma}_1$ [n x n]

The outputs, $\underline{y}k$, are commonly expressed as a (linear, stationary) combination of the state :

$$\underline{y}_k = \underline{H}\,\underline{x}_k \qquad (8.2)$$

where for p outputs, $\underline{H}$ has dimension [p x n]

The particular formulation of (8.1) and (8.2) may vary according to the task in hand. That is, the parameters in the system matrices may for example differ if the equations are formulated for identification or for control design. These alternative "canonical" (meaning standardized and convenient) forms have identical dynamics and are related by matrix transformations. This is discussed in [68, 87]. A canonical form may be obtained which represents the state purely by past inputs and outputs, and is thus equivalent to the input-output forms described below.

(ii) Input-Output forms

The input-output form is related to the classical transfer function. Inputs and outputs are related by some (linear, stationary) combination of dynamic terms. For the discrete-time case this involves the use of terms going back as far as required in discrete time. This may be contrasted to state space models where only one timestep is considered and the concept of a "state" is introduced to "fill in" the missing dynamics.

The input-output equation takes the form

$$\underline{A}(z^{-1})\underline{y}_k = \underline{B}(z^{-1})\underline{u}_k + \underline{C}(z^{-1})\underline{\xi}_k \qquad (8.3)$$

where $\underline{y}$ are the system outputs

$\underline{u}$ are the system inputs

$\underline{\xi}$ are noise or disturbance inputs

k denotes a discrete time instant

$\underline{A}$, $\underline{B}$, $\underline{C}$ are vectors of polynomials in the unit delay operator z^{-1}:

$$z^{-n}.\underline{y}_k = \underline{y}_{k-n} \qquad (8.4)$$

The above model consists of an autoregressive (AR) combination of past outputs and a moving-average (MA) combination of control inputs, and is thus known as an "ARMA" model. A useful extension is the "integrated" (ARIMA) form:

$$\underline{A}(z^{-1})\,\Delta\underline{y}_k = \underline{B}(z^{-1})\,\Delta\underline{u}_k + \underline{C}(z^{-1})\,\underline{\xi}_k \qquad (8.5)$$

where the model is now expressed in terms of control and output moves rather than absolute values. The advantage of this approach is realised when developing controllers for systems which are subject to step-like disturbances in $\underline{\xi}$ and for which zero control input $\underline{u}$ does not lead to zero output $\underline{y}$ [84]. For systems with dead time longer than the sample interval (say d intervals) the control input term in (8.5) becomes

$$\Delta\underline{u}_{k-d}$$

Whichever form of model is chosen, its parameters (ϕ, Γ, Γ_1, for state space, $\underline{A}$, $\underline{B}$, $\underline{C}$, for ARIMA) must be obtained either from physical understanding of the system or by direct identification. In most practical situations the latter approach must be adopted because the system is complex and/or important dynamic factors such as friction/viscous damping cannot reliably be modelled.

8.2.2 Identification techniques

A detailed description of the many available identification and parameter estimated methods would not be appropriate here, but may be found in modern control texts, for example [68, 85]. A summary of the principles and problems involved is given as background to the technique used for the 520DCE work.

The fundamental approach is to excite the system inputs, and to predict and measure the corresponding states and/or outputs of the system. The model parameters are then systematically adjusted to optimise the match between system and model.

In practice the identification process has many variables, particularly the choice of model order and structure (single input-output or multivariable), type of excitation, parameter estimation algorithm and definition of the best system-model match. The process tends to be iterative, changing the model order to improve the match, possibly changing the parameter estimation algorithm to suit different system dynamics or noise/disturbance effects. A practical illustration of the comparative complexity of several commonly-used identification methods applied to different systems is given in [86].

The choice of input signal type depends upon the system and the identification process to be used. For example in vibration analysis, impulses or a sequence of sine waves are commonly used, giving a non-parametric model (impulse response or frequency response function). Parameter estimation may then be performed remotely on this intermediate model. In process control open-loop step response tests may be used. For non-linear systems these impulsive inputs are not ideal since they have a high "crest factor", that is, requiring a high peak input signal level to transmit a given level of input "energy" to the system. Since the need for an acceptable signal-to-noise ratio sets a lower limit on the energy required, inputs with a high crest factor are likely to exacerbate non-linearity problems.

The alternative, adopted for the DCE work, is to use a pseudo-random binary sequence (PRBS) input. This has a low crest factor, and can easily be computer-generated. As will be seen later, this is convenient since the identification process can be fully automated, with input signal generation and parameter estimation being carried out simultaneously.

Having obtained parametric models, in state space or input-output form, a range of possible control design methods is available. These are reviewed in the following subsections, in the context of engine control.

8.2.3 State space control design

A state space model is amenable to control designs ranging from classical pole-placement to more advanced optimal control methods. This approach will be illustrated by a simple example of Diesel engine speed control:

(i) The system

The dynamic equation for the continuous system, making the simplifying assumptions of linearity and ideal torque response to fuelling (neglecting cyclic combustion) may be written :

$$\frac{d(Ne)}{dt} = \frac{K_t . u_f}{J} - \frac{\gamma_L}{J} \qquad (8.6)$$

Where Ne is engine speed

γ_L is engine load torque

J is referred inertia

u_f is fuelling control input

K_t is the linearised engine brake torque/fuelling gain

Equation (8.6) is in continuous state space form :

$$\dot{\underline{x}} = \underline{F}\,\underline{x} + \underline{G}\,\underline{u} + \underline{G}_1\,\underline{W} \qquad (8.7)$$

$$\underline{y} = \underline{H}\,\underline{x}$$

with state $\underline{x} = x = Ne$

input $\underline{u} = u = uf$

disturbance W = W = τ_L

output $\underline{y} = \mathbf{y} \equiv x$

(all scalars in this example)

that is, $\dot{x} = \frac{Kt}{J} \cdot U - \frac{1}{J} \cdot W$ (8.7a)

$y = x$

The equations (8.7a) must be transformed to discrete-time equivalents for direct digital control designs, that is to the form described in subsection 8.2.1 :

$$\underline{x}_{k+1} = \underline{\phi}\,\underline{x}_k + \underline{\Gamma} u_k + \underline{\Gamma}_1 w_k \qquad (8.1)$$

$$\underline{y}_k = \underline{H}\,\underline{x}_k \qquad (8.2)$$

The transformation is a standard technique, based on solving equation (8.7) over one sample period; details may be found in [68]. The result depends upon the behaviour of the control input u in the inter-sample period. Digital-to-analogue converters used in microprocessor-based control systems commonly hold a fixed level between samples, referred to as zero-order hold (ZOH). Making this assumption, and remembering that time delays due to cyclic combustion have been neglected, the following relations are obtained:

$$\underline{\phi} = \underline{I} + \underline{F}\,T\,\underline{\Psi}$$
$$\underline{\Gamma} = \underline{\Psi}_T\,\underline{G}$$
$$\underline{\Gamma}_1 = \underline{\Psi}_T\,\underline{G}_1 \qquad (8.8)$$

where I is the identity matrix

T is the sample interval

$\underline{\Psi} = \underline{I} + \underline{F}T/2! + \underline{F}^2T^2/3! + \ldots$

In this example :

$$\underline{\phi} = \phi = 1 \quad \text{(F is zero)}$$

$$\underline{\Gamma} = \Gamma = \frac{Tk_t}{J} \tag{8.8a}$$

$$\underline{\Gamma}_1 = \Gamma_1 = \frac{-T}{J}$$

so that the discrete-time model is :

$$x_{k+1} = x_k + \frac{Tk_t}{J}.u_k - \frac{T}{J}.W_k \tag{8.9}$$

$$y_k = x_k$$

It should be noted that the above manipulation was required when starting from a physical model. If identification techniques were used, then the discrete-time parameters (coefficients in equation (8.9)) would be obtained directly.

(ii) Control design

The principle of state space control is to feed back some linear combination of the state at each sample instant:

$$\underline{U}_k = -\underline{K}\,\underline{x}_k \tag{8.10}$$

Where K is a matrix of feedback gains. In this single input, single state case,

$$u = -k_f.x \tag{8.10a}$$

Substituting (8.10a) into (8.9) gives the closed loop model :

$$X_{k+1} = \left[\frac{1-Tk_t\ k_f}{J}\right].x_k - \frac{T}{J}.W_k \tag{8.11}$$

For pole placement design an expression in the frequency domain is required. For the discrete-time case the Z- transform expression is used (the z operator was described in subsection 8.2.1). The z-transform of (8.11) is

$$z\,X(z) = X(z).\left[\,1 - \frac{T\,k_t\,k_f}{J}\right] - \frac{T}{J}.W(z) \qquad (8.12)$$

and the characteristic equation of (8.12) has determinant :

$$\left| z - 1 + \frac{T\,k_t\,k_f}{J} \right| = 0 \qquad (8.13)$$

Therefore, given a desired z-plane root (closed-loop pole) location B,

$$B = 1 - \frac{T\,k_t\,k_f}{J} \qquad (8.13a)$$

may be used to select the feedback gain K_f. Note that the controller sample interval T must be defined at this stage. If K_f is too large, B will become less than (-1, j0), outside the region of stability (a unit circle centred on the origin) in the z-plane. As K_f is reduced to zero, B tends to (1,j0).

Alternatively, "optimal" control methods may be used. These have particular advantages in designing controllers for systems having multiple control inputs. The controllers are optimal in that they minimise some cost function, which for the state space model has the form :

$$J = \frac{1}{2}\sum_{k=0}^{N}\left[\,\underline{x}_k^T \cdot \underline{Q}_1 \cdot \underline{x}_k + \underline{u}_k^T \cdot \underline{Q}_2 \cdot \underline{u}_k\,\right] \qquad (8.14)$$

where $\underline{x}$ and $\underline{u}$ are state and control input vectors as before, and $\underline{Q}_1$, $\underline{Q}_2$ are matrices weighting their relative "cost" over some discrete-time interval k = (0,N). It will be seen that a very similar cost function is used with input-output models.

It should be noted that (8.14) is constrained by the relationship between x and u implied in the state space model, equation (8.1). The solution may be found using the method of Lagrange multipliers, and is well-documented [68,85] but lengthy.

The design specification has been transferred from pole placement (or similar graphical interpretation) to choice of the loss matrices $\underline{Q}_1$ and $\underline{Q}_2$. Optimal control design will be discussed further, for the input-output model case, in the next subsection.

(iii) Observer design

In the simple design example used above, only one state variable (engine speed) was used. In general the controller may use states which will not be measured. In this case an "observer" is used to estimate unmeasured states from available information. If the "observed" state is denoted $\hat{\underline{x}}$, then the control law becomes

$$\underline{u}_k = -\underline{K}\,\hat{\underline{x}}_k \qquad (8.15) \quad (\text{cf. } 8.10)$$

that is, control action depends on observed rather than measured states. Observed states may be used even where measured data is available, acting as a filter of signal noise. The ideal observer would model the system dynamics in the same way as they have been modelled above:

$$\hat{\underline{x}}_{k+1} = \underline{\Phi}.\hat{\underline{x}}_k + \underline{\Gamma}.\underline{u}_k + \underline{\Gamma}_I\underline{w}_k \qquad (8.16)$$

In general the observer will be inaccurate, because the parameters of (8.16) are not exact and because the noise/disturbance inputs W may be unknown. A feedback loop is included to correct the observer. The difference between the observer predicted output :

$$\hat{\underline{y}}_k = \underline{H}\,\hat{\underline{x}}_k \qquad (8.17)$$

and the measured output $\underline{y}_k$ is used, as shown in fig. 8.1 (for the speed control example). Thus the observer equation is :

$$\hat{\underline{x}}_{k+1} = \underline{\phi}.\hat{\underline{x}}_k + \underline{\Gamma}.\underline{u}_k + \underline{\Gamma}_1.W_k + \underline{L}\,[\underline{y}_k - \underline{H}\hat{\underline{x}}_k] \qquad (8.18)$$

The observer correction feedback gains $\underline{L}$ are selected either by pole placement or by optimal techniques, as for $\underline{K}$; in this case it is the dynamics of the prediction error :

$$[\underline{x} - \hat{\underline{x}}]_{k+1}$$

which are controlled.

(iv) Feedforward

The above design does not incorporate any feedforward (demand) input. Fig. 8.2 shows a complete controller (control law/observer/feedforward) schematic. The feedforward, r_k, is incorporated directly in the control equation:

$$\underline{u}_k = -\underline{K}\,\underline{x}_k + Nr_k \qquad (8.19)$$

and commonly is also incorporated in the observer equation, so that the direct effect of feedforward changes upon the observer error can be "tuned out". This is discussed further in [43], and again the general theories are covered by modern control texts.

8.2.4 Input-output models control design

Like the state-space model, the input-output model may be used in a range of control design methods. As observed in subsection 8.2.1 this model is a form of transfer function, expressed as a rational equation in the discrete time operator z^{-1}. It can therefore directly be used with the classical methods such as pole placement or root locus design again using the correct interpretation of regions in the z-plane. In addition a simple bilinear transformation may be used to map the Z-transform into the so-called w-plane [68,79], which closely resembles the continuous S-plane. Conventional gain and phase margin design rules may then be followed, as was described in [43] for the engine speed control example.

Cost function-based (optimal) methods may again be used, treating the past inputs and outputs as the system state. One cost function-based approach which has quite recently been explored, and for which good stability, robustness and ease of tuning have been claimed, is long-range predictive control (LRPC). Several independently-derived, but similar, LRPC methods are compared in [88]. A single generalised LRPC theory [89] has been reported which encompasses the various related LRPC methods. Furthermore the same workers have explained relationships with state-space optimal design methods and other simpler techniques [90, 91].

The principles of LRPC are illustrated in Fig. 8.3, and explained below [88].

(i) at each sampling instant, the system outputs over some future time horizon (say 1 sample periods) are predicted, using some system model. Clearly these outputs will depend upon (unknown) future control outputs.

(ii) As shown in fig. 8.3 for a single-input, single output case, different postulated future control inputs lead to different predicted process outputs. Here the inputs are taken to be constant up to the prediction horizon; this simplifies the problem but will be seen not to restrict the solution. A future control strategy is selected which moves the predicted output towards the feedforward setpoint in some optimal way (that is, according to some cost function). It may be noted that future changes in the feedforward setpoint are taken into account (if known), as shown in the figure. This is chiefly of use in process control, but has been used in control of transient engine testbeds [92].

(iii) The optimum control input is then used, but only at the current time. At the next sample interval the procedure is repeated with new data. Thus the postulated fixed future control input is not a constraint; the prediction and control horizons "recedes" at each sample time and the optimal control path is continually adapted.

LRPC techniques were adopted in the DCE work for reasons described below, so precise details will be given later in this chapter.

8.2.5 Model selection for DCE work

Two forms of parametric models for control design have been described in the preceding subsections. The model identification process, and control design methods appropriate to each model, have also been introduced.

In general the state space approach has the broader capabilities since input-output models are essentially particular cases of state space models. In physical terms, systems may be visualised where feedback of

outputs only is insufficient to achieve control of the system. The concept of controllability (and observability, which is very closely related) is useful for complex systems, where theoretical tests on a state space model may be applied if physical understanding is difficult. This is discussed in the literature [68].

For the DCE it was clear from physical understanding, as well as the previous successful use of PID-type control, that input-output models would be acceptable. This would give the following advantages in this case:

(i) Since the identification methods use input-output data, the identified model could be used directly for control design, without transformation.

(ii) A promising technique (LRPC) was available for optimal control using and input-output model, requiring less computation than the formal state space solution.

8.3 DCE IDENTIFICATION

8.3.1 Method and Implementation

8.3.1.1 General approach

As discussed in Chapter 5, the dynamic simulation SIMDCE was intended for use in all phases of the DCE control study. At this stage SIMDCE had been used successfully to develop a PID-type controller for the 520DCE, and had been shown accurately to predict 520DCE dynamic responses. The current phase of control design was therefore also carried out using SIMDCE- this gave the following advantages :

(i) Possibilities of damage to the prototype during identification tests were precluded, along with any resulting delays to the research programme.

(ii) Installation of a turbine torquemeter for further steady-state mapping could proceed in parallel

(iii) Certain DCE conditions (for example fixed output shaft speed) may be simulated, but are not easily achieved on the prototype. Furthermore, experimental problems such as signal noise and analogue conversion accuracy were eliminated from the identification task.

(iv) The simulation may be run as slowly as required, allowing the identification process to be carried out recursively, in time with the model. Experimental identification would require input-output data to be stored and processed later which is less elegant.

Identification techniques were referred to in subsection 8.2.2. A recursive least square (RLS) method was used, described in the next subsection. In comparative studies of identification methods [86], least squares methods were found to be reliable and reasonably light in computation, but susceptible to parameter "bias" (error between the mean values of estimated parameters and their true values) in the presence of noise. Fortunately this problem was eliminated in the use of simulated rather than experimental data. One advantage of least squares methods is that little initialisation is necessary; more complex methods with noise compensation require several important factors to be set a priori.

8.3.1.2 Recursive Least Squares (RLS) method [68,85]

The principles of the RLS method are outlined below, for a single input, single output ARMA (subsection 8.2.1) model without noise. This model is : $A(z^{-1})Yk = B(z^{-1})Uk$ [from (8.3)]

The predicted output at discrete time k is then :

$$y_k^* = a_1 Y_{k-1} + a_2 Y_{k-2} + \ldots + a_n Y_{k-n} + b_1 u_{k-1} + \ldots + b_n u_{k-n} \qquad (8.20)$$

The output prediction error is then

$$Y_k - Y_k^* = e(\hat{\underline{\theta}}_k) \text{ (say)} \tag{8.21}$$

where $e(\hat{\underline{\theta}}_k)$ denotes the error which is a function of the estimated parameter vector at time k, $\hat{\underline{\theta}}_k$:

$$\hat{\underline{\theta}}_k = [a_1\ a_2 \cdots a_n\ b_1\ b_2 \cdots b_n]_k \tag{8.22}$$

(that is, the parameters of $\underline{A}$ and $\underline{B}$).

If the measured input and output values used in (8.20) are denoted

$$\underline{\phi} = [Y_{k-1}\ Y_{k-2} \cdots Y_{k-n}\ u_{k-1} \cdots u_{k-n}] \tag{8.23}$$

Then the error equation (8.21) can be written

$$\begin{aligned} e(\hat{\underline{\theta}}_k) &= Y_k - Y_k^* \\ &= Y_k - \underline{\phi}_k \cdot \hat{\underline{\theta}}_k \end{aligned} \tag{8.24}$$

If a set of such errors is computed over a discrete time period

$$k = 0,1\ldots,N$$

then the least squares principle is to find the parameter vector $\underline{0}$ which minimises the sum of squares of the errors:

$$\text{minimise } J = \sum_{k=0}^{N} e^2\ (\hat{\underline{\theta}}_k) \tag{8.25}$$

The standard least squares solution is to expand (8.25) using (8.24), and take derivatives with respect to $\hat{\underline{\theta}}$. The derivatives should be zero at the minimum (quadratic function). The result may be expressed :

$$[\underline{\phi}]^T[\underline{\phi}][\underline{\theta}_{LS}] = [\underline{\phi}]^T[Y] \tag{8.26}$$

where the square brackets denote the matrices obtained by collecting each vector over the time period k=0,1,...,N of the summation, and where the subscript LS denotes the "least squares" set of parameters.

Recursive least square (RLS) is an extension of the above. Rather than collect a set of data vectors and solve the least squares equation in

one step, the parameter estimates are recursively improved at each sample time. Weighting may be introduced to reduce the importance of old data, either to improve convergence upon final values or to track changing parameters of a non-stationary system. While the principle is unchanged, the derivation of the logic for the recursive computation is quite lengthy, and details may be found in the references.

8.3.1.1 Implementation and validation

The identification method (input signal generation and RLS algorithm) was developed into a set of FORTRAN routines suitable for incorporation into SIMDCE. The purpose and structure of the individual subroutines is shown in Fig. 8.4 (code listings are included in appendix (7)) and explained below :

(i) ACTL

This is the main controlling routine, which interfaces with SIMDCE. In fact (referring to Chapter 5, Fig. 5.5) it is simply inserted as the controller subroutine, and no other changes to SIMDCE are required. If the DCE is not at steady-state then ACTL calls IPGEN to return fixed control inputs, if steady then ACTL calls IDENT to carry out identification.

(ii) IPGEN

Assigns either fixed values or pseudo-random binary sequence (PRBS) values to the control inputs as appropriate. Offsets and PRBS amplitude scaling are set in a data file so they may easily be changed.

(iii) IDENT

Carries out RLS identification. Slightly different versions were written for ARMA and ARIMA models (the ARIMA case is listed in Appendix 7). Operating parameters such as the recursion

"forgetting" factors are set in an external data file. Repeated matrix manipulation is required, so IDENT uses subroutines TMAT, MMULT, SMULT, MSUB (explained in Fig. 8.4). At each time step IDENT obtains a new PRBS bit from subroutine "PRBS", and passes it to IPGEN.

(iV) "PRBS"

Generates a wideband random bit sequence, giving a 0 or 1 at each sample interval. The routine is based upon a "Numerical Recipes" function [93].

Considerable computation is involved, particularly in the RLS algorithm (subroutine IDENT). It was therefore good practice to verify the correctness of the algorithm and the coding on a simple system before applying it to SIMDCE. A short driver program was written to initialise arrays used in the identification subroutines, simultaneously run a discrete time process model and the identification routines, and finally write the parameter estimate history to disk.

Two process models were investigated, both linear single input, single output ARMA models. The first was a test case from [86], a second order model with non-minimum phase response (that is, initial output response to a control input may be in the opposite sense to the final response).

Initial problems were encountered with apparently rather poor identification of the test cases, but no faults could be found in the identification code. It was decided to adapt the routines for inclusion in SIMDCE and proceed cautiously with the identification of DCE parameters. As will be discussed below these parameters appeared sensible - later investigation of the test program discovered an error

in updating the model state vector, which error was not repeated in SIMDCE. With the vector update corrected in the test program, the parameters of both test cases were identified exactly.

8.3.2 DCE Results

8.3.2.1 VG nozzle - boost model

The PID-type 520DCE controller used the turbine VG nozzles to control steady-state compressor speed and transient boost pressure. In both cases system airflow fundamentally was controlled. As explained in Chapter 7, the choice of compressor speed as the controlled variable at steady-state was somewhat nominal; boost could equally well be used if the schedule of optimum setpoints were mapped onto a new base of independent variables. It was therefore decided that the forthcoming controllers should explicitly control boost at steady-state as well as during transients. This would mean that a single model of the response of boost to the control inputs could be used for the controller design, rather than separate models of boost and compressor speed response. Hence the first identified model was a single input, single output (SISO) model of the response of boost pressure (at turbine inlet) to VG position control input (thus including actuator closed-loop dynamics).

As indicated earlier, an ARIMA form was chosen, that is, using control and output moves rather than absolute values :

$$A(z^{-1})\ \Delta y_{boost\ k} = B(z^{-1})\,\Delta u_{VG\ k} \qquad (8.28)$$

The DCE simulation was made to appear effectively as a continuous system simply by running the dynamic model with a timestep much shorter than the sample interval of the identifier. At this stage the sample interval must be specified; it is subject to two considerations :

(i) It is convenient to obtain the identified model at the sampling rate at which the future control system using it will operate. When implemented on the 520DCE prototype using the Dell PC-AT compatible, the PID-type controller cycled at 580Hz (Chapter 4). In view of the large increase in computation with the proposed LRPC control design, it was conservatively estimated that a rate of 50Hz could be achieved with the same hardware. This fixed hardware "cost" seemed a fair basis on which to compare alternative control designs.

(ii) The quality of the identified model may improve with reduced sampling frequency. In certain cases it may therefore be preferable to obtain a discrete time model at one frequency, and use sampled-data theory to convert to a model at a different controller frequency. This approach is sometimes used in adaptive controllers, known as dual-rate control [94] - a major advantage is that the required computational power for real-time identification is directly proportional to the sampling frequency.

In view of the above, identification was initially carried out at a 50Hz sampling rate.

The model order must also be chosen. From experience with the dynamic simulation model in SIMDCE it was known that the VG positional dynamics (actual : feedforward position) could be approximated to a second order response, while the major boost response was fundamentally first order (volume filling). It was anticipated that a second order identified model for the combined dynamics would be sufficient, given the inherent limitation of using a linearised model of a non-linear system. The appropriate model order is also related to the sampling frequency ; slower sampling filters out higher order dynamics from the sampled data.

The DCE operating range was subdivided to cope with the anticipated non-stationary dynamics. For the purposes of identification, fuel rack and VG control inputs would be set open-loop. Therefore the output load condition should take the form of output shaft speed control to give stability. Furthermore, with output shaft speed fixed the load conditions at steady-state are primarily dependent upon the open-loop rack position. Identification was carried out at low output shaft speeds and two fuel rack positions, as shown in Fig. 8.5, thus covering the important regions of the DCE speed/load range. The choice of fixed output shaft speed is conveniently a simple approximation to a practical vehicle applications, where driveshaft speed changes slowly in comparison to engine/compressor speeds and boost pressure. It should be noted that this still leaves the probability that the VG : boost parameters will vary with mean VG position. However, since the experimental and simulation work load had shown that controlled VG position was typically 8-10V (80-100 per cent of maximum restriction), all identification tests were carried out with a VG base setting of 9V, and non-stationarity was neglected over the reduced range of normal operation.

The PRBS amplitude was chosen as +/-1V, about the 9V base value. The identified ARIMA parameters for the four conditions are shown in table 8.1, where the identified model had the form

$$\Delta Y_k + a_1 \Delta Y_{k-1} + a_2 \Delta Y_{k-2} = b_1 \Delta U_{k-1} + b_2 \Delta U_{k-2} \qquad (8.29)$$

where ΔY denotes boost changes, ΔU denotes VG control moves.

From the initial values of zero (used in the absence of a priori knowledge), the parameters converged to their final values within approximately 1000 samples. A small forgetting factor was used in the

recursion; larger values led to oscillation of the parameter estimates with little reduction in the time take to approach their final values.

The results show that the autoregressive parameters (a_1,a_2) are almost stationary over the operating range. The control input parameters (b_1,b_2) are nearly constant over the output shaft speed range, but increase by a factor of approximately 3 from the low to high rack positions.

Returning to a physical understanding of the system, the increased sensitivity of boost to VG input changes at higher rack positions is thought to be due to the higher compressor speeds and bypass flows. With a higher general level of system airflow, a given VG control move - and thus change in turbine swallowing capacity - will cause a greater change in boost pressure (volume filling effect).

For the purposes of control design (described later), it was felt that this identified variation in dynamic response did not immediately justify a controller with gains scheduled according to rack position. Accordingly, approximate mean values were chosen for a_1 and a_2, along with the higher values of b_1 and b_2 (table 8.1), for use over the whole DCE operating range.

A second set of identification runs was carried out at an increased sample rate of 100Hz. These parameters obtained for possible use in the event that satisfactory control could not be achieved at 50Hz (simulated results for the PID-type controller had - as described in Chapter 7 - shown significant deterioration in control performance with the controller rate reduced to 50Hz). The 100Hz results are shown in table

8.2. The same trends are seen as at 50Hz. The autoregressive terms (a_1,a_2) are almost stationary, while the control input terms (b_1,b_2) vary only with rack position, not with output shaft speed. In this case b_1 increases by a factor of 2.5. At this higher frequency the autoregressive terms become increasingly dominant over the control input terms. The physical interpretation of this trend is that as the sampling interval diminishes the system has less time to react to control input changes, and its state at the next sample depends more upon its previous state.

It was planned as an initial step to design a boost controller using the identified model with a simple design method such as pole placement. If this design proved acceptable then it would give confidence in the identified model before moving on to less well-understood LRPC design methods. For the simpler method an ARMA model would be required, similar to the above (second order) ARIMA model of equation (8.29) but with absolute control and input values :

$$Y_k + a_1 Y_{k-1} + a_2 Y_{k-2} = b_1 U_{k-1} + b_2 U_{k-2} \qquad (8.30)$$

It was noted that if the above model were also identified at 50Hz then the concept of "fixed control cost" would be lost, since the number of computations for the pole placement design would be similar to that for the PID-type design which was run at 580Hz. However, in order to achieve a meaningful "validation" of the 50Hz model for use in the LRPC design methods, it was sensible to retain the 50Hz sampling rate for the ARMA case.

The ARMA model was identified at the same four conditions as the ARIMA case, again using a 9V median VG position with +/ -1V PRBS amplitude.

The results are shown in table 8.3. Once again it is seen that the autoregressive parameters (a_1,a_2) are reasonably constant, while the control response parameters (b_1,b_2) vary chiefly with rack position, by a factor of about three. For control design purposes, mean values of a_1 and a_2 and the values of b_1 and b_2 were again chosen, as shown in table 8.3. With an ARMA model it is possible to examine steady-state gains. Taking equation (8.29) and noting by definition that at steady-state

$$Y_k = Y_{k-1} = Y_{k-2} = Y_s, \text{ say}$$

and $$U_{k-1} = U_{k-2} = U_s, \text{ say}$$

then $$Y_s/U_s = (b_1 + b_2)/(1 + a_1 + a_2) \qquad (8.31)$$

If we then take the median VG position used in the identification (and typically during optimum operation of the DCE)

$$U_s = 9 \text{ [Volts]}$$

we obtain the steady-state boost values Y_s at the identification conditions from the appropriate identified parameters, as shown in table 8.4. Each value agreed well with the median boost pressure seen in the main SIMDCE output data files, and simply reflects the variation in steady-state boost which occurs over the DCE range. Although there are appreciable non-linearities in the "path" between steady-state fuelling and boost pressure (engine brake torque is a non-linear function of fuelling, and boost pressure is a non-linear function of compressor torque), nevertheless steady-state boost depends strongly upon rack position, as was discussed in Chapter 3. The main conclusion is that the identification method obtained accurate values of steady-state gains. With the chosen parameter values for the ARMA model, designs based on this model will overestimate steady-state boost at light loads. It should be noted that this variation could be handled by treating rack

position as an external disturbance $\underline{\xi}$ in the general ARMA equation (section 8.2.1) :

$$\underline{A}(z^{-1})\ \underline{Y}_k = \underline{B}(z^{-1})\ \underline{U}_k + \underline{C}(z^{-1})\ \underline{\xi}_k \qquad (8.3)$$

and identifying $\underline{C}(z^{-1})$, which in this case describes how boost varies with rack position. However, since rack position is an input over which we have control (rather than a truly external disturbance), a multivariable approach may be adopted. This is discussed in the next subsection.

The use of the above models for DCE control design is described in subsection 8.4.

8.3.2.2 Multivariable model

As discussed in the introduction to this section, and noted above, the DCE is amenable to a multivariable control approach. The main control loops ("direct coupling"), as used in the PID-type controller, are the control of boost by VG input and the control of engine speed by rack input. The "cross-coupling" loops are thus the effect of rack upon boost response and steady-state boost (seen in the previous subsection), and the effect of VG control input upon engine speed.

The principles of the recursive least squares identification method used in this work were outlined earlier for the single input, single output (SISO) case. The multivariable case is a straightforward extension, using input and output vectors $\underline{u}$, $\underline{y}$ rather than scalars at each sample instant, and similarly extending the parameter arrays to matrices, mutatis mutandis. The increase in computation is, however, significant, going with the square of the number of inputs or outputs. An alternative is to build up the multivariable model from a set of SISO

models. For a linear stationary system the results would be identical. With non-linearity there might be some discrepancies between the results, depending upon the severity of the non-linearities and the cross-coupling. In this case both approaches have the inherent limitation that a linear method is being applied to a non-linear system.

For the DCE it was considered that non-linearity was not great, and that therefore the multiple SISO approach would give acceptable results. This had the advantage that only minor changes were required to the existing identification code.

Identification tests of the remaining direct-coupled pair and of the two cross-coupled pairs are described in turn below, followed by their combination into a multivariable model.

(i) Rack : Engine speed model

As for the VG:boost dynamics, the appropriate form of the rack:engine speed linearised model was indicated by the non-linear model used in SIMDCE. Again the actuator closed-loop positional dynamics were approximately second order, while the major dynamics of engine speed response to engine torque changes were first order (rotational inertia). The final term was the Diesel torque delay. As discussed in Chapter 5 this is physically a pure time delay of variable length (depending upon engine speed and controller synchronisation with the engine cycle) with some influence of the cyclic combustion, but was approximated by a first order lag.

This give a fourth order response, which is clearly over-complex since the first-order inertia dynamics predominate. Control

studies on a turbocharged heavy-duty Diesel engine [82,83] had found basically a first order response of speed to fuel rack position from tests in the frequency range 0-10Hz. Identification of a first order ARIMA model in the present case gave somewhat low and unstable control input parameters over the range of conditions, possibly due to the relatively high sampling frequency of 50Hz. For comparison, the range of firing frequencies for the 520DCE is 50-130Hz under loaded conditions (1000-2600 rev/min). It was simple to incorporate a time delay (of one sampling period for the worst case at 50Hz firing frequency) in the model, but since (a) the delay was simulated as a first order element, and (b) actuator dynamics were equally important, a second order model without time delay was used. This was the same form (equation 8.29) as used for the VG:boost response, and gave stable parameter estimates, which are shown in table 8.5. It should be noted that throughout this set of runs the VG position was fixed at the 9V median position used in the VG:boost identification. The same median rack positions (6V and 9V) also were used in subdividing the DCE operating range, though of course for these tests the rack control input was perturbed, with a PRBS amplitude of +/-1V about these median positions.

The results show little parameter variation, except for a 25 per cent attenuation of the control input response (b_1,b_2) at the high speed, high load condition. It should be reiterated that all feedback control and limiting loops (such as fuel/boost ratio limiting and governor run-out) had been removed. This fall-off in response is therefore mainly attributable to the reduction in engine thermal efficiency with low air/fuel ratios (AFR) described

in Chapter 5. At this condition fuelling is obviously high and boost is barely adequate, such that changes in fuelling invoke reduced changes in torque owing to low AFR. For similar reasons, larger PRBS amplitude would give non-linearity problems at all conditions since (at this relatively fast sampling rate) large fuelling increases would give low AFR, owing to the slow dynamic boost response.

The use of the ARIMA model form with input-output moves rather than absolute values removes the major problem of variation of steady-state gain with loading conditions. The remaining limitation on the model is that the dynamic response is directly dependent upon the inertia referred to the engine shaft. For a conventional engine plus stepped transmission the load inertia (vehicle and drivetrain inertia) referred to the engine shaft changes with the square of the gear ratio selected. In a typical heavy-duty application the spread of ratios gives a change of two orders of magnitude in referred inertia. In the DCE the engine is connected to the load via a floating epicyclic, such that the engine speed can change independently of output shaft speed, and load inertia has a relatively small influence.

Thus in a vehicle the DCE engine speed dynamics may change by a small factor (with changes in vehicle load, or driveshaft torque convertor ratio), but this is a fraction of the variation caused by a stepped transmission. Fortunately in vehicle applications loose speed control is acceptable, so that stability can always be achieved. Conversely, in applications requiring isochronous governing (such as generating sets), the inertia is constant.

(ii) VG : Engine speed model

This is the first of the cross-coupling models. With experience from the above direct-coupling identification work, a second order ARIMA model was used. Furthermore, only the two most extreme conditions, namely high speed/high rack and low speed/low rack were tested. Again a VG median setting of 9V, with PRBS amplitude of +/-1V was used. The results are shown in table 8.6. The trends follow those for the effect of VG upon boost, where the control input terms (b_1,b_2) increase with rack position. The sense of these terms is negative, that is increased VG restriction depresses engine speed. This was expected by physical reasoning : greater VG restriction increases boost pressure and compressor torque. Increased compressor torque implies increased engine load and thus a reduction in engine speed.

The magnitudes of the parameters b_2 at each condition exceed those of b_1. That is, the current engine speed is more strongly affected by changes in VG control input two sample periods ago. This may reflect the additional lag in this coupling: VG changes affects boost pressure (volume dynamics) while the corresponding change in epicyclic torque levels affects engine speed (inertia dynamics).

The general magnitude of the cross-coupling (VG) effect upon engine speed is a factor of 5-10 lower than that of the direct-coupling (rack) effect (table 8.5) over the identification range, in terms of the change in engine speed [rev/min] to change in control input [Volts]. Compounded with this are the "useful" ranges of the control inputs (or actuator positions). For the

rack actuator, fuelling varies almost linearly over a 7V range from 3-10V. For the VG actuator typically only a 2V range from 8-10V gives a useful change in swallowing capacity, though VG could be made to have a greater influence with the reduced turbine size discussed in Chapter 7. Thus the rack control input will have a dominant effect upon engine speed.

(iii) Rack : Boost model

This is the second cross-coupling model. Once again a second order ARIMA model was used. The VG control input was fixed at 9V, and the rack control input was given +/-1V PRBS excitation about the median positions. The results, for the two extreme conditions, are shown in table 8.7, Some instability was seen in the estimate of b_2; the values given are mean values over a large number of consecutive samples.

The magnitudes of b_1 and b_2 may be compared to those for the direct-coupling (VG) model (table 8.1). In this case the direct-coupled parameters are roughly a factor of 5 greater in the case of b_1, while the picture for b_2 is rather unclear. The argument of relative "useful" control input ranges applied in (ii) above now applies in reverse, so that the cross-coupling effect of rack upon boost appears significant. This is consistent with steady-state relationships which have been explained earlier. Epicyclic torques are directly related to fuelling, and boost pressure is almost proportional to compressor (epicyclic) torque. That is, at steady-state, boost is a function of rack position more than VG position.

(iv) Multivariable model

As explained at the start of this subsection, the multivariable model is a combination of the four SISO models identified above. The multivariable form is, from equation (8.3):

$$\begin{bmatrix} A_{11}(z^{-1}) & A_{12}(z^{-1}) \\ A_{21}(z^{-1}) & A_{22}(z^{-1}) \end{bmatrix} \begin{bmatrix} \Delta Y_{eng.speed} \\ \Delta Y_{boost} \end{bmatrix}_K^T = \begin{bmatrix} B_{11}(z^{-1}) & B_{12}(z^{-1}) \\ B_{21}(z^{-1}) & B_{22}(z^{-1}) \end{bmatrix} \begin{bmatrix} \Delta U_{rack} \\ \Delta U_{vg} \end{bmatrix}_K^T \tag{8.32}$$

where each of the polynomials in z^{-1} comes from the appropriate SISO model, using the parameter values for control design shown in tables 8.1, 8.5, 8.6 and 8.7. To be explicit, the polynomials are:

$$A_{11}(z^{-1}) = 1 - 1.45z^{-1} + 0.53z^{-2}$$
$$B_{11}(z^{-1}) = 0.32z^{-1} + 0.078z^{-2} \qquad \text{(table 8.5)}$$

$$A_{12}(z^{-1}) = 1 - 1.88z^{-1} + 0.94z^{-2}$$
$$B_{12}(z^{-1}) = 0.048z^{-1} - 0.075z^{-2} \qquad \text{(table 8.6)}$$

$$A_{21}(z^{-1}) = 1 - 1.25z^{-1} + 0.44z^{-2}$$
$$B_{21}(z^{-1}) = 0.004z^{-1} + 0.007z^{-2} \qquad \text{(table 8.7)}$$

$$A_{22}(z^{-1}) = 1 - 1.30z^{-1} + 0.50z^{-2}$$
$$B_{22}(z^{-1}) = 0.020z^{-1} + 0.005z^{-2} \qquad \text{(table 8.1)}$$

In the next section, parametric control designs are discussed, using the SISO and multivariable models identified above.

8.4 PARAMETRIC DCE CONTROL DESIGNS

8.4.1 Deadbeat Boost Control

As a straightforward baseline for control designs using parametric models, a "deadbeat" SISO boost controller was designed, using the VG:boost ARMA model identified for this purpose (subsection 8.3.2.1).

This is a form of pole-placement control, and is computationally similar to digital PID control, being based on a combination of past output errors and control inputs. For a theoretical nth order system with a perfectly-identified linear model, deadbeat control will move the output to the setpoint (feedforward) value within n timesteps. In practice (with modelling inaccuracies, actuator saturation, etc.) deadbeat control gives good setpoint tracking, though the approach to the setpoint may be erratic [84]. The design rules may be found in [84, 85] and will not be described here; the method gives a fixed control equation directly from identified model parameters.

The structure of the DCE controller with deadbeat boost control is shown in Fig. 8.6. A listing of the controlled subroutine for SIMDCE, "DBC1.FOR", is given in appendix (4), part 4.2. The controller is similar to the finalised PID-type controller described in Chapter 7, with the exceptions that

(i) boost is controlled at all times, rather than control of compressor speed at steady-state, and of boost during transients only

(ii) the boost loop now uses deadbeat control

In Chapter 7, standardised transients were chosen for the comparison of different controllers. These included a driver demand step :

Driver demand step 50-100 per cent (5-10V), 500Nm load torque

and a load step

Driver demand 70 per cent (7V), load step 500-1000Nm

In both cases only the dynamometer inertia was simulated. In terms of the identified model this was a "worst case", in that the identification had been carried out at fixed output shaft speed (infinite load

inertia). However, as explained earlier no large variations from the identified models were anticipated with load inertia changes for the DCE. Simulation of low inertia transients would nevertheless provide an extreme test of the general applicability (and thus practical value) of the identified model.

Fig. 8.7 shows the driver demand step response with deadbeat boost control. A fixed transient boost setpoint of 3 bar was used, and the controller gave very close regulation to this during the transient (Fig. 8.7a). At approximately 4.5 seconds engine speed approaches the full driver demand value, and boost is rapidly brought down to the scheduled 'optimum' steady-state value. Beyond approximately 5 seconds engine and compressor speeds fall gradually to their final steady-state values. The scheduled feedforward boost is unchanged, but the actual boost falls as compressor speed (massflow) falls. The controller increases the VG restriction to compensate but reaches the actuator limit at approximately 7 seconds (Fig. 8.7b).

The brief "dip" in VG restriction (and thus boost) at 7 seconds was thought to be due to the extremely non-linear constraint of the VG actuator limit interfering with the action of the deadbeat algorithm. However, the undershoot at 4.5 seconds (where the boost setpoint suddenly reduces) is a fair indication of the performance of the deadbeat design.

The comparable response with the PID-type controller is shown in Fig. 8.8 (just eight important parameters are included). It should be noted that because of discrepancies between the steady-state scheduling of compressor speed (used in the PID-type case) and boost (used in the

deadbeat case), the initial conditions differ slightly. In addition transient boost setpoints for the PID-type case varied with the absolute fuelling limit, which makes comparison difficult, but overall the two designs gave similar performance. In consequence, the output shaft speed responses were very similar.

Fig. 8.9 shows the load step with deadbeat boost control (in this case transient begins at zero seconds). Over the first 0.5 seconds VG control action (Fig. 8.9b), and thus boost (Fig. 8.9a) oscillate. Three factors alter the boost setpoint (scheduled on an output shaft speed : torque base) here : first load torque increases, thus output shaft speed falls - both changing the scheduled setpoint. Then as engine speed falls, transient control is involved, changing the setpoint to 3 bar. The deadbeat controller performs poorly until the setpoint has stabilised. It must be noted that the plots are based on data recorded at 0.1 second intervals, and surely mask higher frequency VG and boost oscillations.

Engine speed has recovered at 1.7 seconds and there is a transition to the higher optimum boost pressure. However, there is again an initial dip in VG restriction and boost. The VG position is below the 10V limit, so there are no extenuating reasons for this. Overall the load acceptance is better than that achieved with PID-type control (Fig. 8.10), but this is chiefly attributable to the aforementioned difference in the transient boost setpoints used by the two controllers.

In summary, deadbeat boost control gave tight setpoint control, with DCE transient responses similar to those achieved using PID-type control. Control input instabilities occurred at some conditions, which would

probably be unacceptable in a practical vehicle application for reasons of actuator wear plus noticeable hunting of boost pressure and torques. Deadbeat designs are perhaps better suited to process control, where the emphasis is on rapid tracking of occasional setpoint changes rather than smooth response to continual setpoint changes.

8.4.2 LRPC : Boost Control

The principles of long-range predictive control (LRPC) were introduced in subsection 8.2.4, with references to the literature. An LRPC boost controller was designed, as described below.

LRPC is an optimal control technique, in that the control sequence is computed to minimise some quadratic cost function of the form :

$$J = \sum_{K=1}^{\ell} [e^2(t+k) + \beta^2 \, \Delta u^2(t+k)] \qquad (8.33)$$

where $e = r - y$, r is the feedforward reference (setpoint)

y is the output

Δu is the control input move

β is some control cost weighting factor

k denotes the number of discrete time instants (sample intervals) from the current time t

ℓ is the (finite) horizon of the cost function

If the future errors and control moves are written as vectors

$$\underline{e} = [\underline{r}-\underline{y}] \; 0 \; [e(t+2),\ldots, e(t+l)]^T$$

$$\underline{\Delta u} = [\, u(t+1), \; u(t+2),\ldots, \; u(t+l)]^T$$

then equation (8.33) can be written in vector form :

$$J = \underline{e}^T . \underline{e} + B^2 . \underline{\Delta u}^T . \underline{\Delta u} \qquad (8.33a)$$

It may be noted that the horizons of the error $\underline{e}$ and the control moves $\underline{\Delta u}$ are both $k = 1,\ldots,\ell$ here. Shorter horizons may be used for the control moves to reduce computation, and reduce control activity by postulating zero control moves beyond the horizon [89]. The latter effect may of course also be achieved by increasing β, such that control action is costed more highly in relation to output errors.

The minimum solution to equation (8.33a) is constrained, in as much as the future errors $\underline{e}$ are dependent upon the control input sequence $\underline{\Delta u}$. The relation between any postulated control input and future outputs must therefore be known. The output at a discrete time instant, y(t), can be approximated by means of the discrete finite impulse response (FIR) h(j), defined by :

$$y(t) = \sum_{j=1}^{N} h(j).u(t-j) \qquad (8.34)$$

Thus given h(j) the predicted output y* at k timesteps in the future can be written as :

$$y^*(t+k) = \underline{h}^T.\underline{u} \qquad (8.34a)$$

where $\underline{h} = [h(1), h(2),\ldots,h(N)]^T$

$\underline{u} = [u(t+k-1), u(t+k-2),\ldots,u(t+k-N)]^T$

Now the FIR may for example be obtained by sampling the system response

$u(t+k)$, $k=1,2,\ldots$

to a unit impulse

$u(t+k-j) = 1$, $j=N$

$= 0$, $0 \leq j < N$.

To put this in context, the boost pressure would be sampled in response to an impulse at the VG control input. However, since we already have an identified model of the VG : boost response (systematically built up from RLS identification tests over the operating range), it is sensible to derive the FIR from this. As noted earlier, the ARIMA form is preferred since it avoids the problem of deviation in steady-state gains. The FIR (which involves absolute values u and y) may be obtained from the ARIMA model (involving Δu and Δy) as follows :

Step response coefficients may be defined by [90]:

$$s(0) = 0;\ s(j) = s(j-1) + h(j),\ j=1,2,\ldots,N \qquad (8.35)$$

or, $$h(j) = s(j) - s(j-1),\ j=1,2,\ldots,N \qquad (8.35a)$$

The output of a step response model is taken to be the superposition of the responses to an infinite set of past control moves, each consisting of a step function added to the previous set:

$$y(t) = s(1).\Delta u(t-1) + s(2).\Delta u(t-2)+\ldots$$

$$= \sum_{j=1}^{\infty} [s(j).\ u(t-j)] \qquad (8.36)$$

To obtain a relation with the FIR coeffieicnts h(j), note that the output at time (t-1) may similarly be written

$$y(t-1) = \sum_{j=1}^{\infty} [s(j).\ u(t-j-1)] \qquad (8.36a)$$

subtracting gives

$$y(t) = y(t-1) + s(1).\Delta u(t-1) + \sum_{j=1}^{\infty} [(s(j+1)-s(j)).\Delta u(t-j-1)] \qquad (8.36a)$$

Now $s(1) = h(1)$ from (8.35).

and $s(j+1)-s(j) = h(j+1)$ from (8.35a)

substituting into (8.37) gives

$$y(t) = y(t-1) + h(1).\Delta u(t-1) + \sum_{j=1}^{\infty} [h(j+1).\Delta u(t-j-1)]$$

$$= y(t-1) + \sum_{j=1}^{\infty} [h(j).\Delta u(t-j-1)] \qquad (8.38)$$

In practice there is some finite number (N) of steps after which the output can be assumed to settle; that is, the h(j) becomes negligible. So (8.38) can approximately be written :

$$y(t) = y(t-1) + \sum_{j=1}^{N} [h(j).\Delta u(t-j)] \qquad (8.38a)$$

or $$\Delta y(t) = \sum_{j=1}^{N} [h(j)\,\Delta u(t-j)] \qquad (8.38b)$$

Equation (8.38b) shows that the FIR coefficients may be found by putting a unit step input u into the identified ARIMA model :

$$\Delta u(t-j) = 1, \quad j=N$$

$$= 0, \quad 0 \leq j < N$$

and computing the output changes $\Delta y(t)$ over N sample periods. The coefficients are then simply equal to the output change at each step.

Using this approach, FIR coefficients were obtained from the VG : boost ARIMA model. After 8 samples, the coefficients became negligible, so N=8 was chosen.

Having obtained $\underline{h}$, we can now use equation (8.34a). This showed that at each timestep the predicted future outputs $y^*(t+k)$ up to the prediction horizon $k=\ell$ may be calculated (if the horizon ℓ exceeds N, then y^* remains constant beyond N), postulating no future input changes. This gives a vector $\underline{y}^*$.

However, if future control moves are to be included in the solution, the vector of predicted outputs becomes :

$$\underline{y} \leftarrow [\underline{y}^* + \underline{H}.\ \underline{\Delta u}] \tag{8.39}$$

where $\underline{\Delta u} = [\ u(t),\ u)t+1),\ldots,\ u(t+\ell-1)\ ]^T$

$$\underline{H} = \begin{bmatrix} h(1) & & & O \\ h(2) & h(1) & & \\ \vdots & \vdots & \ddots & \\ h(\ell) & h(\ell-1) & \ldots & h(1) \end{bmatrix}$$

(note $\underline{H}$ has dimensions ℓ x ℓ in general. Again where ℓ exceeds N, elements beyond N are zero).

The least-squares optimal solution to the cost function equation (8.33), subject to the relation between future control inputs and future outputs, equation (8.39) is [88, 68]:

$$\underline{\Delta u} = (\underline{H}^T.\underline{H} + \beta^2\underline{I})^{-1}\ .\underline{H}^T.\ (\underline{r}-\underline{y}^*) \tag{8.40}$$

where $\underline{I}$ is the identity matrix.

The vector $\underline{\Delta u}$ is the series of future control moves which moves the predicted output y^* towards future reference inputs (setpoints) r in the optimal way. The final crucial point is that only the first element of $\underline{\Delta u}$ is used, giving the next control input :

$$u(t) = u(t-1) + \Delta u(t) \tag{8.41}$$

and the control equation (8.40) is computed again at each sample interval. The horizon of the cost function thus recedes at each step.

Note that unless adaptive control (real-time identification of the system model) is used, the system model parameters are fixed and therefore so are the impulse response coefficients. The matrix manipulation

$$(\underline{H}^T\underline{H} + \sqrt{\beta^2}.\underline{I})^{-1}.\underline{H}^T$$

in equation (8.40) may then be pre-computed, and the control law reduces to one array multiplication, done at each timestep.

In some forms of LRPC the FIR model is used both in the control solution and in the prediction of future outputs for the calculation of future output errors. In the present case the identified ARIMA model was used directly. The (fixed) parameter vector was combined with recursively-updated input/output data to predict outputs up to the model order (two steps ahead). Predictions beyond the model order up to the costing horizon used recursive updates of predicted output moves and absolute values in parallel.

The equations were coded into SIMDCE subroutine "LRPC.FOR", listed in Appendix (4) part 4.3. As for the deadbeat control case, the VG control inputs was used to control boost at all conditions. Engine speed control, and the various limiting controls, were again identical to the PID-type controller. The costing horizon was chosen to be equal to the limit of the FIR, at 8 sample intervals ahead. This was a compromise between robust stability with a long horizon [89], and computational load. The control cost weighting factor $\sqrt{\beta^2}$ was set from the main SIMDCE data file to facilitate tuning of the controller. Finally, the future boost setpoints $\underline{r}$ were taken to be equal to the current setpoint, since a vehicle control system can have no knowledge of future operating conditions.

Controller performance was assessed using the simulated transients used for previous designs, namely

(i) 5Ø-1ØØ per cent (5-1Ø V) driver demand step, 5ØØNm load

(ii) 7Ø per cent (7 V) driver demand, 5Ø-1ØØØNm load step

- both with the dynamometer inertia.

Initial runs with zero control cost ($\beta_2 = Ø$) led to oscillatory control inputs, as anticipated. Gradually increasing β_2 achieved smooth control. The weighting has the effect of attenuating the control inputs, and this improves stability as in conventional feedback of well-behaved systems.

The driver demand step response (fig. 8.11) was very similar to the deadbeat control case (fig.8.7), however, the unwanted dips in boost seen for the deadbeat case were entirely absent. Very tight regulation to the boost setpoints was achieved. Output shaft speed response was identical to the deadbeat case, and thus similar again to the PID-type case.

The load step response (fig.8.12) was superior to the deadbeat case (fig.8.9). The VG restriction was kept at the maximum throughout the first second of the transient, so that boost rose immediately and engine and output shaft speeds fell less sharply. Nevertheless both controllers achieved the 3 bar boost setpoint within the same time - this was due to the inherent differential supercharging effect of the DCE with falling output shaft speed; in the deadbeat case extra bypass flow was generated over the first Ø.5s which was then rapidly "converted" to boost as the VG nozzles were closed. However, the better load acceptance in the LRPC case enabled transition back to steady

state (maximum efficiency) control at approximately 1.3s, compared to 1.9s for the deadbeat case. Furthermore the unwanted deadbeat control oscillations were again absent in the LRPC case.

In summary, the LRPC design gave very smooth and tight boost control, leading to similar driver demand step response and improved load acceptance in comparison with the PID-type controller. Tuning was reduced to a single parameter (control cost weighting), which may be considered to trade off control response and stability. Clearly this was not an exhaustive trial, but the transient steps were large, and the inertia condition was as far away as possible from that at which the system model was identified, testing the robustness of the method.

8.4.3 Multivariable LRPC

The development of a multivariable LRP Controller was carried out in three stages. First an acceptable LRPC design was achieved for the rack : engine speed SISO loop. Secondly this and the above VG : boost SISO LRP Controller were used simultaneously, to provide a baseline for the final multivariable LRP Controller.

8.4.3.1 Rack : engine speed LRPC

The initial rack : engine speed LRP Controller was designed in the same way as the VG : boost controller described above. In the PID-type controller, 100 per cent (10V) driver demand was interpreted as an engine speed demand of 2800 rev/min, giving an 8 per cent "runout" above the rated engine speed of 2600 rev/min. This gave loose, stable control, analogous to a mechanical governor. However, LRPC gives

setpoint tracking, so for this design 1ØØ per cent driver demand was interpreted as an engine speed demand of 26ØØ rev/min. The VG control input was fixed at 9V so that the engine speed control could be assessed alone at this stage.

Using the standard driver demand step (5 - 1ØV at 5ØØNm load) as the test case, persistent control oscillations were seen. A typical case is shown in fig.8.13. Large control cost weighting factors were required to smooth these oscillations. In view of the performance achieved by the boost LRP Controller, these problems were unexpected. The identified rack : engine speed model was checked by incorporating it into the validation program mentioned in subsection 8.3.1.3. The engine speed response predicted by the identified model to a sequence of rack control inputs was very similar to that predicted by SIMDCE under the same conditions. Confidence in the identified model was thus re-affirmed.

The large control inputs were attributed to the discrepancy between the costing horizon (8 sample intervals equates to Ø.16s at 5Ø Hz) and the open-loop response of engine speed; that is the control design aimed for unachievable closed-loop dynamics. To reduce oscillation around setpoints a large control cost weighting was introduced, while to reduce overshoot with step changes in the driver demand setpoint a more realistic reference model was introduced, as described below.

The output error vector

$$\underline{e} = \underline{r} - \underline{y}^{*} \qquad \text{(from 8.33)}$$

was re-defined as

$$\underline{e} = \underline{y}_{mr} - \underline{y}^{*}$$

where $\underline{y}_{mr}$ is a model reference vector. The reference model is chosen such that for a rapid change in the feedforward r, y_{mr} changes in a way which the predicted output y^{*} could realistically be expected to follow. A first order reference model was chosen:

$$y_{mr}(t+k) = \alpha . y_{mr}(t+k-1) + (1-\alpha).r(t) \qquad (8.42)$$

where $\alpha = e^{-\gamma/Ts}$

T_s = sampling interval (Ø.Ø2s)

γ = a chosen time constant

A factor $\gamma/T_s = Ø.1$ was chosen, implying that for an instantaneous step change in driver demand (r), the feedforward (y_{mr}) will cover this step over a Ø.2s period.

This gave smooth and nevertheless tight engine speed control, as shown in results discussed in the next subsection.

8.4.3.2 Dual SISO LRPC

The two single input, single output (SISO) LRP Controllers developed above were next used simultaneously, with no compensation for cross-coupling. The response to the standard driver demand step (fig.8.14) was practically identical to that for the previous case with conventional engine speed control (fig.8.11). Rack and VG control inputs were well-behaved, boost was tightly controlled to the setpoints

with slight over- and under-shoot, and engine speed response was smooth and stable.

The standard load step response (fig.8.15) was slightly improved (compared with fig.8.12), owing to the absence of engine speed droop. The higher final engine speed gave a higher final output shaft speed. Both control inputs were again well-behaved.

Given the excellent control performance obtained with these two independent SISO loops, it seemed that little could be gained by multivariable compensation. The control method was sufficiently robust to handle non-linearities such as actuator limits and fuel/boost ratio (smoke) limits, and to overcome cross-coupling effects. However, the multivariable extension was tested, for completeness.

8.4.3.3 Multivariable (decoupling) LRPC

In this context, "multivariable" control involves the co-ordination of the two SISO loops to improve their performance. In the LRPC design this may be done by extending the SISO ARIMA models and impulse response (FIR) models to incorporate the cross-coupling terms, as explained below.

Each SISO ARIMA model output prediction may be written:

$$\Delta y^{*}(k) = -a_1 . \Delta y(k-1) - a_2 . \Delta y(k-2) + b_1 . \Delta u(k-1) + b_2 . \Delta u(k-2) \quad \text{(from 8.29)}$$

which in vector form is:

$$\Delta y^{*}(k) = \underline{\phi}_k^T . \underline{\theta}_k \qquad (8.43)$$

where $\underline{\phi}_k = [\, a_1 \quad a_2 \quad b_1 \quad b_2 \,]^T$ (parameter vector)

$$\underline{\theta}_k = [-\Delta y(k-1) \quad -\Delta y(k-2) \quad \Delta u(k-1) \quad \Delta u(k-2)]^T$$

(data vector)

To incorporate the cross-coupling effect of the other control input (denoted $\Delta u'$, say), the parameter vector is extended to

$$\underline{\phi}_{mv} = [a_1 \quad a_2 \quad b_1 \quad b_2 \quad b'_1 \quad b'_2]^T$$

where b'_1, b'_2 are the control input parameters of the appropriate cross-coupling model, and the data vector is extended to

$$\underline{\theta}_{k\,mv} = [-\Delta y(k-1) \quad -\Delta y(k-2) \quad \Delta u(k-1) \quad \Delta u(k-2) \quad \Delta u'(k-1) \quad \Delta u'(k-2)]^T$$

The output prediction is then

$$\Delta y^*_k = \underline{\phi}^T_{k\,mv} \cdot \underline{\theta}_{k\,mv} \qquad (8.43a)$$

The FIR models may be extended in a similar way, so that predictions beyond the model order also include cross-coupling effects.

The optimal solution given by the control equation (8.40) with the extended vectors thus accounts for the cross-coupling influence of past control inputs.

A listing of the subroutine in which this was implemented ("MVPC.FOR") is given in Appendix 4 part 4.4.

The standard driver demand step response (fig.8.16) was similar to that obtained without decoupling compensation (fig.8.14), but with slight oscillation of the VG control and very slight oscillation of the rack control. The compensation appeared in fact to have created a feedpath between the two loops which slightly worsened the controller

performance.

The standard load step response (fig.8.17) was practically identical to that without decoupling (fig.8.15). In this transient the control inputs happened never to change simultaneously - each one was constrained at the 10V actuator limit whenever the other was changing. Thus the prediction models saw no cross-coupling input moves.

In summary, this brief evaluation of decoupling LRP Control could not improve upon the very good performance already achieved with independent LRPC loops. However, a slightly different aspect of multivariable control, namely the optimal control of multiple outputs by a smaller number of inputs, was also of interest as discussed in the next section.

8.5 PRACTICAL APPLICATIONS OF OPTIMAL CONTROL

For research purposes, transient control of the DCE has involved the regulation of two parameters (engine speed and boost pressure) for maximum response, using two primary control inputs (rack and VG). In a practical vehicle application, emissions legislation and commercial demands for low route fuel consumption would extend the list of important system outputs to:

(i) "response"
(ii) fuel efficiency
(iii) emissions.

"Response" fundamentally means torque response. In the DCE case torque response demand was implied by the strategy of boost (3 bar) demand, which was known generally to enable the fastest output torque response; a similar strategy is commonly used in transient control of VG turbocharged engines.

Fuel efficiency is usually ignored in transient operation; its deterioration is accepted in favour of maximum response.

Emissions may, for the purposes of this discussion, be restricted to NOx and particulates - these being of greatest legislative concern - and smoke.

The engine controller will influence all of the five major operating parameters listed above, generally with the use of fewer control inputs. The 520DCE prototype has three control inputs (fuel rack, VG and injection timing) which are all significant. Injection timing has previously been accepted as having secondary importance, but its effect upon emissions is major, and in turn the optimisation of NOx / particulates by injection timing control might allow fuelling increases under some conditions. VG turbocharged engines with electronic fuel injection equipment (FIE) have control inputs analogous to the 520DCE.

In principle, torque, fuel efficiency and emissions responses to each control input may be represented as identified models. There will, however, be non-linearity and non-stationarity problems with all these parameters, which may require localised linear models to be obtained over schedules of points in the engine / actuator operating ranges. If useable linearised models can be achieved, the optimal control methods (such as LRPC) enable a complex multivariable task like the above (3

inputs, 5 outputs) to be handled in a systematic way. Thus transient response can be optimised within emissions constraints, and furthermore transient fuel consumption may also be considered.

The cost function required is a multivariable case of equation (8.33a):

$$J = \underline{E}^T . \underline{Q}_1 . \underline{E} + \underline{\Delta U}^T . \underline{Q}_2 . \underline{\Delta U} \quad (8.33b)$$

where $\underline{E} = [\ \underline{e}_1\ \ \underline{e}_2\ \ldots\ \underline{e}_n\ ]$ for n outputs

$\underline{e} = [\ e(t+1)\ \ e(t+1)\ \ldots\ e(t+1)\ ]$ for cost horizon 1.

That is, $\underline{\Delta E}$ is a matrix composed of n vectors of output errors, up to a costing horizon of 1 sample periods.

Similarly $\underline{\Delta U} = [\ \underline{\Delta u}_1\ \ \underline{\Delta u}_2\ \ldots\ \underline{\Delta u}_m\ ]^T$ for m inputs

$\underline{\Delta u} = [\ \Delta u(t+1)\ \ \Delta u(t+2)\ldots\ \Delta u(t+1)]$ for cost horizon 1

That is, $\underline{\Delta U}$ is a matrix composed of m vectors of control input moves, up to the costing horizon.

$\underline{Q}_1$, $\underline{Q}_2$ are weighting matrices for the relative cost of the various input moves and output errors.

The output error e (being the difference between the feedforward setpoint and the corresponding output) clearly is dependent on the choice of the setpoint. It would therefore seem reasonable to vary the setpoint in accordance with some a priori knowledge of what is realistically achievable at a given operating condition. For example, fuel efficiency setpoints might simply be scheduled as the steady state optimum levels achieved. Thus the effect of the chosen fuel efficiency

error cost factor in Q_1 would remain reasonably constant over the engine operating range.

One programme of research to reduce transient emissions of a VG turbocharged engine by optimal VG control was recently reported in [9]; however, the final implementation was simplified to boost control, since the identified emissions models showed that maximum boost was always desireable. Fuel efficiency was not considered, and this deteriorated. Theoretical work on a marine engine control system [67], using optimal control of fuelling for fuel efficiency, achieved improved efficiency under transient conditions compared to open loop and PI speed control.

There is clearly some potential for the use of optimal methods in powertrain control, given the continual demand for better efficiency and transient response within tighter emissions constraints, and the increasing interest in electronic FIE and VG turbochargers. However, the increased complexity of the controller must be justified by worthwhile performance (response, emissions, efficiency) improvements and/or reduced development time.

List of Figures

List of Tables

TABLE 8.1

VG : Boost ARIMA parameters, 50 Hz

DCE CONDITION		PARAMETERS			
No/s [rev/min]	Rack [V]	a 1	a 2	b 1	b 2
2900	9	-1.30	0.50	0.021	0.005
2900	6	-1.12	0.44	0.007	0.002
1100	9	-1.32	0.51	0.022	0.006
1100	6	-1.29	0.50	0.009	0.002
Values used for control design:		-1.3	0.5	0.02	0.005

TABLE 8.2

VG : Boost ARIMA parameters, 100Hz

DCE CONDITION		PARAMETERS			
No/s [rev/min]	Rack [V]	a 1	a 2	b 1	b 2
2900	9	-1.70	0.78	0.0049	0.0019
2900	6	-1.62	0.74	0.0019	0.0006
1100	9	-1.74	0.80	0.0051	0.0019
1100	6	-1.71	0.80	0.0021	0.0008

TABLE 8.3

VG :Boost ARMA parameters, 50Hz

DCE CONDITION		PARAMETERS			
No/s [rev/min]	Rack [V]	a 1	a 2	b 1	b 2
2900	9	-1.48	0.58	0.030	0.008
2900	6	-1.32	0.38	0.011	0.002
1100	9	-1.50	0.60	0.030	0.008
1100	6	-1.39	0.50	0.014	0.004
Values used for control design:		-1.45	0.55	0.03	0.008

TABLE 8.4

VG : Boost model steady state values

DCE CONDITION		ARMA MODEL STEADY STATE BOOST AT VG = 9V
No/s [rev/min]	Rack [V]	[bar]
2900	9	3.42
2900	6	1.95
1100	9	3.42
1100	6	1.47
Using values chosen for control design purposes:		3.42

TABLE 8.5

Rack:engine speed ARIMA parameters, 50Hz

DCE CONDITION		PARAMETERS			
No/s [rev/min]	Rack [V]	a 1	a 2	b 1	b 2
2900	9	-1.44	0.54	0.255	0.059
2900	6	-1.46	0.52	0.320	0.077
1100	9	-1.44	0.52	0.325	0.078
1100	6	-1.45	0.54	0.350	0.080
Values used for control design:		-1.45	0.53	0.32	0.078

TABLE 8.6

VG:engine speed ARIMA parameters, 50Hz

DCE CONDITION		PARAMETERS			
No/s [rev/min]	Rack [V]	a 1	a 2	b 1	b 2
2900	9	-1.86	0.925	-0.048	-0.075
1100	6	-1.89	0.960	-0.024	-0.030
Values used for control design:		-1.88	0.94	-0.048	-0.075

TABLE 8.7

Rack : Boost ARIMA parameters, 50Hz

DCE CONDITION		PARAMETERS			
No/s [rev/min]	Rack [V]	a 1	a 2	b 1	b 2
2900	9	-1.29	0.48	0.0041	0.007
1100	6	-1.22	0.40	0.0023	0.0005
Values used for control design:		-1.25	0.44	0.004	0.007

PREDICTION OBSERVER - FUNCTION SCHEMATIC

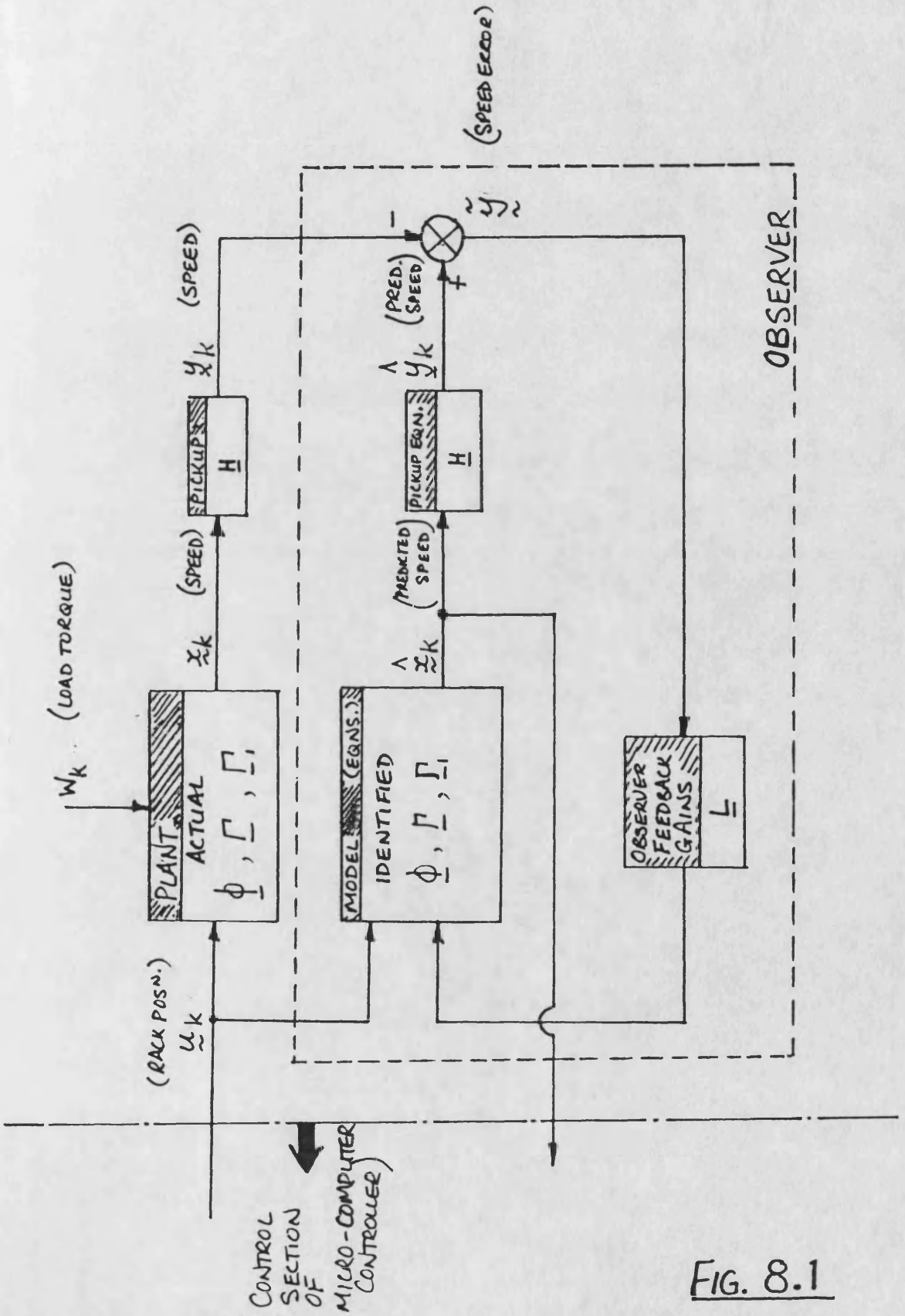

FIG. 8.1

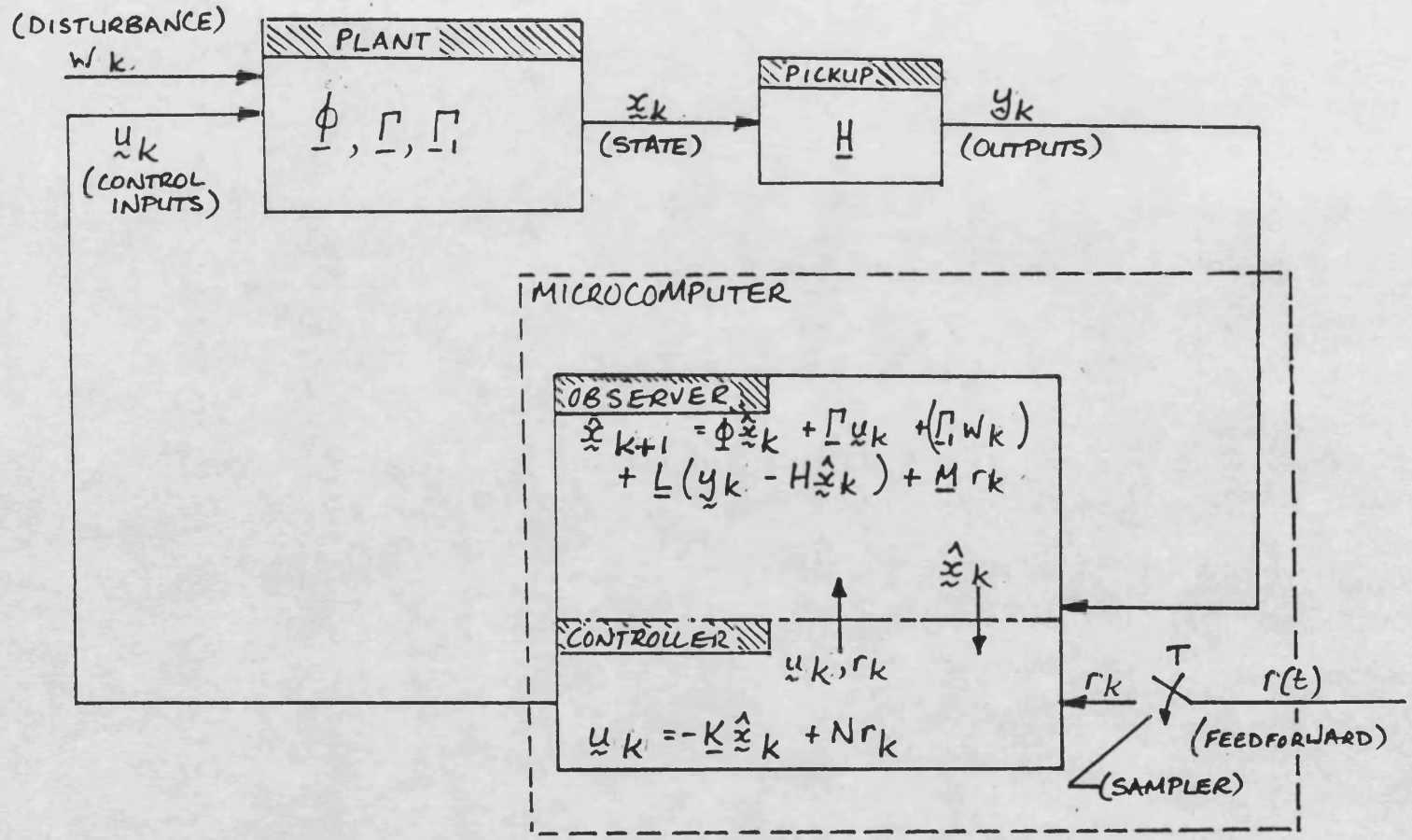

FIG. 8.2

CONTROLLER - FUNCTION SCHEMATIC

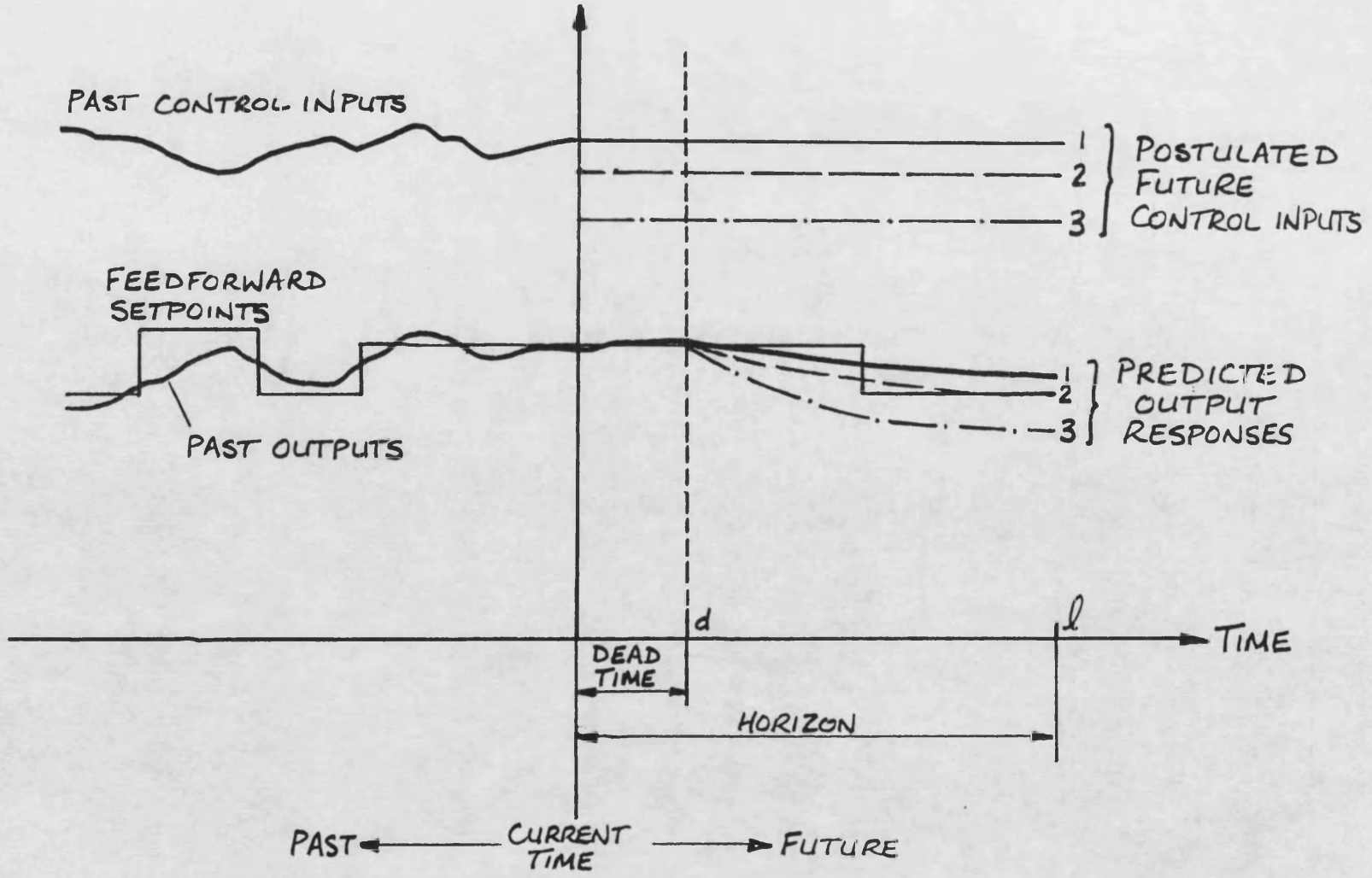

FIG. 8.3 LONG RANGE PREDICTIVE CONTROL - PRINCIPLES

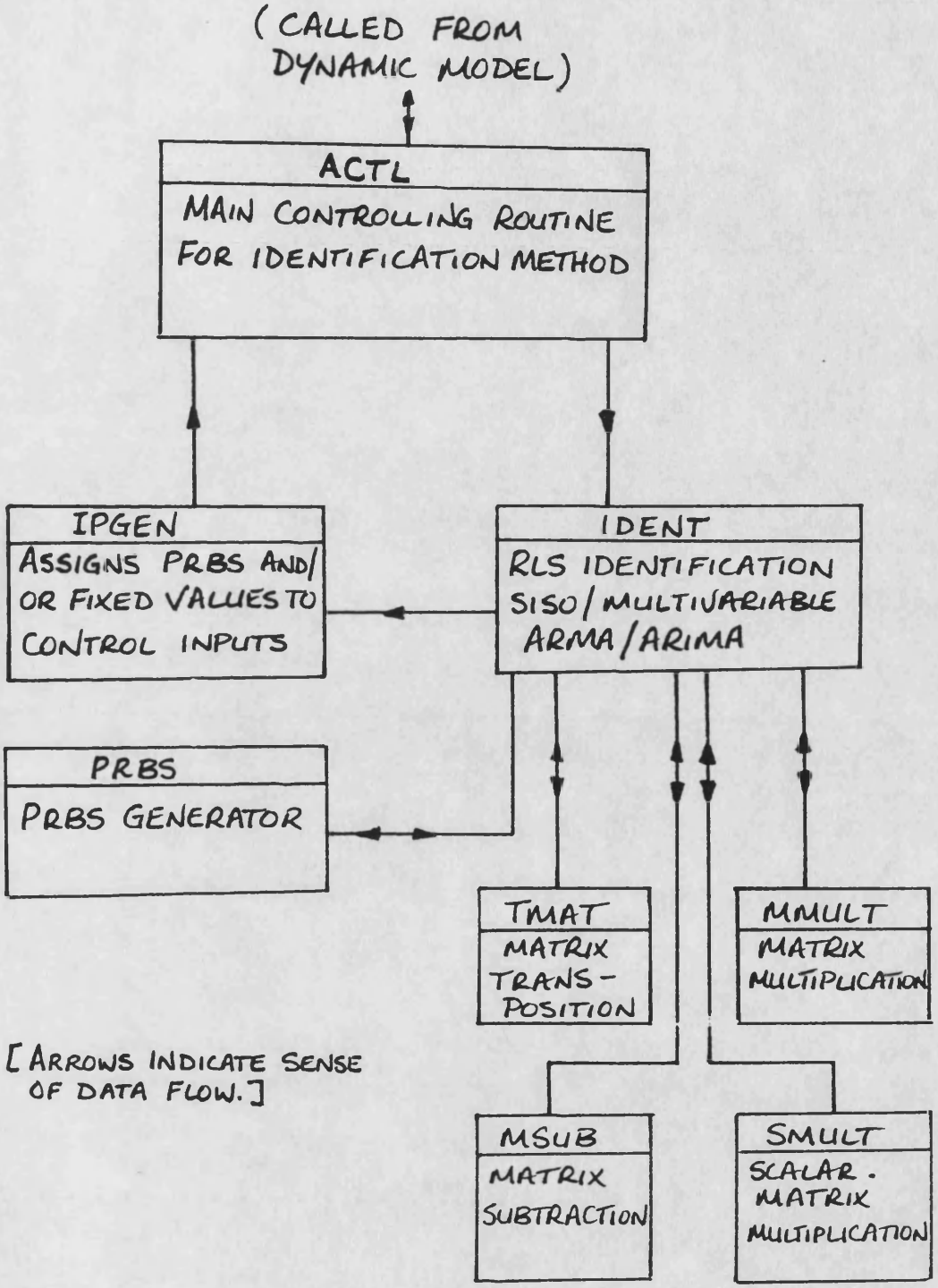

FIG. 8.4 IDENTIFICATION ROUTINES

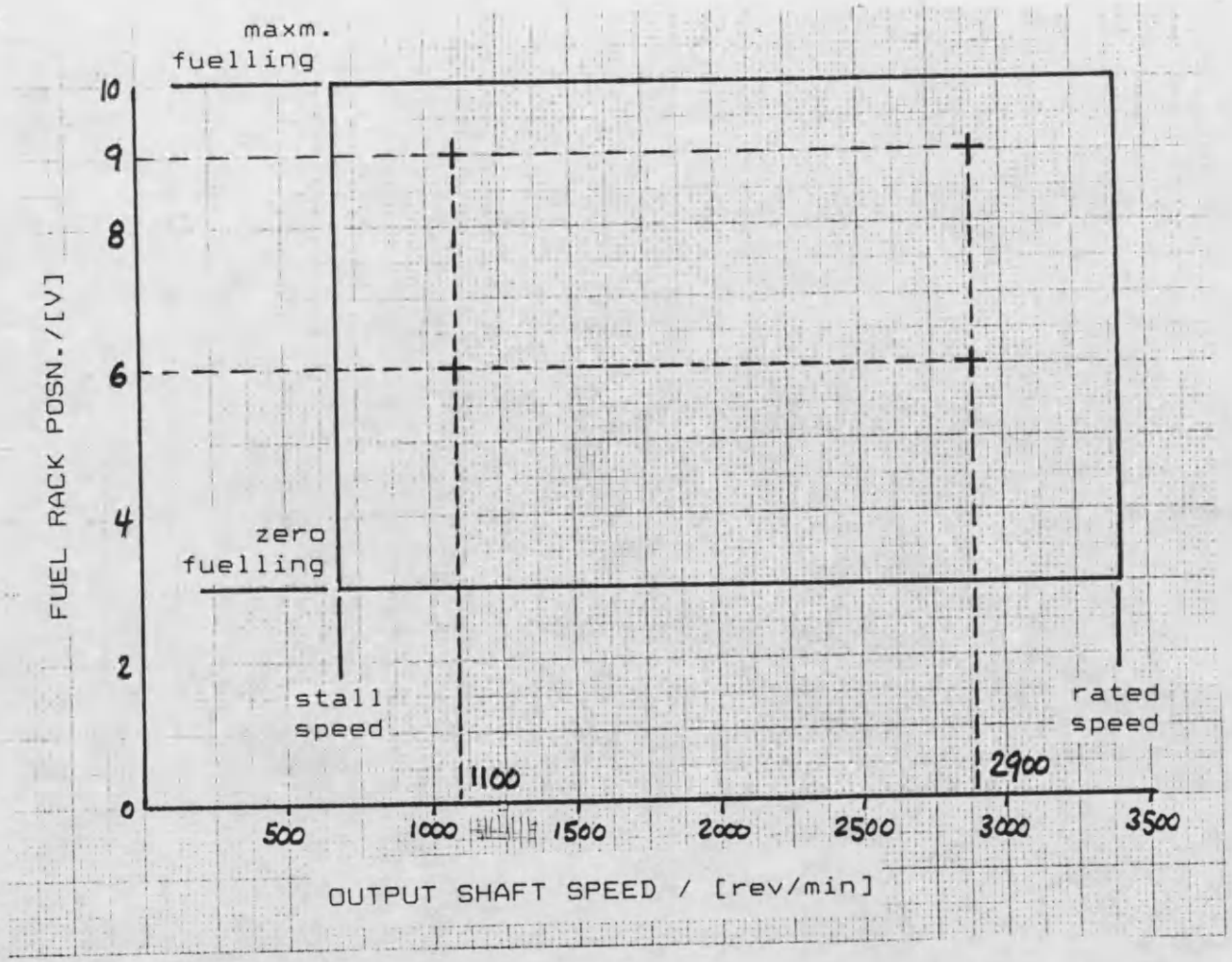

+ identification carried out at these 4 points.

Note: fuelling starts at 3 V for mechanical reasons.

FIG. 8.5 IDENTIFICATION POINTS IN DCE SPEED : RACK OPERATING RANGE

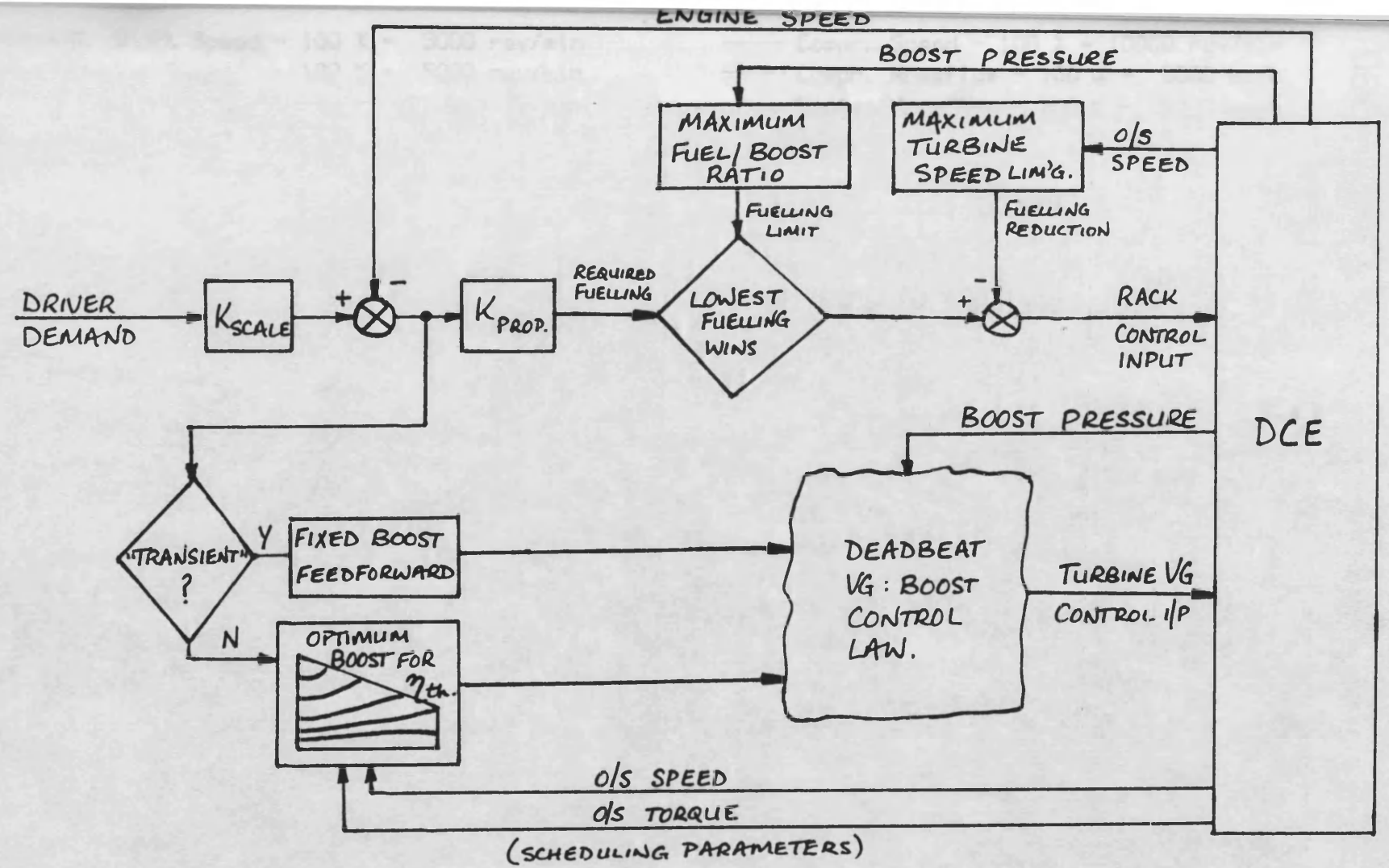

FIG. 8.6 CONTROLLER SCHEMATIC - DEADBEAT BOOST CONTROL.

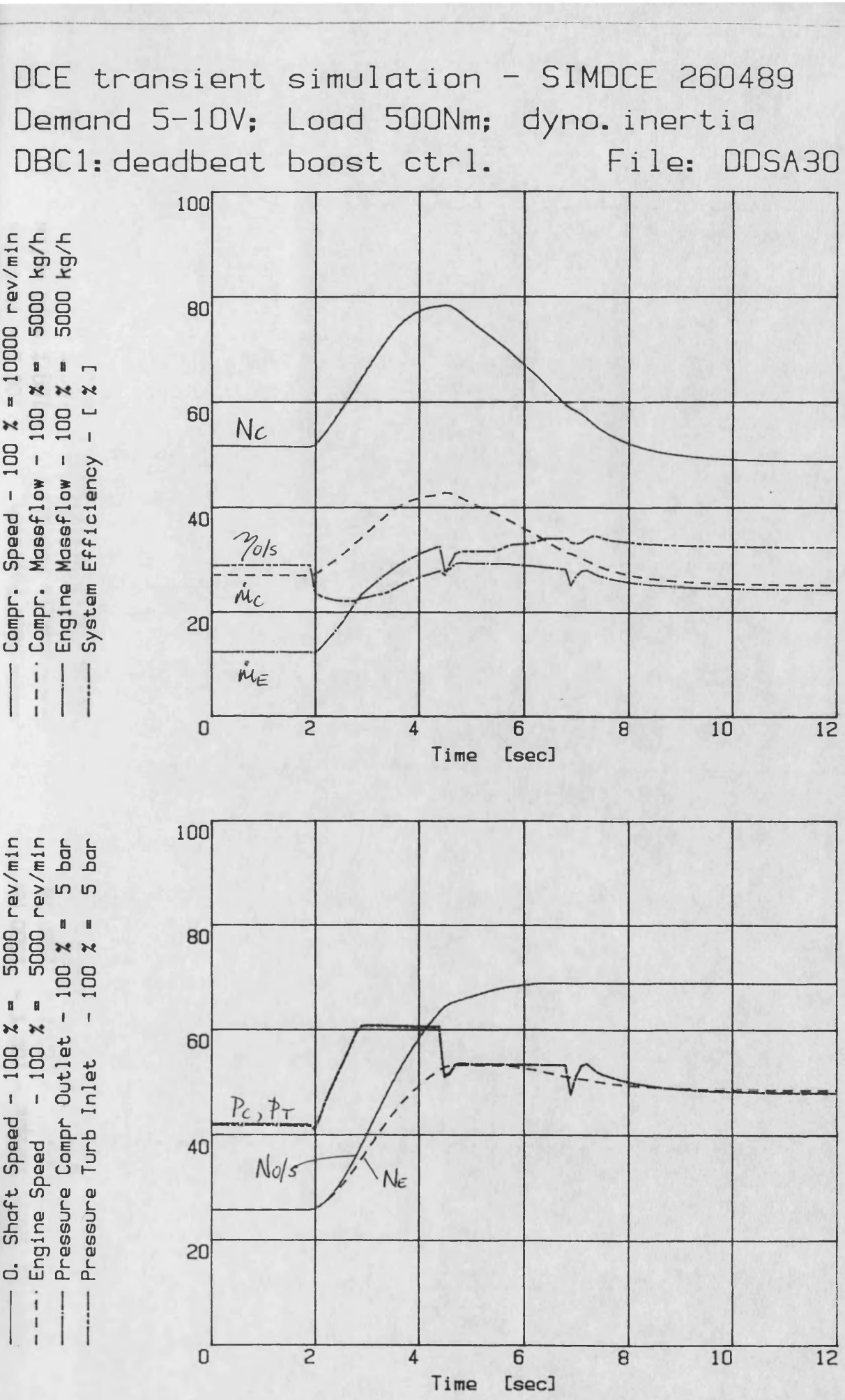

FIG. 8.7A driver demand step - deadbeat boost control

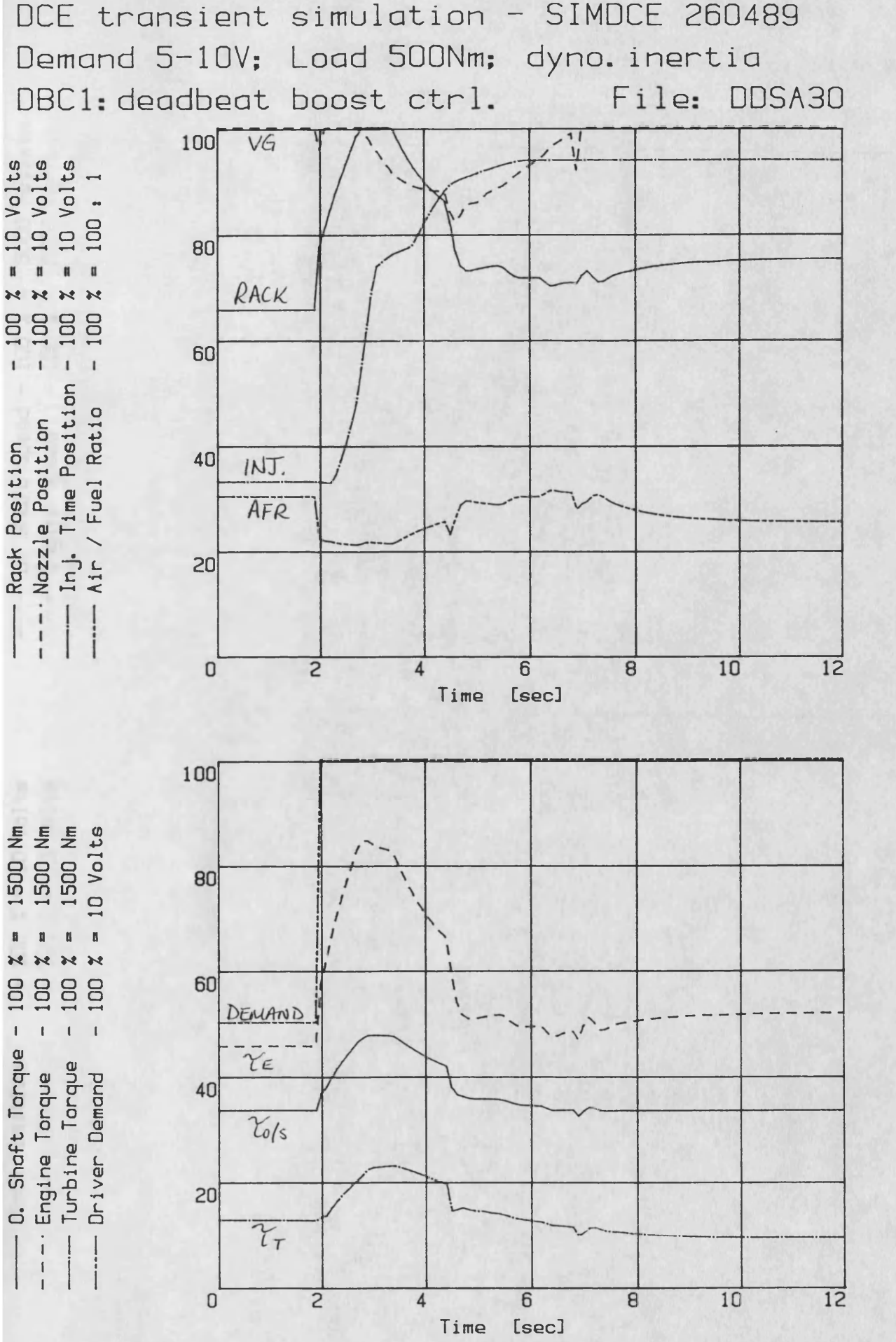

FIG. 8.7B. driver demand step - deadbeat boost control

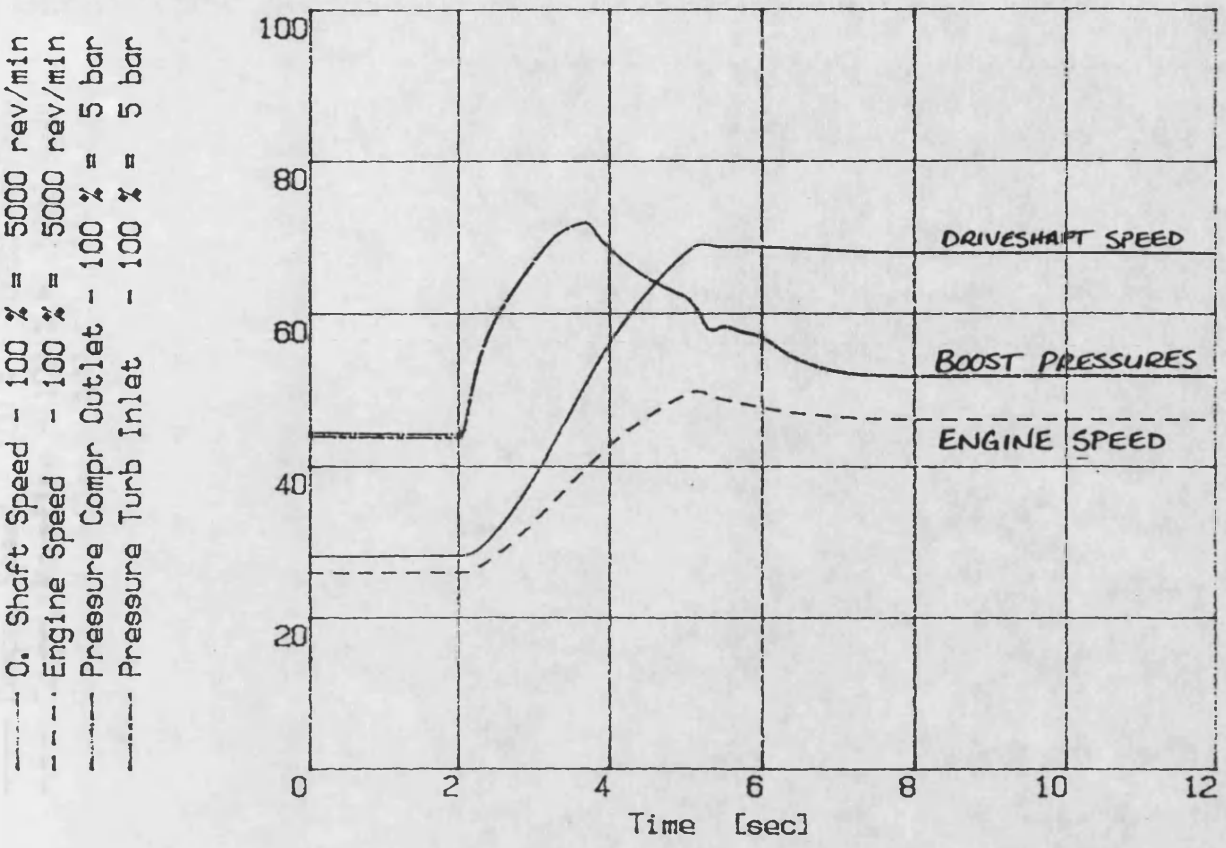

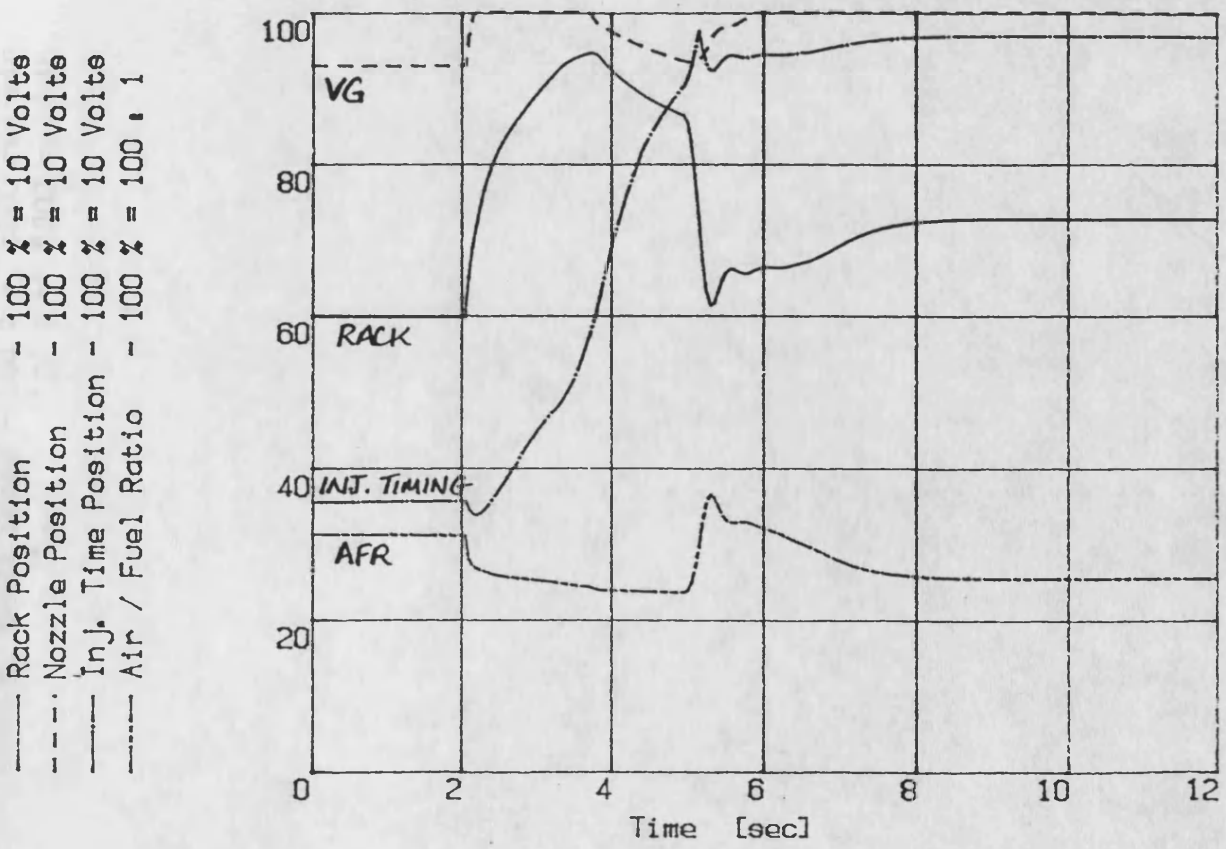

FIG. 8.8 driver demand step - PID-type control

DCE transient simulation - SIMDCE 260489
Demand 7V; Load 500-1000Nm; dyno. inertia
DBC1: deadbeat boost ctrl. File: dlsb1.

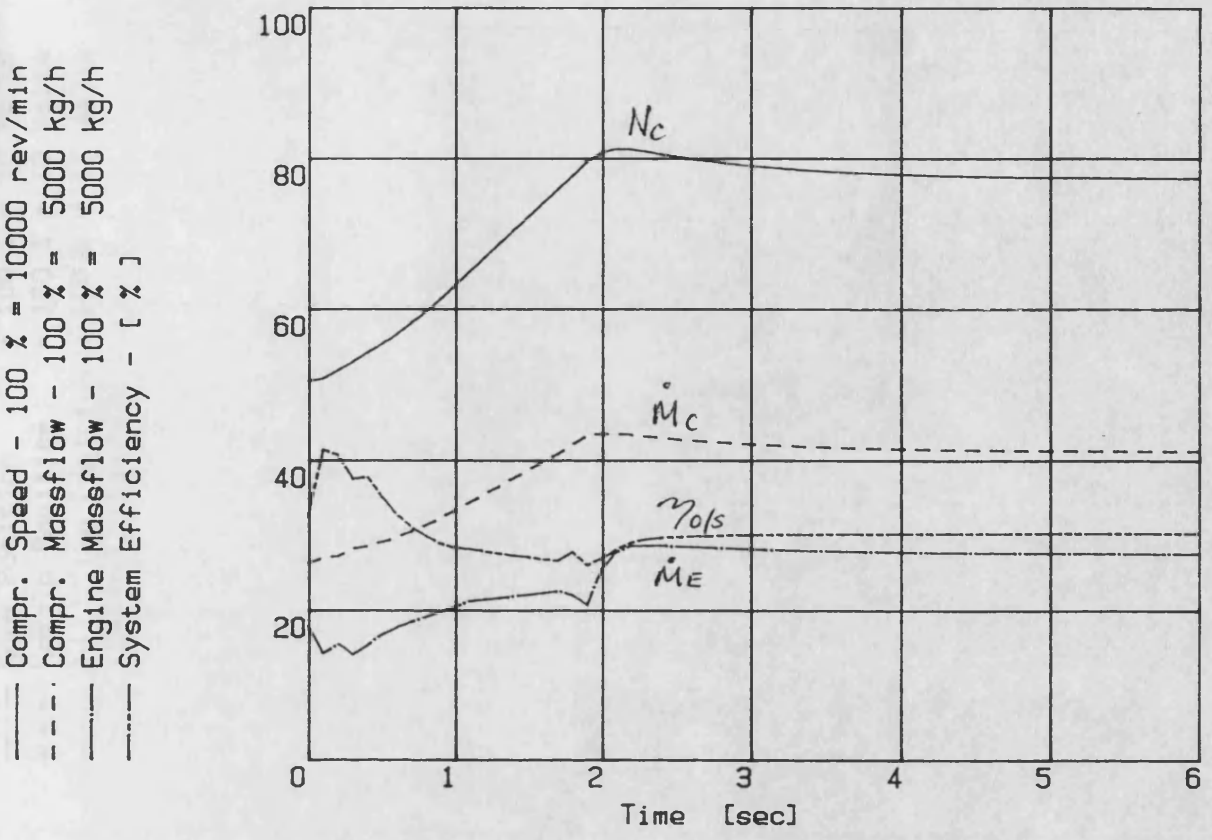

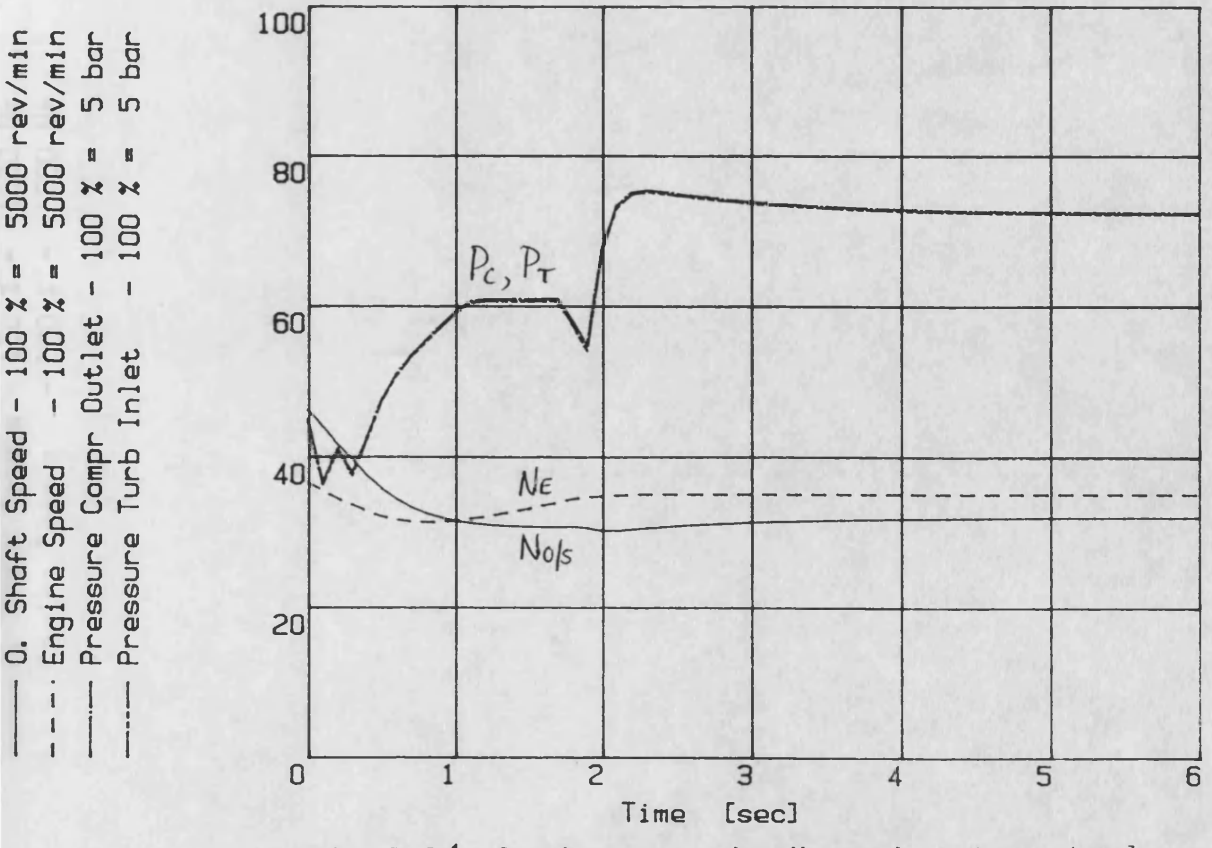

FIG. 8.9A load step - deadbeat boost control

DCE transient simulation - SIMDCE 260489
Demand 7V; Load 500-1000Nm; dyno. inertia
DBC1: deadbeat boost ctrl. File: dlsb1.

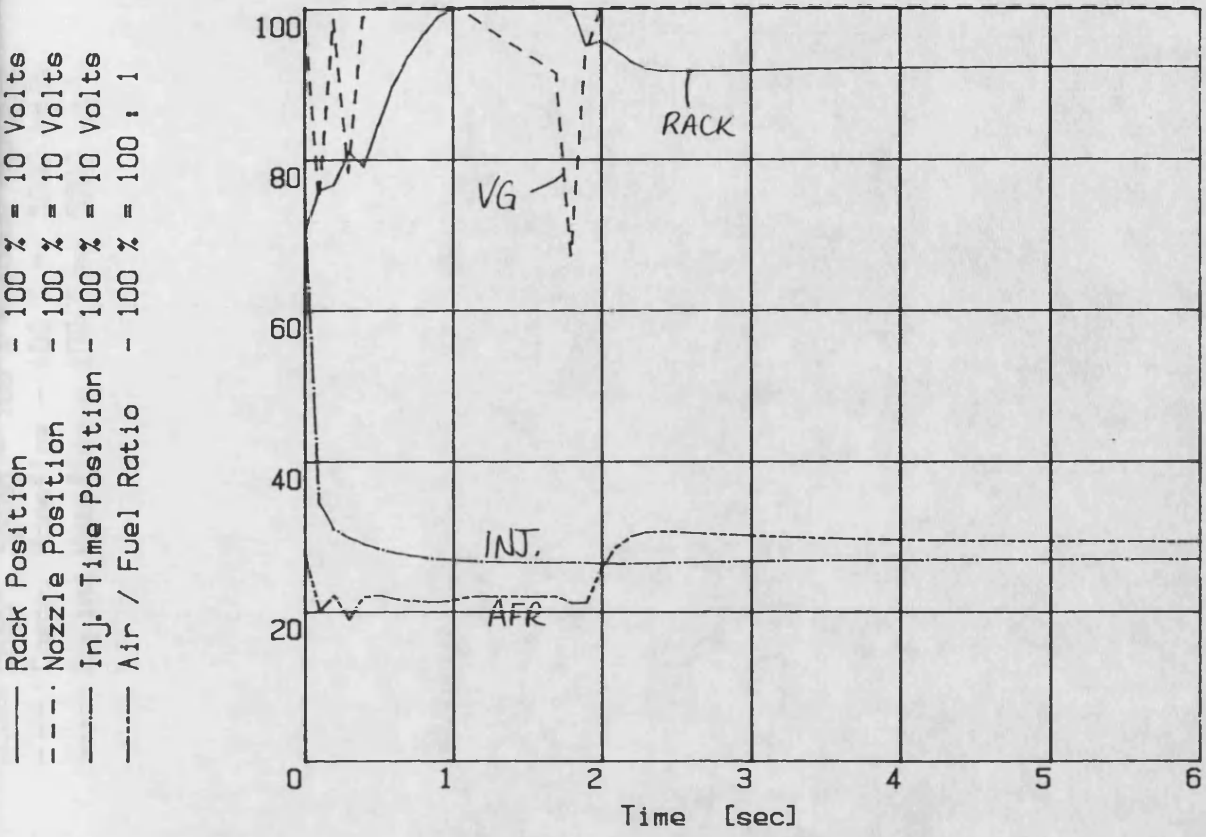

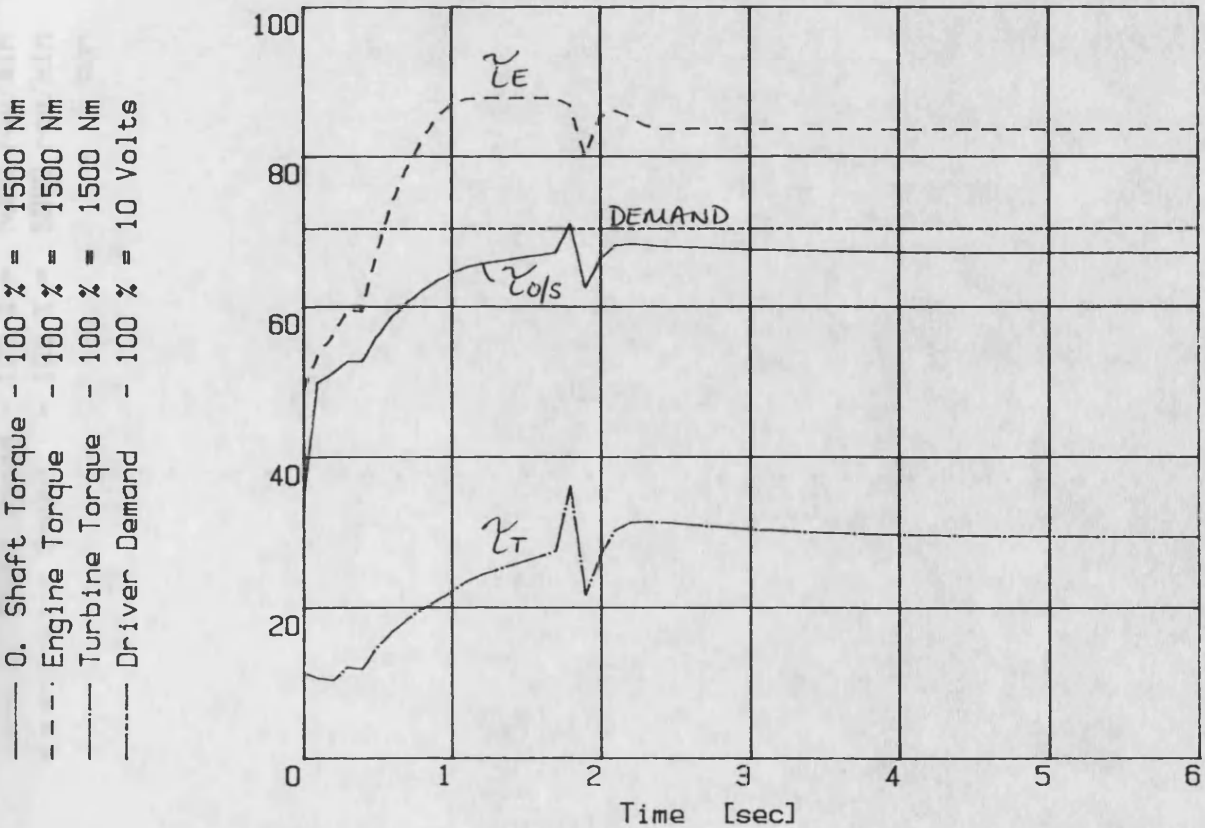

FIG. 8.9B load step - deadbeat boost control

DCE transient simulation - SIMDCE 170289
Demand step 7- 7V; Load step 500-1000Nm
CTLRK2: low AFR File: LSB2.DAT

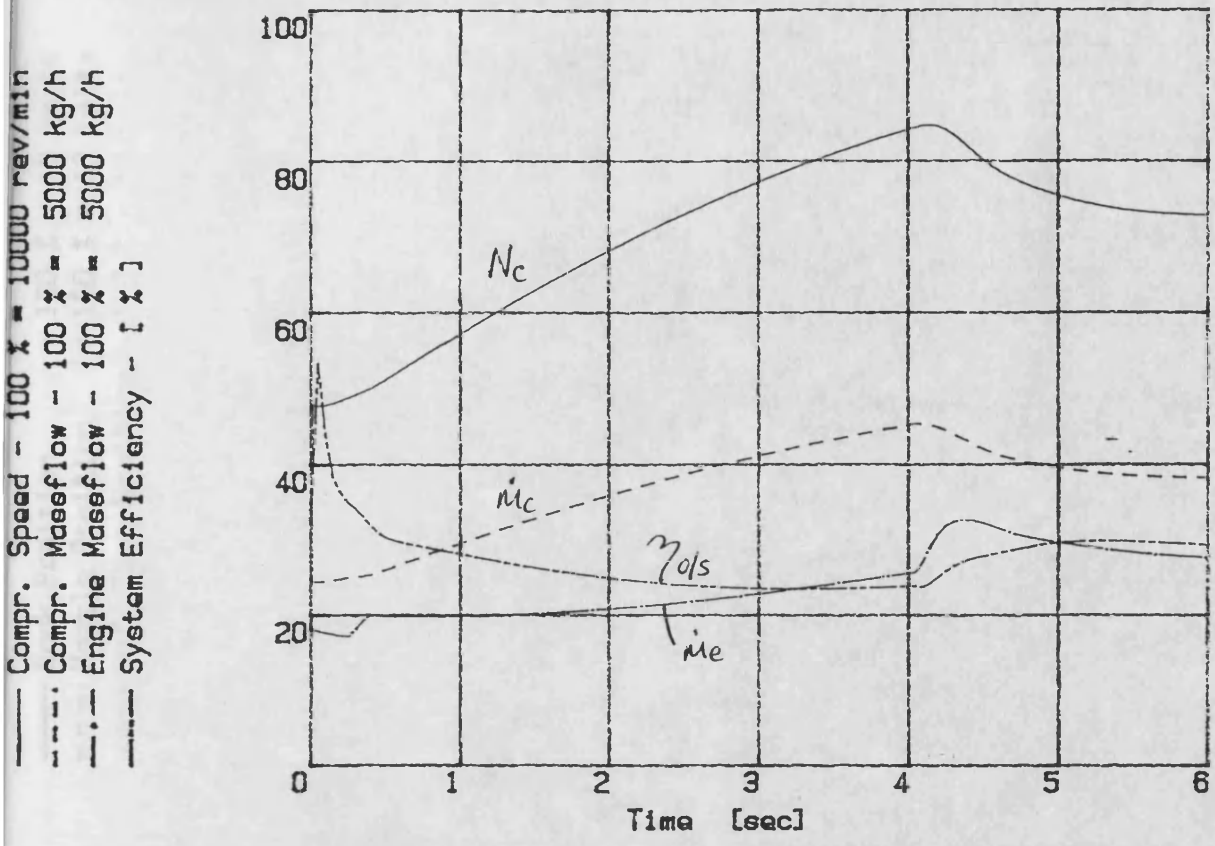

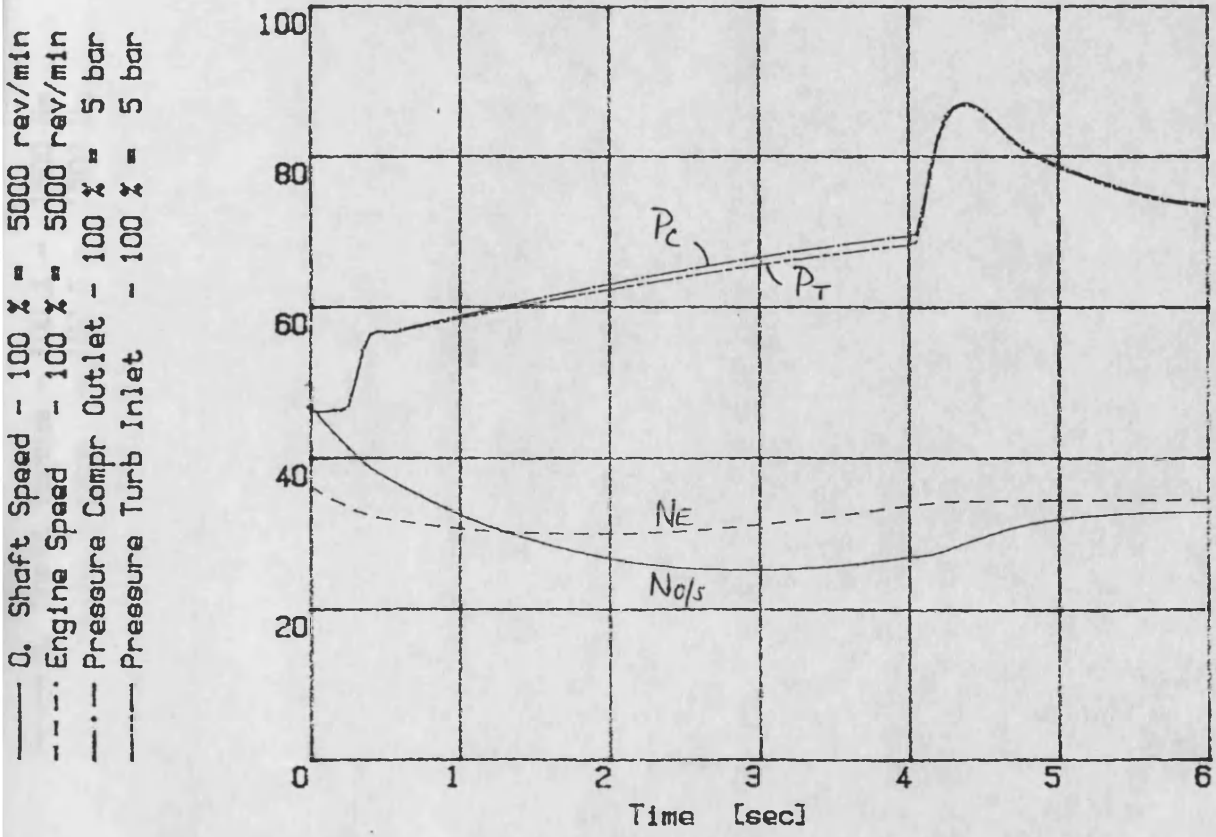

FIG. 8.10A load step - PID-type control

DCE transient simulation - SIMDCE 170289
Demand step 7- 7V; Load step 500-1000Nm
CTLRK2: low AFR File: LSB2.DAT

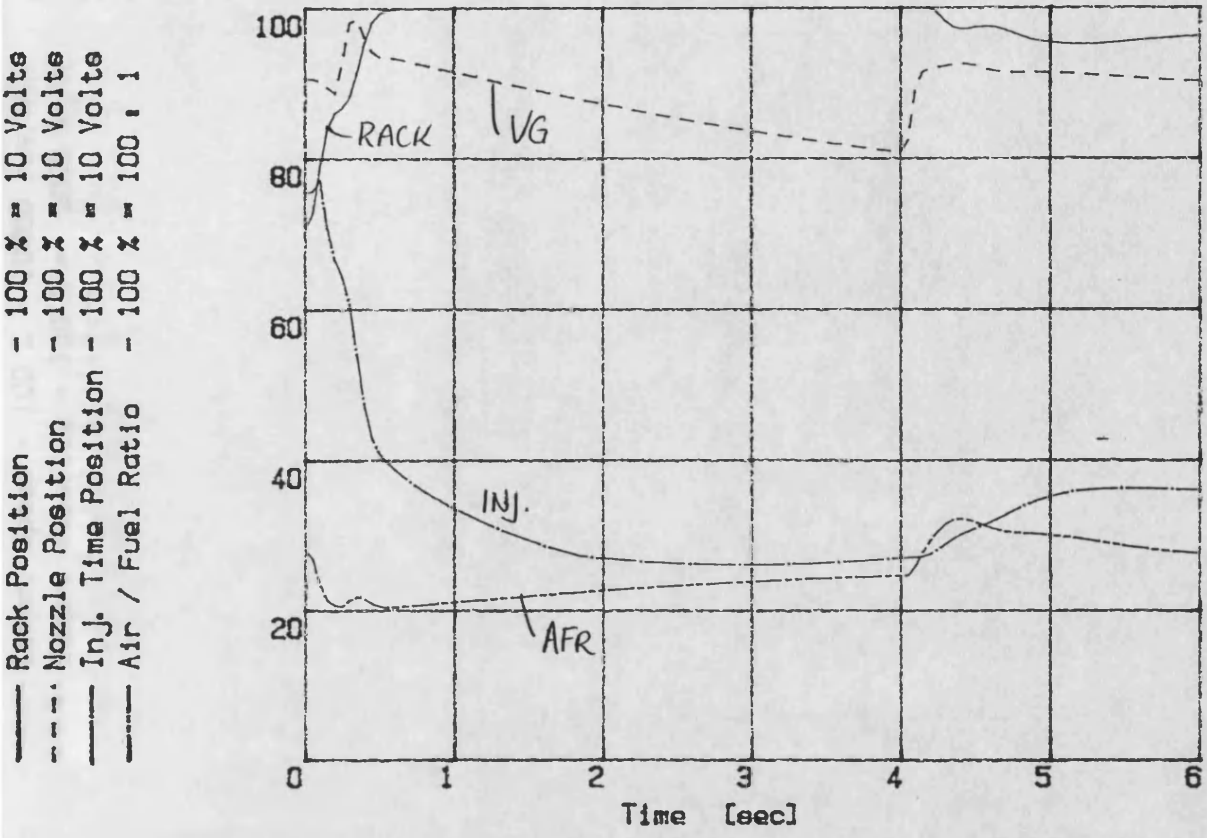

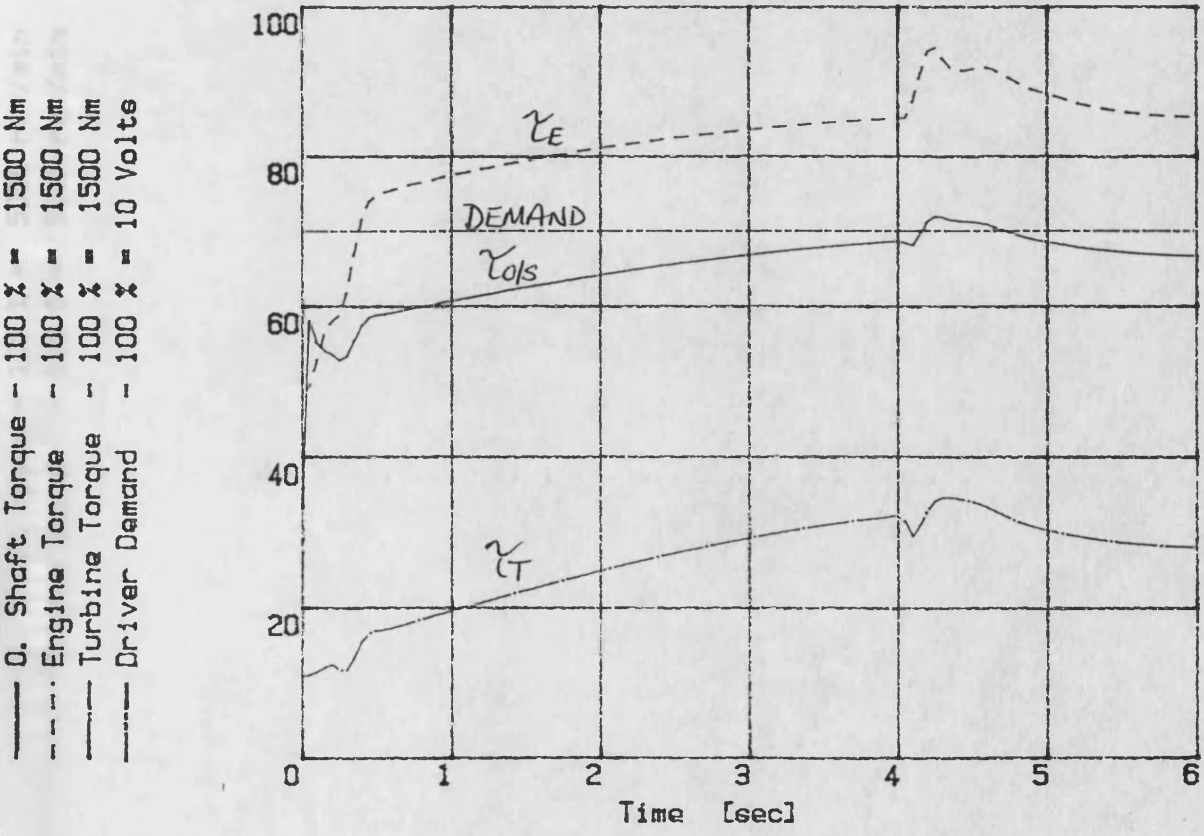

FIG. 8.10B load step - PID-type control

DCE transient simulation - SIMDCE 310489
Demand 5-10V; Load 500Nm; dyno. inertia
LRPC3: ARIMA model File: DDSA42.DAT

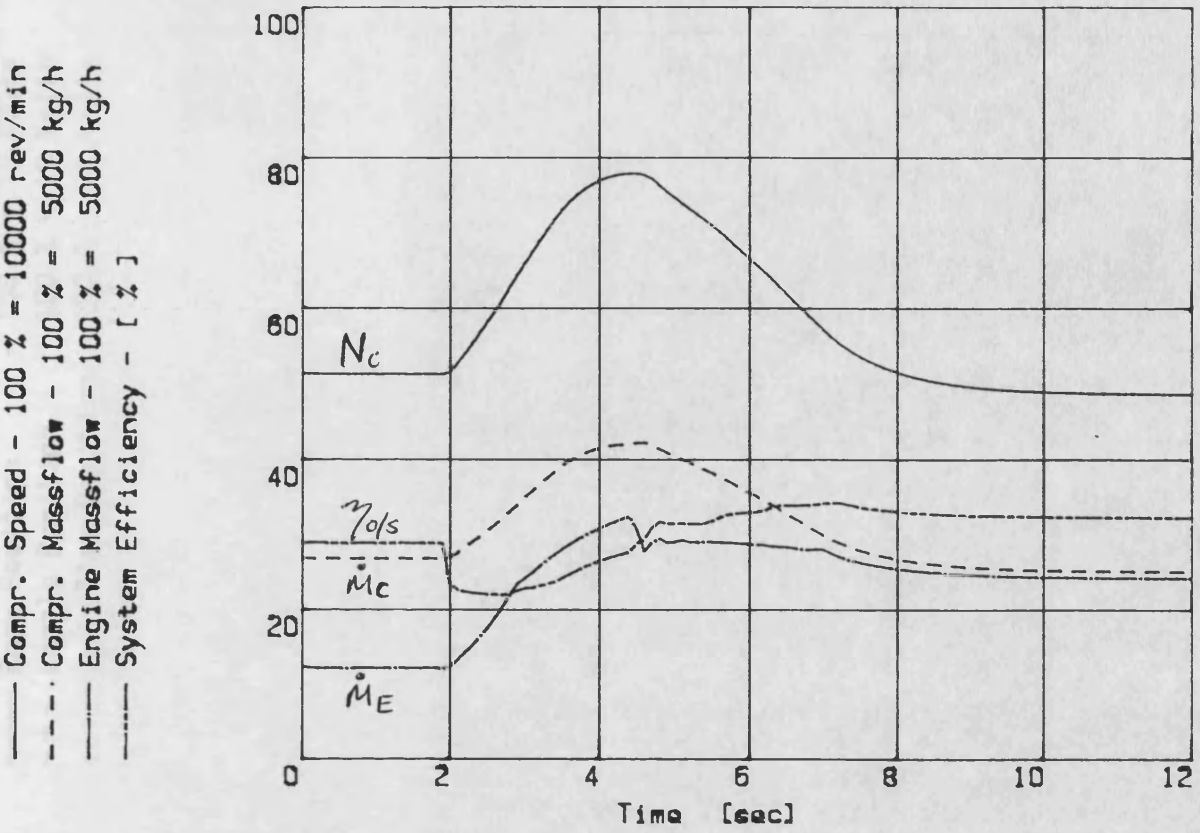

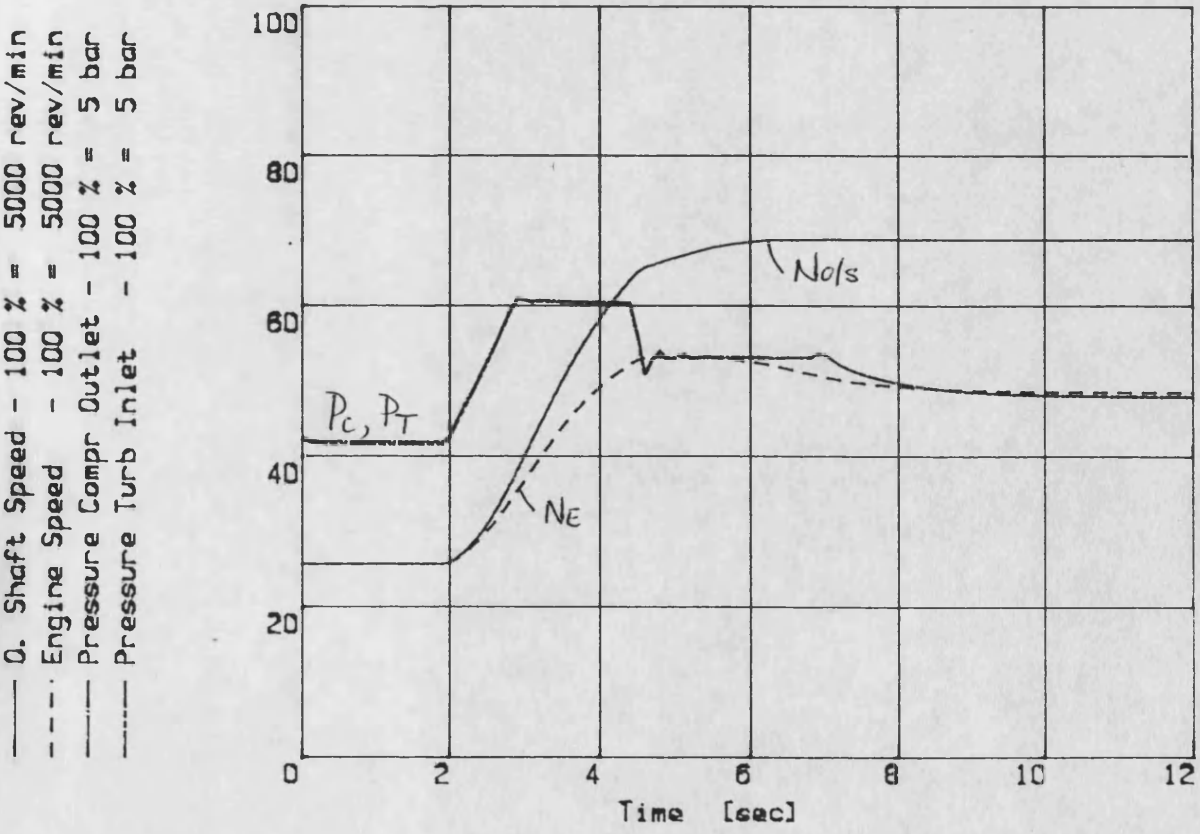

FIG. 8.11A driver demand step - LRPC boost control

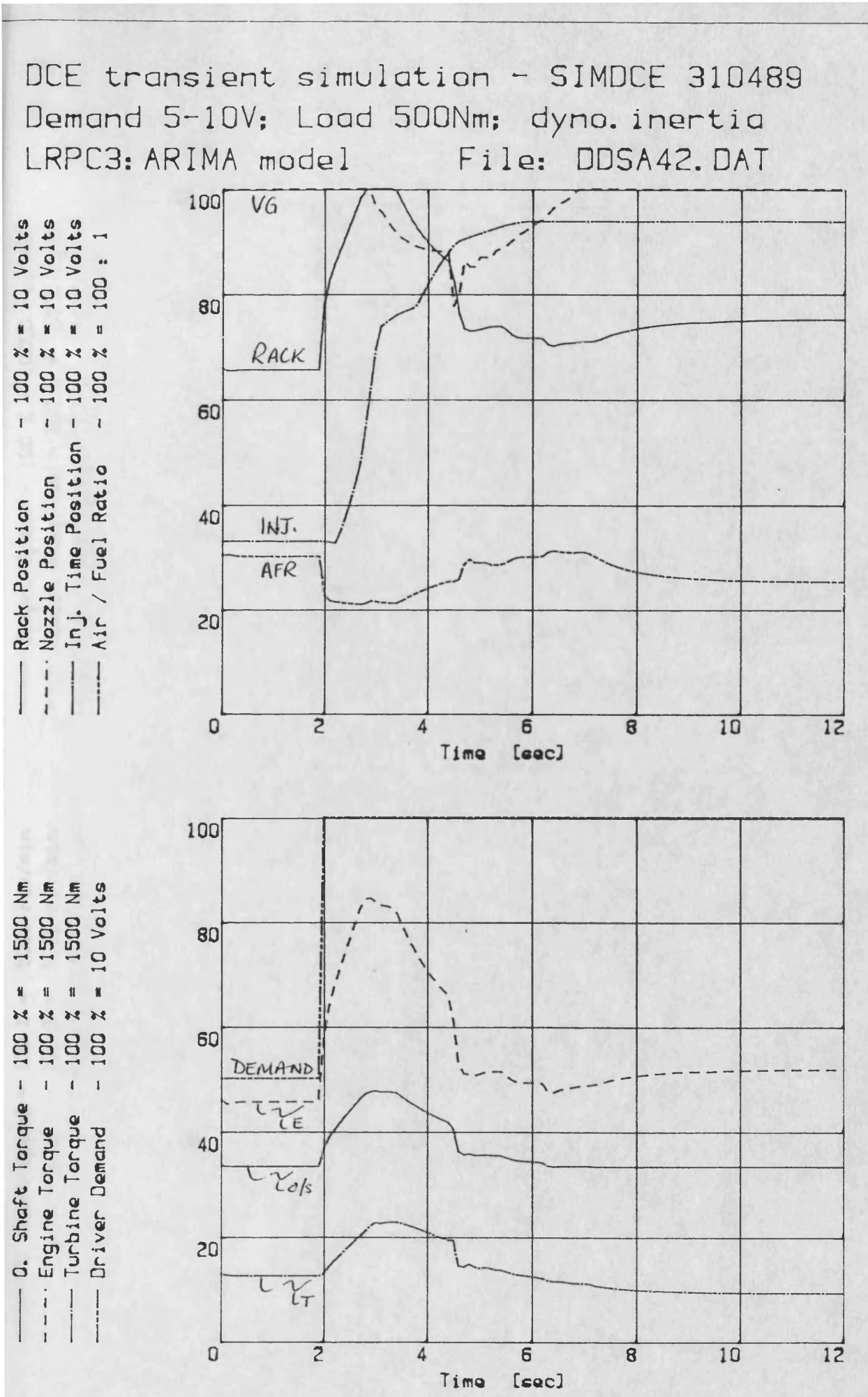

FIG. 8.11B driver demand step - LRPC boost control

DCE transient simulation - SIMDCE 310489
Demand 7V; Load 500-1000Nm; dyno. inertia
LRPC3: ARIMA model File: dlsb2.dat

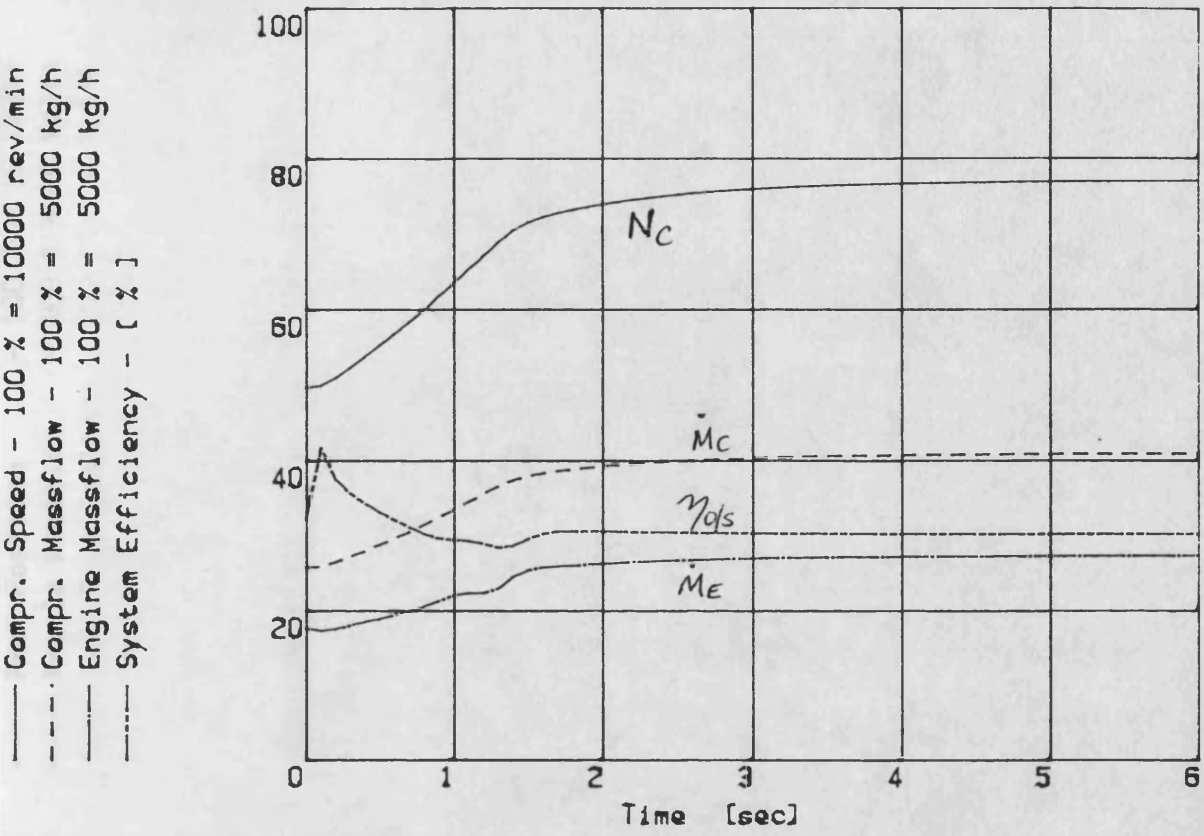

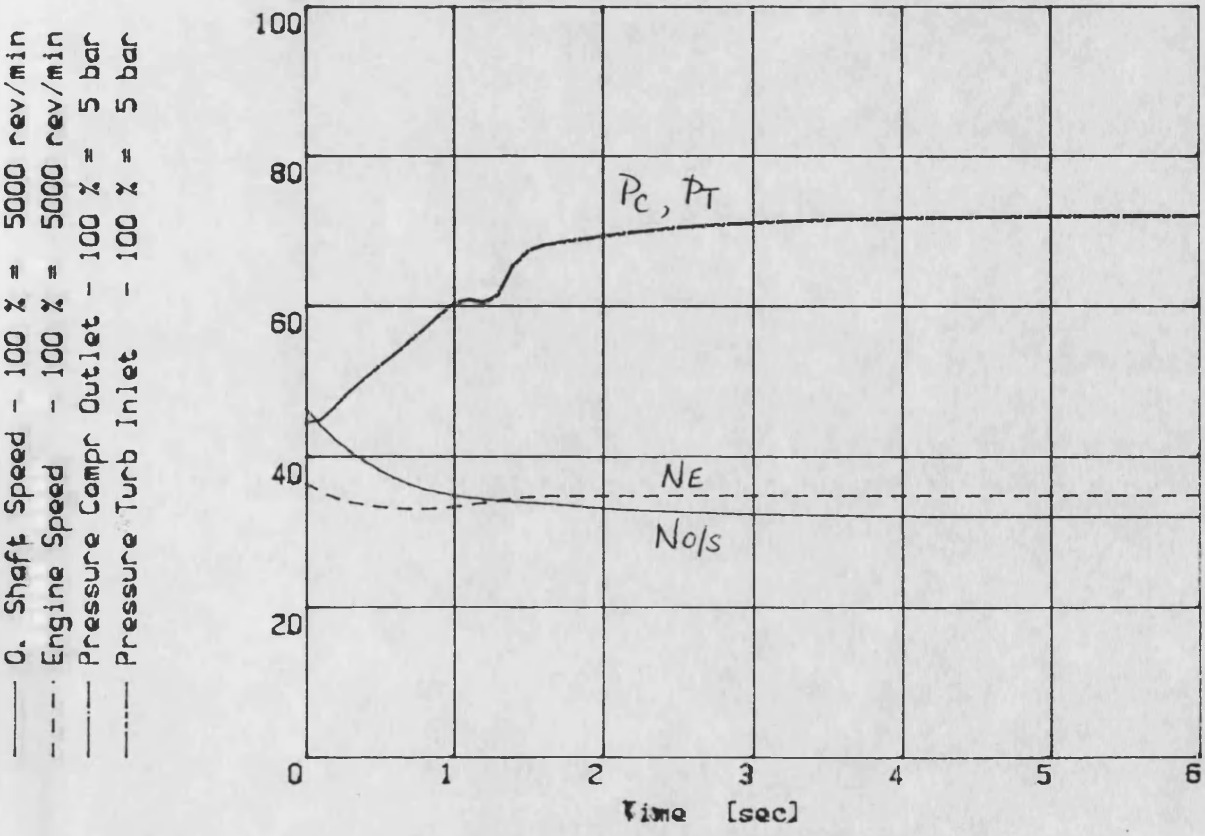

FIG. 8.12A load step - LRPC boost control

DCE transient simulation - SIMDCE 310489
Demand 7V; Load 500-1000Nm
LRPC3: ARIMA model File: dlsb2.dat

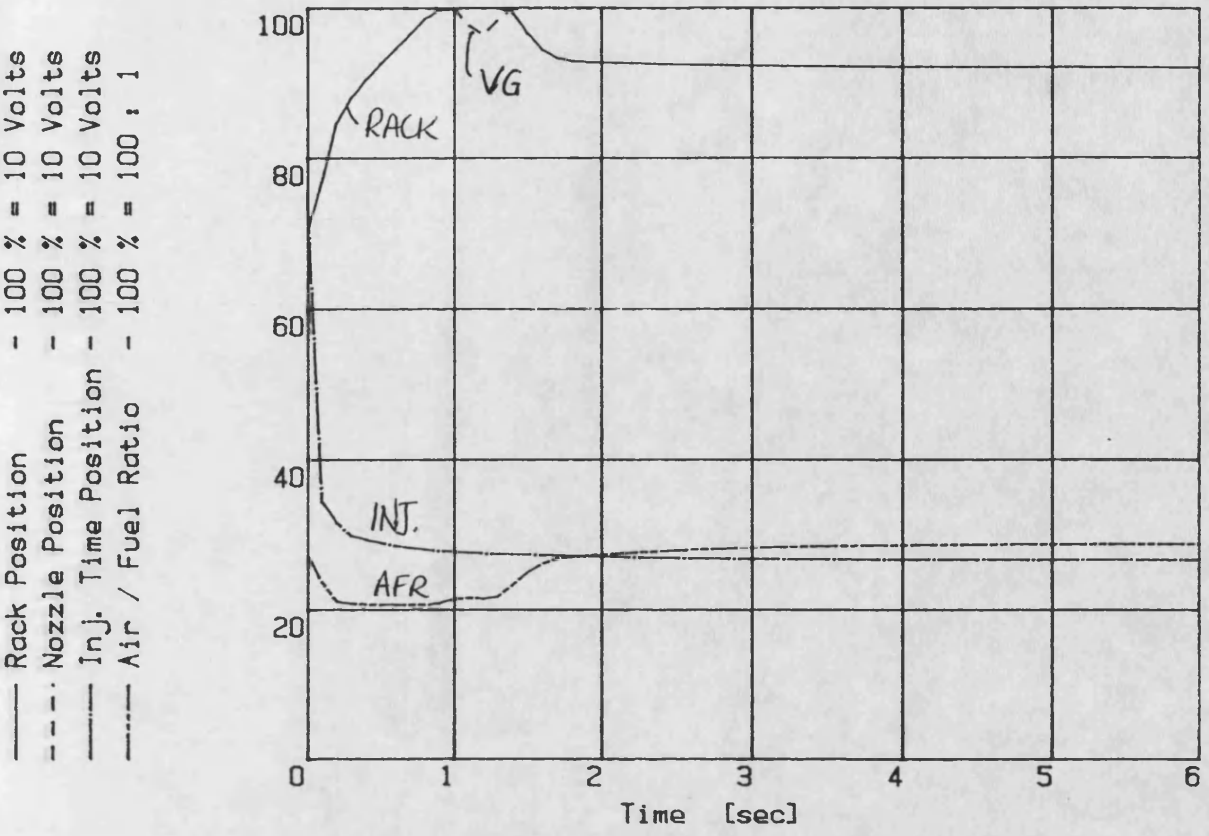

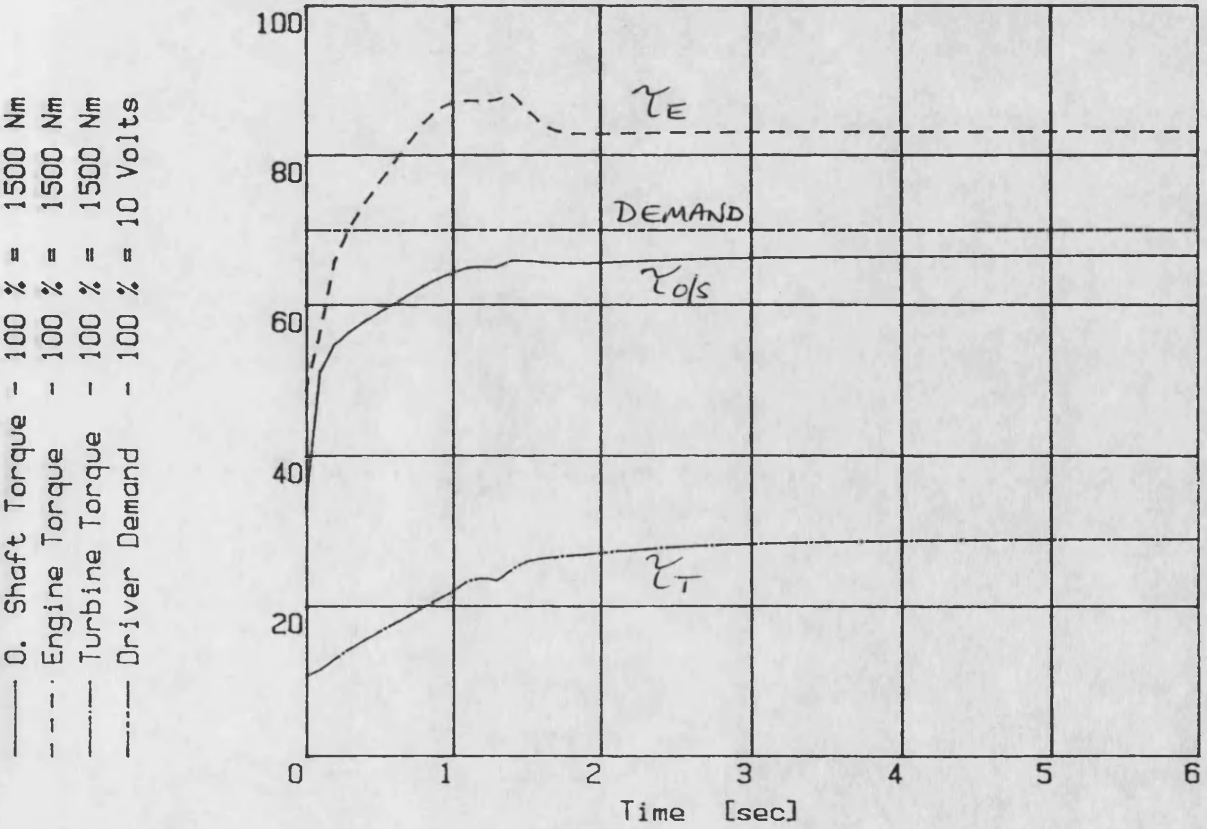

FIG. 8.12 *B* load step - LRPC boost control

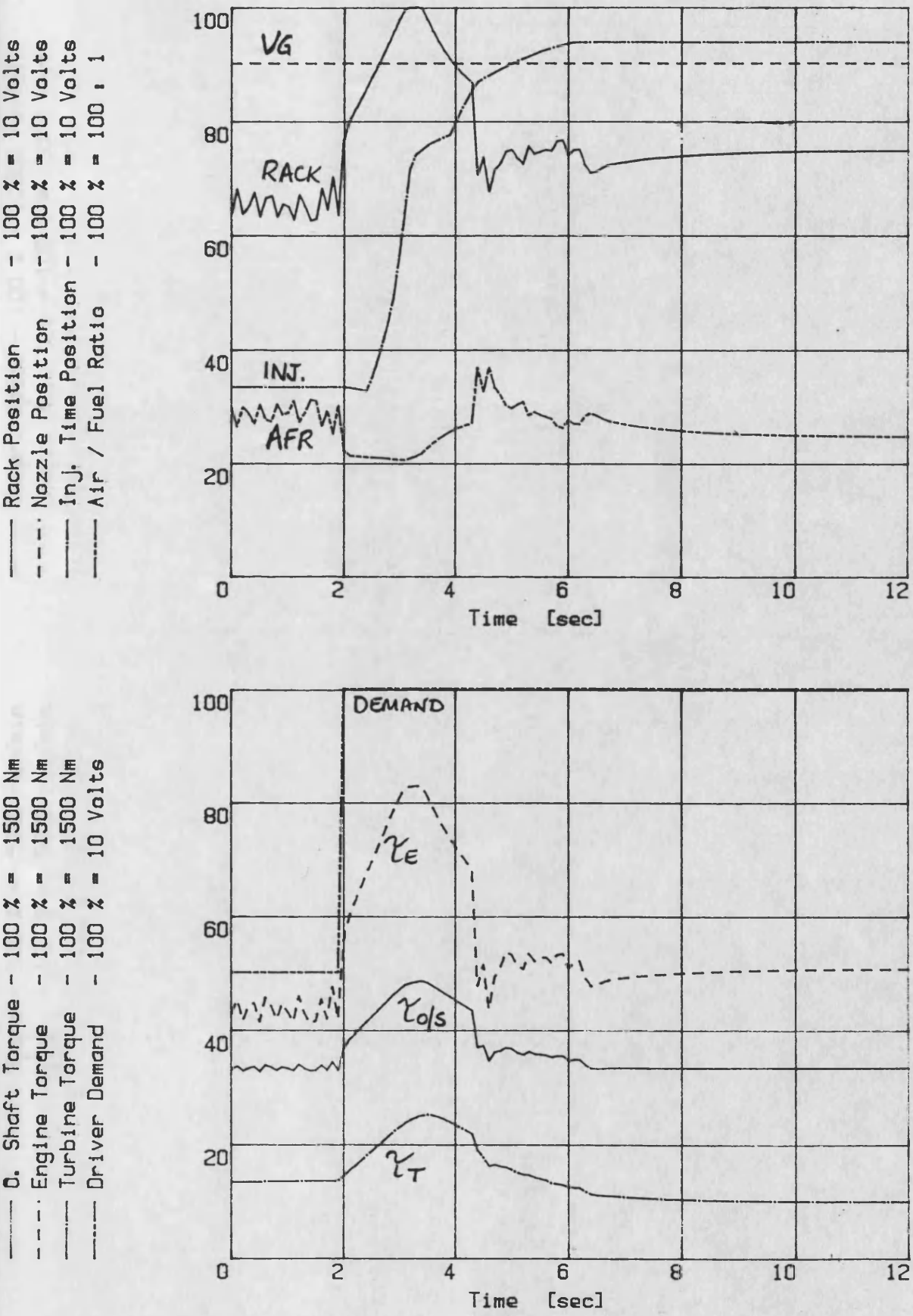

FIG. 8.13 driver demand step - initial engine speed LRPC

DCE transient simulation - SIMDCE 110589
Demand 5-10V; Load 500Nm; dyno. inertia
MVPC5: 2 siso loops. File: ddsa50

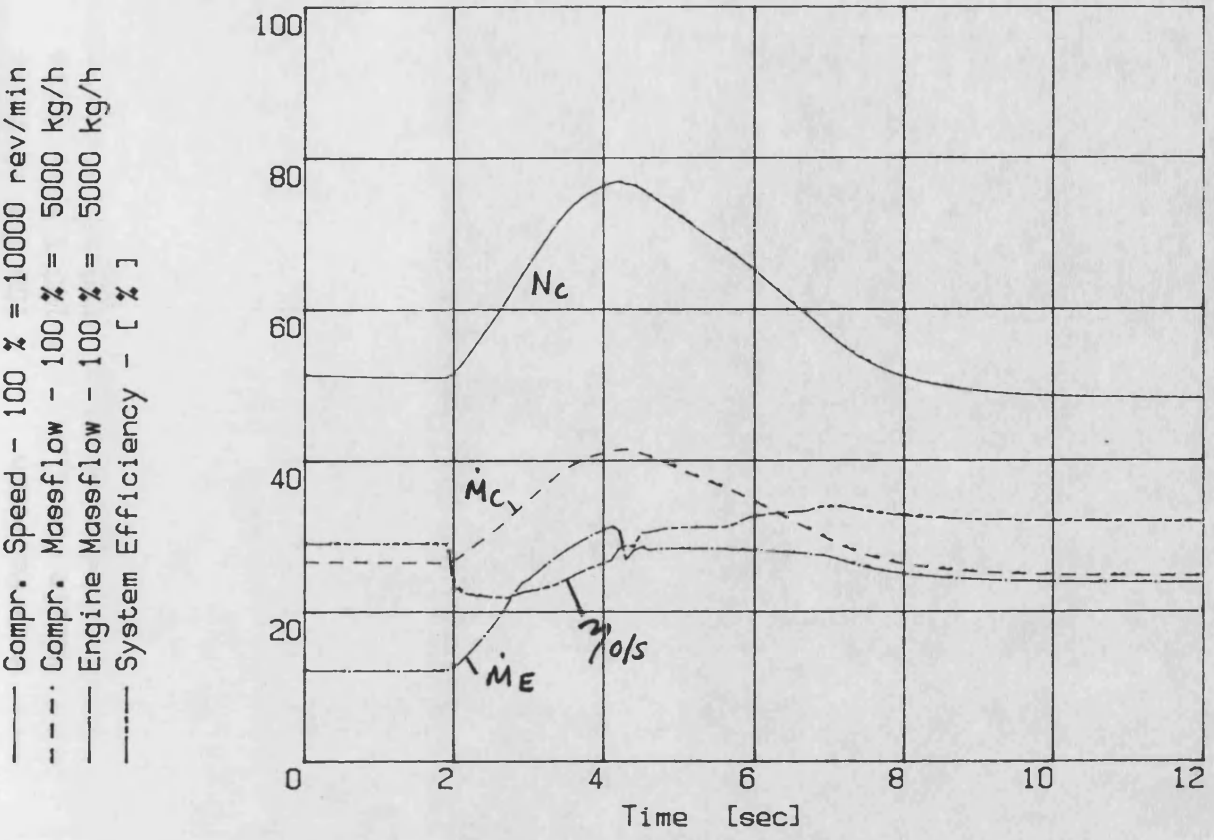

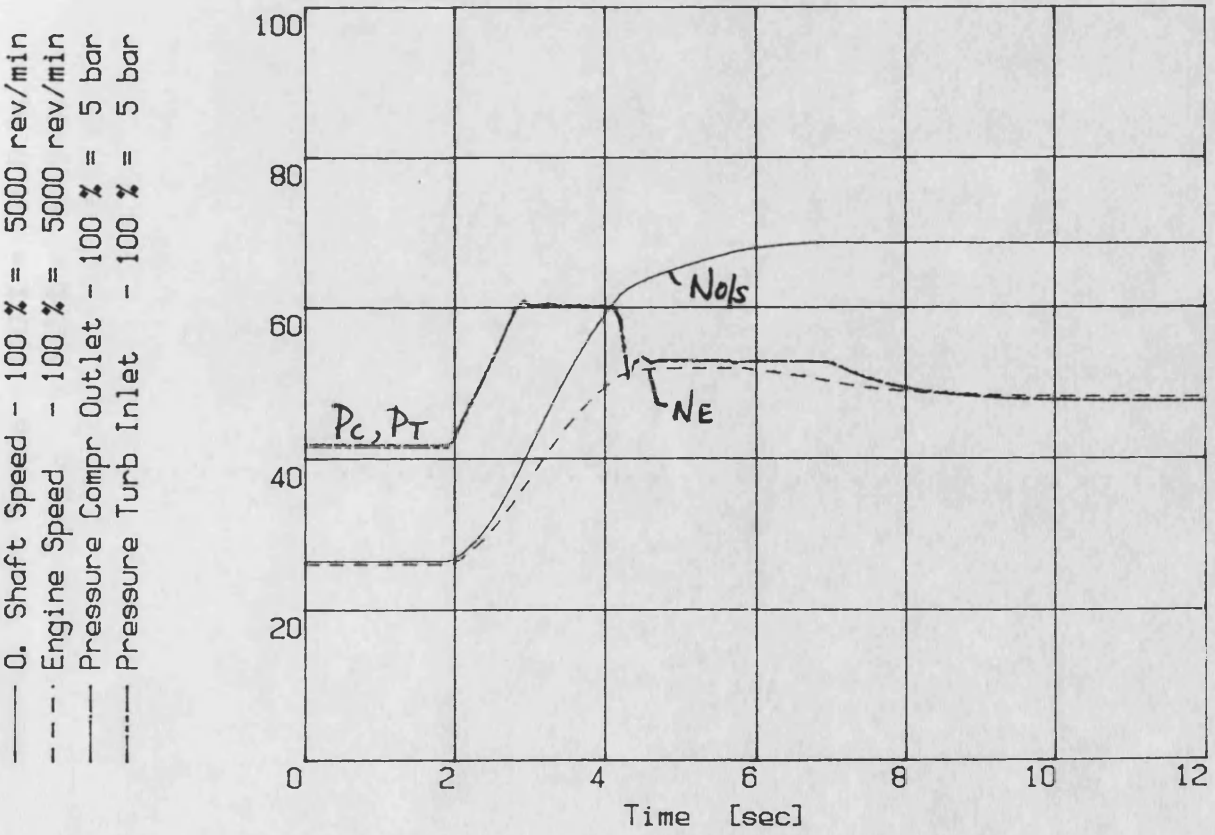

FIG. 8.14**A** driver demand step - dual LRPC

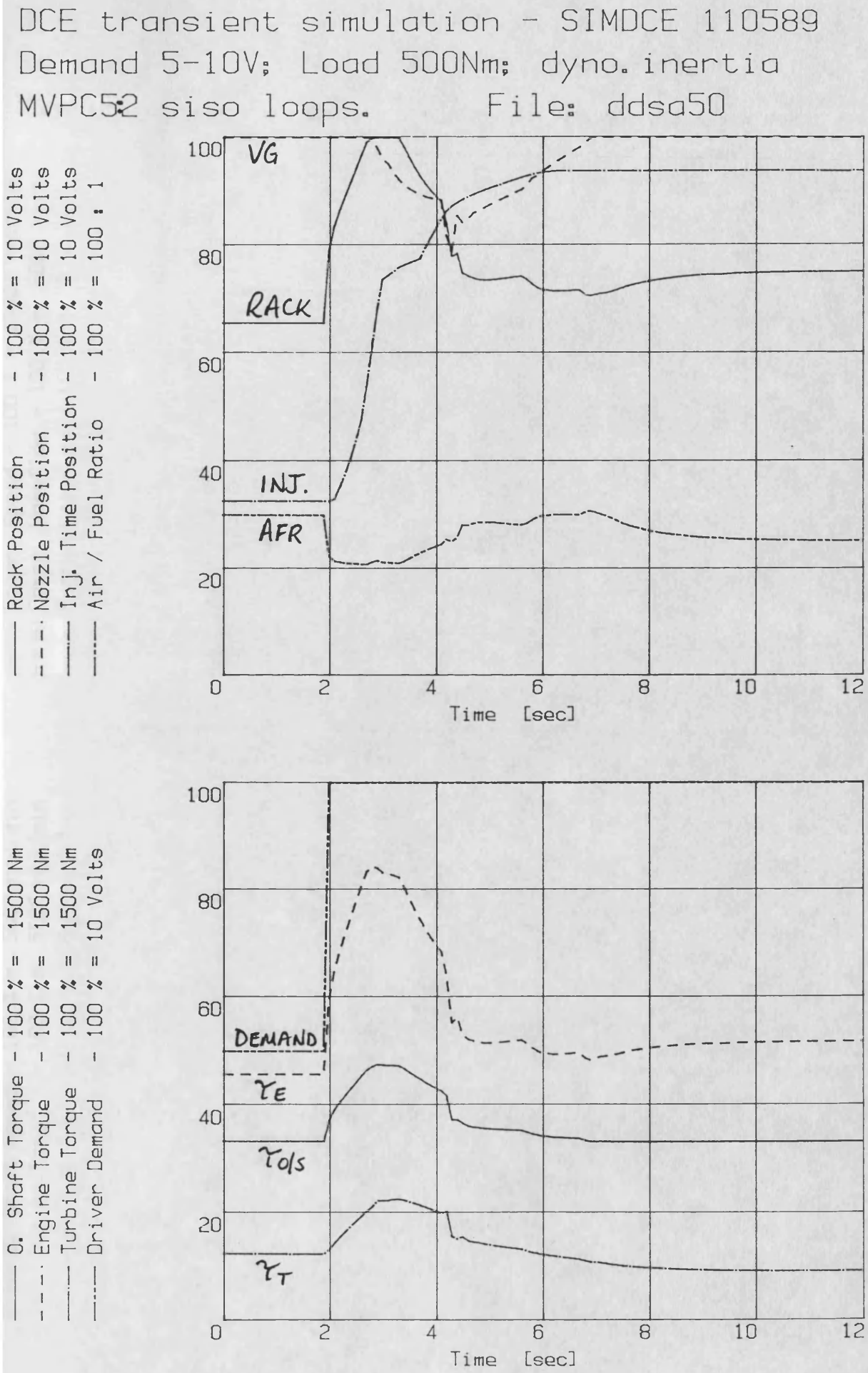

FIG. 8.14B driver demand step - dual LRPC

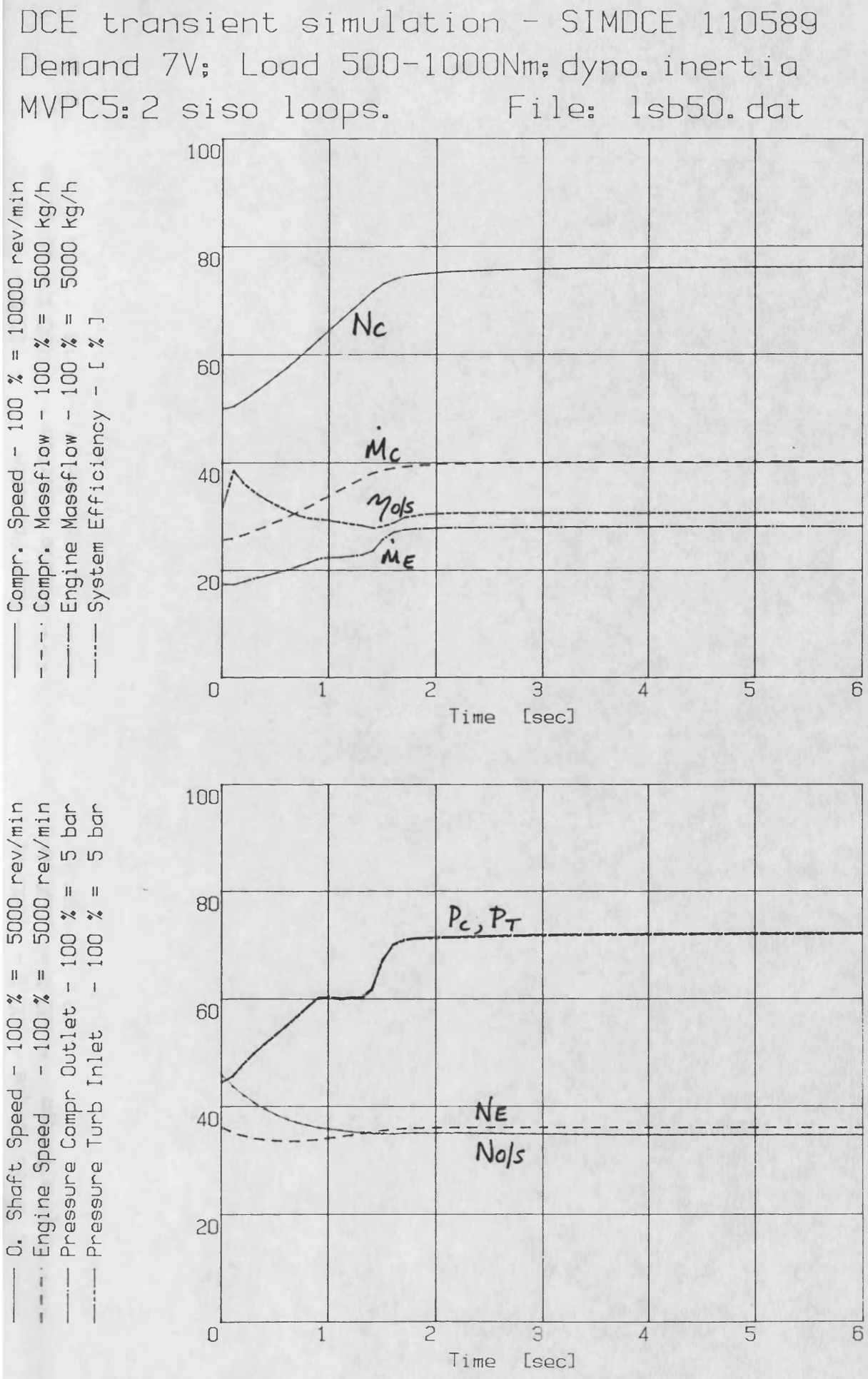

FIG. 8.15A load step - dual LRPC

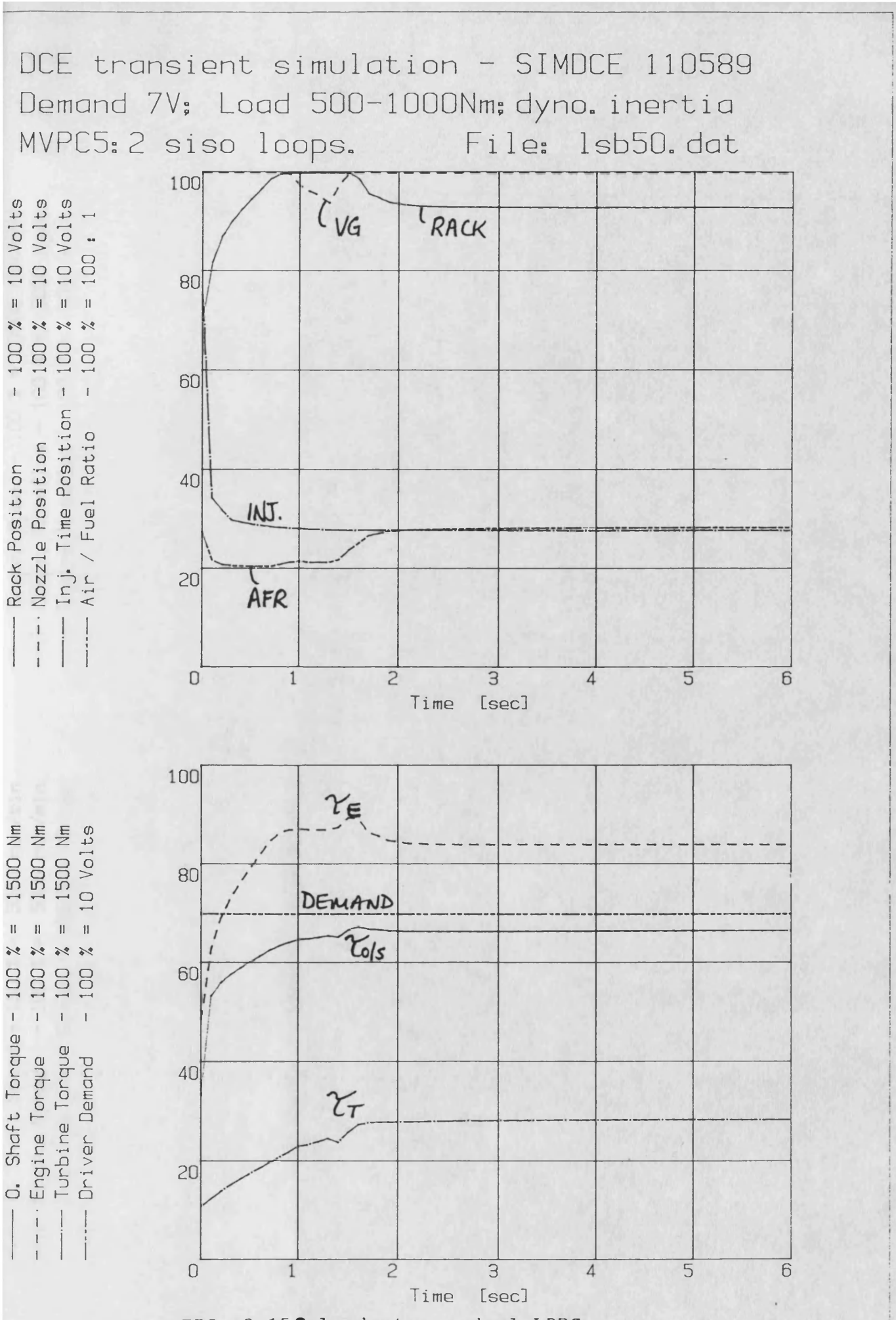

FIG. 8.15B load step - dual LRPC

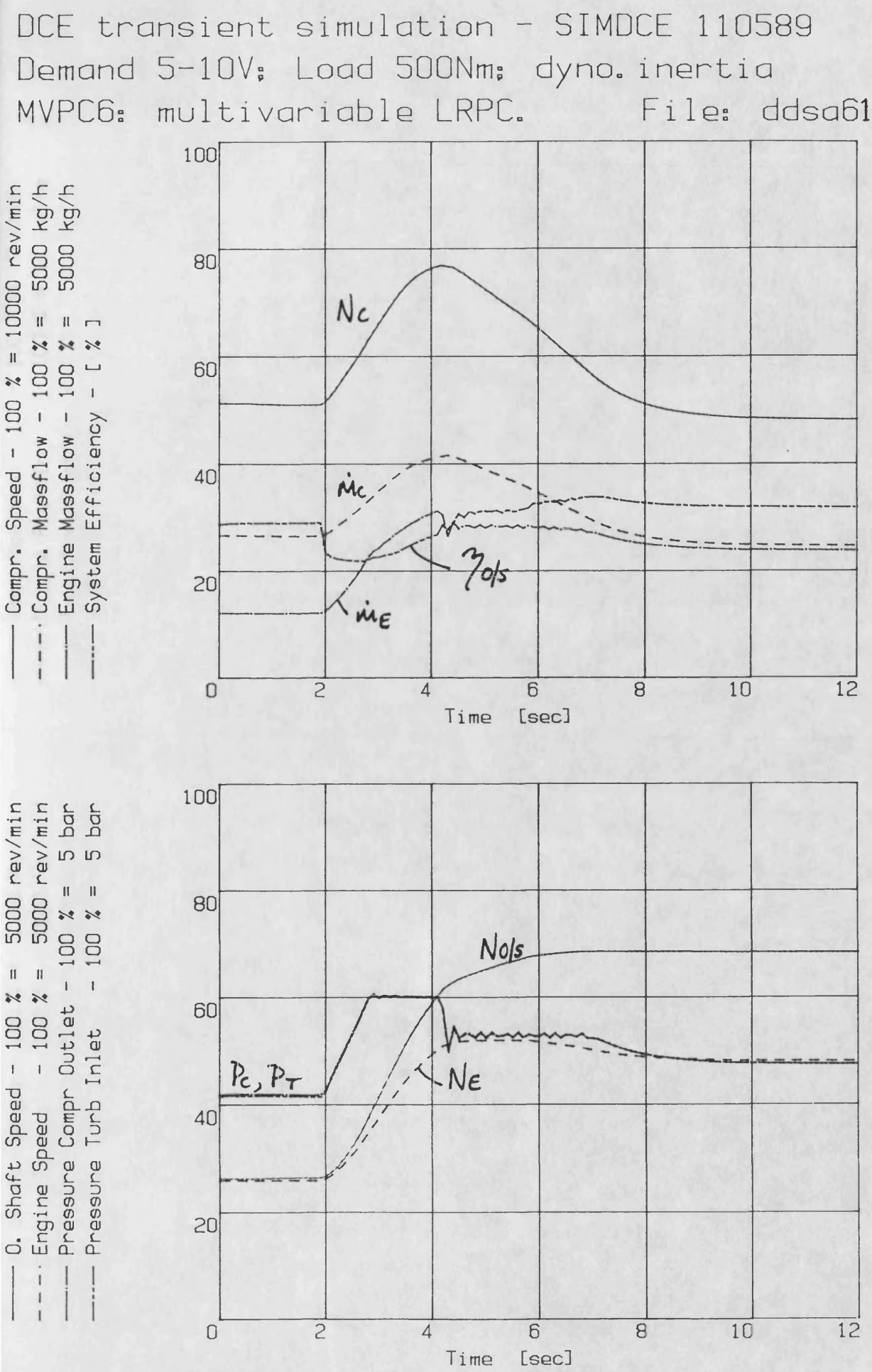

FIG. 8.16A driver demand step - multivariable LRPC

DCE transient simulation - SIMDCE 110589
Demand 5-10V; Load 500Nm; dyno. inertia
MVPC6: multivariable LRPC File: ddsa61

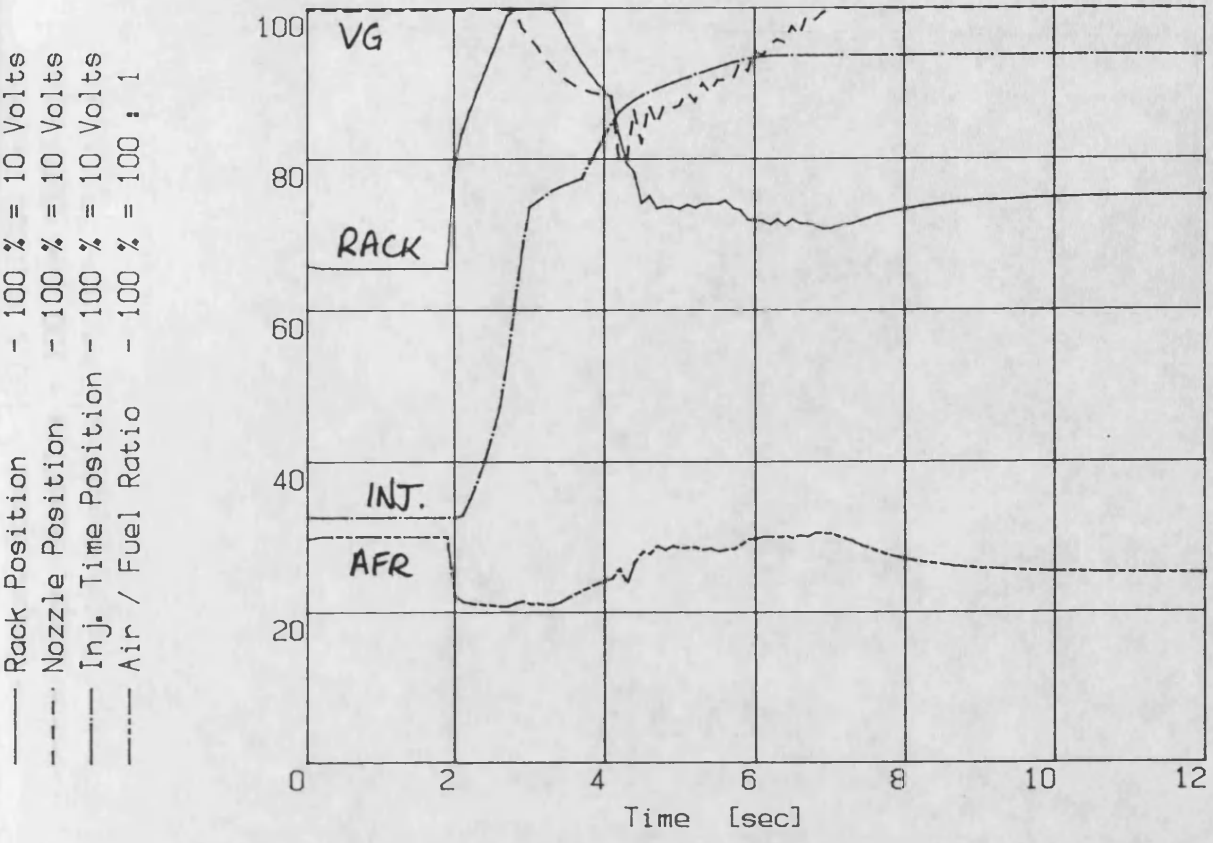

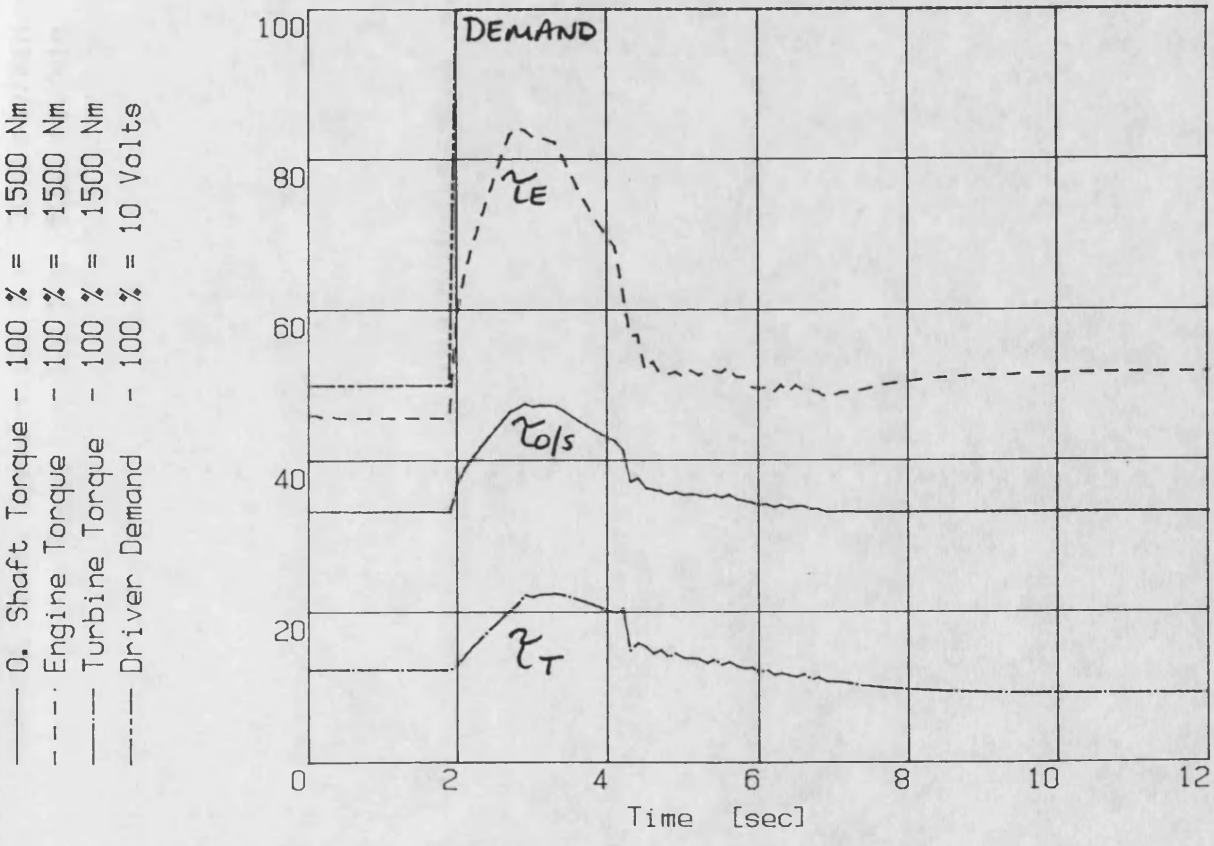

FIG. 8.16B driver demand step - multivariable LRPC

DCE transient simulation - SIMDCE 110589
Demand 7V; Load 500-1000Nm; dyno. inert.
MVPC6: multivariable LRPC File: lsb61.

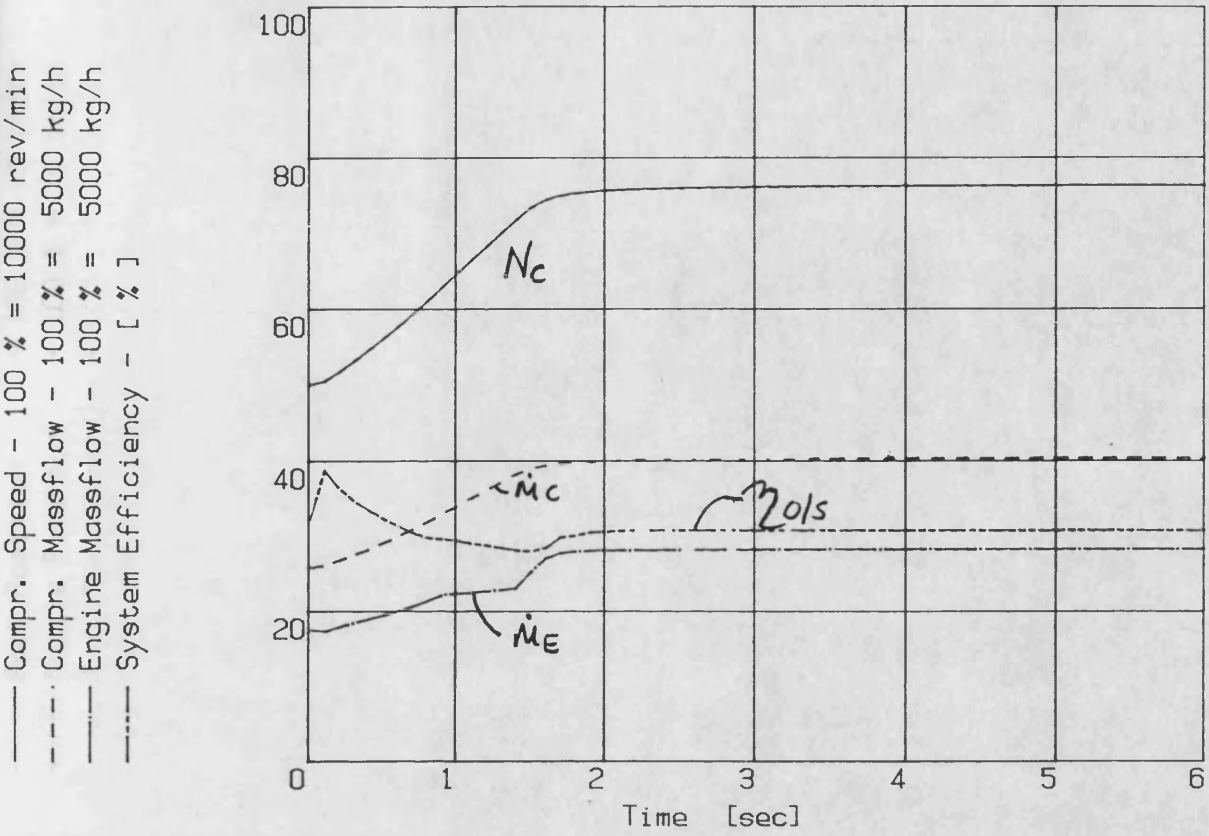

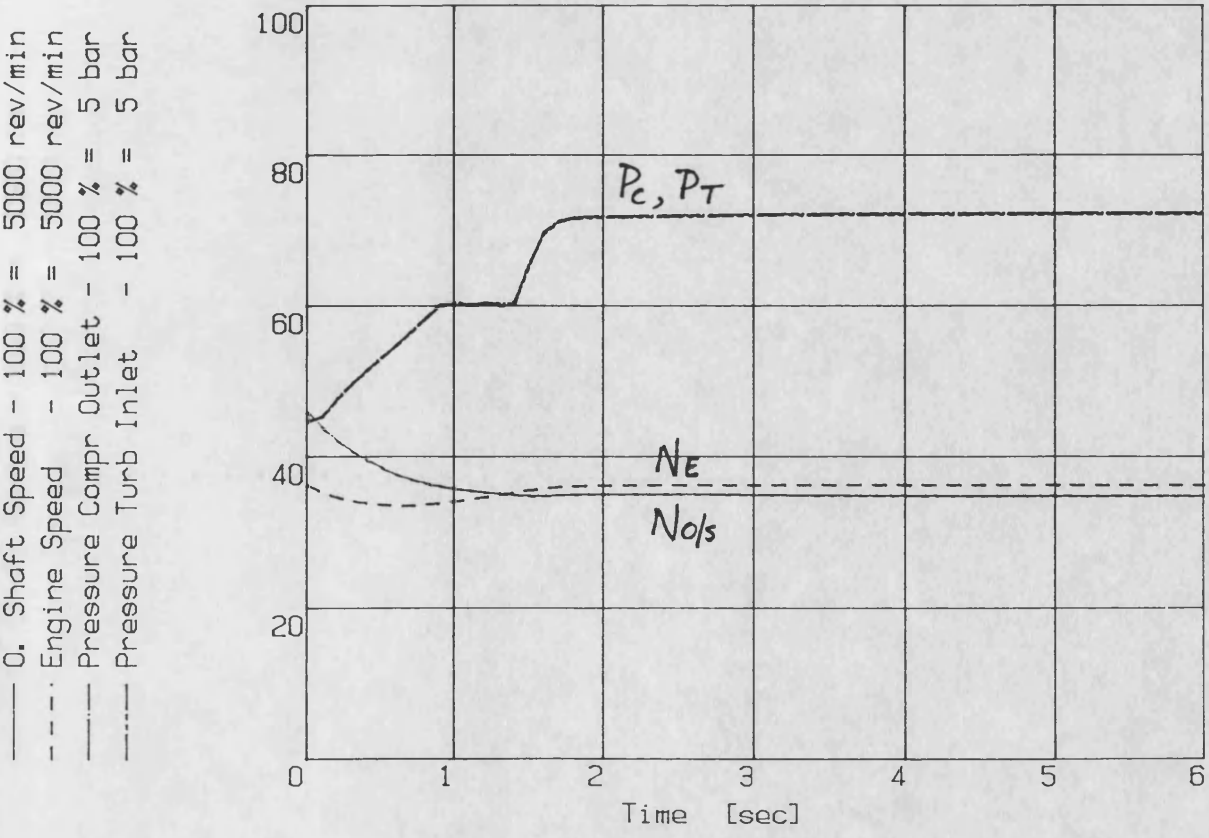

FIG. 8.17A load step - multivariable LRPC

DCE transient simulation - SIMDCE 110589
Demand 7V; Load 500-1000Nm; dyno inert.
MVPC6: multivariable LRPC File: lsb61.

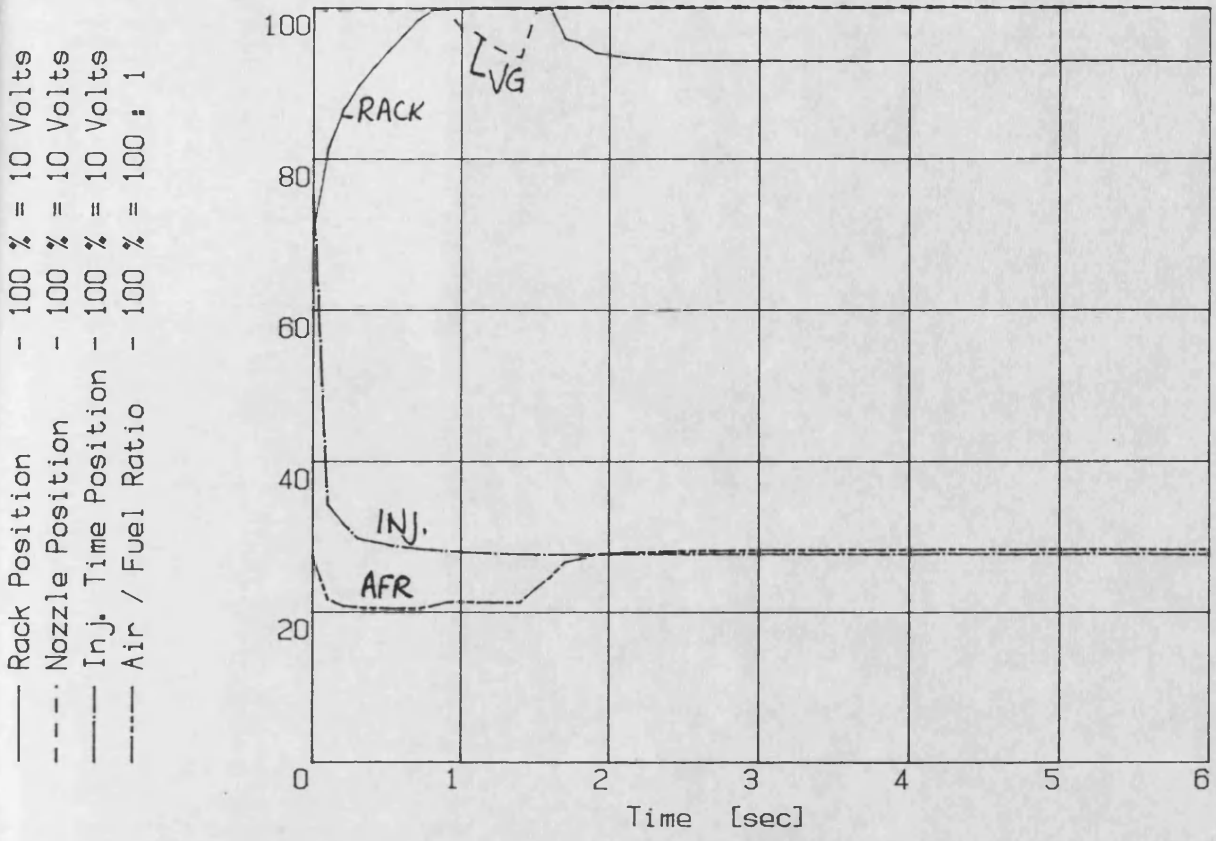

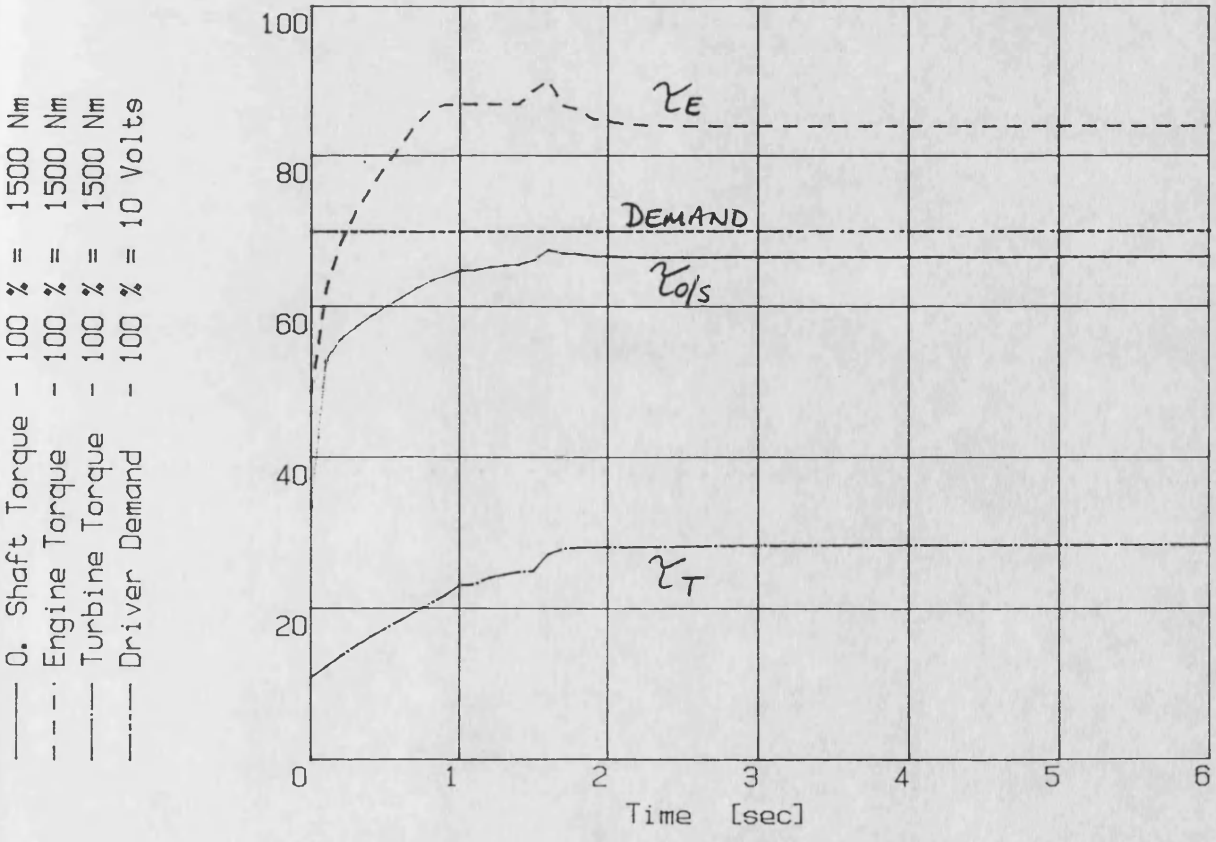

FIG. 8.17B load step - multivariable LRPC

9. CONCLUSIONS AND RECOMMENDATIONS

9.1 THE DCE

9.1.1 Steady state performance

9.1.2 Transient performance

9.1.3 Future work

9.2 CONTROL DESIGN

9.2.1 Design techniques

9.2.2 Summary of designs

9. CONCLUSIONS AND RECOMMENDATIONS

9.1 THE DCE

The findings of this research with regard to the steady state and transient performance of the DCE are summarised in turn below, followed by recommendations for future work on the DCE concept.

9.1.1 Steady state performance

The maximum torque curve and output shaft efficiencies of the 52ØDCE prototype were well below design predictions. The reasons for this were identified as:

(i) Very low turbine powers - the turbine was an untested design, having been modified from a standard component to suit 52ØDCE pressure ratios of up to 4. Furthermore, its swallowing capacity was high, such that the VG mechanism operated near full restriction at optimum steady state DCE conditions. Flow conditions at turbine inlet would therefore be unsatisfactory.

(ii) Excessive charge cooler pressure losses - this gives a general loss of system efficiency since some compressor work is effectively wasted in providing a higher delivery pressure than is obtained at engine inlet. Maximum torque is also reduced since the engine operates at reduced air/fuel ratio, meeting the thermal limit sooner. Engine efficiencies were good, and gearbox losses were acceptable, though a correctly engineered design for the 52ØDCE ratings would probably give slighlty lower losses. The experimental results gave no reason to dispute simulation predictions; despite the relatively high pressure ratios and the use of VG nozzles it should be possible to develop a suitable radial

turbine with the efficiency characteristics assumed in the simulations.

9.1.2 Transient performance

Simulation and experimental work identified two important factors in maximising the transient response of the DCE:

(i) Having sufficient VG (swallowing capacity) restriction, in order to "convert" bypass air flow rapidly into increased boost pressure, thus allowing increased engine fuelling and torque.

(ii) Having a wide margin between steady state engine air/fuel ratios (AFR) and the minimum AFR allowable within smoke limits. This margin determines the transient excess of engine over compressor power and thus the acceleration of the engine and compressor. Clearly however, this margin cannot be increased simply by matching for high design point AFR, as this implies reduced system efficiency (excessive compressor work with limited utilisation in engine and turbine of the extra boost) and reduced power density.

The relative importance of these factors depends upon the operating condition. At light loads, engine and compressor acceleration is required in order to increase output shaft power; VG restriction is ineffective because bypass flow is already low. At higher loads with significant bypass flow, VG restriction becomes useful.

A variable bypass valve seems unnecessary where turbine VG is available. However, in a DCE design with a fixed geometry turbine, variable bypass closure might be useful, particularly in transients.

Simulation of overrunning output shaft and very light load conditions indicated potential difficulties with compressor reversal and reverse

bypass flow. This may be overcome by a compressor brake (also improving the "engine braking" capability of the DCE) and bypass valve arrangements, but subsequent acceleration from these conditions was poor. It was noted that the simulation of simple transients might give a misleading or incomplete impression of the behaviour of a DCE in a practical application. Dynamic vehicle/route simulation is the most reliable approach, since it will cover all possible conditions, naturally emphasising those which occur most frequently in a given application.

9.1.3 Future work

The DCE concept is now at a stage where component matching and control strategies are well understood, and awaits the gradual development of its component parts in terms of performance (for example, turbomachinery efficiency), durability and cost, leading to the point where their combination into a DCE becomes commercially viable. However, three areas require attention:

(i) Light load/engine braking conditions

The evidently poor acceleration of the DCE from these conditions, predicted by the simple dynamic simulation in this thesis, should be verified by other simulations. Its effect upon vehicle/route performance should then be assessed, again by a fully dynamic simulation. The best practical form of the compressor brake and bypass valve arrangements should also be considered.

(ii) Compressors

Compressor developments for the high pressure ratios and wide flow range requirements of the DCE should be monitored. Current centrifugal

compressors are far short of the required flow range, so a compact high efficiency positive displacement compressor is required (with acceptable cost and durability).

(iii) Turbines

The development of VG turbines and of compound turbine arrangements is now quite widespread in the automotive field. However, typical pressure ratios for a single radial turbine are up to approximately 3, beyond which two-stage turbocharging may be adopted. Therefore, high pressure ratio automotive-size turbine developments should also be monitored.

Other aspects of the DCE, such as high engine ratings and high cylinder pressures (20 bar and 150 bar respectively in the 520DCE) will be perfectly acceptable in heavy-duty Diesel engine designs in the very near future.

Further work on the 520DCE prototype is not recommended, though the testing and development of individual components (in line with (ii) and (iii) above) may be worthwhile. Any future prototype should be in a "pre-production" form suitable for vehicle evaluation rather than a research form; further research would be more effective by simulation.

9.2 CONTROL DESIGN

9.2.1 Design techniques

A simple dynamic simulation, based on a limited number of dynamic state variables, with quasi-steady calculations or empirical relationships for other variables, achieved good dynamic (and reasonable steady state) accuracy with very short run times. This proved to be an invaluable tool for control system design and testing.

Two design approaches were used:

(i) Intuitive tuning of PID-type loops

(ii) Identification of major system responses (including multivariable cross-coupling) followed by systematic control design.

In both cases the simulation was used extensively. In the first case the control strategies and control loops were chosen and refined by simulation, before successful microcomputer-based implementation on the prototype. In the second case the simulation model was used for identification purposes, and the resulting control designs were then evaluated by simulation.

9.2.2 Summary of designs

(i) Strategies

The optimum transient VG (swallowing capacity) control strategy was not clear-cut. The optimum balance between boost and massflow depends upon turbine energy utilisation as well as engine and compressor powers. Increased restriction (up to the point where bypass flow is reduced to zero) gives higher boost and lower massflow. This enables increased

engine fuelling and thus torque, but potentially at the expense of lower turbine power.

Ultimately the solution - given sufficient development time - might be to schedule transient VG control setpoints for optimum response, in the same way as optimum efficiency schedules are used at steady state.

(ii) PID-type control

Acceptable control performance was obtained with intuitively-tuned PID-type loops. Owing to the non-linearities and non-stationarities (response changes with operating condition) of the system, rather low control gains were used to ensure stability at all conditions. Unfortunately it was difficult to assess losses in DCE output shaft efficiency due to the slightly "loose" control, because turbine performance had been improved between the original mapping and the implementation of the microcomputer-based controller. However, no significant deteriorations were seen.

(iii) Predictive control

Further controllers were designed using identified system models and predictive control methods. As expected, the identified models were non-stationary (non-linearity was inherently neglected in the identification method, but small excitation signals were used to minimise these effects), but it was possible to use fixed parameters over the whole operating range, since the predictive control method is quite robust.

As tested by simulation, the predictive control design gave much tighter (yet stable) control than the simpler PID-type loops. However, DCE

transient response (as measured by output shaft torque or speed response) was similar.

Using the identified models it was possible to compensate for multivariable cross-coupling between the main control loops. However, this seemed slightly to degrade the already excellent control performance of the single input - single output loops. This is surprising, but was attributed to failure to account for constraints on the rack and VG control inputs (chiefly physical limits of maximum fuelling and VG restriction, plus smoke-limiting restriction of the rack) in the multivariable compensation calculations. In other circumstances - where the cross-coupling is stronger, or where these control input non-linearities do not exist - multivariable compensation could be worthwhile, and is easily incorporated in predictive control designs.

REFERENCES

1. Hales JM & MP May
"Transient cycle emissions reduction at Ricardo-1988 and beyond"
SAE 860456, 1986

2. Beckman D
"Aftercooling for detonation and thermal load reduction"
Ricardo Consulting Engineers, 1980

3. Ball WF
"Some effects of injection pressure on quiescent direct injection Diesel combustion" Ricardo Consulting Engineers, 1980

4. Ghadiri-Zareh MS & FJ Wallace
"Variable geometry vs.two-stage turbocharging of high output Diesel engines" IMechE C63/78, 1978

5. Needham JR & MH Sandford
"A truck engine for the 1990's" ASME 87-ICE-50, 1987

6. Wallace FJ, RJB Way & A Baghery
"Variable geometry turbocharging-the realistic way forward"
SAE 810336, 1981

7. Wallace FJ, D Howard & EW Roberts
"Variable geometry turbocharging - optimisation and control under steady-state conditions" IMechE C97/86, 1986

8. Wallace FJ et al
"Variable geometry turbocharging of a large truck Diesel engine"
SAE 860452, 1986

9. Pilley AD et al
"Optimization of heavy-duty Diesel engine transient emissions by advanced control of a variable geometry turbocharger"
SAE 890395, 1989

10. Borila YG
"A sequential turbocharging method for highly-rated truck Diesel engines" SAE 860074, 1986

11. Roberts EW
"Variable geometry turbocharging - optimisation and control"
Ph.D thesis, University of Bath 1984

12. Roessler M & KR Swenson
"Variable nozzle turbochargers for medium speed Diesel engines"
SAE 880119, 1988

13. O'Connor GF & MM Smith
"Variable nozzle turbochargers for passenger car applications"
SAE 880121, 1988

14. Wilson DE
"The design of a low specific fuel consumption turbocompound engine" SAE 860072, 1986

15. Brands MC et al
"Vehicle testing of Cummins turbocompound Diesel engine"
SAE 810073, 1981

16. "Hino's new ceramic turbocompound engine with CVT"
Japan Autotech report, No.226, 1985

17. Rogers GFC & YR Mayhew
"Engineering thermodynamics,Work and Heat transfer" Longman 1980

18. French CCJ et al
"Ceramics for reciprocating internal combustion engines"
Ricardo Consulting Engineers, 1983

19. Bryzik W & R Kamo
"TACOM/Cummins adiabatic engine program" SAE 830314, 1983

20. Kamo R & W Bryzik
"Cummins/TARADCOM adiabatic turbocompound engine program"
SAE 810070, 1981

21. Rogers GFC, H Cohen & HIH Saravanamuttoo
"Gas turbine theory" Longman 1975

22. Winterbone DE, N Munro & PMG Lourtie
"A preliminary study of the design of a controller for an automotive gas turbine" ASME 73-GT-14, 1973

23. Winterbone DE, N Munro & DJ Nuske
"A multivariable controller for an automotive gas turbine"
ASME gas turbine conference, March 1979

24. "Automotive engine alternatives"
Ed. RL Evans, Plenum 1987

25. Sjoestroem S
"Scania transport simulation system" Saab-Scania 1978

26. Tarabad M
"Transmissions for passenger cars and commercial vehicles"
University of Bath, 1984

27. Greenwood CJ
"Integration of a commercial vehicle regenerative braking driveline" IMechE C196/86, 1986

28. Wallace FJ & M Tarabad
"Engine transmission systems for the heavy goods vehicle and the passenger-carrying bus" IMechE 31/83, 1983

29. Dawson JG, WJ Hayward & PW Glamman
"Some experiences with a differentially-supercharged Diesel engine" Proc.IMechE 1963/4, 178 pt.2A,157.

30. Wallace FJ
"Operating characteristics of compound engine schemes for traction purposes based on opposed-piston two-stroke engines and differential gearing" IMechE P2(b)/63, 1963

31. Wallace FJ et al
"The differential compound engine - a new integrated engine transmission system concept for heavy vehicles"
IMechE C47/83, 1983

32. Wallace FJ et al
"Design and performance characteristics of the laboratory differential compound engine at Bath University"
IMechE C196/86, 1986

33. Kainz A et al
"A new concept for electronic Diesel engine control"
SAE 860141, 1986

34. Seibt A et al
"An innovative electronic Diesel engine management system"
SAE 880486, 1988

35. Farr MK
"Electronic controls for John Deere Diesel engines"
SAE 890391, 1989

36. Prince DJ
"Design,build and steady-state test of a differential compound engine" Ph.D thesis, University of Bath 1987

37. Howard D
"The design of control systems for Diesel engines"
Ph.D thesis, University of Bath 1987

38. Tarabad M
"Epicyclic gearset" University of Bath 1982

39. Wallace FJ, M Tarabad & D Howard
"Design and performance studies for a 1000hp military version of the differential compound engine" IMechE C194/86, 1986

40. Wallace FJ, MS Ghadiri-Zareh & M Rezaian
"Steady-state performance predictions for the Cummins L10 engine as the power unit for the differential compound engine"
Cummins Engine Co. DCE project 3rd progress report, Bath 1987

41. Wallace FJ,MS Ghadiri-Zareh & D Dang
"Steady-state characteristics of L10DCE with fixed geometry turbine" Cummins Engine Co.DCE project 7th prog.report,Bath 1987

42. Watson N & MS Janota
"Turbocharging the internal combustion engine" MacMillan 1982

43. Hall J
"Development and control analysis of a DCE" transfer report, University of Bath, Feb.1988

44. BS1042 : "Flow measurement"

45. RTI-860 user's manual, Analog Devices 1987

46. RTI-802 user's manual, Analog Devices 1987

47. Labtech Notebook manual (version 4), Lab.Technologies Corp. 1988

48. Roelle T
"Untersuchung des instationaeren betriebsverhaltens eines differentialverbundmotors" Diplomarbeit D8890ST,Hanover Univ.,1989

49. Papadopoulos J
"Experimental and analytical optimisation studies on the differential compound engine" MSc.dissertation, Univ.of Bath 1987

50. Wong HY
"Heat transfer for engineers" Longman.

51. Anderson U
"Acceleration response of a variable geometry turbocharged 32t truck" MSc.thesis, University of Bath 1984

52. AIP-24 manual, Blue Chip Technology 1987

53. AOP-8 manual, Blue Chip Technology 1987

54. Zhou Dequan, M Rezaian & FJ Wallace
"Transient response and route simulations for heavy vehicles with alternative engine-transmission systems" SAE 890393, 1989

55. Wallace FJ et al
"Performance of inward radial flow turbines under steady flow conditions with special reference to high pressure ratios and partial admission" IMechE vol.184, 1970

56. Huckvale S
"The simulation of heavy vehicle transmission systems incorporating epicyclic gear trains and hydrostatic elements" Ph.D thesis, University of Bath, 1978

57. Charlton SJ
"SPICE -Simulation Program for Internal Combustion Engines" University of Bath, 1986

58. Rezaian M
"Modelling of engine-transmission systems for heavy vehicles" Ph.D thesis, University of Bath, 1988

59. Benson RS et al
"Comparison of experimental and simulated transient responses of a turbocharged Diesel engine" SAE 730666, 1973

60. Jennings MJ et al
"A dynamic simulation of the Detroit Diesel electronic control system in heavy duty truck powertrains" SAE 861959, 1986

61. Shan-Chin Tsai & MR Goyal
"Dynamic turbocharged Diesel engine model for control analysis and design" SAE 860455, 1986

62. Rackmil CN & PN Blumberg
"Dynamic simulation of a turbocharged/intercooled Diesel engine with rack-actuated electronic fuel control system"
SAE 890394, 1989

63. Flower JO & PA Hazell
"Sampled data theory applied to the modelling and control analysis of compression-ignition engines - Part II"
Int.Journal Control Vol.13 No.4, 1971

64. Massey BS
"Mechanics of fluids" Van Nostrand Reinhold 1975

65. Sjoestroem S
"Rational use of energy in road transport"
proc. SAE Int. west coast mtg., 1977

66. Urban CM
"Dynamometer simulation of truck & bus road horsepower for transient emissions" SAE 840349, 1984

67. Hendricks E & NK Poulsen
"Minimum energy control of a large Diesel engine" SAE 861191,1986

68. Franklin GF & JD Powell
"Digital control of dynamic systems" Addison-Wesley 1980

69. Charlton SJ, AD Jones & AR Daniels
"Multiprocessor simulation of Diesel engines for condition monitoring applications" IMechE C10/87, 1987

70. Schumer MA & K Steiglitz
"Adaptive step size random search" IEEE trans.AC-13, 1968

71. Reklaitis GV et al
"Engineering optimisation: methods and applications" Wiley 1983

72. Bunday BD
"Basic optimisation methods" Arnold 1984

73. Powell MD
"On search directions for minimisation algorithms"

Mathematical Progress 4(2),p193-201, 1973

74. Nelder JA & R Mead
"A simplex method for function minimisation"
Computer Journal 7,p308-313, 1965

75. White CL et al
"Adaptive control and optimisation of Diesel engines for variable quality fuels" CIMAC D-98, 1989

76. Leonard HJ
"Control of airflow and fuel injection parameters in Diesel engines" Ph.D thesis, University of Bath 1989

77. Rosenbrock HH
"Computer-aided control system design" Academic Press 1974

78. Hall J & FJ Wallace
"Control design for a differential compound engine"
SAE 890392, 1989

79. Katz P
"Digital control using microprocessors" Prrentice-Hall 1981

80. Wallace FJ & MS Ghadiri-Zareh
"Transient response of the Cummins L10DCE power unit"
Cummins engine Co. DCE project 5th progress report,Bath,Mar.1987

81. Wallace FJ et al
"Engine-assisted braking"
Cummins Engine Co. DCE project 9th progress report, Bath, 1987

82. Backhouse R & DE Winterbone
"Dynamic behaviour of a turbocharged Diesel engine"
SAE 860453, 1986

83. Winterbone DE & S Jai-In
"Control studies of an automotive turbocharged Diesel engine with variable geometry turbine" SAE 880485, 1988

84. "Implementation of self-tuning control"
Ed. K Warwick, IEE series, Peregrinus 1988

85. Isermann R
"Digital control systems" Springer-Verlag 1981

86. Isermann R et al
"Comparison and evaluation of six on-line identification and parameter estimation methods with three simulated processes"
Paper E-1, proc. 3rd IFAC symposium on identification, 1973

87. Leigh JR
"Applied digital control" Prentice-Hall 1985

88. De Keyser RMC et al
"A comparative study of self-adaptive long-range predictive control methods" Automatica 24 (2), 1987

89. Clarke DW, C Mohtadi & PS Tuffs
"Generalized predictive control - Part I. The basic algorithm"
Automatica 23 (2), 1987

90. Clarke DW, C Mohtadi & PS Tuffs
"Generalized predictive control - Part II. Extensions and interpretations" Automatica 23 (2), 1987

91. Clarke DW & C Mohtadi
"Properties of generalized predictive control"
proc.10th IFAC world congress, Vol.X, 1988

92. Noble AD, AJ Beaumont & AS Mercer
"Predictive control applied to transient engine testbeds"
SAE 880487, 1988

93. Press WH et al
"Numerical recipes" Cambridge University Press 1986

94. Hung CC et al
"A dual-rate adaptive digital Smith predictor"
Automatica 25 (1), 1989

APPENDICES

1. DTR - data reduction code listing
2. AMI - control program code listing
3. Dynamic simulation - functional specification
4. SIMDCE code listings
5. Actuator dynamics
6. Difference equations for Diesel engine torque delay
7. Identification routines code listings

APPENDIX 1

```
      PROGRAM DTR
C DCE data reduction; esp.for turbine performance mapping.
C Last change JH 210689
C Written: J Hall  17th April 1989
C Code:    Microsoft FORTRAN Version 4.1
C Machine: PC-AT compatibles
C
      INTEGER I,I1
C turbine raw and processed data
C TTIN1,TTIN2,TTOUT1,TTOUT2,PTIN,PTOUT,ALFA,TORT
C NT,NDNT,WTTEMP,WTMEAS,MT,NDMT,BSR,PRAT,TISEFF,TOVEFF
C engine raw and proc.data
C NE,TORENG,QFUEL,TFUEL
C MFUEL,WE
C compressor raw and proc.data
C NC,PCIN,PCOUT,TCIN,TCOUT
C MC,WC
C system raw and proc.data
C NOS,TOROS
C WOS,WUN,TRANEF
C ambient data
C PATM
C
C o/p data file arrays (raw and proc.data)
      REAL RAW(20,5),PROC(21,5)
C date,header,o/p filename
      CHARACTER*1  C
      CHARACTER*6  DATE
      CHARACTER*30 HEADER
      CHARACTER*10 FNAME
C initialise
      I=1
C read header etc
      WRITE(*,601)
  601 FORMAT(10(/))
      WRITE(*,603)
      WRITE(*,605)
  603 FORMAT(9X,'  DTR - turbine testing data reduction')
  605 FORMAT(9X,'  ------------------------------------'//)
      WRITE(*,607)
  607 FORMAT('    Enter header(30char):')
      READ(*,'(A30)') HEADER
      WRITE(*,609)
  609 FORMAT('    Enter date (ddmmyy) :')
      READ(*,'(A6)') DATE
      WRITE(*,611)
  611 FORMAT('    Enter Atm.pres.[bar]:')
      READ(*,*) RAW(20,I)
C
   20 CONTINUE
C
      WRITE(*,613) I
  613 FORMAT(///' TEST POINT ',I1,'  Please input data as prompted
C
      WRITE(*,615)
  615 FORMAT(' input SPEEDS [rev/min]:')
      WRITE(*,617)
  617 FORMAT(' engine speed:')
      READ(*,*) RAW(1,I)
```

```
      WRITE(*,619)
  619 FORMAT(' output speed:')
      READ(*,*) RAW(2,I)
      WRITE(*,621)
  621 FORMAT(' compr. speed:')
      READ(*,*) RAW(3,I)
      WRITE(*,623)
  623 FORMAT(//'  input TORQUES [Nm]:')
      WRITE(*,625)
  625 FORMAT(' engine torque :')
      READ(*,*) RAW(4,I)
      WRITE(*,627)
  627 FORMAT(' output torque :')
      READ(*,*) RAW(5,I)
      WRITE(*,629)
  629 FORMAT(' turbine torque:')
      READ(*,*) RAW(6,I)
C
      WRITE(*,631)
  631 FORMAT(//'  input TEMPERATURES [deg.K]:')
      WRITE(*,633)
  633 FORMAT(' turbine plenum A4:')
      READ(*,*) RAW(7,I)
      WRITE(*,635)
  635 FORMAT(' turbine plenum A5:')
      READ(*,*) RAW(8,I)
      WRITE(*,637)
  637 FORMAT(' turbine flange A6:')
      READ(*,*) RAW(9,I)
      WRITE(*,639)
  639 FORMAT(' turbine pipe   A8:')
      READ(*,*) RAW(10,I)
      WRITE(*,641)
  641 FORMAT(' compr. plenum  A1:')
      READ(*,*) RAW(11,I)
      WRITE(*,643)
  643 FORMAT(' compr.  inlet  B2:')
      READ(*,*) RAW(12,I)
      WRITE(*,645)
  645 FORMAT(' fuel(flowmtr)temp:')
      READ(*,*) RAW(13,I)
C
      WRITE(*,647)
  647 FORMAT(//'  input PRESSURES [units as prompted]:')
      WRITE(*,649)
  649 FORMAT(' compr.plenum [barg] :')
      READ(*,*) RAW(14,I)
      WRITE(*,651)
  651 FORMAT(' turb.plenum(BNC2)[V]:')
      READ(*,*) RAW(15,I)
      WRITE(*,653)
  653 FORMAT(' comp.inlet dp[cmH2O]:')
      READ(*,*) RAW(16,I)
      WRITE(*,655)
  655 FORMAT(' exh.back pres.[cmHg]:')
      READ(*,*) RAW(17,I)
C
      WRITE(*,657)
  657 FORMAT(//'  input other data:')
      WRITE(*,659)
  659 FORMAT(' fuel flowrate[V]:')
      READ(*,*) RAW(18,I)
```

```
      WRITE(*,661)
  661 FORMAT(' Nozzles posn.[V]:')
      READ(*,*) RAW(19,I)
C set all patm s equal
      RAW(20,I)=RAW(20,1)
C
      WRITE(*,663)
  663 FORMAT(//' input complete: hit any key to check it')
      READ(*,'(A1)') C
C
   30 CONTINUE
C echo all i/p data to screen for checking/corrections
      CALL UPSCRN(RAW,I)
C and get modifications one-by-one
      WRITE(*,671)
  671 FORMAT(///' Enter [C] to make changes OR [P] to process data:
      READ(*,'(A1)') C
      IF(C.EQ.'P'.OR.C.EQ.'p') THEN
         WRITE(*,673)
  673    FORMAT(' processing data...')
         CALL DATPRO(RAW,PROC,I)
         I=I+1
      ELSE
C input changes
   40    CONTINUE
         WRITE(*,675)
  675    FORMAT(/' Enter number (1-19) of entry to change:')
         READ(*,*) I1
         IF(I1.LT.1 .OR. I1.GT.19) GOTO 40
         WRITE(*,677)
  677    FORMAT(' Enter new value:')
         READ(*,*) RAW(I1,I)
C loop back for more changes
         GOTO 30
      END IF
C loop back for next test point (max 5)
      IF(I.LT.5) THEN
         WRITE(*,680)
  680    FORMAT(/' Any more test points ([y]/n)?')
         READ(*,'(A1)') C
      ELSE
         C='n'
      END IF
      IF(C.NE.'N'.AND.C.NE.'n') GOTO 20
C have input,checked & processed all data. now write to file
      WRITE(*,681)
  681 FORMAT(//' Data ready; enter o/p filename (10char):')
      READ(*,'(A10)') FNAME
      OPEN(UNIT=4,FILE=FNAME,STATUS='NEW')
      WRITE(4,700)
  700 FORMAT(6X,'[output from dtr: DCE turbine tests]'/)
      WRITE(4,701) HEADER,DATE
  701 FORMAT(4X,A30,4X,A6)
      WRITE(4,702) RAW(20,1)
  702 FORMAT(/' atmospheric pres. ',G10.3,'bar')
      WRITE(4,703)
  703 FORMAT(' SPEEDS [rev/min]')
      WRITE(4,704) (RAW(1,I1),I1=1,I)
  704 FORMAT(' Engine',5(G10.3))
      WRITE(4,706) (RAW(2,I1),I1=1,I)
  706 FORMAT(' O/P   ',5(G10.3))
      WRITE(4,708) (RAW(3,I1),I1=1,I)
```

```
  708   FORMAT(' Compr.',5(G10.3))
        WRITE(4,709)
  709   FORMAT(' TORQUES [Nm]')
        WRITE(4,710) (RAW(4,I1),I1=1,I)
  710   FORMAT(' Engine',5(G10.3))
        WRITE(4,712) (RAW(5,I1),I1=1,I)
  712   FORMAT(' O/P    ',5(G10.3))
        WRITE(4,714) (RAW(6,I1),I1=1,I)
  714   FORMAT(' Turbn.',5(G10.3))
        WRITE(4,715)
  715   FORMAT(' TEMPERATURES [deg.C]')
        WRITE(4,716) (RAW(7,I1),I1=1,I)
  716   FORMAT(' TrbIN1',5(G10.3))
        WRITE(4,718) (RAW(8,I1),I1=1,I)
  718   FORMAT(' TrbIN2',5(G10.3))
        WRITE(4,720) (RAW(9,I1),I1=1,I)
  720   FORMAT(' TbOUT1',5(G10.3))
        WRITE(4,722) (RAW(10,I1),I1=1,I)
  722   FORMAT(' TbOUT2',5(G10.3))
        WRITE(4,724) (RAW(11,I1),I1=1,I)
  724   FORMAT(' CmpOUT',5(G10.3))
        WRITE(4,726) (RAW(12,I1),I1=1,I)
  726   FORMAT(' Cmp.IN',5(G10.3))
C
        WRITE(4,727)
  727   FORMAT(' PRESSURES [bar]')
        WRITE(4,728) (RAW(16,I1),I1=1,I)
  728   FORMAT(' Cmp.IN',5(G10.3))
        WRITE(4,730) (RAW(14,I1),I1=1,I)
  730   FORMAT(' CmpOUT',5(G10.3))
        WRITE(4,732) (RAW(15,I1),I1=1,I)
  732   FORMAT(' Trb.IN',5(G10.3))
        WRITE(4,734) (RAW(17,I1),I1=1,I)
  734   FORMAT(' TrbOUT',5(G10.3))
C
        WRITE(4,735)
  735   FORMAT(' MASSFLOWS [kg/min]')
        WRITE(4,736) (PROC(6,I1),I1=1,I)
  736   FORMAT(' Compr.',5(G10.3))
        WRITE(4,738) (PROC(7,I1),I1=1,I)
  738   FORMAT(' Fuel   ',5(G10.3))
        WRITE(4,740) (PROC(8,I1),I1=1,I)
  740   FORMAT(' Turbn.',5(G10.3))
C
        WRITE(4,741)
  741   FORMAT(' POWERS [kW]. Note Turb:[M]torqmtr,[H]enthalpy')
        WRITE(4,742) (PROC(1,I1),I1=1,I)
  742   FORMAT(' Engine',5(G10.3))
        WRITE(4,744) (PROC(5,I1),I1=1,I)
  744   FORMAT(' Compr.',5(G10.3))
        WRITE(4,746) (PROC(3,I1),I1=1,I)
  746   FORMAT(' Trb[M]',5(G10.3))
        WRITE(4,748) (PROC(4,I1),I1=1,I)
  748   FORMAT(' Trb[H]',5(G10.3))
        WRITE(4,750) (PROC(2,I1),I1=1,I)
  750   FORMAT(' O/P    ',5(G10.3))
        WRITE(4,752) (PROC(19,I1),I1=1,I)
  752   FORMAT(' Losses',5(G10.3))
        WRITE(4,754) (PROC(20,I1),I1=1,I)
  754   FORMAT(' Eftran',5(G10.3))
        WRITE(4,753) (PROC(21,I1),I1=1,I)
  753   FORMAT(' o/sSFC',5(G10.3))
```

```
C
      WRITE(4,755)
  755 FORMAT(' TURBINE PARAMETERS [bar,K,kg,kW,min as appropriate]
      WRITE(4,756) (RAW(19,I1),I1=1,I)
  756 FORMAT(' Noz[V]',5(G10.3))
      WRITE(4,758) (PROC(10,I1),I1=1,I)
  758 FORMAT(' ExpRat',5(G10.3))
      WRITE(4,760) (PROC(11,I1),I1=1,I)
  760 FORMAT(' NDflow',5(G10.3))
      WRITE(4,762) (PROC(12,I1),I1=1,I)
  762 FORMAT(' NDspd.',5(G10.3))
      WRITE(4,764) (PROC(13,I1),I1=1,I)
  764 FORMAT(' U/c   ',5(G10.3))
      WRITE(4,766) (PROC(14,I1),I1=1,I)
  766 FORMAT(' Eflsen',5(G10.3))
      WRITE(4,768) (PROC(15,I1),I1=1,I)
  768 FORMAT(' Efnett',5(G10.3))
C
      CLOSE(UNIT=4,STATUS='KEEP')
C
      STOP
      END
C
C
      SUBROUTINE DATPRO(RAW,PROC,I)
C data reduction
      INTEGER I,I1,I2,J
      REAL RAW(20,5),PROC(21,5)
      REAL R(7),M(8),M1(7)
      REAL KW(8),CMM(7)
      REAL PRC,IEFACT
      DATA R(1),R(2),R(3),R(4) /1.686,2.023,2.382,2.727/
      DATA R(5),R(6),R(7) /3.043,3.435,3.635/
      DATA M(1),M(2),M(3),M(4) /.006343,.007803,.00862,.010512/
      DATA M(5),M(6),M(7) /.01097,.01196,.01246/
      DATA M1(1),M1(2),M1(3) /.004269,.004219,.004177/
      DATA M1(4),M1(5),M1(6) /.004202,.004177,.004219/
      DATA CMM(1),CMM(2),CMM(3) /35.68,35.06,34.77/
      DATA CMM(4),CMM(5),CMM(6) /34.66,34.42,34.25/
      DATA KW(1),KW(2),KW(3),KW(4) /46.92,58.66,66.76,80.23/
      DATA KW(5),KW(6),KW(7) /85.61,99.4,105.85/
C
      I1=I
C convert pressure inputs to abs.[bar]pressures
      RAW(14,I1)=RAW(14,I1) + RAW(20,I1)
      RAW(15,I1)=RAW(15,I1)*.3 + RAW(20,I1)
      RAW(16,I1)=RAW(20,I1) - RAW(16,I1)/1020.
      RAW(17,I1)=RAW(17,I1)/76. + RAW(20,I1)
C compr.pres.ratio
      PRC=RAW(14,I1)/RAW(16,I1)
C convert temps to [K] (except fuel temp)
      DO 30 I2=7,12
         RAW(I2,I1)=RAW(I2,I1)+273.
   30 CONTINUE
C scale other i/ps to engineering units: Qfuel [cm3/min]
      RAW(18,I1)=RAW(18,I1)*.4
C massflows [kg/min]: compr.,+ fuel, =turb.
C compr.vol.flow by interpoln from set of CompAir data
C first calc inter/extrapoln factor on basis of pres.ratio PRC
      DO 21 J=1,6
         IF(R(J).GT.PRC) GOTO 70
   21 CONTINUE
```

```
      J=6
      GOTO 80
 70   IF(J.LT.2) J=2
 80   IEFACT=(PRC-R(J-1))/(R(J)-R(J-1))
      M1(7)=M1(J-1)+IEFACT*(M1(J)-M1(J-1))
      CMM(7)=CMM(J-1)+IEFACT*(CMM(J)-CMM(J-1))
      PROC(6,I1)=CMM(7)+M1(7)*(RAW(3,I1)-9000.)
C massflow (NB density at inlet conditions, also note p[bar])
      PROC(6,I1)=PROC(6,I1)*RAW(16,I1)*348.3/RAW(12,I1)
C fuel massflow
      PROC(7,I1)=RAW(18,I1)*(.841+.002*(RAW(13,I1)-15.)/3.)
C compr.+ fuel = turbine massflow at steady state
      PROC(8,I1)=PROC(6,I1)+PROC(7,I1)
C
C powers [kW]: eng.,o/p,turb(meas.),compr.(mapped),turb(thermodyn.)
      PROC(1,I1)=RAW(1,I1)*RAW(4,I1)/9549.3
      PROC(2,I1)=RAW(2,I1)*RAW(5,I1)/9549.3
      PROC(3,I1)=RAW(2,I1)*14.67*RAW(6,I1)/9549.3
C compressor power from CompAir test data by interpoln (values at
C data points exactly as used in DCETABB).
C interpoln done above for massflow calcs-same principles apply
      DO 22 J=1,7
         IF(R(J).GT.PRC) GOTO 60
 22   CONTINUE
      J=7
      GOTO 90
 60   IF(J.LT.2) J=2
 90   IEFACT=(PRC-R(J-1))/(R(J)-R(J-1))
      M(8)=M(J-1)+IEFACT*(M(J)-M(J-1))
      KW(8)=KW(J-1)+IEFACT*(KW(J)-KW(J-1))
      PROC(5,I1)=M(8)*(RAW(3,I1)-7850.)+KW(8)
      PROC(4,I1)=PROC(8,I1)*1.147*( RAW(7,I1)+RAW(8,I1)
     >             -RAW(9,I1)-RAW(10,I1) )/120.
C unaccounted power and effective total transmission efficiency
      PROC(19,I1)=PROC(1,I1)+PROC(3,I1)-PROC(5,I1)-PROC(2,I1)
      PROC(20,I1)=PROC(2,I1)/(PROC(2,I1)+PROC(19,I1))
C o/p shaft BSFC (kg/kWh)
      PROC(21,I1)=60.*PROC(7,I1)/PROC(2,I1)
C turbine params:
C pres.ratio,NDmassflow,NDspd,U/c,isen.effy,overall effy. [bar,rpm,kg
      PROC(10,I1)=RAW(15,I1)/RAW(17,I1)
      PROC(11,I1)=PROC(8,I1)*SQRT((RAW(7,I1)+RAW(8,I1))/2.)/RAW(15,
      PROC(12,I1)=RAW(2,I1)*14.67/SQRT( (RAW(7,I1)+RAW(8,I1))/2. )
      PROC(13,I1)=RAW(2,I1)*14.67*8.977E-3/ SQRT( 2.*1147*RAW(7,I1)
     >             *( 1.- (1./PROC(10,I1))**.25 ) )
      PROC(14,I1)=(1.- (RAW(9,I1)+RAW(10,I1))/(RAW(7,I1)+RAW(8,I1))
     >             (1.- (1./PROC(10,I1))**.25)
      PROC(15,I1)=PROC(14,I1)*PROC(3,I1)/PROC(4,I1)
C
      RETURN
      END
C
C
      SUBROUTINE UPSCRN(RAW,I)
C refresh screen with updated inputs
      INTEGER I
      REAL RAW(20,5)
C simply need to put up all inputs,with index numbers and current va
      WRITE(*,101) 1,RAW(1,I)
 101  FORMAT(4X,I3,2X,' Engine speed:',G10.3)
      WRITE(*,103) 2,RAW(2,I)
 103  FORMAT(4X,I3,2X,' Output speed:',G10.3)
```

```
      WRITE(*,105) 3,RAW(3,I)
105   FORMAT(4X,I3,2X,' Compr. speed:',G10.3)
      WRITE(*,107) 4,RAW(4,I)
107   FORMAT(4X,I3,2X,' Engine torq.:',G10.3)
      WRITE(*,109) 5,RAW(5,I)
109   FORMAT(4X,I3,2X,' Output torq.:',G10.3)
      WRITE(*,111) 6,RAW(6,I)
111   FORMAT(4X,I3,2X,' Turbine torq:',G10.3)
      WRITE(*,113) 7,RAW(7,I)
113   FORMAT(4X,I3,2X,' Trb.Tin [A4]:',G10.3)
      WRITE(*,115) 8,RAW(8,I)
115   FORMAT(4X,I3,2X,' Trb.Tin [A5]:',G10.3)
      WRITE(*,117) 9,RAW(9,I)
117   FORMAT(4X,I3,2X,' Trb.Tout[A6]:',G10.3)
      WRITE(*,119) 10,RAW(10,I)
119   FORMAT(4X,I3,2X,' Trb.Tout[A8]:',G10.3)
      WRITE(*,121) 11,RAW(11,I)
121   FORMAT(4X,I3,2X,' Cmp.Tout[A1]:',G10.3)
      WRITE(*,123) 12,RAW(12,I)
123   FORMAT(4X,I3,2X,' Cmp.T in[B2]:',G10.3)
      WRITE(*,125) 13,RAW(13,I)
125   FORMAT(4X,I3,2X,' Fuel Temp.  :',G10.3)
      WRITE(*,127) 14,RAW(14,I)
127   FORMAT(4X,I3,2X,' Comp.Del.pres[bar g]:',G10.3)
      WRITE(*,129) 15,RAW(15,I)
129   FORMAT(4X,I3,2X,' Turb.Inl.pres.[BNC2]:',G10.3)
      WRITE(*,131) 16,RAW(16,I)
131   FORMAT(4X,I3,2X,' Comp.Inl.Depr[cmH2O]:',G10.3)
      WRITE(*,133) 17,RAW(17,I)
133   FORMAT(4X,I3,2X,' Exh.back pres.[cmHg]:',G10.3)
      WRITE(*,135) 18,RAW(18,I)
135   FORMAT(4X,I3,2X,' Fuel Vol.flowrate[V]:',G10.3)
      WRITE(*,137) 19,RAW(19,I)
137   FORMAT(4X,I3,2X,' Turb.Nozzles Posn[V]:',G10.3)
C
      RETURN
      END
```

```
        ami2.c       */
DCE micro-controller */
version 2  using steady-state schedule settings plus separate*/
boost control transient strategy.*/
last change made: JH Ø8Ø289*/
written: J Hall   Jan. 1989*/
code   : Microsoft C5.1 and QuickC
machine: Dell 2ØØ (8Ø286 AT-compatible), running MS-DOS
i/o    : Blue Chip Technology AIP-24,AOP-8 PC-bus boards
ADC and DAC connections are as follows:
ADC Ø=demand 1=nos  2=neng  3=ncomp  4=pcomp  5=texh  6=xrack
DAC Ø=urack  1=unoz 2=utim

nclude<stdio.h>
nclude<conio.h>
in()
      {
      long put();    /*function declarations*/
      long get();
      long pull();
      long offset();
      long racklm();
      long demand,nos,neng,ncomp,pcomp,texh,xrack;
      long urack,unoz,utim;
      long fuel,desfl,maxfl,scrlm,flredn;
      long ncsch;
      long kne,knc,kfbr,knoslm,kbstlm,ktexlm,ktrbst;
      long ncarr  [6] [9]; /*height x width of schedule arrays*/
      long timarr [6] [9];
      long idlnoz=1ØØØ;    /*fixed 5V nozzle setting at Idle*/
      long idltim=12ØØ;    /*  "   6V timing        "       */
      int i,j;
      int txflag=Ø;
      int serch=1;         /*signal error checking enabled*/
      int rsigok=1;        /*rack signal ok*/
      char reply;
      FILE *fptr;  /*pointer to file*/
      /*open data file amidat*/
      if( (fptr=fopen("amidat.doc","r"))==NULL)
         {
         printf("Can't open data file amidat.doc\n\n");
         exit();
         }
      /*read control gains:note these are scaled *1ØØ for discrimination
      fscanf(fptr,"%ld %ld %ld",&kne,&knc,&kfbr);
      fscanf(fptr,"%ld %ld %ld",&knoslm,&ktrbst,&ktexlm);
      /*read schedules for steady-state Ncomp and stat.inj.timing*/
      for(i=Ø;i<6;i++)       /*6 lines of data,one per fuelling division
         {
         for(j=Ø;j<9;j++)    /*each line has 9 speed divisions*/
            {
            fscanf(fptr,"%ld",&ncarr[i] [j]);
            /*scale from Ø-12ØØØrev/min to Ø-2ØØØdecimal*/
            ncarr[i] [j] = ncarr[i] [j]/6;
            }
         }
      for(i=Ø;i<6;i++)
```

```
    {
    for(j=Ø;j<9;j++)
       {
       fscanf(fptr,"%ld",&timarr[i] [j]); /*already scaled to dec.*/
       }
    }
fclose(fptr);
printf("\n\n\n\n\n\n\n\n\n\n\n\n\n");
printf("                 _____________________________________________\n");
printf("            |_____________________ AMI _____________________|\n");
printf("            |                                               |\n");
printf("            |           DCE micro-controller                |\n");
printf("            |   (version2 : transient boost control)        |\n");
printf("            |_______________________________________________|\n");
printf("\n\n\n");
printf("                 _____________________________________________\n");
printf("            | AMI performs                                  |\n");
printf("            | (i)  single operator i/p control of DCE.      |\n");
printf("            | (ii) interactive bumpless transfer from       |\n");
printf("            |      manual to computer control.              |\n");
printf("            | (iii)single-key jump to Idle condition        |\n");
printf("            |      in emergency.                            |\n");
printf("            | (iv) bumpless transfer from Idle to           |\n");
printf("            |      manual control.                          |\n");
printf("            |_______________________________________________|\n");
printf("\n\n");
printf("                 _____________________________________________\n");
printf("            |_____PRESS__ANY__KEY__TO__CONTINUE_____|\n");
reply=getch();
printf("\n\n\n\n\n\n\n\n\n\n\n");
printf("                 _____________________________________________\n");
printf("            |_SIGNAL_ERROR_CHECKING_____________________|\n");
printf("            |                                               |\n");
printf("            | Signal error checking is incorporated to      |\n");
printf("            | minimise dangers of signal short or open      |\n");
printf("            | circuits.  For program development this       |\n");
printf("            | may be disabled:                              |\n");
printf("            |_______________________________________________|\n");
printf("            | HIT [D] TO DISABLE SIGNAL ERROR CHECKING      |\n");
printf("            |_HIT_ANY_OTHER_KEY_TO_RETAIN_CHECKING_____|\n");
printf("\n\n\n\n\n\n\n");
reply=getch();
if(reply=='d' || reply=='D') serch=Ø;
printf("\n\n\n\n\n");
printf("                 _____________________________________________\n");
printf("            |_OPERATOR  INSTRUCTIONS____________________|\n");
printf("            |                                               |\n");
printf("            | DCE must be at normal operating temps,        |\n");
printf("            | and operating in the following control        |\n");
printf("            | modes:                                        |\n");
printf("            | Engine: manual SPEED mode (black master       |\n");
printf("            |         knob set to SPEED).                   |\n");
printf("            |   Load: manual, any mode.                     |\n");
printf("            |                                               |\n");
printf("            | Also ensure that the Engine RACK control      |\n");
printf("            | MANual/EXTernal switch is set to EXT.         |\n");
printf("            |                                               |\n");
printf("            | The RACK LIMIT pot. may be set to any         |\n");
printf("            | level;this will of course restrict the        |\n");
printf("            | max. dyno. load the DCE can support.          |\n");
printf("            |_______________________________________________|\n");
printf("            |_____PRESS__ANY__KEY__TO__CONTINUE_____|\n");
```

```
printf("\n\n\n\n\n");
reply=getch();
printf("\n\n\n\n\n\n\n\n\n\n\n");
printf("                 _____________________________________________\n");
printf("                ¦ Ensure that all i/o connections have been¦\n");
printf("                ¦ correctly made.Signal loss at most inputs¦\n");
printf("                ¦ will cause fuelling/nozzle restrictions  ¦\n");
printf("                ¦ or  automatic jump to an Idle condition  ¦\n");
printf("                ¦ and/or stall at high loads.Overboosting &¦\n");
printf("                ¦ Component overspeeding will NOT occur as ¦\n");
printf("                ¦ a result of any signal loss.             ¦\n");
printf("                ¦ Diagnostic messages will be given.       ¦\n");
printf("                ¦___________________________________________¦\n");
printf("                ¦_____PRESS__ANY__KEY__TO__CONTINUE_______¦\n");
printf("\n\n\n\n\n\n\n\n");
reply=getch();
printf("\n\n\n\n\n\n\n\n");
printf("                 _____________________________________________\n");
printf("                ¦_________________IMPORTANT!_________________¦\n");
printf("                ¦(i) The automatic shutdown system and the  ¦\n");
printf("                ¦    3 manual shutdown buttons are enabled  ¦\n");
printf("                ¦    at all times.                          ¦\n");
printf("                ¦(ii)Peak cylinder pres.(max.150bar)is not  ¦\n");
printf("                ¦    explicitly controlled, and should be   ¦\n");
printf("                ¦    monitored by the operator.If exceeded  ¦\n");
printf("                ¦    whilst in computer control mode,       ¦\n");
printf("                ¦    reduce DEMAND,or hit [I] for Idle mode¦\n");
printf("                ¦___________________________________________¦\n");
printf("\n\n\n");
printf("                 _____________________________________________\n");
printf("                ¦ PRESS [A] TO START INTERACTIVE BUMPLESS   ¦\n");
printf("                ¦ TRANSFER TO MICROCOMPUTER CONTROL,  or    ¦\n");
printf("                ¦ PRESS ANY OTHER KEY TO EXIT TO DOS.       ¦\n");
printf("                 ---------------------------------------------\n");
printf("\n\n\n");
reply=getch();
if(reply!='a' && reply!='A') exit(0);
nos=get(1);
if(nos<320 && serch==1)   /*=nt to 550rev/min*/
   {
   printf("\n    STOP: faulty o/p shaft speed signal.\n\n");
   exit();
   }
xrack=get(6);
/*should be in range about 1-10V*/
if((xrack<200 || xrack>2020) && serch==1)
   {
   printf("\n    STOP: faulty rack position signal.\n\n");
   exit();
   }
/*move DCE to current sched.Ncomp.  Schedules are based on     */
/*fuelling:rack-fuelling correln from exptal mapping 300189*/
fuel = (17*(xrack-600)) / 14;
ncsch = 6*pull(ncarr,nos,fuel); /*sched.Nc ,in rev/min*/
printf("\n\n\n\n\n\n\n\n");
printf("                  ___________________________________\n");
printf("                 ¦ Bring COMPRESSOR speed to %ld rpm¦\n",ncsch);
printf("                 ¦ using manual NOZZLE control pot.  ¦\n");
printf("                 ¦___________________________________¦\n");
printf("                 ¦__THEN_PRESS_ANY_KEY_TO_CONTINUE___¦\n");
printf("\n\n\n\n\n\n\n\n\n\n");
reply=getch();
```

```
/*-------------------------------------*/
/*condition will have changed: re-read*/
/*-------------------------------------*/
nos=get(1);
neng=get(2);
/*engine speed signal should be in range 600-3000rpm*/
if((neng<400 || neng>2000) && serch==1)
   {
   printf("\n    STOP: faulty engine speed signal.\n\n");
   exit();
   }
xrack=get(6);
if((xrack<200 || xrack>2020) && serch==1)
   {
   printf("\n    STOP: faulty rack position signal.\n\n");
   exit();
   }
fuel = (17*(xrack-600)) / 14;
/*now have current No/s,rack,fuel & Neng. Calc scheduled inj.timing*
/*and nozzle settings, and the Demand setting for bumpless transfer*
/*the reqd demand pot.setting is calc.from the current engine speed*
/*and the computer engine speed ctrl gain,to give a rack demand =to*
/*the current rack position,so there will be no bump on switchover.*
demand=((((100*fuel)/kne) + neng)*75)/14;    /*gains prescaled x100*
if(demand>10000) demand=10000;  /*[mV]*/
ncomp=get(3);
if(ncomp<83 && serch==1)   /*500rpm*/
  {
  printf("\n    STOP: faulty compressor speed signal.\n\n");
  exit();
  }
ncsch=pull(ncarr,nos,fuel);
unoz=(knc*(ncomp-ncsch))/100+offset(nos,fuel);
if(unoz>2000) unoz=2000;   /*ctrl range is 0-10V ie 0-2000dec.*/
if(unoz<0)    unoz=0;
utim=pull(timarr,nos,fuel);
printf("\n\n\n");
printf("                 _____________________________________\n");
printf("                | Set TIMING control to %ld     mV  |\n",utim*5);
printf("                | Set NOZZLE control to %ld     mV  |\n",(unoz*5))
printf("                | Set DEMAND control to %ld     mV  |\n",demand);
printf("                | CHECK:                            |\n");
printf("                | Demand switch set to MANual input |\n");
printf("                | Rack switch set to EXTernal input |\n");
printf("                |-----------------------------------|\n");
printf("                | When ready to transfer to computer|\n");
printf("                | (Auto.) control, carry out the    |\n");
printf("                | following steps in the order given:\n");
printf("                |                                   |\n");
printf("                | 1.press [A]                       |\n");
printf("                | 2.switch TIMING control to COMPuter\n");
printf("                | 3.switch NOZZLE control to COMPuter\n");
printf("                | 4.switch Engine ctrl mode selector|\n");
printf("                |   (black rotary switch) to RACK   |\n");
printf("                | 5.hit [SPACEBAR] for runtime menu |\n");
printf("                |___________________________________|\n\n\n");
lbl4:
reply=getche();  /*look for the [A] instruction*/
if(reply!='A' && reply!='a')
   {
   if(reply=='X' || reply=='x') {exit();}
   printf("\n        WARNING: key pressed was not [A]; \n");
```

```
   printf("        Re-enter, or press [X] to eXit program\n");
   goto lbl4;
   }
printf("\n");
/*now run Auto. ctrl. until operator hits [I] to go to Idle    */
/*loop until key is pressed. Only check buffer for contents    */
/*when kbhit flags keystroke has been made,otherwise getch will*/
/*wait for input at each loop*/
while(reply!='I' && reply!='i')
   {
   if( kbhit() )
      {
      reply=getch();
      if(reply==' ')   /*spacebar hit - put up menu*/
         {
         printf("\n\n\n\n");
printf("                 _____________________________________________\n")
printf("           ¦              ______¦__AMI__¦_______              ¦\n"
printf("           ¦           ¦__DCE microcontroller_¦               ¦\n"
printf("           ¦-------------------------------------------------¦\n"
printf("           ¦ DCE in auto.control. Operator input is via      ¦\n"
printf("           ¦ Demand pot. only. If Pmax >150 bar reduce       ¦\n"
printf("           ¦ Demand or hit[I]to drop to Idle(see below).     ¦\n"
printf("           ¦_________________________________________________¦\n"
printf("     _____________________________   _____________________________
printf("    ¦________SHUTDOWN___________¦  ¦__________IDLE_____________

printf("    ¦ the automatic shutdown & ¦  ¦ hit [I] key to drop DCE

printf("    ¦ the 3 red manual shutdown¦  ¦ to fixed fast Idle. NB

printf("    ¦ buttons are active at all¦  ¦ reduce Load if nec. to

printf("    ¦ times.                   ¦  ¦ avoid stalling the DCE.

printf("    ¦__________________________¦  ¦_____________________________

printf("                 _____________________________________________\n");
printf("           ¦___Return_to_MANUAL_control_(-via IDLE)____¦\n")
printf("           ¦ ensure Load is low (100-300 Nm),bring the ¦\n")
printf("           ¦ Engine speed to about 1200rpm using Demand¦\n")
printf("           ¦ pot. Then hit [I] key.                    ¦\n")
printf("           ¦_______________________________________________¦\n")
         }
      }
   /*-----Auto ctrl statements-----*/
   /*engine speed control*/
   demand=get(0);
   /*10Vdemand=2800rpm cf 10Vneng=3000rpm, so demand is rescaled*/
   demand = (demand*14)/15;
   neng=get(2);
   /*first check for signal loss, let Ne<400rpm be signal loss*/
   if(neng<267 && serch==1)
      {
      printf("\n WARNING: Ne apparently <400rpm. SWITCHING TO IDLE'
      printf("\n          CONTROL MODE, WITH FIXED 2V RACK SETTING'
      reply='I';
      }
   /*min loaded engine speed 800rpm so impose eng.idle spd.ctrl. *,
   /*if demand and speed drop too low set demand to minimum;if Ne*,
   /*below 850rpm (567dec) increase gain with droop(lever action)*,
   if(neng>567)
```

```
            {
            fuel =( kne*(demand - neng) )/100;
            }
         else
            {
            if(demand<567) {demand=567;}
            fuel =(kne * ((demand-neng) * (867-neng))/300)/100;
            }
         desfl=fuel; /*before constraints are imposed*/
         /*rack limit*/
         scrlm = racklm(neng);
         if(fuel>scrlm) {fuel=scrlm;}
         /*smoke-limiting (based on a max. fuel/boost ratio kfbr)*/
         /*ass.typical 1000mbar Patm at Wolfson test cell.*/
         /*scaling is 4bar=10v=2000dec so 1000mbar=500dec.*/
         pcomp = 500 + get(4);
         maxfl=(kfbr*pcomp)/100;
         if(fuel > maxfl) {fuel = maxfl;}
         /*output shaft speed limiting (reduce fuel with excess speed)*/
         /*rated speed 3409rpm,start limiting above 3300rpm(=1885dec.)*/
         nos=get(1);
         if(nos>1885)
            {
            flredn= knoslm*((nos-1885)/10)*((nos-1885)/10);
            fuel = fuel - flredn;
            desfl=desfl - flredn;
            }
         /*cut fuelling to limit exh.temp.  680deg C=6.8V=1360dec.*/
         if(txflag==0)
           {
           texh=-get(5); /*texh signal came via x10 inverting amplifier*/
           /*check for o/c at this input- crosstalk will push signal up*/
           if(texh>1900)    /*950deg C impossible*/
             {
             texh=0;       /*ignore faulty i/p*/
             txflag=1;     /*flag to not read texh in future*/
             printf("\n\n\n       ");
             printf("WARNING: Exh.temp signal unrealistically high");
             printf("\n         Texh-based fuel restriction disabled\n");
             }
           }
         if(texh>1360) {fuel = fuel - (ktexlm*(texh-1360))/100;}
         /*finally constrain min.rack posn demand to zero*/
         if(fuel<0) {fuel=0;}
         /*convert fuelling to equiv.rack position using correlation*/
         /*from experimental mapping and put out rack demand to DAC0*/
         urack = (14*fuel)/17 + 600;
         put(urack,0);
         /*now we want the fuelling for scheduling. This is based on
           sampled rack posn, not on fuel control o/p, since this is
           both more accurate and smoother, due to damping in pump*/
         if(rsigok==1)
            {
            xrack=get(6);
            if((xrack<0 || xrack>2100) && serch==1 )
               {
               printf("\n WARNING: Rack signal faulty-Using Rack demand c
stead");

               rsigok=0;   /*(so message is only put up once)*/
               }
            /*rack signal sensible. convert to equiv.fuelling*/
            fuel = (17*(xrack-600)) / 14;
```

```
      }
   /*offset+Prop. nozzle control*/
   ncomp=get(3);
   /*check signal.say <500rpm is signal loss*/
   if(ncomp<83 && serch==1)
      {
      printf("\n WARNING: Nc apparently <500rpm. SWITCHING TO IDLE");
      reply='I';
      }
   /*pull s-s optimum compressor speed from schedule*/
   /*SWITCH between st.state & transient control*/
   if(desfl>=scrlm)
      {
      unoz = (ktrbst*(100*scrlm/kfbr - pcomp))/100 + offset(nos,fuel
      }
   else
      {
      unoz = ( knc*(ncomp-ncsch) )/100 + offset(nos,fuel);
      }
   /*finally,constrain to 0-10V ie 0-2000dec*/
   if(unoz>2000) {unoz=2000;}
   if(unoz<0)    {unoz=0;   }
   /*put nozzle demand out to DAC1*/
   put(unoz,1);
   /*static inj.timing control is positional only- no feedback*/
   /*pull s-s optimum setting from schedule in timarr*/
   utim=pull(timarr,nos,fuel);
   /*put timing demand out to DAC2*/
   put(utim,2);
   }
/*get here if operator hit [I] key or if signal check set reply=I*/
/*transfer immediately to Idle condition, and display the */
/*operator's current instructions and options*/
printf("\n\n\n");
printf("    ___________________________________________________\n")
printf("   |                 _______|__AMI__|_______           |\n"
printf("   |               |__DCE microcontroller__|           |\n"
printf("   |---------------------------------------------------|\n"
printf("   | DCE is in Idle mode. There are no operator inputs.|\n"
printf("   | The auto.shutdown system and the 3 red manual     |\n"
printf("   | shutdown buttons are active. To return to MANUAL  |\n"
printf("   | control, follow the sequence below. To return to  |\n"
printf("   | AUTO.control, you must go via MANUAL control.     |\n"
printf("   |---------------------------------------------------|\n"
printf("   |   PRESS [M] TO GET INSTRUCTIONS FOR BUMPLESS      |\n"
printf("   |   TRANSFER TO MANUAL CONTROL MODE.                |\n"
printf("   |___________________________________________________|\n"
printf("\n\n\n");
while(reply!='S' && reply!='s')
   {
   if( kbhit() )
      {
      reply=getch();
      if(reply=='m' || reply=='M')
         {
         printf("\n\n\n\n\n\n");
printf("          ___________________________________________\n");
printf("         | For bumpless transfer to MANUAL control,  |\n");
printf("         | carry out the following sequence:         |\n");
printf("         |-------------------------------------------|\n");
printf("         | 1.check that Engine SPEED control is      |\n");
printf("         |   switched to MANual                      |\n");
```

```
        printf("        ¦ 2.set Engine SPEED  pot. to 5 Volts      ¦\n");
        printf("        ¦ 3.set NOZZLE control pot.to 5 Volts      ¦\n");
        printf("        ¦ 4.set TIMING control pot.to 6 Volts      ¦\n");
        printf("        ¦ 5.switch TIMING control to MANual        ¦\n");
        printf("        ¦ 6.switch NOZZLE control to MANual        ¦\n");
        printf("        ¦ 7.switch Engine control mode selector    ¦\n");
        printf("        ¦   (black rotary switch) to SPEED         ¦\n");
        printf("        ¦------------------------------------------¦\n");
        printf("        ¦ DCE is then under fully MANUAL control.  ¦\n");
        printf("        ¦ hit [S] to Stop controller. Re-run AMI   ¦\n");
        printf("        ¦ for transfer back to AUTO. control.      ¦\n");
        printf("        ¦__________________________________________¦\n");
              }
           }
        /*fast Idle mode control*/
        /*fixed speed demand,with fixed nozzle posn.*/
        neng=get(2);
        if(neng<267 && serch==1)
           {
           urack=400;   /*fixed small fuelling to give gentler but
                         definite stall if Ne signal is lost (400dec=2
           }
        else
           {
           fuel=(kne*(900-neng))/100;  /*'Idle'Demand is 4.5V ie900dec
           if(fuel<0) fuel=0;
           scrlm = racklm(neng);
           if(fuel>scrlm) fuel=scrlm;  /*limit max fuelling*/
           /*convert to equiv.rack setting*/
           urack = (14*fuel)/17 + 600;
           }
        put(urack,0);
        put(idlnoz,1);   /*set noz.fixed posn*/
        put(idltim,2);   /*set fixed static timing */
        }
     exit(0);
     }
/* get() */
/* reads a given channel from ADC */
long get(chan)
unsigned chan;
     {
     unsigned padc=512; /*ADC base address*/
     int val,lobyte,hibyte,topfour,adcbusy;
     long valong;
     outp(padc,chan);  /*select channel, with unity gain*/
     outp(padc+1,0);   /*start conversion*/
     do
        {
        lobyte=inp(padc+2);  /*read first 8bits of input*/
        hibyte=inp(padc+3);  /*read high 4bits+busybit+dig.i/p bit*/
        topfour=hibyte & 15; /*filter low nibl from high byte*/
        adcbusy=hibyte & 32; /*adc busy if hibyte bit5 is set*/
        }
     while(adcbusy==32);       /*rpt above until bit5 clear*/
     /*sample twice to ensure ADC hardware awake and clean*/
     outp(padc,chan);  /*select channel, with unity gain*/
     outp(padc+1,0);   /*start conversion*/
     do
        {
        lobyte=inp(padc+2);  /*read first 8bits of input*/
        hibyte=inp(padc+3);  /*read high 4bits+busybit+dig.i/p bit*/
        topfour=hibyte & 15; /*filter low nibl from high byte*/
        adcbusy=hibyte & 32; /*adc busy if hibyte bit5 is set*/
```

```
        }
      while(adcbusy==32);        /*rpt above until bit5 clear*/
      val=lobyte + 256*topfour; /*scale top nibl correctly*/
      val=(val-2047);           /*offset since ADC is bipolar*/
      valong=(long)val;         /*must return long integer*/
      return(valong);  /*decimal 0-2047 value returned to main*/
      }
/* put() */
/* puts contents of a given variable out to a given DAC*/
long put(outvar,outch)
long outvar;      /*variable to be output */
unsigned outch;   /*DAC channel to be used*/
      {
      unsigned pdac=768;  /*DAC base addr=300H*/
      int val,lobyte,hibyte,dummy;
      /*scale to 12bit unipolar (0-4095) from 12bit bipolar ((0)-2047)*/
      val=(int)(2*outvar);
      if(val>4095) {val=4095;}
      if(val<2)    {val=2;}          /*BCT board unreliable below 4mV*/
      hibyte = val/256;              /*split 12bits into 2 bytes*/
      lobyte = val - 256*hibyte;
      outp(pdac + 2*outch, lobyte); /*2 bytes per chan.,starting at pdac*/
      outp(pdac + 2*outch + 1, hibyte);
      dummy=inp(pdac + 15);          /*update (all) DACs*/
      }
/* pull() */
/* pulls scheduled value from given array at given index position*/
long pull(array,spd,fuel)
long array [6] [9];
long spd,fuel;/*schedules mapped on y(=fuel) - x(=spd) basis*/
      {
      long pulled;
      long xspd,ispd,ispdp,spdrem,xfuel,ifuel,ifuelp,fulrem;
      long scr1,scr2,scr3;
      /*scale spd and fuel to axes of arrays*/
      /*work with integers scaled *1000 rather than f.p.to interpolate.*/
      /*this gives more than adequate accuracy cf.the resolution of the*/
      /*experimental mapping on which the schedule arrays are based.   */
      {xspd=((spd-393)*8000)/1557;} /*sched on No/s basis*/
      xfuel=(fuel*5)/2;  /*max result is 5000*/
      ispd=xspd/1000;
      if(ispd<0) {ispd=0;}  /*arrays indexed starting from zero*/
      ifuel=xfuel/1000;
      if(ifuel<0) {ifuel=0;}
      spdrem=xspd - 1000*ispd;
      fulrem=xfuel - 1000*ifuel;
      ispdp=ispd + 1;
      ifuelp=ifuel + 1;
      if(ispdp>8) ispdp=8;
      if(ifuelp>5) ifuelp=5;
      /*get settings at the nearest array entries*/
      scr1=array[ifuel] [ispd];
      scr2=array[ifuelp] [ispd];
      /*lin.intrp.between these*/
      scr3=1000*scr1 + (scr2-scr1)*fulrem;
      /*nearest array entries at next pt.*/
      scr1=array [ifuel] [ispdp];
      scr2=array [ifuelp] [ispdp];
      /*lin.intrp.between these*/
      scr1=1000*scr1 + (scr2-scr1)*fulrem;
      /*lin.intrp.in 2nd dimension between the 2 intrp.points*/
      pulled=(scr3 + (scr1-scr3)*spdrem/1000) / 1000;
```

```
      return (pulled);  /*scheduled value pulled is returned*/
      }
* offset() */
* calcs current offset for nozzles for offset+prop. control from */
* from existing data, positional pattern is unclear.Use fixed 9V */
ong offset(nos,fuel)
ong nos,fuel;
      {
      long offval;
      offval=1800;
      return (offval);
      }
* racklm() */
* default max.rack limit as a fnc of engine speed. Based on steady-state*/
* experimental data at thermal/mech.limits of engine.Abs.BMEP limit is  */
* 20bar (req.c.180mg/inj).Max.power 266kW (based on orig.design limits).*/
* fuel is limited to levels which should keep engine within both limits.*/
ong racklm(neng)
ong neng;
      {
      long defmax;
      if(neng>1297)       /*nominally limit to 266kW*/
         {
         defmax = 2334600/neng;
         }
      else                /*nominally limit to 20bar BMEP*/
         {
         defmax = 1800;   /*1800dec=180mg/inj gives c.20bar*/
         }
      return (defmax);
      }
```

APPENDIX 3

DYNAMIC SIMULATION - FUNCTIONAL SPECIFICATION

Part 3 of this thesis covers the development and use of a dynamic simulation for optimisation and control studies. When the specification was drawn up, it was anticipated that these studies might extend to two engine systems, namely:

(i) The DCE, having electronically-controlled fuelling, turbine VG and injection timing in prototype form, with provision for bypass closure control and conceptual use of a turbine CVT.

(ii) VG turbocharged Diesel engines, in particular the Leyland TL11 rig, having electronic fuelling, VG and timing controls, plus charge air temperature control.

The basic specification for the simulation was:

(i) To have readily interchangeable dynamic models and controller routines.

(ii) To have setpoint inputs and loading conditions analogous to practical experimental inputs and/or vehicle applications.

It should be noted that these determined the layout of the simulation but left the compromise of dynamic/thermodynamic accuracy and execution speed open for each dynamic model. The general program structure required is shown in fig.1. The main program segment should communicate with the control and engine/transmission subroutines such that it needs no changes when these subroutines are replaced to model alternative systems. In particular, the system states and control inputs should be represented in a non-specific way, eg. as elements of arrays with room for expansion. The array elements can then be

interpreted in different ways by different models.

The decision whether to employ transient control strategies or steady-state control including extremal (self-optimising) algorithms can be made by the main program on the basis of data from the dynamic model and/or the duty cycle.

The duty cycle subroutine should -as indicated above- accept input in a form analogous to testbed/vehicle inputs, typically one or more "demands" from the operator, plus a load torque level. In the vehicle case an equivalent driveshaft torque may be generated from input road conditions and vehicle data by a further subroutine. Note that if vehicle drivetrain/chassis/tyre dynamics are of interest these must be incorporated in the engine/transmission model.

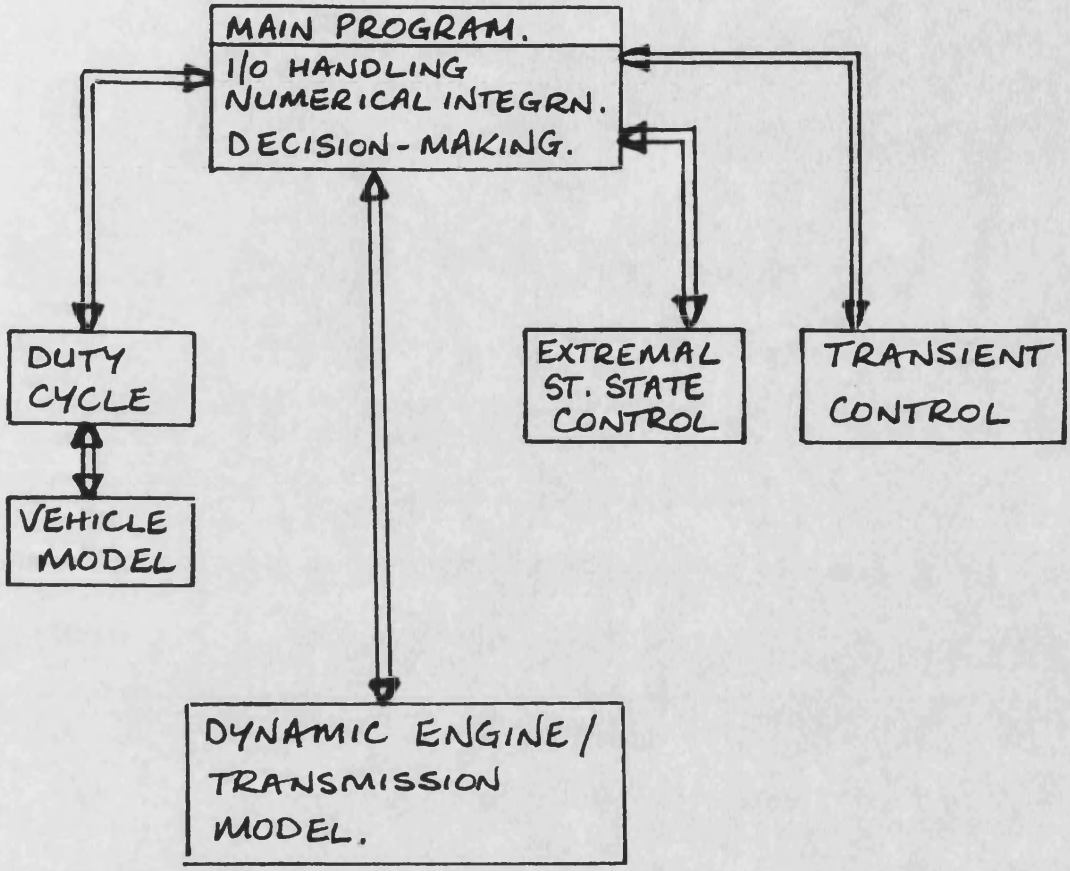

FIG. 1 DYNAMIC SIMULATION - OUTLINE STRUCTURE

APPENDIX 4

SIMDCE code listings and example data files

Part:

1. DCECON.FOR
2. EULER1.FOR
3. DCECSb/c/e.FOR
4. Controller subroutines
5. OPTICa/b.FOR
6. GETSET.FOR
7. RITRPS.FOR
8. VEHICL.FOR
9. WRITOP.FOR
10. PROUTB.FOR
11. DCEMOD.DAT
12. MODES.DAT, SCHEDS.DAT, TRUCK.DAT

PART 1.

```
      PROGRAM DCECON
C
C   ¦-------------------------------------------------------------¦
C   ¦                          DCECON                             ¦
C   ¦ a transient simulation of the Leyland 500 DCE, for use in   ¦
C   ¦ the study of adaptive steady-state, and transient control   ¦
C   ¦ strategies. A simplified dynamic model is used, to give     ¦
C   ¦ representative predicted dynamic behaviour with quick run   ¦
C   ¦ times, rather than absolute thermodynamic accuracy.         ¦
C   ¦ Alternative s.s/transient control strategies (scheduled/    ¦
C   ¦ adaptive & indep.loop/multivariable) can be evaluated by    ¦
C   ¦ linking with different versions of the subroutine "optic"   ¦
C   ¦ and subroutine "ctrlr" .                                    ¦
C   ¦-------------------------------------------------------------¦
C
C  LAST CHANGE 030489 JH
C
C  Written :  J.Hall  Aug.1987
C  Machine :  LSI11/23
C  Code    :  Fortran IV
C  Ported to PC-AT compatibles and made compatible with MicroSoft
C  FORTRAN (77) Version 4.1   Dec.1988.
C
C  Program description
C  -------------------
C  DCECON operates as outlined below:
C
C  1.read input data files
C    a)dcemod.dat - DCE rig data eg component efficiencies,inertias..
C                   and ambient conditions
C    b)scheds.dat - s-s schedules for timing,nozzle ang.,tgr control
C    c)modes.dat - required duty modes (or single condition)
C    d)truck.dat - vehicle and road conditions-REQUIRED ONLY IF MODES
C                  SPECIFIES A VEHICLE SIMULATION IS TO BE RUN.
C  2.get first Demand,N1,T1 etc. condition
C  3.get scheduled tim.,noz./boost,tgr settings from schedule arrays
C  4.establish steady-state at first condition
C  5.run duty cycle
C  6.log data through the set of duty modes.
C
C  variable notation
C  -----------------
C  DCE(8)        array describing dynamic state of DCE.
C  DCEDOT(8)     rates of change of array 'DCE'
C    array elements:SEE DCE MODEL SUBROUTINE CURRENTLY IN USE.
C
C--VARIABLES DECLARATION,(PARAMETER STATEMENTS),COMMONS,INITIALISATIO
C
C       !unless explicity declared below
        IMPLICIT REAL (A-H,J-Z)
        IMPLICIT INTEGER (I)
C
        INTEGER MTSIZE
C
        INTEGER NMODES,NRECS
C       !mode,record no.counters
C
        INTEGER RUNTYP
C       !0 for dyno sim.,1 for vehicle sim.
C
        INTEGER INL,ITOS,INE
C       !array index subscripts for scheduling
C
        INTEGER ISTORE
```

```
C       !array index for record
C
        INTEGER ISS
C       !flag in record =1 for nom.s-s,=0 for nom.transient
        INTEGER*4 IRLSCT
C       !initialisation count in RLS subroutine
        REAL EFFOLD,EFFNEW
C       !o/s brake th.effy previous and current
C
        REAL TIME,DIST
C       !elapsed time[s] and distance[m] covered
C
        INTEGER ITNREC
C       !accumulated no of data records(pointer)
C
        REAL NLSS,NCSS,TLSS,PVOLSS,NEDSS,DEMSS
C       !steady-state limits
C
        REAL RUNTIM,RUNLEN
C       !time or distance for a mode in duty cycle
C
        REAL GRADE,BRAKES
C       !road gradient and braking force[N]in veh.sim
C
        REAL JWHEEL
C       !total wheels/hubs/brks/tyres rotn.inertia[kg.m.m]
C
        REAL K1,K2,K3,K4,K5,K6,K7,K8
C       !controller gains (not nec.all used)
        REAL URACK,UNOZ,U3,U4
C       !controller outputs to DCE model
C
        REAL RECORD(40,350)
C       !no.of recorded variables x max.no.of records
C
        REAL DCE(8),DCEDOT(8)
        REAL DUTARR(20,4)
C       !basic load conditions for each mode;these are
C       DEMAND,TQLOAD,RUNTIM,-      if dyno testing is to be simulate
C       DEMAND,GRADE ,RUNLEN,BRAKES if vehicle simulation.
C
        REAL NOZSCH(20,20)
C       !boost demand nozzle schedule
C
        REAL TIMSCH(20,20)
C       !timing schedule
C
        REAL TGRSCH(20,20)
C       !turbine/output gear ratio schedule
C       arrays used in RLS identification routine&init.here
        REAL P(4,4),THETA(4,1),ONEMAT(4,4)
C       parameter estimate monitor array
        REAL PARMON(4,120)
C
        LOGICAL STEADY
C       !true for steady state,false for trans. as def.above
C
        EXTERNAL DCEMOD
C       !name of model subr. called by Euler.
C
C--COMMON BLOCK-----------------------------------------------------
C--variables which change during run--------------------------------
C
```

```
      COMMON /A/  NENG,AENG,NTURB,AFR,PCOMP,PINMAN
      COMMON /B/  TQENG,TQANN,TQSUN,TQPC,TQCOMP,TQTURB,TQLOAD,TQOUT
      COMMON /C/  MCOMP,MINMAN,MFUEL,MTURB
      COMMON /D/  TINMAN,TEXMAN,TCOMP,TVOL,TVODOT
      COMMON /E/  FPREV,FPREVA,NOZ,NOZA,TGR,TIM,TIMA
      COMMON /F/  DEMAND,URACK,UNOZ,U3,U4,EFFOLD,EFFNEW,ISS
C
C--variables which are fixed for run-----------------------------------
C
      COMMON /G/  PATM,TATM,TCOOL
      COMMON /H/  JCOMP,JTURB,JANN,JOIPC,JOS
      COMMON /I/  KTQC,KMC,KMINMA,KMF,KTQE,KFRIC,KBYPAS
      COMMON /J/ EFCOMP,EFTURB,EFCOOL
      COMMON /K/ CP,R,GAMMA
      COMMON /L/ CGR,OGR
      COMMON /M/ VOLUME,AREABY,TQSTAT,FPREVM
      COMMON /N/ MTARR(6),VFCARR(4,13),WCARR(4,13)
      COMMON /O/ X4,X5
      COMMON /P/ ISEED
      COMMON /DCE/    DCE
      COMMON /SCHEDS/ NOZSCH,TIMSCH,TGRSCH,IXSIZE,IYSIZE
      COMMON /GAINS/  K1,K2,K3,K4,K5,K6,K7,K8
      COMMON /OUT/  RECORD,DUTARR,DT,ISTORE,NMODES,RUNTYP
      COMMON /RLS/  P,THETA,ONEMAT,IRLSCT
      COMMON /PU/   PARMON,IMON
C
C--INITIALISE----------------------------------------------------------
C
      DATA TIME,DIST,ICOUNT,ITNREC /0.,0.,0,0/
C     DATA DCE(8) /0./
      DATA DCEDOT(1),DCEDOT(2),DCEDOT(3) /1.,1.,0./
      DATA DCEDOT(4),DCEDOT(5),DCEDOT(6),DCEDOT(7),DCEDOT(8)
     +     /0.,0.,0.,0.,0./
C
      ISS=0
      ISEED=12345
      IRLSCT=0
C
C-----intro.message----------------------------------------------------
C
      WRITE  (*, 600)
C
C-----read dce data from files DCEMOD.DAT,SCHEDS.DAT and MODES.DAT-----
C
      WRITE  (*, 601)
      OPEN   (UNIT = 4, FILE = 'DCEMOD.DAT', STATUS = 'OLD')
      READ   (4,401) (MTARR(I),I=1,6)
      DO 5 I=1,13
           READ (4,*) DUMMY,(VFCARR(I1,I),I1=1,4)
5     CONTINUE
      READ   (4,405)
405   FORMAT(3(/))
      DO 8  I=1,13
           READ (4,*) DUMMY,(WCARR(I1,I),I1=1,4)
8     CONTINUE
      READ  (4,405)
      READ  (4,*) KTQC,KMC,KMINMA,KMF,KTQE,KFRIC,KBYPAS
      READ  (4,405)
      READ  (4,*) EFCOMP,EFTURB,EFCOOL
      READ  (4,405)
      READ  (4,*) CGR,OGR
      READ  (4,405)
      READ  (4,*) JCOMP,JTURB,JANN,JOIPC,JOS
```

```
      READ  (4,405)
      READ  (4,*) CP,R,GAMMA
      READ  (4,405)
      READ  (4,*) TCOOL,TATM,PATM,VOLUME,AREABY,TQSTAT,FPREVM
      READ  (4,405)
      READ  (4,*) K1,K2,K3,K4,K5,K6,K7,K8
C
      CLOSE (UNIT = 4, STATUS = 'KEEP')
C
C
C identification routines array init. (use depends on CTRLR version)
        DO 6,ILP1=1,4
C       set up init.state vector all ero
            THETA(ILP1,1)=0.
            DO 4,ILP2=1,4
               IF(ILP1.EQ.ILP2) THEN
C                 set up init.variance array diagonal
                  P(ILP1,ILP2)=K5
C                 also set up identity matrix onemat
                  ONEMAT(ILP1,ILP2)=1.
               ELSE
                  P(ILP1,ILP2)=0.
                  ONEMAT(ILP1,ILP2)=0.
               END IF
  4         CONTINUE
  6     CONTINUE
C
C--read schedules for timing,nozzles and CVT control-----------------
C
      WRITE (*,603)
603   FORMAT(//' reading control schedules from SCHEDS.DAT')
C
      OPEN (UNIT=4, FILE='SCHEDS.DAT', STATUS='OLD', ERR=991)
C
      READ (4,*) IXSIZE,IYSIZE
C     !actual no.of sched array entries
C     note same no.of entries for each schedule
C     check entries dont overfill arrays:
C
      IF (IXSIZE .GT. 20 .OR. IYSIZE .GT. 20)  STOP
     +   'DCECON: schedule arrays overfilled'
C
      DO 10 I=1,IYSIZE
           READ(4,*) (NOZSCH(I1,I),I1=1,IXSIZE)
10    CONTINUE
      DO 11 I=1,IYSIZE
           READ(4,*) (TIMSCH(I1,I),I1=1,IXSIZE)
11    CONTINUE
      DO 14 I=1,IYSIZE
           READ(4,*) (TGRSCH(I1,I),I1=1,IXSIZE)
14    CONTINUE
C
      CLOSE  (UNIT = 4, STATUS = 'KEEP')
C
C--read the duty cycle to be run-------------------------------------
C
      WRITE  (*, 605)
605   FORMAT (//' reading duty cycle from MODES.DAT')
      OPEN   (UNIT=4, FILE='MODES.DAT', STATUS='OLD', ERR=992)
C
      READ  (4,*) NMODES
C
C     (20 is current size of duty array DUTARR)
```

```
      IF (NMODES.GT.20) STOP  'error in MODES.DAT - too many modes'
C
      READ  (4,*) RUNTYP
      DO 15 I=1,NMODES
            READ(4,*) (DUTARR(I,I1),I1=1,4)
C           !read demand,tqload/grade,runtim/runlen,-/brakes
15    CONTINUE
C     Initialisation- ok for single and two-volume models
      READ(4,*) (DCE(I),I=1,7),PCOMP
C     init.guess for Nc,Nl,Pvol,actuator states and Pcomp.
      DCE(8) = PCOMP
C     Initialise other ctrl states
      X4 = 0.
      X5 = 1.
C
      READ(4,*) DT,TINT,RECINT
C
      CLOSE(UNIT=4, STATUS='KEEP')
C
C
C--read truck & road data if required
      IF(RUNTYP.EQ.1) GOTO 16
      GOTO 12
16    CONTINUE
            WRITE   (*, 607)
607         FORMAT  (//' note-vehicle simulation being run')
            DEMAND=DUTARR(1,1)
            GRADE=DUTARR(1,2)
            BRAKES=DUTARR(1,4)
            OPEN  (UNIT=4, FILE='TRUCK.DAT', STATUS ='OLD', ERR=993)
            READ  (4,*) GVW,CDA,KTYRE,RAXRAT,TYRDIA,WNDSPD,JWHEEL
            CLOSE (UNIT = 4, STATUS = 'KEEP')
C
C  replace jos read from dcemod.dat with value based on truck params
C
            JPROP= 0.5
C           !propshaft+diff.i/p gears inertia-typical value
C
C           input Jwheel must be referred to rel.speed of output shaft
            JWHEEL=JWHEEL/(RAXRAT*RAXRAT)
C
C  refer vehicle mass to effective output shaft rotn.inertia
            JREF=GVW*TYRDIA*TYRDIA/(4.*RAXRAT*RAXRAT)
            JOS=JREF+JPROP+JWHEEL
C           ![kg.m.m]
C  calc initial load condition from truck data and initial o/s speed
            CALL VEHICL(DCE(2),GRADE,BRAKES,GVW,CDA,KTYRE,RAXRAT,TYRDI
     >                  WNDSPD,TQLOAD)
      GOTO 20
12    CONTINUE
            WRITE(*, 609)
609         FORMAT(//' note-dyno simulation being run')
            DEMAND=DUTARR(1,1)
            TQLOAD=DUTARR(1,2)
20     CONTINUE
C
C
C
C
C--now have initial condition in terms of demand & o/s spd,load------
C--run dynamic model until other params stabilise,ie establish s-s---
C
        ICOUNT=0
```

```
        ISFLAG=2
C
C--get scheduled control settings for the instantaneous condition-----
C--note-scheds in terms of nload and demand values,not nload,tqload---
C
C       !start of loop
24      CONTINUE
        CALL GETSET
C
C--returns scheduled settings for current nload/demand condition------
C--can now run a timestep of the model with inst.ctrl settings--------
C
        CALL EULER(DCE,DCEDOT,8,DT,DCEMOD,TINT,TIME)
C
        ICOUNT=ICOUNT+1
        ITYPE=ICOUNT/100
        IF (ITYPE*100.EQ.ICOUNT) WRITE (*, 611) ICOUNT
611     FORMAT(//' establishing initial condition-',I5,' iterations')
C
        IF (ITYPE*100.EQ.ICOUNT) WRITE(*, 612) (DCE(I),I=1,4),DCE(6)
612     FORMAT(' Nc=',G11.4,' No/s=',G11.4,' Pvol=',G11.4,' Xrack=',
     +       G11.4,' Xnoz=',G11.4)
C  check for convergence (must be within limits for 2 SUCCESSIVE loops
C  set isflag to 2 if at any time the convergence criterion is not met
        IF (ABS(DCEDOT(1)).GT.20.0) GOTO 28
C  o/s accn (dcedot(2)) depends on Jo/s so adjust conv.limit
        IF (ABS(DCEDOT(2)).GT.20.) GOTO 28
        IF (ABS(DCEDOT(3)).GT.1.)   GOTO 28
C
C       if here then conv.crit.met-check if 2nd time
        ISFLAG=ISFLAG-1
        IF (ISFLAG.GT.1) GOTO 24
C       !dont reset isflag.run another loop
C       if here then conv.crit.met 2 successive times.
        GOTO 32
C
28      CONTINUE
        ISFLAG=2
        GOTO 24
C
32      CONTINUE
C       !init.cond established; iss=1 flags that steady-state=TRUE
        ISS=1
C
C
C       put start point conds into record array
C       !array pointer for Record
        ISTORE=1
        WRITE (*, 613)
613     FORMAT(///' converged on start condition-record this data')
C
        CALL WRITOP(TIME,DIST,DCE,DCEDOT)
C
        WRITE(*, 614)
614     FORMAT(///' running duty cycle')
C
C--transient run or steady-state optimisation 'micro-transient'-------
C
        INREC=0
        INSTEP=RECINT/DT
C
        DO 70 IMODE=1,NMODES
              DEMAND=DUTARR(IMODE,1)
```

```
            IF(RUNTYP.EQ.0) GOTO 34
            IF(RUNTYP.EQ.1) GOTO 36
34          CONTINUE
            TQLOAD=DUTARR(IMODE,2)
            RUNTIM=DUTARR(IMODE,3)
            GOTO 38
6           CONTINUE
            GRADE=DUTARR(IMODE,2)
            RUNLEN=DUTARR(IMODE,3)
            BRAKES=DUTARR(IMODE,4)
38          CONTINUE
C
C
C--run dynamic model as appropriate for the type of simulation--------
C
            IF (RUNTYP.EQ.0) GOTO 42
            IF (RUNTYP.EQ.1) GOTO 48
C
C-----------Dyno simulation statements--------------------------------
42          CONTINUE
            INREC=RUNTIM/RECINT
C           !no of records in this mode
C
            DO 44 IREC=1,INREC
                  DO 46 I=1,INSTEP
C  --------------------get schedule settings--------------------------
                     CALL GETSET
C                    call dyn.model via numerical integration routine
                     CALL EULER(DCE,DCEDOT,8,DT,DCEMOD,TINT,TIME)
C
46                CONTINUE
C                 put data into record array
C
                  ISTORE=ISTORE+1
C                 !record array index pointer
C
C                 check array not full
                  IF(ISTORE.GT.349) GOTO 90
C
                  DIST=0.
C                 !test beds don't move
                  CALL WRITOP(TIME,DIST,DCE,DCEDOT)
C
44          CONTINUE
C           !jump past road statements
            GOTO 66
C
C-----------Road simulation statements--------------------------------
48          CONTINUE
60          CONTINUE
C           !distance complete for this mode
            IF(DIST.GE.RUNLEN) GOTO 64
            DO 56 I=1,INSTEP
C                 get sched.ctrl settings
                  CALL GETSET
C                 call vehicl to calculate equiv.tqload from current
C                 condition
                  CALL VEHICL(DCE(2),GRADE,BRAKES,GVW,CDA,KTYRE,
     +                  RAXRAT,TYRDIA,WNDSPD,TQLOAD)
C                 call dynamic model with these ctrl settings
C
C                 !to calc approx mean speed over timestep
                  DUM1=DCE(2)
```

```
C
                    CALL EULER(DCE,DCEDOT,8,DT,DCEMOD,TINT,TIME)
                    DIST=DIST+(DCE(2)+DUM1)*.02618*TYRDIA*DT/RAXRAT
56            CONTINUE
C             write data to record array
              ISTORE=ISTORE+1
              IF(ISTORE.GT.349) GOTO 90
              CALL WRITOP(TIME,DIST,DCE,DCEDOT)
C
              GOTO 60
C             !next (recint)
C
64            CONTINUE
C             !road sim.-distance complete for current mode
C
66            CONTINUE
C             !dyno sim.-time complete for current mode
C
70      CONTINUE
C       !Imode ie current mode completed
C
C--duty cycle(all modes)completed-----------------------------------
C
90      CONTINUE
C       !jumped here if record array became full during run
        IF (ISTORE.GT.349) WRITE (*, 615) IMODE
615     FORMAT (//' run stopped in mode',I3,' as record array is full')
C
C--write record of run to file--------------------------------------
C
        CALL PROUT
C
        CALL PLOT1(RECINT)
        CALL PLOT2
        STOP ' finished'
990     CONTINUE
        STOP ' DCECON: error opening DCEMOD.DAT'
991     CONTINUE
        STOP ' DCECON: error opening SCHEDS.DAT'
992     CONTINUE
        STOP ' DCECON: error opening MODES.DAT'
993     CONTINUE
        STOP ' DCECON: error opening TRUCK.DAT'
C
C  401    FORMAT (7(/),6(F4.2,3X),41(/))
401     FORMAT (7(/),6(F4.2,3X),7(/))
600     FORMAT (5(/),'      SIMDCE - DCE dynamic simulation',3(/))
601     FORMAT (2(/),' reading DCEMOD.DAT')
        END
```

PART 2.

```
      SUBROUTINE EULER(X,XDOT,ISIZE,DT,MODEL,TINT,TIME)
C  ------------------------------------------------------------------
C :                            EULER1.FOR                            :
C : NUMERICAL INTEGRATION OF STATES RATES OF CHANGE ARRAY            :
C : using the predictor-corrector method                             :
C :-----------------------------------------------------------------:
C
C  transferred to PC-AT from DEC LSI11/23   151288
C  LAST CHANGE 161288 JH
C
C  VARIABLE LIST:
C  X             state-vector (array representing models dynamic state)
C  XDOT          rates of change of X with time
C  X1            X at step n+1
C  XDOT1         XDOT at step n+1
C  ISIZE         size of above arrays
C  DT            time step used for integration
C  MODEL         subroutine used to obtain XDOT at state X
C
C ------------------------------------------------------------------
C
      IMPLICIT REAL (A-H,J-Z)
      IMPLICIT INTEGER (I)
      DIMENSION X(8),XDOT(8),X1(8),XDOT1(8),X1NEW(8)
      EXTERNAL MODEL
C
      ERRLIM=.005
C     pred-corr convergence crit.
      ITS=0
C     pred-corr iteration counter
C
C-------------------------------------------------------------------
C  using X and XDOT at step n
C  calculate auxiliary array X1 at step n+1
C-------------------------------------------------------------------
C
      DO 10 I=1,ISIZE
      X1(I)=X(I)+DT*XDOT(I)
10    CONTINUE
C
C-------------------------------------------------------------------
C  PREDICTOR-CORRECTOR LOOP
C  Call MODEL to obtain auxiliary array XDOT1 at step n+1.
C  Recalculate auxiliary array X1 at step n+1 using average XDOT
C  Repeat process until convergence obtained.DT is passed in call
C  for use in calc.'torque delay'term in engine model. JH.
C-------------------------------------------------------------------
C
15    CONTINUE
      CALL MODEL(X1,XDOT1,DT,TINT,TIME)
      DO 20 I=1,ISIZE
C           update X1 using average XDOT
            X1NEW(I)=X(I)+(DT/2)*(XDOT(I)+XDOT1(I))
20    CONTINUE
C
C-------------------------------------------------------------------
C     test for convergence but only on main dyn.states.
      DO 22 I=1,3
          ERROR=ABS((X1NEW(I)-X1(I))/X1(I))
C         convergence error
22    CONTINUE
      IF (ERROR.GT.ERRLIM) GOTO 25
C     continue iterating
```

```
      GOTO 35
C     leave pred-corr loop
C-----------------------------------------------------------------------
25    CONTINUE
      ITS=ITS + 1
      IF(ITS.LE.20) GOTO 27
      ITS=0
      ERRLIM=100.*ERRLIM
C     relax conv.crit. after 20 iterations
      WRITE (*, 600)
600   FORMAT(' EULER: pred.-corr. convergence limit relaxed')
27    CONTINUE
      DO 30 I=1,ISIZE
C           reset X1 array for next iteration
            X1(I)=X1NEW(I)
30    CONTINUE
      GOTO 15
C
C-----------------------------------------------------------------------
C  update X and XDOT for next time step
C-----------------------------------------------------------------------
C
35       CONTINUE
         DO 40 I=1,ISIZE
         X(I)=X1NEW(I)
         XDOT(I)=XDOT1(I)
40       CONTINUE
C
         TIME=TIME+DT
C
         RETURN
         END
```

PART 3.1

```
      SUBROUTINE DCEMOD(DCE,DCEDOT,DT,TINT,TIME)
C
C ¦-------------------------------------------------------------¦
C ¦                                                             ¦
C ¦                          DCECSB.FOR                         ¦
C ¦    simple dynamic model of Leyland 520 DCE prototype rig    ¦
C ¦                                                             ¦
C ¦-------------------------------------------------------------¦
C
C  last change 130389 JH
C
C  (subroutine DCEMOD for control study simulation DCECON)
C
C  Epicyclic speed and torque relationships represent the
C  current gear trains used in the Ley.500 prototype.(overall ie
C  component-component ratios CGR,OGR are input from DCEMOD.DAT file.)
C  Quasi-steady and linearised non-dynamic calculations are matched
C  to experimental data from L500DCE, component stand-alone data
C  and,where necessary, more thermodyn.accurate simulation.
C  This simulation
C  is intended for use in developing multivariable control systems for
C  transient and steady-state operation.The model incorporates the
C  dynamic responses of the electro-hydraulic (servo-valve) actuators
C  and positional control feedback loops used on the prototype rig to
C  set fuel pump rack and turbine nozzle positions, with a view to
C  investigating proposed analog/digital controllers for the rig.
C
C  dynamic equations give :
C  ----------------------
C  1. compressor acceleration
C  2. output acceleration
C  3. rate of pressure change in volume (mass storage in volume)
C
C  all other variables are calculated using simple approximations
C  which assume no dynamics ie. no time lag between inputs and
C  outputs.
C
C  assumptions:
C  -----------
C  single volume
C  planet accelerations neglected
C  gearbox losses approximated
C  perfect mixing in volume
C
C  variable notation:
C  -----------------
C  DCE(8)        array describing dynamic state of DCE rig.
C  DCEDOT(8)     rates of change of array 'DCE'
C    array elements:
C    DCE states                              explanation:
C                1    NCOMP & ACOMP         compressor
C                2    NLOAD & ALOAD         o/p shaft
C                3    PVOL  & PVODOT        pres.in control volume
C                8    integral(XERROR)dt  &  XERROR
C    Control system states
C                4    XRACK & DXRACK        rack actuator posn,velocity
C                5    YRACK & DYRACK        rack act.velocity and  deriv.
C                6    XNOZ  & DXNOZ         nozzle act. posn.and velocity
C                7    YNOZ  & DYNOZ         nozzle act.velocity and deriv.
C    NB DXRACK and YRACK are identical; so are DXNOZ and YNOZ.
C       Units are Volt, Volt/s and Volt/s/s.
C  TQ            torques (Nm)
C  W             powers (usually KW*60)-ie [kJ/min] JH
C  N             speeds (rpm)
```

```
C  A             acceleration (rpm/sec)
C  P             pressures (Bar)
C  PR            pressure ratio
C  M             massflows (kg/min)
C  VF            volume flow (cubic ft./min)
C  X             linear posn [m]
C  Q             flowrate [m3/s]
C  VEL           air velocity (m/sec)
C  T             temperatures (deg.K)
C  J             inertias (Nm.sec/rpm)
C  K             linear gains (output/input)
C  EF            efficiency
C  RO            density (kg/m**3)
C  AREA          area (m**2)
C  VOLUME        litres
C  VOMASS        mass stored in volume
C  FPINJ         fuel per inj. [mg/inj]
C  FPREV         fuel per rev. (kg.*10000)(=mg/inj.*100*2/6  JH)
C  FPREVA
C  FPREVM        max.rack in terms of fuel per rev.(NOT ALWAYS USED)
C  NOZ           nozzle setting IN VOLTS (0-10V)
C  NOZA          nozzle angle(deg.)ass.good,linear,calibration.
C  TIM           static timing in VOLTS(0=full ret.,10=full adv.,std.=7
C  TIMA          corresp. SNL in msBTDC at the current engine condition
C
C  suffix notation:
C  ---------------
C  ENG           engine
C  ANN           annulus
C  SUN           sun
C  PC            planet carrier
C  COMP          compressor
C  TURB          turbine
C  LOAD          load parameters
C  OUT           output-shaft conditions
C  ATM           atmospheric conditions
C  VOL           conditions in volume
C  FUEL          fuel
C  INMAN         conditions in inlet manifold
C  EXMAN         conditions in exhaust manifold
C  COOL          intercooler cooling medium
C  IND           indicated
C  FRIC          friction
C  STAT          static (fixed) offset
C  DOT           rate of change w.r.t. time
C  ARR           signifies array name
C  SCH           signifies schedule array
C  DEM           demanded
C
C-----------------------------------------------------------------------
C SPECIFICATION STATEMENTS, COMMONS, INITIALISATION
C-----------------------------------------------------------------------
C
C
      IMPLICIT REAL (A-H,J-Z)
      IMPLICIT INTEGER (I)
      INTEGER MTSIZE
      DIMENSION DCE(8),DCEDOT(8)
C
C  common block variables which change with time
      COMMON /A/  NENG,AENG,NTURB,AFR,PCOMP,PINMAN
      COMMON /B/  TQENG,TQANN,TQSUN,TQPC,TQCOMP,TQTURB,TQLOAD,TQOUT
      COMMON /C/  MCOMP,MINMAN,MFUEL,MTURB
```

```
      COMMON /D/  TINMAN,TEXMAN,TCOMP,TVOL,TVODOT
      COMMON /E/  FPREV,FPREVA,NOZ,NOZA,TGR,TIM,TIMA
      COMMON /F/  DEMAND,URACK,UNOZ,U3,U4,EFFOLD,EFFNEW,ISS
C
C  common block variables which are constant for each run
      COMMON /G/  PATM,TATM,TCOOL
      COMMON /H/  JCOMP,JTURB,JANN,JOIPC,JOS
      COMMON /I/  KTQC,KMC,KMINMA,KMF,KTQE,KFRIC,KBYPAS
      COMMON /J/ EFCOMP,EFTURB,EFCOOL
      COMMON /K/ CP,R,GAMMA
      COMMON /L/ CGR,OGR
      COMMON /M/ VOLUME,AREABY,TQSTAT,FPREVM
      COMMON /N/ MTARR(6),VFCARR(4,13),WCARR(4,13)
C
C     !initialise: size of MTARR and engine acceleration
      DATA MTSIZE/6/
C
C  fuel calorific value [kJ/kg] - torque/fuelling correction
C  (see engine eqns)
      AENG = 1.
      CALVAL=42500.
C
C-----------------------------------------------------------------------
C  RENAME DYNAMIC STATE VARIABLES (FOR READABILITY)
C-----------------------------------------------------------------------
C
      NCOMP=DCE(1) / 60.
      NLOAD=DCE(2) / 60.
      PVOL=DCE(3)  * 1.E+5
      XRACK=DCE(4)
      YRACK=DCE(5)
      XNOZ=DCE(6)
      YNOZ=DCE(7)
C
C-----------------------------------------------------------------------
C  GET CONTROL INPUTS FOR CURRENT OPERATING POINT
C  note: ctrlr is called every TINT seconds-for analog ctrl TINT=DT
C-----------------------------------------------------------------------
C
C
      TFRAC=AMOD(TIME+DT/2.,TINT)
      IF (TFRAC.GT.0..AND.TFRAC.LE.DT) THEN
           CALL CTRLR(DCE,XERROR)
      END IF
C
C-----------------------------------------------------------------------
C
      NENG  = NENG / 60.
      PCOMP = PCOMP * 1.E+5
C
C-----------------------------------------------------------------------
C  COMPRESSOR CALCULATIONS -- EMPIRICAL DATA PULLED FROM 2-D ARRAYS
C-----------------------------------------------------------------------
C
C     compressor pressure ratio
      PRCOMP = PCOMP /ATM
C
C  check array indices are in limits
      IF (NCOMP .LT. -3.)    STOP 'program stopped - NComp reversal'
      IF (NCOMP .GE. 236.)   STOP 'program stopped - NCOMP too high'
      IF (PRCOMP .LE. 0. )   STOP 'program stopped - PRCOMP is zero'
      IF (PRCOMP .GE. 4.4)   STOP 'program stopped - PRCOMP too high'
```

```
      IF (PVOL .LE. 0.)       STOP 'program stopped - Pvol is zero'
C
C     calculate compressor volume flow (FAD)  VFCOMP  [cu m./min]
      NCNORM = (NCOMP*60. + 200.)/4800. + 1.
      PRNORM = (PRCOMP + .0343)/.3448 + 1.
      VFCOMP = ( RITRP2(NCNORM,PRNORM,VFCARR,4,13) )/35.315
C
C     ROA is the ambient air density in kg/cubic m
      ROA = PATM / (287.1 * TATM)
C
C     compressor massflow in Kg/min
      MCOMP = VFCOMP * ROA
C
C     compressor power [W]
      WCOMP = 745.7*RITRP2(NCNORM,PRNORM,WCARR,4,13)
C
C     compressor torque [NM]
      TQCOMP = WCOMP / (6.2824 * NCOMP)
C
C  isentropic outlet temp.(TCOMP), isentropic comp. work (WCISEN)
C  and hence isentropic efficiency (EFCOMP)
       TCOMP = TATM * (PRCOMP)**((GAMMA-1)/GAMMA)
       WCISEN= MCOMP * CP * (TCOMP-TATM)
       IF(WCOMP.NE.0.) THEN
          EFCOMP= WCISEN / (WCOMP * 0.06)
C         calculate actual outlet temp. using isentropic efficiency
          TCOMP=TATM + (TCOMP-TATM)/EFCOMP
       ELSE
          TCOMP=TATM
       END IF
C
C-----------------------------------------------------------------------
C  INTERCOOLER
C-----------------------------------------------------------------------
C pres.drop [N/m2] approxn from exptal results as fnc of flowrate
       PINMAN=PCOMP - 1750.*MINMAN
C thermostat holds around 50deg.C Charge Air Temp
       TINMAN=323.
C
C-----------------------------------------------------------------------
C  ENGINE EQUATIONS
C-----------------------------------------------------------------------
C
C  speed from epicyclic equation [rev/s]
       NENG = NCOMP / CGR + NLOAD / OGR
C
C  airflow through engine from perfect gas equation  [KG/MIN]
       MINMAN = KMINMA * (PINMAN * 1E-5) * (NENG * 60.) / TINMAN
C  rack ctrl i/p Urack from controller gives rack posn/vel via dynamic
C  first impose mech.constraints
       IF(XRACK.GT.10.) XRACK=10.
       IF(XRACK.LT.0.)  XRACK=0.
C
C      !rack vel(1st ord.)
       DXRACK=YRACK
C
C      !rack accn(2nd ord)
       DYRACK=-2000.*XRACK-120.*YRACK+2000.*URACK
C
C  model needs actual posn ie XRACK. This comes from num.int.,so is on
C  integration step behind.Hence timestep must be << time consts of DC
C  and control system being modelled.
C  fuelling (per rev) comes from pump calibration based on exptal data
```

```
C  XRACK posn.calib.in Volts. As mapped 30-01-89.
C  Fuelling [mg/inj]
      FPINJ=170.*(XRACK - 3.)/7.
      IF(FPINJ.LT.0.) FPINJ=0.
C  Fuel per rev.[kgE-4/rev]
      FPREVA=FPINJ * .03
C
C     !fuel massflow  [KG/MIN]
      MFUEL = KMF * FPREVA * (NENG * 60.)
C
C     Calculation of Air/Fuel Ratio, avoiding division by zero
C     base AFR on clean air only, not recirc.exh.gases
      IF(MBYPAS.GE.0.) THEN
C        +ve byp.flow, so all engine air is clean
         IF(MFUEL.EQ.0.) THEN
            AFR=100.
         ELSE
            AFR = MINMAN / MFUEL
         END IF
      ELSE
C        -ve byp.flow, so only comp.del.air is clean
         IF(MFUEL.EQ.0.) THEN
            AFR=100.
         ELSE
            AFR = MCOMP / MFUEL
         END IF
      END IF
C
C  relative efficiency ass.to drop linearly with AFR below AFR=30
      IF (AFR.LT.30.) THEN
          EFREL = 1. - 0.02 * (30. - AFR)
      ELSE
          EFREL = 1.
      END IF
C
C  engine torque proportional to FPREV and relative efficiency EFREL
C  note:calval/42500 allows corrn for different fuels,keeps same KTQE
C  Hazell & Flower torque delay correln incorporated as difference eqn
C
C     !expected torque (assumed no delay)
      TQX=KTQE*FPREVA*CALVAL*EFREL/42500.
      EAT = EXP ((- NENG * 60.) * DT / 13.)
C  NB on overrun,realistic to have torque drop off IMMEDIATELY,not in
C  a first order way.
C
      IF(TQX.GE.TQIND) THEN
C        current tq is combn.of tq at last timestep
C        and ideal torque based on current fuelling
         TQIND=EAT*TQIND + (1-EAT)*TQX
      ELSE
C        set to expected tq on overrun
         TQIND=TQX
      END IF
C
C
C     !friction torque(loosely Chen&Flynn)
      TQFRIC = TQSTAT + KFRIC * (NENG * 60.)
C
C     !brake torque
      TQENG=TQIND-TQFRIC
C  correct brake torque for non-optimum start of combn.(would have pre
C  to correct ind.torque,but exptal data not readily available) JH
C
```

```
C NB actuator dynamics comparable to rack/noz.,but effects of timing
C  secondary,therefore dynamics neglected.Convert static ctrl i/p U3
C  corresp.dynamic timing
C  st.of inj [msBTDC] (empirical correln based on JH 520DCE expt
      TIMA = 167. * (1.1784 * U3 + 7.275) / (NENG * 60.)
C
C  delay [ms] (empirical correln based on data from a 121 6cyl
C  TCA DI truck diesel operating at similar BMEPs to the 520DCE.):
      DELAY = 0.0001 * (22040. - 5.78 * (NENG * 60.) - 3.32 * TQENG)
C
C  start of combn [msBTDC]:
      SOC=TIMA-DELAY
C
C  relative effy (based on approx.observation that(i)optimum st.combn
C  the above engine was always about 0.7msBTDC,and that(ii)the relativ
C  drop in brake th.effy with deviation (in deg.CA) from this optimum
C  similar over the operating range of the engine.
      EFCOMB = 1. - 0.0000462 * (NENG * 60.) * (SOC-0.7)
C
C  corrected torque is thus
      TQENG = TQENG * EFCOMB
C
C  and although efcomb=fnc(tqeng),iteration is not worthwhile!
C
C       WENG  is the engine power in  KW*60
      WENG = TQENG * (NENG * 60.) * 2. * 3.142 / 1000.
      MEXMAN=MINMAN+MFUEL
C  calc.exh.temp. this involves either a combn temp rise(CTRISE) or a
C  motored temp rise(MTRISE)where the engine behaves as a recip.compr.
C  With +ve WENG:
C
C       !pwr to exh.=0.9*eng. power
      CTRISE=0.9*WENG/(CP*MEXMAN)
C  With no fuelling(ass.Isentropic comprn.):
      IF(PVOL/PINMAN .GT. 1.) THEN
         MTRISE=TINMAN*((PVOL/PINMAN)**((GAMMA-1.)/GAMMA)-1.)
      ELSE
C       ass. air is never cooled,even by expansion thro engine
         MTRISE = 0.
      END IF
C  temp rise set always > or = motored rise:
      IF(CTRISE.GE.MTRISE) THEN
         TEXMAN=TINMAN+CTRISE
      ELSE
         TEXMAN=TINMAN+MTRISE
      END IF
C
C-----------------------------------------------------------------------
C  BYPASS CALCULATIONS - variable closure modelled,leaving 1% "leakage"
C  area at nominal fully closed setting to allow model to work
C  ie with a single control volume and straightforward engine treatment
C-----------------------------------------------------------------------
C
C  MBYPAS is the bypass mass flow [kg/min]
      MBYPAS=MCOMP-MINMAN
C
C  ROBYP is the bypass air density in kg/cubic m (287.1 = R in J/kg K)
      ROBYP = PCOMP / (287.1 * TCOMP)
C  control i/p U4: 0V=fully open, 10V=fully closed NB 1%leakage assumec
C
C       lim slewrt(closing too fast)
      IF(((U4-X4)/DT).GT.20.) X4=X4+20.*(U4-X4)
C
```

```
C        (opening too fast)
         IF(((X4-U4)/DT).GT.20.) X4=X4-20.*(U4-X4)
C
C        no slewrt lim. required
         IF(ABS((U4-X4)/DT).LE.20.) X4=U4
C
C        absolute posn limits
         IF(X4.GT.10.) X4=10.
         IF(X4.LT. 0.) X4= 0.
C
C        areaby is unrestr.pipe area
         ABYP=AREABY*(1.-.099*X4)
C
C        gas velocity [m/s] in bypass
         VELBYP = MBYPAS / (ABYP * ROBYP * 60.)
C
C        compressor pressure = volume pressure + delta pressure in byp.
         IF(VELBYP.GE.0.) THEN
            PCOMP = PVOL + (KBYPAS * ROBYP * VELBYP*VELBYP)
         ELSE
C           with reverse byp.flow pvol exceeds pcomp
            PCOMP = PVOL - (KBYPAS * ROBYP * VELBYP*VELBYP)
         END IF
C
C-------------------------------------------------------------------------
C  VOLUME TEMPERATURE ASSUMING CONSTANT Cp AND PERFECT MIXING
C              NB if byp.flow -ve, (recirculating), then volume temp
C  same as exhaust temp.Also NB NOT dynamically calculated. JH 20.7.88
C-------------------------------------------------------------------------
C
         IF(MBYPAS.GE.0.0) THEN
            TVOL=(MEXMAN*TEXMAN + MBYPAS*TCOMP) / (MEXMAN+MBYPAS)
         ELSE
            TVOL=TEXMAN
         END IF
C
C-------------------------------------------------------------------------
C  TURBINE CALCULATIONS
C-------------------------------------------------------------------------
C
C  mech.constraints on noz.actuator
         IF(XNOZ.GT.10.) XNOZ=10.
         IF(XNOZ.LT.0.)  XNOZ=0.
C  actuator dynamics (revised gain for crit. damping  260788)
C
C        !actuator vely
         DXNOZ=YNOZ
C
C        !act. accn.
         DYNOZ=-1600.*XNOZ -80.*YNOZ +1600.*UNOZ
C
C  convert posn setting to equiv.nozzle angle BASED ON EXPTAL DATA
C  TO MODEL DATA MATCHING  OF CHOKED N-D MASSFLOWS          jh130389
         NOZA=7.+1.5*(10.-XNOZ)
C
C--nozzle position set-now do thermodynamics-------------------------
C
C  non-dimensional turbine speed  [rpm/rt.K]
         NTURB = (NLOAD * 60.) * TGR / SQRT(TVOL)
C  note effect of turbine CVT seen in above eqn.
C--MODEL-BASED TURBINE MASSFLOW---------------------------------------
C  shift pressure ratio axis linearly with speed
```

```
      PTADJ = PVOL/PATM - 1.3 - (NTURB-1675.)*5.E-4
C
C  chokes when PTADJ is over 1.25; interpoln below 1.25
      IF(PTADJ .GE. 1.25) THEN
         MTURB=37.* NOZA
      ELSE
         PTNORM=PTADJ/0.25+1.
C        non-dim massflow from predicted turbine swal. capacity
         MTURB=RITRP1(PTNORM,MTARR,MTSIZE)*NOZA
      END IF
C
C  dimensionalise to [kg/min]
      MTURB = MTURB * (PVOL * 1.E-5) / SQRT(TVOL)
C  !!reduced turb.size JH150589
      mturb=mturb*.7
C  turbine isen.effy from peak value in data file and U/c-based red.
C  tip speed [m/s] (Nload [rev/s],tgr [-],rotor tip dia.0.17145m)
      TIPVEL=NLOAD*TGR*.5386
C  isentropic expansion outlet gas vel [m/s], ass. stat.T,p = stagn.T,
C  scale peak effy (efturb) according to blade speed ratio (tipvel/gas
C  opt. bsr=.68 for C-045;effy redn away from .68 based on Napier data
C  True turb pres ratio based on typical back pres.
      PTURB = PVOL/(PATM*1.02)
      IF( PTURB .GT. 1.) THEN
         GASVEL=SQRT(2000.*CP*TVOL*(1.- (1./PTURB)
     >             **((GAMMA-1.)/GAMMA) ) )
         TISEFF=EFTURB*(TIPVEL/GASVEL)*(2.- TIPVEL/GASVEL/.68)/.68
C        turbine work [kJ/min] where tiseff=isentropic efficiency
         WTURB = MTURB * CP * TVOL * (1. - (1./PTURB)
     >              **((GAMMA-1.)/GAMMA) ) * TISEFF
      ELSE
         WTURB = 0.
      END IF
C  turbine torque NB REFERRED TO O/S SPEED by excluding factor of tgr.
C  note Wturb[kJ/min],Nload[rev/s]thus need factor of 60 [s/min]
C
C  thermodynamic turbine torque [Nm]
      TQTURB = WTURB * 1000. / ((NLOAD * 60.) * 2. * 3.1412)
C  consideration of turbine+shaft acceleration and geartrain efficienc
C  gives dynamic turbine torque delivered at o/p shaft. NB the accn tq
C  is calculated at turbine shaft then referred to o/s speed,to ensure
C  that sim.of CVT at o/s would treat turb.train inertias correctly.
      TQTAPP = 0.92 * (TQTURB -  (JTURB* ALOAD*TGR )*TGR )
C
C-----------------------------------------------------------------------
C  RATE OF CHANGE OF PRESSURE WITH TIME (VOLUME DYNAMICS)
C-----------------------------------------------------------------------
C
C  mass stored in volume from perfect gas equation [kg]
C  using R = 287.1 J/kg K
      VOMASS = ( PVOL * (VOLUME * 1.E-3)) / (287.1 * TVOL)
C  rate of change of VOMASS (mass storage equation) [kg/min]
      VOMDOT=(MCOMP+MFUEL-MTURB)
C  energy equation (quasi-steady open system) used to get rate of ch.o
C  heat transfer and KE neglected,so d(mu)/dt = SUM{d(mh)/dt}
C  first decide what bypass gas temp is (=Tcomp if +ve, Tvol if -ve fl
      IF(MBYPAS.GE.0.) THEN
         TBYP=TCOMP
      ELSE
         TBYP=TVOL
      END IF
C  mean Cp,Cv used for all flows for simplicity
C  note tvodot [deg.K/min]
```

```
      TVODOT=( (MEXMAN*TEXMAN + MBYPAS*TBYP - MTURB*TVOL)*GAMMA
     >  - VOMDOT*TVOL ) / VOMASS
C  rate of change of PVOL from VOMDOT and TVODOT..
C  ..combined with perfect gas eqn (varied units and /6 gives [bar/sec]
        PVODOT=(VOMDOT*TVOL + TVODOT*VOMASS)*R / (VOLUME*6.)
C
C-----------------------------------------------------------------------
C  TORQUE AND ACCELERATION EQUATIONS (INERTIA DYNAMICS)
C-----------------------------------------------------------------------
C
C  annulus torque
        TQANN = TQENG - (JANN * AENG)
C
C  input compressor torque (sun torque referred to compressor speed)
        TQSUN = 0.96 ** 2 * TQANN / CGR
C
C  input torque into planet carrier(referred to output shaft speed)
        TQPC  = TQANN / OGR
C
C  consideration of planet carrier and idler inertiae gives dynamic tq.
        TQPC  = 0.96 ** 3 * (TQPC - JOIPC * ALOAD)
C  developed o/p tq is sum of dynamic pc & turbine tqs
        TQOUT = TQPC + TQTAPP
C
C  output shaft acceleration
        ALOAD = (TQOUT - TQLOAD) / JOS
C
C  compressor acceleration
        ACOMP = (TQSUN - TQCOMP) / JCOMP
C  eng accn from epicyclic eqn
        AENG = ACOMP / CGR + ALOAD / OGR
C
C-----------------------------------------------------------------------
C  ASSIGN RATES OF CHANGE TO ARRAY DCEDOT
C-----------------------------------------------------------------------
C
        DCEDOT(1)=ACOMP * 60. / (2. * 3.1412)
        DCEDOT(2)=ALOAD * 60. / (2. * 3.1412)
        DCEDOT(3)=PVODOT
        DCEDOT(4)=DXRACK
        DCEDOT(5)=DYRACK
        DCEDOT(6)=DXNOZ
        DCEDOT(7)=DYNOZ
C
C       !DCE(8) is integral of error (in this model)
        DCEDOT(8)=XERROR
C
C  Reconversion from SI units into initial units
C  [bar,rev/min]
        PCOMP  = PCOMP  * 1.E-5
        NENG = NENG * 60.
        AENG = AENG * 60.
C
        RETURN
        END
```

PART 3.2

```
      SUBROUTINE DCEMOD(DCE,DCEDOT,DT,TINT,TIME)
C  ------------------------------------------------------------------
C ¦                                                                  ¦
C ¦                            DCECSC.FOR                            ¦
C ¦     simple dynamic model of Leyland 520 DCE prototype rig        ¦
C ¦     plus notional compressor sprag clutch.                       ¦
C ¦                                                                  ¦
C  ------------------------------------------------------------------
C
C  last change 150389 JH
C
C  (subroutine DCEMOD for control study simulation DCECON)
C
C  version C incorporates compressor overrunning clutch model (not
C  fitted to prototype), using an extra dynamic state to separate
C  compressor and comp.drive train dynamics.
C
C  dynamic equations give :
C  ----------------------
C  1. compressor drivetrain (sun) acceleration
C  2. output acceleration
C  3. rate of pressure change in volume (mass storage in volume)
C  4. compressor acceleration
C
C  all other variables are calculated using simple approximations
C  which assume no dynamics ie. no time lag between inputs and
C  outputs.
C
C  variable notation:
C  -----------------
C  DCE(8)       array describing dynamic state of DCE rig.
C  DCEDOT(8)    rates of change of array 'DCE'
C    array elements:
C    DCE states                              explanation:
C                1   NCDRV & ACDRV           compressor drive shaft
C                                            ie sun dyn.ref to comp.shaft
C                2   NLOAD & ALOAD           o/p shaft
C                3   PVOL  & PVODOT          pres.in control volume
C                8   NCOMP & ACOMP           compressor
C    Control system states
C                4   XRACK & DXRACK          rack actuator posn,velocity
C                5   YRACK & DYRACK          rack act.velocity and  deriv.
C                6   XNOZ  & DXNOZ           nozzle act. posn.and velocity
C                7   YNOZ  & DYNOZ           nozzle act.velocity and deriv.
C    NB DXRACK and YRACK are identical; so are DXNOZ and YNOZ.
C       Units are Volt, Volt/s and Volt/s/s.
C-----------------------------------------------------------------------
C SPECIFICATION STATEMENTS, COMMONS, INITIALISATION
C-----------------------------------------------------------------------
C
C
        IMPLICIT REAL (A-H,J-Z)
        IMPLICIT INTEGER (I)
        INTEGER MTSIZE
        DIMENSION DCE(8),DCEDOT(8)
C
C  common block variables which change with time
        COMMON /A/  NENG,AENG,NTURB,AFR,PCOMP,PINMAN
        COMMON /B/  TQENG,TQANN,TQSUN,TQPC,TQCOMP,TQTURB,TQLOAD,TQOUT
        COMMON /C/  MCOMP,MINMAN,MFUEL,MTURB
```

```
      COMMON /D/  TINMAN,TEXMAN,TCOMP,TVOL,TVODOT
      COMMON /E/  FPREV,FPREVA,NOZ,NOZA,TGR,TIM,TIMA
      COMMON /F/  DEMAND,URACK,UNOZ,U3,U4,EFFOLD,EFFNEW,ISS
C
C  common block variables which are constant for each run
      COMMON /G/  PATM,TATM,TCOOL
      COMMON /H/  JCOMP,JTURB,JANN,JOIPC,JOS
      COMMON /I/  KTQC,KMC,KMINMA,KMF,KTQE,KFRIC,KBYPAS
      COMMON /J/  EFCOMP,EFTURB,EFCOOL
      COMMON /K/  CP,R,GAMMA
      COMMON /L/  CGR,OGR
      COMMON /M/  VOLUME,AREABY,TQSTAT,FPREVM
      COMMON /N/  MTARR(6),VFCARR(4,13),WCARR(4,13)
C
C     !initialise: size of MTARR and engine acceleration
      DATA MTSIZE/6/
C
C  fuel calorific value [kJ/kg] - torque/fuelling correction
C  (see engine eqns)
      AENG = 1.
      CALVAL=42500.
C
C-----------------------------------------------------------------------
C  RENAME DYNAMIC STATE VARIABLES (TO HELP PROGRAM READABILITY)
C-----------------------------------------------------------------------
C
      NCDRV=DCE(1) / 60.
      NCOMP=DCE(8) / 60.
      NLOAD=DCE(2) / 60.
      PVOL=DCE(3)  * 1.E+5
      XRACK=DCE(4)
      YRACK=DCE(5)
      XNOZ=DCE(6)
      YNOZ=DCE(7)
C
C-----------------------------------------------------------------------
C  GET CONTROL INPUTS FOR CURRENT OPERATING POINT
C  note: ctrlr is called every TINT seconds-for analog ctrl TINT=DT
C-----------------------------------------------------------------------
C
C
      TFRAC=AMOD(TIME+DT/2.,TINT)
      IF (TFRAC.GT.0..AND.TFRAC.LE.DT) THEN
           CALL CTRLR(DCE,XERROR)
      END IF
C
      NENG  = NENG / 60.
      PCOMP = PCOMP * 1.E+5
C
C-----------------------------------------------------------------------
C  COMPRESSOR CALCULATIONS -- EMPIRICAL DATA PULLED FROM 2-D ARRAYS
C-----------------------------------------------------------------------
C
C     compressor pressure ratio
      PRCOMP = PCOMP / PATM
C
C  check array indices are in limits
      IF (NCOMP .LT. -3.)    STOP 'program stopped - NComp reversal'
      IF (NCOMP .GE. 236.)   STOP 'program stopped - NCOMP too high'
      IF (PRCOMP .LE. 0. )   STOP 'program stopped - PRCOMP is zero'
      IF (PRCOMP .GE. 4.4)   STOP 'program stopped - PRCOMP too high'
      IF (PVOL .LE. 0.)      STOP 'program stopped - Pvol is zero'
```

```
C
C      calculate compressor volume flow (FAD)  VFCOMP  [cu m./min]
       NCNORM = (NCOMP*60. + 200.)/4800. + 1.
       PRNORM = (PRCOMP + .0343)/.3448 + 1.
       VFCOMP = ( RITRP2(NCNORM,PRNORM,VFCARR,4,13) )/35.315
C
C      ROA is the ambient air density in kg/cubic m
       ROA = PATM / (287.1 * TATM)
C
C      compressor massflow in Kg/min
       MCOMP = VFCOMP * ROA
C
C      compressor power [W]
       WCOMP = 745.7*RITRP2(NCNORM,PRNORM,WCARR,4,13)
C
C      compressor torque [NM]
       TQCOMP = WCOMP / (6.2824 * NCOMP)
C
C  isentropic outlet temp.(TCOMP), isentropic comp. work (WCISEN)
C  and hence isentropic efficiency (EFCOMP)
        TCOMP = TATM * (PRCOMP)**((GAMMA-1)/GAMMA)
        WCISEN= MCOMP * CP * (TCOMP-TATM)
        IF(WCOMP.NE.0.) THEN
           EFCOMP= WCISEN / (WCOMP * 0.06)
C          calculate actual outlet temp. using isentropic efficiency
           TCOMP=TATM + (TCOMP-TATM)/EFCOMP
        ELSE
           TCOMP=TATM
        END IF
C
C-------------------------------------------------------------------------
C  INTERCOOLER
C-------------------------------------------------------------------------
C pres.drop [N/m2] approxn from exptal fnc of flowrate [kg/min]
        PINMAN=PCOMP - 1750.*MINMAN
C thermostat holds around 50deg.C Charge Air Temp
        TINMAN=323.
C
C-------------------------------------------------------------------------
C  ENGINE EQUATIONS
C-------------------------------------------------------------------------
C
C  speed from epicyclic equation [rev/s]
        NENG = NCDRV / CGR + NLOAD / OGR
C
C  airflow through engine from perfect gas equation  [KG/MIN]
        MINMAN = KMINMA * (PINMAN * 1E-5) * (NENG * 60.) / TINMAN
C  rack ctrl i/p Urack from controller gives rack posn/vel via dynamics
C  first impose mech.constraints
        IF(XRACK.GT.10.) XRACK=10.
        IF(XRACK.LT.0.)  XRACK=0.
C
C       !rack vel(1st ord.)
        DXRACK=YRACK
C
C       !rack accn(2nd ord)
        DYRACK=-000.*XRACK-120.*YRACK+2000.*URACK
C
C  model needs actual posn ie XRACK. This comes from num.int.,so is on
C  integration step behind.Hence timestep must be << time consts of DC
C  and control system being modelled.
C  fuelling (per rev) comes from pump calibration based on exptal data
C  XRACK posn.calib.in Volts. As mapped 30-01-89.
```

```
C  Fuelling [mg/inj]
       FPINJ=170.*(XRACK - 3.)/7.
C  Fuel per rev.[kgE-4/rev]
       FPREVA=FPINJ * .03
C
C      !fuel massflow  [KG/MIN]
       MFUEL = KMF * FPREVA * (NENG * 60.)
C
C     Calculation of Air/Fuel Ratio, avoiding /zero on overrun.
C     base AFR on clean air only, not recirc.exh.gases
      IF(MBYPAS.GE.0.) THEN
C        +ve byp.flow, so all engine air is clean
         IF(MFUEL.EQ.0.) THEN
            AFR=200.
         ELSE
            AFR = MINMAN / MFUEL
         END IF
      ELSE
C        -ve byp.flow, so only comp.del.air is clean
         AFR = MCOMP / MFUEL
      END IF
C
C  relative efficiency ass.to drop linearly with AFR below AFR=30
      IF (AFR.LT.30.) THEN
          EFREL = 1. - 0.01 * (30. - AFR)
      ELSE
          EFREL = 1.
      END IF
C
C  engine torque proportional to FPREV and relative efficiency EFREL
C  note:calval/42500 allows corrn for different fuels,keeps same KTQE
C  Hazell & Flower torque delay correln incorporated as difference eqn:
C
C      !expected torque (assumed no delay)
       TQX=KTQE*FPREVA*CALVAL*EFREL/42500.
       EAT = EXP (- NENG * 60. * DT / 13.)
C  NB on overrun,realistic to have torque drop off IMMEDIATELY,not in
C  a first order way.
C
       IF(TQX.GE.TQIND) THEN
C           current tq is combn.of tq at last timestep
C           and ideal torque based on current fuelling
            TQIND=EAT*TQIND + (1-EAT)*TQX
       ELSE
C           set to expected tq on overrun
            TQIND=TQX
       END IF
C
C
C      !friction torque(loosely Chen&Flynn)
       TQFRIC = TQSTAT + KFRIC * (NENG * 60.)
C
C      !brake torque
       TQENG=TQIND-TQFRIC
C  correct brake torque for non-optimum start of combn.(would have pre:
C  to correct ind.torque,but exptal data not readily available) JH
C
C  NB actuator dynamics comparable to rack/noz.,but effects of timing
C  secondary,therefore dynamics neglected.Convert static ctrl i/p U3 tc
C  corresp.dynamic timing
C  st.of inj [msBTDC] (empirical correln based on 520DCE expt data):
       TIMA = 167. * (1.1784 * U3 + 7.275) / (NENG * 60.)
C
```

```
C  delay [ms] (empir. correln based on data from 12l 6cyl swirling
C  TCA DI truck diesel operating at similar BMEPs to the 520DCE.):
       DELAY = 0.0001 * (22040. - 5.78*(NENG*60.)-3.32*TQENG)
C
C  start of combn [msBTDC]:
       SOC=TIMA-DELAY
C
C  relative effy (based on approx.observn that(i)opt. st.combn for
C  the above engine was always about 0.7msBTDC,and(ii)the relative
C  drop in brake th.effy with deviation [deg.CA] from optimum was
C  similar over the operating range of the engine.
       EFCOMB = 1. - 0.0000462 * (NENG * 60.) * (SOC-0.7)
C
C  corrected torque is thus
       TQENG = TQENG * EFCOMB
C
C  and although efcomb=fnc(tqeng),iteration is not worthwhile!
C
C  WENG  is the engine power in  KW*60
       WENG = TQENG * (NENG * 60.) * 2. * 3.142 / 1000.
       MEXMAN=MINMAN+MFUEL
C  calc.exh.temp. this involves either a combn temp rise(CTRISE) or a
C  motored temp rise(MTRISE)where the engine behaves as a recip.compr.
C  With +ve WENG:
C
C       !pwr to exh.=0.9*eng. power
       CTRISE=0.9*WENG/(CP*MEXMAN)
C  With no fuelling(ass.Isentropic comprn.):
       IF(PVOL/PINMAN .GT. 1.) THEN
          MTRISE=TINMAN*((PVOL/PINMAN)**((GAMMA-1.)/GAMMA)-1.)
       ELSE
C      ass. air is never cooled,even by expansion thro engine
          MTRISE = 0.
       END IF
C  temp rise set always > or = motored rise:
       IF(CTRISE.GE.MTRISE) THEN
          TEXMAN=TINMAN+CTRISE
       ELSE
          TEXMAN=TINMAN+MTRISE
       END IF
C
C-----------------------------------------------------------------------
C  BYPASS CALCULATIONS - variable closure modelled,leaving 1% "leakage'
C  area at nominal fully closed setting to allow model to work
C     with a single control volume and straightforward engine treatmen'
C-----------------------------------------------------------------------
C
C  MBYPAS is the bypass mass flow [kg/min]
       MBYPAS=MCOMP-MINMAN
C
C  ROBYP is the bypass air density in kg/cubic m
       ROBYP = PCOMP / (287.1 * TCOMP)
C  control i/p U4: 0V=fully open,10V=ful. closed NB 1%leakage ass.
C
C       lim slewrt(closing too fast)
       IF(((U4-X4)/DT).GT.20.) X4=X4+20.*(U4-X4)*DT
C
C       (opening too fst)
       IF(((X4-U4)/DT).GT.20.) X4=X4-20.*(U4-X4)*DT
C
C       no slewrt lim. required
       IF(ABS((U4-X4)/DT).LE.20.) X4=U4
C
C       absolute posn limits
```

```
      IF(X4.GT.10.) X4=10.
      IF(X4.LT. 0.) X4= 0.
C
C     areaby is unrestr.pipe area
      ABYP=AREABY*(1.-.099*X4)
C
C     gas velocity [m/s] in bypass
      VELBYP = MBYPAS / (ABYP * ROBYP * 60.)
C
C     compressor pressure = volume pressure + delta p in bypass
      IF(VELBYP.GE.0.) THEN
         PCOMP = PVOL + (KBYPAS * ROBYP * VELBYP*VELBYP)
      ELSE
C        with reverse byp.flow pvol exceeds pcomp
         PCOMP = PVOL - (KBYPAS * ROBYP * VELBYP*VELBYP)
      END IF
C
C-----------------------------------------------------------------------
C  VOLUME TEMPERATURE ASSUMING CONSTANT Cp AND PERFECT MIXING OF EXH. &
C  BYPASS FLOW. NB if byp.flow -ve, (recirculating), then volume temp
C  same as exhaust temp.Also NB NOT dynamically calculated. JH 20.7.88
C-----------------------------------------------------------------------
C
      IF(MBYPAS.GE.0.0) THEN
         TVOL=(MEXMAN*TEXMAN + MBYPAS*TCOMP) / (MEXMAN+MBYPAS)
      ELSE
         TVOL=TEXMAN
      END IF
C
C-----------------------------------------------------------------------
C  TURBINE CALCULATIONS
C-----------------------------------------------------------------------
C
C  mech.constraints on noz.actuator
      IF(XNOZ.GT.10.) XNOZ=10.
      IF(XNOZ.LT.0.)  XNOZ=0.
C  actuator dynamics (revised gain for crit. damping  260788)
C
C     !actuator vely
      DXNOZ=YNOZ
C
C     !act. accn.
      DYNOZ=-1600.*XNOZ -80.*YNOZ +1600.*UNOZ
C
C  convert posn setting to equiv.nozzle angle BASED ON EXPTAL
C  cf MODEL DATA MATCHING  OF CHOKED N-D MASSFLOWS  jh130389
      NOZA=7.+1.5*(10.-XNOZ)
C
C--nozzle position set-now do thermodynamics--------------------------
C
C  non-dimensional turbine speed  [rpm/rt.K]
      NTURB = (NLOAD * 60.) * TGR / SQRT(TVOL)
C  note effect of turbine CVT seen in above eqn.
C--MODEL-BASED TURBINE MASSFLOW---------------------------------------
C  shift pressure ratio axis linearly with speed
      PTADJ = PVOL/PATM - 1.3 - (NTURB-1675.)*5.E-4
C
C  chokes when PTADJ is over 1.25; interpoln below 1.25
      IF(PTADJ .GE. 1.25) THEN
         MTURB=37.* NOZA
      ELSE
         PTNORM=PTADJ/0.25+1.
```

```
C          non-dim massflow from predicted turbine swal. capacity
           MTURB=RITRP1(PTNORM,MTARR,MTSIZE)*NOZA
        END IF
C
C  dimensionalise to [kg/min]
        MTURB = MTURB * (PVOL * 1.E-5) / SQRT(TVOL)
C  turbine isen.effy from peak val.in data file and U/c-based redn.
C  tip speed [m/s] (Nload [rev/s],tgr [-],rotor tip dia.0.17145m)
        TIPVEL=NLOAD*TGR*.5386
C  isentropic expansion outlet gas vel [m/s], ass.stat.T,p=stag.T,p
C  scale peak effy (efturb) according to blade spd ratio(tipvel/gasvel)
C  opt. bsr=.68 for C-045;effy redn away from .68 based on Napier data.
C  True turb pres ratio based on typical back pres.
        PTURB = PVOL/(PATM*1.02)
        IF( PTURB .GT. 1.) THEN
           GASVEL=SQRT(2000.*CP*TVOL*(1.- (1./PTURB)
     >              **((GAMMA-1.)/GAMMA) ) )
           TISEFF=EFTURB*(TIPVEL/GASVEL)*(2.- TIPVEL/GASVEL/.68)/.68
C          turbine work [kJ/min] where tiseff=isentropic efficiency
           WTURB = MTURB * CP * TVOL * (1. - (1./PTURB)
     >              **((GAMMA-1.)/GAMMA) ) * TISEFF
        ELSE
           WTURB = 0.
        END IF
C  turbine torque NB REFERRED TO O/S SPEED by excluding factor of tgr.
C  note Wturb[kJ/min],Nload[rev/s]thus need factor of 60 [s/min]
C
C  thermodynamic turbine torque [Nm]
        TQTURB = WTURB * 1000. / ((NLOAD * 60.) * 2. * 3.1412)
C  consideration of turbine+shaft acceleration and geartrain effy
C  gives dynamic turbine torque delivered at o/p shaft.NB accn tq
C  is calculated at turbine shaft then referred to o/s spd,to ensure
C  that sim.of CVT at o/s would treat turb.train inertias correctly.
      TQTAPP = 0.92 * (TQTURB -  (JTURB* ALOAD*TGR )*TGR )
C
C-----------------------------------------------------------------------
C  RATE OF CHANGE OF PRESSURE WITH TIME (VOLUME DYNAMICS)
C-----------------------------------------------------------------------
C
C  mass stored in volume from perfect gas equation [kg]
C  using R = 287.1 J/kg K
      VOMASS = ( PVOL * (VOLUME * 1.E-3)) / (287.1 * TVOL)
C  rate of change of VOMASS (mass storage equation) [kg/in]
      VOMDOT=(MCOMP+MFUEL-MTURB)
C  energy equation (quasi-steady open system) used to get rt.ch.of Tvol
C  heat transfer and KE neglected,so d(mu)/dt = SUM{d(mh)/dt}
C  first decide what bypass gas temp is(Tcomp if +ve,Tvol if -ve flow)
      IF(MBYPAS.GE.0.) THEN
         TBYP=TCOMP
      ELSE
         TBYP=TVOL
      END IF
C  mean Cp,Cv used for all flows for simplicity
C  note tvodot [deg.K/min]
      TVODOT=( (MEXMAN*TEXMAN + MBYPAS*TBYP - MTURB*TVOL)*GAMMA
     >  - VOMDOT*TVOL ) / VOMASS
C  rate of change of PVOL from VOMDOT and TVODOT..
C  ..combined with perfect gas eqn (varied units and /6 gives [bar/sec
        PVODOT=(VOMDOT*TVOL + TVODOT*VOMASS)*R / (VOLUME*6.)
C
C-----------------------------------------------------------------------
C  TORQUE AND ACCELERATION EQUATIONS (INERTIA DYNAMICS)
```

```
C-----------------------------------------------------------------------
C
C  annulus torque
      TQANN = TQENG - (JANN * AENG)
C
C  input compressor torque (sun torque referred to compressor speed)
      TQSUN = 0.96 ** 2 * TQANN / CGR
C
C  input torque into planet carrier(referred to output shaft speed)
      TQPC  = TQANN / OGR
C
C  consideration of planet carrier and idler inertiae gives dynamic tq.
      TQPC  = 0.96 ** 3 * (TQPC - JOIPC * ALOAD)
C  developed o/p tq is sum of dynamic pc & turbine tqs
      TQOUT = TQPC + TQTAPP
C
C  output shaft acceleration
      ALOAD = (TQOUT - TQLOAD) / JOS
C
C  compressor and comp.train accelerations (overrunning clutch)
C  Note:separate comp train inertias either side of clutch,which is ass
C  to run at compressor speed.Jcomp=96% of total, Jtrain=4% of total.
C  First assume clutch disengaged - compressor overrunning - and calc
C  comp. and drive train accns independently.
C  then go on to impose accn compatibility if necessary.
      ACDRV = TQSUN / (JCOMP*.04)
      ACOMP = -TQCOMP / (JCOMP*.96)
C  now if compr.not overrunning,clutch must be engaged.
      IF((NCOMP.LE.NCDRV) .AND. (ACOMP.LT.ACDRV)) THEN
C        re-synch speeds exactly (dce()array is passed to num.int.)
         DCE(8) = DCE(1)
C        comp accel less than drive shaft is imposs.:treat as engagec
C        clutch.NB comp."pulling" torque cannot be transm. by clutch
C        but is "seen" by drive train because it red. comp.dyn.torque
         ACDRV = (TQSUN-TQCOMP) / JCOMP
         ACOMP = ACDRV
      END IF
C
C  eng accn from epicyclic eqn
      AENG = ACDRV / CGR + ALOAD / OGR
C
C-----------------------------------------------------------------------
C  ASSIGN RATES OF CHANGE TO ARRAY DCEDOT
C-----------------------------------------------------------------------
C
      DCEDOT(1)=ACDRV * 60. / (2. * 3.1412)
      DCEDOT(8)=ACOMP * 60. / (2. * 3.1412)
      DCEDOT(2)=ALOAD * 60. / (2. * 3.1412)
      DCEDOT(3)=PVODOT
      DCEDOT(4)=DXRACK
      DCEDOT(5)=DYRACK
      DCEDOT(6)=DXNOZ
      DCEDOT(7)=DYNOZ
C
C  Reconversion from SI units into initial units
C  [bar,rev/min]
      PCOMP  = PCOMP  * 1.E-5
      NENG = NENG * 60.
      AENG = AENG * 60.
C
      RETURN
      END
```

```
      SUBROUTINE DCEMOD(DCE,DCEDOT,DT,TINT,TIME)
C  ____________________________________________________________
C  :                                                           :
C  :                          DCECSE.FOR                       :
C  :       2 volume dynamic model of DCE (matched to L520DCE)  :
C  :                                                           :
C  -------------------------------------------------------------
C
C  last change 230389 JH
C
C  (subroutine DCEMOD for control study simulation DCECON)
C  Version E  based on version B,with flap-regulated compressor bypass,
C  and engine bypass flap valve to prevent reverse flow. Model uses TWO
C  control volumes, at comp.outlet and turbine inlet.
C
C  dynamic equations give :
C  ----------------------
C  1. compressor acceleration
C  2. output acceleration
C  3. rate of pressure change in  2 volumes (mass storage)
C
C  all other variables are calculated using simple approximations
C  which assume no dynamics ie. no time lag between inputs and
C  outputs.
C
C  assumptions:
C  -----------
C  Two volumes
C  planet accelerations neglected
C  gearbox losses approximated
C  perfect mixing in volumes
C
C  variable notation:
C  -----------------
C  DCE(8)        array describing dynamic state of DCE rig.
C  DCEDOT(8)     rates of change of array 'DCE'
C    array elements:
C    DCE states                              explanation:
C                1   NCOMP & ACOMP           compressor
C                2   NLOAD & ALOAD           o/p shaft
C                3   PVOL  & PVODOT          pres.in turb. side control vol.
C                8   PCOMP & PCODOT               "   comp.        "
C    Control system states
C                4   XRACK & DXRACK          rack actuator posn,velocity
C                5   YRACK & DYRACK          rack act.velocity and  deriv.
C                6   XNOZ  & DXNOZ           nozzle act. posn.and velocity
C                7   YNOZ  & DYNOZ           nozzle act.velocity and deriv.
C    NB DXRACK and YRACK are identical; so are DXNOZ and YNOZ.
C       Units are Volt, Volt/s and Volt/s/s.
C-------------------------------------------------------------------
C SPECIFICATION STATEMENTS, COMMONS, INITIALISATION
C-------------------------------------------------------------------
C
C
        IMPLICIT REAL (A-H,J-Z)
        IMPLICIT INTEGER (I)
        INTEGER MTSIZE
        DIMENSION DCE(8),DCEDOT(8)
C
C  common block variables which change with time
      COMMON /A/  NENG,AENG,NTURB,AFR,PCOMP,PINMAN
      COMMON /B/  TQENG,TQANN,TQSUN,TQPC,TQCOMP,TQTURB,TQLOAD,TQOUT
```

```
      COMMON /C/  MCOMP,MINMAN,MFUEL,MTURB
      COMMON /D/  TINMAN,TEXMAN,TCOMP,TVOL,TVODOT
      COMMON /E/  FPREV,FPREVA,NOZ,NOZA,TGR,TIM,TIMA
      COMMON /F/  DEMAND,URACK,UNOZ,U3,U4,EFFOLD,EFFNEW,ISS
C
C  common block variables which are constant for each run
      COMMON /G/  PATM,TATM,TCOOL
      COMMON /H/  JCOMP,JTURB,JANN,JOIPC,JOS
      COMMON /I/  KTQC,KMC,KMINMA,KMF,KTQE,KFRIC,KBYPAS
      COMMON /J/ EFCOMP,EFTURB,EFCOOL
      COMMON /K/ CP,R,GAMMA
      COMMON /L/ CGR,OGR
      COMMON /M/ VOLUME,AREABY,TQSTAT,FPREVM
      COMMON /N/ MTARR(6),VFCARR(4,13),WCARR(4,13)
      COMMON /O/ X4,X5
C
C     !initialise: size of MTARR and engine acceleration
      DATA MTSIZE/6/
C
C  fuel calorific value [kJ/kg] - torque/fuelling correction
C  (see engine eqns)
      AENG = 1.
      CALVAL=42500.
C
C-----------------------------------------------------------------------
C  RENAME DYNAMIC STATE VARIABLES (TO HELP PROGRAM READABILITY)
C-----------------------------------------------------------------------
C
      NCOMP=DCE(1) / 60.
      NLOAD=DCE(2) / 60.
      PVOL =DCE(3) * 1.E+5
      PCOMP=DCE(8) * 1.E+5
      XRACK=DCE(4)
      YRACK=DCE(5)
      XNOZ =DCE(6)
      YNOZ =DCE(7)
C
C-----------------------------------------------------------------------
C  GET CONTROL INPUTS FOR CURRENT OPERATING POINT
C  note: ctrlr is called every TINT seconds-for analog ctrl TINT=DT
C-----------------------------------------------------------------------
C
C
      TFRAC=AMOD(TIME+DT/2.,TINT)
      IF (TFRAC.GT.0..AND.TFRAC.LE.DT) THEN
           CALL CTRLR(DCE,XERROR)
      END IF
C
      NENG  = NENG / 60.
C
C-----------------------------------------------------------------------
C  COMPRESSOR CALCULATIONS -- EMPIRICAL DATA PULLED FROM 2-D ARRAYS
C-----------------------------------------------------------------------
C
C     compressor pressure ratio
      PRCOMP = PCOMP / PATM
C
C  check array indices are in limits
      IF (NCOMP .LT. -3.)    STOP 'program stopped - NComp reversal'
      IF (NCOMP .GE. 236.)   STOP 'program stopped - NCOMP too high'
      IF (PRCOMP .LE. 0. )   STOP 'program stopped - PRCOMP is zero'
      IF (PRCOMP .GE. 4.4)   STOP 'program stopped - PRCOMP too high'
      IF (PVOL .LE. 0.)      STOP 'program stopped - PVOL is zero'
```

```
      IF (PVOL/PATM.GE.4.5)  STOP 'program stopped - PVOL too high'
C
C     calculate compressor volume flow (FAD)  VFCOMP  [cu m./min]
      NCNORM = (NCOMP*60. + 200.)/4800. + 1.
      PRNORM = (PRCOMP + .0343)/.3448 + 1.
      VFCOMP = ( RITRP2(NCNORM,PRNORM,VFCARR,4,13) )/35.315
C
C     ROA is the ambient air density in kg/cubic m
      ROA = PATM / (287.1 * TATM)
C
C     compressor massflow in Kg/min
      MCOMP = VFCOMP * ROA
C
C     compressor power [W]
      WCOMP = 745.7*RITRP2(NCNORM,PRNORM,WCARR,4,13)
C
C     compressor torque [NM]
      TQCOMP = WCOMP / (6.2824 * NCOMP)
C
C  isentropic outlet temp.(TCOMP), isentropic comp. work (WCISEN)
C  and hence isentropic efficiency (EFCOMP)
       TCOMP = TATM * (PRCOMP)**((GAMMA-1)/GAMMA)
       WCISEN= MCOMP * CP * (TCOMP-TATM)
       IF(WCOMP.GE.0.) THEN
          EFCOMP= WCISEN / (WCOMP * 0.06)
C         calculate actual outlet temp. using isentropic efficiency
          TCOMP=TATM + (TCOMP-TATM)/EFCOMP
       ELSE
          TCOMP=TATM
       END IF
C
C-----------------------------------------------------------------------
C  COMPRESSOR BYPASS
C-----------------------------------------------------------------------
C  modelled as byp.with same dia.and fric.coeffs as engine bypass.
C  flap valve admits inflow, prevents outflow. Slewrate lims.
C  valve posn.:
       IF(PCOMP.GT.PATM) THEN
C         comp.byp.closed/closing
          U5 = 1.
       ELSE
C         open(ing)
          U5 = 0.
       END IF
C  slewrate limit: full travel .2 sec
       IF( (U5-X5)/DT .GT. 1000.) THEN
          X5=X5 + 1000.*DT
       ELSE IF( (X5-U5)/DT .GT. 1000.) THEN
          X5=X5 - 1000.*DT
       ELSE
          X5=U5
       END IF
C  posn limits
       IF(X5 .LT. 0.) X5=0.
       IF(X5 .GT. 1.) X5=1.
C  corresp.comp.bypass area
       ACBYP=AREABY*(1.-X5)
C  now calc flowrate: ass. fric.factor constant.
C  ass. pres & temp always as for +ve flow
       IF(PAM.GE.PCOMP) THEN
          MCBYP= KBYPAS * ACBYP * SQRT( (PATM-PCOMP)*ROA )
       ELSE
C         reverse dp for sqrt computation
```

```
            MCBYP=-KBYPAS * ACBYP * SQRT( (PCOMP-PATM)*ROA )
         END IF
C
C-----------------------------------------------------------------------
C  INTERCOOLER
C-----------------------------------------------------------------------
C pres.drop [N/m2] approxn from exptal fnc of flowrate [kg/min]
         PINMAN=PCOMP - 1750.*MINMAN
C thermostat holds around 50deg.C Charge Air Temp
         TINMAN=323.
C
C-----------------------------------------------------------------------
C  ENGINE EQUATIONS
C-----------------------------------------------------------------------
C
C  speed from epicyclic equation [rev/s]
         NENG = NCOMP / CGR + NLOAD / OGR
C
C  airflow through engine from perfect gas equation  [KG/MIN]
         MINMAN = KMINMA * (PINMAN * 1E-5) * (NENG * 60.) / TINMAN
C  rack ctrl i/p Urack from controller gives rack posn/vel via dynamics
C  first impose mech.constraints
         IF(XRACK.GT.10.) XRACK=10.
         IF(XRACK.LT.0.)  XRACK=0.
C
C        !rack vel(1st ord.)
         DXRACK=YRACK
C
C        !rack accn(2nd ord)
         DYRACK=-2000.*XRACK-120.*YRACK+2000.*URACK
C
C  fuelling (per rev) comes from pump calibration based on exptal data
C  XRACK posn.calib.in Volts. As mapped 30-01-89.
C  Fuelling [mg/inj]
         FPINJ=170.*(XRACK - 3.)/7.
C  Fuel per rev.[kgE-4/rev]
         FPREVA=FPINJ * .03
C
C        !fuel massflow  [KG/MIN]
         MFUEL = KMF * FPREVA * (NENG * 60.)
C
C     Calculation of Air/Fuel Ratio, avoiding div.by zero on overrun.
C     neglect recirc.exh.gases since will be very small dilution
         IF(MFUEL.EQ.0.) THEN
C           nom.fuel flow allows afr to be calcd (shows up zero minman)
            AFR= MINMAN / (MFUEL+.001)
         ELSE
            AFR = MINMAN / MFUEL
         END IF
C
C  relative efficiency ass.to drop linearly with AFR below AFR=30
         IF (AFR.LT.30.) THEN
            EFREL = 1. - 0.02 * (30. - AFR)
         ELSE
            EFREL = 1.
         END IF
C
C  engine torque proportional to FPREV and relative efficiency EFREL
C  note:calval/42500 allows corrn for different fuels,keeps same KTQE
C  Hazell & Flower torque delay correln incorporated as difference eqn
C
C        !expected torque (assumed no delay)
         TQX=KTQE*FPREVA*CALVAL*EFREL/42500.
```

```
      EAT = EXP ((- NENG * 60.) * DT / 13.)
C  on overrun,realistic to have torque drop off immediately,not in
C  a first order way.
C
      IF(TQX.GE.TQIND) THEN
C          current tq is combn.of tq at last timestep
C          and ideal torque based on current fuelling
           TQIND=EAT*TQIND + (1-EAT)*TQX
      ELSE
C          set to expected tq on overrun
           TQIND=TQX
      END IF
C
C
C     !friction torque(loosely Chen&Flynn)
      TQFRIC = TQSTAT + KFRIC * (NENG * 60.)
C
C     !brake torque
      TQENG=TQIND-TQFRIC
C  correct brake torque for non-optimum start of combn.(would have pref
C  to correct ind.torque,but exptal data not readily available) JH
C
C  NB actuator dynamics comparable to rack/noz.,but effects of timing
C  secondary,therefore dynamics neglected.Convert static ctrl i/p U3 -
C  corresp.dynamic timing
C  st.of inj [msBTDC] (empirical correln based on 520DCE expt):
      TIMA = 167. * (1.1784 * U3 + 7.275) / (NENG * 60.)
C
C  delay [ms] (empirical correln based on data from  121 6cyl
C  TCA DI truck diesel operating at similar BMEPs to the 520DCE.):
      DELAY = 0.0001 * (22040. - 5.78 * (NENG * 60.) - 3.32 * TQENG)
C
C  start of combn [msBTDC]:
      SOC=TIMA-DELAY
C
C  relative effy (based on approx.observation that(i)opt st.combn for
C  the above engine was always about 0.7msBTDC,and that(ii)the relative
C  drop in brake th.effy with deviation (in deg.CA) from optimum was
C  similar over the operating range of the engine.
      EFCOMB = 1. - 0.0000462 * (NENG * 60.) * (SOC-0.7)
C
C  corrected torque is thus
      TQENG = TQENG * EFCOMB
C
C  and although efcomb=fnc(tqeng),iteration is not worthwhile!
C
C     WENG  is the engine power in  KW*60
      WENG = TQENG * (NENG * 60.) * 2. * 3.142 / 1000.
      MEXMAN=MINMAN+MFUEL
C  calc.exh.temp. this involves either a combn temp rise(CTRISE) or a
C  motored temp rise(MTRISE)where the engine behaves as a recip.compr.
C  With +ve WENG:
C
C     !pwr to exh.=0.9*eng. power
      CTRISE=0.9*WENG/(CP*MEXMAN)
C  With no fuelling(ass.sentropic comprn.):
      IF(PVOL/PINMAN .GT. 1.) THEN
         MTRISE=TINMAN*((PVOL/PINMAN)**((GAMMA-1.)/GAMMA)-1.)
      ELSE
C     ass. air is never cooled,even by expansion thro engine
         MTRISE = 0.
      END IF
```

```
C  temp rise set always > or = motored rise:
      IF(CTRISE.GE.MTRISE) THEN
         TEXMAN=TINMAN+CTRISE
      ELSE
         TEXMAN=TINMAN+MTRISE
      END IF
C
C-----------------------------------------------------------------------
C  COMPRESSOR SIDE VOLUME DYNAMICS AND THERMODYNAMICS
C-----------------------------------------------------------------------
C
C  temperature: NB comp.bypass gas
C  flow ass. to be in the intended dirn of flow for simplicity.
      TCVOL=(MCOMP*TCOMP+MCBYP*TATM) / (MCOMP+MCBYP)
C  mass storage (ass.total system vol is split 50/50 comp.    /turb
      CVMASS=PCOMP*VOLUME*.5E-3/(287.1*TCVOL)
      CVMDOT=MCOMP+MCBYP-MINMAN-MEBYP
C  temp.r.o.c.from open system energy eqn negl ht.transfer and KE, and
C  again ass. bypass temps are those for flow in intended dirn.[degK/m
      TCVDOT=( (MCOMP*TCOMP+MCBYP*TATM-MINMAN*TCVOL-MEBYP*TCVOL)
     >          *GAMMA - CVMDOT*TCVOL ) / CVMASS
C  pres. r.o.c. from pg eqn
      PCODOT=(CVMDOT*TCVOL + TCVDOT*CVMASS)*R / (VOLUME*3.)
C
C-----------------------------------------------------------------------
C  ENGINE BYPASS
C-----------------------------------------------------------------------
C  flap valve closure modelled, fully open if
C  +ve bypass flow, full closure if flow reverses.
C  Incorp.slew rate limiting to improve stability around zero flow
C  MEBYP is ENG.bypass mass flow [kg/min]
C
      IF(PCOMP.GE.PVOL) THEN
C        flap moves open-ultimate posn.is U4, slewrate-ltd posn.X4
         U4 = 0.
      ELSE
         U4 = 1.
      END IF
C  slew rate limits (full travel in .2 sec)
      IF( (U4 - X4)/DT .GT. 1000.) THEN
         X4 = X4 + 1000.*DT
      ELSE IF( (X4 - U4)/DT .GT. 1000.) THEN
         X4 = X4 - 1000.*DT
      ELSE
         X4 = U4
      END IF
C  posn.limits
      IF(X4 .LT. 0.) X4 = 0.
      IF(X4 .GT. 1.) X4 = 1.
C  corresp.engine bypass area
      AEBYP = AREABY * (1. - X4)
C  gas density ass.flow in +ve dirn.
      ROEBYP = PCOMP/(287.1*TCVOL)
C  massflow(pipe friction model)
      IF(PCOMP.GE.PVOL) THEN
         MEBYP= KBYPAS * AEBYP * SQRT( (PCOMP-PVOL)*ROEBYP )
      ELSE
         MEBYP=-KBYPAS * AEBYP * SQRT( (PVOL-PCOMP)*ROEBYP )
      END IF
C
C-----------------------------------------------------------------------
C  TURBINE SIDE VOLUME TEMPERATURE (needed in turbine calcs.)
C-----------------------------------------------------------------------
```

```
C  volume temp. ass const Cp
C
      IF(MEBYP .GT. 0.) THEN
C        perfect mixing of eng.exh. and eng.byp.flows
         TVOL=(MEXMAN*TEXMAN + MEBYP*TCVOL) / (MEXMAN+MEBYP)
      ELSE
C        turb.side volume only sees eng.exh.gas
         TVOL=TEXMAN
      END IF
C
C-----------------------------------------------------------------------
C  TURBINE CALCULATIONS
C-----------------------------------------------------------------------
C
C  mech.constraints on noz.actuator
      IF(XNOZ.GT.10.) XNOZ=10.
      IF(XNOZ.LT.0.)  XNOZ=0.
C  actuator dynamics (revised gain for crit. damping  260788)
C
C     !actuator vely
      DXNOZ=YNOZ
C
C     !act. accn.
      DYNOZ=-1600.*XNOZ -80.*YNOZ +1600.*UNOZ
C
C  convert posn setting to equiv.nozzle angle BASED ON EXPTAL DATA
C  TO MODEL DATA MATCHING  OF CHOKED N-D MASSFLOWS         jh130389
      NOZA=7.+1.5*(10.-XNOZ)
C
C--nozzle position set-now do thermodynamics--------------------------
C
C  non-dimensional turbine speed  [rpm/rt.K]
      IF(TVOL.LE.0.) STOP ' STOP - turb.volume temp < 0 deg.K'
      NTURB = (NLOAD * 60.) * TGR / SQRT(TVOL)
C  note effect of turbine CVT seen in above eqn.
C--MODEL-BASED TURBINE MASSFLOW---------------------------------------
C  shift pressure ratio axis linearly with speed
      PTADJ = PVOL/PATM - 1.3 - (NTURB-1675.)*5.E-4
C
C  chokes when PTADJ is over 1.25; interpoln below 1.25
      IF(PTADJ .GE. 1.25) THEN
         MTURB=37.* NOZA
      ELSE
         PTNORM=PTADJ/0.25+1.
C        non-dim massflow from predicted turbine swal. capacity
         MTURB=RITRP1(PTNORM,MTARR,MTSIZE)*NOZA
      END IF
C
C  dimensionalise to [kg/min]
      MTURB = MTURB * (PVOL * 1.E-5) / SQRT(TVOL)
C  turbine isen.effy from peak value in data file and U/c-based red.
C  tip speed [m/s] (Nload [rev/s],tgr[-],rotor tip dia.0.17145m)
      TIPVEL=NLOAD*TGR*.5386
C  isentropic expansion outlet gas vel [m/s], ass.stat.T,p=stag.T,p
C  scale peak effy (efturb) according to blade spd ratio(tipvel/gasvel
C  opt. bsr=.68 for C-045;effy redn away from .68 based on Napier data
C  True turb pres ratio based on typical back pres.
      PTURB = PVOL/(PATM*1.02)
      IF( PTURB .GT. 1.) THEN
         GASVEL=SQRT(2000.*CP*TVOL*(1.- (1./PTURB)
     >              **((GAMMA-1.)/GAMMA) ) )
         TISEFF=EFTURB*(TIPVEL/GASVEL)*(2.- TIPVEL/GASVEL/.68)/.68
C        turbine work [kJ/min] where tiseff=isentropic efficiency
```

```
            WTURB = MTURB * CP * TVOL * (1. - (1./PTURB)
     >              **((GAMMA-1.)/GAMMA) ) * TISEFF
         ELSE
            WTURB = 0.
         END IF
C  turbine torque NB REFERRED TO O/S SPEED by excluding factor of tgr.
C  note Wturb[kJ/min],Nload[rev/s]thus need factor of 60 [s/min]
C
C  thermodynamic turbine torque [Nm]
         TQTURB = WTURB * 1000. / ((NLOAD * 60.) * 2. * 3.1412)
C  consideration of turbine+shaft acceleration and geartrain effy
C  gives dynamic turbine torque delivered at o/p shaft. NB accn tq
C  is calculated at turbine shaft then referred to o/s spd,to ensure
C  that sim.of CVT at o/s would treat turb.train inertias correctly.
         TQTAPP = 0.92 * (TQTURB -  (JTURB* ALOAD*TGR )*TGR )
C
C-----------------------------------------------------------------------
C  TURBINE SIDE VOLUME DYNAMICS AND THERMODYNAMICS
C-----------------------------------------------------------------------
C  Note: turb.side vol.temp (TVOL) calc.above (before turbine modelling
C  mass stored in volume from perfect gas equation [kg]
C  using R = 287.1 J/kg K
         VOMASS = ( PVOL * (VOLUME * .5E-3)) / (287.1 * TVOL)
C  rate of change of VOMASS (mass storage equation) [kg/min]
         VOMDOT=(MEBYP+MEXMAN-MTURB)
C  energy equation (quasi-steady open system) used to get  roc of Tvol
C  heat transfer and KE neglected,so d(mu)/dt = SUM{d(mh)/dt}
C  ass. bypass gas temp is that for intended +ve flow
C  mean Cp,Cv used for all flows for simplicity
C  note tvodot [deg.K/min]
         TVODOT=( (MEXMAN*TEXMAN + MEBYP*TCVOL - MTURB*TVOL)*GAMMA
       >  - VOMDOT*TVOL ) / VOMASS
C  rate of change of PVOL from VOMDOT and TVODOT..
C  combined with perfect gas eqn (varied units,50%vol.&/3 =[bar/s])
         PVODOT=(VOMDOT*TVOL + TVODOT*VOMASS)*R / (VOLUME*3.)
C
C-----------------------------------------------------------------------
C  TORQUE AND ACCELERATION EQUATIONS (INERTIA DYNAMICS)
C-----------------------------------------------------------------------
C
C  annulus torque
         TQANN = TQENG - (JANN * AENG)
C
C  input compressor torque (sun torque referred to compressor speed)
         TQSUN = 0.96 ** 2 * TQANN / CGR
C
C  input torque into planet carrier(referred to output shaft speed)
         TQPC  = TQANN / OGR
C
C  consideration of planet carrier and idler inertiae gives dynamic tq
         TQPC  = 0.96 ** 3 * (TQPC - JOIPC * ALOAD)
C  developed o/p tq is sum of dynamic pc & turbine tqs
         TQOUT = TQPC + TQTAPP
C
C  output shaft acceleration
         ALOAD = (TQOUT - TQLOAD) / JOS
C
C  compressor acceleration
         ACOMP = (TQSUN - TQCOMP) / JCOMP
C  eng accn from epicyclic eqn
         AENG = ACOMP / CGR + ALOAD / OGR
C
```

APPENDIX
PART 4.2

```
      SUBROUTINE CTRLR(DCE,XERROR)
C
C     ------------------------------------------------------------------
C     |                                                                |
C     |                            DBC1.FOR                            |
C     |  subroutine of dcecs_.generates positional control outputs for |
C     |  rack,noz. as fnc.of demand input,current operating state,and  |
C     |  if appropriate, scheduled setting from dcecon/getset.this     |
C     |  version uses single variable(SIO)ctrl loops, setting rack as  |
C     |  a boost-limited allspeed governor, and controlling boost by   |
C     |  dead-beat 2nd order control of nozzle posn demand.            |
C     ------------------------------------------------------------------
C
C     last change 250489 JH
C
C     Written : J.Hall  25 Apr.1989
C     Machine : PC-AT compatibles
C     Code    : Microsoft FORTRAN 77
C
C
      IMPLICIT REAL (A-H,J-Z)
C     ..unless explicitly re-declared below
      IMPLICIT INTEGER(I)
C
      DIMENSION DCE(8),DCEDOT(8)
C     variables which change during run
      COMMON /A/  NENG,AENG,NTURB,AFR,PCOMP,PINMAN
      COMMON /E/  FPREV,FPREVA,NOZ,NOZA,TGR,TIM,TIMA
      COMMON /F/  DEMAND,URACK,UNOZ,U3,U4,EFFOLD,EFFNEW,ISS
      COMMON /GAINS/ K1,K2,K3,K4,K5,K6,K7,K8
C
C     note demand is 'drivers'feedfwd input (from modes.dat),Noz,tim,tgr ar
C     internally-generated feedfwds (eg for boost or cvt control)
C     note Urack,Unoz,U3,U4 are the controller O/Ps (ie plant ctrl I/Ps)
C
C     ------------------------------------------------------------------
C
C     ---SPEED GOVERNOR-------------------------------------------------
C     L520 DCE speed dem.range 0-10v corresp.to 0-(k5*10)rev/min.(Rated
C     speed 2600rpm,min.loaded speed 1000rpm).Droop set by prop.gain K1
      NEDEM=K5*DEMAND
C     (equivalent speed demand)
C     low idle speed ctrl (idle c.900rpm) 1000rpm allows some droop
      IF(NENG.LT.1000. .AND. NEDEM.LT.1000.) NEDEM=1000.
      IF(NENG.LT.1000.) FPINJ=.08*K1*(NEDEM-NENG)**2
C     fuelling gain increases with idle speed deficit ('lever action')
C     set fuelling demand (FPINJ) above idle speed
      IF(NENG.GE.1000.) FPINJ=K1*(NEDEM-NENG)
C     ass.fuel is to be fully shut off on overrun
      IF(FPINJ.LT.0.) FPINJ=0.
C     unconstrained rack demand (before any limiting action)
      XREQD=FPINJ
C     max.fuelling-absolute limits partly based on exptal eng.data 191288
      IF(NENG.LE.1946.) ABMXFL=180.
C     180 mg/inj is enough for 20bar BMEP
      IF(NENG.GT.1946.) ABMXFL=350280./NENG
C     run along 266kW power line
      IF(FPINJ.GT.ABMXFL) FPINJ=ABMXFL
C     AFR limiting (fuelling part)-limit boost/fuelling ratio. Should stay
C     below K7 mg/inj(FPINJ) per Bar abs. (pcomp)  110488
```

```
      MXFUEL=K7*PCOMP
      IF(FPINJ.GT.MXFUEL) FPINJ=MXFUEL
C
C  ---O/S SPEED LIMITING-----------------------------------------------
C  o/s must be constrained from overspeeding-this is best done by
C  ctrlling fuel i/p.start limiting at 335Ø,aim to have zero fuelling
C  by 342Ørpm (this defines K6, which is set in dcemod.dat).
C
      NOSRED=Ø.
      IF(DCE(2).GT.335Ø.) NOSRED=K6*((DCE(2)-335Ø.)**2)
      FPINJ=FPINJ-NOSRED
C  also reduce xreqd to avoid running in tr.ctrl mode at limiting No/s
      XREQD=XREQD-NOSRED
C
C  Finally check that above reduction has not set urack < Øv limit
      IF(FPINJ.LT.Ø.) FPINJ=Ø.
C  convert to rack setting which gives this fuelling (correln 3ØØ189)
      URACK=3. + FPINJ/24.286
C  but max rack (physical) =1ØV so dont ask for more
      IF(URACK.GT.1Ø.) URACK=1Ø.
C  -------------------------------------------------------------------
C
C  ---NOZZLE CONTROL---------------------------------------------------
C  At Steady-State:
C     deadbeat control of boost pressure for best Effy (scheduled)
C  At Transient:
C  If desired fuelling<abs.max.fuelling limit the above s-s ctrl applies
C  If desired rack ctrl o/p >=abs.max.fuelling,
C  Nozzles are used to keep boost at level reqd for absolute max.
C  engine fuelling, ie 3 bar.
C  NB higher nozzle volts (UNOZ) implies more closure.
C
C    detect transient...
      IF(XREQD.GE.ABMXFL) THEN
C       transient control strategy
        WBST=3.
      ELSE
C       steady-state control strategy (NOZ is sched.boost pressure)
        WBST=NOZ
      END IF
C  deadbeat control: 2nd order so update past errors..
      ERRKM2=ERRKM1
      ERRKM1=ERRK
C  ..and compute current error
      ERRK=WBST-DCE(3)
C  update past control i/ps..
      UNZKM2=UNZKM1
      UNZKM1=UNOZ
C  ..and compute current control i/p
      UNOZ=.79*UNZKM1+.211*UNZKM2+26.32*ERRK-38.2*ERRKM1+14.5*ERRKM2
C  ctrl limits are Ø-1ØV (actuator saturation)
      IF(UNOZ.LT.Ø.)  UNOZ=Ø.
      IF(UNOZ.GT.1Ø.) UNOZ=1Ø.
C
C  -------------------------------------------------------------------
C  ---TIMING CONTROL---------------------------------------------------
C  optimum st.state static timing [Volts] is TIM (fr.common block)
      U3=TIM
C
C  ---CVT and BYPASS CONTROL not used----------------------------------
      U4=Ø.
      RETURN
      END
```

APPENDIX
PART 4.3

```
      SUBROUTINE CTRLR(DCE,XERROR)
C
C ┌──────────────────────────────────────────────────────────────┐
C │                          LRPC.FOR                            │
C │  subroutine of dcecs_.generates positional control outputs for │
C │  rack,noz. as fnc.of demand input,current operating state,and │
C │  if appropriate, scheduled setting from dcecon/getset.this   │
C │  version uses single variable(SIO)ctrl loops, setting rack as │
C │  a boost-limited allspeed governor, and controlling boost by │
C │  Long-Range Predictive Control of nozzle posn.               │
C └──────────────────────────────────────────────────────────────┘
C
C  last change 310489 JH
C
C  Written : J.Hall  31 Apr.1989
C  Machine : PC-AT compatibles
C  Code    : Microsoft FORTRAN 77
C
C
      IMPLICIT REAL (A-H,J-Z)
C     ..unless explicitly re-declared below
      IMPLICIT INTEGER(I)
C
      DIMENSION DCE(8),DCEDOT(8)
      REAL H(8),PSI(4),PSIP(4),TH(4)
      REAL YPRED(8),DYPRED(8)
      REAL HTH
C  variables which change during run
      COMMON /A/  NENG,AENG,NTURB,AFR,PCOMP,PINMAN
      COMMON /E/  FPREV,FPREVA,NOZ,NOZA,TGR,TIM,TIMA
      COMMON /F/  DEMAND,URACK,UNOZ,U3,U4,EFFOLD,EFFNEW,ISS
      COMMON /GAINS/ K1,K2,K3,K4,K5,K6,K7,K8
C
      DATA H(1),H(2),H(3),H(4) /.Ø2,.Ø76,.Ø89,.Ø78/
      DATA H(5),H(6),H(7),H(8) /.Ø58,.Ø38,.Ø21,.ØØ8/
      DATA HTH /.Ø255/
      DATA TH(1),TH(2),TH(3),TH(4) /-1.3,.49,.Ø2,.Ø5/
C  note H(j) are impulse response coefficients over 8 future steps;
C       HTH is  Transp(H).(H);
C       THeta are identified ARIMA 2nd order model parameters;
C       PSI are ARIMA states, PSIp are states at the next timestep
C       pred.using ARIMA model.
C
C  note demand is 'drivers'feedfwd input (from modes.dat),Noz,tim,tgr a
C  internally-generated feedfwds (eg for boost or cvt control)
C  note Urack,Unoz,U3,U4 are the controller O/Ps (ie plant ctrl I/Ps)
C
C  ------------------------------------------------------------------
C
C  ---SPEED GOVERNOR-----------------------------------------------
C  L52Ø DCE speed dem.range Ø-1Øv corresp.to Ø-(k5*1Ø)rev/min.(Rated
C  speed 26ØØrpm,min.loaded speed 1ØØØrpm).Droop set by prop.gain K1
      NEDEM=K5*DEMAND
C       (equivalent speed demand)
C  low idle speed ctrl (idle c.9ØØrpm) 1ØØØrpm allows some droop
      IF(NENG.LT.1ØØØ. .AND. NEDEM.LT.1ØØØ.) NEDEM=1ØØØ.
      IF(NENG.LT.1ØØØ.) FPINJ=.Ø8*K1*(NEDEM-NENG)**2
C  fuelling gain increases with idle speed deficit ('lever action')
C  set fuelling demand (FPINJ) above idle speed
```

```
      IF(NENG.GE.1000.) FPINJ=K1*(NEDEM-NENG)
C  ass.fuel is to be fully shut off on overrun
      IF(FPINJ.LT.0.) FPINJ=0.
C  unconstrained rack demand (before any limiting action)
      XREQD=FPINJ
C  max.fuelling-absolute limits partly based on exptal eng.data 191288
      IF(NENG.LE.1946.) ABMXFL=180.
C       180 mg/inj is enough for 20bar BMEP
      IF(NENG.GT.1946.) ABMXFL=350280./NENG
C       run along 266kW power line
      IF(FPINJ.GT.ABMXFL) FPINJ=ABMXFL
C  AFR limiting (fuelling part)-limit boost/fuelling ratio. Should stay
C  below K7 mg/inj(FPINJ) per Bar abs. (pcomp)  110488
      MXFUEL=K7*PCOMP
      IF(FPINJ.GT.MXFUEL) FPINJ=MXFUEL
C
C  ---O/S SPEED LIMITING-----------------------------------------------
C  o/s must be constrained from overspeeding-this is best done by
C  ctrlling fuel i/p.start limiting at 3350,aim to have zero fuelling
C  by 3420rpm (this defines K6, which is set in dcemod.dat).
C
      NOSRED=0.
      IF(DCE(2).GT.3350.) NOSRED=K6*((DCE(2)-3350.)**2)
      FPINJ=FPINJ-NOSRED
C  also reduce xreqd to avoid running in tr.ctrl mode at limiting No/s
      XREQD=XREQD-NOSRED
C
C  Finally check that above reduction has not set urack < 0v limit
      IF(FPINJ.LT.0.) FPINJ=0.
C  convert to rack setting which gives this fuelling (correln 300189)
      URACK=3. + FPINJ/24.286
C  but max rack (physical) =10V so dont ask for more
      IF(URACK.GT.10.) URACK=10.
C  ------------------------------------------------------------------
C
C  ---NOZZLE CONTROL---------------------------------------------------
C  At Steady-State:
C     deadbeat control of boost pressure for best Effy (scheduled)
C  At Transient:
C  If desired fuelling<abs.max.fuelling limit the above s-s ctrl applies
C  If desired rack ctrl o/p >=abs.max.fuelling,
C  Nozzles are used to keep boost at level reqd for absolute max.
C  engine fuelling, ie 3 bar.
C  NB higher nozzle volts (UNOZ) implies more closure.
C
C    detect transient...
      IF(XREQD.GE.ABMXFL) THEN
C       transient control strategy
        WBST=3.
      ELSE
C       steady-state control strategy (NOZ is sched.boost pressure)
        WBST=NOZ
      END IF
C  future o/p predictions up to horizon 1=8, using postulated ctrl.move
C
C  predns up to model order using ARIMA model directly:
C  update state vector (right-shift old data & introduce latest data)
C  NB here we use ctrl scenario that Unoz is unchanged in future.
      DYJ=DCE(3)-YJM1
      DUJM1=UNOZ-UJM1
      PSI(2)=PSI(1)
      PSI(1)=-DYJ
```

```
      PSI(3)=Ø.
      PSI(4)=DUJM1
C  update y (o/p) for next time (will then be Y j-1)
      YJM1=DCE(3)
C  next o/p move from current state, and model params
      DYPRED(1)=Ø.
      DO 2Ø I=1,4
         DYPRED(1)=DYPRED(1) + PSI(I)*TH(I)
 2Ø   CONTINUE
C  get o/p position predn from o/p move predn
      YPRED(1)=DYPRED(1)+DCE(3)
C  construct one-step ahead pred.state vector psip from psi and
C  dypred(1), and postulated future controls (ie moves=Ø.)
      PSIP(1)=-DYPRED(1)
      PSIP(2)=-DYJ
      PSIP(3)=Ø.
      PSIP(4)=Ø.
C  and thus predict 2 step ahead o/p move using ARIMA model and
C  one step ahead pred.state (NB param.vector fixed)
      DYPRED(2)=Ø.
      DO 1Ø I=1,4
         DYPRED(2)=DYPRED(2) + PSIP(I)*TH(I)
 1Ø   CONTINUE
C  the pred.2 step ahead o/p posn is
      YPRED(2)=DYPRED(2)+YPRED(1)
C
C  predns from >model order up to predn horizon use recursive updates
C  of dy and y in parallel:
      DO 3Ø I=3,8
         DYPRED(I)=-TH(1)*DYPRED(I-1) -TH(2)*DYPRED(I-2)
         YPRED(I) =YPRED(I-1) + DYPRED(I)
 3Ø   CONTINUE
C  ctrl is min.of predicted cost.Assumptions:
C  i)  future ref.i/ps = current ref.i/p WBST
C  ii) MAC/GPC type cost fnc.;K3=control cost weighting factor
C  iii)'control horizon'(GPC concept) =1
C  soln is  H.(w-ypred)/(H'.H + K3)
C  first compute H.(w-ypred)
      SCRB=Ø.
      DO 4Ø I=1,8
         SCRB=SCRB + H(I)*(WBST-YPRED(I))
 4Ø   CONTINUE
C  H'.H + K3 is
      SCRA = HTH + K3
C  record current ctrl posn for next time (will then be U j-1)
      UJM1=UNOZ
C  and comp. next step min.cost (optimal) control move..
      DUNOZ=SCRB/SCRA
C  ..and thus new ctrl posn.
      UNOZ = UNOZ+DUNOZ
C
C  ctrl limits are Ø-1ØV (actuator saturation)
      IF(UNOZ.LT.Ø.)  UNOZ=Ø.
      IF(UNOZ.GT.1Ø.) UNOZ=1Ø.
C
C  ------------------------------------------------------------
C  ---TIMING CONTROL-------------------------------------------
C  optimum st.state static timing [Volts] is TIM (fr.common block)
      U3=TIM
C
C  ---CVT and BYPASS CONTROL not used--------------------------
      U4=Ø.
      RETURN
      END
```

```
      SUBROUTINE CTRLR(DCE,XERROR)
C
C  ------------------------------------------------------------------
C  |                                                                |
C  |                            MVPC.FOR                            |
C  |  subroutine of dcecs_.generates positional control outputs for |
C  |  rack,noz. as fnc.of demand input,current operating state,and  |
C  |  if appropriate, scheduled setting from dcecon/getset.this     |
C  |  version uses Multivariable Long-Range Predictive Control of   |
C  |  Engine speed and Boost by rack and nozzle inputs.             |
C  ------------------------------------------------------------------
C
C  last change 080589 JH
C
C  Written : J.Hall  5 May 1989
C  Machine : PC-AT compatibles
C  Code    : Microsoft FORTRAN 77
C
C
       IMPLICIT REAL (A-H,J-Z)
C      ..unless explicitly re-declared below
       IMPLICIT INTEGER(I)
C
       DIMENSION DCE(8),DCEDOT(8)
       REAL H(8,2),PSI(4,2),PSIP(4,2),TH(4,2)
       REAL YPRED(8,2),DYPRED(8,2)
       REAL W(2)
C  variables which change during run
       COMMON /A/  NENG,AENG,NTURB,AFR,PCOMP,PINMAN
       COMMON /E/  FPREV,FPREVA,NOZ,NOZA,TGR,TIM,TIMA
       COMMON /F/  DEMAND,URACK,UNOZ,U3,U4,EFFOLD,EFFNEW,ISS
       COMMON /GAINS/ K1,K2,K3,K4,K5,K6,K7,K8
C
       DATA H(1,1),H(2,1),H(3,1),H(4,1) /.223,.213,.204,.195/
       DATA H(5,1),H(6,1),H(7,1),H(8,1) /.186,.178,.170,.163/
       DATA H(1,2),H(2,2),H(3,2),H(4,2) /.02,.076,.089,.078/
       DATA H(5,2),H(6,2),H(7,2),H(8,2) /.058,.038,.021,.008/
       DATA HTH1,HTH2 /.2965,.0255/
       DATA TH(1,1),TH(2,1),TH(3,1),TH(4,1) /-.956,0.,.223,0./
       DATA TH(1,2),TH(2,2),TH(3,2),TH(4,2) /-1.3,.49,.02,.05/
C  note H(j,i) are impulse response coefficients over j future steps;
C       i=1:Neng/Urack   i=2:Boost/Unoz
C       THeta(i) are identified ARIMA 1st/2nd order model parameters anc
C       PSI(i) are ARIMA states, PSIp are states at the next timestep
C       pred.using ARIMA models, where i=1 are for Ne/Urack model,
C       i=2 are for Boost/Unoz model.
C       HTH is transpose(H).H, precomputed since constant.
C  note demand is 'drivers'feedfwd input (from modes.dat),Noz,tim,tgr a)
C  internally-generated feedfwds (eg for boost or cvt control)
C  note Urack,Unoz,U3,U4 are the controller O/Ps (ie plant ctrl I/Ps)
C
C  ------------------------------------------------------------------
C
C  ---ENGINE SPEED-----------------------------------------------------
C  L520 DCE speed dem.range 0-10v corresp.to 0-(k5*10)rev/min.(Rated
C  speed 2600rpm,min.loaded speed 1000rpm).
       W(1)=K5*DEMAND
C      (speed reference i/p ie setpoint)
C  low idle speed ctrl (idle c.900rpm)
       IF(NENG.LT.900. .AND. W(1).LT.900.) W(1)=900.
C
C  ---BOOST------------------------------------------------------------
C  At Steady-State:
```

```
C      boost pressure for best Effy (scheduled)
C   At Transient:
C   If desired fuelling<abs.max.fuelling limit the above s-s ctrl applies
C   If desired rack ctrl o/p >=abs.max.fuelling,
C      Nozzles are used to keep boost at level reqd for absolute
C      max.engine fuelling, ie 3 bar.
C   NB higher nozzle volts (UNOZ) implies more closure.
C
C     detect transient...NB xreqd is one step behind since rack and
C   nozzle controls are computed together rather than sequentially.
           IF(XREQD.GE.ABMXFL) THEN
C          transient control strategy
             W(2)=3.
           ELSE
C          steady-state control strategy (NOZ is sched.boost pressure)
             W(2)=NOZ
           END IF
C
C   current setpoints W(i) for engine speed and boost computed.
C   ---MULTIVARIABLE CONTROL-----------------------------------------
C
C   future o/p predictions up to horizon l=8, using postulated ctrl.moves
C
C   predns up to model order using ARIMA model directly:
C   update state vector (right-shift old data & introduce latest data)
C   NB here we use ctrl scenario that Urack,Unoz unchanged in future.
C   Speed/Rack ARIMA states are DY1,DU1(j) and PSI(j,1)
           DY1J=NENG-Y1JM1
           DU1JM1=URACK-U1JM1
C   Boost/Nozzles states DY2,DU2(j) and PSI(j,2)
           DY2J=DCE(3)-Y2JM1
           DU2JM1=UNOZ-U2JM1
C   state vectors: first for eng.speed o/p..
           PSI(1,1)=-DY1J
           PSI(3,1)=DU1JM1
           PSI(2,1)=Ø.
           PSI(4,1)=Ø.
C   ..then for boost o/p
           PSI(2,2)=PSI(1,2)
           PSI(1,2)=-DY2J
           PSI(3,2)=Ø.
           PSI(4,2)=DU2JM1
C   update y (o/ps) for next time (will then be Y j-1)
           Y1JM1=NENG
           Y2JM1=DCE(3)
C   predict future o/p moves from current states, and model params
           DO 25 IA=1,2
              DYPRED(1,IA)=Ø.
              DO 2Ø I=1,4
                 DYPRED(1,IA)=DYPRED(1,IA) + PSI(I,IA)*TH(I,IA)
  2Ø          CONTINUE
  25       CONTINUE
C   get o/p position predns from o/p move predns.
           YPRED(1,1)=DYPRED(1,1)+NENG
           YPRED(1,2)=DYPRED(1,2)+DCE(3)
C   construct one-step ahead pred.state vector psip(j,i) from psi(j,i)
C   and dypred(1,i), and postulated future controls (ie moves=Ø.)
           PSIP(1,1)=-DYPRED(1,1)
           PSIP(2,1)=Ø.
C
           PSIP(1,2)=-DYPRED(1,2)
           PSIP(2,2)=-DY2J
C   (note states 3,4 are zero as postulated and are thus not used)
```

```
C  and thus predict 2 step ahead o/p moves using ARIMA models and
C  one step ahead pred.states (NB param.vectors fixed)
        DO 15 IA=1,2
           DYPRED(2,IA)=Ø.
           DO 1Ø I=1,2
              DYPRED(2,IA)=DYPRED(2,IA) + PSIP(I,IA)*TH(I,IA)
  1Ø       CONTINUE
C          the pred.2 step ahead o/p posns are
           YPRED(2,IA)=DYPRED(2,IA)+YPRED(1,IA)
  15    CONTINUE
C
C  predns from >model order up to predn horizon use recursive updates
C  of dy and y in parallel:
        DO 3Ø I=3,8
          DO 35 IA=1,2
            DYPRED(I,IA)=-TH(1,IA)*DYPRED(I-1,IA)-TH(2,IA)*DYPRED(I-2,IA
            YPRED(I,IA) =YPRED(I-1,IA) + DYPRED(I,IA)
  35      CONTINUE
  3Ø    CONTINUE
C  ctrl is min.of predicted cost.Assumptions:
C  i)  future ref.i/ps = current ref.i/ps WNE,WBST
C  ii) MAC/GPC type cost fnc.;k3,k4=control cost weighting factors
C  iii)'control horizon'(GPC concept) =1
C  soln is  H'.(w-ypred)/(H'.H + Beta.I), computed SEPARATELY for each
C  output.
C
C  first compute 2off H.(w-ypred) and  H'.H + Beta.
        SCRA1=HTH1 + K3
        SCRA2=HTH2 + K4
        SCRB1=Ø.
        SCRB2=Ø.
        DO 4Ø I=1,8
           SCRB1=SCRB1 + H(I,1)*( W(1)-YPRED(I,1) )
           SCRB2=SCRB2 + H(I,2)*( W(2)-YPRED(I,2) )
  4Ø    CONTINUE
C
C  record current ctrl posns for next time (will then be U j-1)
        U1JM1=URACK
        U2JM1=UNOZ
C  and comp. next step min.cost (optimal) control moves..
        DU1=SCRB1/SCRA1
        DU2=SCRB2/SCRA2
C  ..and thus new ctrl posns.
        URACK= URACK+ DU1
        UNOZ = UNOZ + DU2
C
C  rack must be within engineering and actuator limits:
C  corresp.fuelling (do limiting this way for compat.with earlier work)
        FPINJ=24.286*(URACK-3.)
        XREQD=FPINJ
C  absolute fuelling limit (2Øbar or 266kW nominally)
        IF(NENG.LE.1946) THEN
           ABMXFL=18Ø.
        ELSE
           ABMXFL=35Ø28Ø./NENG
        END IF
        IF(FPINJ.GT.ABMXFL) FPINJ=ABMXFL
C  smoke limiting (boost based)
        SLMXFL=K7*PCOMP
        IF(FPINJ.GT.SLMXFL) FPINJ=SLMXFL
C  o/s max.speed limiting: limit from 335Ørev/min up, as defined by K6.
        IF(DCE(2).GT.335Ø.) THEN
```

```
            NOSRED=K6*((DCE(2)-335Ø.)**2)
            FPINJ=FPINJ-NOSRED
C           also reduce xreqd to preclude running in trans.ctrl at lim.No
            XREQD=XREQD-NOSRED
         END IF
C
C  equiv.rack posn is
         URACK=3.+FPINJ/24.286
C  actuator limits Ø-1ØV
         IF(URACK.GT.1Ø.) THEN
            URACK=1Ø.
         ELSE IF(URACK.LT.Ø.) THEN
            URACK=Ø.
         END IF
C  nozzle ctrl limits are Ø-1ØV (actuator saturation)
         IF(UNOZ.GT.1Ø.) THEN
            UNOZ=1Ø.
         ELSE IF(UNOZ.LT.Ø.) THEN
            UNOZ=Ø.
         END IF
C
C  ------------------------------------------------------------------
C  ---TIMING CONTROL-------------------------------------------------
C  optimum st.state static timing [Volts] is TIM (fr.common block)
         U3=TIM
C
C  ---CVT and BYPASS CONTROL not used--------------------------------
C        U4=Ø.
C
         RETURN
         END
```

OPTICA.FOR

subroutine of dcecon. generates control settings for DCE at steady-state to optimise BSFC within engineering limits. a heuristic method is used, in this case an adaptive step size random search, varying nozzle angle and injection timing (fixed turbine gear ratio).

last change 131087 JH

Written : J.Hall Sep.1987

Machine : DEC LSI11/23
Code : Fortran IV

Subroutine description

OPTIC(A) takes current operating params from common block and from dynamic state array 'DCE', and generates trial moves of turbine noz. angle and inj.timing to optimise o/s brk.th.effy. it is called by dcecon during periods of operation which are nominally steady-state. the trial moves are slew rate-limited to be more realistic, however, the dynamics of typical actuators are not modelled below these limits.

```
      SUBROUTINE OPTIC(DCE,DCEDOT,ICALL,NCSS,NLSS,PVOLSS,DT)

      IMPLICIT REAL (A-H,J-Z)
      IMPLICIT INTEGER(I)

      DIMENSION DCE(4),DCEDOT(4)
      DIMENSION VEC0(2),VEC1(2),VECY(2),VECS(2) !elements nozang,timing

      COMMON NENG,AENG,NTURB,AFR,PCOMP,PINMAN
      COMMON TQENG,TQANN,TQSUN,TQPC,TQCOMP,TQTURB,TQLOAD,TQOUT
      COMMON MCOMP,MINMAN,MFUEL,MTURB
      COMMON TINMAN,TEXMAN,TCOMP,TVOL,TVODOT
      COMMON FPREV,FPREVA,NOZ,NOZA,TGR,TIM,TIMA
      COMMON DEMAND,EFFOLD,EFFNEW,ISS

      COMMON PATM,TATM,TCOOL
      COMMON JENG,JCOMP,JLOAD
      COMMON KTQC,KMC,KMINMA,KMF,KTQE,KFRIC,KBYPAS
      COMMON EFCOMP,EFTURB,EFCOOL
      COMMON CP,R,GAMMA
      COMMON CGR,OGR
      COMMON VOLUME,AREABY,TQSTAT,FPREVM
      COMMON MTARR(6),VFCARR(4,13),WCARR(4,13)
      COMMON K1,K2,K3

      KS=0.618 !success step size scale factor---WAS 1.618---
      KF=0.618 !failure ---------- " ----------
      KL=0.2   !step size factor-----------------WAS 0.4-----
      IMAX=6   !max no of failed trial moves before step size is reduced
```

```
C
      CALVAL=42500.  !kJ/kg
C
C     set reasonable actuator slew rate limits(tho' no control
C     dynamics included).nozzle 20V/s,timing 20V/s.maxm moves are thus
      DNOZ=100.*DT
      DTIM=100.*DT
C
C  check whether first call
C
      IF(ICALL.EQ.1) GOTO 10
      IF(ICALL.GT.1) GOTO 20
 10   CONTINUE      !ICALL=1 statements
        EFFNEW=.006283*DCE(2)*TQOUT/(MFUEL*CALVAL) !baseline
        INCOM=0
        GOTO 42
C
C  not first call-was previous move complete or slewrate-limited?
C
 20   CONTINUE      !ICALL>1 statements
        IF(INCOM.EQ.1) GOTO 34
        IF(INCOM.EQ.0) CONTINUE
C
C  check whether DCE has stabilised (def.by 3 dyn.state variables)
C
        ISTAB=1
        IF(ABS(DCEDOT(1)).GT.NCSS) ISTAB=0
        IF(ABS(DCEDOT(2)).GT.NLSS) ISTAB=0
        IF(ABS(DCEDOT(3)).GT.PVOLSS) ISTAB=0
C
C  take appropriate action
C
        IF(ISTAB.EQ.0) GOTO 90   !return same settings until stable
        IF(ISTAB.EQ.1) CONTINUE
C
C  now have fully-made last move,and stable DCE. execute the
C  adap.step-size random search algorithm
C
      EFFOLD=EFFNEW
      EFFNEW=.006283*DCE(2)*TQOUT/(MFUEL*CALVAL)
      GOTO 40
C
C
 42   CONTINUE
        VECO(1)=NOZ
        VECO(2)=TIM
C       (no tgr control)
 25     CONTINUE !generate random vector for trial move
        VECS(1)=RAN(IRAND1,IRAND2)
        VECS(2)=RAN(IRAND1,IRAND2)
C       randomise the sign (+/-)
        SGN1=RAN(IRS1,IRS2)
        SGN2=RAN(IRS1,IRS2)
C       normalise to a unity ampl.vector
        SCRAT1=VECS(1)*VECS(1)
        SCRAT2=VECS(2)*VECS(2) + SCRAT1
        SCRAT1=SQRT(SCRAT2)
        VECS(1)=VECS(1)/SCRAT1
        VECS(2)=VECS(2)/SCRAT1
C       impose signs from above
        IF(SGN1.LT.0.5) VECS(1)=-VECS(1)
        IF(SGN2.LT.0.5) VECS(2)=-VECS(2)
C
        VEC1(1)=VECO(1)+KL*VECS(1)
        VEC1(2)=VECO(2)+KL*VECS(2)
```

```
30          CONTINUE
            generate trial vector
            VECY(1)=VECO(1)+KS*(VEC1(1)-VECO(1))
            VECY(2)=VECO(2)+KS*(VEC1(2)-VECO(2))
            check vector within bounds of actuation/engineering limits
            IF(VECY(1).GT.10..OR.VECY(1).LT.0.) GOTO 50 !nozzle [Volts]
            IF(VECY(2).GT.10..OR.VECY(2).LT.0.) GOTO 50 !timing [Volts]
            assign to controls
            NOZTRY=VECY(1)
            TIMTRY=VECY(2)
            TGR=14.67
34        CONTINUE !jump here if prev.trial move was incomplete

            check moves against slew rate limits calc. above
            in each case flag if trial move incomplete this time
            INCON=0
            INCOT=0
            INCOM=0
            IF((NOZTRY-NOZ).GT.DNOZ.OR.(NOZ-NOZTRY).GT.DNOZ) INCON=1
            IF((TIMTRY-TIM).GT.DTIM.OR.(TIM-TIMTRY).GT.DTIM) INCOT=1
            if slew lims not exceeded set noz=noztry etc
            IF(INCON.EQ.0) NOZ=NOZTRY
            IF(INCOT.EQ.0) TIM=TIMTRY
            IF(INCON.EQ.1.OR.INCOT.EQ.1) INCOM=1
            IF((NOZTRY-NOZ).GT.DNOZ) NOZ=NOZ+DNOZ
            IF((NOZ-NOZTRY).GT.DNOZ) NOZ=NOZ-DNOZ
            IF((TIMTRY-TIM).GT.DTIM) TIM=TIM+DTIM
            IF((TIM-TIMTRY).GT.DTIM) TIM=TIM-DTIM



            GOTO 90 !return to dcecon with these settings

40        CONTINUE !optic previously active-has BSFC results to compare

            IF(EFFNEW.GT.EFFOLD) GOTO 44
            IF(EFFNEW.LE.EFFOLD) GOTO 46
44          CONTINUE
            IFAILS=0 !reset failure counter
            KL=KS*KL !increase step size
            VEC1(1)=VECY(1)
            VEC1(2)=VECY(2)
            GOTO 30
46          CONTINUE
            IFAILS=IFAILS+1
50          IF(IFAILS.GT.IMAX) KL=KF*KL !reduce step size
            IF(IFAILS.GT.IMAX) IFAILS=0 !reset failure counter
          GOTO 25

90        RETURN
          END
```

```
C  ------------------------------------------------------------
C  |                                                          |
C  |                        OPTICB.FOR                        |
C  |  subroutine of dcecon.generates control settings for DCE |
C  |  at steady-state to optimise BSFC within engineering     |
C  |  limits. a heuristic method is used, in this case a      |
C  |  binary step hill-climbing search,varying nozzle angle   |
C  |  and injection timing (fixed turbine gear ratio).        |
C  |                                                          |
C  ------------------------------------------------------------
C
C  last change 151087 JH
C
C  Written : J.Hall  Oct.1987
C  Machine : DEC LSI11/23
C  Code    : Fortran IV
C
C  Subroutine description
C  ----------------------
C  OPTIC(B) takes current operating params from common block and from
C  dynamic state array 'DCE',and generates trial moves of turbine noz.
C  angle and inj.timing to optimise o/s brk.th.effy. it is called by
C  dcecon during periods of operation which are nominally steady-state.
C  the trial moves are slew rate-limited to be more realistic,however,
C  the dynamics of typical actuators are not modelled below these limits.
C
C
      SUBROUTINE OPTIC(DCE,DCEDOT,ICALL,NCSS,NLSS,PVOLSS,DT)
C
      IMPLICIT REAL (A-H,J-Z)
      IMPLICIT INTEGER(I)
C
      DIMENSION DCE(4),DCEDOT(4)
C
      COMMON NENG,AENG,NTURB,AFR,PCOMP,PINMAN
      COMMON TQENG,TQANN,TQSUN,TQPC,TQCOMP,TQTURB,TQLOAD,TQOUT
      COMMON MCOMP,MINMAN,MFUEL,MTURB
      COMMON TINMAN,TEXMAN,TCOMP,TVOL,TVODOT
      COMMON FPREV,FPREVA,NOZ,NOZA,TGR,TIM,TIMA
      COMMON DEMAND,EFFOLD,EFFNEW,ISS
C
      COMMON PATM,TATM,TCOOL
      COMMON JENG,JCOMP,JLOAD
      COMMON KTQC,KMC,KMINMA,KMF,KTQE,KFRIC,KBYPAS
      COMMON EFCOMP,EFTURB,EFCOOL
      COMMON CP,R,GAMMA
      COMMON CGR,OGR
      COMMON VOLUME,AREABY,TQSTAT,FPREVM
      COMMON MTARR(6),VFCARR(4,13),WCARR(4,13)
      COMMON K1,K2,K3
C
C     set reasonable actuator slew rate limits(tho' no control
C     dynamics included).nozzle 20V/s,timing 20V/s.maxm moves are thus
      DNOZMX=100.*DT
      DTIMMX=100.*DT
C
C  set up step sizes
      KB=.8 !base step size=8% of range(0-10V)-same for both variables
      KR=-.5 !halve step size & reverse dirn if sfc gets worse
      KM=KB/8.  !min size;allows 3 reversals before tries next variable
C
C  check whether first call
      IF(ICALL.GT.1) GOTO 20
 30   CONTINUE      !ICALL=1 statements
      INCOM=0
      EFFNEW=DCE(2)*TQOUT/MFUEL
      IVAR=1
 40   CONTINUE
```

```
        KC=KB !initialise step size
        IF(IVAR.EQ.1) NOZD=NOZ+KC
        IF(IVAR.EQ.2) TIMD=TIM+KC
C  constrain this initial step within range of actuation,but if exceeds
C  take no other action. note 1st step +ve,so can only go >10V,never <0V.
        IF(NOZD.GT.10.) NOZD=10.
        IF(TIMD.GT.10.) TIMD=10.
        GOTO 90
C
 20     CONTINUE      !ICALL>1 statements
        IF(INCOM.EQ.1) GOTO 90
C  check whether DCE stable
        ISTAB=1
        IF(ABS(DCEDOT(1)).GT.NCSS) ISTAB=0
        IF(ABS(DCEDOT(2)).GT.NLSS) ISTAB=0
        IF(ABS(DCEDOT(3)).GT.PVOLSS) ISTAB=0
        IF(ISTAB.EQ.0) GOTO 100  !return same settings until stable
        EFFOLD=EFFNEW
        EFFNEW=DCE(2)*TDOUT/MFUEL
C  last move complete-compare sfc s
        IF(EFFNEW.LT.EFFOLD) GOTO 70
C  otherwise make same step again
        IF(IVAR.EQ.1) NOZD=NOZ+KC
        IF(IVAR.EQ.2) TIMD=TIM+KC
C  check set pt within limits
        IF(NOZD.GT.10..OR.NOZD.LT.0.) GOTO 70
        IF(TIMD.GT.10..OR.TIMD.LT.0.) GOTO 70
        GOTO 90
C
 70     CONTINUE
        KC=KC*KR
        IF(ABS(KC).LT.KM) GOTO 80 !step size reduced to limit
        IF(IVAR.EQ.1) NOZD=NOZ+KC
        IF(IVAR.EQ.2) TIMD=TIM+KC
        GOTO 90
C
 80     CONTINUE
        IVAR=IVAR+1           !change variable
        IF(IVAR.EQ.3) IVAR=1 !just two variables controlled
        GOTO 40
C
C  limit slew rates
C
 90     CONTINUE
        INCON=0
        INCOT=0
        INCOM=0
        DNOZ=NOZD-NOZ
        DTIM=TIMD-TIM
        IF(ABS(DNOZ).GT.DNOZMX) INCON=1
        IF(ABS(DTIM).GT.DTIMMX) INCOT=1
C       if slew lims not exceeded set noz=nozd etc
        IF(INCON.EQ.0) NOZ=NOZD
        IF(INCOT.EQ.0) TIM=TIMD
C       if slew lims exceeded set move=maxm,and flag INCOMplete move
        IF(INCON.EQ.1.OR.INCOT.EQ.1) INCOM=1
        IF(DNOZ.GT.DNOZMX) NOZ=NOZ+DNOZMX
        IF(DNOZ.LT.-DNOZMX) NOZ=NOZ-DNOZMX
        IF(DTIM.GT.DTIMMX) TIM=TIM+DTIMMX
        IF(DTIM.LT.-DTIMMX) TIM=TIM-DTIMMX
C
 100    RETURN
        END
```

```
      IF(IY.EQ.IYSIZE) IYY=IYSIZE
C  look up settings
      NOZ1=NOZSCH(IX,IY)
      NOZ2=NOZSCH(IXX,IY)
      TIM1=TIMSCH(IX,IY)
      TIM2=TIMSCH(IXX,IY)
      TGR1=TGRSCH(IX,IY)
      TGR2=TGRSCH(IXX,IY)
C  lin.intrpln
      NOZ3=NOZ1+(NOZ2-NOZ1)*XREM
      TIM3=TIM1+(TIM2-TIM1)*XREM
      TGR3=TGR1+(TGR2-TGR1)*XREM
C  lin intrpln at next pt in array
      NOZ1=NOZSCH(IX,IYY)
      NOZ2=NOZSCH(IXX,IYY)
      TIM1=TIMSCH(IX,IYY)
      TIM2=TIMSCH(IXX,IYY)
      TGR1=TGRSCH(IX,IYY)
      TGR2=TGRSCH(IXX,IYY)
      NOZ4=NOZ1+(NOZ2-NOZ1)*XREM
      TIM4=TIM1+(TIM2-TIM1)*XREM
      TGR4=TGR1+(TGR2-TGR1)*XREM
C  lin intrp between two intrp pts
      NOZ=NOZ3+(NOZ4-NOZ3)*YREM
      TIM=TIM3+(TIM4-TIM3)*YREM
      TGR=TGR3+(TGR4-TGR3)*YREM
C  NB! noz need not be simply noz.posn. setting-could be eg boost
C  setting or comp.speed setting. pass back to dcecon
      RETURN
      END
```

PART 7

```
      REAL FUNCTION RITRP1(XNORM,YARR,ISIZE)
C
C  ---------------------------------------------------------------
C  RITRPS - 1D,2D interpolation functions concatenated into one file
C  ---------------------------------------------------------------
C  1-D INTERPOLATION FUNCTION
C  given XNORM this routine returns a value for Y from the
C  array YARR. XNORM is X normalised to a real number on
C  the same scale as the array indices.Y and YARR are of
C  type REAL.
C
      IMPLICIT REAL (A-H,J-Z)
      IMPLICIT INTEGER (I)
      DIMENSION YARR(ISIZE)
C
C     ! integer part of XNORM
      IXINT=INT(XNORM)
C
C     ! fractional part of XNORM
      XFRAC=ABS(XNORM-IXINT)
      Y1=YARR(IXINT)
      Y2=YARR(IXINT+1)
C
C     ! linear interpolation
      RITRP1=Y1+(Y2-Y1)*XFRAC

      RETURN
      END

    FUNCTION  RITRP2(XNORM,YNORM,ZARR,IXSIZE,IYSIZE)
C
C  2-D INTERPOLATION FUNCTION
C  given X and Y values this routine returns a value for Z from
C  the 2-D array ZARRAY. X and Y must be normalised to real
C  numbers on the same scale as the array indices.
C  2-D interpolation is achieved by doing three 1-D interpolations

      IMPLICIT REAL (A-H,J-Z)
      IMPLICIT INTEGER (I)
      DIMENSION ZARR(IXSIZE,IYSIZE)
C
C     ! integer part of XNORM
      IXINT=INT(XNORM)
C
C     ! fractional part of XNORM
      XFRAC=ABS(XNORM-IXINT)
      IYINT=INT(YNORM)
      YFRAC=ABS(YNORM-IYINT)

C  first 1-D interpolation, keeping Y constant
      Z1=ZARR(IXINT,IYINT)
      Z2=ZARR(IXINT+1,IYINT)
C
C     ! linear interpolation
      Z3=Z1+(Z2-Z1)*XFRAC
C  second 1-D interpolation, keeping Y constant
      Z1=ZARR(IXINT,IYINT+1)
      Z2=ZARR(IXINT+1,IYINT+1)
      Z4=Z1+(Z2-Z1)*XFRAC
C  final 1-D interpolation, keeping X constant
      RITRP2=Z3+(Z4-Z3)*YFRAC

      RETURN
      END
```

PART 8.

```
      SUBROUTINE VEHICL(NLOAD,GRADE,BRAKES,GVW,CDA,KTYRE,RAXRAT,
     +                  TYRDIA,WNDSPD,TQLOAD)
C
C  ---------------------------------------------------------------
C  |                                                             |
C  |                        VEHICL.FOR                           |
C  |  subroutine of dcecon.calculates load torque for current    |
C  |  road speed and conditions with given vehicle data          |
C  |                                                             |
C  ---------------------------------------------------------------
C
C  last change 230987 JH
C
C  Written : J.Hall  Sep.1987
C  Machine : DEC LSI11/23
C  Code    : Fortran IV
C  ported to PC-AT/Microsoft FORTRAN v.4.1 Dec.88
C
C  Subroutine description
C  ----------------------
C  VEHICL takes vehicle/road data via dcecon from input file truck.dat.
C  calculates the tractive effort at the current road speed and convert
C  this to a load torque at the output shaft.
C  The tractive effort comprises aero.drag,tyre drag and gradient force
C  in addition,braking is simply included as an extra tractive drag.
C
C
      IMPLICIT REAL(A-H,J-Z)
      IMPLICIT INTEGER(I)
C
C     calc road speed from current nload  [m/s]
C
      SPEED=0.05236*NLOAD*TYRDIA/RAXRAT
C
C     aerodynamic drag  [N]
C
      EAERO=0.6125*CDA*(SPEED+WNDSPD)*(SPEED+WNDSPD)
C
C  tyre drag(based on SAE J688-1986 handbook)rolling resistance coeff
C  Cr=C1+C2.v where C1=.0076[-],C2=.0002014[s/m].(Efr=m.g.Cr.ktyre).
C  NB no allowance for effect of no.of axles on drag in this correln.
C  Tyre drag/[N]:
C
      ETYRE=(.0746+.00197*SPEED)*KTYRE*GVW
C
C  climbing force(note grade in % = 100 x sin(angle to horiz.))
C
      EGRD=.0981*GVW*GRADE
C
C  total tractive effort (including wheel braking forces) is then
C
      EFFORT=EAERO+ETYRE+EGRD+BRAKES
C
C  convert to equiv.torque at output shaft,ass. 0.95 final drv.effy
C
      TQLOAD=EFFORT*TYRDIA*.5/(RAXRAT*.95)
C
      RETURN
      END
```

PART 9

```
      SUBROUTINE WRITOP(TIME,DIST,DCE,DCEDOT)
```

```
                          WRITOP.FOR
    subroutine of dcecon.writes current data to log array
```

```
last change 220688 JH

Written : J.Hall  Sep.1987
Machine : DEC LSI11/23
Code    : Fortran IV
Transfer: to PC-AT compatibles and FORTRAN77 Dec88
Subroutine description
----------------------
WRITOP takes various data from common block, and puts it in data
log array RECORD along with current time/distance covered and
current dynamic state of the rig (DCE,DCEDOT).

      !unless exlicitly re-declared below
      IMPLICIT REAL (A-H,J-Z)
      IMPLICIT INTEGER(I)
      INTEGER  ISTORE,NMODES,RUNTYP

      DIMENSION RECORD(40,350),DUTARR(20,4)
      DIMENSION DCE(8),DCEDOT(8)
      variables which change during run
      COMMON /A/  NENG,AENG,NTURB,AFR,PCOMP,PINMAN
      COMMON /B/  TQENG,TQANN,TQSUN,TQPC,TQCOMP,TQTURB,TQLOAD,TQOUT
      COMMON /C/  MCOMP,MINMAN,MFUEL,MTURB
      COMMON /D/  TINMAN,TEXMAN,TCOMP,TVOL,TVODOT
      COMMON /E/  FPREV,FPREVA,NOZ,NOZA,TGR;TIM,TIMA
      COMMON /F/  DEMAND,URACK,UNOZ,U3,U4,EFFOLD,EFFNEW,ISS
      COMMON /OUT/ RECORD,DUTARR,DT,ISTORE,NMODES,RUNTYP
      COMMON /MAX/ TORMAX,PRMAX,MASMAX,NMAX,NCMAX,NTMAX

      !MJ/kg as in dcecon
      CALVAL=42500.

      TORMAX = MAX (TQOUT,TQENG,TORMAX)
      PRMAX  = MAX (PCOMP,PRMAX)
      MASMAX = MAX (MINMAN,MCOMP,MASMAX)
      NMAX   = MAX (DCE(2),NENG,NMAX)
      NCMAX  = MAX (DCE(1),NCMAX)
      NTMAX  = MAX (DCE(2)*TGR,NTMAX)

      RECORD(1,ISTORE)=DEMAND
      RECORD(2,ISTORE)=TQLOAD
      RECORD(3,ISTORE)=DCE(1)
      RECORD(4,ISTORE)=DCE(2)
      RECORD(5,ISTORE)=DCE(3)
      RECORD(6,ISTORE)=MTURB * 60.
      RECORD(7,ISTORE)=DCEDOT(1)
      RECORD(8,ISTORE)=DCEDOT(2)
      RECORD(9,ISTORE)=DCEDOT(3)
      RECORD(10,ISTORE)=NOZ
      RECORD(11,ISTORE)=NOZA
      RECORD(12,ISTORE)=PINMAN * 1.E-5
      RECORD(13,ISTORE)=TIM
      RECORD(14,ISTORE)=TIMA
      RECORD(15,ISTORE)=TGR
      RECORD(16,ISTORE)=FPREVA
```

```
        RECORD(17,ISTORE)=NENG
        RECORD(18,ISTORE)=AENG
C  get true turbine speed-Nturb is non-dim.
        TURBSP=DCE(2)*TGR
        RECORD(19,ISTORE)=TURBSP
        IF(AFR.LE.100.) THEN
           RECORD(20,ISTORE)=AFR
        ELSE
           RECORD(20,ISTORE)=100.
        END IF
        RECORD(21,ISTORE)=TQENG
        RECORD(22,ISTORE)=TQOUT
        RECORD(23,ISTORE)=TEXMAN
        IF(TQOUT.NE.0. .AND. MFUEL.NE.0.) THEN
           RECORD(24,ISTORE)=.006283 * DCE(2) * TQOUT / (MFUEL*CALVAL)
        ELSE
           RECORD(24,ISTORE)=100.
        END IF
        RECORD(25,ISTORE)=MFUEL * 60.
        RECORD(26,ISTORE)=TIME
        RECORD(27,ISTORE)=DIST
        RECORD(28,ISTORE)=MCOMP * 60.
C
C       calc.bypass flow (not explicitly passed in common block)
C
        MBYPAS=MCOMP-MINMAN
C
        RECORD(29,ISTORE)=MBYPAS * 60.
        RECORD(30,ISTORE)=DCE(4)
        RECORD(31,ISTORE)=URACK
        RECORD(32,ISTORE)=DCE(6)
        RECORD(33,ISTORE)=UNOZ
        RECORD(34,ISTORE)=U4
        RECORD(35,ISTORE)=PCOMP
        RECORD(36,ISTORE)=MINMAN * 60.
        RECORD(37,ISTORE)=TQTURB
C
      WRITE(*, 601) ISTORE
601   FORMAT(//' data logged for record number',I4)
C
        RETURN
        END
```

```
      SUBROUTINE PROUT
C  ------------------------------------------------------------------
C  :                                                                :
C  :                          PROUTB.FOR                            :
C  :     subroutine of dcecon.prints data log compactly to file     :
C  :                                                                :
C  ------------------------------------------------------------------
C
C  last change: 310389 JH
C
C  Written: J.Hall  Oct.1987
C  Modified T.Roelle for compatibility with plotting software
C  Machine: PC-AT compatibles
C  Code   : FORTRAN 77
C
C  Subroutine description
C  ----------------------
C  PROUT takes arrays of the simulation duty cycle,the run parameters eg
C  control loop gains,integration timestep etc.,and the record of data
C  through the simulation run, then writes required data to output file.
C-----------------------------------------------------------------------
C
C     STATEMENTS CONCERNING VARIABLE DECLARATION
C     ==========================================
C
      COMMON /OUT/    RECORD,DUTARR,DT,ISTORE,NMODES,RUNTYP
      COMMON /PU/     PARMON,IMON
      COMMON /CHARS/ FILE
C
      REAL       RECORD(40,350),DUTARR(20,4),DT
      REAL       PARMON(4,120)
      INTEGER    IMON
      INTEGER    ISTORE,NMODES,RUNTYP,N
      CHARACTER FILE*11,NFILE*11
C
C     DETERMINATION AND INSTALLATION OF THE OUTPUT FILE, DEFAULT NAME
C     ===============================================================
C     IS SIMOUT.DAT
C     =============
C
      FILE = 'SIMOUT.DAT'
      WRITE  (*, 1000)
      READ   (*, 2000) NFILE
      IF     (NFILE .NE. ' ') FILE = NFILE
      WRITE  (*, 3000) FILE
      OPEN   (UNIT=8, FILE=FILE)
C
C     WRITING OF FIRST SHEET
C     ======================
C
      CALL HEADER
      WRITE  (8,4000)
      DO 20  N = 1,ISTORE
             WRITE (8,5000) N, RECORD(4,N),RECORD(17,N),RECORD(3,N),
     +                         RECORD(19,N),RECORD(8,N),RECORD(18,N)
20    CONTINUE
      WRITE  (8,6000)
      WRITE  (8,*) CHAR(12)
C
C     WRITING OF SECOND SHEET
C     =======================
C
```

```
      CALL HEADER
      WRITE  (8,7000)
      DO 30  N = 1,ISTORE
             WRITE (8,8000) N, RECORD(2,N),RECORD(22,N),RECORD(21,N),
     +                         RECORD(26,N),RECORD(27,N),RECORD(20,N)
30    CONTINUE
      WRITE  (8,6000)
      WRITE  (8,*) CHAR(12)
C
C     WRITING OF THIRD SHEET
C     ======================
C
      CALL HEADER
      WRITE (8,9000)
      DO 40  N = 1,ISTORE
             WRITE (8,10000) N, RECORD(36,N),RECORD(28,N),RECORD(6,N),
     +                         RECORD(29,N),RECORD(25,N),RECORD(7,N)
40    CONTINUE
      WRITE  (8,6000)
      WRITE  (8,*) CHAR(12)
C
C     WRITING OF FOURTH SHEET
C     =======================
C
      CALL HEADER
      WRITE (8,11000)
      DO 50  N = 1,ISTORE
             WRITE (8,12000) N, RECORD(5,N),RECORD(9,N),RECORD(35,N),
     +                         RECORD(12,N),RECORD(23,N),RECORD(24,N)
50    CONTINUE
      WRITE  (8,6000)
      WRITE  (8,*) CHAR(12)
C
C     WRITING OF THE FIFTH SHEET
C     ==========================
C
      CALL HEADER
      WRITE (8,13000)
      DO 60  N = 1,ISTORE
             WRITE (8,14000) N, RECORD(10,N),RECORD(11,N),RECORD(13,N),
     +                         RECORD(15,N),RECORD(32,N),RECORD(33,N)
60    CONTINUE
      WRITE  (8,6000)
      WRITE  (8,*) CHAR(12)
C
C     WRITING OF THE SIXTH SHEET
C     ==========================
C
      CALL HEADER
      WRITE (8,15000)
      DO 70  N = 1,ISTORE
             WRITE (8,16000) N, RECORD(14,N),RECORD(16,N),RECORD(30,N),
     +                         RECORD(31,N),RECORD(34,N),RECORD(1,N)
70    CONTINUE
      WRITE  (8,6000)
      WRITE  (8,*) CHAR(12)
C
      CLOSE (UNIT=8, STATUS='KEEP')
      WRITE  (*,17000)
C
1000  FORMAT (//,3X,'ENTER FILENAME IF NEW OUTPUT FILE IS DESIRED',
     +         ' (DEFAULT : SIMOUT.DAT)')
2000  FORMAT (A10)
```

```
3000  FORMAT (//,3X,'  THE OUTPUT FILE IS : ',A11)
4000  FORMAT (1X,'STEP',' OS SPEED',' ENG SPEED',' COMP SPEED',
     +                ' TURB SPEED',' OS ACCEL',' ENG ACCEL',/,
     +             5X,'  REV/MIN','  REV/MIN','  REV/MIN',
     +                '  REV/MIN',' REV/MIN/S',' REV/MIN/S')
5000  FORMAT (2X,I3,4(6X,F6.0),2(6X,F6.1))
6000  FORMAT (/////)
7000  FORMAT (1X,'STEP',' LOAD TORQUE',' OS TORQUE',' ENG TORQUE',
     +                ' ELAPS TIME',' DISTANCE',' A/F RATIO',/,
     +             5X,'       NM','       NM','       NM',
     +                '        S','        M','      [-]')
8000  FORMAT (2X,I3,3(7X,F5.0),3(6X,F6.1))
9000  FORMAT (1X,'STEP',' ENG MASSFL',' COMP MASSFL',' TURB MASSFL',
     +                ' BYP MASSFL',' FUEL MASSFL',' COMP ACCEL',/,
     +             5X,'     KG/H','     KG/H','     KG/H',
     +                '     KG/H','     KG/H',' REV/MIN/S')
10000 FORMAT (2X,I3,6(5X,F7.1))
11000 FORMAT (1X,'STEP','   PR VOL',' PR VOL DOT','   PR COMP',
     +                ' PR IN MANIF',' T OUT MANIF',' OS BR EFF',/,
     +             5X,'       BAR','      BAR/S','       BAR',
     +                '       BAR','         K','       [-]')
12000 FORMAT (2X,I3,4(6X,F6.3),7X,F5.1,7X,F5.3)
13000 FORMAT (1X,'STEP',' SCH FF NOZ',' NOZ ANGLE',' SCHED TIM',
     +                ' SCH FF TGR',' NOZZLE POS',' NOZ CONTR',/,
     +             5X,'       [-]','   DEGREES','       V',
     +                '       [-]','         V','       V')
14000 FORMAT (2X,I3,6(3X,F9.3))
15000 FORMAT (1X,'STEP','       SNL',' Q INJ/REV','  RACK POS',
     +                ' RACK C POS',' CONTR IP U4','    DEMAND',/,
     +             5X,'   MS BTDC',' KG E-4/REV','       V',
     +                '         V','         V','       V')
16000 FORMAT (2X,I3,6(5X,F7.3))
17000 FORMAT (//,3X,'THE OUTPUT FILE IS COMPLETE')
C ------------------------------------------------------------------
C --ADDITIONAL SECTION TO WRITE PARAMETER ESTIMATE HISTORY TO DISK---
C ------------------------------------------------------------------
C Written: JH 310389
      OPEN(UNIT=8,FILE='PEST  .DAT')
      WRITE(8,900)
900   FORMAT(/,9X,' PARAMETER ESTIMATE HISTORY',/)
      DO 901 I=1,IMON
        WRITE(8,902) PARMON(1,I),PARMON(2,I),PARMON(3,1),PARMON(4,I)
901   CONTINUE
902   FORMAT(2X,' a1:',G10.3,' a2:',G10.3,' b1:',G10.3,' b2:',G10.3)
      CLOSE(UNIT=8,SATUS='KEEP')
C
      RETURN
      END

      SUBROUTINE HEADER
C
C     WRITES THE HEADER WITH THE BASIC DATA OF A SIMULATION RUN
C     =========================================================
C     ON TOP OF EVERY SHEET OF THE OUTPRINT - CALLED BY PROUT
C     =======================================================
C
      COMMON /GAINS/ K1,K2,K3,K4,K5,K6,K7,K8
      COMMON /OUT/   RECORD,DUTARR,DT,ISTORE,NMODES,RUNTYP
C
      REAL    K1,K2,K3,K4,K5,K6,K7,K8,RECORD(40,350),DUTARR(20,4),DT
      INTEGER I,J,ISTORE,NMODES,RUNTYP
C
```

```
      WRITE  (8,1000)
      IF (RUNTYP.EQ.0) THEN
              WRITE  (8,2000)
                  ELSE
                  WRITE  (8,3000)
      END IF
      WRITE  (8,4000)
C
      DO 10 I=1,NMODES
              WRITE(8,5000) I,(DUTARR(I,J),J=1,4)
10    CONTINUE
C
      WRITE  (8,6000) K1,K2,K3,K4
      WRITE  (8,7000) K5,K6,K7,K8
      WRITE  (8,8000) DT
C
1000  FORMAT (///,15X,'DCE SIMULATION RESULTS',/,15X,22('='))
2000  FORMAT (/,1X,' DYNAMOMETER SIMULATION')
3000  FORMAT (/,1X,' VEHICLE SIMULATION')
4000  FORMAT (1X,' DUTY CICLE FROM FILE MODES.DAT:',/)
5000  FORMAT (1X,' MODE:',I2,': DEM.:',G10.4,'TQLOAD/GRD:',G11.4,
     +         'RUNTIM/LEN:',G8.2,'BRKS:',G7.1)
6000  FORMAT (/,1X,' CONTROL LOOP GAINS: K1=',G11.4,',K2=',G11.4,
     +         ',K3=',G11.4,',K4=',G11.4)
7000  FORMAT (1X,' CONTRAL LOOP GAINS: K5=',G11.4,',K6=',G11.4,
     +         ',K7=',G11.4,',K8=',G11.4)
8000  FORMAT (/,1X,' INTEGRATION TIMESTEP: ',G11.4,' [SEC]')
C
      RETURN
      END
```

APPENDIX 4
PART II

DCEMOD.DAT - system model data & control gains

DCECS- DATA FILE - Leyland 520 DCE

TURBINE CHARACTERISTIC :- non-dimensional massflow vs. pressure ratio

pressure ratio					
0.0	.25	.50	.75	1.0	1.25
massflow (kg/min)*(deg.K**.5)/(bar)					
0.0	23.1	31.0	34.4	36.4	37.4

COMPRESSOR CHARACTERISTICS (CompAir data)

volume flow FAD [cu.ft./min.]

	speed			
press. ratio	-200	4600	9400	14200
-.0343	-72.5	687.5	1447.5	2207.5
.3105	-82.5	670.	1422.5	2175.
.6553	-92.5	652.5	1397.5	2142.5
1.0001	-102.5	635.	1372.5	2110.
1.3449	-112.5	617.5	1347.5	2077.5
1.6897	-122.5	600.	1322.5	2045.
2.0345	-132.5	582.5	1297.5	2012.5
2.3793	-127.5	580.	1287.5	1995.
2.7241	-145.	570.	1285.	2000.
3.0689	-140.	567.5	1275.	1982.5
3.4137	-152.5	557.5	1267.5	1977.5
3.7585	-165.	547.5	1260.	1972.5
4.1033	-177.5	537.5	1252.5	1967.5

compressor power consumption in horse power

	speed			
press. ratio	-200	4600	9400	14200
-.0343	-11.	-15.	-19.	-23.
.3105	-10.	-5.	0.	5.
.6553	-9.	5.	19.	33.
1.0001	-8.	15.	38.	61.
1.3449	-7.	25.	57.	89.
1.6897	-6.	35.	76.	117.
2.0345	-5.	45.	95.	145.
2.3793	-3.5	52.5	108.5	164.5
2.7241	-7.	62.	131.	200.
3.0689	-4.5	66.	136.5	207.
3.4137	2.5	80.5	158.5	236.5
3.7585	9.5	95.	180.5	266.
4.1033	16.5	109.5	202.5	295.5

factors for linearised models

KTQC	KMC	KMINMA	KMF	KTQE	KFRIC	KBYPAS
32.	0.0045	1.315	1.E-4	295.	0.040	2.1

CONT'D/

APPENDIX 4
PART II

/CONT'D.

efficiencies (turbine:peak efficiency)

EFCOMP	EFTURB	EFCOOL
0.70	0.80	0.80

gear ratios

CGR	OGR
8.798	1.841

inertias in kgm2 - JOS re-calc if vehicle sim., JTURB ref.to turb.

JCOMP	JTURB	JANN	JOIPC	JOS
0.18013	8.71E-3	0.1353	0.1561	14.

gas properties

CP	R	GAMMA
1.03	0.287	1.39

general data

TCOOL	TATM	PATM	VOLUME	AREABY	TQSTAT	FPREVM
300.	293.	1.E+5	40.	0.0050	48.	6.00

control loop gains

K1	K2	K3	K4	K5	K6	K7	K8
.674	0.1	50.	.13	260.	.00588	60.	.0

APPENDIX 4
PART 12

MODES.DAT - simulation type,duty cycle & init.states

```
2                   !no.of modes in cycle
0                   !0=dyno.,1=vehicle sim.
4.4,210.,.4,0.      !mode 1:demand,load tq.,run time,-.
10.,210.,5.7,0.     !mode 2:----------- " ------------
note:for veh.sim.these are: demand,gradient,mode distance,brake eff.
3200.,1430.,1.43,5.2,0.,10.,0.,1.43 !initial guesses for dyn.states;
Ncomp,No/s,Pvol,Xrack,Vrack,Xnoz,Vnoz,Pcomp for DCECS- models
.001,.02,.1         !timestep,ctrl.interval,data recording interval
```

SCHEDS.DAT - setpoint schedules

```
9,6                                    !dimensions of schedules
1.,1.,1.,1.,1.,1.,1.,1.,1.
1.65,1.64,1.64,1.63,1.63,1.63,1.65,1.65,1.65
2.4,2.4,2.4,2.4,2.3,2.3,2.3,2.3,2.3
3.,3.,3.,3.,2.9,3.,3.,3.,3.              ! 9x6 boost schedule
3.5,3.7,3.7,3.7,3.6,3.6,3.4,3.2,3.
4.,4.,4.,4.,3.8,3.6,3.4,3.2,3.
4,4,4,4.2,5.8,7.5,6.5,7,7
4,4,4,4.2,5.8,7.5,6.5,7,8
4,3.6,3.5,4.6,7.2,7.2,7,8,9              ! 9x6 stat.timing schedule
3.4,3.2,3,5,7.5,8,8.5,9.2,9.75
2.2,2.5,2.8,3.8,5,6,7.1,8.2,9
1.25,1.9,2.5,2.75,3,4,5.5,7,8.25
14.67,14.67,14.67,14.67,14.67,14.67,14.67,14.67,14.67
14.67,14.67,14.67,14.67,14.67,14.67,14.67,14.67,14.67
14.67,14.67,14.67,14.67,14.67,14.67,14.67,14.67,14.67
14.67,14.67,14.67,14.67,14.67,14.67,14.67,14.67,14.67  !fixed turb.
14.67,14.67,14.67,14.67,14.67,14.67,14.67,14.67,14.67  !gear ratio
14.67,14.67,14.67,14.67,14.67,14.67,14.67,14.67,14.67
```

TRUCK.DAT - vehicle parameters

```
32000.,7.65,0.7,6.78,1.056,0.,15.
  a     b   c    d    e   f   g
```

a: vehicle mass [kg]
b: frontal area [m2]
c: drag.coeff.Cd [-]
d: rear axle ratio
e: tyre rolling dia.[m]
f: wind speed [m/s]
g: total wheel/tyre/brakes/hub inertia [kg m2]

APPENDIX 5

ACTUATOR DYNAMICS

The major DCE controls (fuel rack and turbine VG nozzle position) use electrohydraulic actuators each comprising an analog positional control circuit driving a Moog 76-338 servovalve, which admits a 1200psi hydraulic supply to a bi-directional ram. In order to design a digital control system, the dynamics of these actuators must be quantified.

Moog approximate the response of their servovalves to a second-order transfer function, typically with a damping ratio of 0.7 and 90deg. phase lag at 200Hz. The general form is thus:

$$\frac{\text{ram velocity}}{\text{servovalve current}} = G_v(s) = \frac{1}{1 + \tau_2 . s + \tau_1^2 . s^2}$$

therefore Arg. $G_v(i\omega) = \tan^{-1} \{ \omega \tau_2 / (1 - \omega^2 . \tau_1^2) \}$

and damping ratio $c = \tau_2 / 2.\tau_1$

These give $\tau_2 = 1.1$ ms and $\tau_1 = 0.8$ ms.

So $$Gv(s) = \frac{k_v}{1 + s/900 + s^2/1562500}$$

where s is the Laplace variable, and where k_v is the dc gain given by the maximum ram velocity (servovalve maximum flowrate at 1200psi supply pressure and low load pressure, divided by ram piston area) at the maximum servovalve current.

From Moog data the rated flow is 43 l/min and rated current is 8mA.

For the fuel rack ram, piston diameter is 12mm.

Thus $k_v = 800$ [m/As].

If the ram is assumed to act as a pure integrator,

ram position = ram velocity / s

Thus the overall actuator open loop transfer function is

$$\frac{\text{ram position}}{\text{driver current}} = G_a(s) = \frac{800}{s.(1 + s/900 + s^2/1562500)}$$

For stability the actuators work closed-loop; for DCE control system design the actuator overall (ie. closed-loop) transfer function (OTF) is therefore required. Position feedback is provided by LVDT with suitable scaling, as shown in fig.1. LVDT response is "flat" in the frequency range of interest, as is that of the analog board op-amps. Both are therefore represented as gains only.

Referring to the nomenclature of fig.1, the OTF is:

$$\frac{\text{ram position}}{\text{setpoint}} = G_c(s) = \frac{kc \,.\, Ga(s)}{1 + k_f . k_c . G_a(s)}$$

The theoretical OTF for the rack actuator is sketched (Bode plot) in fig.2, scaled to a dc gain of 0 dB. The theoretical response is excellent up to about 600Hz, much better than required for the application.

The above analysis excludes mechanical/hydraulic resonances. Approximate calculations of the ram load resonance frequency, given by

$$f_1 = 2\pi \sqrt{k_0 / m}$$

where k_0 is the hydraulic stiffness

m is the inertia referred to the ram

gave f_1 as approximately 1.3kHz for the rack actuator (cf. for example the highest DCE engine firing frequency of 130Hz). These effects were therefore thought negligible.

The frequency responses of both actuators were measured to check this analysis. The tests were done on the closed loops, exciting the feedforward (setpoint) input, and taking the response from the LVDT feedback signal rather than fit separate accelerometers. The equipment is listed below:

Excitation: Feedback Ltd. FG601 function generator

Response: ac LVDT and Sangamo CA-1 conditioning card

Data capture: Iwatsu DS6121 digital storage oscilloscope. 8 bit resolution, 20MHz clock rate.

The measured rack and VG actuator closed-loop transfer functions are sketched in figs.3 and 4 respectively (NB the frequency scales are shifted by one decade cf. the theoretical response of fig.2). The measured frequency responses were poorer than expected. In terms of the 90deg. phase lag frequency:

Theoretical	Rack OTF	700rad/s (110Hz)
Measured	Rack OTF	40rad/s (6.5Hz)
Measured	VG OTF	100rad/s (16Hz)

The reason for the low rack 90deg. lag frequency is probably the sliding friction damping effect of the close-tolerance fuel pump components. The measured phase responses fall below 180deg., however, a second-order approximation was considered adequate when fitting parametric models to the data.

For dynamic simulation a state space model is required, that is a set of first-order differential or difference equations. These were obtained as described below.

From the above analysis (for the theoretical case) we know that

$$\tau_a^2 \cdot \ddot{q} + \tau_b \cdot \dot{q} + q = k_v \cdot i \qquad (1)$$

where i is the servovalve current
q is the oil flowrate to ram
k_v = oil flowrate per unit valve current

(and $\tau_a^2 = 1/1562500$, $\tau_b = 1/900$ were obtained above)

Also $$x = k_j \cdot q \qquad (2)$$

where x is the ram velocity
k_j = 1 / ram piston area

Also, $$i = k_i \cdot e \qquad (3)$$

where u is the setpoint
r is the ram position feedback
e is the error signal u-r
k_i is the error gain

Finally, $$r = k_f \cdot x \qquad (4)$$

where x is the ram position
k_f is the feedback scaling

Thus we have a set of equations (1)-(4) describing the state of the system. In state space form we require 3 first order equations (the theoretical system response is third-order).

Define a new state $y = \dot{q}$

then $\ddot{q} = \dot{y}$

(1) can then be re-arranged as:

$$\dot{y} = (k_i \cdot k_v \cdot u - k_i \cdot k_v \cdot k_f \cdot x - \tau_b \cdot y - q)/\tau_a$$

(2) is $\dot{x} = k_j \cdot q$

and $\dot{q} = y$ as defined above.

So we have 3 state equations; the states are x (ram position), q (oil flowrate) and y (rate of change of flowrate). The setpoint or feedforward input is u. In matrix form:

$$\begin{bmatrix} \dot{x} \\ \dot{y} \\ \dot{q} \end{bmatrix} = \begin{bmatrix} 0 & 0 & k_j \\ -k_i.k_v.k_f/ & -\tau_b/\tau_a & -1 \\ 0 & 1 & 0 \end{bmatrix} . \begin{bmatrix} x \\ y \\ q \end{bmatrix} + \begin{bmatrix} 0 \\ k_i.k_v/\tau_a \\ 0 \end{bmatrix} . u$$

and these equations may be incorporated into a dynamic simulation. The simulation must carry three new states for each actuator. This is the theoretical actuator model - as noted above, second-order models were identified from the experimental data - described below.

A graphical approach to parameter estimation was adopted. Candidate parametric models were plotted on Bode and Nyquist diagrams for comparison with the measured data, to get the best match of amplitude and phase responses. To facilitate the process, an interactive program was written on a DEC LSI11/23 microcomputer to produce log gain, phase and real/imaginary components of candidate models in half-decade steps over the frequency range of interest. A typical result, comparing the measured rack response and a second-order model, is shown in fig.5. For a second-order model, good starting values for the time constants may be obtained by some simple observations about the Nyquist plot . The best parameter estimates so obtained were then reduced to state space models in the same way as the theoretical model example above. The final models were:

(i) Rack:

$$\begin{bmatrix} \dot{v} \\ \dot{x} \end{bmatrix}_{RACK} = \begin{bmatrix} -120 & -2000 \\ 1 & 0 \end{bmatrix} . \begin{bmatrix} v \\ x \end{bmatrix}_{RACK} + \begin{bmatrix} 2000 \\ 0 \end{bmatrix} .u_{RACK}$$

(ii) VG:

$$\begin{bmatrix} \dot{v} \\ \dot{x} \end{bmatrix}_{VG} = \begin{bmatrix} -80 & -1600 \\ 1 & 0 \end{bmatrix} \begin{bmatrix} v \\ x \end{bmatrix}_{VG} + \begin{bmatrix} 1600 \\ 0 \end{bmatrix} .u_{VG}$$

where x = actuator position
v = actuator velocity
u = setpoint (feedforward position demand)

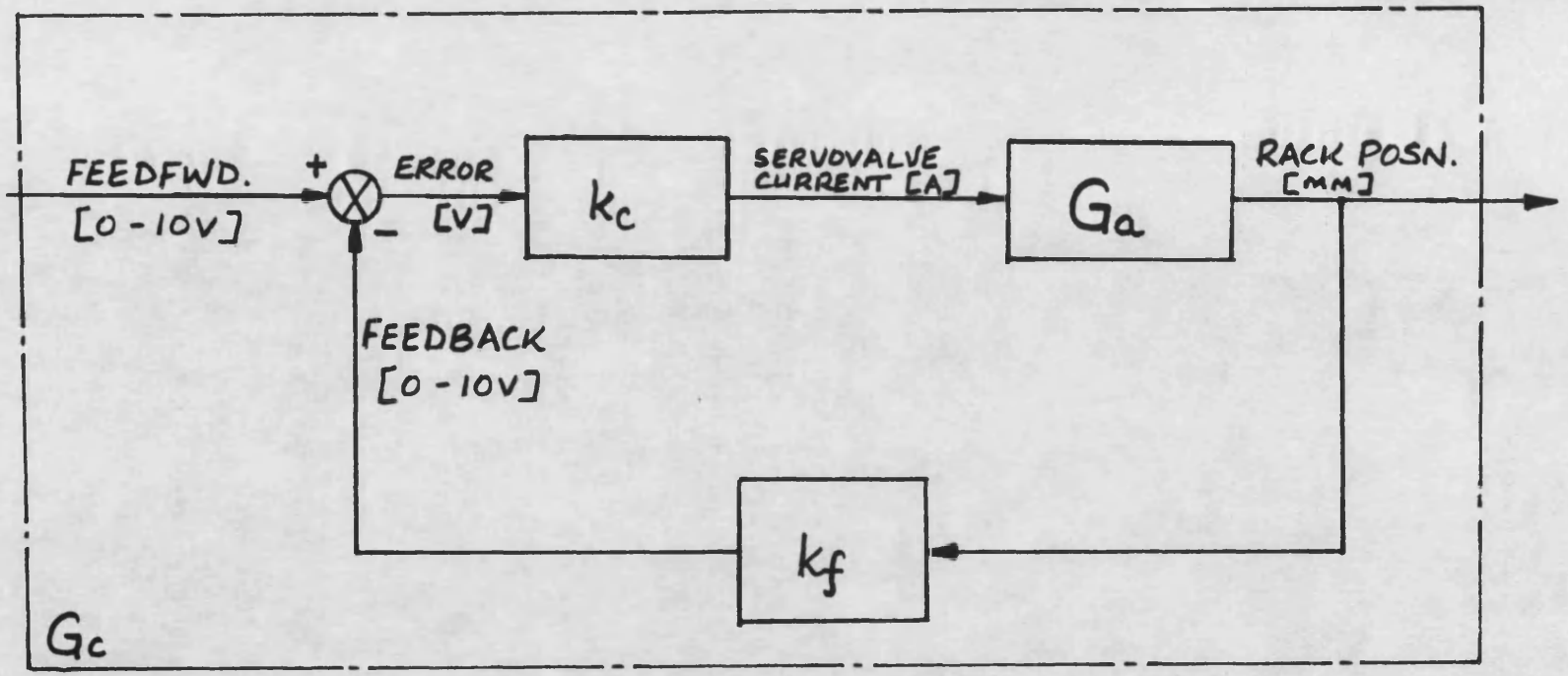

k_c : ANALOG BOARD CONTROL GAIN
k_f : FEEDBACK SCALING
G_a : ACTUATOR OPEN-LOOP FREQUENCY RESPONSE
G_c : CLOSED LOOP FREQUENCY RESPONSE

FIG. 1 ELECTROHYDRAULIC ACTUATOR – BLOCK DIAGRAM

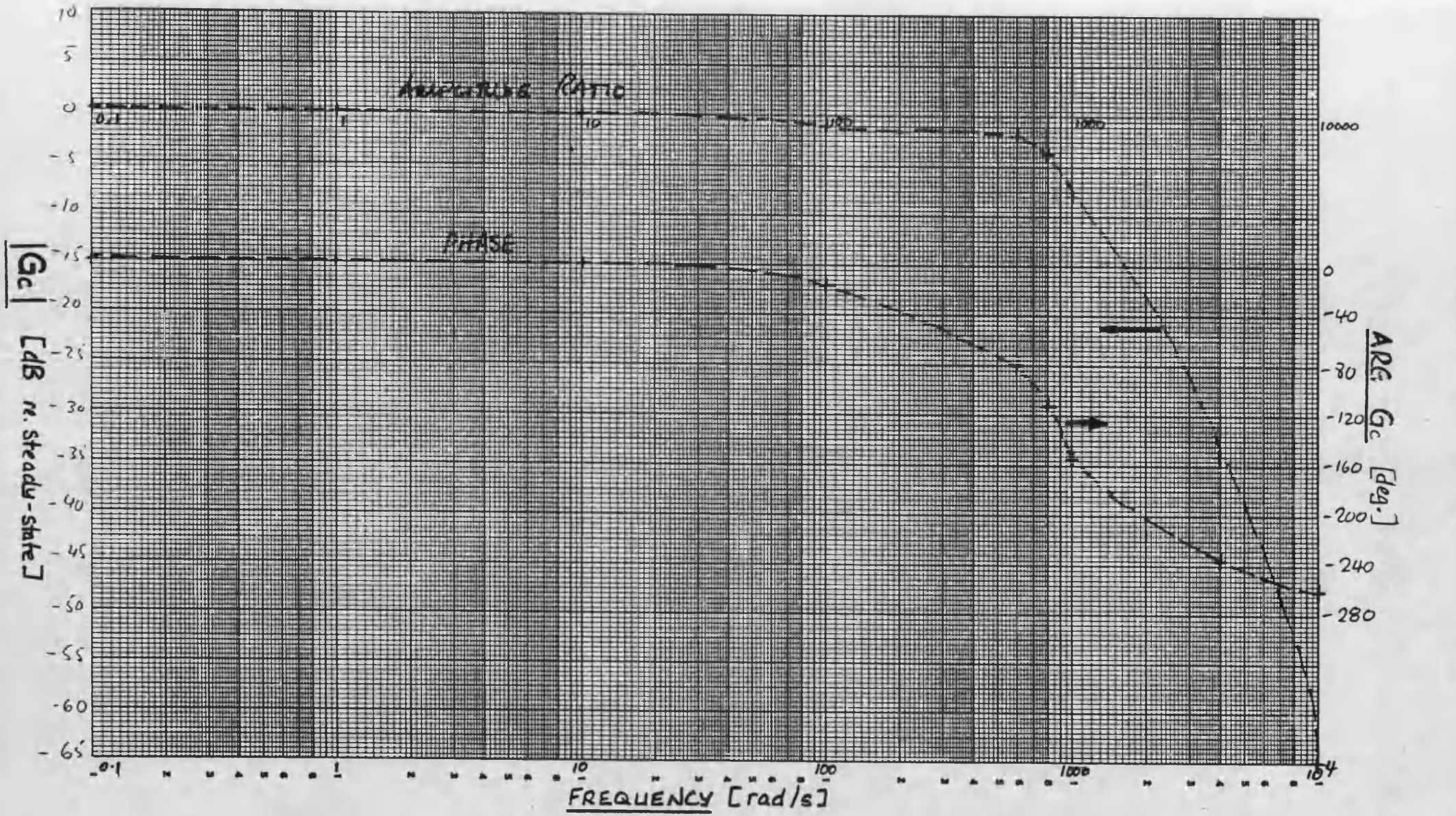

THEORETICAL RACK ACTUATOR CLOSED-LOOP RESPONSE – BODE PLOT

FIG. 2

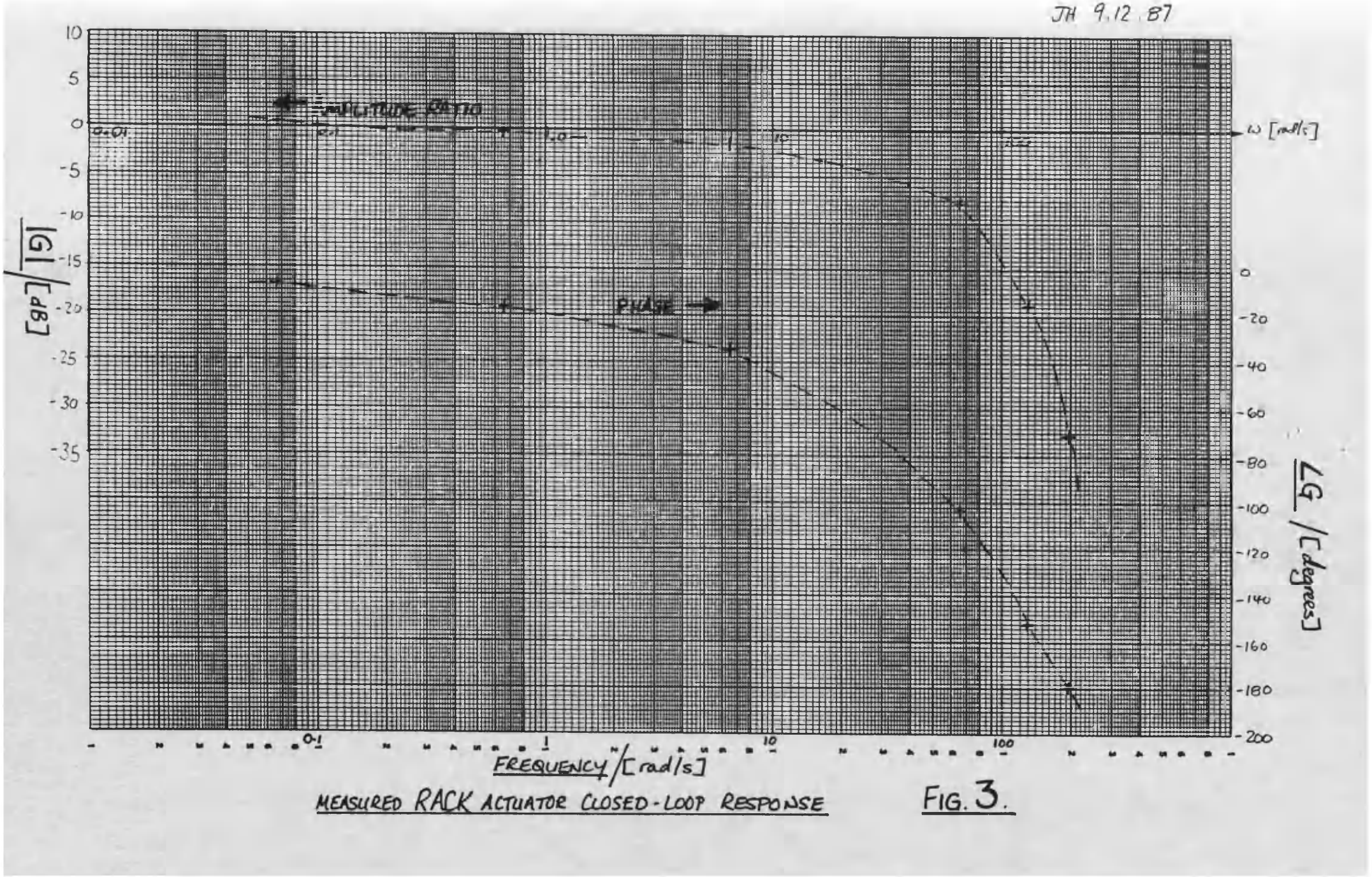

MEASURED RACK ACTUATOR CLOSED-LOOP RESPONSE

FIG. 3.

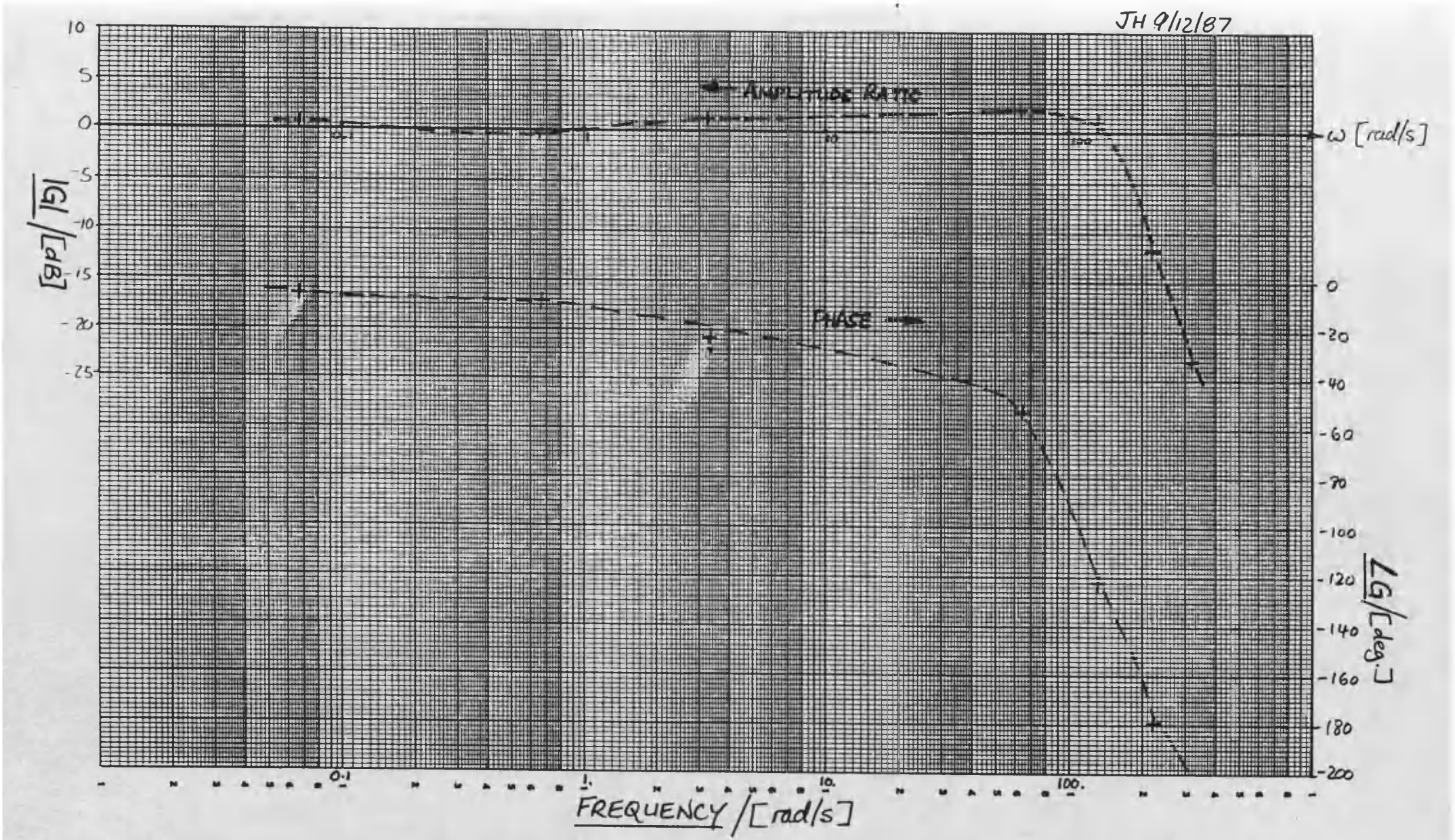

MEASURED TURBINE NOZZLES ACTUATOR CLOSED-LOOP RESPONSE

FIG. 4

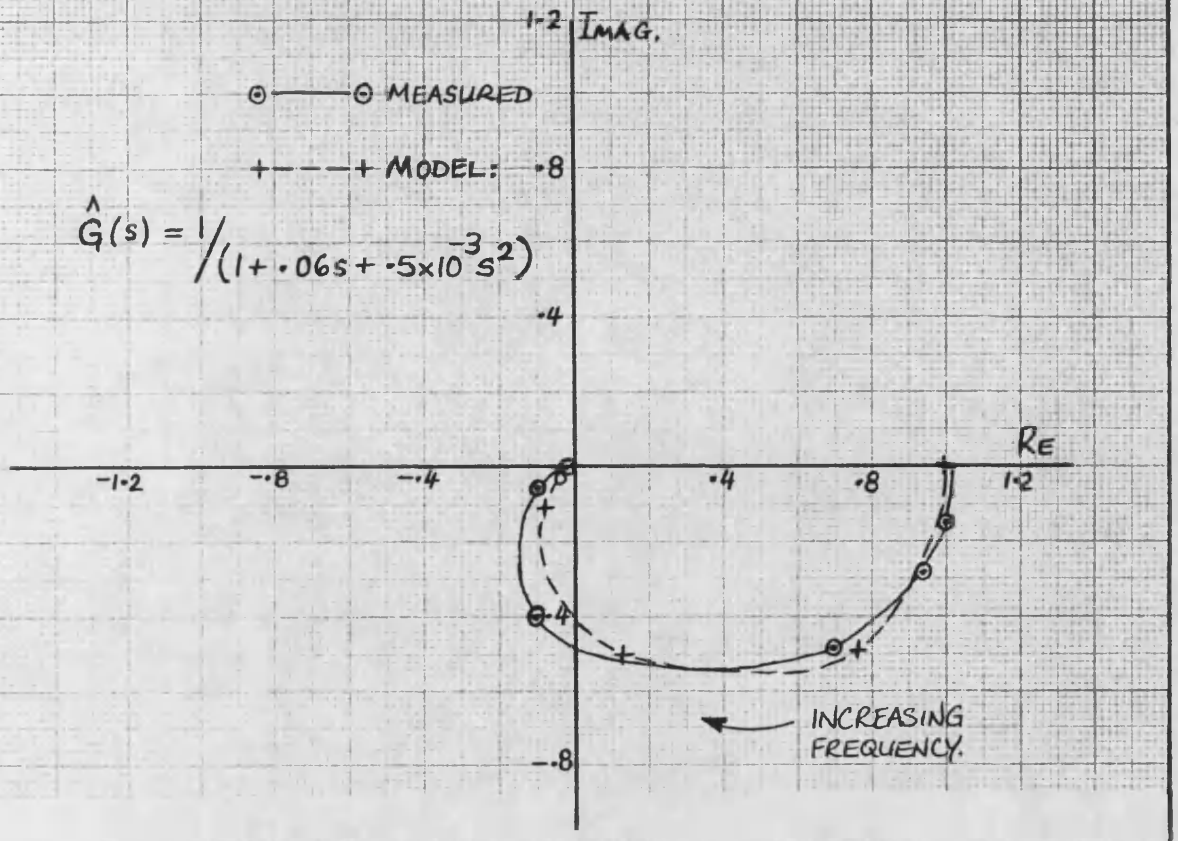

RACK : MEASURED FREQUENCY RESPONSE

GAIN	PHASE [ms]	log Gain	Gain [dB]	T [ms]	phase [deg]	-phase [deg]
.98	440	-8.7739e-3	-0.175	9520	-16.6	16.600
.837	92	-0.077	-1.540	960	-34.5	34.500
.404	27.6	-0.394	-7.880	95.2	-104	104.000
1.059	2000	0.025	0.500	93200	-7.7	7.700
.023	16.2	-1.638	-32.760	32.4	-180	180.000
.114	20.4	-0.943	-18.860	48.2	-152	152.000

RACK: "BEST FIT" SECOND ORDER PARAMETRIC MODEL.

DC GAIN: 1.000
1st ORDER TIME CONST.: 0.6000E-01
2nd ORDER TIME CONST.: 0.5000E-03

Freq[rad/s]	[Hz]	Gain[dB]	Phase[deg]	REAL	IMAG.
0.10E-01	0.159E-02	-0.1085E-05	-0.3438E-01	1.000	-0.6000E-03
0.32E-01	0.503E-02	-0.1165E-04	-0.1087	1.000	-0.1897E-02
0.10	0.159E-01	-0.1191E-03	-0.3438	1.000	-0.6000E-02
0.32	0.503E-01	-0.1129E-02	-1.087	0.9997	-0.1897E-01
1.0	0.159	-0.1128E-01	-3.435	0.9969	-0.5984E-01
3.2	0.503	-0.1116	-10.80	0.9698	-0.1849
10.	1.59	-1.012	-32.29	0.7525	-0.4752
32.	5.03	-5.855	-75.24	0.1299	-0.4928
0.10E+03	15.9	-17.16	56.31	-0.7692E-01	-0.1154
0.32E+03	50.3	-34.41	21.17	-0.1775E-01	-0.6872E-02
0.10E+04	159.	-54.02	6.856	-0.1975E-02	-0.2375E-03
0.32E+04	503.	-73.99	2.174	-0.1998E-03	-0.7582E-05
0.10E+05	0.159E+04	-93.98	0.6875	-0.2000E-04	-0.2400E-06

FIG. 5

RACK ACTUATOR PARAMETER ESTIMATION

APPENDIX 6

DIFFERENCE EQUATIONS FOR DIESEL ENGINE TORQUE DELAY

The design of a Diesel engine speed controller may need to account for the delay between control action and engine response due to cyclic combustion. This can be done by including an approximation to the delay in the plant dynamic equations. An alternative is to develop the difference equations for the system based on a state space model with delay:

$$\underline{x}(t) = \underline{F}.\underline{x}(t) + \underline{G}.\underline{u}(t - \delta) \qquad (1)$$

$$y(t) = \underline{H}.\underline{x}(t) \qquad (2)$$

where δ is the delay between action and effect.

Taking the general solution to eqn.(1) and working in discrete time, the following difference equation is found (Ref.1 below):

$$\left.\begin{aligned} \underline{x}(k+1) &= \underline{\Phi}.\underline{x}(k) + \underline{\Gamma}_a.\underline{u}(k) + \underline{\Gamma}_b.\underline{u}(k+1) \\ \text{where} \quad \underline{\Gamma}_a &= \Phi(m).\ \underline{\Psi}(T-m).(T-m).\underline{G} \\ \underline{\Gamma}_b &= \underline{\Psi}(m).m.\underline{G} \end{aligned}\right\} \quad (2) \quad \text{for } \delta < T$$

and where m is defined by

$$\delta = l.T + m \ , \ (l \text{ integer, } m \text{ real, } T \text{ is sample period})$$

that is, δ is separated into a number (l) of sample periods and a remainder (m). For the general case of $\delta > T$ $(l > 1)$ the difference equation becomes more complex and it is necessary to invent more states to eliminate "old" values of u from the equation.

Difficulty arises for an engine in choosing an appropriate δ (and thus the appropriate form of eqn.(2)). Assuming a controller sample interval of (say) T = Ø.ØØ2 sec, the following range of l,m is possible for the Leyland 5ØØ engine:

"Worst case": control output just after an injection, engine speed 8ØØ rev/min. Assume half stroke to "torque production".

δ = Ø.Ø25s (time between injections) + Ø.Ø19s (9Ø deg.crank)

= Ø.Ø44s.

T = Ø.Ø2s therefore l = 2, m = Ø.ØØ2s.

"Best case": control output just before injection, 26ØØ rev/min. Again assume half stroke to "torque production".

δ = Øs + Ø.ØØ6s (9Ø deg.crank) = Ø.ØØ6s

T = Ø.Ø2s therefore l = Ø, m = Ø.ØØ6s.

The above illustrates the variation over a typical range of operation. Not surprisingly, there is a similar decision to be made when using a continuous approximation to the delay, for example in choosing a time constant for a first-order lag approximation as outlined below.

The "sampling" delay of a 6 cylinder 4 stroke Diesel engine, due to cyclic combustion, may be approximated by a first-order lag (Ref.2):

$$G_d(s) = \frac{1}{k_d.s + 1} = \frac{\alpha}{s + \alpha}$$

where α = engine speed [rev/min] / 13.

This may be discretised using the impulse invariant transform (Ref.3)

$$z = e^{sT}$$

where T is now the integration timestep of the discrete computation. The result is

$$G_d(z) = \alpha.z / (z - e^{-\alpha.T})$$

$$= \alpha / (1 - e^{-\alpha.T} .z^{-1})$$

We expect a unity steady-state gain, that is the actual torque will eventually equal the ideal torque at a given fuelling. However,

$$G_{d\ [st.state]} = \alpha / (1 - e^{-\alpha.T})$$

so to match the steady-state gain we use

$$G'_d(z) = \frac{1 - e^{-\alpha.T}}{\alpha} \cdot \frac{\alpha}{1 - e^{-\alpha.T}.z^{-1}}$$

or

$$\frac{Y(z)}{X(z)} = \frac{1 - e^{-\alpha.T}}{1 - e^{-\alpha.T}.z^{-1}} \qquad (3)$$

where y(t) = actual engine torque
x(t) = ideal torque corresponding to instantaneous fuelling.

The above equation (3) may be re-arranged:

$$Y(z).(1 - e^{-\alpha.T}.z^{-1}) = (1 - e^{-\alpha.T}).X(z)$$

this gives a difference equation (z^{-1} represents a unit time delay)

$$y(k) = e^{-\alpha.T}.y(k-1) + (1 - e^{-\alpha.T}).x(k)$$

Thus the current actual torque y(k) may be calculated from the current fuelling (which gives x(k)) and the actual torque at the last timestep y(k-1). The model should calculate the factor $e^{-\alpha T}$ at each timestep (ie. based on length T of timestep and current α =engine speed/13) for maximum accuracy.

References:

1. Franklin GF & JD Powell

   "Digital control of dynamic systems" Addison-Wesley 1980.

2. Flower JO & PA Hazell

   "Sampled data theory applied to the modelling and control analysis of compression ignition engines - Part II"

   Int.J.Control 13(4), 1971.

3. Katz P

   "Digital control using microprocessors" Prentice-Hall 1981.

APPENDIX 7.
PART 1.

```
   SUBROUTINE CTRLR(DCE,XERROR)
```

```
                          ACTLb2.FOR
  subroutine of DCEcs- in simdce. Open loop control of rack and
  nozzles (and timing). PRBS excitation of rack or nozzle ctrl,
  Recursive Least-Squares identification of Engine speed or Turb
  inlet pres.response. 2nd ord.ARIMA model used in each case.
```

```
 last change 26Ø489 JH

 Written : J.Hall  26 Apr.1989 (based on ACTLb1.)
 Machine : PC-AT compatibles
 Code    : Microsoft FORTRAN 77 Vers.4.1


      IMPLICIT REAL (A-H,J-Z)
      ..unless explicitly re-declared below
      IMPLICIT INTEGER(I)

      DIMENSION DCE(8),DCEDOT(8)
 variables which change during run
      COMMON /A/  NENG,AENG,NTURB,AFR,PCOMP,PINMAN
      COMMON /E/  FPREV,FPREVA,NOZ,NOZA,TGR,TIM,TIMA
      COMMON /F/  DEMAND,URACK,UNOZ,U3,U4,EFFOLD,EFFNEW,ISS
      COMMON /L/  CGR,OGR

 ---CONTROL/IDENTIFICATION----------------------------------------
 SISO RLS param.est.for input-output 2nd order model
 Note 1:not all params in call may be used,but are included for
 possible future use.
 Note 2:identification is done here so that corresponding ctrl
 input and system output are sampled.
      IF(ISS.EQ.1) THEN
         do prbs,control and identification via rls12
         CALL IDENT(URACK,UNOZ,DCE,NENG)
      ELSE
         just do fixed control until process stable at start pt.
         CALL IPGEN(Ø)
      END IF

      RETURN
      END
```

```
      SUBROUTINE IPGEN(IBIT)
```

```
 generates control inputs to process/plant model on basis of
 ibit, which may be PRBS.
```

```
last change 26Ø489
Written JH Ø7Ø489
PC-AT compat.; Microsoft FORTRAN 4.1
      IMPLICIT REAL (A-H,J-Z)
```

```
      IMPLICIT INTEGER(I)

      COMMON /A/  NENG,AENG,NTURB,AFR,PCOMP,PINMAN
      COMMON /E/  FPREV,FPREVA,NOZ,NOZA,TGR,TIM,TIMA
      COMMON /F/  DEMAND,URACK,UNOZ,U3,U4,EFFOLD,EFFNEW,ISS
      COMMON /GAINS/ K1,K2,K3,K4,K5,K6,K7,K8

 ---NOZZLE CONTROL-----------------------------------------------------
 direct feedfwd nozzle demand Ø-1ØV
      UNOZ=DEMAND

 ---RACK CONTROL-------------------------------------------------------
 fixed posn = K1 Volts during initialisation of DCE condition.
 PRBS, amplitude (+/-)K2 Volts about K1 Volts median setting during
 identification.
      IF(ISS.EQ.1) THEN
      run prbs input
         IF(IBIT.EQ.Ø) THEN
            URACK=K1-K2
         ELSE
            URACK=K1+K2
         END IF
      ELSE
      stay at median posn
         URACK=K1
      END IF

 ---TIMING CONTROL-----------------------------------------------------
 optimum st.state static timing [Volts] is TIM (fr.common block)
      U3=TIM

 ---CVT and BYPASS CONTROL not used------------------------------------
 bypass wide open
      U4=Ø.


      RETURN
      END

-----------------------------------------------------------------------
-----------------------------------------------------------------------

      SUBROUTINE PRBS(IBIT)
 ---------------------------------------------------------------------
 ¦ prbs generator. uses primitive polyn.mod.2,in this case 18th order, ¦
 ¦ to generate a wideband random bit sequence .                        ¦
 ---------------------------------------------------------------------
 last change 31Ø389
 Written: JH 31Ø389 based on Numerical Recipes function IRBIT1.
 Code   : MicroSoft FORTRAN Version 4.1
 Machine: PC-AT compatibles

      LOGICAL NEWBIT
      INTEGER ISEED,IBIT
      INTEGER*4 IB1,IB2,IB5,IB18
 set up polynom. with pwrs of 2
      PARAMETER(IB1=1, IB2=2, IB5=16, IB18=131Ø72)
      COMMON /P/ ISEED

      NEWBIT = IAND(ISEED,IB18) .NE. Ø
      IF(IAND(ISEED,IB5).NE.Ø) NEWBIT=.NOT.NEWBIT
      IF(IAND(ISEED,IB2).NE.Ø) NEWBIT=.NOT.NEWBIT
```

```
      IF(IAND(ISEED,IB1).NE.Ø) NEWBIT=.NOT.NEWBIT
 shake the seed
      ISEED = IAND( ISHFT(ISEED,1) , NOT(IB1) )
 random bit
      IF(NEWBIT) THEN
         IBIT=1
         ISEED=IOR(ISEED,IB1)
      ELSE
         IBIT=Ø
      END IF

      RETURN
      END

------------------------------------------------------------------------
------------------------------------------------------------------------

      SUBROUTINE IDENT(URACK,UNOZ,DCE,NENG)
 ------------------------------------------------------------------------
¦---------------------------- RLS12b ------------------------------¦
 ------------------------------------------------------------------------
¦ recursive least squares identification of 2nd order 1-variable      ¦
¦ ARIMA input-output model                                            ¦
 ------------------------------------------------------------------------
 last change 270489
 Written: J Hall April 1989, based on RLS12a.for
 Code   : MicroSoft FORTRAN version 4.1
 Machine: PC-AT compatibles

      IMPLICIT REAL (A-H,J-Z)
      IMPLICIT INTEGER (I)
      INTEGER*4 IRLSCT

      COMMON /GAINS/ K1,K2,K3,K4,K5,K6,K7,K8
      COMMON /RLS/   P,THETA,ONEMAT,IRLSCT
      COMMON /PU/    PARMON,IMON

      DIMENSION DCE(8),PARMON(4,12Ø)
      DIMENSION P(4,4),ONEMAT(4,4)
      DIMENSION THETA(4,1),PSI(4,1),PSIT(4,1),L(4,1),SCRF(4,1)
      DIMENSION SCRA(4,1),SCRB(1,1),SCRC(4,4),SCRD(4,4),SCRE(1,1)

      IRLSCT=IRLSCT+1
      IF(IRLSCT.LT.3) THEN
         initialise state vector:
         update state vector (ARIMA model). right-shift last data,
         and put new data in left-hand end of each partition.
         new control,o/p MOVES are:
         DY=DCE(3)-YOLD
         DU=URACK-UOLD
         PSI(2,1)=PSI(1,1)
         PSI(1,1)=-DY
         PSI(4,1)=PSI(3,1)
         PSI(3,1)=DU
         update ctrl/o/p positions for next time
         YOLD=DCE(3)
         UOLD=URACK

      ELSE
      do recursive estimation
      update input values
         PSI(4,1)=PSI(3,1)
         PSI(3,1)=DU
```

```
C           calc correction gain matrix L (in several stages)
            CALL MMULT(P,4,4,PSI,4,1,SCRA)
            CALL TMAT(PSI,4,1,PSIT)
            CALL MMULT(PSIT,1,4,SCRA,4,1,SCRB)
            IF(K8.EQ.Ø. .OR. K7.EQ.Ø.) STOP ' RLS12:STOP: K7 or K8=Ø'
            DUM2=1./K8
            CALL SMULT(SCRB,1,1,DUM2,SCRE)
            DUM1=K8 * ( (1./K7 + SCRE(1,1)) )
            IF(DUM1.EQ.Ø.) STOP ' RLS12:STOP: /Ø in L array update calcs.'
            DUM1=1./DUM1
            CALL SMULT(SCRA,4,1,DUM1,L)
C           ("collect" new data here ie DCE(3),unoz)
C           recursively update parameter vector estimate
            CALL MMULT(PSIT,1,4,THETA,4,1,SCRB)
C           CARIMA model update is: theta=theta + L.(dy-psi.theta)
C           first compute new ctrl,o/p moves (we need dy, not y) :
            DY=DCE(3)-YOLD
            DU=URACK-UOLD
            DUM1=-(DY - SCRB(1,1))
            CALL SMULT(L,4,1,DUM1,SCRA)
            CALL MSUB(THETA,SCRA,4,1,SCRF)
C           write updated theta (scrf)into theta using smult for convenience
            DUM1=1.
            CALL SMULT(SCRF,4,1,DUM1,THETA)
C           update estimate variance array P
            CALL MMULT(L,4,1,PSIT,1,4,SCRC)
            CALL MSUB(ONEMAT,SCRC,4,4,SCRD)
            CALL MMULT(SCRD,4,4,P,4,4,SCRC)
            CALL SMULT(SCRC,4,4,DUM2,P)
C           update the ARIMA state vector
            PSI(2,1)=PSI(1,1)
            PSI(1,1)=-DY
C           update the ctrl and o/p positions for next time:
            YOLD=DCE(3)
            UOLD=URACK
C           get next PRBS bit (ibit)...
            CALL PRBS(IBIT)
C           ..and use it to generate next control input(s)
            CALL IPGEN(IBIT)
C           (note-everything but ibit passed thro common blocks)
         END IF
C
C write param.estimates to array periodically - start pt and every
C (k6)th update thereafter.
C
         IF(IRLSCT.EQ.3 .OR. MOD((IRLSCT+3),K6).EQ.Ø) THEN
            IF(IRLSCT.EQ.3) IMON=Ø
            IMON=IMON+1
            IF(IMON.LE.12Ø) THEN
               DO 5 I=1,4
                  PARMON(I,IMON)=THETA(I,1)
  5            CONTINUE
            ELSE
               WRITE(*,9Ø6)
 9Ø6           FORMAT(/' RLS12:WARNING: param.array PARMON is full')
            END IF
         END IF
C
         RETURN
         END
```

```
      SUBROUTINE MMULT(A,NRA,NCA,B,NRB,NCB,C)
C  ------------------------------------------------------------------
C ¦ matrix multiplication  [C]=[A].[B]                               ¦
C  ------------------------------------------------------------------
C  last change Ø30489
C  written: JH Ø30489
C  code   : MicroSoft FORTRAN vers.4.1
C  machine: PC-AT compat.
C
      INTEGER NRA,NCA,NRB,NCB
      INTEGER I,J,K
      REAL A(NRA,NCA),B(NRB,NCB),C(NRA,NCB)
C
      IF(NCA.NE.NRB) STOP 'MMULT: matrix dims.incompatible'
C
      DO 1Ø I=1,NRA
         DO 2Ø J=1,NCB
            C(I,J) = Ø.
            DO 3Ø K=1,NCA
               C(I,J) = C(I,J) + A(I,K)*B(K,J)
 3Ø         CONTINUE
 2Ø      CONTINUE
 1Ø   CONTINUE
C
      RETURN
      END
C ------------------------------------------------------------------
C
      SUBROUTINE TMAT(A,NRA,NCA,B)
C  ------------------------------------------------------------------
C ¦ matrix transpose [B] = [A]T                                      ¦
C  ------------------------------------------------------------------
C  last change Ø30489
C  written JH Ø30489
C
      INTEGER NRA,NCA,I,J
      REAL A(NRA,NCA),B(NCA,NRA)
C
      DO 1Ø I=1,NRA
         DO 2Ø J=1,NCA
            B(J,I) = A(I,J)
 2Ø      CONTINUE
 1Ø   CONTINUE
C
      RETURN
      END
C ------------------------------------------------------------------
C
      SUBROUTINE SMULT(A,NRA,NCA,K,B)
C  ------------------------------------------------------------------
C ¦ matrix scaling  [B] = k.[A]  where k scalar                       ¦
C  ------------------------------------------------------------------
C  last change Ø30489
C  written  JH Ø30489
C
      INTEGER NRA,NCA,I,J
      REAL K
```

```
      REAL A(NRA,NCA),B(NRA,NCA)
C
      DO 1Ø I=1,NRA
         DO 2Ø J=1,NCA
            B(I,J) = K * A(I,J)
2Ø       CONTINUE
1Ø    CONTINUE
C
      RETURN
      END
C ------------------------------------------------------------------
C
      SUBROUTINE MSUB(A,B,NRA,NCA,C)
C  ----------------------------------------------------------------
C ¦ matrix subtraction [C] = [A] - [B]                            ¦
C  ----------------------------------------------------------------
C  last change Ø30489
C  written  JH Ø30489
C
      INTEGER NRA,NCA,I,J
      REAL A(NRA,NCA),B(NRA,NCA),C(NRA,NCA)
C
      DO 1Ø I=1,NRA
         DO 2Ø J=1,NCA
            C(I,J)=A(I,J)-B(I,J)
2Ø       CONTINUE
1Ø    CONTINUE
C
      RETURN
      END
```